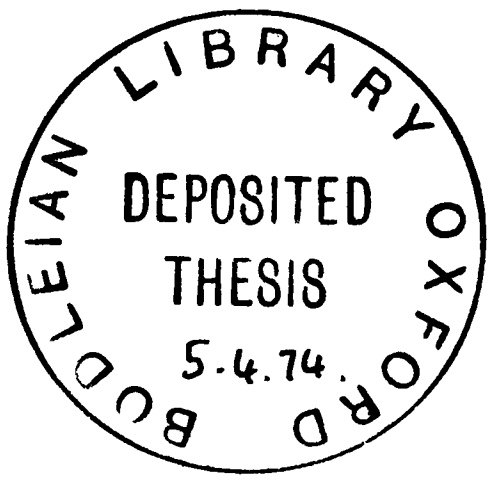
THESIS SUBMITTED FOR THE DEGREE OF DOCTOR OF PHILOSOPHY
UNIVERSITY OF OXFORD

MINERAL EQUILIBRIA IN THE LEVEN SCHISTS NEAR FORT WILLIAM, INVERNESS-SHIRE

by

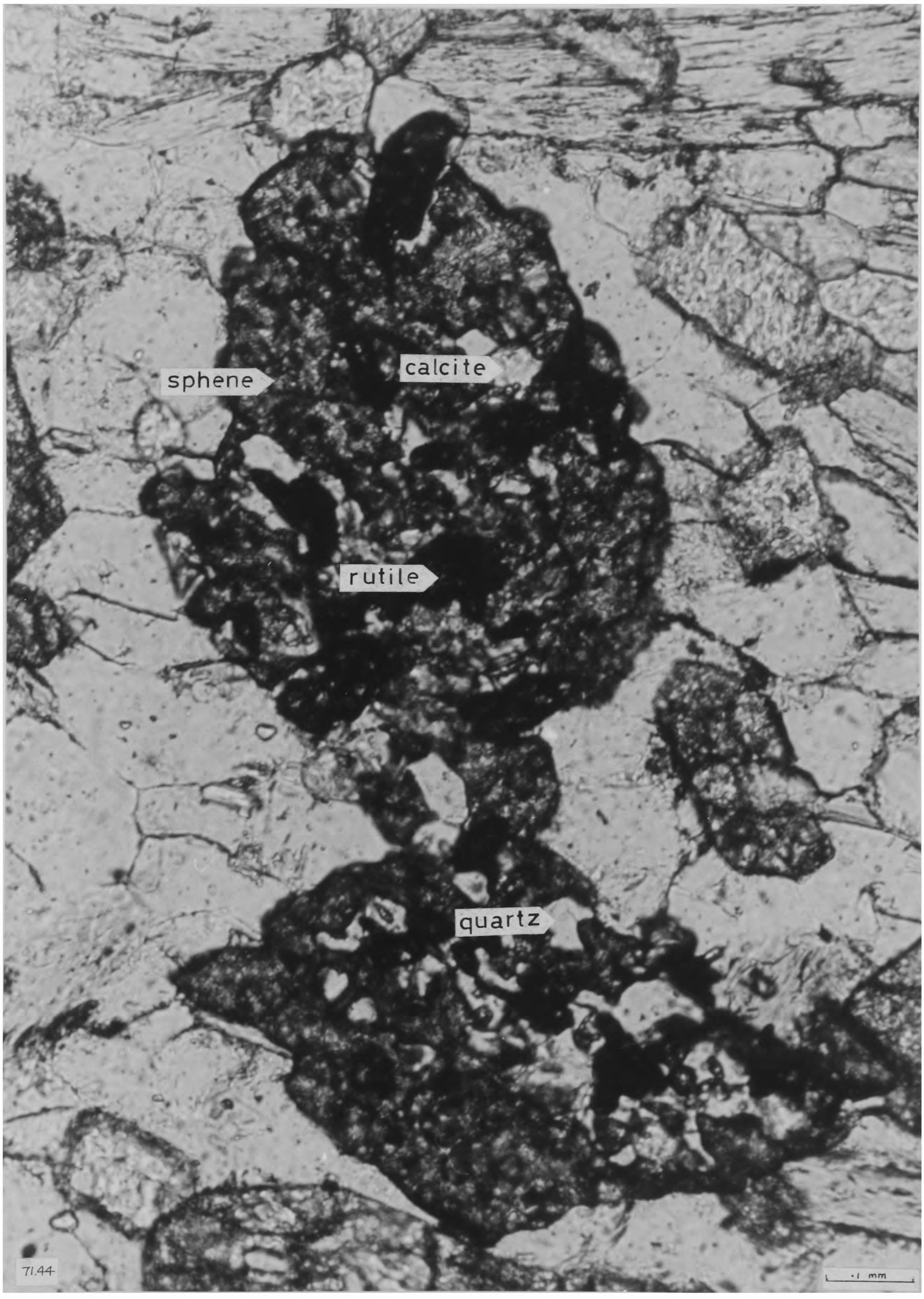
ROGER POWELL



Oriel College
and
Department of Geology and Mineralogy,
Oxford

1973

FRONTISPIECE



sphene → rutile + calcite + quartz

ABSTRACT

Models of upper mantle and crustal processes relating to metamorphism can be proposed if the distribution of temperature and pressure during a metamorphic event is known. Knowledge of the distribution of temperature and pressure during the Dalradian metamorphism in the west and south west Scottish Highlands has not materially increased since Elles and Tilley (1930) applied Barrow's (1912) zones to this area. This study was initiated to improve this situation.

Rocks from an area 3 miles by 2 miles, east and south east of Spean Bridge, 15 miles east of Fort William, Inverness-shire, were studied to find the conditions of metamorphism, temperature and pressure and the composition and behaviour of the fluid phase attending metamorphism. The rocks are siliceous dolomites, carbonate-bearing pelites (calc-pelites), Ca - rich, but carbonate - free pelites, graphitic pelites and graphitic calc-pelites of the Leven Schists metamorphosed in the garnet zone of the epidote amphibolite facies. Characteristic assemblages are :

pelites: quartz-oligoclase-biotite-chlorite-muscovite-garnet-epidote-ilmenite

siliceous dolomites: quartz-oligoclase-phlogopite-chlorite-talc-tremolite-calcite-dolomite-rutile

calc-pelites: quartz-oligoclase-biotite-chlorite or muscovite-epidote-calcite-calcite-dolomite-sphene and/or rutile

The rocks show a considerable variety of assemblages which appear to be in textural equilibrium. The preponderance of low variance assemblages and the occurrence of apparently incompatible assemblages, even on a thin section scale, suggest that the fluid phase composition was buffered by the assemblage. The relationship of fluid pressure to solid pressure and the composition of the fluid phase are discussed and

it is concluded that $P_{fluid} = P_{total}$ and $P_{CO_2} + P_{H_2O} = P_{fluid}$ are good approximations except in the graphitic rocks where methane was an important component of the fluid phase. The metamorphic variables that control the assemblages are considered to be temperature, pressure and X_{CO_2} (and X_{CH_4} in the graphitic rocks).

The descriptions and calculations on the assemblages are considered in terms of a model system, K_2O-CaO-MgO-Al_2O_3-SiO_2-CO_2-H_2O, with the phases quartz, anorthite, calcite, dolomite, talc, tremolite, clinochlore, muscovite, phlogopite, clinozoisite and grossularite which are components of minerals found in the assemblages.

A thermodynamic background for the calculation of metamorphic conditionsis presented. The calculations are only as reliable as the thermodynamic data. The errors on the best calorimetric determinations of enthalpies of minerals become unacceptably large when applied to the enthalpy change of a reaction because the enthalpy of reaction is often an order of magnitude smaller than the enthalpy of individual minerals. The corollary is that precise relative thermodynamic data can be calculated from experimentally reversed reactions. A calculation method is presented and is used to derive themodynamic data for the model system phases and, in addition, forsterite, enstatite, sphene, wollastonite, annite, Fe-chlorite, almandine, Fe-staurolite, Fe-chloritoid and Mg-cordierite. These data and the activities of the model system components in microprobe analysed minerals are used to infer the metamorphic conditions.

The % $MgCO_3$ in calcite in equilibrium with dolomite provides a geothermometer with the experimental calibration of the calcite-dolomite solvus in $MgCO_3$-$CaCO_3$ by Goldsmith and Newton (1969). The natural carbonates contain iron, but Fe is shown to have little or no affect on the solvus. About 20 calcites from each of seven calcite-dolomite bearing rocks were probe analysed to apply the calcite-dolomite geothermometer.

There is evidence from the area of two metamorphic events, a main event affecting the whole area and a late event affecting only the siliceous dolomites.

The calcites from the rocks, apart from the siliceous dolomites show a narrow range of composition, representing a temperature of 546°C at 2 kbars or 530°C at 6 kbars. There is no indication of a temperature gradient across the area. The analysed assemblages are all univariant in the model system; one variable, temperature, is fixed, so that the others can be calculated.

1. A graphitic assemblage

quartz-oligoclase-biotite-chlorite-clinozoisite-tremolite-calcite-dolomite-graphite

is univariant if the fluid phase contained methane. Applying the calcite temperature, this assemblage formed at about 5.6 kbars with $X_{CH_4} = 0.30$ and $X_{CO_2} = 0.40$.

2. Two calc-pelitic assemblages

quartz-oligoclase-biotite-chlorite-epidote-calcite-dolomite

quartz-oligoclase-biotite-muscovite-epidote-calcite-dolomite

give pressures of 4.8 and 5.0 kbars and $X_{CO_2} = 0.55$ and 0.60 respectively.

3. The fine grained parts of the siliceous dolomites appear not to have been affected by the late event. Two different assemblages

quartz-oligoclase-tremolite-talc-dolomite-clinochlore

quartz-oligoclase-tremolite-calcite-dolomite-clinochlore

give pressures of 4.5 and 4.7 kbars and X_{CO_2} of 0.3 and 0.8 respectively.

4. The carbonate-free pelitic assemblages are compositionally far removed from the model system. Although they are model invariant (if $X_{CO_2} = 0$), reactions that intersect to form the invariant point do not converge in the pressure range of metamorphism. This is interpreted as being due to the failure of the method for calculating activities

at this degree of dilution.

The conditions of metamorphism for the main metamorphic event from 1, 2 and 3 above are concluded to be about 5 kbars at 535°C with variable fluid phase composition.

The siliceous dolomites have been recrystallised along irregular surfaces on which large tremolites are developed. The assemblage in the coarse grained part of the siliceous dolomites is model invariant,

quartz-albite-phlogopite-talc-chlorite-tremolite-calcite-dolomite

This represents metamorphic conditions of about 420°C and 1 kbar. The calcites from the siliceous dolomites have a wide spread in $\%MgCO_3$. This is interpreted as re-equilibration at a lowertemperature than the main event, probably between 400° and 450°C. Fluid inclusion studies (by Mr F.W. Smith , Durham University) on a semi-conformable quartz vein from within the area defines a pressure temperature band for the formation of the quartz vein. This intersects the band of calcite temperatures and corresponds with the calculated conditions for the siliceous dolomite assemblage. The late metamorphic event, at about 420°C and 1 kbar, is interpreted as a late flushing through of the area by magmatic or metamorphic fluids along fractures through the pelites and into the more permeable rocks along minor planes of weakness to form the coarse assemblage of the siliceous dolomites and partly re-equilibrate the calcites.

The distribution of sphene and rutile in calcite-quartz bearing assemblages cannot be interpreted as equilibrium if the above calculations are correct. For sphene to have been stable, the X_{CO_2} must have been less than 0.03. It is considered that sphene is metastable in many of the calcite-quartz bearing assemblages, casting some doubt upon the conclusions of Ernst (1971) on the fluid phase composition during the Franciscan and Sanbagawa metamorphism.

References

Barrow, G., 1912, Proc. Geol. Ass. 23, 268-73

Elles, G.L., and Tilley, C.E., 1930, Trans. R. Soc. Edinb.56, 621-46

Ernst, W.G., 1972, Geochim. cosmochim. Acta 36, 497-504

Goldsmith, J.R., and Newton, R.C., 1969, Am. J. Sci. 267-A, 160-190.

LIST OF CONTENTS

		page number
CHAPTER 1 :	INTRODUCTION	1
CHAPTER 2 :	THERMODYNAMIC PRINCIPLES	6
	Laws of thermodynamics	12
	Gibbs fundamental equation	15
	Meaning of dn_i	16
	Thermodynamic potentials	16
	Equilibrium and stability	19
	Chemical equilibrium using chemical potentials	20
	Phase rule	21
	Gases	22
	Activity	25
	Equilibrium constant	27
	Gibbs energy	28
	Activity coefficients	32
CHAPTER 3 :	PRACTICAL THERMODYNAMICS	42
	Main data sources	42
	Methods of calulation	46
	Gas data	51
	H_2O	51
	CO_2	53
	O_2	56
	H_2	56
	Gas mixtures	58
	$CO_2 - H_2O$	58
	CH_4-CO_2 and CH_4-H_2O	60
	$H_2 - H_2O$ and $H_2 - CO_2$	61
	O_2 in C - H - O	61

Data for solid phases 63

magnesite 66

dolomite 66

talc 68

diopside 73

wollastonite 73

forsterite 76

orthoenstatite 76

sphene 78

tremolite 80

minerals that contain aluminium 82

muscovite 84

clinochlore 85

phlogopite 89

cordierite 89

annite . 92

grossularite 92

zoisite and clinozoisite 94

iron chlorite 97

almandine 97

iron staurolite 99

iron chloritoid 102

Activity coefficients of solid mixtures 104

halite - sylvite again 111

magnesiowustites 111

calcite-dolomite 118

enstatite - diopside 127

hercynite - magnetite 128

CHAPTER 4 : THE ROCKS 129

lithologies 129

Model system 133

Textures 142

Analytical data 144

Assemblages 147

Group 1: talc + tremolite subgroup 147

Group 1: tremolite + clinozoisite subgroup 154

Group 1: amphibole bearing garnet pelite subgroup 158

Group 2: carbonate-free subgroup 163

Group 2: carbonate-present subgroup 174

Discussion of Bailey (1934) 181

Fluid inclusions 183

CHAPTER 5 : METAMORPHIC CONDITIONS 186

Activites 186

Model for metamorphic conditions 188

equilibrium 188

pressure 189

distribution of conditions 191

Metamorphic conditions 192

calcite-dolomite geothermometry 192

model system calculations 203

rutile-sphene relations 231

iron analogue to the model system 236

Reaction paths 236

Summary, implications and conclusions 240

APPENDIX 1 : NOTATION 263

APPENDIX 2 : DERIVATION OF THE FUGACITY POLYNOMIAL FOR H_2O 265

APPENDIX 3 : COMPUTER PROGRAMS 274

APPENDIX 4 : THERMODYNAMIC DATA 329

APPENDIX 5 : ANALYSES 364

LIST OF REFERENCES 243

LIST OF PLATES

			page
Chapter 1		-	
Chapter 2		-	
Chapter 3		-	
Chapter 4	1	B100: an example of a siliceous dolomite	149
	2	71.79: an example of a hornblende-bearing garnet pelite	159
	3	70.80: an example of a garnet pelite	167
	4	B375: an example of a carbonate-bearing pelite	169
	5	B235: an example of a carbonate-bearing garnet pelite	176

LIST OF TABLES

			page
Chapter 1		-	
Chapter 2		-	
Chapter 3	1	CO_2 polynomial coefficients	54
	2	O_2 polynomial coefficients	54
	3	Oxygen buffers	62
	4	AQC model mixing parameters for calcite I and II from 0.5 to 10.0 kbars	124
Chapter 4	1	Assemblage lists	134
	2	All the reactions in the model system	141
	3	Occurrence of possible assemblages in the ta-tr free model system	162

LIST OF FIGURES

		page
Chapter 1		
1	Location of Spean Bridge	3
2	Geography of Spean Bridge	4
Chapter 2	-	
Chapter 3		
1	Pressure-temperature fields of applicability of the three P-V-T polynomials of Burnham et al. (1969)	44
2	Pressure-temperature fields of applicability of the reduced variable equations of Rhyzenko and Volkov (1971)	45
3	Comparison of approximations for calculating equilibrium temperatures of reactions	52
4	Pressure temperature fields of literature P-V-T data for CO_2	55
5	Magnesite reaction	67
6	Dolomite reaction	69
7	Talc reaction	71
8	Talc reaction	72
9	Diopside reaction	74
10	Wollastonite reaction	75
11	Forsterite reaction	77
12	Sphene reaction	79
13	Tremolite reaction	81
14	Muscovite reaction	86
15	Clinochlore reaction	88
14a	Phlogopite reaction	90
16	Cordierite reaction	93
17	Grossularite reaction	95
18	Zoisite reaction	96
19	Fe chlorite reaction	98

20	Almandine reaction	100
21	Fe Staurolite reaction	101
22	Fe chloritoid reaction	103
23	Plots of literature data used to calculate orthopyroxene activity coefficients	108
24	Diagrammatic comparison of the R model activity coefficients and the orthopyroxene activity coefficients	110
28	Temperature dependence of the AQC model mixing parameter, W_G, for NaCl - KCl	112
29	Comparison of AQC model and SR model and experimentally determined enthalpies of mixing for NaCl - KCl	113
25	Comparison of the R, QC and AQC model mixing parameter for magnesiowustites	115
26	Comparison of the experimentally determined magnesiowustite activities with calculated AQC model activities at 1100°C	116
27	Comparison of the experimentally determined magnesiowustite activities with calculated AQC model activities at 1300°C	117
30	ln X_{MgCO_3} in calcite in equilibrium with dolomite against reciprocal temperature at 1 bar	120
31	Calcite I - calcite II - aragonite diagram	121
32	AQC model mixing parameters, W_H and W_S for calcite I and II as a function of pressure	125

Chapter 4

1	Geological map of area studied	130
2	Bailey's structural interpretation of the area studied	131
3	Specimen locations of rocks in Table 1	138
4	Occurence of amphibole bearing model univariant and divariant assemblages	148

5	Textures 1	152
6	Textures 2	153
7	Textures 3	156
8	Textures 4	160
9	Occurence of model univariant and divariant assemblages with epidote but without garnet	164
10	Occurence of model univariant and divariant assemblages with garnet but without epidote	165
11	Occurence of model univariant and divariant assemblages with garnet and epidote	166
12	Textures 5	170
13	Textures 6	171
14	Textures 7	177
15	Analyses across a zoned garnet in B376	182
16	Fluid inclusion results	184

Chapter 5

1	Distribution of Fe between calcite and dolomite	194
2	Correlation between Mg and Fe in calcite	195
3	Histogram of % $MgCO_3$ in calcite; B100	196
4	Histogram of % $MgCO_3$ in alcite: 71.16	197
5	Histogram of % $MgCO_3$ in calcite: 71.19	198
6	Histogram of % $MgCO_3$ in calcite: 71.26	199
7	Histogram of % $MgCO_3$ in calcite: 71.42	200
8	Histogram of % $NgCO_3$ in calcite: 71.44	201
9	Histogram of % $MgCO_3$ in calcite: 71.64	202
10	Talc + tremolite subgroup, model system, μ_{H_2O} - μ_{CO_2}, topology 1	205
11	Talc + tremolite subgroup, model system, μ_{H_2O} - μ_{CO_2}, topology 2	206

12 Talc + tremolite subgroup, model system, P-T-X_{CO_2}, calculated activities, plagioclase = oligoclase: B100 207

13 Talc + tremolite subgroup, T-X_{CO_2} at 1 Kbar, calculated activites, plagioclase = albite: B100 209

14 Talc + tremolite subgroup, T-X_{CO_2} at 1.5 kbars, calculated activities, plagioclase = albite: B100 210

15 Summary of the evidence for the late metamorphic event 211

16 Tremolite + clinozoisite subgroup, model system, μ_{H_2O}-μ_{CO_2}, Topology 1 212

17 Tremolite + clinozoisite subgroup, model system, μ_{H_2O}-μ_{CO_2}, Topology 2 213

18 Tremolite + clinozoisite subgroup, T-X_{CO_2} at 4 kbars, model system 214

19 Tremolite + clinozoisite subgroup, T - X_{CO_2} at 6 kbars, model system 215

20 Tremolite + clinozoisite subgroup, P-T-X_{CO_2}, calculated activities, 0 % CH_4: 71.19 216

21 Tremolite + clinozoisite subgroup, P-T-XCO_2, calculated activities, 25% CH_4: 71.19 217

22 Tremolite + clinozoisite subgroup, P-T-X_{CO_2}, calculated activities, 50% CH_4: 71.19 218

23 Tremolite + clinozoisite subgroup, P and T against - ln (1 - X_{CH_4}): 71.19 219

24 Garnet pelite amphibole bearing subgroup, P-T at 0% CO_2, calculated activities: 71.19 221

25 Group 2, model system, $\mu_{H_2O} - \mu_{CO_2}$, Topology 1 222

26 " " " " " 2 223

27 " " " " " 3 224

28 " " " " " 4 225

29	Group 2, model system, $\mu_{H_2O} - \mu_{CO_2}$, Topology 5	226
30	" " " " " 6	227
31	Group 2, T - X_{CO_2} at 4 kbars, model system	228
32	Group 2, T - X_{CO_2} at 6 kbars, model system	229
33	Carbonate-free subgroup: P-T at 0%CO_2, calculated activities 70.48, 71.85, 72.3, 72.6	230
34	Carbonate-present subgroup P-T-X_{CO_2}, calculated activities: 71.64 and 71.42	232
35	Carbonate-present subgroup, P-T-X_{CO_2} - X_{CH_4}, calculated activities: B376	233
36	Carbonate-present subgroup, $-\ln(1-X_{CH_4})$ against pressure at 535°C, for B376	234
37	Summary of evidence for the P-T conditions of the main metamorphic event	235
38	Sphene reaction at 4, 5 and 6 kbars	237

Acknowledgements

I thank particularly Dr S.W. Richardson for showing me how to study metamorphic rocks and for much encouragement and guidance. Discussions with A. Middleton, A. Bath, Dr R.K. O'Nions, Dr E.R. Oxburgh, L. Knight and F.W. Smith helped clarify my ideas. I thank Professor G.M. Brown for permission to use the Durham Geoscan Mk II electron probe microanalyser and Dr A. Reckett for providing excellent tuition in its operation. I thank F.W. Smith for the fluid inclusion studies on a quartz vein from my area.

I am grateful to R. Holland for many thin sections, S. Baker for the plates, and Miss S. Fraser and Miss G. Saxon for making a very good job of typing from my handwriting.

I am indebted to Marjorie, my wife, without whose help and moral support this thesis would not have come into being. I thank her particularly for the excellent diagrams.

The work was done during the tenure of a N.E.R.C. studentship.

CHAPTER 1

INTRODUCTION

Introduction

Barrow's (1893, 1912) pioneer studies of the Dalradian metamorphic rocks from the south east Highlands represent the first attempt to bring precision to the study of metamorphism. He introduced a zonal classification for increasing metamorphic grade based on the first appearance of a set of minerals (biotite, garnet, staurolite, kyanite and then sillimanite). The lower part of this sequence was applied to the central and south west Highlands by Elles and Tilley (1930). Studies since then have added considerably to the body of data on the assemblages from the south east, central and south west Highlands (Wiseman (1934), Chinner (1960), McNamara (1965), Atherton (1966), Mather (1970)).

Barrow (1893, 1912) regarded his zones as concentric parts of the aureoles of intrusions of gneissic 'older granites' which are abundant in the higher grade rocks of the south east Highlands. This has been reiterated by Harker (1932) and, in a different guise, by Read (1935) and Kennedy (1948). Elles and Tilley (1930) reject this interpretation because of the absence of the 'older granite' in the south west Highlands. They follow Read (1923) in suggesting that depth of burial was primarily responsible for metamorphism.

It would be necessary to have a detailed structural and metamorphic picture of the Scottish Highlands to understand the metamorphism in terms of crustal and mantle processes. The structure has to be known so that large post metamorphic folds and faults can be returned. The distribution of temperature and pressure and the behaviour of the fluid phase during metamorphism are required if thermal models are to be constructed.

Zonal sequences, although useful for descriptive purposes, cannot

usually be quantified for zones defined by the first appearance of a mineral. Its appearance may be strongly dependant on rock composition. Chinner (1966) gives an approximate distribution of temperatures and pressures for the south east and east Highlands. This is based on the distribution of andalusite, kyanite and sillimanite with the well known aluminium silicate phase diagram (eg. Richardson et al. (1969)) and the distribution of migmatites.

In the west and south-west Highlands, no aluminium silicates are present because the rocks are below the staurolite zone and are compositionally below the garnet-chlorite tie line in the AFM projection (Thompson(1957)). The understanding of the temperature and pressure distribution has not materially increased in this area since Elles and Tilley (1930).

This study was initiated to improve this situation. A short field season looking at rocks from Loch Creran to Roybridge indicated that the most helpful rocks outcropped to the east and south of Spean Bridge in the streams and rivers, Fig 1 and 2. These rocks, siliceous dolomites, calc-pelites, graphitic pelites, and graphitic calc-pelites are a part of the Ballapell Foundation of Bailey (1934). He subdivides the sequence into the Ballachulish Slate, Ballachulish Limestone and Leven Schists. This is unsubstantiated as discussed in Chapter 3; all the rocks are considered to be part of the Leven Schists (sensu lato).

An unusual feature of the rocks is the large proportion of low variance assemblages. This increases the number of reactions which can be written between the components of the minerals and so increases the opportunities for calculating metamorphic conditions. Thermodynamic data ~~is~~ are required for the calculations. Reliable data for some minerals has been tabulated in the literature (eg. Robie and Waldbaum (1968)). For other minerals there ~~is~~ are either no data or the data ~~is~~ are unreliable. Data for those minerals has been calculated from published experimentally reversed reactions. These data and activities calculated from electron

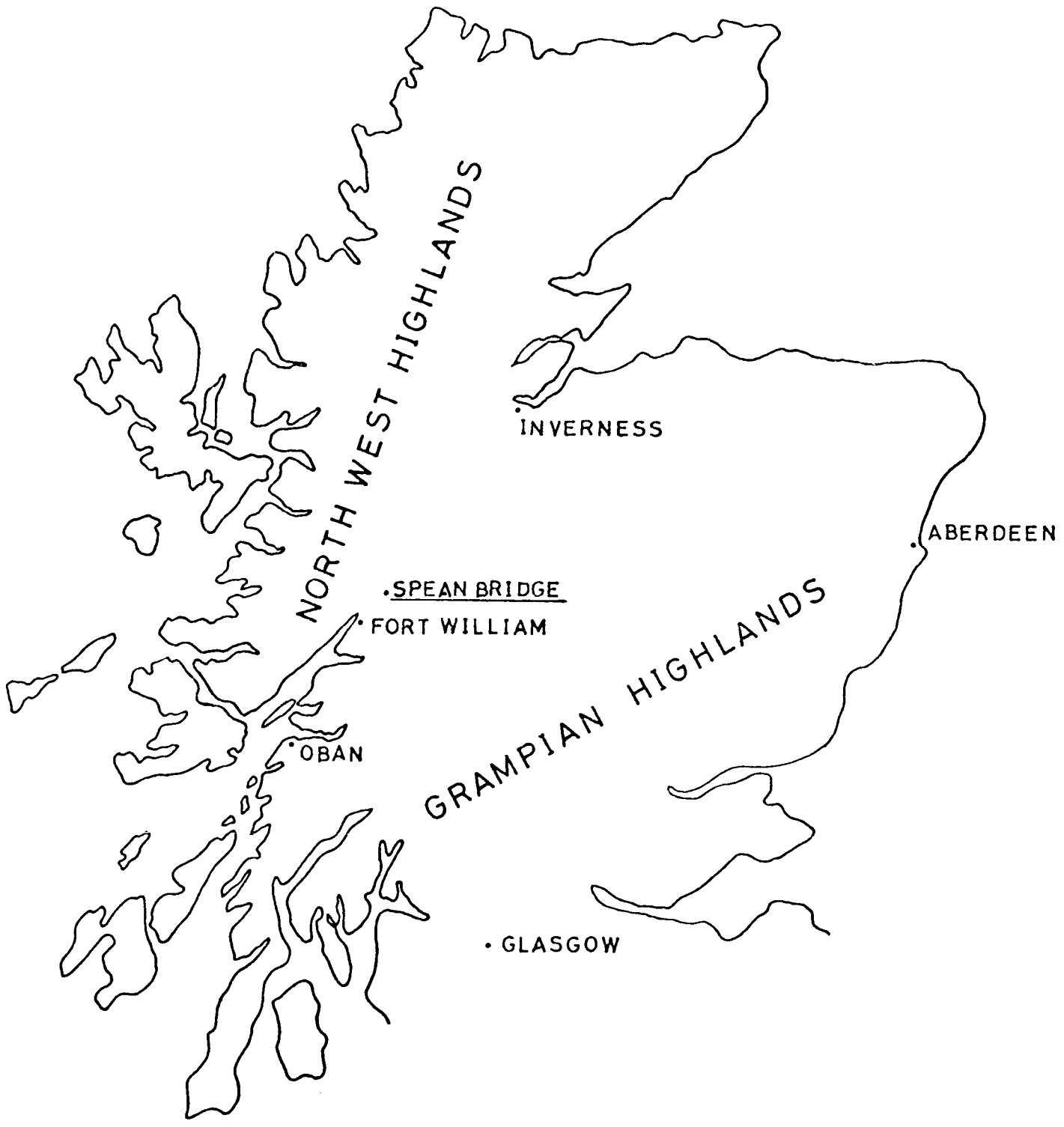


Fig 1:-Location of Spean Bridge

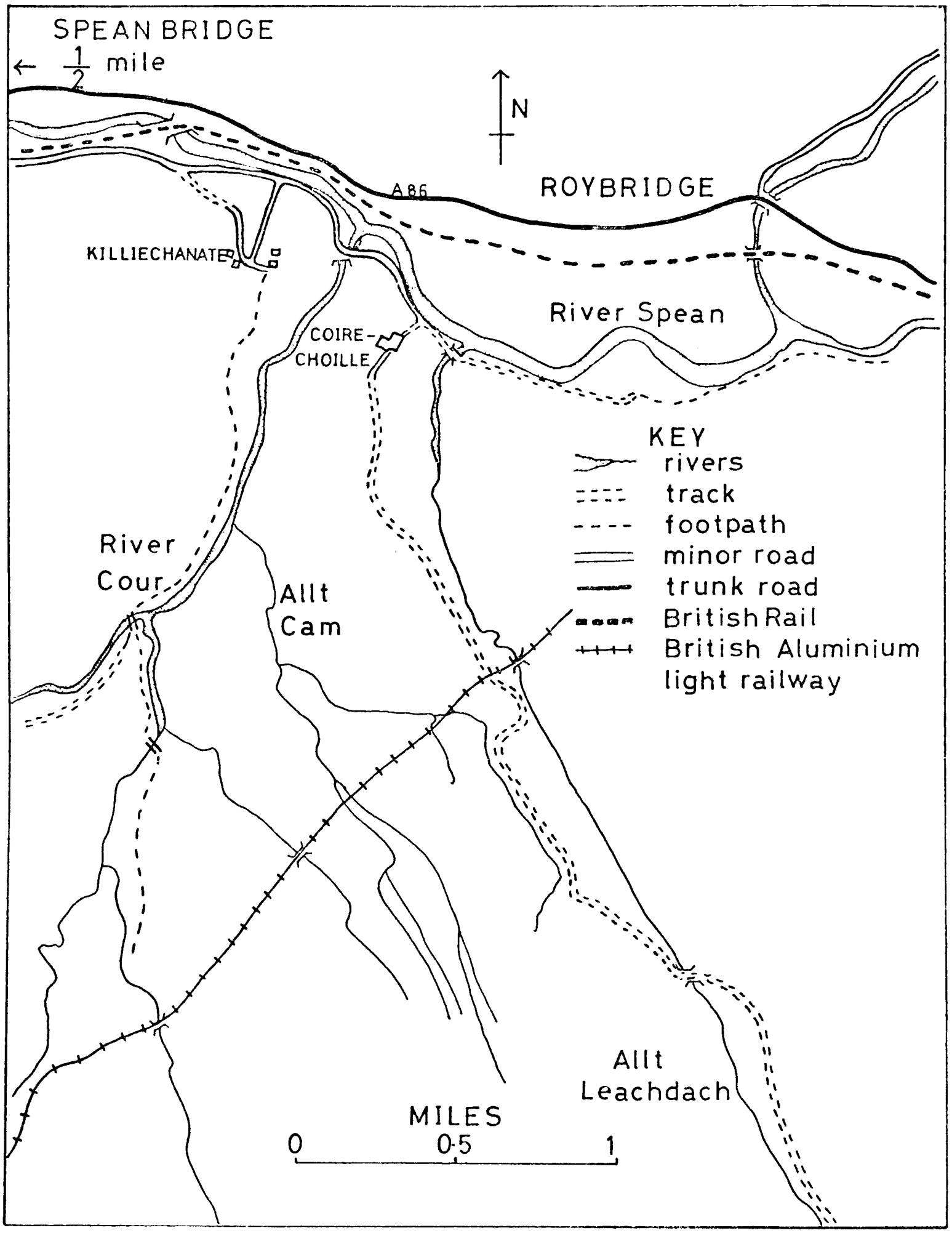


Fig 2 :-Geography of Spean Bridge area.

probe analyses for the minerals from the lowest variance assemblages are used to calculate the conditions of metamorphism.

Figures, plates and tables are numbered consecutively in each chapter and are referred to by their chapter number only from outside the chapter in which it appears.

CHAPTER 2

THERMODYNAMIC PRINCIPLES

THERMODYNAMIC PRINCIPLES

The aim of this chapter is to provide a groundwork for the following chapters where thermodynamic methods will be applied to the Spean Bridge metamorphic rocks. The development starts at the beginning with the so called 'laws' of thermodynamics. This approach has been adopted so that a (metamorphic) geologist without a formal thermodynamics background may appreciate the thermodynamics used later and see where the conventional thermodynamics in geology comes from. Also, it is the approach I had to take to unravel some of the inconsistencies in the thermodynamics used in the geological literature and so that I could develop methods to study my rocks. Discussion of the geological relevance of the assumptions made in this chapter will be left to the next chapters.

The development given in this chapter is compounded from Haase (1971), Munster (1970), Callen (1960), Denbigh (1968), and Lewis and Randall (1961). However, some points treated obliquely or unsatisfactorily by the above are clarified, and an unambiguous notation is provided and summarised in Appendix 1.

In thermodynamics a number of terms are used in a precise way. The majority are set out below, while some are introduced later.

A system is any macroscopic portion of matter that is under consideration. The boundaries of the system are defined in such a way that the system may be considered as isolated, thermally insulated, closed, or open. The surroundings of a system is the rest of the physical world as it may influence the system being considered. The term subsystem is used for any homogenous macroscopic part of a system.

isolated system: there can be no exchange of matter or energy between an isolated system and its surroundings.

thermally insulated system: there can be no exchange of thermal energy or matter between a thermally insulated system and its surroundings.

closed system: there can be exchange of energy but not exchange of matter between a closed system and its surroundings.

open system: there can be exchange of both energy and matter between an open system and its surroundings.

homogeneous system: the intensive properties are independent of location in a homogeneous system. A homogeneous system consists of a single phase.

heterogeneous system: a system consisting of several phases is called a heterogeneous system. A heterogeneous system is called a discontinuous system by Haase (1971) as opposed to a continuous system in which the intensive variables vary over macroscopic parts of the system.

The state of a system is the condition of the system as represented by the macroscopic properties of the system, called state variables. The state of a system is determined by any set of state variables (the independent state variables) such that the result of any further measurement of state variables (the dependent state variables) in the system can be calculated. The dependent state variables can be expressed as functions of the chosen set of independent state variables. Haase (1971) considers the state variables in two groups, the external coordinates (position coordinates of the system in, for example, a gravitational field) and internal state variables (properties of the system isolated from its surroundings). The assumption is made from now on that the system is not affected by any external

fields. The state variables that will be considered are the internal state variables; these fall in two groups, the extensive and the intensive variables.

The extensive variables are the state variables that depend on the quantity of the subsystem considered. If the masses or mole numbers of all the substances in the subsystem are increased by a certain factor, then, for constant intensive variables, the extensive variables increase by the same factor. It follows that extensive variables are additive. Volume obviously comes in this category.

The intensive variables have been defined in two non-equivalent ways:-

Munster (1970 p.49) defines intensive variables as state variables which are capable of contact equilibrium. Contact equilibrium is the attainment of equal values of the intensive properties in adjacent subsystems.

The usual definition (eg. Prigogine and Defay 1954) is that intensive variables are state variables that do not depend on the quantity of subsystem considered. The definitions are only equivalent for homogeneous systems. Certain quantities, derived from extensive variables by division by mass (specific quantities), by number of moles (molar quantities), or by volume (generalised density), are intensive variables only on the second definition for the general case of a heterogeneous system. Variables which are intensive only by Munster's definition will be called intensive variables (for example, pressure and temperature), while those variables which are intensive only by the second definition will be called derived intensive variables (for example, molar volume and density). Derived intensive, intensive, and extensive variables have a clear mathmatical meaning.

Consider a function $f = f(a_1, a_2, a_3 \ldots\ldots a_r)$. It is said to be t^{th} degree homogeneous if

$$f(ka_1, ka_2, ka_3 \ldots\ldots ka_r) = k^t f(a_1, a_2, a_3 \ldots\ldots a_r) \qquad (1)$$

From which by differentiating with respect to k and setting k = 1,

$$\sum_{i=1}^{r} \left(\frac{\partial f}{\partial a_i}\right)_{a_j\,(j\neq i)} a_i = tf \qquad (2)$$

This relation is known as Euler's theorem (eg Bowman and Gerard 1967, p.149).

For t=1, from (1)

$$f(ka_1, ka_2, ka_3 \ldots\ldots ka_r) = kf(a_1, a_2, a_3 \ldots\ldots a_r)$$

If the a_i are identified with the mole numbers n_i, it is clear that extensive variables are first degree homogeneous functions in the mole numbers, (other variables being constant).

For t=0, from (1)

$$f(ka_1, ka_2, ka_3 \ldots\ldots ka_r) = f(a_1, a_2, a_3 \ldots\ldots a_r)$$

Again, identifying a_i with n_i, it is clear that intensive variables are zeroth degree homogeneous in the mole numbers, (other variables being constant).

For an extensive variable Z, of an r component phase, from (2),

$$\sum_{i=1}^{r} \left(\frac{\partial Z}{\partial n_i}\right)_{n_j(j\neq i)} n_i = Z \qquad (3)$$

For an intensive variable Y of an r component phase

$$\sum_{i=1}^{r} \left(\frac{\partial Y}{\partial n_i}\right)_{n_j\,(j\neq i)} n_i = 0 \qquad (4)$$

Expressions (3) and (4) are used later.

The derived intensive variables are now considered:-

mean molar quantities, for an extensive property Z in an r component phase, are defined by

$$z = Z/\sum_{i=1}^{r} n_i \tag{5}$$

For r=1, this reduces to z=Z/n where z is now called the molar Z. If Z is identified with n_i then z is x_i, the mole fraction of i,

$$x_i = n_i / \sum_{i=1}^{r} n_i \quad \text{note that} \quad \sum_{i=1}^{r} x_i = 1 \tag{6}$$

Similarly if Z is identified with the volume V then z is v, the molar volume.

$$v = V / \sum_{i=1}^{r} n_i$$

partial molar quantities for an extensive property Z in an r component phase, other variables being constant, are defined by

$$z_i = \left(\frac{\partial Z}{\partial n_i}\right)_{n_{j(j\neq i)}}$$

This may now be used to simplify Euler's theorem for an extensive variable Z

$$Z = \sum_{i=1}^{r} \left(\frac{\partial Z}{\partial n_i}\right)_{n_{j(j\neq i)}} \qquad n_i = \sum_{i=1}^{r} z_i n_i \tag{7}$$

By setting $k = 1 / \sum_{i=1}^{r} n_i$ in (1), and from (6), (7)

$$z = \sum_{i=1}^{r} z_i x_i \tag{8}$$

By comparing (8) with (3) it is clear that mean molar quantities are first degree homogenous in the mole fractions, although, from the way they are defined they are zeroth degree homogenous functions in the mole numbers.

Similarly it can be shown that partial molar quantities are first degree homogenous in the mole fractions and zeroth degree homogenous in the mole numbers. For example, using volume V, these four statements can be summarised by:- (9)

$$V = \sum_{i=1}^{r} v_i x_i \qquad 0 = \sum_{i=1}^{r} v_i n_i \qquad V_i 0 = \sum_{i=1}^{r} \left(\frac{\partial v_i}{\partial x_i}\right) x_j (j \neq i) \qquad 0 = \sum_{i=1}^{r} \left(\frac{\partial v_i}{\partial n_i}\right) n_i$$

To derive partial molar quantities from experimentally determined mean molar quantities, it is necessary to have an equation relating them. Munster (1970, p.105) shows that for a partial molar quantity z_i in an r component phase

$$z_i = z - \sum_{j=1}^{r\,(j\neq i)} x_j \left(\frac{\partial z}{\partial x_j}\right)_{x_k (k \neq j)} \tag{10}$$

For example, for volume, in a binary between components 1 and 2

$$v_1 = v - x_2 \left(\frac{\partial v}{\partial x_2}\right)$$

$$v_2 = v - x_1 \left(\frac{\partial v}{\partial x_1}\right) \tag{11}$$

An <u>equilibrium state</u> is one in which the intensive variables are independent of time through internal causes; if the system became isolated the intensive variables would not vary with time. It has been found that the size of the set of independent state variables is a minimum in an equilibrium state.

stable equilibrium: the system is in an equilibrium state and there is no other state more stable.

metastable equilibrium: the system is in an equilibrium state and is stable relative to all states whose intensive variables are infinitesimally different, but is less stable

than at least one state which is finitely different.

unstable equilibrium: the system is in an equilibrium state but is unstable relative to a state whose intensive variables are infinitesmally different.

internal (mosaic, local) equilibrium: a subsystem is in equilibrium but the system is not.

Component The term component will be used in a way unfamiliar to geologists. A component of a phase is a chemical entity that can be independently added to or subtracted from the phase. Thus a component has the same meaning as an end member as used in mineralogy. For example Mg_2SiO_4 and Fe_2SiO_4 are components of olivine while FeO, MgO, SiO_2 are not.

Laws of thermodynamics

Thermodynamics, as a part of theoretical physics, is one of a group of phenomenonological theories in which only macroscopically measurable quantities are considered and the 'laws' of the theory are derived from experience of macroscopic phenomena; they are 'rules of experience'.

The zeroth law can be stated as follows:-

if two systems are both in thermal equilibrium with a third system, they are in thermal equilibrium with each other (due to Caratheodory, 1909).

The systems have a property in common related to 'hotness', called empirical temperature, equal between two systems in thermal equilibrium.

The first law can be stated simply in two parts, the work done on a thermally insulated system is independent of the source of work and the path through which the system passes from the initial to the final state

and the work done on a closed system is not necessarily equal to the increase of the energy of the system.

The first part of the formulation, due to Caratheodory, gives the change of the energy of the system, called the internal energy, U, between two states, A and B, as:-

$$\int_A^B dU = \Delta U = U_B - U_A = w \quad \text{thermally insulated system} \qquad (12)$$

The second part of the formulation, due to Born (1921), gives an unambiguous definition of heat, q, as

$$q = \Delta U - W \qquad \text{closed system}$$

Considering all the work done by the system involves only volume changes then

$$dW = -PdV$$

so that

$$dQ = dU + PdV \qquad (13)$$

Embodied in the first law and expressed by (12) is the independence of path of the internal energy change between two states. This can be expressed mathematically using total differentials.

For a differentiable function $f(a_1, a_2, a_3 \ldots a_r)$, the total (exact, complete) differential, written df, is defined as:-

$$df = \left(\frac{\partial f}{\partial a_1}\right)_{a_{i(i\neq1)}} da_1 + \left(\frac{\partial f}{\partial a_2}\right)_{a_{i(i\neq2)}} da_2 + \ldots + \left(\frac{\partial f}{\partial a_r}\right)_{a_{i(i\neq r)}} da_r$$

$$= \sum_{i=1}^{r} x_i da_i \qquad \text{where } x_i = \left(\frac{\partial f}{\partial a_i}\right)_{x_{j(j\neq i)}} \qquad (14)$$

for example, in Bowman and Gerard (1967, p.148, 194)

Three important situations arise:

(i) When can a function, equal to $\sum_{i=1}^{r} Y_i dx_i$, where $Y_i = Y_i (x_1, x_2 \ldots x_4)$ be written as a total differential,

$$df = \sum_{i=1}^{r} Y_i dx_i \quad \text{if} \quad \frac{\partial Y_i}{\partial x_j} = \frac{\partial Y_j}{\partial x_i}$$, the reciprocity relation

This condition is necessary and sufficient for the given function to be written as a total differential.

(ii) when can a differential dZ be written as a total differential,

In general $\int_A^B dZ \neq Z_B - Z_A$, however if $\int_A^B dZ = Z_B - Z_A$ then

$dZ = df(x_1, x_2, x_3 \ldots x_r)$, and, if z is differentiable,

$$\text{then } dz = \sum_{i=1}^{r} x_i dx_i \quad \text{where } x_i = \left(\frac{\partial f}{\partial x_i}\right)_{x_j(j\neq i)} \tag{16}$$

In words, if z is a function of a set of variables then z can be written as a total differential in these variables.

From (12) and (16), dU is a total differential, so that

$$dU = \sum_{i=1}^{r} x_i da_i \quad \text{where } x_i = \left(\frac{\partial U}{\partial a_i}\right)_{a_j(j\neq i)} \tag{17}$$

where a_i (i=1,2,3 ... r) is a set of independent state variables. This set appears in the formulation of the second law below.

The <u>second</u> law can be formulated most concisely as a set of mathematical statements containing the necessary and sufficient information to cover the 'rules of experience' involved. The connection between experience and mathematical expression is less straightforward than for the other laws of thermodynamics.

There exists an extensive variable, entropy, S, a function of the state variables internal energy U, volume V, and mole numbers n_i in an homogeneous system such that

$$TdS = dU + PdV + \sum_{i=1}^{r} T\left(\frac{\partial S}{\partial n_i}\right)_{U,V,n_j(j\neq i)} \tag{18}$$

where $\mu_i = -T\left(\frac{\partial S}{\partial n_i}\right)_{U,V,n_j(j\neq i)}$ is called the chemical potential

T is the thermodynamic temperature.

Also that, for a thermally insulated system

$$dS \geq 0 \tag{19}$$

Caratheodory (1909) shows the equivalence of the empirical temperature introduced in the zeroth law and the thermodynamic temperature introduced in the second law.

The <u>third</u> law (or Nernst heat theorem, due to Nernst (1906)) is given by Wilks (1971) as

> The contribution to the entropy of a system in internal equilibrium by each aspect (translational motion, rotational motion, disorder of magnetic moments etc) tends to zero as the temperature tends to absolute zero.

The third law provides a means of defining the absolute or third law entropy of a system and this will be considered later.

Gibbs fundamental equation

Equation (18) is called Gibbs fundamental equation and it can be written in two forms

$$dS = \frac{1}{T} dU + \frac{P}{T} dV - \sum_{i=1}^{r} \frac{\mu_i}{T} dn_i \qquad \text{entropy representation} \qquad (20)$$

$$dU = TdS - PdV + \sum_{i=1}^{r} \mu_i \, dn_i \qquad \text{energy representation} \qquad (21)$$

and the following important properties can be noted:-

(i) both representations are characteristic functions of the system. they contain every statement that thermodynamics can make about the system.

(ii) because dS and dU depend only on extensive properties and are extensive themselves, then for one mole of a phase

$$ds = \frac{1}{T} du + \frac{P}{T} dv - \sum_{i=1}^{r} \frac{\mu_i}{T} dx_i \qquad (22)$$

$$du = Tds - Pdv + \sum_{i=1}^{r} \mu_i \, dx_i \qquad (23)$$

(iii) both representations provide definitions of the intensive variables P, T, μ_i because both dU and dS are total differentials. Thus

$$dS = \left(\frac{\partial S}{\partial U}\right)_{V,n_i} dU + \left(\frac{\partial S}{\partial V}\right)_{U,n_i} dV + \left(\frac{\partial S}{\partial n_i}\right)_{U,V,n_{j(j\neq i)}} \qquad (24)$$

comparing (24) and (20)

$$\left(\frac{\partial S}{\partial U}\right)_{V,n_i} = \frac{1}{T}, \quad \left(\frac{\partial S}{\partial V}\right)_{u,n_i} = \frac{P}{T}, \quad \left(\frac{\partial S}{\partial n_i}\right)_{U,V,n_{j(j\neq i)}} = \mu_i \qquad (25)$$

Also

$$dU = \left(\frac{\partial U}{\partial S}\right)_{V,n_i} dS + \left(\frac{\partial U}{\partial V}\right)_{s,n_i} dV + \left(\frac{\partial U}{\partial n_i}\right)_{S,V,n_{j(j\neq i)}} dn_i \qquad (26)$$

comparing (26) and (21)

$$\left(\frac{\partial U}{\partial S}\right)_{V,n_i} = T, \quad \left(\frac{\partial U}{\partial V}\right)_{S,n_i} = -P, \quad \left(\frac{\partial U}{\partial n_i}\right)_{V,S,n_{j(j\neq i)}} = \mu_i \qquad (27)$$

and from the reciprocity relation (15), the useful relations

$$\left(\frac{\partial \mu_i}{\partial P}\right)_{T n_i} = \left(\frac{\partial V}{\partial n_i}\right)_{P,T,n_{j(j\neq i)}} = v_i \qquad (28)$$

$$\left(\frac{\partial \mu_i}{\partial T}\right)_{P,n_i} = \left(\frac{\partial S}{\partial n_i}\right)_{PT,n_{j(j\neq i)}} = s_i \qquad (29)$$

(iv) both representations are homogeneous functions of the first degree in all the independent variables; this follows from (ii) above. Therefore, from (1) and (18)

$$U = TS - PV + \sum_{i=1}^{r} \mu_i n_i \qquad (30)$$

Meaning of dn_i

At this point it is relevant to consider what dn_i means in (18) and subsequent expressions. The mole number of component i in phase j, dn_i^j, in a heterogeneous system, may vary by:-

(i) chemical reactions in the phase, $d_1 n_i^j$

(ii) exchange of matter with other phases in the system, $d_2 n_i^j$

(iii) exchange of matter with the surroundings of the system, $d_3 n_i^j$

so that $dn_i^j = d_1 n_i^j + d_2 n_i^j + d_3 n_i^j$

In a closed system $d_3 n_i^j = 0$ and $dn_i^j = d_1 n_i^j + d_2 n_i^j$

For a closed phase $d_3 n_i^j = d_2 n_i^j$ and $dn_i^j = d_1 n_i^j$

Unless otherwise stated the system being considered is closed, so that dn_i^j refers to chemical reactions or exchange reactions between or within phases.

Thermodynamic potentials

Whereas the fundamental equation holds the maximum possible amount of information about a system, it is clumsy because the independent variables are all extensive properties which are usually measurable or controllable only with great difficulty. It would be useful to have functions which hold the same information as the fundamental equation but have the intensive variables as independent variables. This can be

achieved using Legendre transforms.

Consider a function $f = f(a_1, a_2, a_3 \ldots a_r)$, which according to (14) can be written

$$df = \sum_{i=1}^{r} X_i da_i \text{ where } X_i = \left(\frac{\partial f}{\partial a_i}\right)_{a_j (j \neq i)}$$

f can be considered as a hypersurface in (r+1) dimensional space, and the derivative X_i is a partial slope of this hypersurface. The hypersurface can be represented by the locus of points given by f or as the envelope of the tangent hyperplanes (Callen 1960, Fig. 5.5).

The partial Legendre transform of f, to replace the independent variables a_i (i = 1,2 ... m; m<r) by the partial derivatives X_i (i = 1,2 ... m; m<r), is written $f\{X_1, X_2 \ldots X_m\}$ and is defined as

$$f\{X_1, X_2 \ldots X_m\} = f - \sum_{i=1}^{m} X_i a_i \qquad (31)$$

and if f is first degree homogeneous function, from (31) and (2)

$$f\{X_1, X_2 \ldots X_m\} = \sum_{i=m+1}^{r} X_i a_i \qquad (32)$$

The partial Legendre transform provides a new function f′ with the desired properties.

$$f\{X_1, X_2 \ldots X_m\} = f'(X_1, X_2 \ldots X_m, a_{m+1}, a_{m+2} \ldots a_r)$$

The thermodynamic potentials, Helmholz potential A, enthalpy H and Gibbs energy G are defined as partial Legendre functions of the internal energy U.

Helmholz potential $A \equiv U\{T\} = U - TS \qquad (33)$

Enthalpy $H \equiv U\{P\} = U + PV \qquad (34)$

Gibbs energy $G \equiv U\{T,P\} = U + PV - TS = H - TS \qquad (35)$

The useful forms of the Gibbs fundamental equation appear on writing the total differential of (33-35) and substituting (21)

$$dA = -SdT - PdV + \sum_{i=1}^{r} \mu_i dn_i \qquad (36)$$

$$dH = TdS + VdP + \sum_{i=1}^{r} \mu_i dn_i \qquad (37)$$

$$dG = -SdT + VdP + \sum_{i=1}^{r} \mu_i dn_i \qquad (38)$$

A number of useful relations are obtained when these equations are compared with (14). From (14) and (36)

$$\left(\frac{\partial A}{\partial T}\right)_{V,n_i} = -S \;,\; \left(\frac{\partial A}{\partial V}\right)_{T,n_i} = -P \;,\; \left(\frac{\partial A}{\partial n_i}\right)_{V,T,n_j(j\neq i)} = \mu_i \qquad (39)$$

From (14) and (37)

$$\left(\frac{\partial H}{\partial S}\right)_{P,n_i} = -T \;,\; \left(\frac{\partial H}{\partial P}\right)_{S,n_i} = V \;,\; \left(\frac{\partial H}{\partial n_i}\right)_{P,S,n_j(j\neq i)} = \mu_i \qquad (40)$$

From (14) and (38)

$$\left(\frac{\partial G}{\partial T}\right)_{P,n_i} = -S \;,\; \left(\frac{\partial G}{\partial P}\right)_{T,n_i} = V \;,\; \left(\frac{\partial G}{\partial n_i}\right)_{P,T,\,n_j(j\neq i)} = \mu_i \qquad (41)$$

Further relations are produced using the reciprocity relation (15).

The usefulness of a particular function depends on the system being considered. The Helmholz potential will be most useful for constant volume systems, whereas the enthalpy will be most useful for constant entropy systems. The usual conditions of interest in chemistry and geology are constant temperature and pressure, therefore the Gibbs energy is the thermodynamic potential developed here.

From (31) and (32) it is clear that if a function f is a t^{th} degree homogenous function then the partial Legendre transform of f is also a t^{th} degree homogenous function in those variables not transformed. Therefore, from (20) and (32) or directly from (35)

$$G = \sum_{i=1}^{r} n_i\mu_i \qquad (42)$$

For a one component phase $= G/n = g$ and the chemical potential has the meaning of Gibbs energy per mole.

A property of Legendre transforms is that if every independent variable of a function is transformed, then the resulting function is equal to zero. Therefore

$$U\{S,V,n_i\} = 0 = U - ST - PV - \sum_{i=1}^{r} \mu_i n_i \quad \text{cf.(31)}$$

Differentiating and substituting (20)

$$SdT - VdP + \sum_{i=1}^{r} n_i d\mu_i = 0 \qquad (45)$$

This expression is known as the Gibbs - Duhem equation and relates all

the intensive variables. At constant temperature and pressure, it reduces to

$$\sum_{i=1}^{r} n_i d\mu_i = 0 \quad \text{or} \quad \sum_{i=1}^{r} x_i d\mu_i = 0 \tag{46}$$

The latter expression is important in within phase equilibria and will be used later.

Equilibrium and stability

The explicit statement of the equilibrium and stability conditions for a system are due to Gibbs and are contained in the second law

for equilibrium $(dS)_U = 0$; for stability $(d^2S)_u < 0$ or, entropy is a maximum in stable or metastable equilibrium or, the equivalent

for equilibrium $(dU)_S = 0$; for stability $(d^2U) < 0$ or, internal energy is a minimum in stable or metastable equilibrium.

Callen (1960, ch.6) shows that partial legendre transforms of the internal energy, U, will have the same equilibrium and stability conditions as U, as long as the new independent variables produced by the transform are constant and superimposed on the system by its surroundings. Therefore

$\{dG = 0\ d^2G > 0\}_{P,T}$ or, Gibbs energy is a minimum in stable or metastable equilibrium, for constant superimposed temperature and pressure.

For a heterogenous system of s phases and r components Munster (1970, p.110) shows that the equilibrium conditions are

$$\begin{aligned} T^1 &= T^2 = T^3 = \ldots\ldots\ldots\ldots = T^s \\ P^1 &= P^2 = P^3 = \ldots\ldots\ldots\ldots = P^s \\ \mu_i^1 &= \mu_i^2 = \mu_i^3 = \ldots\ldots\ldots\ldots = \mu_i^s \quad (i = 1,2,3 \ldots . r) \end{aligned} \tag{48}$$

This is the property of contact equilibrium ascribed to intensive variables by Munster (1970) Although the chemical potential can be considered as the partial molar Gibbs energy and so therefore is a derived intensive variable, in obeying contact equilibrium, the chemical

potential is a true intensive variable. The property of contact equilibrium by the chemical potential is the basis for the discussion of equilibrium in heteregeneous systems.

Chemical equilibrium using chemical potentials

The equilibrium conditions for a chemical reaction can be derived from (48). Consider a reaction

$$\sum_{k=1}^{t} A_k M_k = 0$$

in a heterogeneous system of s phases and r components, where A_k are the components and M_k are the stoichiometric numbers of the components in the reaction, and t is a subset of r. It is irrelevant whether this reaction takes place within one phase or between components of several phases.

If δG^j is a small displacement of Gibbs energy of phase j; then at equilibrium, from (47)

$$\sum_{j=1}^{s} \delta G^j = 0 = -\sum_{j=1}^{s} S^j \delta P^j + \sum_{j=1}^{s} V^j \delta P^j + \sum_{j=1}^{s} \sum_{i=1}^{r} \mu_i^j \delta n_i \qquad (49)$$

At equilibrium

$$\sum_{j=1}^{s} \delta T^j = 0 \quad \text{and} \quad \sum_{j=1}^{s} \delta P^j = 0 \qquad (50)$$

and for the non reacting components

$$\sum_{j=1}^{s} \delta n_i^j = 0 \quad (i = 1,2 \ldots r;\ i \neq k) \qquad (51)$$

for the reacting components, displacements of mole numbers are related by the stoichiometric numbers to displacement of other mole numbers, so that

$$\sum_{j=1}^{s} \frac{\delta n_{k1}^j}{M_{k1}} = \sum_{j=1}^{s} \frac{\delta n_{k2}^j}{M_{k2}} \qquad (k1, k2 = 1, 2 \ldots t) \qquad (52)$$

substituting (50-51) into (49) using (48)

$$\sum_{k=1}^{t} \mu_k \left(\sum_{j=1}^{s} dn_k^j \right) = 0 \qquad (53)$$

Replacing δn_k^j by δn_t^j by substituting (52) into (53)

$$\sum_{k=1}^{t} M_k \mu_k \left(\sum_{j=1}^{s} \delta n_t^j \right) = 0$$

since the displacements of δn_t^j are arbitrary, this can only be satisfied for

$$\sum_{k=1}^{t} M_k \mu_k = 0 \qquad (54)$$

This important relation provides the means of considering chemical reactions in homogeneous and heterogeneous systems.

Phase rule

An important tool in the treatment of phase equilibria is the phase rule (due to Gibbs, eg. Denbigh 1966). This expresses the number of degrees of freedom (the number of variables that can be independently altered) of a system in terms of the number of phases, number of components, and the possible reactions between the components.

Consider a heterogenous system of P phases each containing C components, then for equilibrium between the phases, the equations (48) provide (P-1)(C+2) equations between the P(C-1+2) temperatures and pressures of the phases, and the chemical potentials for the components in the phases. Now (54) provides one more equation between the chemical potentials for each independent reaction between the components. For R independent reactions the number of degrees of freedom or variance W is given by

$$\begin{aligned} W &= P(C-1+2) - (C+2)(P-1) - R \\ &= (C-R) + 2 - P \end{aligned} \qquad (55)$$

For systems in which some phases do not contain all the components, the number of chemical potentials is decreased but the same number of chemical potential equations also disappear so that the relation (55)

stays the same. If a W variant system is considered at constant pressure and temperature it can be considered as (W-2) variant for those conditions. Similarly, if the chemical potentials of n components are controlled externally to a W variant system, then it can be considered as (W-n) variant.

Gases

The thermodynamics of gases is a fundamental part of basic thermodynamics; it provides the introduction to the useful functions, activity and activity coefficient, which give the thermodynamic relations in gas, liquid, and solid mixtures.

Ideal gases

The gas law, $Pv=RT$, applies to an invented substance, the ideal gas. The relation can be derived from statistical mechanics for a system in which there is no interaction between the atoms or molecules in the system. This state is thought to be approached by all substances when $P \to 0$ and the atoms or molecules become infinitely separated. As a first approximation many gases obey the gas law at low pressures and high temperatures (for example H_2O is almost an ideal gas above $700^{\circ}C$ at 100 bars).

Gas mixtures which obey the gas law obey Dalton's law of partial pressures

$$p_i = RT/v_i \text{ where } p_i = x_i P, \text{ the partial pressure of component i} \qquad (56)$$

The chemical potential of i can be introduced by substituting (56) in (28)

$$\left(\frac{\partial \mu_i}{\partial P}\right)_{Tn_i} = V_i = RT/p_i \qquad (57)$$

Integrating at constant composition and temperature (these conditions apply for all expressions with the form of (58))

$$\int_{\mu_i'}^{\mu_i} d\mu_i = RT \int_{p_i'}^{p_i} \frac{dp_i}{p_i} = RT \int_{p_i'}^{p_i} d\ln p_i$$

$$\mu_i = \mu_i' + RT \ln p_i/p_i' = \mu_i' + RT \ln P/P' + RT \ln x_i/x_i' \qquad (58)$$

Where μ_i', an integration constant, is the chemical potential of i at pressure p_i' at the same T. For a one component system, (58) becomes

$$\mu = \mu' + RT \ln P/P' \qquad (59)$$

Real gases

For real gases, Lewis (1901) introduced a ficticious pressure, which he called the fugacity, so that an equation similar to (58) could be written for the fugacity, with the condition that the fugacity equals the pressure when the gas becomes ideal; or

$$\mu_i = \mu_i' + RT \ln f_i/f_i' \text{ and } f_i/p_i \to 1 \text{ as } P \to 0 \qquad (60)$$

or for a one component system

$$\mu = \mu' + RT \ln f/f' \text{ and } f/P \to 1 \text{ as } P \to 0 \qquad (61)$$

To evaluate fugacities for a gas, it is necessary to have a relation between fugacity and the PVT data for the gas.

From (60) and (28) at constant temperature and composition.

$$d\mu_i = RT\, d \ln f_i = v_i dP$$

subtracting $RT\, d\ln p_i$ from both sides

$$\begin{aligned} RT\, d\ln f_{i/p_i} &= v_i dP - RT\, d\ln p_i \\ &= v_i dP - RT\, d\ln P - x_i \\ &= (v_i - \frac{RT}{P})\, dP \end{aligned}$$

Integrating at constant T and composition from P=0 to P=P

$$RT\ln (f_i/p_i)_{P=P} - RT\ln(f_i/p_i)_{P=0} = \int_0^P (v_i - \frac{RT}{P})dP$$

and, from the limiting relation in (60)

$$RT\ln f_i = RT\ln p_i + \int_0^P (v_i - \frac{RT}{P})dP \qquad (62)$$

or, for a one component gas

$$RT \ln f = RT \ln P + \int_0^P (v - \frac{RT}{P})dP \qquad (63)$$

In practice the gas approaches ideality at a finite pressure and the integrations can be performed from this pressure to the pressure of interest. Calculation of fugacities require volume measurements d own to pressures at which the gas approaches ideality at each temperature.

Tunell (1931) examines Lewis' definition of fugacity and finds mathematical rigour lacking. He redefines fugacity in terms of (63) and Lewis' definition can be derived from this.

The superscript in (58,59) and (60,61) refers to conditions, called the standard state, which are chosen for convenience for the system being considered. There are some natural choices:-

1. pure component i at 1 bar pressure and the temperature of interest; the superscript ^{o} will be used.
2. pure component i at the pressure and temperature of interest; the superscript * will be used.
3. pure component i as a hypothetical ideal gas at 1 bar and the temperature of interest; the superscript ^{oo} will be used.
4. pure component i as a hypothetical ideal gas at the pressure and temperature of interest, the superscript ** will be used.

$$\text{or, } \mu_i = \mu_i^{o} + RT \ln f_i/f_i^{o} \qquad (64)$$

$$\mu_i = \mu_i^{*} + RT \ln f_i/f_i^{*} \qquad (65)$$

$$\mu_i = \mu_i^{oo} + RT \ln f_i/1 \qquad (66)$$

$$\mu_i = \mu_i^{**} + RT \ln f_i/P \qquad (67)$$

It would be convenient to write f_i as a function of f_i^{*} and x_i only. This is only possible for the limiting condition where the interspecies molecular interactions are the same as the intraspecies molecular interactions, when the mixing is said to be ideal. Then

$$f_i = f_i^{*} x_i \qquad (68)$$

This is known as Raoult's law. Although this is approximately true for some binary systems (for example $C_2H_4Br_2$ - $C_3H_6Br_2$), in general it is only true for the solvent in the limit of infinite dilution of the solutes. Whereas for ideal binary systems both components obey Raoult's law, for non-ideal solutions if the solvent obeys Raoult's law (which is almost always the case for dilute solutions) then it can be shown that the solute obeys Henry's law.

$f_i = L_i x_i$ where L_i is Henry's law constant for i and is a function of temperature, pressure, and the nature of the solvent and solute. (69)

Activity

Considering (60), it is often impossible or inexpedient to determine f_i and f_i' for a component in, for example, an almost involatile solid. However for the correct choice of standard state, the ratio f_i/f_i' , called the activity a_{ti}, the activity of component i for the standard state t, can be used for gas, liquid and solid mixtures. From (64-67) and the definition:-

$$a_{1i} = f_i/f_i^{\circ} \quad \text{and} \quad \mu_i = \mu_i^{\circ} + RT \ln a_{1i} \tag{70}$$

$$a_{2i} = f_i/f_i^{*} \quad \text{and} \quad \mu_i = \mu_i^{*} + RT \ln a_{2i} \tag{71}$$

$$a_{3i} = f_i \quad \text{and} \quad \mu_i = \mu_i^{\circ\circ} + RT \ln a_{3i} \tag{72}$$

$$a_{4i} = f_i/P \quad \text{and} \quad \mu_i = \mu_i^{**} + RT \ln a_{4i} \tag{73}$$

Activity a_{4i} is often called the fugacity coefficient, it is one way that gas fugacities are sometimes tabulated.

It would be most convenient to represent a_{ti} as a function of a_{ti} and x_i only, substituting (68) into (70-73) for ideal mixing.

$$a_{1i} = f_i/f_i^{o} = f_i^{*}x_i/f_i^{o} = a_{1i}^{*}x_i \text{ and } \mu_i = \mu_i^{o} + RT \ln a_{1i}^{*}x_i \quad (74)$$

$$a_{2i} = f_i/f_i^{*} = f_i^{*}x_i/f_i^{*} = x_i \quad \text{and } \mu_i = \mu_i^{*} + RT \ln x_i \quad (75)$$

$$a_{3i} = f_i = f_i^{*}x_i = a_{3i}^{*}x_i \text{ and } \mu_i = \mu_i^{oo} + RT \ln a_{3i}^{*}x_i \quad (76)$$

$$a_{4i} = f_i/P = f_i^{*}x_i/P = a_{4i}^{*}x_i \text{ and } \mu_i = \mu_i^{**} + RT \ln a_{4i}^{*}x_i \quad (77)$$

For non-ideal mixtures, the activity coefficients γ_{ti} are introduced so that (70-73) still hold. They account for the non-ideality of the mixture, and equal one when the mixture becomes ideal. They are defined by

$$\gamma_{1i} = a_{1i}^{*}/x_i \quad (78)$$

$$\gamma_{2i} = a_{2i}/x_i \quad (79)$$

$$\gamma_{3i} = a_{3i}/a_{3i}^{*}x_i \quad (80)$$

$$\gamma_{4i} = a_{4i}/a_{4i}^{*}x_i \quad (81)$$

By equating the chemical potentials for pairs of equations (74-77) and mole fractions for pairs of equations (70-73) it is possible to express μ^{o}, μ^{*}, μ^{oo}, μ^{**} in terms of each other, for example:- $\mu_i^{o} = \mu_i^{*} + RT \ln f_i^{*}/f_i^{o}$ (82)

and to express a_{1i}, a_{2i}, a_{3i}, a_{4i} in terms of each other, for example:-

$$a_{1i} = a_{2i}f_i^{o}/f_i^{*} \quad (83)$$

From all the relations similar to (83), it is clear that

$$\gamma_{1i} = \gamma_{2i} = \gamma_{3i} = \gamma_{4i} = \gamma_i$$

so the chemical potential of a component i in a non-ideal mixture for the 4 standard states is

$$\mu_i = \mu_i^{o} + RT \ln a_{1i}^{*}x_i\gamma_i \quad (84)$$

$$\mu_i = \mu_i^{*} + RT \ln x_i\gamma_i \quad (85)$$

$$\mu_i = \mu_i^{oo} + RT \ln a_{3i}^{*}x_i\gamma_i \quad (86)$$

$$\mu_i = \mu_i^{**} + RT \ln a_{4i}^{*}x_i\gamma_i \quad (87)$$

Equilibrium constant

The equilibrium condition for a chemical reaction $\sum_{k=1}^{t} A_k M_k = 0$ is (55) $\sum_{k=1}^{t} \mu_k M_k$ in a heterogenous or homogenous system.

Substituting (70-74) into (55)

$$\sum_{k=1}^{t} M_k \left(\mu_k^{o} + RT \ln a_{1k}\right) = 0 \tag{88}$$

$$\sum_{k=1}^{t} M_k \left(\mu_k^{*} + RT \ln a_{2k}\right) = 0 \tag{89}$$

$$\sum_{k=1}^{t} M_k \left(\mu_k^{oo} + RT \ln a_{3k}\right) = 0 \tag{90}$$

$$\sum_{k=1}^{t} M_k \left(\mu_k^{**} + RT \ln a_{4k}\right) = 0 \tag{91}$$

rearranging (88-91)

$$-\frac{\Delta G_k^{o}}{RT} \equiv -\sum_{k=1}^{t} \frac{\mu_k^{o} M_k}{RT} = \sum_{k=1}^{t} \ln a_{1k}^{M_k} = \ln K_1 \tag{92}$$

$$-\frac{\Delta G_R^{*}}{RT} \equiv -\sum_{k=1}^{t} \frac{\mu_k^{*} M_k}{RT} = \sum_{k=1}^{t} \text{in } a_{2k}^{M_k} = \ln K_2 \tag{93}$$

$$-\frac{\Delta G_R^{oo}}{RT} \equiv -\sum_{k=1}^{t} \frac{\mu_k^{oo} M_k}{RT} = \sum_{k=1}^{t} \ln a_{3k}^{M_k} = \ln K_3 \tag{94}$$

$$-\frac{\Delta G_R^{**}}{RT} \equiv -\sum_{k=1}^{t} \frac{\mu_k^{**} M_k}{RT} = \sum_{k=1}^{t} \ln a_{4k}^{M_k} = \ln K_4 \tag{95}$$

where K_t is the equilibrium constant for the reaction for the standard state t. ΔG_R is the Gibbs energy change for the reaction as written if each component occurred as a separate phase; it is the Gibbs energy change obtained by summing the relevant literature data for the pure components.

The extra subscript t appears in the last two sections to emphasize the point that a_{ti} and so therefore K_t and ΔG_R are dependent on the standard state chosen. It is worth being explicit at the expense of a slightly heavy notation. Confusion arises when one author uses ΔG_R^{o} in the sense used here and another uses it in the sense of ΔG_R^{oo} or ΔG_R^{**}, when the intention is not always defined.

The value of the equilibrium constant formulation is that it relates the Gibbs free energy of reaction for the pure components to the phases of the system in which they occur. To actually apply (92-95) it is necessary to know the behaviour of the mixtures, which involves knowing the activity coefficients of the components in the phases, and the Gibbs energies of the pure components in the reaction. Gibbs energies and activity coefficients are covered in the next two sections.

Gibbs energy

In thermodynamics the most useful functions are not always easily measurable. The change of molar Gibbs energy for a phase between different temperatures and pressures can be calculated from the molar volume v as a function of temperature and pressure and from the molar heat capacity at constant pressure c_P, the heat required to raise the temperature of the system by $1^{\circ}C$ at constant pressure, as a function of temperature at each pressure.

From (13), (21), (37) and (20)

$$cp = \left(\frac{\partial q}{\partial T}\right)_P = \left(\frac{\partial h}{\partial T}\right)_P = T\left(\frac{\partial s}{\partial T}\right)_P \qquad (96)$$

Introducing an unambiguous notation for the change in g, h, or s for phase A between temperatures T_1 and T_2 and pressures P_1 and P_2:-

$$\Delta g_A \ (p_1 \rightarrow p_2 \text{ bars}, \ T_1 \rightarrow T_2 \ ^{\circ}K)$$

where, for constant pressure $p_1 \rightarrow p_2$ is replaced by P, the constant pressure, and for constant temperature $T_1 \rightarrow T_2$ is replaced by T the constant temperature.

From (96)

$$\Delta h_A(P, \ T_1 \rightarrow T_2) = \left\{\int_{T_1}^{T_2} c_p \, dT\right\}_P \qquad (97)$$

$$\Delta s_A(P, \ T_1 \rightarrow T_2) = \left\{\int_{T_1}^{T_2} \frac{cp}{T} \, dT\right\}_P \qquad (98)$$

From which

From which

$$\Delta g_A(P,\ T_1 \rightarrow T_2) = \{ \int_{T_1}^{T_2} cp\,dT - T_2 \int_{T_1}^{T_2} \frac{cp}{T}\,dT \}_P \qquad (99)$$

From (41)

$$\Delta g_A(T,\ P_1 \rightarrow P_2) = \{ \int_{P_1}^{P_2} v\,dP \}_T \qquad (100)$$

so that

$$\Delta g_A(T_1 \rightarrow T_2,\ P_1 \rightarrow P_2) = \Delta g_A(P,\ T1 \rightarrow T_2) + \Delta g_A(T_2,\ P_1 \rightarrow P_2) \qquad (101)$$

$\Delta h_A(1\text{ bar}, 298.15 \rightarrow T^oK)$ is usually called the heat content of A at temperature T

$\Delta s_A(1\text{ bar}, 298.15 \rightarrow T^oK)$ is here called the entropy content of A at temperature T

$\Delta g_A(1\text{ bar}, 298.15 \rightarrow T^oK)$ is here called the Gibbs energy content of A at temperature T.

Equations like (99) and (100) define the change of Gibbs energy between different temperatures and pressures, e.g.

$$\Delta g_A(1\text{ bar}, 298.15 \rightarrow T^oK) = g_A(1\text{ bar}, T^oK) - g_A(1\text{ bar}, 298.15^oK)$$

'Absolute' Gibbs energies at a P,T, $g_A(P,T)$, are undefined. Gibbs energies are usually tabulated as Gibbs energies of formation from either the elements or the oxides, i.e. the difference between the Gibbs energy of the phase and the Gibbs energies of the component elements or oxides in some defined state at the stated pressure and temperature. The notation used for Gibbs free energy of formation of A from the elements at P,T will be

$$\Delta_f g_A(el,\ P\text{ bars},\ T^oK)$$

from the oxides at P,T will be

$$\Delta_f g_A(ox,\ P\text{ bars},\ T^oK)$$

The usual tabulated Gibbs energy of formation is the Gibbs energy of formation from the elements at 298.15°K and 1 bar, the elements being in their most stable state.

Unlike enthalpy or Gibbs energy, the entropy of a phase has an absolute value at a particular temperature and pressure as a result of the third law. The absolute or third law entropy is given by

$$s\ (P\ \text{bars},\ T^{o}K) = \{\int_{0}^{T} \frac{cp}{T}\, dT\}_{P} \qquad (102)$$

This entropy can be calculated from low temperature heat capacity measurements.

In the equilibrium constant formulation Gibbs energies are always involved as differences, moreover the differences are balanced with respect to the moles of the elements or oxides in the reaction. The important result of this is that in calculating ΔG_R for (92-95), if a scheme of Gibbs energies of formation are used at one pressure and temperature, then ΔG_R for another pressure and temperature can be simplified by cancellation of terms.

For example, consider the calculation of ΔG_R^{*} for a reaction at a particular temperature T and pressure P, given the Gibbs free energies of the components in the reaction at 298.15°K and 1 bar, and the Gibbs energy contents of the phases and elements which make up the phases.

For a reaction $\sum_k A_k M_k = 0$

The straightforward approach is

$$\Delta G_R^{*}\ (P\ \text{bars},\ T^{o}K) = \sum_k M_k (\Delta_f g(\text{el},\ P\ \text{bars},\ T^{o}K)) \qquad (103)$$

Involving the calculation $\Delta_f g(\text{el},\ P\ \text{bars},\ T^{o}K)$ from $\Delta_f g(\text{el},\ 1\ \text{bar},\ 298.15^{o}K)$ using the Gibbs energy contents, i.e.

$$\Delta_f g_k(\text{el},\ P\ \text{bars},\ T^{o}K) = \Delta_f g_k(\text{el},\ 1\ \text{bar},\ 298.15^{o}K) + \Delta g_k(1 \rightarrow P_{\text{bars}},\ 298.15\ \ T^{o}K) - \sum_{\text{elements}} n_{el} (\Delta g_{el}(1\ P\ \text{bars},\ 198.15\text{-}T^{o}K) \qquad (104)$$

However, this approach can be simplified considerably, in stages

(1) The third term on the RHS of (104) will cancel out in (103)

$$\Delta G_R^{*}\ (P\ \text{bars},\ T^{o}K) = \sum_k M_k \{\Delta_f g_k(\text{el},\ P\ \text{bar},\ 298.15) + g_k(1\text{-}P\ \text{bar},\ 298.15\ T^{o}K)\} \qquad (105)$$

(2) Because g = h - Ts, and because s can have absolute values, the first term in (105) can be split and the entropy part changed from entropy of formation to third law entropy, because the difference will cancel out in the sum

$$\Delta G_R^* \text{ (P bars, } T^oK) = \sum_k M_k \{\Delta_f h_{A_k} \text{(el, 1 bar, 298.15)} - Ts(\text{P bar, } 298.15^oK) \quad (106)$$

$$+ \Delta h_{A_k} (1 \rightarrow \text{P bars, } 298.15 \rightarrow T^oK) - T\Delta S(1 \rightarrow P_{bars}, 298.15 \rightarrow T^oK)\}$$

(3) This can be arranged to give

$$\Delta G_R^* \text{ (P bars, } T^oK) = \sum_k M_k \{\Delta_f h_{A_k} \text{(el, 1 bar, 298.15)} - Ts(\text{1 bar, } T^oK)$$

$$+ \Delta h_{A_k} (\text{1 bar, } 298.15 \rightarrow T^oK) + \Delta g_{A_k} (T, 1 \rightarrow \text{P bar})\} \quad (107)$$

(4) With the observation that v is almost independent of P and T ; using (100)

$$\Delta G_R^* \text{ (P bars, } T^oK) = \sum_k M_k \{\Delta_f h_{A_k} \text{(el, } 298.15^oK, \text{ 1 bar)} + \Delta h_{A_k} (\text{1 bar, } 298.15\text{-}T^oK)$$

$$- Ts_{A_k} (\text{1 bar, } T^oK) + v_{A_k} (P\text{-}1)\} \quad (108)$$

The above line of reasoning has been followed through to show the simplifications possible in calculating ΔG_R. Similar arguments can be applied to any standard state set. Equation (108) expresses ΔG_R^* in terms that can be read from data tabulations eg. Robie and Waldbaum (1968) (ie enthalpy of formation at 298.15°K and 1 bar, heat contents at 1 bar and a range of temperatures, third law entropy at 1 bar and a range of temperatures, and the molar volume).

It is obviously crucial to be aware of the way data compilations are constructed before using them.

Activity coefficients

To use the equilibrium constant formulation (92-95) it is crucial to know a_{it}; which from (79-81), (84-87), involves knowing γ_i, the activity coefficient of the component i in the mixture. For ideal mixtures and very dilute mixtures $\gamma_i \sim 1$; however, in general, γ_i is a function of temperature, pressure and the composition of the mixture.

Activity coefficients can be easily calculated from detailed fugacity or fugacity coefficient tabulations of gas mixtures, using for example (79) and (74).

Where direct calculations are not possible indirect calculation using, for example, solwus data in binary systems may give reliable approximations.

For non-ideal mixtures any empirical power series in the mole fractions can be used to approximate the activity coefficients at a particular temperature and pressure as long as it obeys Raoult's Law (68) and the Gibbs-Duhem equation (46) recast using activity coefficients; from (85) and (46); for a binary:-

$$x_1 \ln\gamma_1 + x_2 \ln \gamma_2 = 0 \qquad (109)$$

The best known power series is due to Margules (1895). He expressed RT ln γ_1 by a power series in x_2, thus fulfilling Raoult's Law. The RT term is included so that the coefficients of the power series have the dimensions of energy. Thus:-

$$\begin{aligned} RT \ln \gamma_1 &= a_1 x_2 + b_1 x_2^2 + c_1 x_2^3 \ldots\ldots \\ RT \ln \gamma_2 &= a_1 x_1 + b_2 x_1^2 + c_2 x_1^3 \ldots\ldots \end{aligned} \qquad (110)$$

Where a_1, a_2, b_1 etc. are coefficients, constants at a particular pressure and temperature.

He showed that if these equations hold over the complete system, then, by the Gibbs-Duhem relation (45), there must be relations between these coefficients, particularly

$$a_1 = a_2 = 0$$

$$b_2 = b_1 + 1/2\ C_1 \ldots. \qquad (111)$$

$$c_2 = -c_1 + \ldots\ldots$$

and so on

Two much used empirical equations based on the Margules equation are obtained by truncating (110) after the quadratic and after the cubic term respectively.

Porter (1921), Hildebrand (1927) and others have shown that the truncation after the quadratic term is adequate to describe many systems of non-electrolytes. For a binary, the equations are

$$RT \ln \gamma_1 = A\, x_2^2$$
$$RT \ln \gamma_2 = A\, x_1^2 \qquad (112)$$

This is referred to as the R model.

Hildebrand (1929) introduced the term 'regular solution' for mixtures which were found experimentally to conform to these equations. By the nature of the equations the system is symmetric in composition.

However many systems are observably unsymmetric. Hardy (1953) and others introduced the cubic term of the Margules equation into the regular solution equations, and called the mixtures 'sub regular'. From (111) and (110), for a binary

$$RT \ln \gamma_1 = b_1 x_2^2 + c_1 x_2^3$$
$$RT \ln \gamma_2 = (b_1 + \tfrac{3}{2} c_1)\, x_1^2 - c_1 x_1^3$$

This can be arranged into the more symmetrical form, Hardy (1953)

$$\ln \gamma_1 = x_2^2 (A + 2x_1 (B-A))$$
$$\ln \gamma_2 = x_1^2 (B + 2x_2 (A-B)) \qquad (113)$$

where $A = b_1 + c_1 = (2b_2 + c_2)/2$

$B = (2b_1 + c_1)/2 = b_2 + c_2$

This is referred to as the SR model.

An alternative approach to the formulation of activity coefficients of mixtures uses statistical thermodynamics (Bethe 1935, Fowler and Guggenheim 1952). These authors and others have attempted to make simplifying assumptions about atomic and molecular arrangements in systems so that activity coefficients can be predicted or calculated.

The observed equilibrium properties of a system depend on the partition function, related to a weighted average of the energies of all the accessible quantum states of the system. The statistical thermodynamics approach to mixtures involves a number of assumptions.

(1) that the partition function can be separated into a translational part and an internal part, the translational part describing the position and motion of the molecules. It implies that the mixing properties are related to the translational part only, as the internal part will be the same in the mixture as in the pure phase.

(2) that for crystalline solids (and for liquids if they may be regarded as consisting of quasilattices) the translational part may be separated into an acoustic part and a configurational part. The configurational part describes the energy of the molecules at rest on their lattice points while the acoustic part describes the vibrational energy of the molecule about the lattice point. It implies that the mixing properties are related to the configurational part only, as the acoustic part will be the same in the mixture as in the phase.

Within statistical mechanics it is easy to write down expressions for the configurational part of the partition function for different distributions and interactions of molecules, and, with the above two assumptions, obtain expressions for the activity coefficients. The validity of the above assumptions is vindicated by the success of the models derived using them.

Guggenheim (1952) defines a 'strictly regular solution' as a mixture satisfying all the conditions for forming an ideal mixture except that the configurational energy is no longer independent of the mutual disposition of the two or more types of molecules, although these molecules are sufficiently alike in size and shape to be interchangeable on the lattice or quasilattice. This means that although the entropy of mixing is the same as for an ideal mixture, the energy required to change a molecule of A for a molecule of B in the lattice, the interchange energy W, is not zero. Guggenheim (1952, ch.4) develops a series of approximations for symmetric mixtures using the parameter W.

The zeroth approximation assumes that the different molecules are distributed completely at random on the lattice, although the energy of mixing is non-zero. The consequence for a binary is that (Guggenheim p.34)

$$\begin{aligned} RT \ln \gamma_1 &= x_2^2 W \\ RT \ln \gamma_2 &= x_1^2 W \end{aligned} \qquad (114)$$

By comparison with (112), A = W and (114) is equivalent to the R model so that Hildebrand's regular solutions have some firm thermodynamic basis.

The first approximation assumes that each molecule interacts only with its z nearest neighbours, where z is the coordination number of the molecule, and that the interactions can be considered in terms of non-interfering pairs. Guggenheim calls this approach the quasi-chemical approximation because the relations between numbers of types of pairs has the same form as for the numbers of molecules of gas species in chemical equilibrium. For a binary (Guggenheim p.40)

$$\ln \gamma_1 = \frac{z}{2} \ln \{1 + \frac{x_2}{x_1} \frac{(\beta-1)}{(\beta+1)}\} \qquad (115)$$

$$\ln \gamma_2 = \frac{z}{2} \ln \{1 + \frac{x_1}{x_2} \frac{(\beta-1)}{(\beta+1)}\} \qquad (116)$$

where $\beta = \{1 + 4x_1x_2 (\exp (2W/zRT) - 1)\}^{\frac{1}{2}}$

This is referred to as the QC model.

Guggenheim (1952) gives further approximations on the same lines as the first approximation but considering non-interfering triplets or quadruplets of sites, instead of pairs. Guggenheim (1969, p.94) points out how insensitive the activity coefficients are to the choice of basic group of sites, and considers that there is little need to venture beyond non-interfering pairs.

For asymmetric mixtures, in which the molecules are not sufficiently similar in shape and size to be simply interchangeable on the lattice, Guggenheim (1952, ch.11) introduces two dependent parameters, called contact factors q_1 and q_2, related to the geometrical relation of one molecule with another and reflecting the difference in shape and size of the molecules. When $q_1 \to 1$, then $q_2 \to 1$ and the mixture becomes a strictly regular solution.

For the zeroth approximation, assuming randomly distributed molecules, by rearranging Guggenheim 1952 11.05. 2, 3, the activity coefficients are:

$$\ln \gamma_1 = -\frac{zq_1}{2} \ln (x_1 + Ax_2) + \left(\frac{Ax_2}{x_1 + Ax_2}\right)^2 \frac{q_1W}{RT} \qquad (117)$$

$$\ln \gamma_2 = \frac{zq_2}{2} \ln \left(x_2 + \frac{x_1}{A}\right) + \left(\frac{x_1}{x_1 + Ax_2}\right)^2 \frac{q_2W}{RT}$$

where $A = q_2/q_1$

Obviously when $q_1 = q_2 = 1$ these equations simplify to (112)

For the first approximation, assuming non-interfering pairs of sites; by rearranging Guggenheim 1952 11.08.9, 10, the activity coefficients are

$$\ln \gamma_1 = \frac{zq_1}{2} \ln \left\{\frac{A_1}{x_1} \left(1 + \frac{A_2}{A_1} \frac{(\beta-1)}{\beta+1}\right)\right\} = \frac{zq_1}{2} \ln \left(\frac{1-KA_2}{x_1}\right)$$

$$\ln \gamma_2 = \frac{zq_2}{2} \ln \left\{\frac{A_2}{x_2} \left(1 + \frac{A_1}{A_2} \frac{(\beta-1)}{(\beta+1)}\right)\right\} = \frac{zq_2}{2} \ln \left(\frac{1-KA_1}{x_2}\right) \qquad (118)$$

where $A_1 = q_1x_1/(q_1x_1 + q_2x_2)$

$A_2 = q_2x_2/(q_1x_1 + q_2x_2)$

$\beta = \{1 + 4A_1A_2(\exp(2W/ZRT) - 1)\}^{\frac{1}{2}}$

$K = 2/(B+1)$

This is referred to as the AQC model

Obviously where $q_1 = q_2 = 1$ these equations simplify to (115). Again higher approximations do not significantly affect the activity coefficients, so they are not considered here.

An important point to note with the above equations (113-118) is that they only apply if the model is true over the complete compositional range. Darken (1967), considering metallic solutions, points out that in the terminal compositional regions of experimentally determined binaries, the solvent closely obeys

$$RT \ln \gamma_1 = Ax_2^2 \qquad (119)$$

but because the central compositional region cannot reasonably be fitted by any polynomial let alone (119), the solute in the same region as (119) obeys

$$RT \ln \gamma_2 = Ax_1^2 + I$$

Where I is an integration constant produced in applying the Gibbs Duhem equation to (119), only when (119) applies across the whole compositional range will $I = 0$.

Most of the discussions in the chemical and metallurgical literature about the form of the mole fraction dependence of the activity coefficients are concerned with fitting experimentally determined activity coefficients by simple functions. Except for a few solution-

mineral cation distribution experiments (e.g. Orville 1972) the only chance of establishing activity coefficients for geologically relevant solid mixtures is by using experimentally determined solvi.

In the statistically based models, at least in simple systems it should be possible to measure or even predict W, q_1 and q_2. An alternative approach, used here, is to consider these as adjustable parameters. Through (48), the chemical potentials of each component are the same in coexisting phases across the solvus. For a binary the two equations provide the opportunity to calculate a maximum of two parameters at each temperature and pressure. For a binary system, a phase A rich in component 1 and phase B rich in component 2, the two equations are

$$\mu_{1A} = \mu_{1B}$$

$$\mu_{2A} = \mu_{2B}$$

Substituting (85)

$$\frac{\mu^*_{1A} - \mu^*_{1B}}{RT} + \ln X_{1A}\gamma_{1A} = \ln X_{1B}\gamma_{1B}$$

$$\frac{\mu^*_{2A} - \mu^*_{2B}}{RT} + \ln X_{2A}\gamma_{2A} = \ln X_{2B}\gamma_{2B} \qquad (120)$$

For each phase the activity coefficients are related by (109), or:-

$$x_{1A}\partial\ln\gamma_{1A} + X_{2A}\partial\ln\gamma_{2A} = 0$$

$$X_{1B}\partial\ln\gamma_{1B} + X_{2B}\partial\ln\gamma_{2B} = 0 \qquad (121)$$

Because the activity coefficients are not completely defined by (120-121), it is possible to reproduce the solvus without producing meaningful activity coefficients. It is obviously necessary to test any model in an experimentally determined system, before being applied to the solvus of an undetermined system.

Equations (120) are the general equations for a solvus between two dissimilar structures; if the structures are closely similar, for example sylvite-halite, then the term involving the standard chemical potentials disappears because

$$\mu^{*}_{1A} \simeq \mu^{*}_{1B}$$

$$\mu^{*}_{2A} \simeq \mu^{*}_{2B}$$

Many chemistry textbooks relate activity coefficients to thermodynamic excess functions. These express the difference between the function for the real system and for the system as an ideal mixture. From (68) and (9) the Gibbs energy of an ideal mixture is

$$g = X_1\mu_1 + X_2\mu_2 = X_1\mu_1^{*} + X_2\mu_2^{*} = X_1RT \ln X_1 + X_2RT \ln X_2$$

For real systems a term involving the activity coefficients must be included, and this gives the excess Gibbs energy of mixing g^{ex}

$$g^{ex} = X_1 RT \ln \gamma_1 + X_2RT \ln \gamma_2 \qquad (122)$$

The thermodynamic expressions that relate g to h, s, v, for a system apply also to g^{ex}; thus

$$\left(\frac{\partial g}{\partial T}\right)^{ex}_{P,n_i} = s^{ex} \quad , \left(\frac{\partial g}{\partial P}\right)^{ex}_{T,n_i} = v^{ex} \quad , \frac{\partial g^{ex}/T}{\partial 1\ /T} = h^{ex}$$

from (11)

$$\mu_1^{ex} = g^{ex} - X_2\frac{\partial g^{ex}}{\partial X_2} \quad \text{and so on} \qquad (123)$$

For each model, given the pressure-temperature dependence for the parameters, it is possible to calculate g^{ex}, s^{ex}, h^{ex}, and v^{ex}. v^{ex} is the only easily measurable quantity; it can be calculated from very accurate molar volume determinations (usually by X-ray determined cell volumes). Such data gives an independent check on

model parameters if the source data is polybaric.

The mixing models described so far can be applied in several ways depending on the mixing process. For liquids and gases the molecules of the components mix together. However in crystalline solids this is usually not the case, the constituent molecules or atoms of the components mix on particular sites in the lattice. Kroger et al (1959) introduce a formalism within which to consider chemical equilibria involving sites in lattices. They use the term structure elements for atoms or atom groups in particular sites in a lattice, and the term building units for stoichiometrically combined structure elements with the property that they can be added to or subtracted from the lattice without violating the stoichiometry of the sites. Thus building units are components and a chemical potential can be written for each. Structure elements are obviously not components and a chemical potential cannot be written for each in the normal way because the definition of a chemical potential, for example (18), involves independent change of n_i , which is not possible for structure elements because the stoichiometry of the sites in the lattice will be destroyed.

However Kroger et al introduce a virtual Gibbs energy, G^V, to be a first order homogeneous function in the mole numbers of structure elements, N_i, defined to equal G for a realizable crystal. By analogy with (42), virtual chemical potentials μ_j^V can then be defined by:-

$$G^V = \sum_j \left(\frac{\partial G^V}{\partial N_j}\right)_{N_j} = \sum_j \mu^V{}_j N_j$$

For the ith component of a lattice, made of S structure elements

$$\mu_i = \frac{\partial G}{\partial n_i} = \frac{\partial G}{\partial n_i} = \sum_{j=1}^{S} \frac{\partial N_j}{\partial n_i} \mu_j{}^V \qquad (124)$$

By analogy with (85)

$$\mu_j^V = \mu_j^{V\,*} + RT \ln X_j \gamma_j \qquad (125)$$

where x_j and γ_j are the mole fraction and chemical potential respectively of j in the site of interest.

From (124) and (125)

$$\mu_i = \sum_{j=1}^{s} \frac{\partial N_j}{\partial n_i} \left(\mu_j^{V*} + RT \ln x_j \gamma_j\right)$$

$$= \mu_i^{*} + RT \sum_{j=1}^{s} \frac{\partial N_j}{\partial n_i} \ln x_j \gamma_j \qquad (126)$$

The relevance of this result can be shown by an example (using standard state 2 throughout and so dropping the extra subscript). Consider the exchange equilibrium between magnesium and iron pyroxenes and olivines. The obvious way to write this exchange reaction is

$$Fe_2SiO_4 + 2\ MgSiO_3 = Mg_2SiO_4 + 2\ FeSiO_3 \qquad (127)$$

Using ideal mixing,

$$\frac{\Delta G^*}{RT}R = \ln x^{ol}_{Mg_2SiO_4} = 2 \ln x^{pyx}_{FeSiO_3} - \ln x^{ol}_{Fe_2SiO_4} - 2 \ln x^{pyx}_{MgSiO_3}$$

However, this assumes that the components are mixing rather than the more reasonable assumption that the cations of the components are mixing on sites in the lattice. Assuming one cation site in the pyroxenes and olivines and applying (126) to each component and combining gives

$$\frac{\Delta G^*}{RT}R = \ln x^{ol,site}_{Mg} + \ln x^{pyx,site}_{Fe} - \ln x^{ol,site}_{Fe} - \ln x^{pyx,site}_{Mg} \qquad (128)$$

If there is no anionic substitution then

$$x^{ol,site}_{Mg} = x^{ol}_{Mg_2SiO_4} \quad \text{etc.}$$

and (127) and (128) can be directly compared.

Comparison of these two models for systems in which the activities of the solid mixtures have been measured will be delayed to the next chapter.

CHAPTER 3

PRACTICAL THERMODYNAMICS

PRACTICAL THERMODYNAMICS

The aim of this chapter is to compile thermodynamic data to calculate conditions of equilibria frozen in the assemblages of rocks. A method of calculation is presented with a review of previously used methods. Some of the thermodynamic data for geologically relevant solid phases, particularly enthalpies of formation, have unacceptably large error brackets. It is suggested that a consistent set of enthalpies of formation may be calculated from experimentally reversed reactions (see also Zen (1969)). I have written a program, THERMOCALC, to retrieve thermodynamic data from experimentally determined temperature brackets and to calculate equilibrium conditions of reactions from the resulting data.

Main data sources

Robie and Waldbaum (1968) brings together the scattered thermodynamic data for geologically relevant phases, giving heat contents, third law entropies, Gibbs energies of formation and enthalpies of formation at ^{o} hundreds of ^{o}K intervals from 298.15^{o}K at 1 atm. Many of the heat contents and entropies are from Kelley (1960) and Kelley and King (1961). Robie and Waldbaum follow Wagman et al. (1965, continuing) in referring the Gibbs energies and enthalpies of formation to

a. the condensed elements in their most stable state at 1 atm. and the temperature of interest

b. the gaseous elements as a hypothetical ideal gas at 1 atm. and the temperature of interest.

Robie and Waldbaum have collected the currently (1968) best available data for heat contents, entropy contents and enthalpies of formation from the elements and list internally consistent tables of

other functions.

The most recent tabulations of 298.15°K, 1 atm. data by Wagman et al. supercede Robie and Waldbaum but no bibliography is supplied so that sources cannot be checked. Naumov et al. (1971) gives an exhaustive tabulation of thermodynamic data for geologists from the Russian and Western literature. Most of the data for silicates is from Kelley (1960), King and Kelley (1961) and Robie and Waldbaum (1968). Stull et al. (1966, 1972) give latm data from 0°K to high temperatures giving a very informative review of data sources with each tabulation. Unfortunately data for few geologically relevant phases are tabulated.

There is no one tabulation of high pressure high temperature gas data. Burnham et al. (1969) gives an invaluable tabulation of data for water from 200 to 1000°C and from 100 bars to 10 kbars. The heat contents and entropy contents are referred to the temperature and pressure of the triple point of water 0.061 bars and 0.01°C. They give the specific volume data in terms of three polynomials in pressure and temperature covering three pressure-temperature fields, see Fig. 1. The situation for other gases is not so good.

Rhyzenko and Volkov (1971) compiles volume data for H_2, N_2, CO, CO_2, and CH_4 and use this to calculate three fugacity coefficient polynomials in reduced temperature T_R (temperature divided by critical temperature) and reduced pressure, P_R (pressure divided by critical pressure) applicable to all the gases in different pressure-temperature ranges, see Fig. 2. This approach depends on the principle of corresponding states, a proposal of van der Waal's that all gases would have the same equation of state in terms of reduced variables. Gases will obey the principle if they are effectively symmetrical, non-polar, and not very light (Guggenheim (1966)). Whereas CO and O_2 conform well, and H_2 and CH_4 less well, the approximation is poor for CO_2 and (particularly) H_2O.

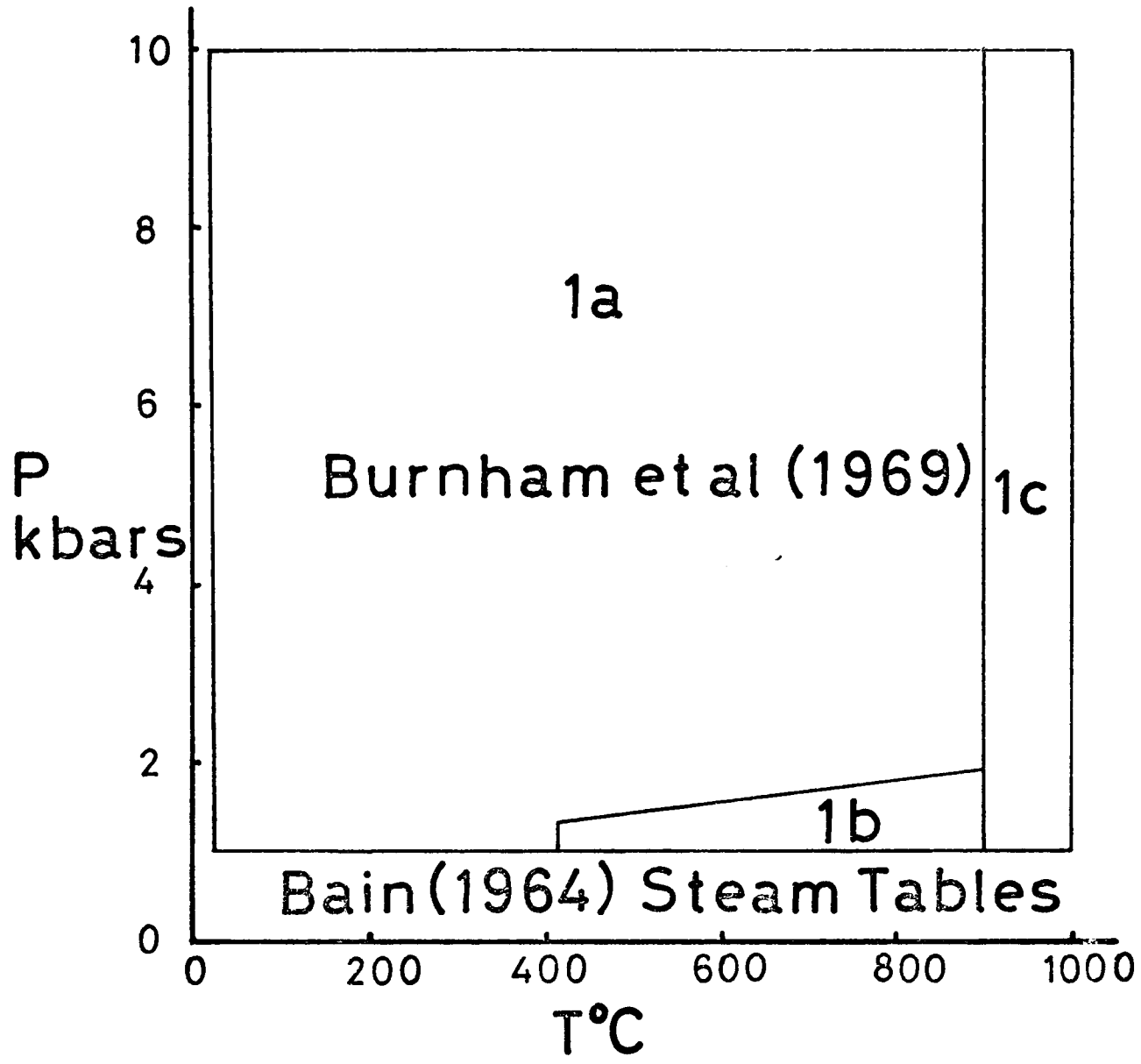


Fig 1 :- Pressure - temperature fields of applicability of the three H_2O P-V-T polynomials of Burnham et al. (1969)

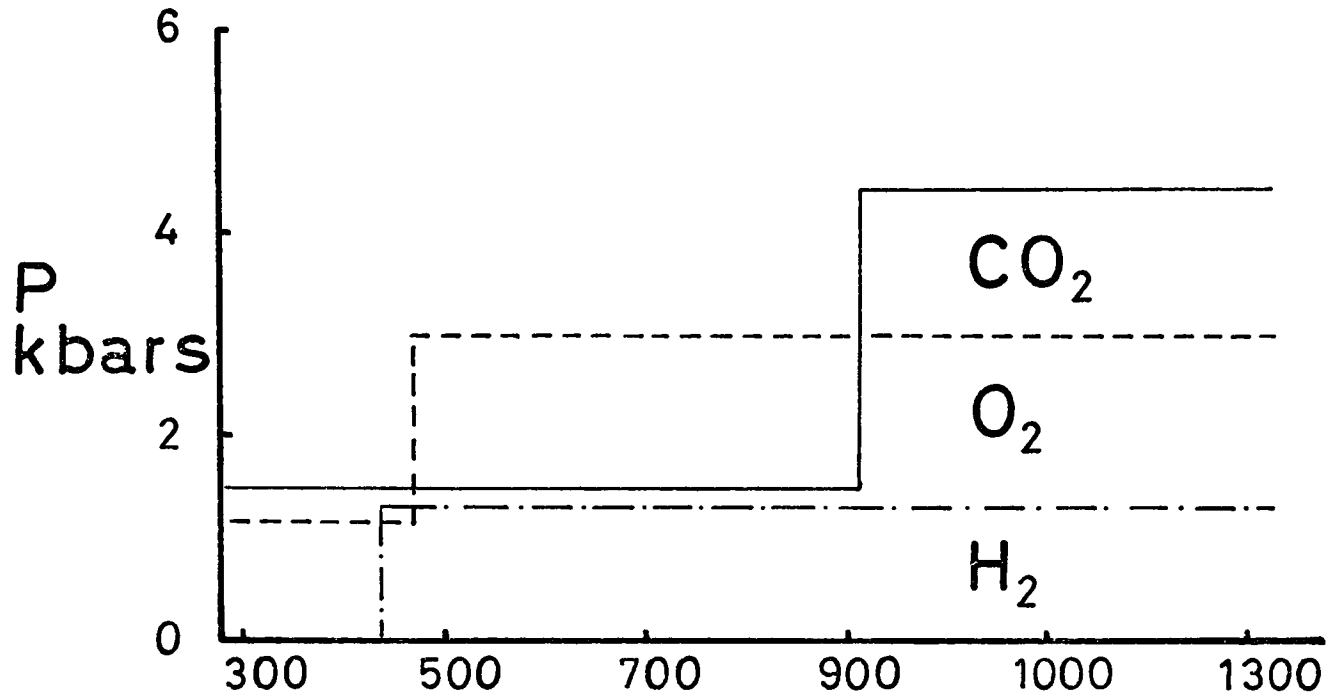


Fig 2:- Pressure - temperature fields of applicability of the reduced variable equations of Rhyzenko and Volkov (1971) for CO_2 O_2 and H_2

Methods of calculation

All methods of calculation of phase equilibria are based on (54) and many on (92-95) and therefore a standard state must be chosen. This choice is dictated by the data sources; obviously it is most convenient to use a standard state involving least alteration of tabulated data.

The standard state chosen combines standard states 2 and 3 (65, 66) from the last chapter. This is a mixed standard state;

(a) for a condensed component: the pure component at the temperature and pressure of interest

(b) for a gaseous component: the hypothetical ideal gas at 1 bar and the temperature of interest.

The advantage of this standard state is that for condensed components the activity of a component in an ideal mixture will equal the mole fraction (75), while for gaseous components the activity of a pure component is numerically equal to the fugacity in bars (although it is dimensionless) (66). The extra subscript on the activity and equilibrium constant can now be dropped. This standard state is used in nearly all thermodynamic studies in the geological literature although rarely is this stated (Anderson (1970) is a ndable exception), and fugacity is nearly always used to mean activity.

Robie and Waldbaum (1968) is used as a basic reference here so that the enthalpies of formation are referred to the same conditions as given in the section on data sources, above.

The method of calculation used later will be outlined here and will be followed by a review of methods which have been used in the geological literature.

Consider a reaction involving t components, the first t_s of which are solid,

$$\sum_{k=1}^{ts} A_k M_k + \sum_{k=ts+1}^{t} A_k M_k = 0 \qquad (129)$$

For each gaseous component k from (86)

$$\mu_k = \mu_k^{oo} + RT \ln f_k^* x_k \gamma_k \qquad (130)$$

For each solid component k, from (85)

$$\mu_k = \mu_k^* + RT \ln x_k \gamma_k \qquad (131)$$

combining (54) with (130, 131)

$$-\frac{\Delta G_R}{RT} = \ln \prod_{k=1}^{ts} (x_k \gamma_k)^{M_k} \cdot \prod_{k=ts+1}^{t} (f_k^* x_k \gamma_k)^{M_k} \qquad (132)$$

with $$\Delta G_R = \sum_{k=1}^{ts} M_k \mu_k^* + \sum_{k=ts+1}^{t} M_k \mu_k^{oo} \qquad (133)$$

Re fering the chemical potentials in (133) to actual literature data, for example, Robie and Waldbaum (1968), gives

$$\mu_k^* = \Delta_f g_k(\text{el, } T^oK, \text{ P bars}) \qquad (134)$$

$$\mu_k^{oo} = \Delta_f g_k(\text{el, } T^oK, \text{ 1 bar}) \qquad (135)$$

Equation (134) can be considered in two parts

$$\mu_k^* = \Delta_f g_k(\text{el, } T^oK, \text{ 1 bar}) + \Delta_f g_k(T^oK, \text{ 1} \rightarrow \text{P bars}) \qquad (136)$$

Combining (133) with (135, 136) gives

$$\Delta G_R = \sum_{k=1}^{t} M_k \Delta_f g_k(\text{el, } T^oK, \text{ 1 bar}) + \sum_{k=1}^{t} M_k \Delta g_k(T^oK, \text{ 1} \rightarrow \text{P bars}) \qquad (137)$$

The last term in this expression involves Δg_k not $\Delta_f g_k$ because the volumes used to calculate the fugacities are not volumes of formation.

The first term can be simplified in the same manner as (103-108) to give

$$\sum_{k=1}^{t} M_k \{\Delta_f h_k(\text{el, } 298.15^oK, \text{ 1 bar}) + \Delta h_k(\text{1 bar, } 298.15 \rightarrow T^oK) - T\Delta S_k(\text{1 bar, } T^oK)\} \qquad (138)$$

The second term involves only condensed phases. Because

$$\Delta g_k(T^oK,\ 1 \rightarrow P \text{ bars}) = \int_1^P v_k dP$$

and the pressure-temperature dependence of the molar volume for condensed phases is negligible for metamorphic pressures, it is a very reasonable approximation to take

$$\int_1^P v_k dP = v_k\ (P-1)$$

Therefore

$$\Delta G_R = \sum_{k=1}^{t} M_k\ (\Delta_f h_k(\text{el},\ 298.15^oK,\ 1 \text{ bar}) + \Delta h_k\ (1 \text{ bar},\ 298.15 \rightarrow T^oK) - T\Delta S_k\ (1 \text{ bar},\ T^oK)) + \sum_{k=1}^{tc} M_k v_k\ (P-1) \qquad (139)$$

Thus ΔG_R can be calculated from tables of enthalpy of formation from the elements at 298.15°K and 1 bar, heat contents and third law entropies at 1 bar and the temperature of interest and molar volumes tabulated in, for example, Robie and Waldbaum. The program THERMOCALC uses this method of calculation. The only approximation in this method is the temperature- pressure independence of the molar volume of condensed phases. The molar volume of quartz, which is more strongly pressure dependent than most silicates (Galdin (1970)), is decreased by only 0.3 cc from 1 bar to 5 kbars (using data of Clark (1966)) or by less than 1%. The contribution of the volume term in (139) is small, so this approximation is justified.

For some phases high temperature heat contents have not been experimentally determined. For these phases it is possible to use the Neumann-Kopp rule, that the heat capacity of a phase is equal to the atomic heats of its component elements. However this is only a good approximation for ionic solids (Denbigh 1968, p.413). A better approximation uses experimentally determined heat capacities for structurally similar phases combined in proportion to the undetermined phase (e.g. Robie and Hemingway 1972). It has been shown that this

additivity breaks down even for ionic solids towards absolute zero. This means that whereas poor approximations of third law entropies can be produced by this additivity method, entropy contents and heat contents can be approximated very well even for silicates, particularly using a volume ratio correction. For example, paragonite = muscovite + high albite - sanidine

given Δh_{musc} (1 bar, 298.15°K $\rightarrow$ T°K) , v_{musc}

$\Delta h_{high\ ab}$ (1 bar, 298.15°K $\rightarrow$ T°K) , $v_{high\ ab}$

Δh_{san} (1 bar, 298.15°K $\rightarrow$ T°K) , v_{san}

and v_{para}

The heat content of paragonite can be approximated by

$$(\Delta h_{musc} - \Delta h_{high\ ab} + \Delta h_{san})\, v_{para}/(v_{musc} - v_{ab} + v_{san})$$

Hemingway and Robie (1972) use this volume correction in estimating the entropy of huntite from calcite and magnesite. The discrepancy between the heat capacity ratio of calcite + magnesite to dolomite in their Fig. 2 is reduced by 50% by applying this volume ratio correction.

It is not obvious what should be used for the heat content of structurally bound water in additivity calculations. Crude calculations on hydrous phases which have been experimentally determined show that at each temperature the necessary heat content is the same as the heat content for ideal gas, H_2O, if the molar volume of ice is used in the volume correction. This approximation has been used in calculating heat contents and entropy contents of hydrous silicates.

Calculation methods used in the geological literature usually involve simplification of (133) whether explicitly stated or not.

Anderson (1970) emphasises that the enthalpy of reaction calculated from experimentally determined equilibria is dependent on the standard

state chosen. The standard state used here is Anderson's standard state 3.

Zen (1969, 1971, 1972, 1973) and Fisher and Zen (1971) have pioneered the serious retrieval of thermodynamic data from published experimental work and Zen has developed his own method for doing this. His method has been adopted by others (e.g. Bird and Anderson) and the approximations within his method are gaining respectability by repetition.

Fisher and Zen (1971) give a detailed account of the method used. The important difference between this and the method used here is that at a stage equivalent to (133) instead of combining the change of Gibbs free energies of formation at 1 bar for the whole reaction they keep separate the term involving the vapour phase. The important consequence of this is that in (138) third law entropies can be used, while in their method it is necessary to use entropies of formation from the elements to calculate the change in entropy for the solids of the reaction. It is obviously more convenient to use third law entropies because they are tabulated in data compilations. Having separated the vapour phase term, they define a Gibbs energy function equal to Gibbs energy of formation at 1 bar and the temperature of interest plus a Gibbs energy content term equal to RT ln f_{H_2O} . This function is tabulated over the region of the water data of Burnham et al. (1969). If the vapour term in Fisher and Zen is not kept separate then it is not necessary to define a new function, and their method reduces to the method used here.

An approximation used by Zen for phases for which heat contents are not known deserves mention. This is

$$\int_{298.15}^{T} \Delta S_{\text{solids}}(1 \text{ bar}, T)\, dT = \Delta S_{\text{solids}}\ (298.15^{\circ}K, 1 \text{ bar})\ (T-298.15)$$

the assumption being that ΔS solids is independent of temperature or that ΔC_p solids = 0. Taking the Neuman - Kopp rule to apply, this approximation is reasonable for reactions not involving vapour components. However if the reaction involves dehydration, decarbonation, oxidation etc., then this approximation is going to be wrong by an amount equal to the entropy of the structurally bound vapour component. For example, for the reaction

$$\text{muscovite} + \text{quartz} \rightleftharpoons \text{sanidine} + \text{kyanite} + H_2O$$

in which the heat contents of the phases are well-known, the approximated temperature is 130°C lower than for the complete calculation at 2 kbars. Using the approximation to the structurally combined water, given earlier the calculated temperature is within 20°C of the temperature from the complete calculation. For a comparison of the curves for this reaction calculated in the different ways, see Fig. 3.

Gas data

One advantage of the chosen standard state is that for gases $a_i = f_i$ so that published fugacity (or fugacity coefficient) equations or tabulations can be used directly. In this section the data sources for the fugacities of pure gases will be evaluated and a 'best available' set of data given.

H_2O

The water data given in Burnham et al (1968) is certainly the best available. It is based on the internationally accepted steam tables (Bain 1964) at low pressures and is supplemented by their own precise high pressure experimental work. It is in excellent agreement with the early work of Bridg man (1935) and of Holser and Kennedy (1958, 1959), and within the stated limits of accuracy of Sharp (1962).

Burnham et al. give three polynomials for PV/M for different

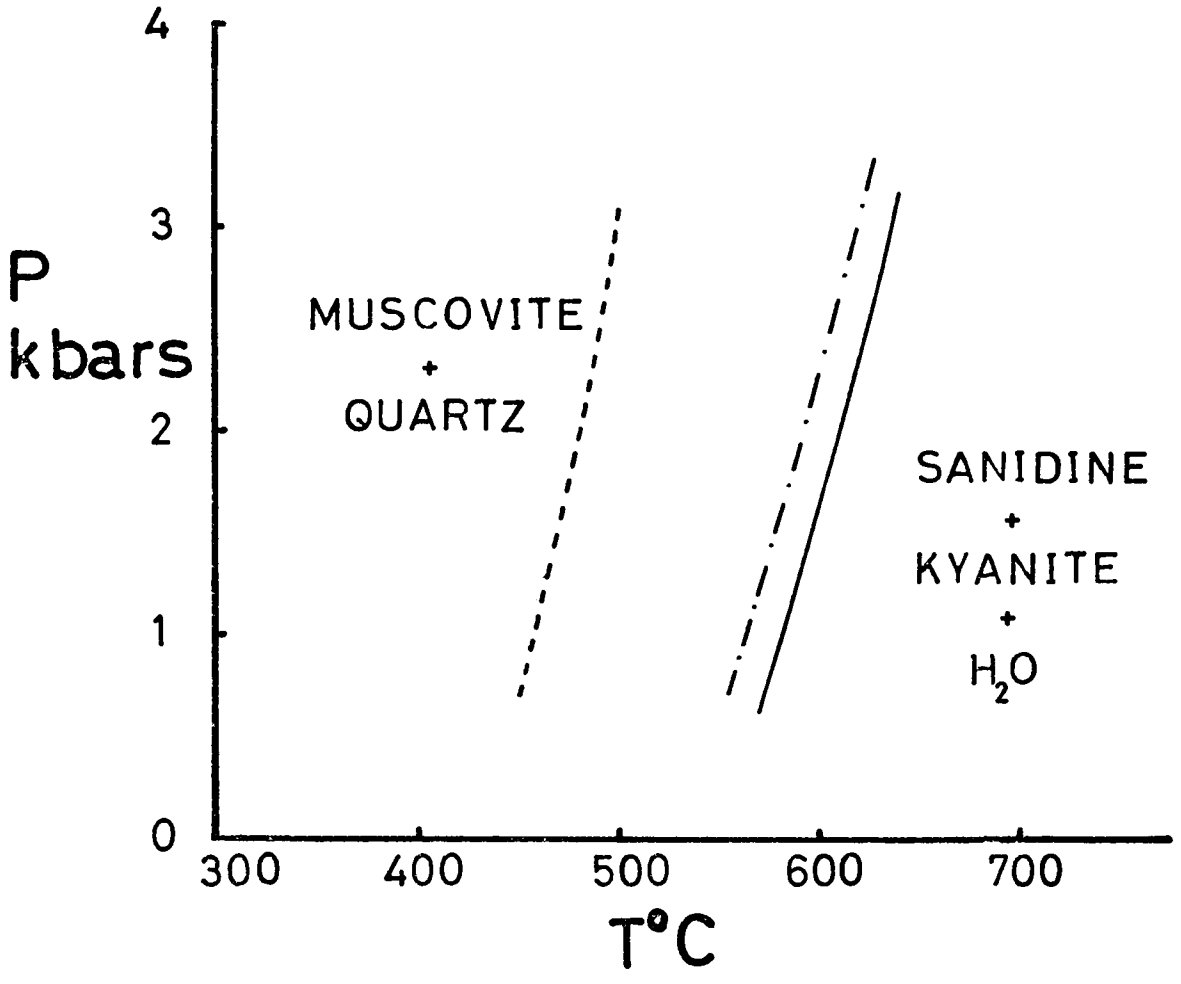


Fig 3 :- Comparison of approximations for calculating equilibrium temperatures of reactions.

—— calculation using heat capacities

-·-·- calculation using approximation suggested here

----- calculation using Zen's approximation

pressure and temperature ranges (Fig. 1). Their main polynomial (1a) applies accurately over the main PT area and is not substantially inaccurate in the PT ranges covered by the other polynomials. Polynomial 1a will be used here. The polynomial has been reconstructed to give a polynomial for ln f_{H_2O} in the form

$$\ln f_{H_2O} = \sum_{i=1}^{10} m_i T^{i-2} \ln P + \sum_{j=1}^{10} \sum_{i=1}^{11-j} n_{ij} T^{i-2} p^{i-1} \qquad (140)$$

with T in hundreds of ^{o}K and P in kbars with the fugacity given in bars. The coefficients and the derivation of this equation are given in Appendix 2. This equation provides the fugacity of water used in all the later calculation.

CO_2

The experimental data for CO_2 is not so reliable nor does it cover the same PT range as the water data. The literature data of McCormick and Schneider (1950), Kennedy (1954), Vukalovitch and Altunin (1965) and Juza et al. (1965) covers various pressure and temperature ranges summarised in Fig. 4.

Rhyzenko and Volkov (1971) have calculated fugacity coefficients from this patchwork of P-V-T measurements and, in their Table 2, compare these with the results from their reduced variable equations (13-15). However, because CO_2 is not ideally suited for reduced variable calculations, the agreement (up to ±20% difference) is poor. Making the assumption that the experimentally determined P-V-T relations are superior to the reduced variable calculation results, I have least squares surface fitted the fugacity coefficients, calculated by Rhyzenko and Volkov from the experimental data, by a polynomial of the form favoured by Rhyzenko and Volkov, using the program FIT (Appendix 3).

Table 1 :-

CO_2 polynomial coefficients

	i = 1	i = 2	i = 3
j = 1	1·01784	0·000	0·000
j = 2	- 0·14329	0·0818242	- 0·0105270
j = 3	0·0036867	- 0·0010585	0·0000040427

Table 2 :-

O_2 polynomial coefficients

	i = 1	i = 2	i = 3
j = 1	1·0000	0·000	0·000
j = 2	0·0124	0·000254	- 0·00005104
j = 3	0·0011089	0·0001998	0·000009393

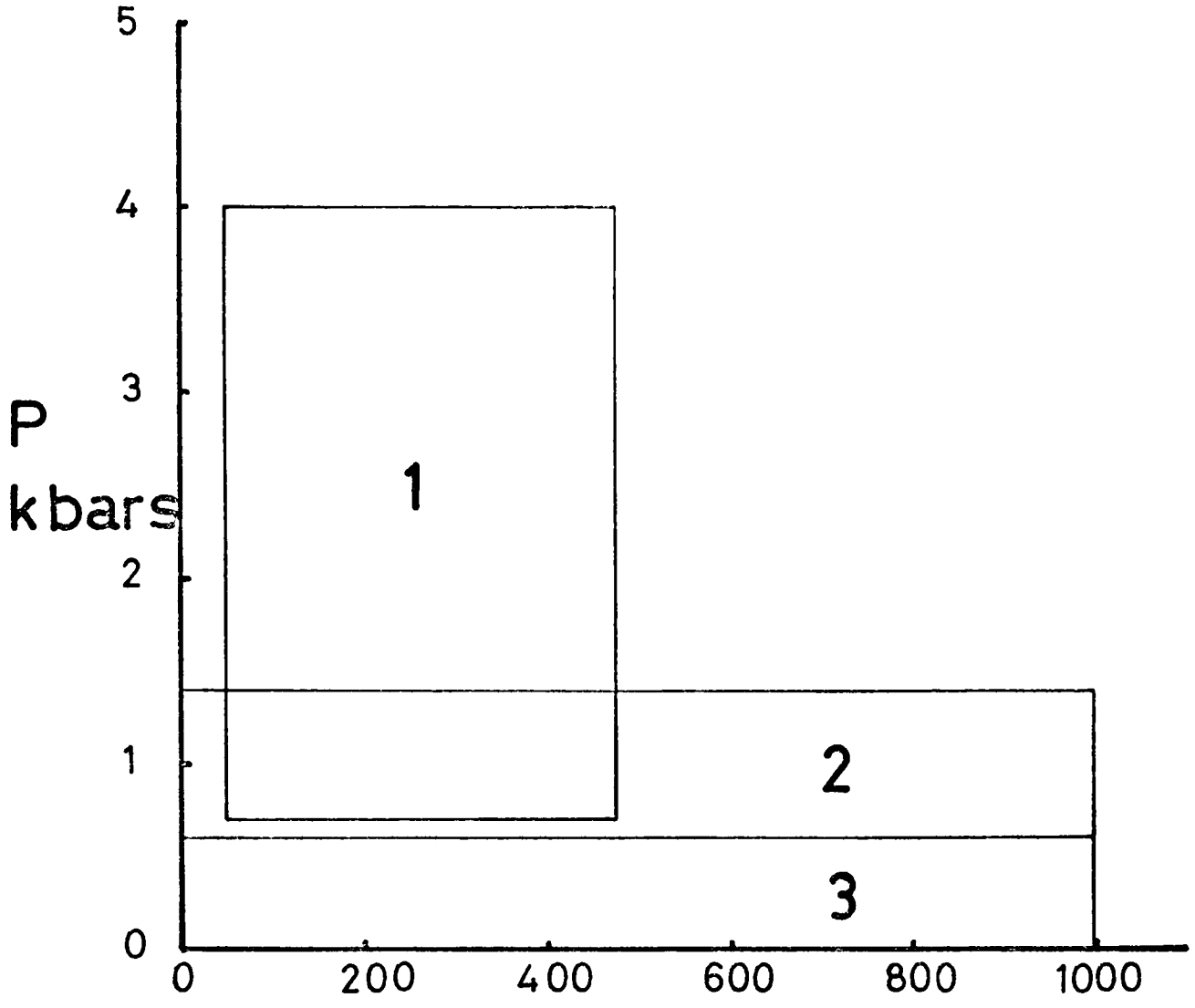


Fig 4 :- Pressure - temperature fields of literature P-V-T data for CO_2

1 - Juza et al (1965)
2 - Kennedy (1954)
3 - Vukalovitch and Altunin (1965)

$$\frac{f}{P}_{CO_2} = \sum_{i=1}^{3}\sum_{j=1}^{3} d_{ij} T_k^{i-1} P_k^{j-1} \quad \text{where } T_k = \frac{T^\circ K}{304.15} \qquad (141)$$

d_{ij} in table 2 $\qquad P_k = \frac{Pbars}{73.8}$

This polynomial fits the data better than 4%. The advantage of a lower order polynomial is that it can be used for extrapolation.

This polynomial is used for calculating the fugacity of CO_2, up to 5 kbars with some confidence of not being incorrect by more than 20%.

O_2

Pressure-volume-temperature data for oxygen at high pressure is limited to Tsiklis et al. (1965) (quoted by Rhyzenko and Volkov) and their data extends only to 400°C. The only choice is to use the appropriate equations from Rhyzenko and Volkov (1971).

$$\frac{f}{P}_{O_2} = \sum_{i=1}^{3}\sum_{j=1}^{3} a_{ij} T_k^{i-1} P_k^{j-1} \quad \text{where } T_k = T^\circ K/154.75$$

a_{ij} in Table 3 $\qquad P_k = Pbars/50.8$

This equation is strictly applicable only above 200°C and up to 3000 bars, but is probably not greatly in error up to 5000 bars, and will be used up to this pressure.

H_2

Shaw and Wones (1964) have reviewed and compiled literature data for the pressure-volume-temperature relations of hydrogen. They introduce a function, from (63)

$$\ln f/P = \int_0^P \left(\frac{v}{RT} - \frac{1}{P}\right) dP = \int_0^P \sigma dP \qquad (142)$$

They fit the function by a polynomial in P and T of the form:

$$\sigma = a - bP - c \exp(-P/300) \qquad (143)$$

where a, b, c are functions of temperature. The third term is an attempt to express the low pressure deviation from linearity of σ against P. Presnall (1968) gives experimentally determined values

of σ for pressures up to 1800 atm. at temperatures from 200° to 600°C. Comparison with (143) shows that b is substantially correct, a is two percent too high, but the third term does not even reproduce the trend of the data at low pressure and high temperature.

I have abandoned the third term and instead use two straight line segments.

$$0 - 500 \text{ atm.} \quad \sigma = a_1 + b_1 P \quad \ln f/P = \{a_1 P + \frac{b_1}{2} P^2\}_0^P$$

$$500 - 1800 \text{ atm.} \quad \sigma = a_2 + b_1 P \quad \ln f/P = a_1 500 + \frac{b_1}{2} 500^2 + \{a_2 P + \frac{b_2}{2} P^2\}_{500}^{P} \tag{144}$$

$$\ln \frac{f}{P}_{H_2} = \{a_1 500 + \frac{b_1}{2} 500^2 - a_2 500 - \frac{b_2}{2} 500^2\} + a_2 P + b_2 P^2 \tag{145}$$

where P is in atmospheres

The term in brackets can be closely approximated by

$$- 1.49* 10^{-5} T + 0.0041 \tag{146}$$

converting the coefficients so that the pressure is in bars

$$\ln \frac{f}{P}_{H_2} = A + BP + CP^2 \tag{147}$$

where $A = -1.49 \times 10^{-5} T + 0.0041$

$B = \exp (-3.8699 T^{\frac{1}{8}} + 0.60493)$

$C = - \exp (-0.1263 T^{\frac{1}{2}} - 15.9537)$

T is in °K

f_{H_2}, P is in bars

The difference between my equation and that given in Shaw and Wones amounts to 2.5% at the highest pressures and temperatures.

This equation will be used for the fugacity of hydrogen. Shaw and Wones claim that their equation is applicable to 3000 atm. Because of the high pressure linearity of σ at each temperature well shown by Presnall's data, the above equation is likely to be applicable to at least that pressure.

Gas mixtures

The characterisation of gas activities in gas mixtures requires knowledge of the fugacity, the mole fraction, and the activity coefficient of the pure gas component in the mixture. In general this activity coefficient will be a function of pressure, temperature and composition of the gas phase.

Fugacities of gases in gas mixtures are calculated from (62)

$$RT \ln \frac{f_i}{P_i} = \int_0^P (v_i - \frac{RT}{P})dP$$

where v_i is the partial molar volume of i calculated from (10). Knowing the fugacity of the pure gas at the same pressure and temperature, f_i^*, allows the calculation of the activity coefficient γ_i from

$$\gamma_i = f_i/f_i^* x_i$$

A huge body of pressure-volume-temperature data is therefore required to calculate activity coefficients for gas mixtures. This does not exist.

$CO_2 - H_2O$

Greenwood (1969) gives pressure-volume-temperature data for $CO_2 - H_2O$ mixtures in the range 0 to 500 bars and 450 to 800°C. If the gas mixture is ideal then the volume of the mixture is linearly related to the volume of the pure gases. His Figs. 4 and 6 show that while at 650°C the gas mixture is approximately ideal (although apparently getting less so to higher pressures), at 450°C the gas mixture is definitely not ideal and becomes more strongly non-ideal to higher pressures.

Rhyzenko and Malinin (1971) give a literature compilation of available experimental data on CO_2 containing binary gas mixtures, including $H_2O - CO_2$. A common feature of these binaries is a negative

deviation from ideality below a pressure independent characteristic temperature and a positive deviation above this temperature. For H_2O - CO_2 this characteristic temperature is about 600°C at 500 bars moving to about 630°C at 1500 bars. At and near the characteristic temperature the mixture is effectively ideal.

Rhyzenko and Malinin (op. cit.) give tables of fugacity coefficients for CO_2 - H_2O mixtures from 400 to 750°C and 400 to a maximum of 2000 bars calculated from literature volume data (mainly of Franck and Todheide (1959)). They emphasise that the calculations are crude and that errors on f_i/P for x_i greater than 0.7 are about ± 5% and between 0.3 and 0.7 about ± 10%, with no meaningful error estimate for x_i less than 0.3.

For this reason the least squares treatment of this data by Barron (1971) is not justified without using a weighting scheme to give preference to the values at high x_i where the likely error is least. He adopts a regular solution model (R model) and gives the parameter w for

$$RT \ln \gamma_{H_2O} = w x^2_{CO_2}$$

$$RT \ln \gamma_{CO_2} = w x^2_{H_2O}$$

The best fit polynomial for w is

$$w = 1243.44 - 1.68096\ P - 1.3983T + 1524.14\ P/T$$

He also gives a polynomial for w linear in pressure and temperature

$$w = 3116.7 + 0.093117P - 3.5528T \quad \text{with P in bars, T in } ^oK \qquad (148)$$

This equation is preferred because a fourth parameter is not justified by the data. The critical point of the solvus in the binary CO_2 - H_2O is effectively independent of pressure above 2000 bars. (Takenouchi and Kennedy 1964). From Thompson (1967) the change of the critical point conditions for the R model is given by

$$\frac{dPc}{dTc} = \frac{d\frac{W}{T}}{d\frac{1}{T}} \Big/ \frac{dw}{dP}$$

Above 2000 bars the denominator must equal zero so that above this pressure equation (148) is used here for the mixing properties of CO_2 - H_2O mixtures with the proviso that P is set equal to 2000 for pressures equal to or greater than 2000 bars.

CH_4 - CO_2 and CH_4 - H_2O

Although in some treatments of mineral equilibria in variable vapour phase systems, the vapour is considered to be binary CO_2 - H_2O (e.g. Greenwood 1967), in fact H_2O and CO_2 are in reaction equilibrium with many species and the vapour phase consists of the components CO_2 - H_2O - H_2 - O_2 - CH_4 - CO and very small amounts of many other hydrocarbons and carbohydrates. French (1966) has considered the vapour phase composition in C-H-O for systems at high temperature and pressure in equilibrium with graphite. An important conclusion of his calculations is that methane is an important, even dominant species, in C-H-O in equilibrium with graphite at temperatures up to about 500°C, moderate to high pressures and moderate to low oxygen fugacities (below the quartz-fayalite-magnetite buffer

The only relevant data on CH_4 - CO_2 and H_2O - CH_4 is given by Reamer et al. (1944) and the former is summarised by Rhyzenko and Malinin. This data extends from 200 to 700 bars and 40 to 240°C. The characteristic temperature is above the upper limit of the experimental data. This means that the only available choice of assuming CH_4 - CO_2 behaves as an ideal mixture is unlikely to be seriously in error for the relatively low temperatures where methane is an important species. The raw CH_4 - H_2O data indicate that the assumption of ideal mixing will not be seriously in error.

H_2 - H_2O and H_2 - CO_2

Hydrogen becomes an important species in C-H-O for moderate to high temperatures and low oxygen fugacities. Krytchevsky and Markov (1940), summarised by Rhyzenko and Malinin, give data for CO_2 - H_2 at pressures to 500 bars and temperatures to 200°C. The characteristic temperature is about 200°C. Again there is no choice but to assume that CO_2 - H_2 is an ideal mixture.

Shaw (1967) gives the deviations from ideality of H_2 - H_2O mixtures at 700°C and 800bars and gives an R model type expression for the activity coefficient for these conditions. The deviation from ideality is not great (for example, 1% at 1 kbar, 650°C and the QFM buffer). Because the mixing conditions are known only for a very limited range of conditions, less error is likely to arise by considering the mixtures as ideal than by trying to use this data beyond the range of its applicability.

O_2 in C-H-O

The fugacity of oxygen at geological temperatures and pressures is extremely small in the system C-H-O because it is controlled by the dissociation reaction of water

$$H_2O \rightleftharpoons H_2 + \tfrac{1}{2}O_2$$

for which the equilibrium constant has been precisely determined by Wagman et al. (1945) and fitted by a polynomial in T°K by Zen (1973) with a maximum deviation of 0.0005.

$$\log K_{H_2O} = \log f_{H_2O}/f_{H_2} f_{O_2}^{\frac{1}{2}} = 12447.90889/T - 1.51609 \log T + 0.00016\ T + 2.00131 \qquad (149)$$

Combining this equation with $P_{H_2} + P_{H_2O} = P_{total}$ it is possible to express the fugacity of H_2 or H_2O in terms of P_{total} and the fugacity of oxygen. For ideal mixing fugacity coefficients are independent of composition. Combining (149) and (150) gives

$$f_{H_2} = f^*_{H_2} \cdot f^*_{H_2O} \,/\, K_{H_2O}\, f_{O_2}^{\frac{1}{2}}\, f^*_{H_2} + f_{H_2O} \qquad (151)$$

$$f_{H_2O} = K_{H_2O}\, f_{H_2}\, f_{O_2}^{\frac{1}{2}} \qquad (152)$$

The fugacity of oxygen is controlled in two main ways in experimental work; by using solid assemblages which buffer the fugacity of oxygen (Eugster 1959, Eugster and Skippen 1967) and by controlling the fugacity of hydrogen directly (Shaw 1963, 1967). The commonly used buffer assemblages and the buffer equations are given in Table 3 in the form

$$\log f_{O_2} = -A/T + B + C(P-1)/T \qquad (153)$$

TABLE 3 OXYGEN BUFFERS

assemblage		A	B	C
HM	Fe_2O_3 - Fe_3O_4	25680	15.953	0.019
	calculated from Haas and Robie (1973), Robie et al (1967)			
HMN	Mn_3O_4 - $Mn_{1-x}O$	25680	13.37	0.080
	Huebner and Sato (1970), corrected to bars			
NNO	Ni - NiO	24930	9.35	0.045
	Huebner and Sato (1970), corrected to bars			
QFM	SiO_2-Fe_2SiO_4-Fe_3O_4	25738	9.00	0.092
	Wones and Gilbert (1969)			
MW	Fe_3O_4 - $Fe_{1-x}O$	32730	13.12	0.083
	Eugster and Wones (1962), from Darken and Gurry (1945)			

These equations will be used in calculating thermodynamic values from oxidation-reduction reactions.

Data for solid phases

As stated in the introduction to this chapter, reversed experimental reactions will be used whenever possible to calculate a consistent set of thermodynamic data. Whereas the enthalpies of solid phases are large, the enthalpies of reaction are up to two orders of magnitude smaller. An acceptable error bracket on the determination of an enthalpy of formation becomes unacceptably large when applied to the enthalpy of reaction.

A result of the relatively small enthalpy of reaction is that equilibrium temperatures of reaction are sensitive to small enthalpy changes of the components in the reaction. Error brackets can be reduced by calculating data from experimentally determined reactions.

The program THERMOCALC, listed and explained in Appendix 3, uses the calculation method given earlier The data for solid phases is input as

$\Delta_f h$ (el, 298.15°K, 1 bar)

s (298.15°K, 1 bar)

v

cp as a function of the form

$$Cp = a + 2bT - c/T^2 \qquad \text{(Kelley 1960)}$$

The heat contents and entropy contents for each phase are calculated from the heat capacity polynomials within the program. The coefficients were calculated from published or calculated heat contents using the program FIT. The lower temperature heat contents were weighted so that the curve passes through 0.0 kcals at 298.15°K. The equations fit the data in most cases to better than 0.5%.

Initially, available literature values for $\Delta_f h$ (el, 298.15°K, 1 bar) and s(298.15°K, 1 bar) were input to the program. For other phases, the entropies were calculated by an additivity method with a volume ratio correction, as suggested earlier, using the entropy of ice for

structurally bound water, (Fyfe et al. 1959), and the enthalpies of formation were guessed.

THERMOCALC has the facility for altering the entropies and enthalpies of formation of components to agree with an experimentally determined reaction. From

$$\frac{dP}{dT} = \frac{\Delta S_R(P,T)}{\Delta V_R(P,T)} \quad \text{and} \quad T_{equil} = \frac{\Delta H_R(P,T)}{\Delta S_R(P,T)}$$

it is clear that the entropy of a component in a reaction controls the dP/dT and the equilibrium temperature of the reaction, while the enthalpy of formation controls only the equilibrium temperature. In theory, it should be possible to calculate entropy data from experimentally reversed reactions for a range of pressures. However, for dehydration and decarbonation reactions, ΔS is largely controlled by the vapour phase and dP/dT are usually large. The result is that dP/dT is insensitive to the entropy of condensed components. Very tightly bracketed experimental work would be required to calculate entropies. Choosing particular temperatures in wide error brackets (e.g. Zen 1972, p.535) must produce unreliable results. When necessary, entropies were calculated here using the additivity method. These entropies are presumed to be correct and THERMOCALC calculates enthalpy corrections.

The method of calculation for each phase involves a number of steps:

1. An experimentally reversed reaction is chosen which has only one phase whose thermodynamic parameters are not known. The data for some minerals cannot be checked using the method adopted here; for these the literature data has to be accepted. Where more than one reaction is available to retrieve data for a particular phase, the relative error on some of the accepted data can be estimated. For example, the stability of paragonite and paragonite + quartz reported by Chatterjee (1970, 1971) and used by Zen (1972) to calculate paragonite data, gives the compatibility of the corundum and aluminium silicate data.

2. The limits of the experimental brackets to the reaction are input to THERMOCALC which calculates by how much the enthalpy of formation of the phase has to be altered for the reaction to pass through the stated temperatures. The enthalpy correction that is adopted is the centre of the overlap of enthalpy correction brackets which correspond to the experimental brackets. The calculation of statistical errors for calculated enthalpies as recommended by Bird and Anderson (1973) lacks point. When an experimental bracket is reported as 500 ± 10°C, for example, this usually means that the reaction was reversed one way at 490°C and the other way at 510°C, and the reaction curve may lie anywhere within the bracket. There is no statistical significance in the ± given. The practice adopted here is to quote a sensitivity of the enthalpy correction to the temperature of the reaction, given in kcals/10°C.

3. For each reaction used the curve calculated using the corrected enthalpy is compared with the experimental brackets.

In the rest of this section, available literature data is reviewed and enthalpy corrections are calculated relative to values tabulated in Robie and Waldbaum (1968) for a range of geologically relevant phases. The final calculated data set is given in Appendix 4. Because many of the enthalpy corrections are dependent on other enthalpy corrections, a scheme is given in Appendix 4 to correct dependent enthalpies in the light of new calorimetric measurements or from redetermined reactions using the quoted sensitivity.

Magnesite

The data for magnesite has been reviewed by Langmuir (1965) and Christ and Hostetler (1970). The heat content and entropy data in Robie and Waldbaum are from Kelley (1960) and Kelley and King (1961). There is a 7.1 kcal range in the literature values for $\Delta_f g$(el, 298.15°K, 1 bar). Langmuir prefers - 241.92 kcals/mole, a value adopted by Wagman et al. (1971), while Robie and Waldbaum prefer - 246.11 kcals/mole.

Christ and Hostetler (1970) redetermine the equilibrium constant for the magnesite dissociation reaction

$$MgCO_3 = Mg^{2+} + CO_3^{2-}$$

and obtain $\Delta_f g$(el, 388.15°K, 1 bar) = -247.84±0.52 kcals/mole, in agreement with Robie and Waldbaum when corrected to 298.15°K, -245.8 ± 0.52 kcals/mole.

The $\Delta_f h$(el, 298,15°K, 1 bar) was calculated from the experimentally reversed decomposition reaction for magnesite of Harker and Tuttle (1955), assuming that the Kelley and King entropy is correct,

$$\underline{MgCO_3} = MgO + CO_2$$

The runs which bracket the univariant line were taken from Harker and Tuttle (1955, Table 4) and input to THERMOCALC. The correction to the Robie and Waldbaum enthalpy of formation is +0.2 kcals/mole (with a sensitivity of 0.25 kcals/10°C). Therefore $\Delta_f h$(el, 298.15°K, 1 bar) becomes -265.81 kcals/mole; within the errors given by Robie and Waldbaum and Christ and Hostetler. This value is adopted here. Fig. 5 shows the experimental brackets and the calculated curve.

Dolomite

Robie and Waldbaum (1968) use the low temperature heat capacity measurements of Stout and Robie (1963) to calculate the high temperature heat contents and entropies of dolomite. Robie and Waldbaum give

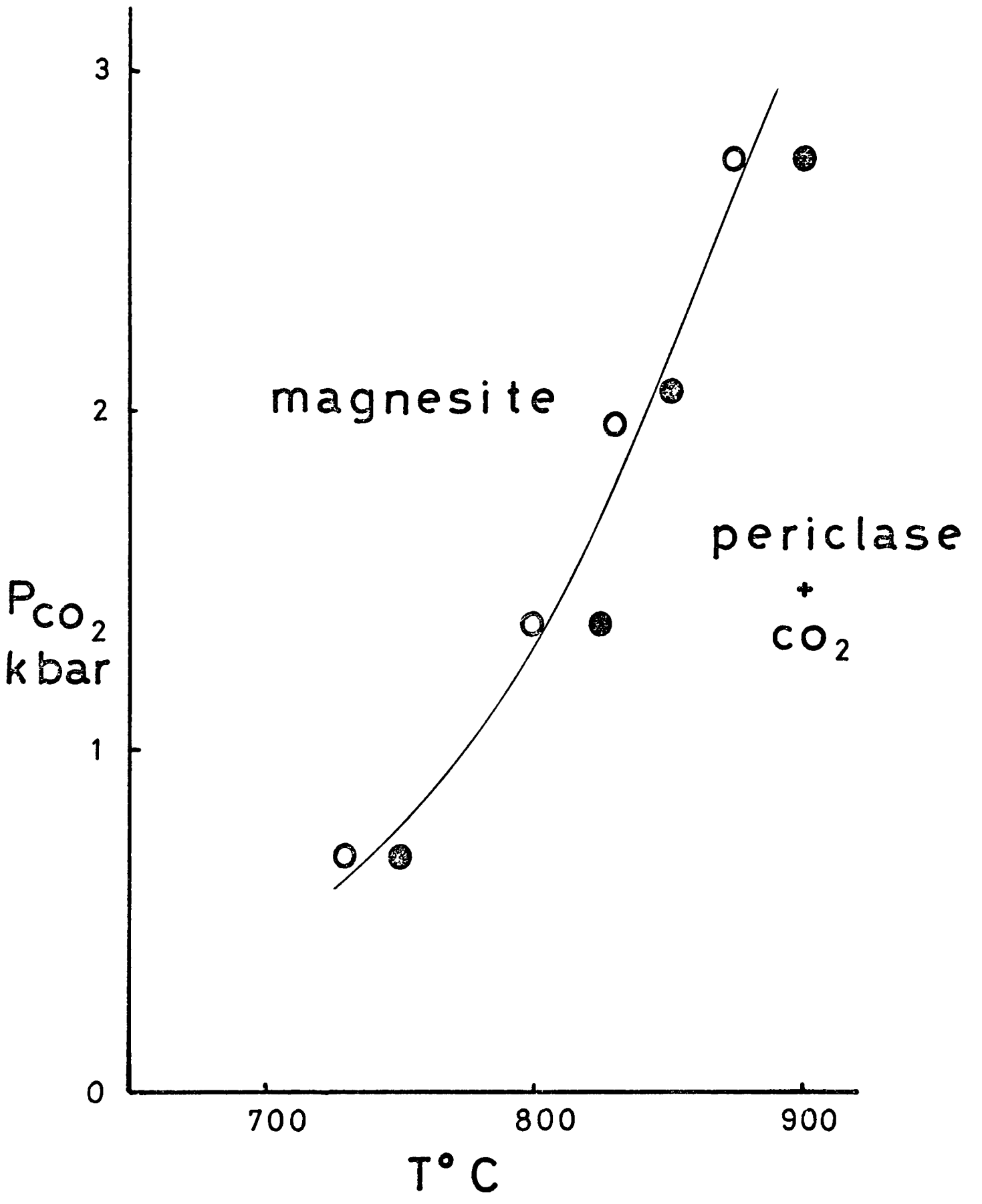


Fig 5 :-MAGNESITE reaction : calculated curve and experimental brackets.
(Harker and Tuttle (1955))

kcal/mole

$\Delta_f h$(el, 298.15°K, 1 bar) = -557.613±0.53 from Robie and Stout. Robie and Hemingway (1973) report a redetermination of this enthalpy without giving the value!

Stout and Robie's value was checked using the dolomite decomposition reaction reversed by Harker and Tuttle (1955),

$$\underline{CaMg(CO_3)_2} = CaCO_3 + MgO + CO_2$$

Most of the runs were long enough to allow equilibration of coexisting calcite and dolomite (see Goldsmith and Newton (1969, p. 173). The activity coefficients for calcite and dolomite calculated in a later section are used in THERMOCALC. The runs which bracket this reaction were taken from Harker and Tuttle (1955, Table 3) and input to THERMOCALC. The enthalpy correction is +0.55 kcals/mole (with a sensitivity of 0.26 kcals/10°C . Therefore $\Delta_f h$(el, 298.15°K, 1 bar) becomes -557.063 kcals/mole; at the upper limit of Stout and Robie's error range. Fig. 6 shows the experimental brackets and the calculated curve.

Talc

Robie and Waldbaum (1968) use the low temperature heat capacity measurements of Robie and Stout (1963) to calculate the high temperature heat contents and entropies of talc. The $\Delta_f g$(el, 298.15°K, 1 bar) of -1324.39 kcals/mole adopted by Robie and Waldbaum comes from Barany (1963) and Robie and Stout (1963). Bricker et al. (1973) report solubility measurements on talc, giving $\Delta_f g$(el, 298,15°K, 1 bar) = -1319.2±1.5. They also reinterpret the solubility measurements on chrysotile by Hostetler and Christ (1968) in terms of incongruent dissolution to talc giving -1321.38 kcals/mole. Bricker et al. also attempt to retrieve data from experimental equilibrium studies. However they assume that the literature values of dolomite and talc are correct. They also assume that the clinoenstatite enthalpy should be adjusted by 1 kcal to apply to orthoenstatite and they adopt the diopside enthalpy of formation of Neuvenon (1952) rather than Kracek

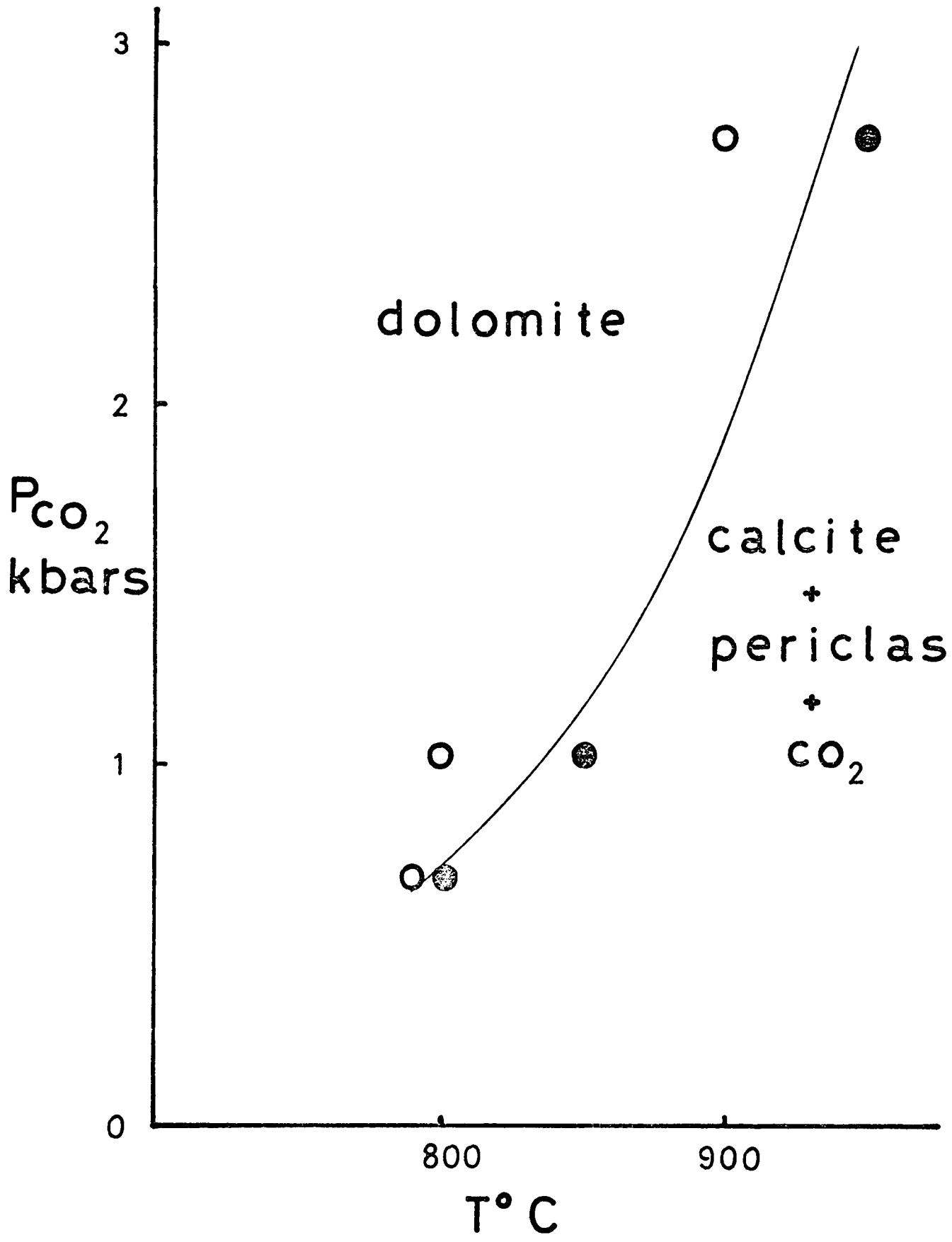


Fig.6 :- DOLOMITE reaction : calculated curve and experimental brackets.
(Harker and Tuttle (1955))

et al. (1952), because it makes their calculations consistent. These assumptions probably negate the values produced although they are in good agreement with the other two values.

A useful reaction to use to improve the talc data would be,

$$3\ MgCO_3 + 4\ SiO_2 + H_2O = \underline{Mg_3Si_4O_{10}(OH)_2} + 3\ CO_2$$

However the only experimental studies are unreversed (Johannes 1969) and the reaction takes place at such low temperatures that equilibrium seems unlikely. However the reaction,

$$3\ CaMg(CO_3)_2 + 4\ SiO_2 + H_2O = \underline{Mg_3Si_4O_{10}(OH)_2} + 3\ CaCO_3 + 3\ CO_2$$

has been reversed at 2 kbars by Gordon and Greenwood (1970) and Skippen (1971). Metz and Puhan (1970), determined this reaction at 1,2,3 and 7 kbars, reversing only one or two runs to the lower temperature assemblage at each pressure.

The runs that bracket this reaction from Table 1 of Gordon and Greenwood were used as input to THERMOCALC. The calculated enthalpy correction is +3.90 kcals/mole (with a sensitivity of 0.6 kcals/10^{o}C). This enthalpy correction is consistent with the less well bracketed results from Metz and Puhan's experiments at 2 and 3 kbars. However, the entropy correction necessary to make the calculated curve pass through their bracket at 1 kbar would require a 15 kcal correction to the enthalpy. It is assumed that the 1 kbar bracket is not properly reversed and the entropy of talc is not altered.

With the enthalpy correction, $\Delta_f h$(el, 298.15^{o}K, 1 bar) becomes -1412.005 kcals/mole, in excellent agreement with Bricker et al. (1973). Fig. 7 and 8 show the experimental brackets of Gordon and Greenwood (1970) and Metz and Puhan (1970) with the calculated curve.

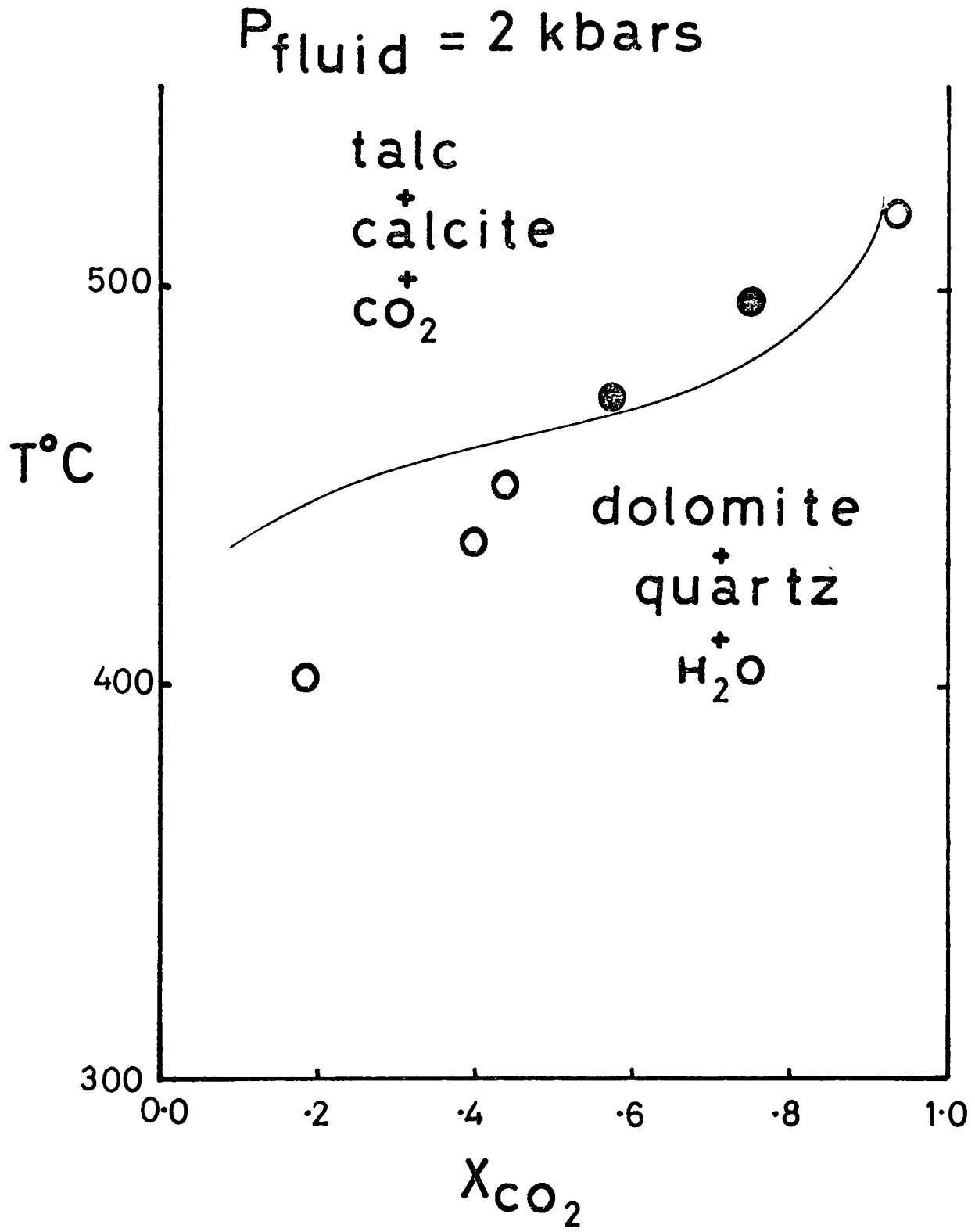


Fig.7:- TALC reaction:
calculated curve and experimental brackets.
(Gordon and Greenwood (1970))

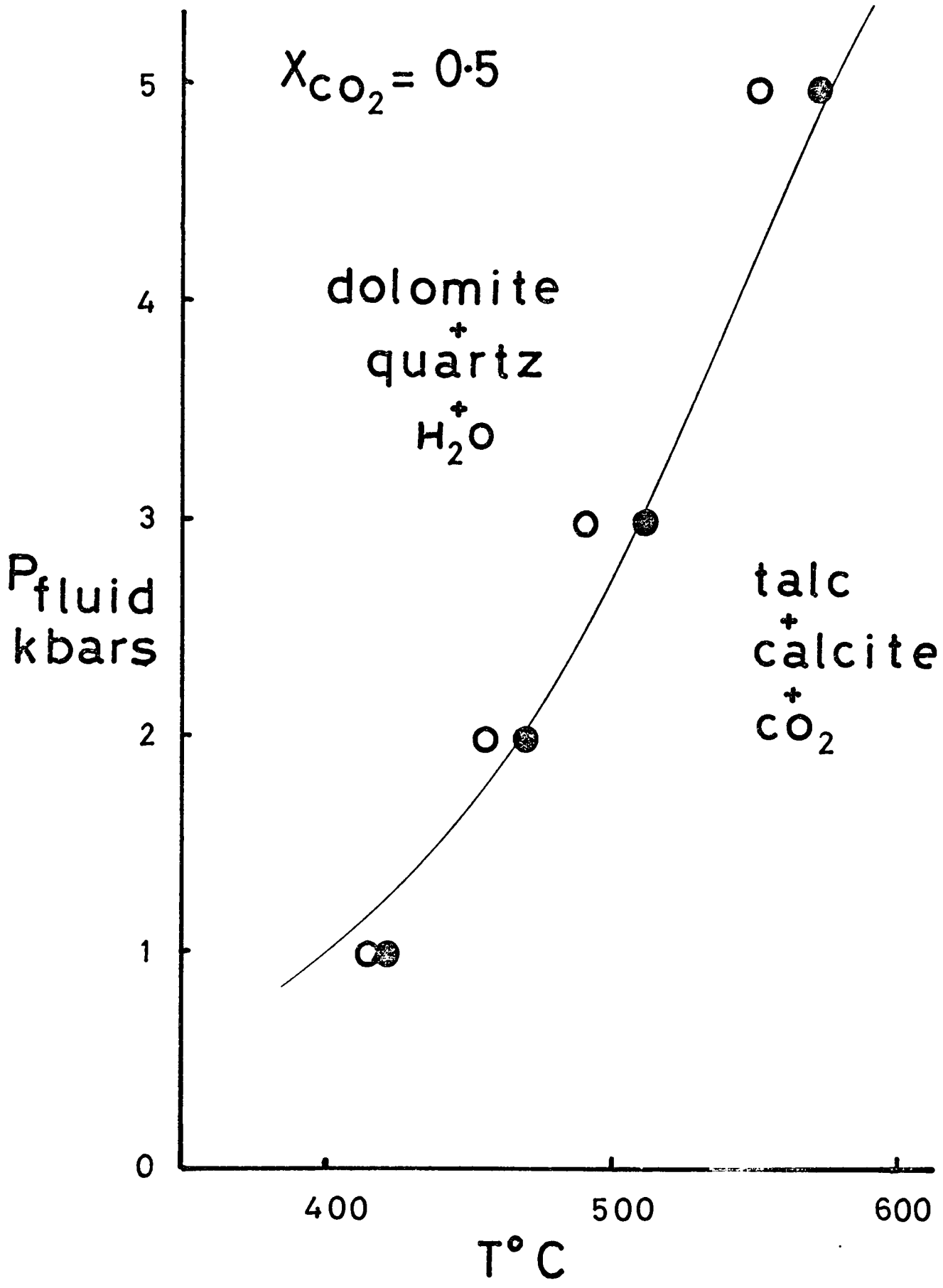


Fig 8 :- TALC reaction :
calculated curve and experimental brackets.
(Metz and Puhan (1970, 1971))

Diopside

The heat contents and entropies in Robie and Waldbaum (1968) are from Kelley (1960) and Kelley and King (1961). For $\Delta_f h$(el, 298.15°K, 1 bar), Robie and Waldbaum give an average of the determinations of Kracek et al. (1953) on a synethetic diopside and Neuvenon (1952) on a natural diopside. There is a 2.51 kcal difference between the two values.

Slaughter et al. (1973) reports the reversal of the reaction

$$\underline{CaMgSi_2O_6} + 2\ CO_2 = CaMg(CO_3)_2 + 2\ SiO_2$$

at 1 kbar, with a wide temperature bracket, 430°-450°C. Skippen calculates this reaction from other reversed reactions in CaO-MgO-SiO_2-H_2O-CO_2 to occur at 460°C. The upper limit of Slaughter's bracket input to THERMOCALC gave an enthalpy correction of +0.8 kcals/mole (with a sensitivity of 0.45 kcals/10°C). The $\Delta_f h$(el, 298.15°K, 1 bar) becomes -766.59 kcals/mole. Fig. 9 shows the Slaughter et al. bracket and Skippen's calculated temperature with the calculated curve.

Wollastonite

The heat contents and entropies in Robie and Waldbaum (1968) are from Kelley (1960) and Kelley and King (1961). The Robie and Waldbaum $\Delta_f h$ (el, 298.15°K, 1 bar) of -390.640 kcal/mole is from Torgeson and Sahama (1948).

Harker and Tuttle (1956) and Greenwood (1967) have reversed the reaction

$$\underline{CaSiO_3} + CO_2 = SiO_2 + CaCO_3$$

The runs that bracket this reaction (Harker and Tuttle (1956) Table 2, Greenwood (1967), Table 2) input to THERMOCALC gave an enthalpy correction of +0.90 kcals/mole (with a sensitivity of 0.20 kcals/10°C). The $\Delta_f h$(el, 298.15°K, 1 bar) becomes -389.54 kcals/mole. Fig. 10 shows the experimental brackets and the calculated curve.

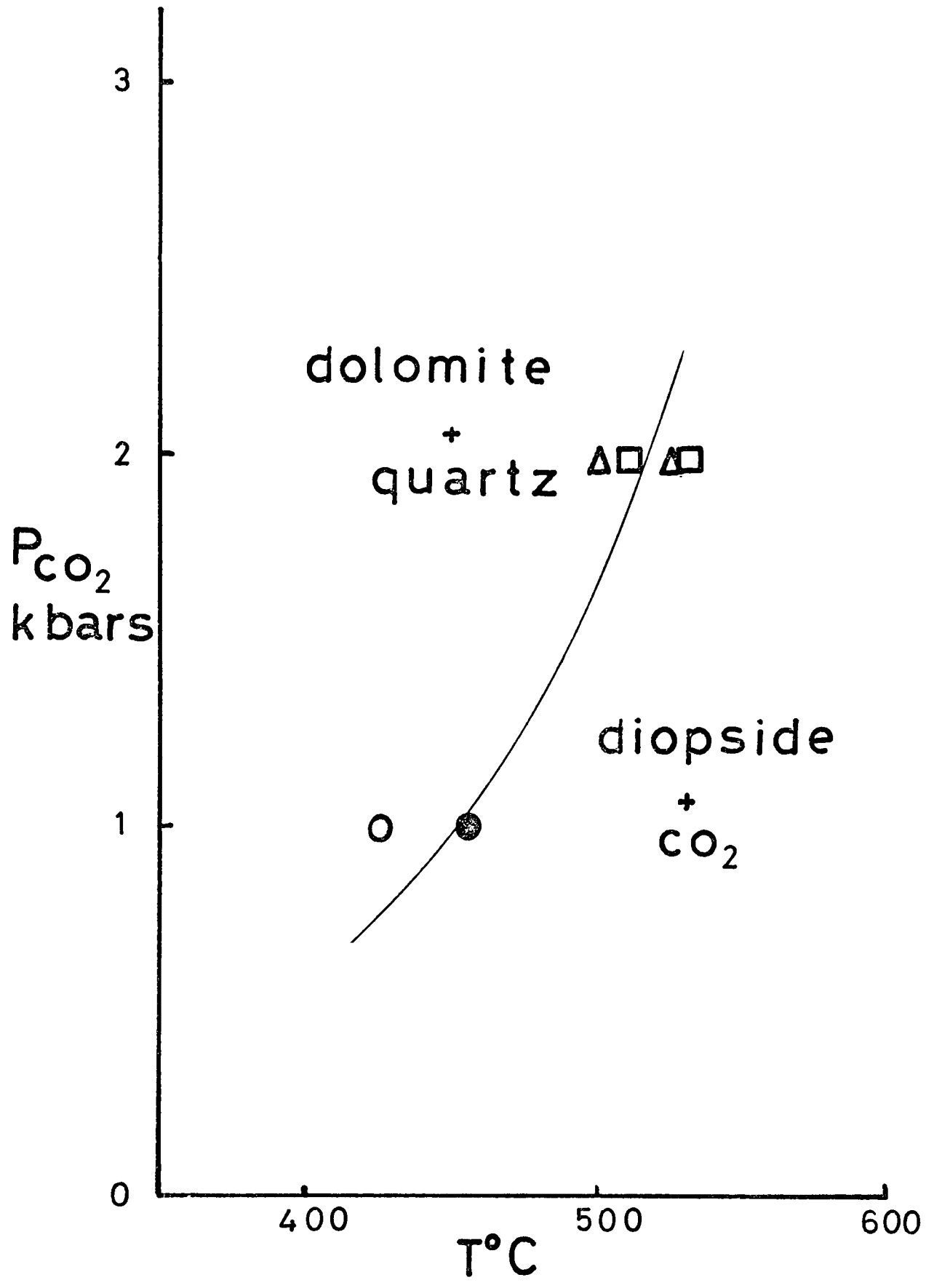


Fig 9 :- DIOPSIDE reaction: calculated curve and experimental brackets.

o ● Slaughter et al. (1973)

□ Skippen (1971)

Δ Metz (1971)

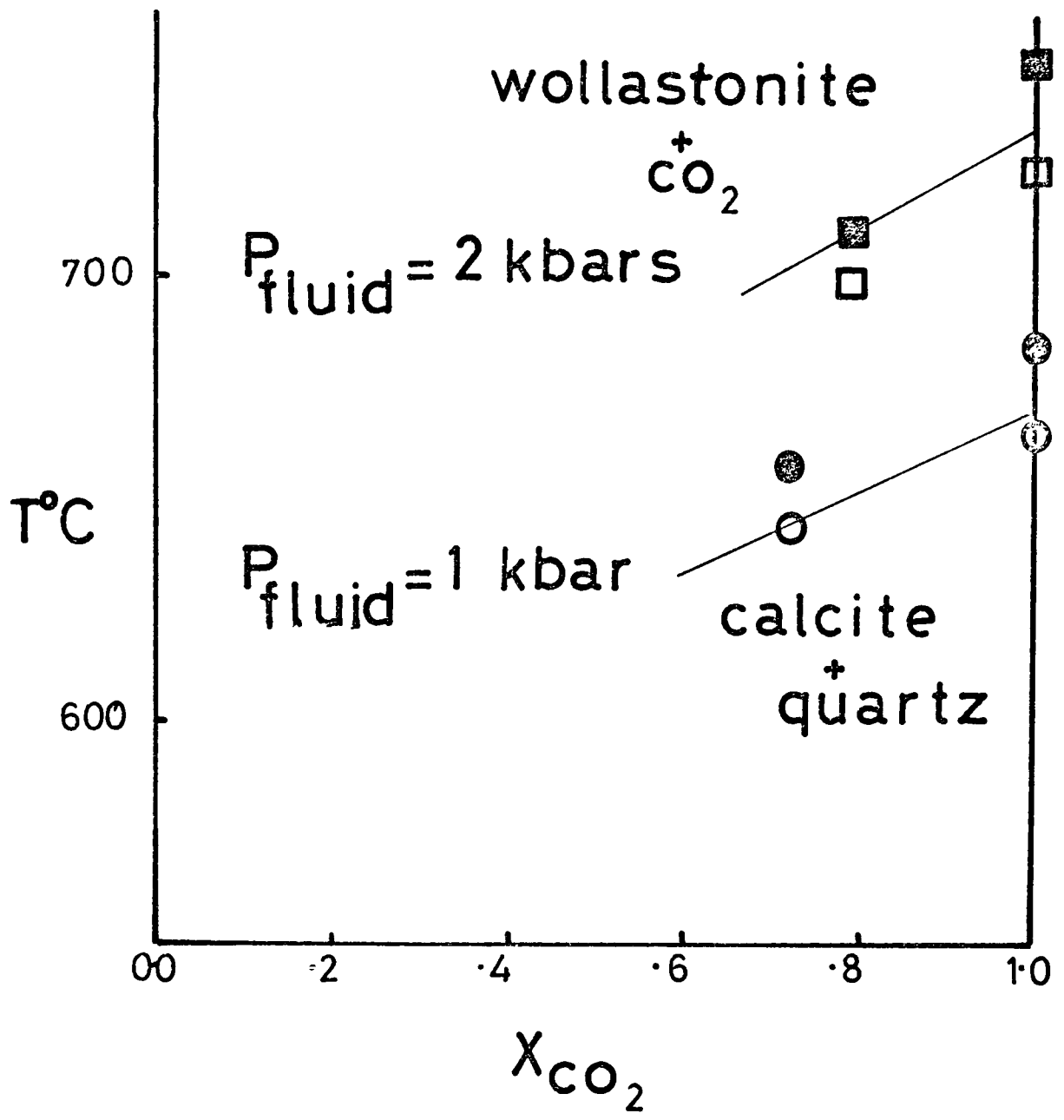


Fig 10 :- WOLLASTONITE reaction: calculated curve and experimental brackets
(Harker and Tuttle (1956))
(Greenwood (1967))

Forsterite

The heat contents and entropies of forsterite in Robie and Waldbaum (1968) are from Kelley (1960) and Kelley and King (1961). The $\Delta_f h$(el, 298.15°K, 1 bar) in Robie and Waldbaum is -520.370 kcals/mole (Torgeson and Sahama 1948).

This value was checked using the reaction

$$4Mg_2SiO_4 + H_2O + 5CO_2 = Mg_3Si_4O_{10}(OH)_2 + 5MgCO_3$$

which was reversed by Greenwood (1967). The runs that bracket this reaction from his Table 4 input to THERMOCALC gave a closely bounded enthalpy correction of +1.70 kcals/mole (with a sensitivity of 0.37 kcals/10°C). The forsterite $\Delta_f h$(el, 298,15°K, 1 bar) becomes -528.670 kcals/mole. Fig. 11 shows the experimental brackets from Greenwood (1967) and the calculated curve.

Orthoenstatite

At metamorphic temperatures and pressures orthoenstatite is the stable form of $MgSiO_3$. All the literature data for $MgSiO_3$ applies to clinoenstatite. The heat contents and entropy of clinoenstatite (Kelley (1960) and Kelley and King (1961)) are unlikely to be much in error if used for orthoenstatite. It has been suggested that the Torgeson and Sahama (1948) measurement of $\Delta_f h$(el, 298.15°K, 1 bar) for clinoenstatite might be corrected by 1 kcal to apply to orthoenstatite (e.g. Skippen (1971), Williams (1971)).

The reaction used to determine the enthalpy of formation of enstatite (orthoenstatite),

$$Mg_2SiO_4 + CO_2 = MgSiO_3 + MgCO_3$$

has been experimentally determined but not reversed at 2 kb by Johannes (1969). However, the unreversed determination of the forsterite-talc-magnesite reaction above is consistent with Greenwood's

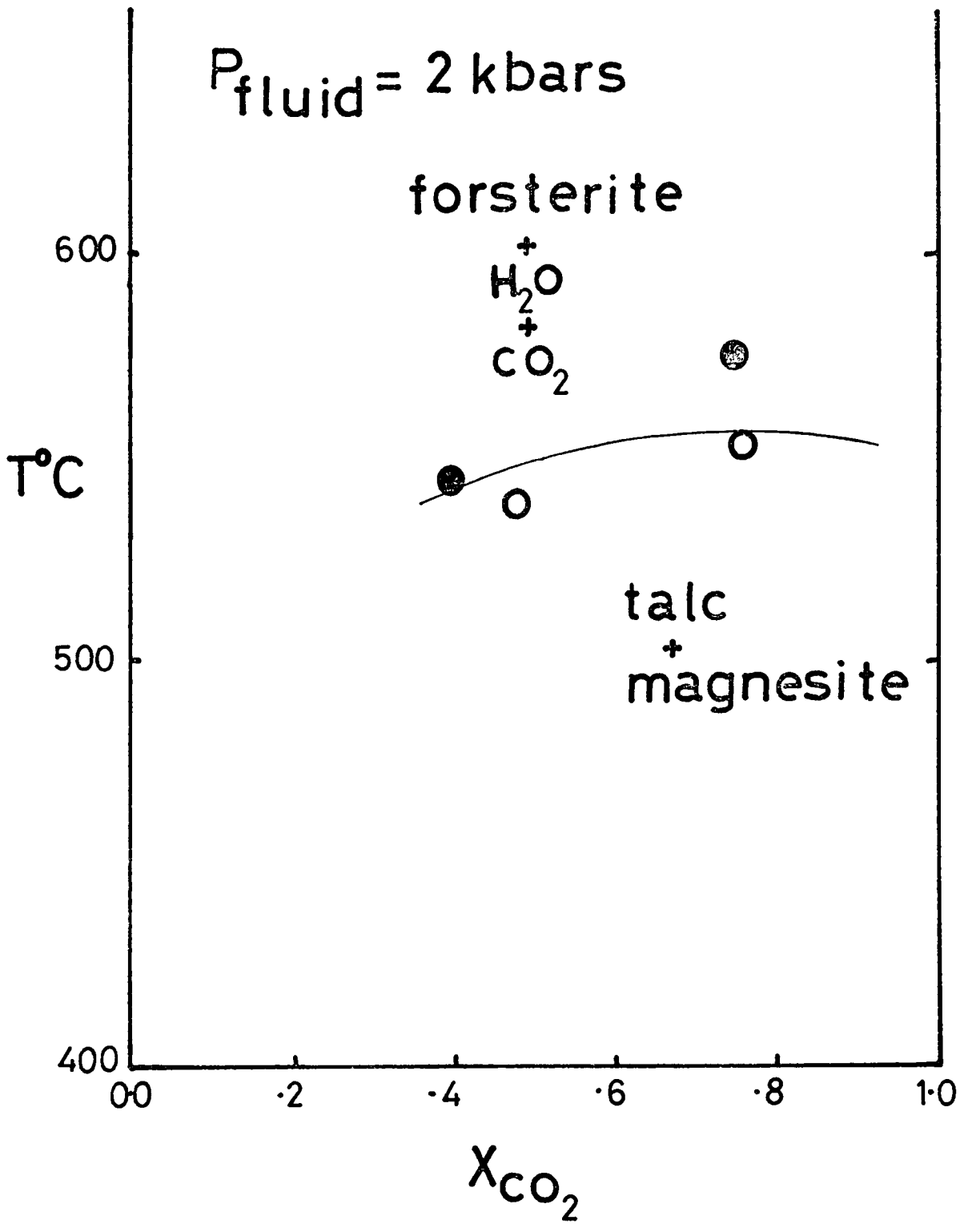


Fig.11:- FORSTERITE reaction : calculated curve and experimental brackets.
(Greenwood (1967))

results although Johannes' temperatures are slightly lower. The upper limit of Johannes' temperature brackets input to THERMOCALC gave an enthalpy correction of +0.2 kcals (with a sensitivity of 0.26 kcals/10°C). The enstatite $\Delta_f h$(el, 298.15°K, 1 bar) becomes -370.03 kcals/mole.

Sphene

The heat content and entropy data in Robie and Waldbaum is from Kelley (1960) and Kelley and King (1961). The enthalpy of formation is from Todd and Kelly (1956). Schuiling and Vink (1967) determined the reaction

$$TiO_2 + CaCO_3 + SiO_2 \rightleftharpoons \underline{CaTiSiO_5}$$

where TiO_2 is the anatase polymorph. The enthalpy difference between the calorimetrically determined enthalpy of formation of rutile (Mah 1957) and the calculated enthalpy of formation of anatase (Robie and Waldbaum, from Osborn (1953)) is 0.1 kcals. However, Navrotsky and Kleppa (1967) calorimetrically determined the heat of reaction of anatase to rutile as -1.24 kcals at 298,15°K and 1 bar. The rutile determination is presumed correct and a value of $\Delta_f h$(el, 298.15°K, 1 bar) anatase = -227.400 kcals/mole is used to calculate the sphene enthalpy correction.

Schuiling and Vink's results from their Table 2 input to THERMOCALC gave an enthalpy correction of +1.18 kcals (with a sensitivity of 0.13 kcals/10°C). $\Delta_f h$(el, 298.15°K, 1 bar) becomes -618.16 kcals/mole. The calculated curve and the experimental results are compared in Fig. 12

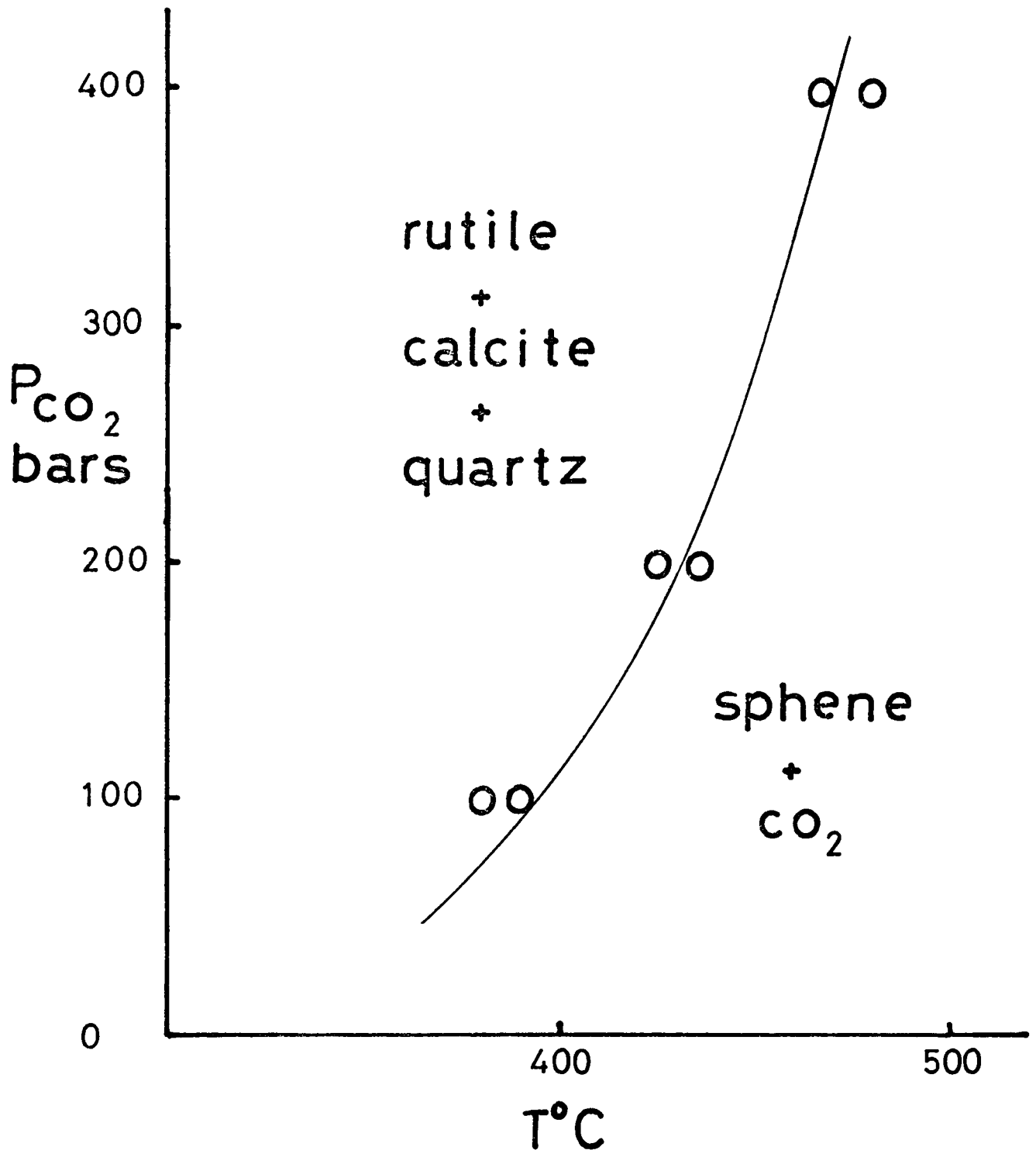


Fig12:-SPHENE reaction:
calculated curve and experimental brackets.
(Schuiling and Vink (1967))

Tremolite

The high temperature heat contents and entropies in Robie and Waldbaum were estimated from low temperature heat capacity measurements. The $\Delta_f h$ (el, 298.15°K, 1bar) is the calorimetric determination by Weeks (1956). Robie and Waldbaum quote an uncertainty of ± 4.14 kcals, on this value; this would give an uncertainty of ± 80°C on the talc-quartz-calcite-tremolite reaction! This reaction

$$5\ Mg_3Si_4O_{10}(OH)_4 + 6\ CaCO_3 + 4SiO_2$$

$$= 3\ \underline{Ca_2Mg_5Si_8O_{22}(OH)_2} + 6CO_2 + 2H_2O$$

has been reversed by Slaughter et al (1973) and calculated by Skippen (1971) for 2 kbars and X_{CO_2} = 0.5 at 440 ± 10°C and 460°4 respectively. The reaction is unsuitable for calculating an enthalpy correction because of the high sensitivity (0.56 kcals / 10°C) and there being only one bracket.

The reaction

$$\underline{Ca_2Mg_5Si_8O_{22}(OH)_2} = 2\ CaMgSi_2O_6 + 3MgSiO_3 + SiO_2 + H_2O$$

has been reversed by Boyd (1959) and Skippen (1971). Skippen provides only one very wide bracket. Boyds results from his Fig 3 (no table of results being given) input to THERMOCALC gave an enthalpy correction of 6.36 kcals / mole (with a sensitivity of 0.17 kcals / 10°C). Fugacity coefficients for diopside and enstatite calculated from the Boyd (1964) solvus by the AQC program were used in this calculation. This enthalpy correction gives a temperature of 455°C for the talc-quartz-calcite-tremolite reaction above.

The $\Delta_f h$ (el, 298.15°K, 1bar) becomes -2946.575 kcals/mole. (1972) Zen calculates a value 4 kcals more negative; however he uses enthalpies of formation of enstatite and diopside as given in Robie and Waldbaum (1968) which need revision as shown above. The calculated curve for the tremolite-enstatite-diopside-quartz reaction compared with Boyd's experiments in Fig 13.

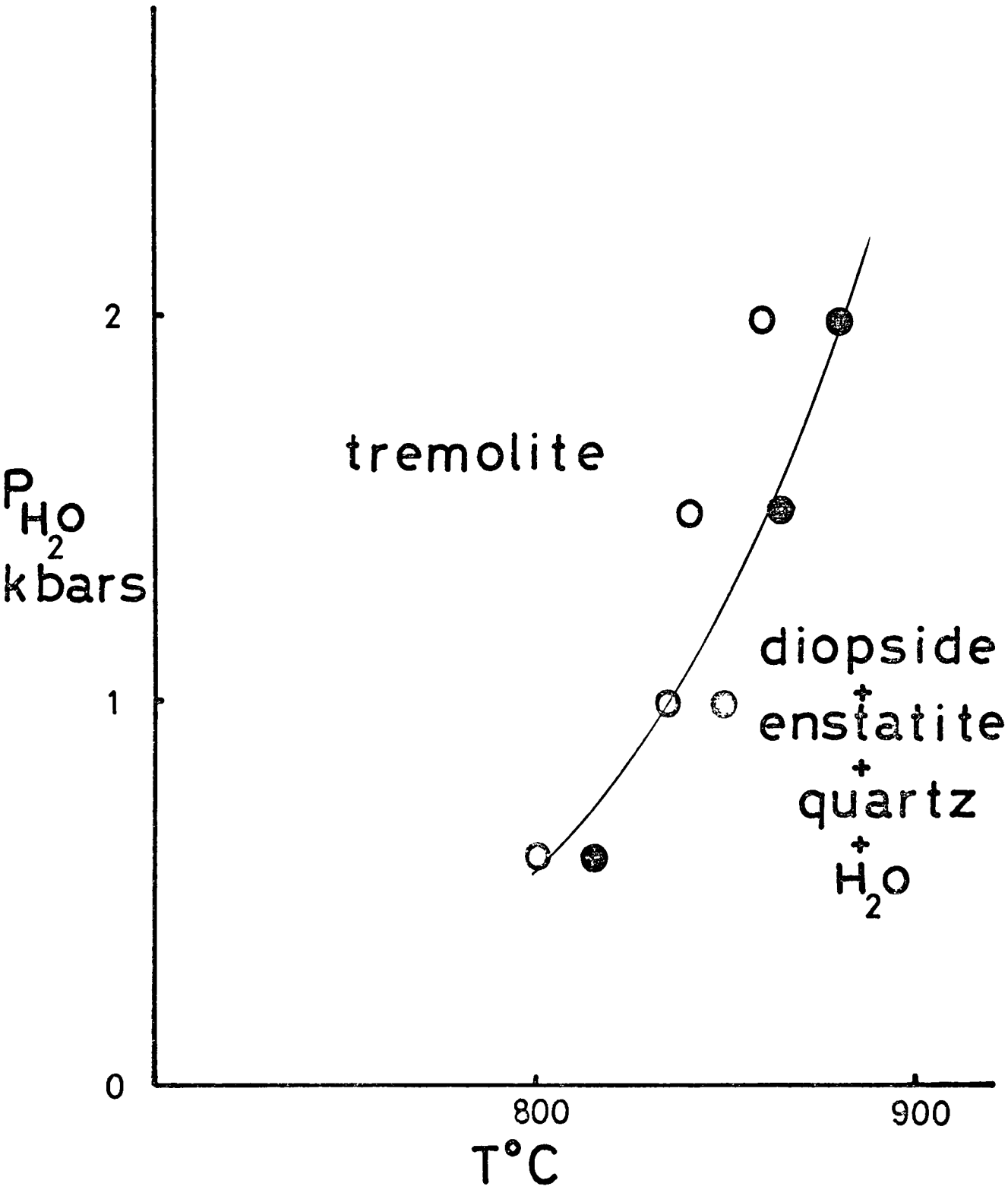


Fig.13:- TREMOLITE reaction: calculated curve and experimental brackets.
(Boyd (1959))

Minerals that contain aluminium

Zen (1969) first pointed out fundamental inconsistences in the thermodynamic data for minerals that contain aluminium. He found a 7 kcal difference in the Gibbs energy of pyrophyllite calculated from the kaolinite-quartz-pyrophyllite reaction and the pyrophyllite-andalusite-quartz reaction. This however assumed that the existing data for kaolinite as well as for andalusite and quartz is correct. The kaolinite data used by Zen comes from the calorimetric measurements of Barany and Kelley (1961).

Zen (1972) showed that the Gibbs energy of formation of muscovite calculated from the muscovite-sanidine-corundum reaction and the muscovite-sanidine-sillimanite-quartz reaction are consistent but are 10 kcals more negative than the calorimetric measurements of Barany (1964) and the solubility measurements of Reesman and Keller (1968). Zen considered that this might be evidence for a 3.5 kcal/mole Al error in the accepted Gibbs energies for corundum and the aluminium silicates. However the determinations of the enthalpy of formation of corundum (see Stull et al. 1972) agree closely and must be more reliable than the calculations from solubility and calorimetric measurements dependent on the Gibbs energies of formation of dissolved species.

Parks (1972) reviews the status of published Gibbs energies of formation of aluminium species in solution and shows that the values are not well known. Zen (1973, pers. comm.) gives two new calorimetric determinations relevant to this problem. The first is an unpublished U.S. Air Force contract report (Gross et al. 1970) on the Gibbs energy of formation of gibbsite tied to metallic Al. The value is consistent with the corundum number but not the $AlCl_3.6H_2O$ number (the important dissolved Al species in calorimetric measurements), indicating a 3 kcal discrepancy in the Gibbs energy of the latter. The second is a

personal communication from Robie to Zen that the Barany Gibbs energy of gibbsite is 3.5 kcals too positive. This means that for minerals containing aluminium the Gibbs energies of formation from measurements tied to $AlCl_3.6H_2O$ rather than corundum will be too positive by 3.0 to 3.5 kcals/mole Al.

For complex hydrated silicates like muscovite and kaolinite, solubility and calorimetric measurements are unlikely to be reliable because of departures from end member compositions and because of the number of dissolved species for which data are required. It is the data for these minerals which can be calculated from experimentally reversed reactions. The main problem arises with data which cannot be checked in this way, particularly the data for the feldspars.

I have applied the arbitrary mean of the above corrections, -3.25 kcals/mole Al to the enthalpies of formation of the phases which were determined by methods tied to the Gibbs energy of $AlCl_3.6H_2O$. The phases with their corrected $\Delta_f h$(el, 298.15°K, 1 bar) are given below.

high albite	$NaAlSi_3O_8$	- 940.396 kcals/mole
anorthite	$CaAl_2Si_2O_8$	-1009.300 kcal/mole
sanicline	$KAlSi_3O_8$	-947.625 kcal/mole

The literature data for the aluminium silicates, andalusite, sillimanite, and kyanite are also used in the following calculations. The enthalpies of formation in Robie and Waldbaum are from Holm and Kleppa (1966). Anderson and Kleppa (1969) have redetermined the sillimanite-kyanite boundary using a more refined experimental method than Holm and Kleppa and the enthalpy of reaction is 0.35 kcals more positive. I have adopted the Holm and Kleppa kyanite enthalpy of formation and corrected the sillimanite and andalusite enthalpies by +0.35 kcals; the $\Delta_f h$(el, 298.15°K, 1 bar) become

sillimanite	-618.300 kcals/mole
andalusite	-619.040 kcals/mole
kyanite	-619.930 kcals/mole

Attempts to calculate the differences between these values from the aluminium silicate phase diagram of Richardson et al. (1969) showed that one of the enthalpies would have to be altered by 0.63 kcals (with a sensitivity of 0.095 kcals/10°C) relative to the others for the three boundaries to pass through their triple point. This correction would imply a 30% error in the Anderson and Kleppa measurement. The three values given above are used in the calculations.

Muscovite

The heat contents and entropies of muscovite in Robie and Waldbaum are from Pankratz (1964) and Weller and King (1963). The $\Delta_f h$(el, 298.15°K, 1 bar) in Robie and Waldbaum is from Barany (1964) and Reesman and Keller (1965) as mentioned earlier. This value should be corrected by -9.75 kcals to correspond to the new determination of $AlCl_3.6H_2O$.

Huang and Keller (1972) determine the Gibbs energy of formation of a non-endmember muscovite by solubility measurements. They calculate the concentration of the species in the solution, rather than assume which species are present. They obtain $\Delta_f g$(el, 298.15°K, 1 bar) = -1399.9 kcals/mole compared with -1330.1 kcals/mole from Robie and Waldbaum; the mole fraction of $KAl_3Si_3O_{10}(OH)_2$ in their muscovite is about 0.84. This enormous difference reflects the importance of the composition of the phase to be dissolved, and highlights the uncertainties in the results of other solubility measurements.

Zen (1972) calculates the muscovite $\Delta_f g$(el, 298.15°K, 1 bar) using the reactions

$$\underline{KAl_3Si_3O_{10}(OH)_2} = KAlSi_3O_8 + Al_2O_3 + H_2O$$

and

$$\underline{KAl_3Si_3O_{10}(OH)_2} + SiO_2 = KAlSi_3O_8 + Al_2SiO_5 + H_2O$$

from Velde (1965) and Day (1970) respectively. However Evans (1965), Althaus et al. (1970) and Kerrick (1972) disagree with Day's results

for the muscovite + quartz reaction. Day uses a textural criterion for the reaction direction while Evans and Kerrick use the weight change of single quartz crystals; it is possible that Day's experiments do not reverse the reaction. Velde (1965), used X-ray diffraction of run products to identify the direction of the muscovite decomposition reaction. By analogy with Day's results his temperatures may be too high. Anderson (1970) showed that a straight line could be put through all of Velde's brackets in a ln f_{H_2O} - 1/T plot. Zen (1972) calculated $\Delta_f g$(el, 298.15°K, 1 bar) from points on Anderson's curve but found an unexplained monotonic difference in the values. The obvious explanations are either that Zen used the wrong entropy for muscovite or that Velde's reversal brackets are unacceptable. The necessary entropy correction is more than 10 cals which seems unlikely by the usually good approximation of the oxide sum for entropy. Velde's results were not used to calculate muscovite data.

At 2 kbars Evans reported 600±10°C and Althaus et al. reported 622°C for the muscovite quartz reaction. A temperature of 610°C is chosen for the 2 kbar point, 30° lower than Day's result at this temperature. The corresponding enthalpy correction beyond the $AlCl_3.6H_2O$ correction is -1.80 kcals. $\Delta_f h$(el, 298.15°K, 1 bar) for muscovite becomes -1432.73 kcals/mole.

The experimental results and the calculated curve are shown in Fig. 14.

Clinochlore

The only literature data for the low Al pure Mg endmember chlorite is a $\Delta_f g$(el, 298.15°K, 1 bar) value of -1954.8 kcals/mole from the solubility measurements of Mackensie and Garrels (1965). Zen (1972) has calculated a third law entropy and an enthalpy of formation from the results of Fawcett and Yoder (1966) on the reaction

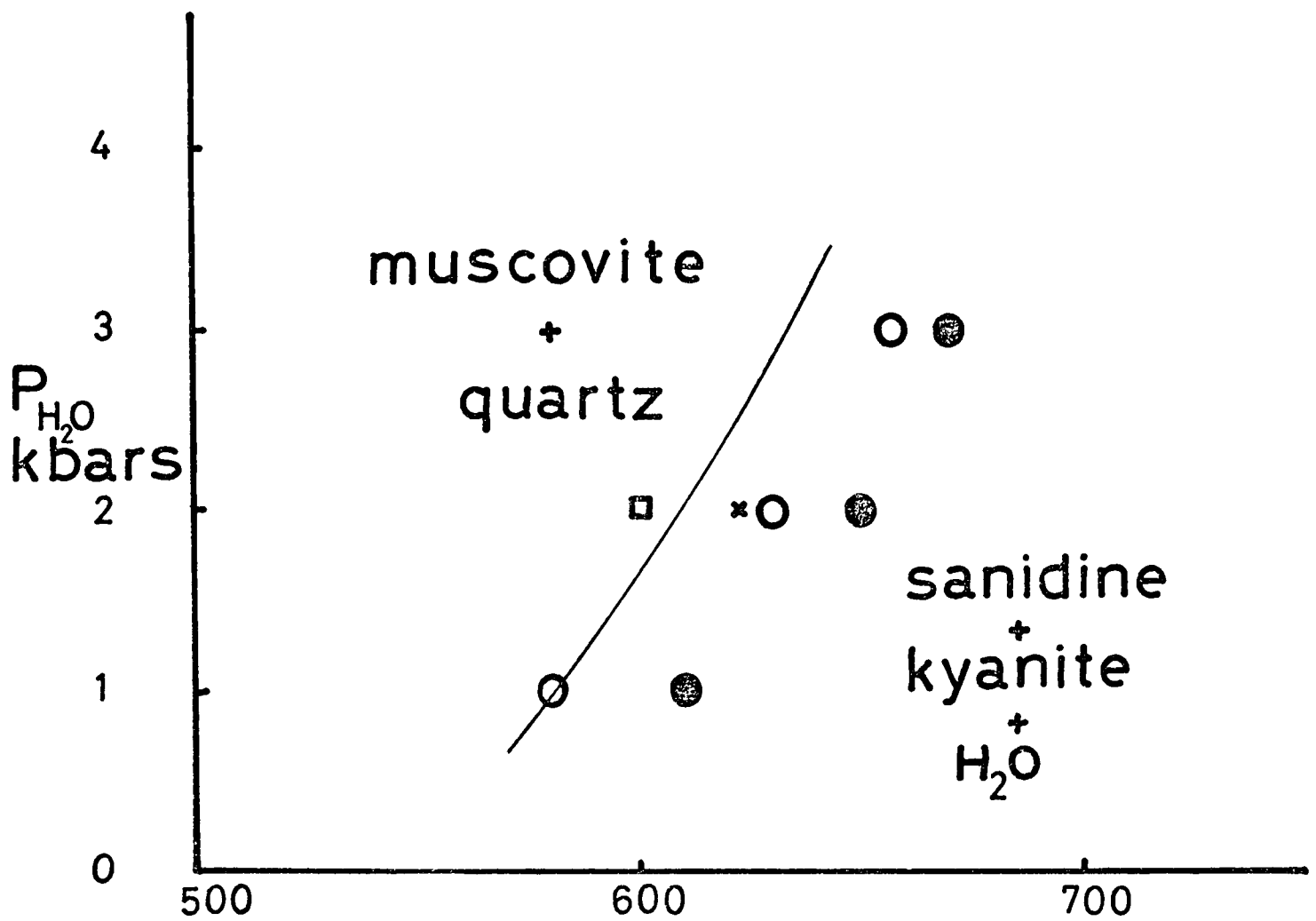


Fig 14:- MUSCOVITE reaction: calculated curve and experimental brackets

o ● questionable reversals of Day (1973)

▫ Evans (1965)

× Althaus et al. (1970)

$$\underline{Mg_5Al_2Si_3O_{10}(OH)_8} = Mg_2SiO_4 + 2MgSiO_3 + MgAl_2O_4 + 4H_2O$$

Apart from using the literature values of forsterite and enstatite, Zen has not taken into account that at the temperatures and pressures of the reaction, the enstatite and clinochlore are more aluminous than written in the equation above. Newton (1972) shows that at 830°C enstatite in equilibrium with sillimanite has 12 mole % Al_2O_3 in solution; this corresponds to a mole fraction of enstatite of 0.88. According to Fawcett and Yoder the chlorites ranged in composition from $Mg_{4.5}Al_{3.5}Si_{2.5}O_{10}(OH)_8$ to $Mg_{3.5}Al_{4.5}Si_{1.5}O_{10}(OH)_2$, the corresponding mole fractions of clinochlore in these chlorites ranging from 0.9 to 0.80.

This reaction was used here. The entropy and heat contents were calculated by the method described earlier. The entropy is in excellent agreement with Zen's value. In the calculations the activity of $MgSiO_3$ in the enstatite and the activity of $Mg_5Al_2Si_3O_{10}(OH)_8$ in the chlorite were calculated using (126). Zen uses only the 10 kbar bracket because the 6 kbar bracket in their Fig. 2 does not correspond with the data given in their Table 2. Zen has to use the upper temperature limit of the 10 kbar bracket and the lower temperature limit of the 5 kbar bracket to retrieve consistent Gibbs energies.

The enthalpy of formation from the 10 kbars, 5 kbars and 3 kbars reversals are all consistent at -2135.5 kcals/mole (with a sensitivity of 0.65 kcals/10°C). Zen's problems were probably caused by the temperature dependence of the error on his entropy approximation. The value calculated here is 7 kcals more negative than Zen's, and nearly 30 kcals more negative than Mackensie and Garrels (1965).

The experimental results and the calculated curve are compared in Fig.15.

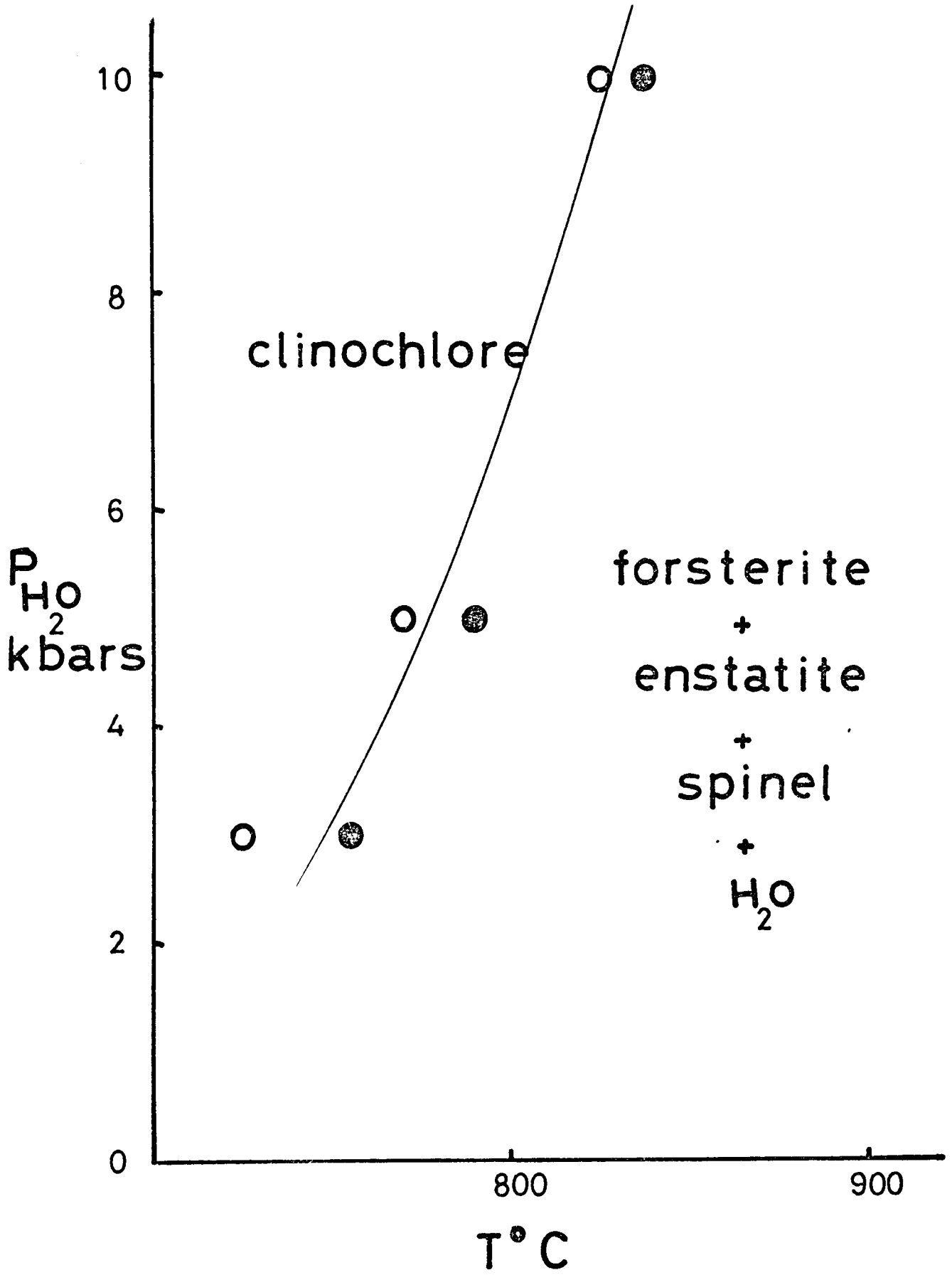


Fig.15:- CLINOCHLORE reaction: calculated curve and experimental brackets.
(Fawcett and Yoder (1966))

Phlogopite

Robie and Waldbaum (1968) give the entropy of phlogopite estimated by Robie[in]. The heat contents and high temperature entropies used here were calculated by the method described earlier.

Bird and Anderson (1973) retrieve the $\Delta_f g$(el, 298,15°K, 1 bar) for phlogopite from the data of Bird and Fawcett (1973) for the reaction

$$3Mg_5Al_2Si_3O_{10}(OH)_2 + 5KAl_3Si_3O_{10}(OH)_2$$

$$\rightleftharpoons \underline{5KMg_3AlSi_3O_{10}(OH)_2} + 8Al_2SiO_5 + SiO_2 + 12H_2O$$

However, apart from using Zen's entropy approximation, they use Zen's calculated Gibbs energy of formation for clinochlore.

The two brackets from Bird and Fawcett (1973) input to THERMOCALC gave an enthalpy of formation of -1495.32 kcals/mole (with a sensitivity of 0.38 kcals/10°C). The experimental brackets and the calculated curve are compared in Fig.14a

Cordierite

Robie and Waldbaum give the heat contents and entropies of cordierite from Weller and Kelley (1963) and Pankratz and Kelley (1964). A considerable problem is the amount of structural water in cordierite (Newton 1973) and it is not stated how much water is contained in Kelley's cordierite samples. The enthalpy of formation of cordierite has not been calorimetrically determined.

Bird and Anderson (1973) have calculated the Gibbs energy of formation of cordierite from the experimental work of Siefert and Schreyer (1970) on the reaction,

$$2Mg_5Al_2Si_3O_{10}(OH)_8 + 8Al_2SiO_5 + 11\ SiO_2 =$$

$$5\ \underline{Mg_2Al_4Si_5O_{18}(OH)_x} + \frac{16-x}{2}\ H_2O$$

Siefert and Schreyer do not analyse the cordierite they used in

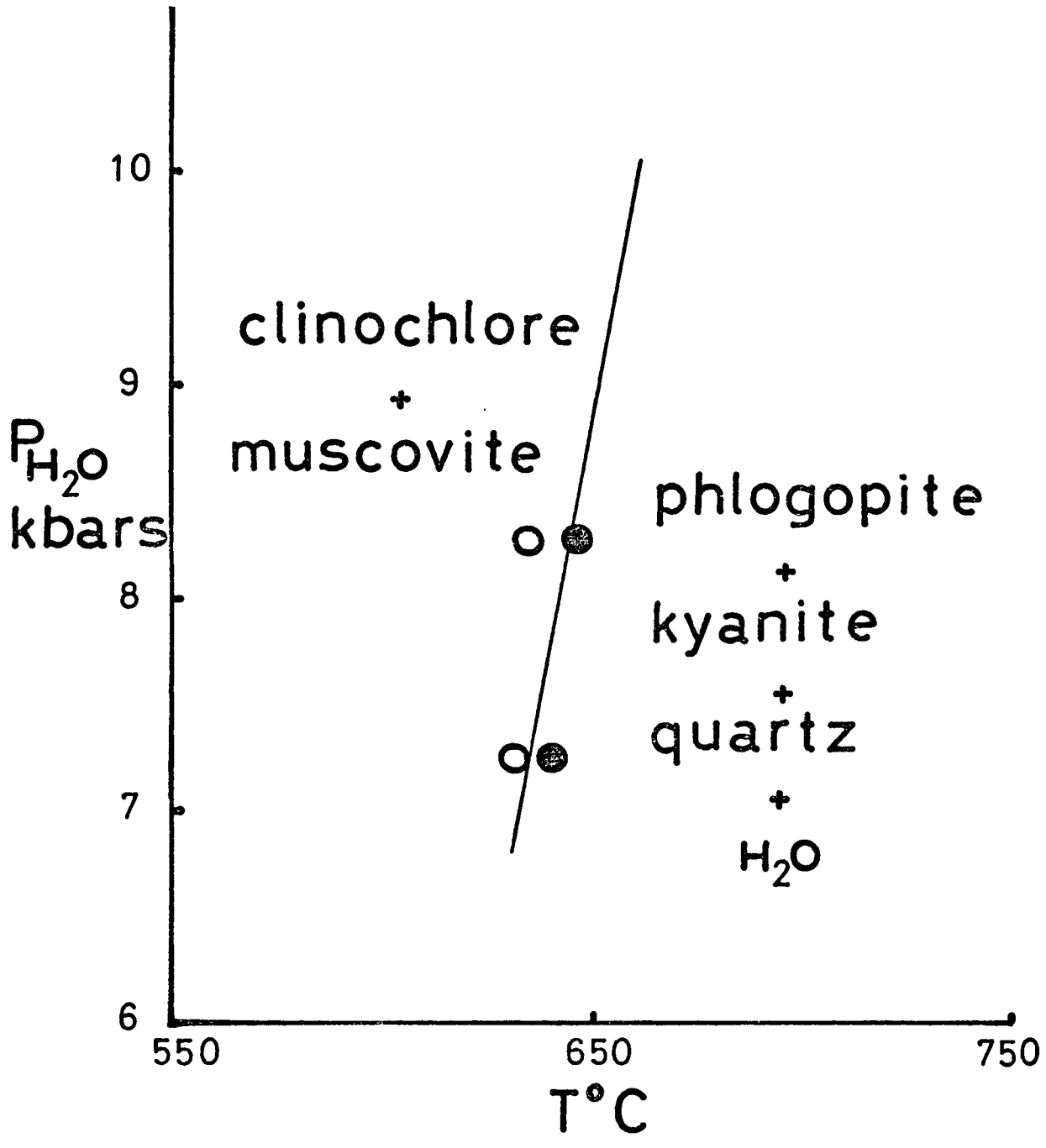


Fig 14A :- PHLOGOPITE reaction: calculated curve and experimental brackets.
(Bird and Fawcett (1973))

their experiments. However, Newton (1972) gives a detailed account of the problem of structural water in cordierites, with particular reference to the cordierites in his experimental reversal of the reaction

$$3\ \underline{Mg_2Al_4Si_5O_{18}(OH)_x} = 2\ Mg_3Si_4O_{10}(OH)_2 + 6\ Al_2SiO_5 + SiO_2 + \left(\frac{4-3x}{2}\right) H_2O$$

Using the experimentally determined slope of this reaction and considering the structural water as zeolitic (Schreyer and Yoder 1964), Newton calculates the water content of the cordierite as 0.75 moles of water, or x = 1.5 in the reaction above on the basis of s (H_2O structural) = 0.85s(H_2O liquid) by analogy with the entropy of analcite and dehydrated analcite (from King and Weller (1961)).

Bird and Anderson assume that x = 1.0 for the purpose of their calculations. It is unfortunate that the enthalpy of formation of cordierite calculated from a reaction is very sensitive to the amount of water in the cordierite. It is less sensitive for reactions involving more water so that Newton's reaction was not used in calculating data for cordierite although his water content is adopted here.

The data for two reactions were input to THERMOCALC to find the enthalpy of formation of cordierite using the entropy of cordierite given in Robie and Waldbaum (1968). Siefert and Schreyer (1970) gives experimental data for the first reaction above where Al_2SiO_5 refers to andalusite and kyanite for the low and high pressure runs respectively. Growth of the lower temperature assemblage seems to be better established than the growth of the upper temperature assemblage. Chernovsky (1973) reports the reversal of the reaction

$$5\ Mg_5Al_2Si_3O_{10}(OH)_8 \rightleftharpoons 10\ Mg_2SiO_4 + 3\ MgAl_2O_4 + \underline{Mg_2Al_4Si_5O_{18}(OH)_x} + \left(\frac{40-x}{2}\right) H_2O$$

for a range of pressures. These two independent reactions give a consistent value for the enthalpy of formation of cordierite as -2224.75 kcals/mole (with a sensitivity of 0.35 kcals/10°C). The calculated curves are compared with the experimental data for these two reactions in Fig. 16. The curves do not fit the ~~curves~~ data over the whole pressure range, the enthalpy was calculated so the fit would be best at the higher pressure of the experiments (5 kbars). The reason for the lack of fit over the pressure range is probably a combination of the inadequacy of the heat contents from Robie and Waldbaum (1968) and the structural water problem.

Annite

Zen (1973) has calculated the entropy and Gibbs energy of formation of annite from the reversed reaction reported by Wones et al. (1972).

$$\underline{K\,Fe_3AlSi_3O_{10}(OH)_2} = K\,AlSi_3O_8 + Fe_3O_4 + H_2$$

Annite synthesised under the most reducing conditions contains 0.3 Fe^{3+} (Hazen and Wones (1972)). Zen calculates data for this annite. Wones' data input to THERMOCALC gave an enthalpy of formation of -1233.9 kcals/mole (with a sensitivity of 0.37 kcals/10°C) for the pure end member annite. The activity of annite was calculated using (126).

Grossularite

The Robie and Waldbaum heat contents and entropies are Waldbaum estimates. The enthalpy of formation in Robie and Waldbaum was apparently calculated by Hays (1967) from his own experimental work in $CaO\text{-}Al_2O_3\text{-}SiO_2\text{-}H_2O$. Boettcher (1970) and Newton (1966) report the reversal of the reaction

$$\underline{Ca_3Al_2Si_3O_{12}} + SiO_2 \rightleftharpoons CaAl_2Si_2O_8 + 2\,CaSiO_3$$

at 3 kbars and Hays (1967) has reversed the reaction at 1200°C on the liquidus. The Boettcher and Newton data input to THERMOCALC gave an

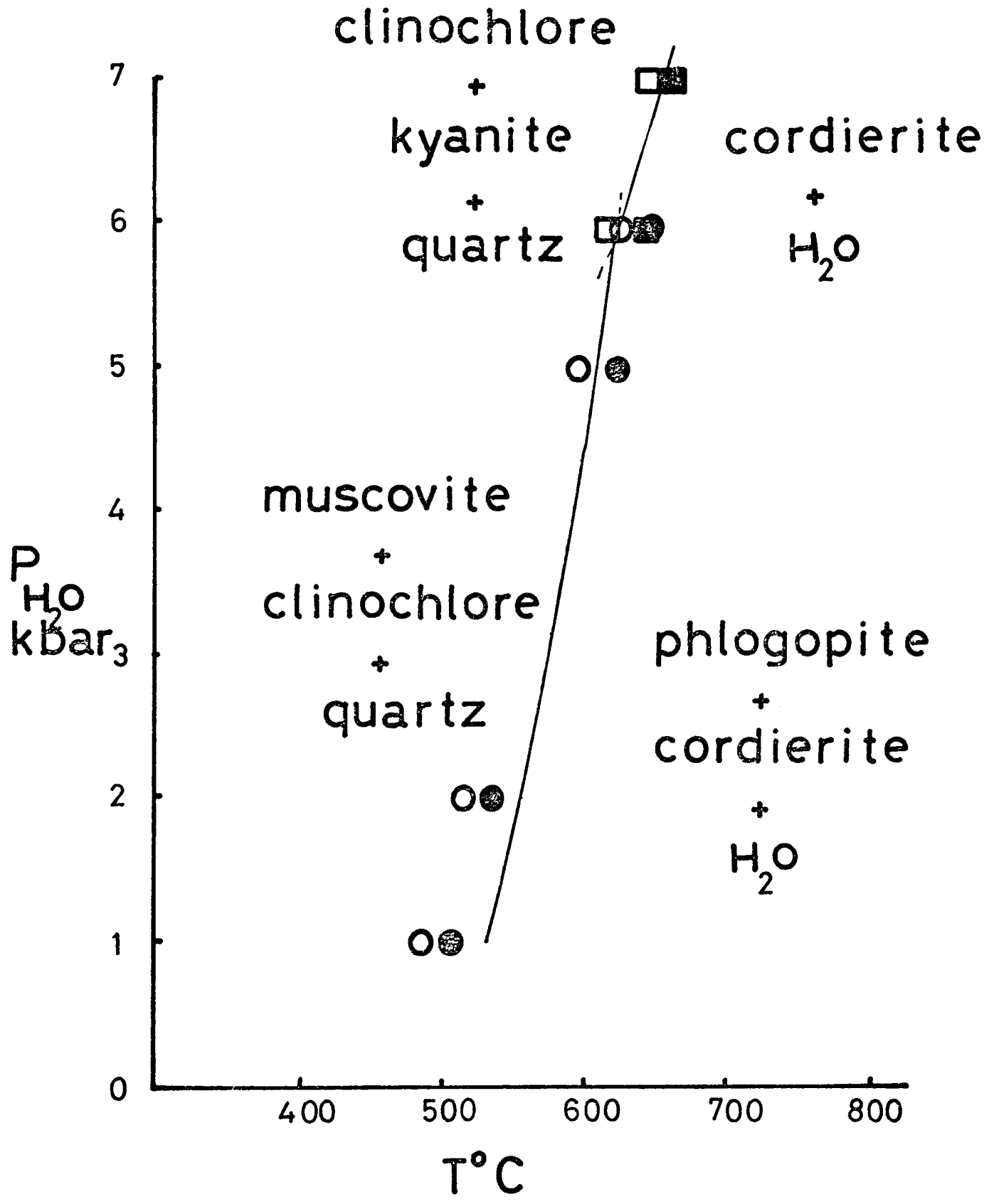


Fig.16 :- CORDIERITE reaction: calculated curve and experimental brackets.
(Siefert and Schreyer (1970))

enthalpy correction of +1.2 kcal/mole (with a sensitivity of 0.21 kcals/10°C). The grossularite $\Delta_f h$(el, 298.15°K, 1 bar) becomes -1587.193 kcals/mole. The experimental brackets and the calculated curve are compared in Fig. 17.

Zoisite and clinozoisite

There is no published calorimetric data for zoisite or clinozoisite. I have calculated the entropy and the heat contents for $Ca_2Al_3Si_3O_{12}(OH)$ by the method described earlier.

Zen (1972) has calculated values for zoisite from Newton's (1966) reversal of the reaction

$$4\ Ca_2Al_3Si_3O_{12}(OH) + SiO_2 = 5\ CaAl_2Si_2O_8 + Ca_3Al_2Si_3O_{12} = 2\ H_2O$$

He calculates the entropy of zoisite from chosen temperatures within each of Newton's brackets. The entropy used here is slightly lower than that adopted by Zen.

Boettcher (1970) also reports the above reaction, his temperature brackets are consistent with Newton's. Boettcher also gives reversal brackets for

$$3\ Ca_2Al_3Si_3O_{12}(OH) = 3\ CaAl_2Si_2O_8 + Al_2O_3 + Ca_3Al_2Si_3O_{12} + 1.5\ H_2O$$

The brackets from these two reactions input to THERMOCALC gave a well-defined $\Delta_f h$(el, 298,15°K, 1 bar) of -1651.65 kcals/mole (with a sensitivity of 0.22 kcals/10°C). The concordance of the calculated values is good evidence for the correction to the anorthite enthalpy of formation given earlier.

The calculated curves and the experimental brackets are compared in Fig. 18.

Clinozoisite is the monoclinic form of $Ca_2Al_3Si_3O_{12}(OH)$. Its molar volume is 136.2 ±.3 compared with 136.5±.3 for zoisite. A small entropy and enthalpy of formation difference between zoisite and clinozoisite would be expected. However, the experimental reversal of the

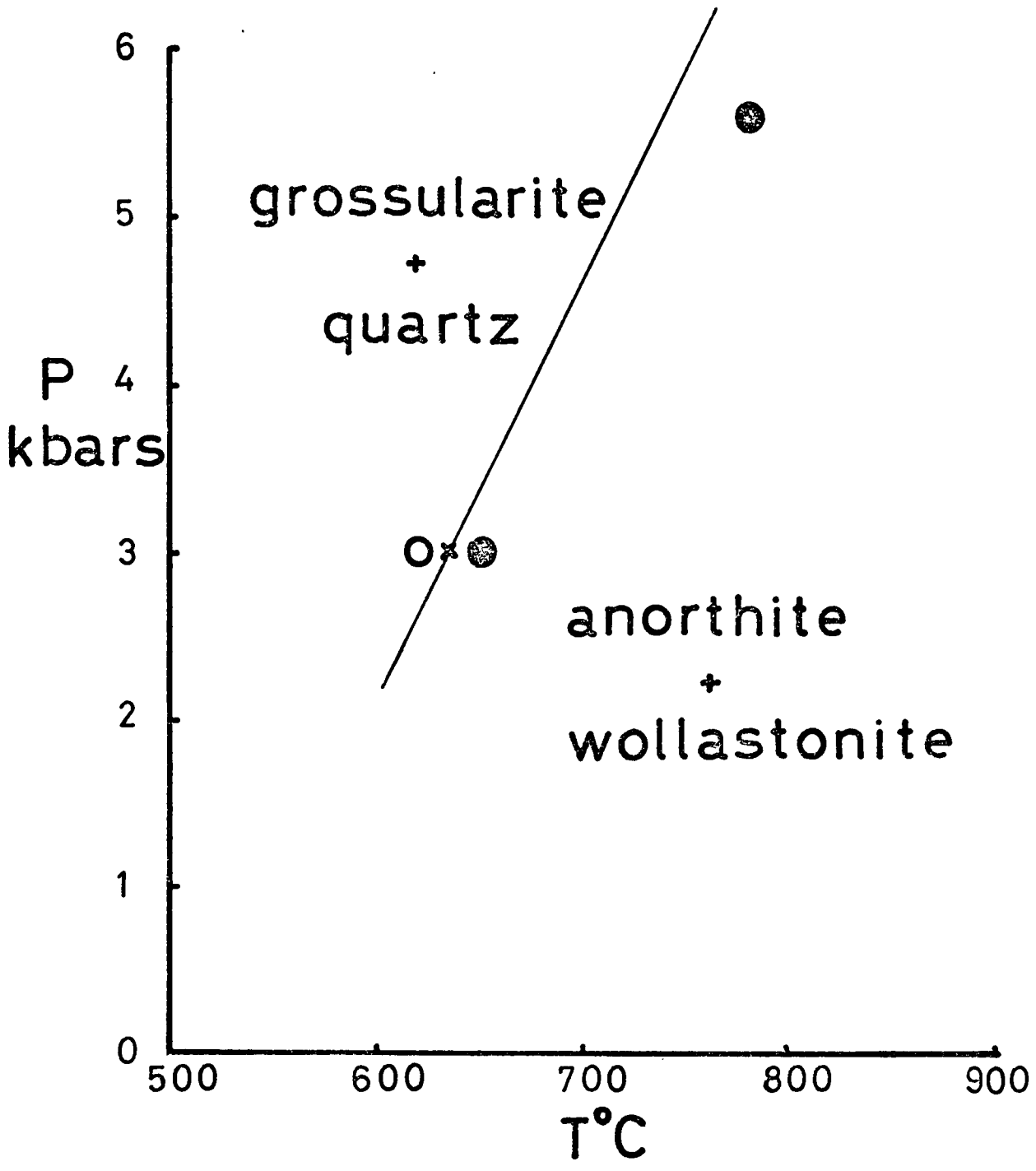


Fig 17 :- GROSSULARITE reaction: calculated curve and experimental brackets.

o ● Boettcher (1970)

× Newton (1966)

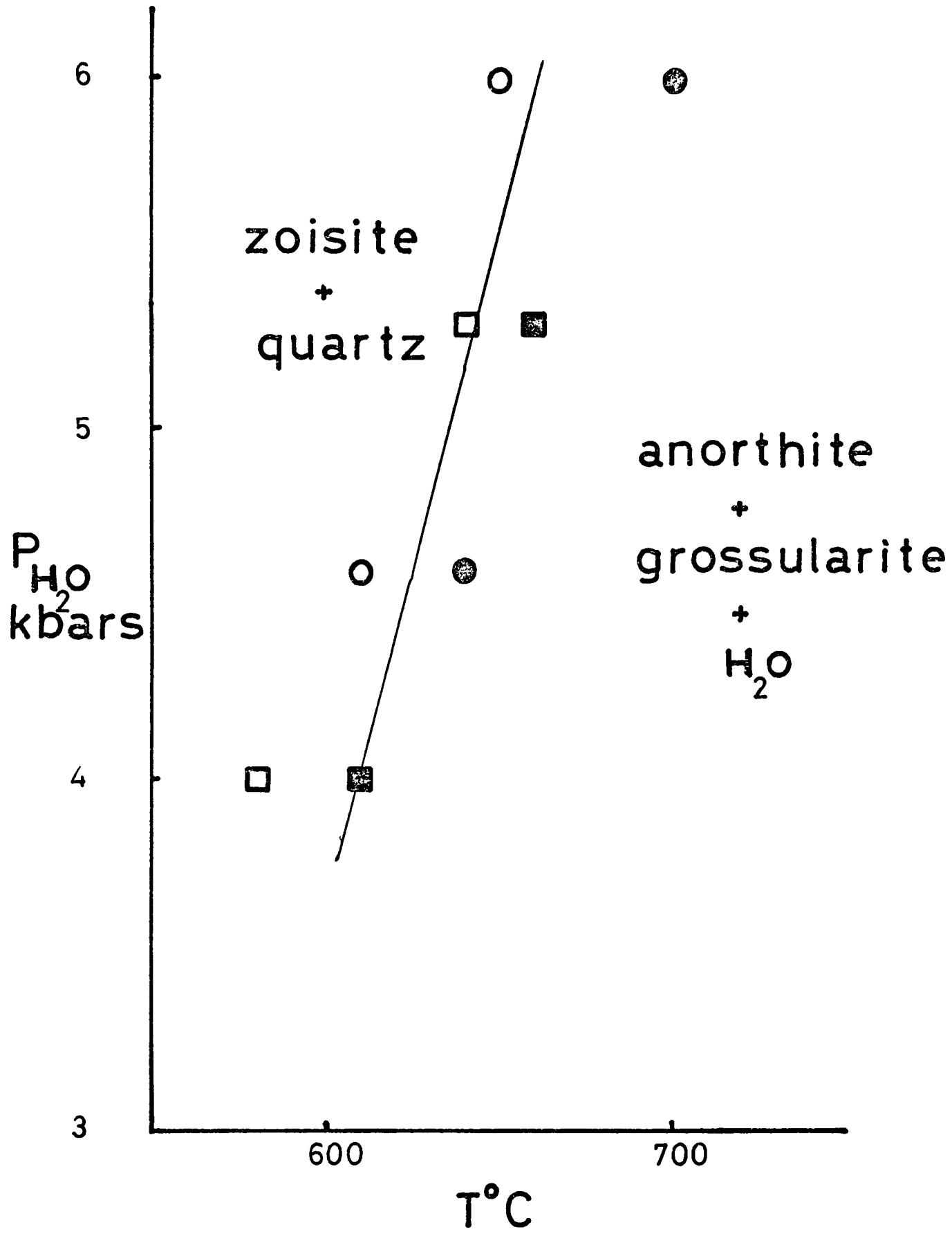


Fig.18:- ZOISITE reaction: calculated curve and experimental brackets.

o ● Newton (1966)

□ ■ Boettcher (1970)

clinozoisite + quartz reaction of Holdaway (1966) shows a rather different dP/dT. This would require an entropy correction of at least 15 cals which necessitates at least a 15 kcals enthalpy correction. In later calculations the zoisite thermodynamic properties are used for clinozoisite.

Iron chlorite

There is no published calorimetric data for the iron analogue of clinochlore, $Fe_5Al_2Si_3O_{10}(OH)_8$, called iron chlorite here. The heat contents and entropies were calculated by the method given earlier, the s(298.15°K, 1 bar) is 141.6 cals/mole.

Hsu (1968) has experimentally reversed the reaction,

$$\frac{2}{3}O_2 + \underline{Fe_5Al_2Si_3O_{10}(OH)_8} = \frac{4}{3}Fe_3O_4 + FeAl_2O_4 + 3\ SiO_2 + 4\ H_2O$$

at a range of pressures, for the NNO buffer. The thermodynamic data for hercynite compiled by Zen (1973) and the activity coefficients for hercynite and magnetite calculated by the QC program are used in this and the following calculation. Hsu's experimental brackets input to THERMOCALC gave an enthalpy of formation,

$\Delta_f h$(el, 298.15°K, 1 bar) of -1732 kcals/mole (with a sensitivity of 1.5 kcals/10°C). The experimental brackets and the calculated curve are compared in Fig. 19.

Almandine

There is no published calorimetric data for almandine. The heat contents and entropy were calculated by the method given earlier, the s(298.15°K, 1 bar) is 68 cals.

Zen (1973) calculates the entropy and enthalpy of formation of almandine using the experimentally reversed reaction (Hsu (1968)).

$$3\ \underline{Fe_3Al_2Si_3O_{12}} + O_2 = 2\ Fe_3O_4 + 3\ FeAl_2O_4 + 9\ SiO_2$$

getting values of 68.3 cals and -1273.56 kcals respectively.

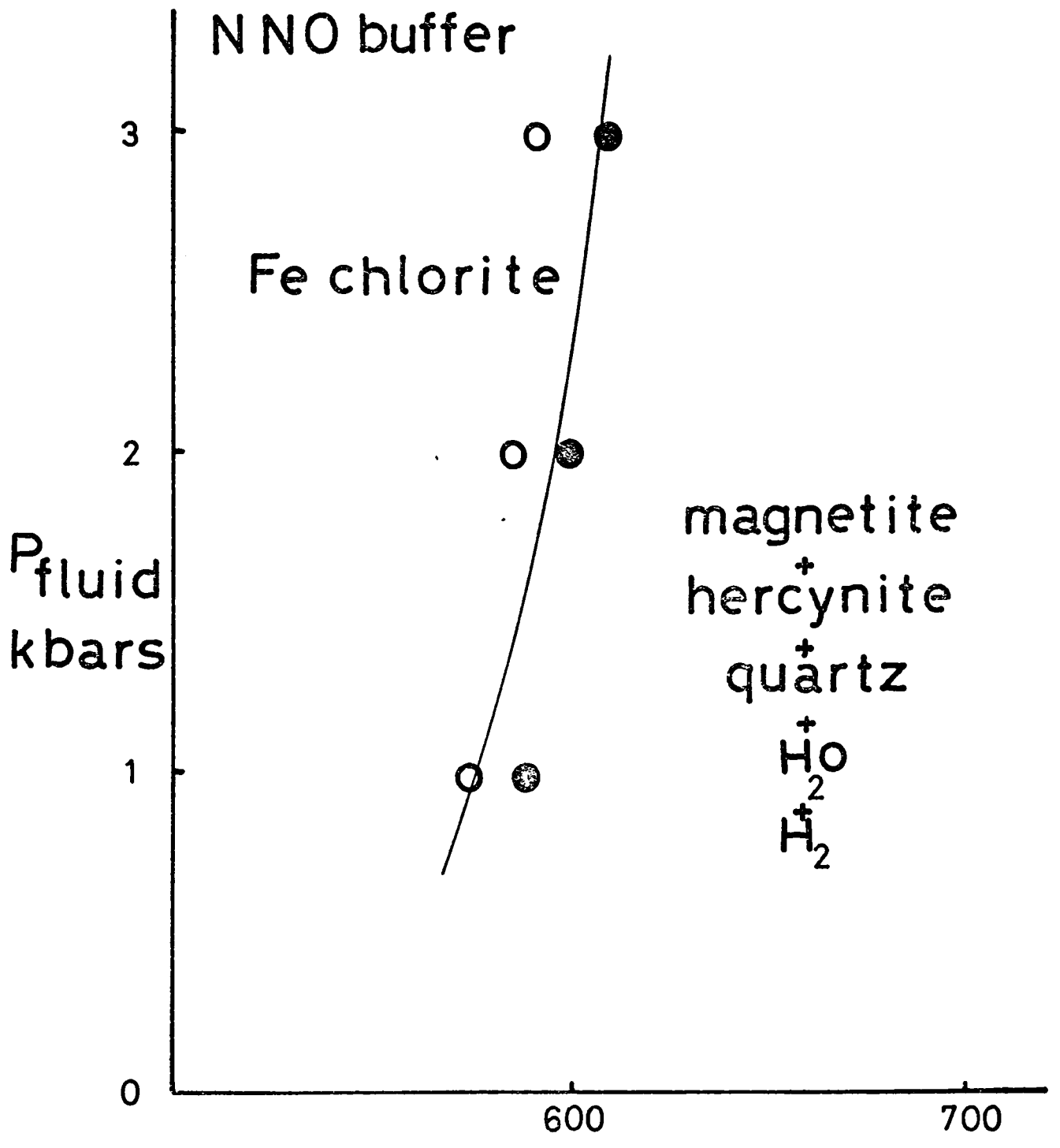


Fig.19:- Fe CHLORITE reaction: calculated curve and experimental brackets.
(Hsu (1968))

This reaction is unsuitable for calculating almandine data because its univariant curve in log f_{O_2} - 1/T is almost parallel to the QFM buffer at which the reaction was determined. A small error in the equation of the buffer curve or the experimental behaviour of the buffer assemblage will cause a large temperature displacement of the reaction, and thus a large displacement of the calculated properties of almandine.

The reaction used here is

$$\frac{1}{3}\,O_2 + Fe_5Al_2Si_3O_{10}(OH)_8 = \underline{Fe_3Al_2Si_3O_{12}} + \frac{2}{3}\,Fe_3O_4 + 4\,H_2O$$

which has been experimentally reversed at the QFM, MI and QFI buffers by Hsu (1968). This reaction crosses the buffer curves at a high angle.

The experimental brackets from Table 4-7 of Hsu input to THERMOCALC gave an enthalpy of formation, $\Delta_f h$(el, 298.15°K, 1 bar) of -1297.5 kcals/mole (with a sensitivity of 0.35 kcals/10°C). The calculated curve and the experimental brackets are compared in Fig. 20.

Iron staurolite

There is no published calorimetric data for Fe-staurolite. There is not even general acceptance of a formula to describe the phase. The formula $Fe_4Al_{18}Si_{7.5}O_{44}(OH)_4$ is adopted (Richardson 1967, but see also Ganguly 1972). The heat contents and entropy were calculated using the method described earlier. The S(298.15°K, 1 bar) is 118.4 cals/mole.

Richardson (1968) has reversed the reaction

$$\underline{6\,Fe_4Al_{18}Si_{7.5}O_{44}(OH)_4} + 25\,SiO_2 = 8\,Fe_3Al_2Si_3O_{12} + 46\,Al_2SiO_5 + 12\,H_2O$$

The experimental brackets for this reaction from his Table 3 input to THERMOCALC gave a $\Delta_f h$(el, 298.15°K, 1 bar) of -5717.5 kcals/mole (with a sensitivity of 2.15 kcals/10°C). The calculated curve and the experimental brackets are compared in Fig. 21.

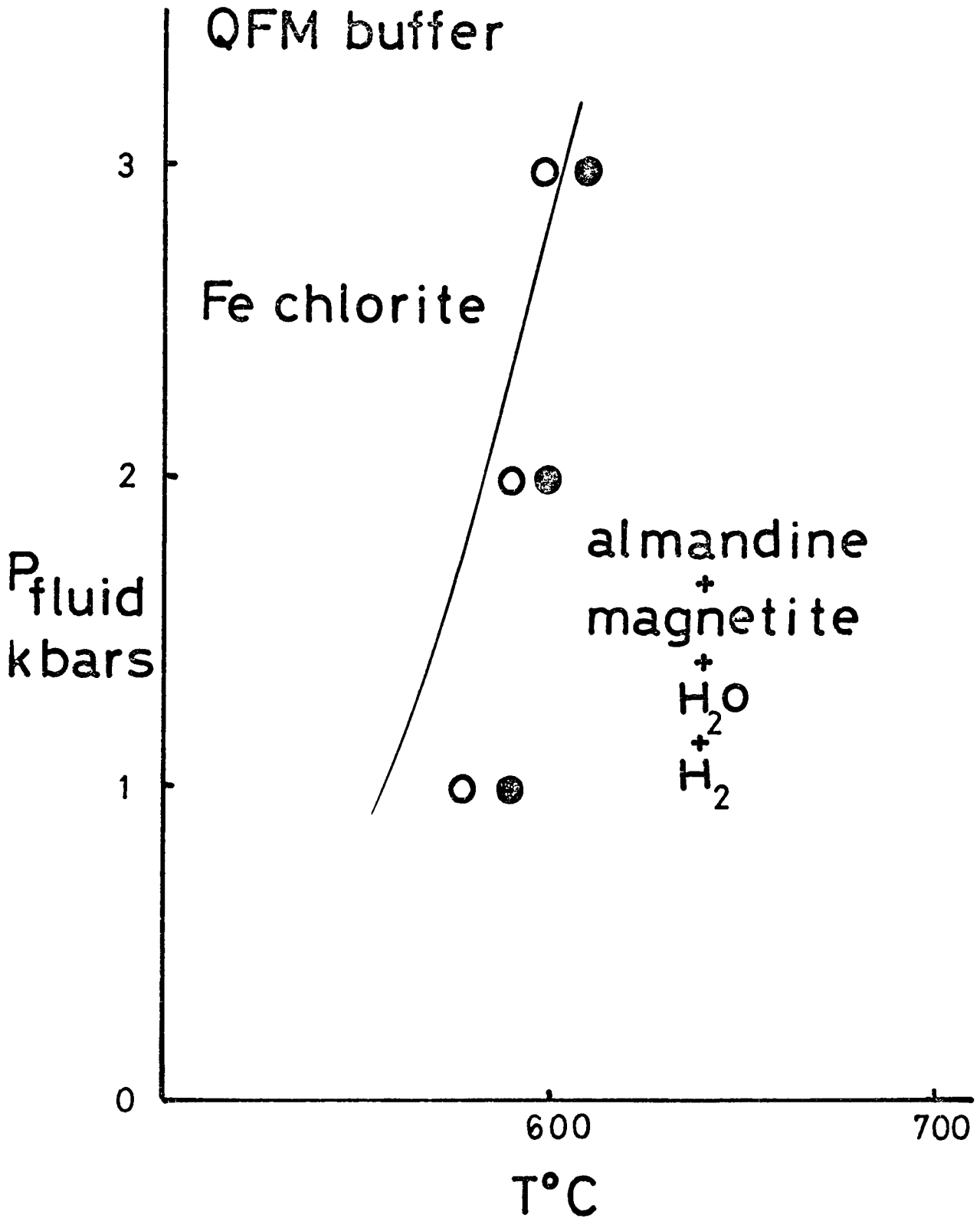


Fig.20 :- ALMANDINE reaction: calculated curve and experimental brackets.
(Hsu (1968))

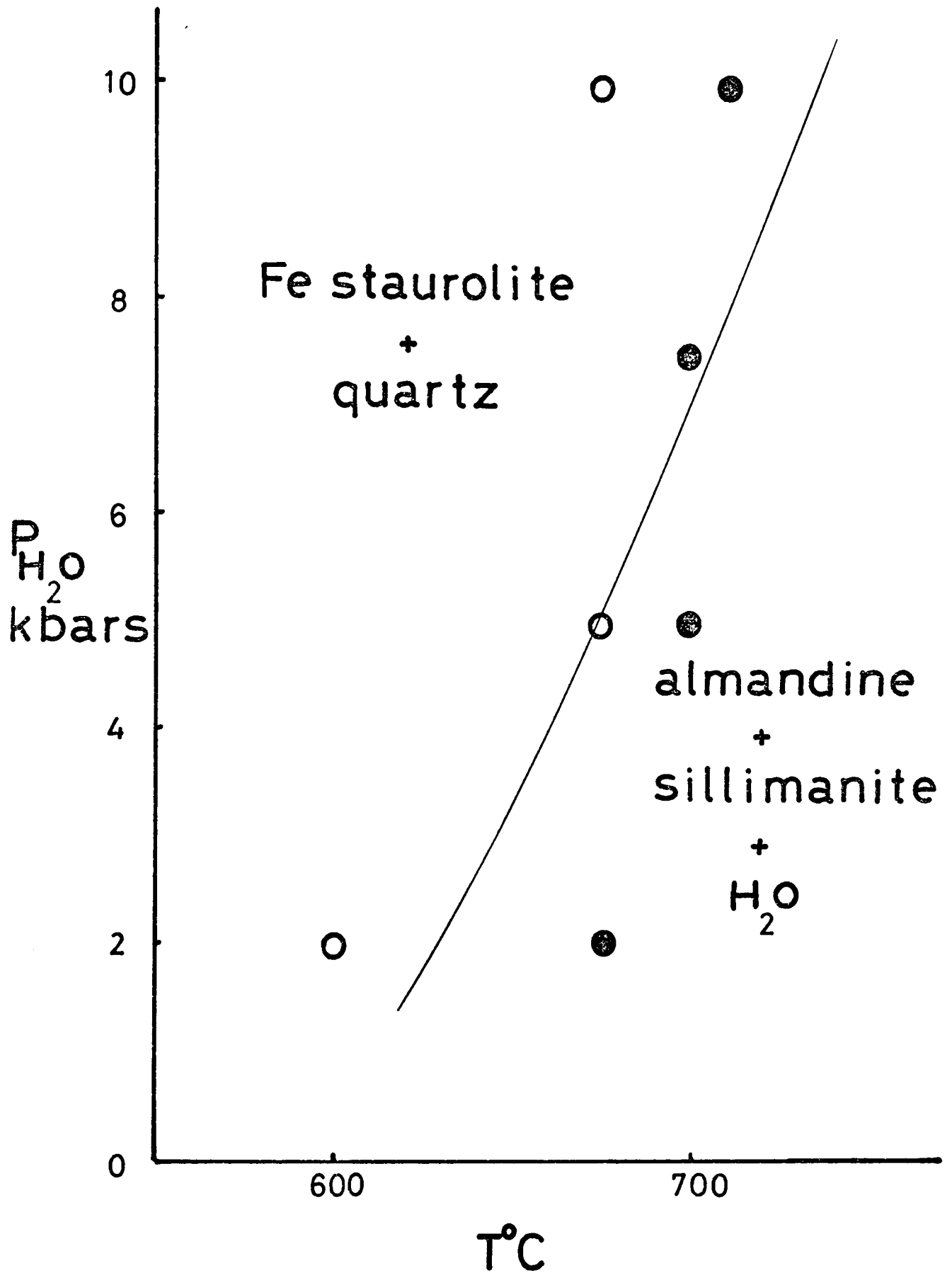


Fig 21:- Fe STAUROLITE reaction: calculated curve and experimental brackets.
(Richardson (1968))

Iron chloritoid

There is no published calorimetric data for $FeAl_2SiO_5(OH)_2$, Fe-chloritoid. The heat contents and entropies were calculated; the S(298.15°K, 1 bar) is 39.10 cals/mole.

Richardson (1968) and Hoschek (1967) have reversed the reaction

$$8\ \underline{FeAl_2SiO_5(OH)_2} + 10\ Al_2SiO_5 \rightleftharpoons 2\ Fe_4Al_{18}Si_{7.5}O_{44}(OH)_4 + 3\ SiO_2 + 4\ H_2O$$

Their results are in good agreement. The experimental brackets input to THERMOCALC gave the enthalpy of formation, $\Delta_f h$(el, 298,15°K, 1 bar) as -748.2 kcals/mole (with a sensitivity of 0.36 kcals/10°C). The calculated curve and the experimental brackets are compared in Fig. 22.

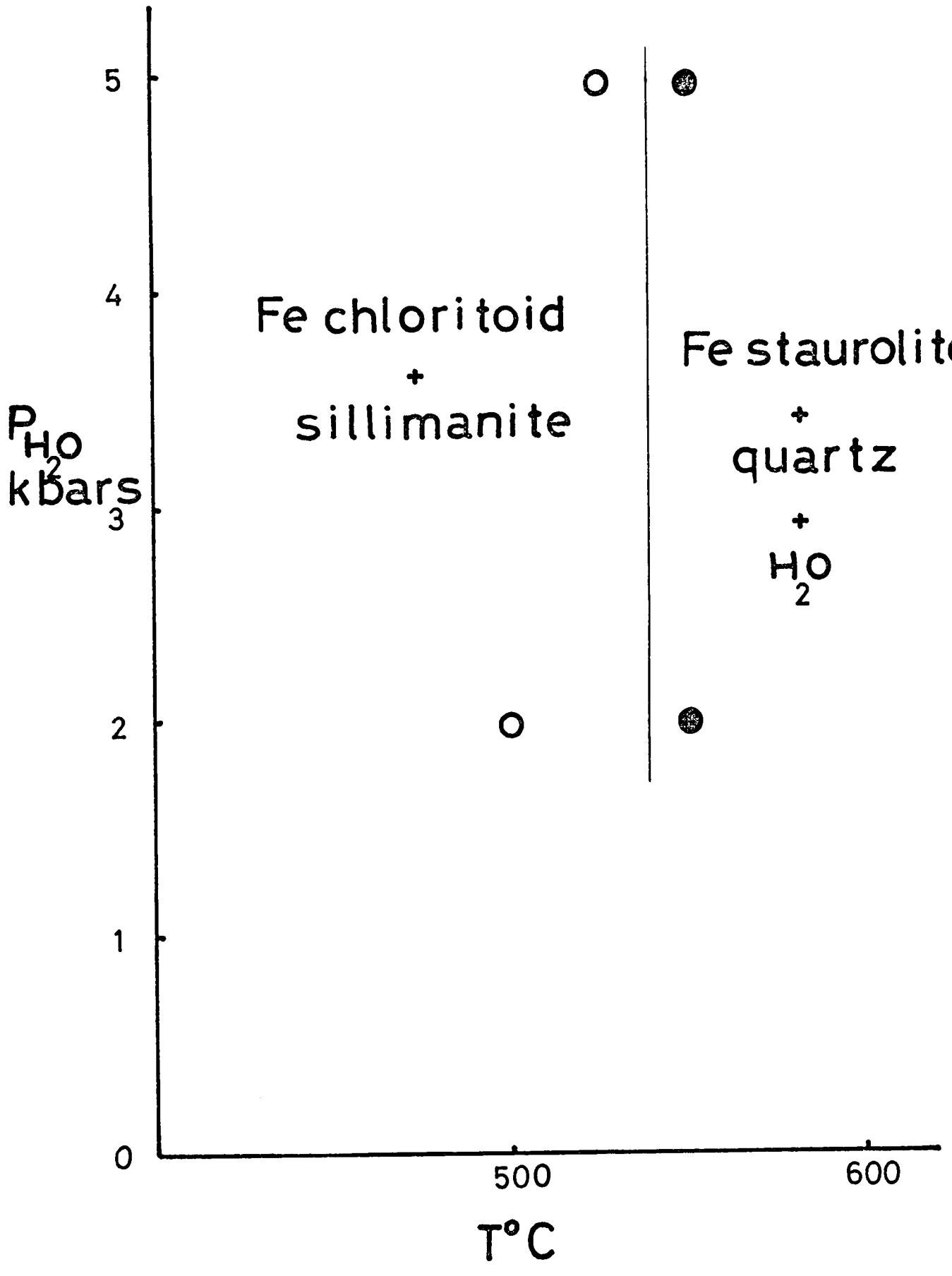


Fig:22:-Fe CHLORITOID reaction: calculated curve and experimental brackets.
(Richardson (1968))

Activity coefficients of solid mixtures

The general theory of activity coefficients has been given in Chapter 2 . In this section the use of the various mixing models in the geological literature will be reviewed, and the models applied to some important systems.

Thompson (1967) introduced mixing models for solid mixtures to the geological literature covering ideal and regular solutions. Within regular solutions he includes symmetric solutions ('regular solutions' of Hildebrand (1927), the R model) and asymmetric solutions ('subregular solutions' of Hardy (1952), the SR model), and extends a suggestive notation for the parameters A, B of (113) used by Carlson and Colburn (1952).

Thompson writes (113) as:-

$$RT \ln \gamma_1 = x_2^2 \{w_{G1} + 2x_1 (w_{G2} - w_{G1})\}$$

$$RT \ln \gamma_2 = x_1^2 \{w_{G2} + 2x_2 (w_{G1} - w_{G2})\}$$

The G subscripts are used because combining this with (122)

$$g^{ex} = x_1 x_2 (w_{G1} x_2 + w_{G2} x_1)$$

From (123)

$$\begin{aligned} v^{ex} &= x_1 x_2 (w_{V1} x_2 + w_{V2} x_1) \\ s^{ex} &= x_1 x_2 (w_{S1} x_2 + w_{S2} x_1) \\ h^{ex} &= x_1 x_2 (w_{H1} x_2 + w_{H2} x_1) \end{aligned} \qquad (154)$$

with $\left(\frac{\partial w_G}{T}\right)_P = w_{S1}$, $\left(\frac{\partial w_{G1}}{P}\right)_T = w_{V1}$, $\frac{\partial w_{G1}}{1/T} = w_{H1}$ and so on, related to equations (123)

If w_{G1} is linear in T then, $w_{S1,2}$ and $w_{H1,2}$ are independent of temperature.

Thompson et al. (1969) and Eugster et al. (1972) apply the SR model to the halite-sylvite and paragonite-muscovite solid mixtures respectively using the experimentally determined solvi. For both of these systems the components are sufficiently similar for the chemical

potential term in (120) to disappear. For each of these binaries of coexisting phases A and B made of components 1 and 2, the equilibrium conditions are

$$RT \ln x_{1A} + x_{2A}^2 (w_{G1} + 2x_{1A}(w_{G2} - w_{G1})) = RT \ln x_{1B} + x_{2B}^2 (w_{G1} + 2 x_{1B}(w_{G2}-w_{G1})$$

$$RT \ln x_{2A} + x_{1A}^2 (w_{G2} + 2x_{2A}(w_{G1} - w_{G2})) = RT \ln x_{2B} + x_{1B}^2 (w_{G2} + 2x_{2B}(w_{G1}-w_{G2}))$$

This is a simultaneous equation in w_{G1} and w_{G2} and can be solved for these two unknowns at each temperature and pressure at which the composition of coexisting phases has been measured. From the pressure-temperature dependence of w_{G1} and w_{G2}, the other mixing parameters, w_{V1}, w_{V2}, w_{S1}, w_{S2}, w_{H1}, w_{H2} can be calculated.

Green (1970) introduced the AQC model to the geological literature in the belief that it described the mixing properties of at least the NaCl-KCl mixtures better than the SR model, based on the limited amount of experimental heat of mixing work done on this system. Unfortunately he has mistranscribed equations from Guggenheim (Ch. 11, 1952). Guggenheim develops an expression for μ_i^{ex} for the AQC model in two stages, the first between the AQC model and the athermal model (1952, ch. 10) and then between the athermal model and an ideal mixture. Green omits this second part so that his equations 13 (and subsequent) are incomplete. Numerically, this error does not make a huge difference to the activity coefficients, the interchange energy w becoming 8% higher for the NaCl-KCl mixtures.

Green gives a useful consideration of the meaning to be attached to q_1 and q_2, the contact factors. He shows that the calculated interchange energies are not strongly dependent on the functional relationship between q_1 and q_2. The importance of this stems from the form of the simultaneous equations giving the equilibrium of coexisting phases A and B composed of components 1 and 2:- From (120) and (118) for structurally similar

phases:-

$$\ln x_{1A} + \frac{zq_1}{2} \ln \left(\frac{1-K_A A_{2A}}{x_{1A}}\right) = \ln x_{1B} + \frac{zq_1}{2} \ln \left(\frac{1-K_B A_{2B}}{x_{1B}}\right)$$

$$\ln x_{2A} + \frac{zq_2}{2} \ln \left(\frac{1-K_A A_{1A}}{x_{2A}}\right) = \ln x_{2B} + \frac{zq_2}{2} \ln \left(\frac{1-K_B A_{1B}}{x_{2B}}\right)$$

Accepting that $\sqrt{q_1 q_2} = 1$ or similar (satisfying the property that when $q_1 \to 1$ then $q_2 \to 1$), this is a pair of equations in 2 unknowns q_1/q_2 and w and so can be solved for them. However, because of the form of the equations it is not possible to separate the variables and solve the equations analytically; they can only be solved iteratively. With the observation that w is insensitive to q_1/q_2 and the intuitive identification of the q's with some function of atomic radius or molar volume, writing

$$\frac{q_1}{q_2} = \frac{v_1^{2/3}}{v_2^{2/3}}$$

simplifies the problem by reducing the variables to w. Each equation can be solved for w, and a numerical expedient is to use an average of these two computed w's as the interchange energy.

Saxena (1972) considering inter- and intra-crystalline equilibrium uses Green's incorrect equations for the AQC model. However, he escapes any numerical error because when he applies the AQC model to the distribution of Fe and Mg between M1 and M2 in orthopyroxenes, he sets q_{1A}, q_{2A}, q_{1B}, $q_{2B} = 1$, thus reducing it to the QC model in which Green's omitted term has cancelled out.

One point made in the last chapter which must be stressed is that to be able to write the usual symmetric expression for the activity coefficient of one component knowing the other, requires that the mixing model applies over the complete compositional range. An example demonstrates this.

Williams (1971) considers the reaction

$$Fe + SiO_2 + \tfrac{1}{2}O_2 = FeSiO_3$$

for which

$$\frac{-\Delta G_R}{RT} = \ln \frac{a_{FS}}{fo_2^{\frac{1}{2}}} = \ln \frac{x_{FS}\gamma_{FS}}{fo_2^{\frac{1}{2}}}$$

rearranging and setting in $\gamma_{FS} = wx_{EN}^2$, the R model (112)

$$\ln x_{FS} - \tfrac{1}{2} \ln fo_2 = -w\,(x_{EN}^2) \quad \frac{-\Delta G}{RT} R$$

A plot of $(\ln x_{FS} - \frac{1}{2} \ln fo_2)$ against (x_{EN}^2) should be linear if this mixing model applies, with -w as the gradient and $-\Delta G_R/RT$ as the intercept. For orthopyroxenes this plot is non linear for $x_{FS} < 0.20$, Fig. 23.

Williams asserts: 'therefore w can be evaluated from the plot of $\log x_{FS} - \frac{1}{2} \log P_{O_2}$ versus $(1-x_{FS})^2$ only in the region where linearity can be demonstrated'. He then calculates w in this way and writes

$$\log \gamma_{FS} = 0.22\,(1-x_{FS})^2$$

However it is then incorrect to write

$$\log \gamma_{EN} = 0.22\,(1-x_{EN})^2$$

because of the following:-

The Gibbs Duhem equation gives

$$x_{FS} d \ln \gamma_{FS} + x_{EN} d \ln \gamma_{EN} = 0$$

so that

$$\ln \gamma_{EN}'' - \ln \gamma_{EN}' = - \int_{x_{FS}'}^{x_{FS}''} \frac{x_{FS}}{x_{EN}} \, d \ln \gamma_{FS}$$

if this integration is performed from $x_{FS} = 0$ then $\ln \gamma_{EN} = 0$ then

$$\ln \gamma_{EN} = \int_{x_{FS} = 0}^{x_{FS} = x_{FS}} \frac{x_{FS}}{x_{EN}} \, d \ln \gamma_{FS}$$

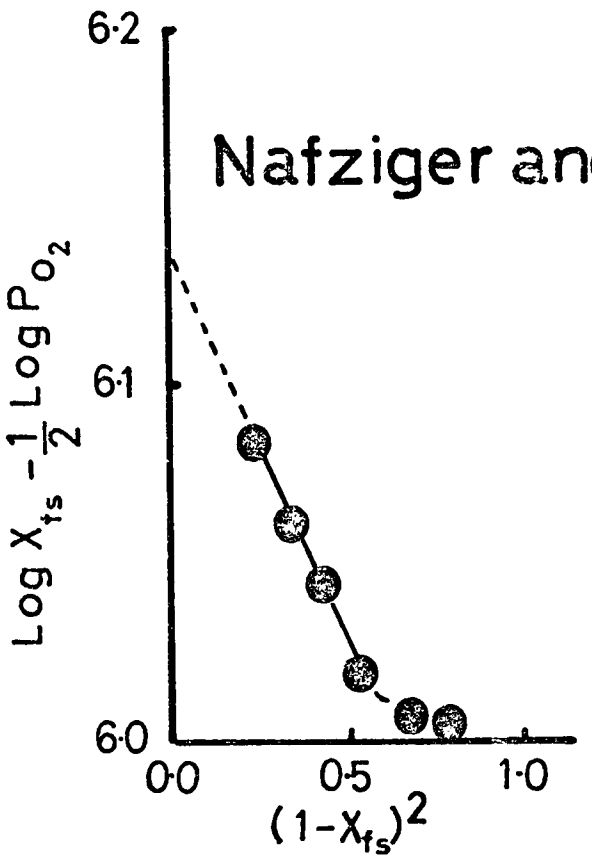
Now if

$$\ln \gamma_{FS} = wx_{EN}^2$$

then $\ln \gamma_{EN} = -\int_0^{x_{FS}} \frac{x_{FS}}{x_{EN}} \, d\,(wx_{EW}^2) = \int_0^{x_{FS}} 2w\, x_{FS}\, d\, x_{FS}$

only if $\ln \gamma_{FS} = wx_{EN}^2$ applies right across the compositional range.

The activity coefficients for $MgSiO_3$ given by Williams 1971 are



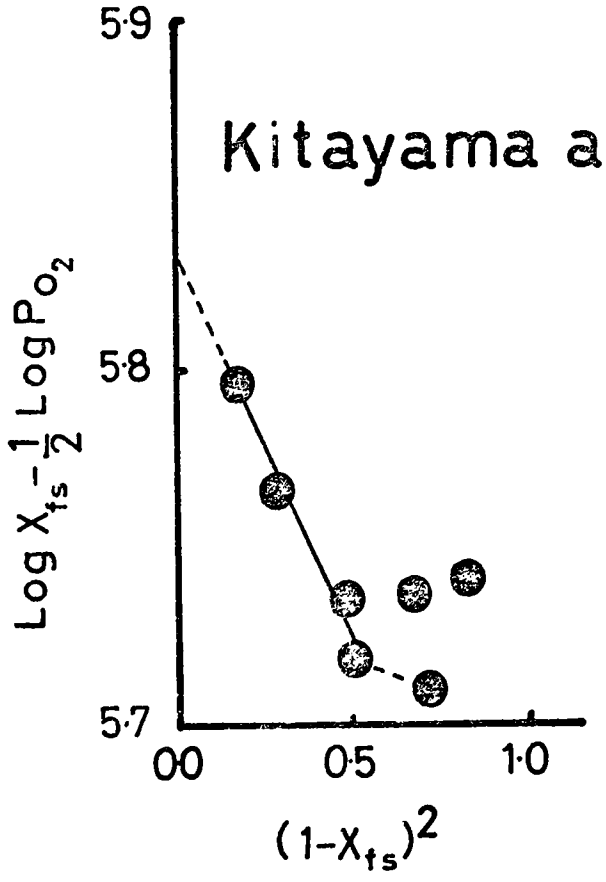


Fig 23:- Plots of literature data used to calculate orthopyroxene activity coefficients, from Williams (1971); see text.

proportional to the area ABC'D' in Fig. 24 whereas they should be proportional to the area ABCD. Therefore the approach of Nafziger and Muan (1967) in simply least squares straight line fitting all the data points and ignoring the curvature on Fig.23 is defensible (particularly as the curvature is not statistically significant for the stated uncertainties).

Various recent papers (e.g. Zen 1973, Froese 1973) have used (simple) mixing models to give activity coefficient expressions for coexisting phases in experimentally determined reactions to aid the extraction of thermodynamic data.

I have written three FORTRAN programs to help consider activity coefficients in solid mixtures:-

ACTIVITY: takes experimentally determined activity coefficients and tries to fit the R, QC, AQC, SR models to them to see which gives the best agreement.

SR: takes the composition of coexisting phases across an experimentally determined solvus and calculates the SR model parameters w_{H1}, w_{H2}, w_{S1} and w_{S2}. This program covers the R model because then $w_{H1} = w_{H2} = w_H$ and $w_{S2} = w_{S1} = w_S$.

QC: takes the composition of coexisting phases across an experimentally determined solvus and calculates the AQC parameter w. The program will calculate the QC parameter w when the input molar volumes for the pure components are set equal to each other; then $q_1 = q_2 = 1$ and the AQC model becomes the QC model.

These programs are explained and listed in Appendix 3.

As pointed out in the last chapter activity coefficients obtained from solvi are dependent on the model chosen. Therefore the applicability of models must be tested on systems in which the mixing properties have been measured. This will now be attempted.

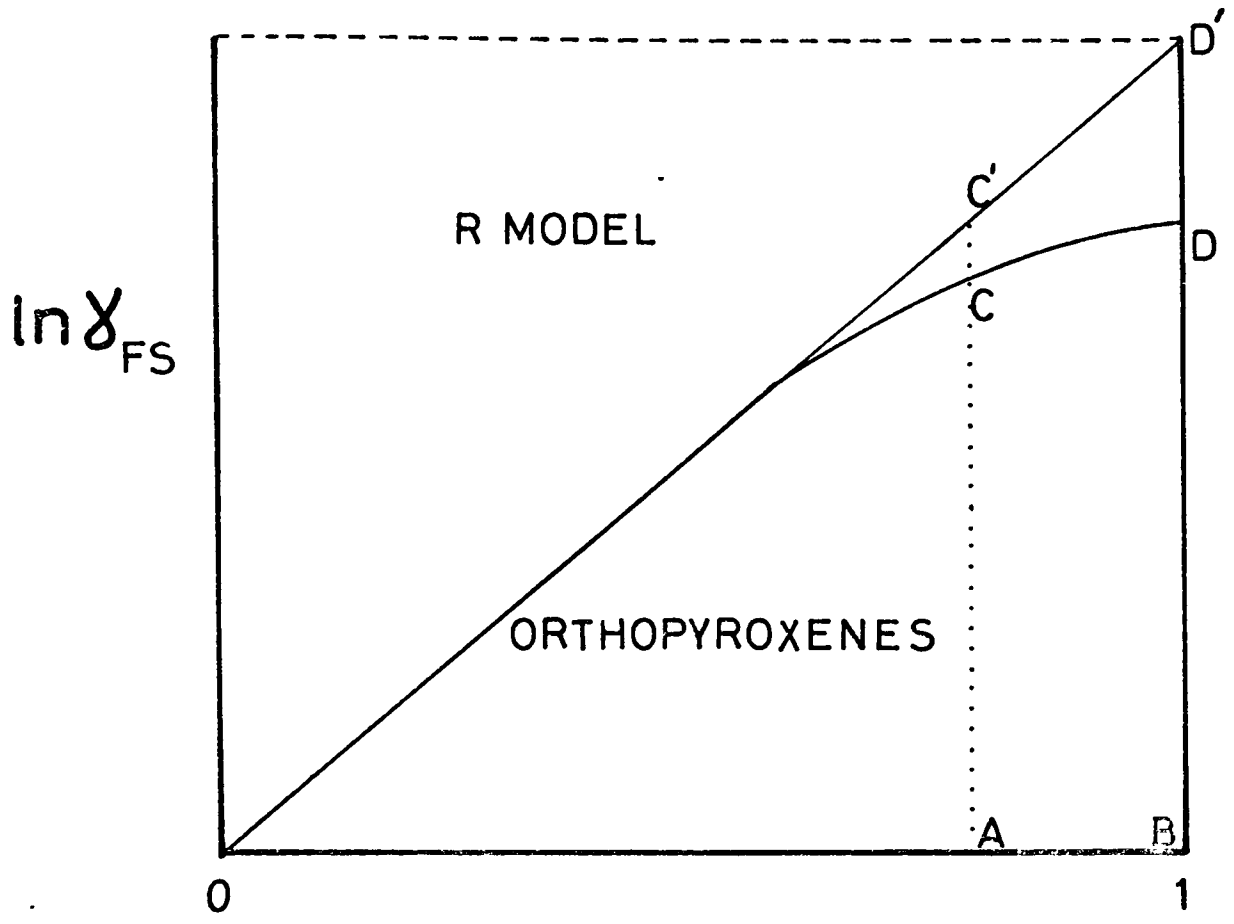


Fig 24 :- Diagrammatic comparison of the R model activity coefficients and the orthopyroxene activity coefficients from : Nafziger and Muan (1967) and Kitayama and Katsura (1968); see text.

Halite-sylvite again

Thompson et al. (1969) and Green (1970) apply the SR and AQC model respectively to the experimentally determined halite-sylvite solvus of Nacken (1918), Bunk (1953) and Barrett et al. (1954).

The SR program was tested with the data used by Thompson et al. (1969), and the program reproduces their SR model parameters. The QC program was tested with Green's incorrect equations and reproduces his results. Using the correct equations, w_G for each data point changes comparatively little, but w_H and w_S are quite different. Fig. 28.

The point of Green's paper was to show that the AQC model fits the enthalpy of mixing experimental data of Barrett et al. (1954) and Lister et al. (1958) better than the SR model. With the correct equations the agreement between the model and the experimental data is even better than by using Green's equations. Fig. 29 .

Thus, it seems that the AQC model is much superior to the SR model in accounting for the mixing properties of halite-sylvite solid mixtures. However, it is unclear how reliable such an almost completely ionic system may be considered as a model for carbonate and silicate mixtures.

Magnesiowustites

Hahn and Muan (1962) give experimental data on pure wustite and magnesiowustite in equilibrium with metallic iron and oxygen at 1100°C and 1300°C. The reaction is

$$2Fe_{0.947}O = 1.894\ Fe(\gamma) + O_2$$

and they give $\log_{P_{O_2}} = 6.496 - 27386/T$ for the endmember univariant reaction. The activity of 'FeO' in a magnesiowustite is then given by

$$a_{FeO} = \left(\frac{P_{O_2}\ \text{for magnesiowustite reaction}}{P_{O_2}\ \text{for endmember reaction}} \right)^{\frac{1}{2}}$$

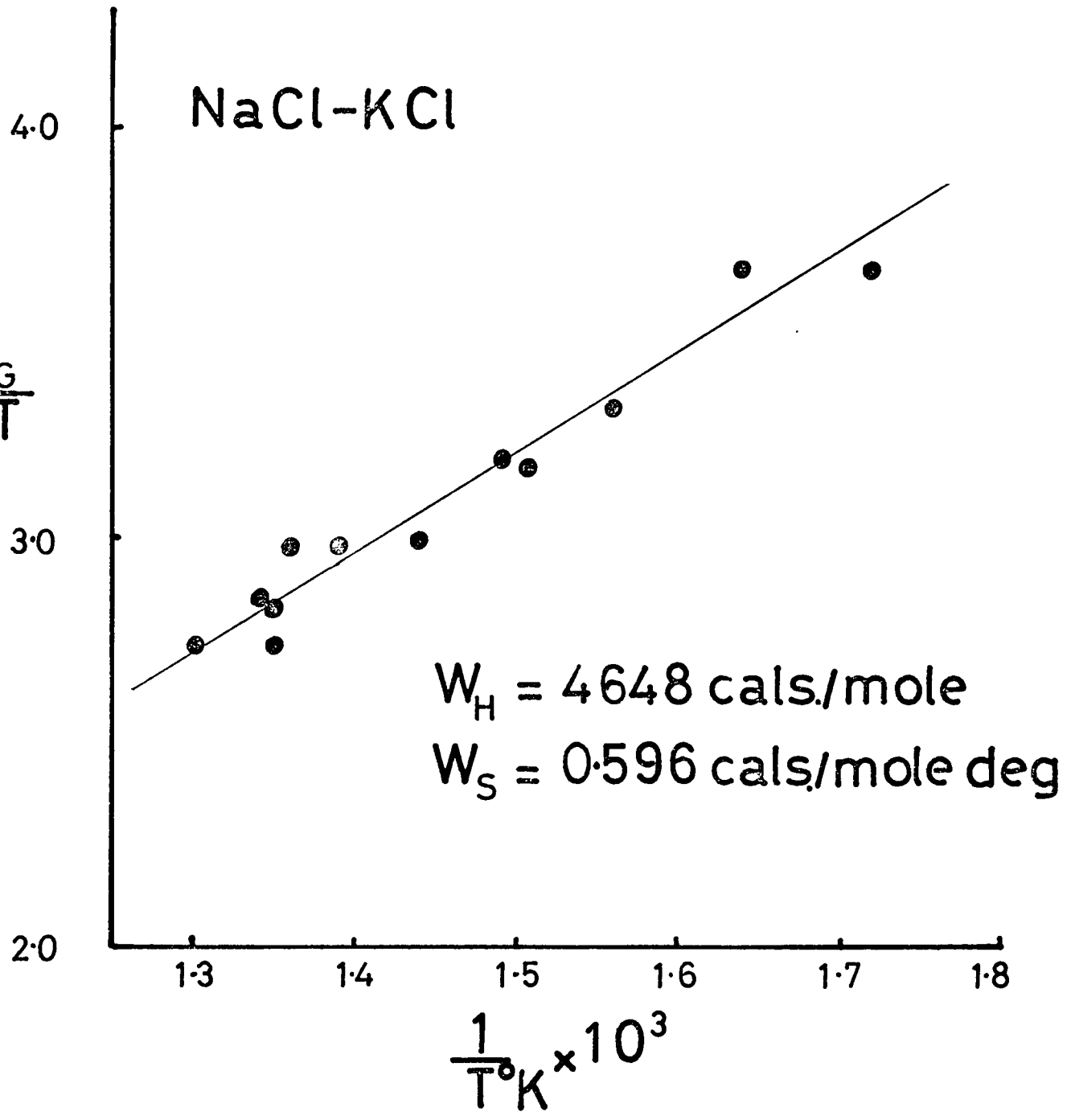


Fig 28:- Temperature dependence of the AQC model mixing parameter, W_G, data selected by : Green (1970)

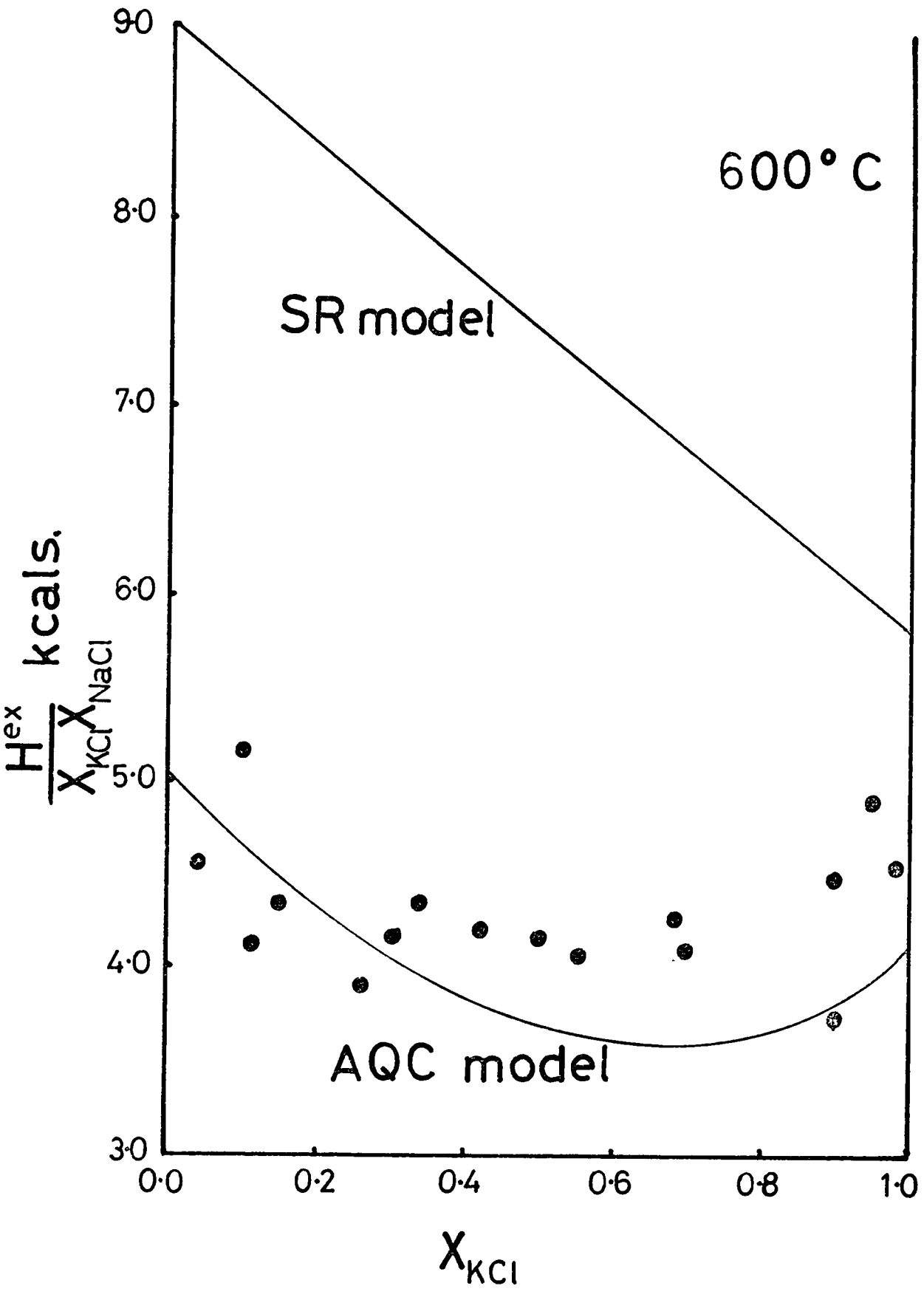


Fig 29 :- Comparison of AQC model, SR model and experimentally determined enthalpies of mixing of NaCl-KCl, data from : Barret et al (1954) and Lister et al (1958).

I have recalculated the activity of FeO in magnesiowustites from their experimental data to see the effect of the stated error of ±0.003 on the X-ray measurement of x_{FeO} and of ±0.02 on the measured log P_{O_2}. The resulting error boxes for x_{FeO} and a_{FeO} were input into ACTIVITY to see which mixing model gave the best fit for the activity coefficients of the magnesiowustites. Of the one parameter models, the AQC model gives the superior fit (Fig. 25 for the 1300°C data) with w_G = 3145 cals/mole for 1100° and 1300°C. Figs. 26 and 27 are activity-concentration plots showing the experimental data as error boxes and the curves predicted by the AQC model with w = 3145 cals/mole.

The magnesiowustites probably provide a much better guide to the mixing properties of silicates, although the size of the error boxes preclude any definitive statement of the best model. However the AQC model does seem to provide the best fit for magnesiowustites (and NaCl-KCl) and it is this model which I adopt to extract activity coefficients from solvi.

Schwer tfeger and Muan (1966), Nafziger and Muan (1967), and others have experimentally determined the equilibrium between olivine, silica, and metallic iron; pyroxene, silica, and metallic iron and olivine-pyroxene exchange equilibrium. However the experimental uncertainty is greater than for the magnesiowustites, and the results are not useful here. For example, Nafziger and Muan use their pyroxene-silica-iron equilibrium data to give activity relations for pyroxenes. They use an R model fit giving

$$w = 0.07 \pm .12 \text{ kcals}$$

and then go on to use this result to calculate the activity relations for olivines! Both mixtures at these conditions (1200°C) are not statistically different from ideal.

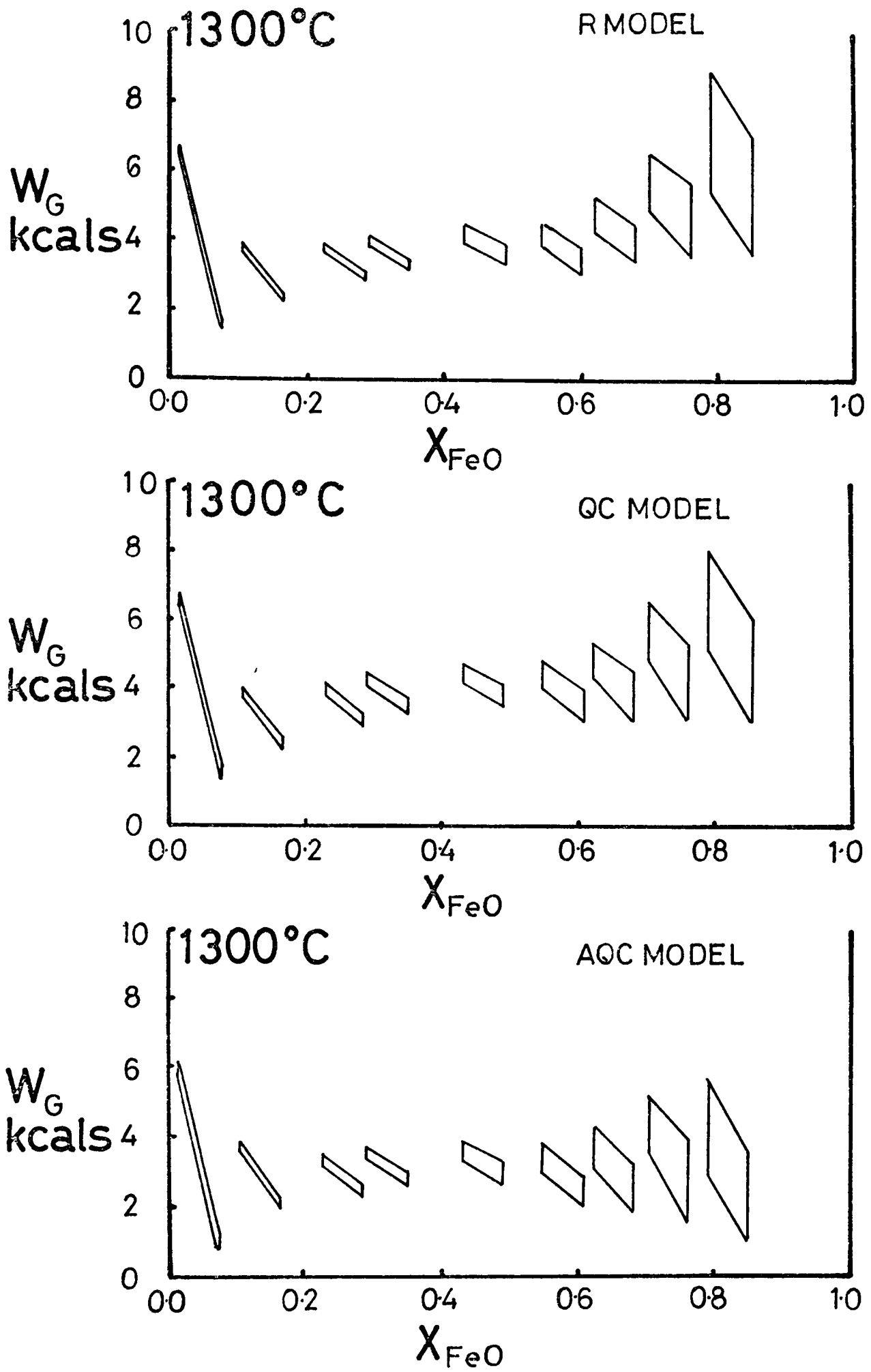


Fig 25 :-Comparison of the R, QC and AQC model mixing parameter for magnesiowustites, data from: Hahn and Muan (1962)

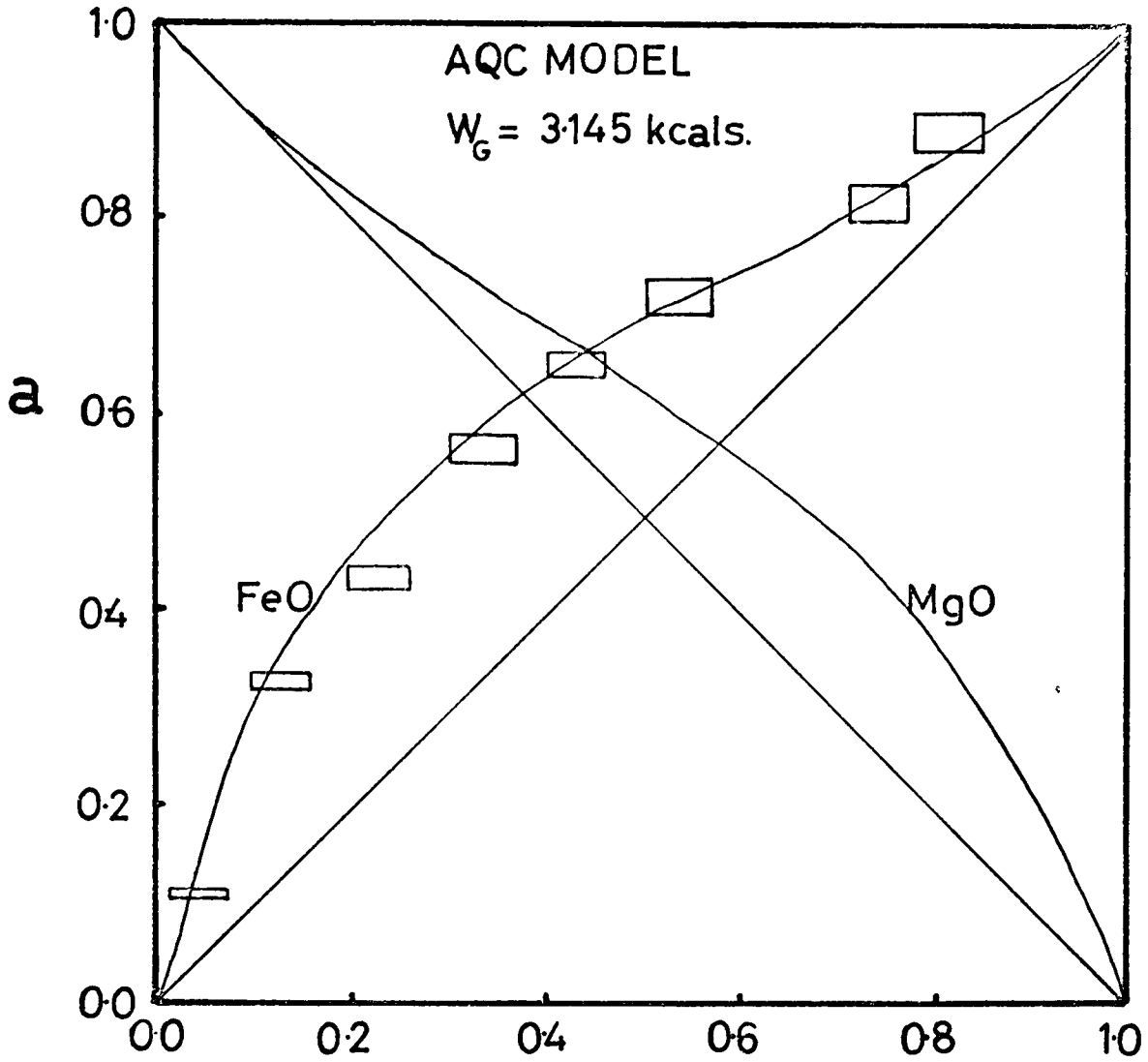


Fig 26 :-Comparison of experimentally determined magnesiowustite activities with calculated AQC model activities at 1100°C, experimental data from Hahn and Muan (1962)

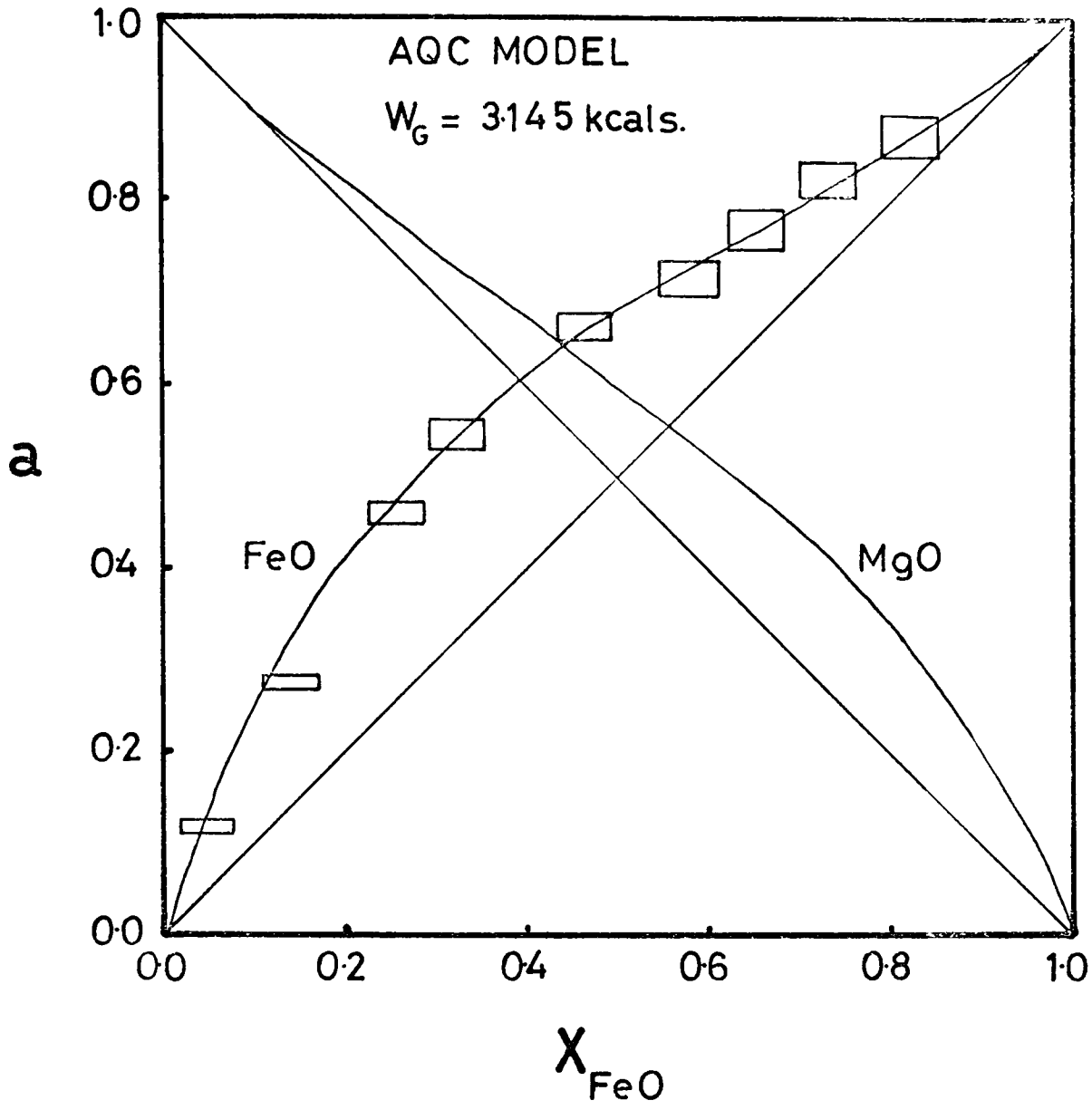


Fig. 27 :-Comparison of experimentally determined magnesiowustite activities with calculated AQC model activities at 1300°C, experimental data from Hahn and Muan (1962).

Calcite-dolomite

The composition of calcite in equilibrium with dolomite can be used as a geothermometer if the solvus has been calibrated. The calcite-dolomite binary has been calibrated in the system $MgCO_3$-$CaCO_3$ by the early work of Harker and Tuttle (1955) and Goldsmith (1959, 1961). More recently Goldsmith and Newton (1969) give the results of a precise calibration of this solvus from 400°C to 960°C and up to 24 kbars. Knowledge of the mixing properties in this system are necessary to calculate equilibrium conditions for reactions involving calcite and dolomite. The first step is to know the pressure-temperature composition of the solvus.

The data given by Goldsmith and Newton (1969) is used exclusively for this purpose for internal consistency in the calculations. The 16 runs at 650°C, 13 runs at 780°C, and 3 runs at each of 500°C and 575°C over a range of pressures provide the pressure dependence of the solvus. Figs. 4 and 5 in Goldsmith and Newton (1969) show that at least at 650°C and 780°C, the mole fraction of $MgCO_3$ in calcite is linear in pressure. The pressure dependence calculated for the four temperatures, weighted proportionally to the number of runs at each temperature, gives, at constant temperature,

$$x^{calcite}_{MgCO_3}\ (1\ bar \quad P\ bars,\ T^oK) = (P-1)\ (0.160\times10^{-8}T - 0.33\times10^{-6})$$

or, for example, 0.0123 per 10 kbars at 650°C.

This equation was used to bring all their data to 1 bar, then the data was least squares straight line fitted by various functions of temperature. No linear function would give a satisfactory fit to all the data, although a plot of $\ln x^{calcite}_{MgCO_3}$ against 1/T gave two straight line segments pivotted at 620°C. The data was split at 620°C and the two sets fitted by this function, giving,

below 600°K, 1 bar $\quad \ln x^{calcite}_{MgCO_3} = 0.8469 - 3090.86 \frac{1}{T}$ with T in °K

above 600°K at 1 bar $\quad \ln x^{calcite}_{MgCO_3} = 1.9679 - 4020.04 \frac{1}{T}$ with T in °K

The experimental data corrected to 1 bar is compared with the values from substitution into these equations in Fig. 30. The composition of calcite in equilibrium with dolomite at any pressure and temperature between 400°C and 900°C and between 1 bar and 20 kbars can be calculated using the above equations.

It is not clear what meaning should be attached to the change of solubility of $MgCO_3$ in calcite at 620°C. Boettcher and Wyllie (1968) and Goldsmith and Newton (1969) show that there is a marked break in the dP/dT of aragonite-calcite at 10 kbars and 480°C which they attribute to the intersection of the calcite I - calcite II transition (an anion order-disorder non-quenchable transition, Jamieson (1957)) with the aragonite-calcite boundary. Linear extrapolation of the X-ray determineded metastable calcite I - calcite II transition at 298°K and 373°K at 15 and 13 kbars respectively (Bridgman 1939, Jamieson 1957) will pass through this point and Goldsmith and Newton continues the boundary to 1 bar and about 1000°C to correspond with the transition reported by Boeke (1912) by a DTA technique.

Goldsmith and Newton made several different attempts to locate the calcite I - calcite II transition on the above suggestion that the transition passes from 10 kbars and 480°C to 1 bar and 1000°C using the solubility of $MgCO_3$ in calcite in equilibrium with dolomite in this region. The runs at 650°C and 780°C at different pressures fail to pick up the expected discontinuity in composition. A DTA approach also failed to locate the transition.

The discontinuity located here at 600°C and 1 bar may be the calcite I - calcite II transition. A possibility is that Boeke (1912) and Jamieson (1957) are correct for the pure $CaCO_3$ system but a consider-

able change in dP/dT for this transition occurs between the pure $CaCO_3$ system and the $CaCO_3$ - $MgCO_3$ system with calcite in equilibrium with dolomite which is much larger than inferred by Goldsmith and Newton

This interpretation is adopted here and is summarised in Fig.31.

Unfortunately the pressure dependence of the solvus is controlled almost completely by the runs at 650°C and 780°C, well within the calcite II field. There is no alternative but to adopt the same pressure dependence equation for calcite I and calcite II. This means that it is not possible to calculate the dP/dT for the calcite I - calcite II transition from the pressure-temperature dependence of the activity coefficients of calcite I and calcite II calculated later to see if the transition will pass through the experimentally determined point/

The theory of activity-composition relations in systems with addition compounds (e.g. dolomite in $MgCO_3$ - $CaCO_3$) is not so straightforward as for normal binary systems (e.g. NaCl-KCl). First, it is necessary to outline the structure of dolomite. Bradley et al. (1953), using powder diffraction methods, refined the crystal structure of dolomite in terms of a planar carbonate group and alternating layers of $CaCO_3$ from calcite and $MgCO_3$ from magnesite. Thus it seems appropriate to consider dolomite-calcite equilibrium in terms of equilibrium between a two site phase (dolomite) and a one site phase (calcite).

Using $\mu_i^{\text{dol Ca}}$ for the chemical potential of i in the Ca rich site and $\mu_i^{\text{dol Mg}}$ for the chemical potential of i in the Mg rich site, equilibrium between calcite and dolomite is given by.

$$\mu_{CaCO_3}^{\text{calcite}} = \mu_{CaCO_3}^{\text{dol Ca}} = \mu_{CaCO_3}^{\text{dol Mg}}$$

$$\mu_{MgCO_3}^{\text{calcite}} = \mu_{MgCO_3}^{\text{dol Ca}} = \mu_{Mg\ CO_3}^{\text{dol Mg}}$$

There is no detailed experimental data on the composition of dolomite coexisting with calcite. The data that exists indicates that there is

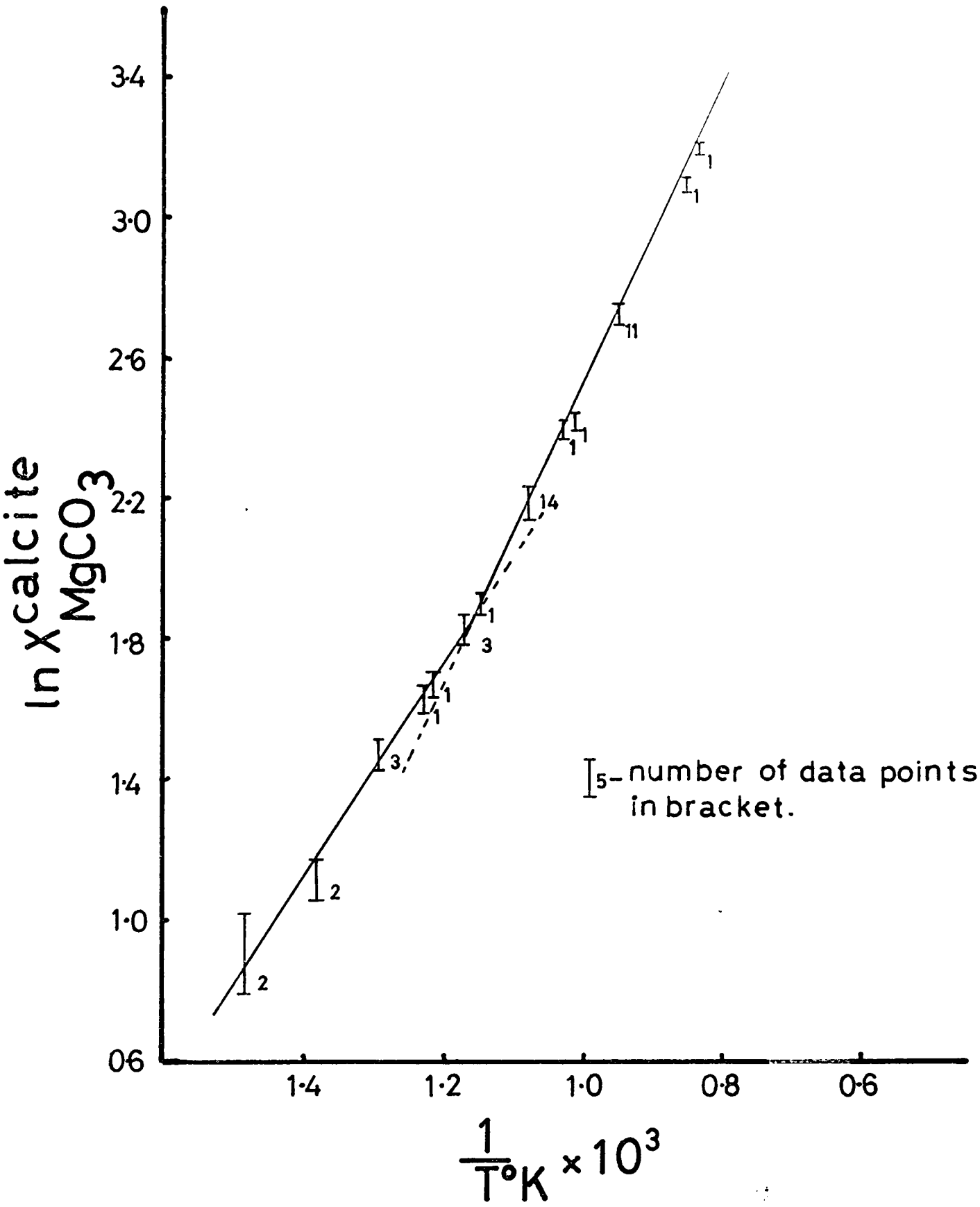


Fig 30 :- $\ln X_{MgCO_3}$ in calcite in equilibrium with dolomite against reciprocal temperature at 1 bar; data from :
Newton and Goldsmith (1968)

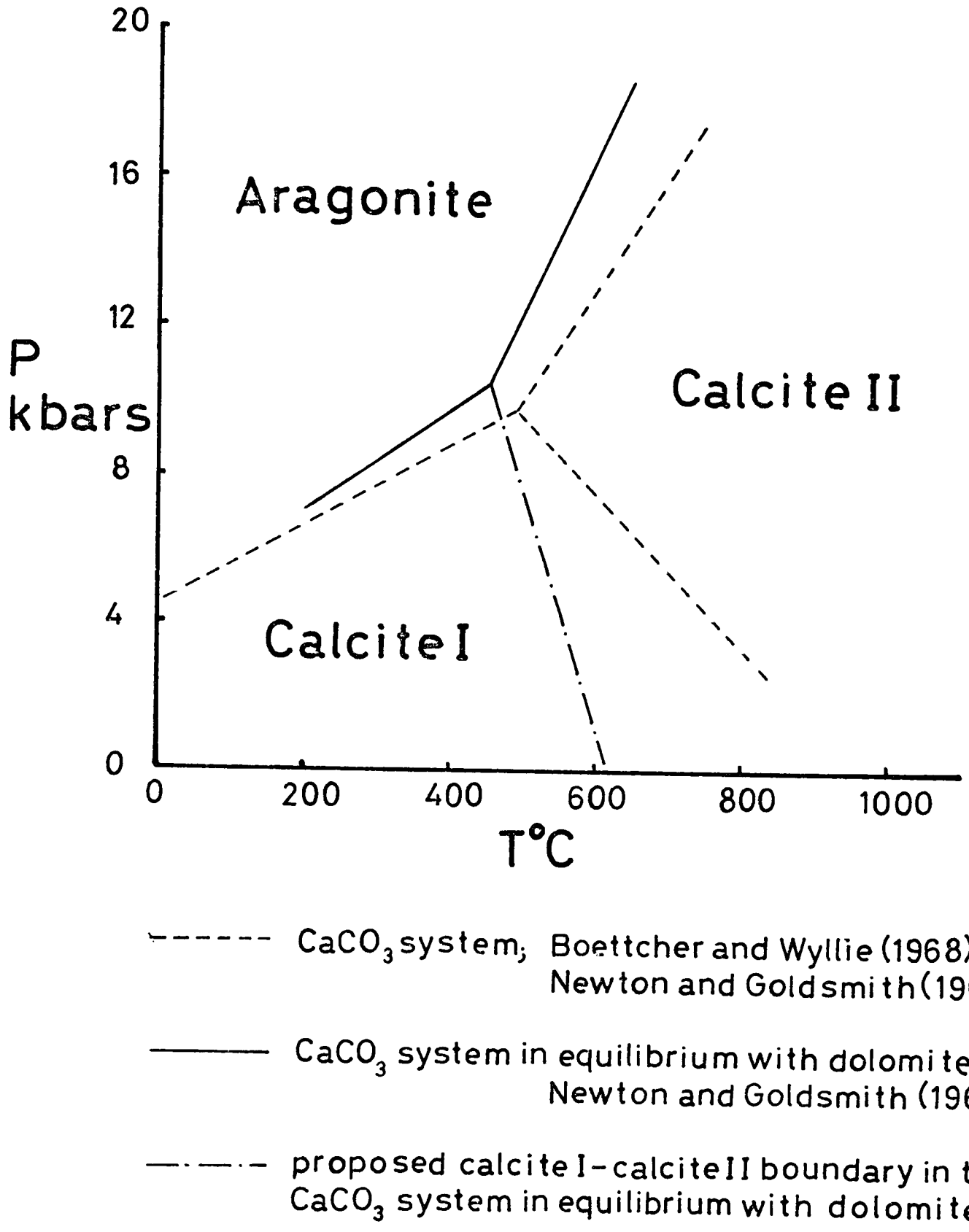


Fig 31 :- CalciteI-calciteII-aragonite phase diagram.

less than 4 mole % excess $CaCO_3$ in dolomite even at 900°C (Harker and Tuttle 1955). In the absence of site population data for dolomites, it will be assumed that dolomite is completely ordered.

From (126)

$$\mu^{dol}_{CaMg(CO_3)_2} = \mu^{dol\ Ca}_{CaCO_3} + \mu^{dol\ Mg}_{MgCO_3}$$

Combining the above three equations

$$\mu^{dol}_{CaMg(CO_3)_2} = \mu^{calcite}_{CaCO_3} + \mu^{calcite}_{MgCO_3}$$

The equilibrium is equivalent to the reaction

$$\text{dolomite} = \text{calcite} + MgCO_3 \text{ calcite}$$

The equilibrium constant formulation for this reaction is

$$-\frac{\Delta G}{RT}R = \ln \frac{a^{calcite}_{CaCO_3}\ a^{calcite}_{MgCO_3}}{a^{dolomite}_{CaMg(CO_3)_2}} \qquad (154)$$

Where ΔG_R is calculated using the Gibbs energy of magnesite for $MgCO_3$ calcite on the basis of their identical crystal structures.

If the standard state for dolomite is defined as the stoichiometric completely ordered solid, and assuming that at the experimental conditions there is no Mg in the Ca site in dolomite, then

$$a^{dolomite}_{CaMg(CO_3)_2} = a^{dol\ Ca}_{CaCO_3}\ a^{dol\ Mg}_{MgCO_3}$$

$$= x^{dol\ Mg}_{MgCO_3}\ \gamma^{dol\ Mg}_{MgCO_3}$$

$$= 2^{*}\ x^{dolomite}_{MgCO_3}$$

assuming activity equals concentration for the Mg site; this is reasonable because, even at 900°C, the excess mole fraction of $CaCO_3$ in dolomite is less than 0.04. For calcite,

$$a^{calcite}_{CaCO_3}\ a^{calcite}_{MgCO_3} = x^{calcite}_{CaCO_3}\ x^{calcite}_{MgCO_3}\ \gamma^{calcite}_{CaCO_3}\ \gamma^{calcite}_{MgCO_3}$$

By assuming that a mixing model applies across the complete composition range, the activity coefficients can be calculated by the AQC model. Given ΔG_R, the mixing parameter w_G can be calculated from (120). The QC program was adapted to this task and was run at 500 bar intervals to 10 kbars for calcite I and calcite II using the solvus equations given above. In all cases w_G is linear in temperature and the parameters w_H and w_S from $w_G = w_H - Tw_S$ for each pressure for calcite I and calcite II are given in Table 4

For calcite I

$$w_H = 2985 - 0.1282\ P$$

$$w_S = -0.664 - 0.000106\ P$$

and for calcite II

$$w_H = 4804 - 0.0725\ P$$

$$w_S = 1.449 - 0.0000429\ P$$

Where P is in bars and w_H and w_S are in cals/mole. The pressure dependence of the mixing parameters of calcite I is largely controlled by the pressure dependence of the solvus of calcite II as mentioned earlier.

The calculated values of w_H and w_S and the straight line fit are compared for calcite I and calcite II in Fig. 32 .

From (154)it is obvious that the mixing parameters depend on the Gibbs energies of calcite, magnesite, and dolomite. This is unfortunate because it will be shown later that these values are not well known. The program was run varying ΔG_R and w_H and w_S were calculated as a function of the difference between the actual ΔG_R and the$\Delta\ G_R$ calculated from the data in Robie and Waldbaum, $\Delta\Delta G_R$, giving,

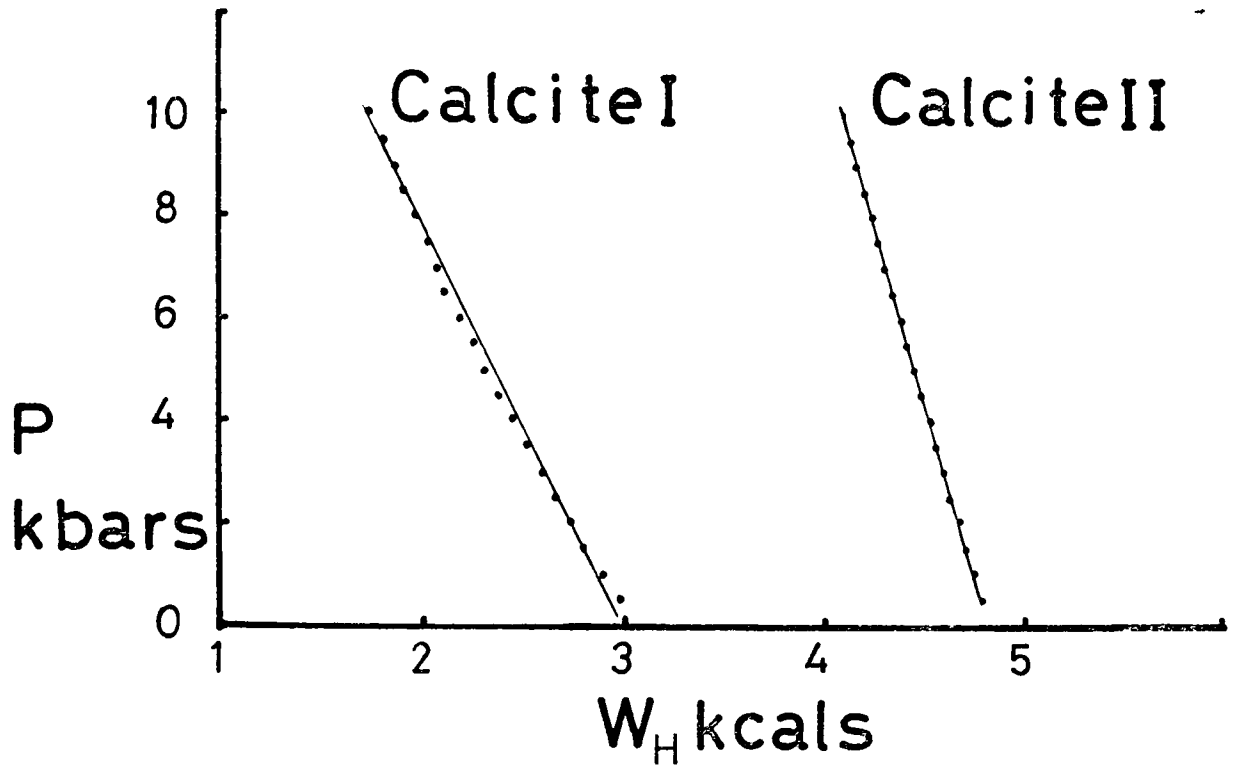
$$\Delta w_H \approx -0.71\ \Delta\Delta G_R$$

$$\Delta w_S \approx -0.61\ \Delta\Delta G_R$$

The equations apply to both calcite I and calcite II.

P kbars	calcite I		calciteII	
	W_H kcals	W_S cals	W_H kcals	W_S cals
10·0	1·754	−1·668	4·094	1·033
9·5	1·806	−1·626	4·122	1·047
9·0	1·856	−1·589	4·157	1·068
8·5	1·906	−1·551	4·190	1·087
8·0	1·960	−1·508	4·225	1·106
7·5	2·013	−1·469	4·261	1·129
7·0	2·067	−1·427	4·291	1·144
6·5	2·126	−1·379	4·319	1·157
6·0	2·184	−1·333	4·360	1·184
5·5	2·245	−1·283	4·398	1·207
5·0	2·310	−1·230	4·433	1·227
4·5	2·374	−1·176	4·470	1·250
4·0	2·440	−1·114	4·511	1·276
3·5	2·514	−1·058	4·545	1·294
3·0	2·584	−0·999	4·583	1·318
2·5	2·660	−0·933	4·619	1·338
2·0	2·735	−0·869	4·658	1·362
1·5	2·814	−0·800	4·706	1·395
1·0	2·899	−0·724	4·738	1·411
0·5	2·981	−0·653	4·783	1·441

Table 4 :- AQC model mixing parameters for calcite I and II from 0·5 to 10·0 kbars



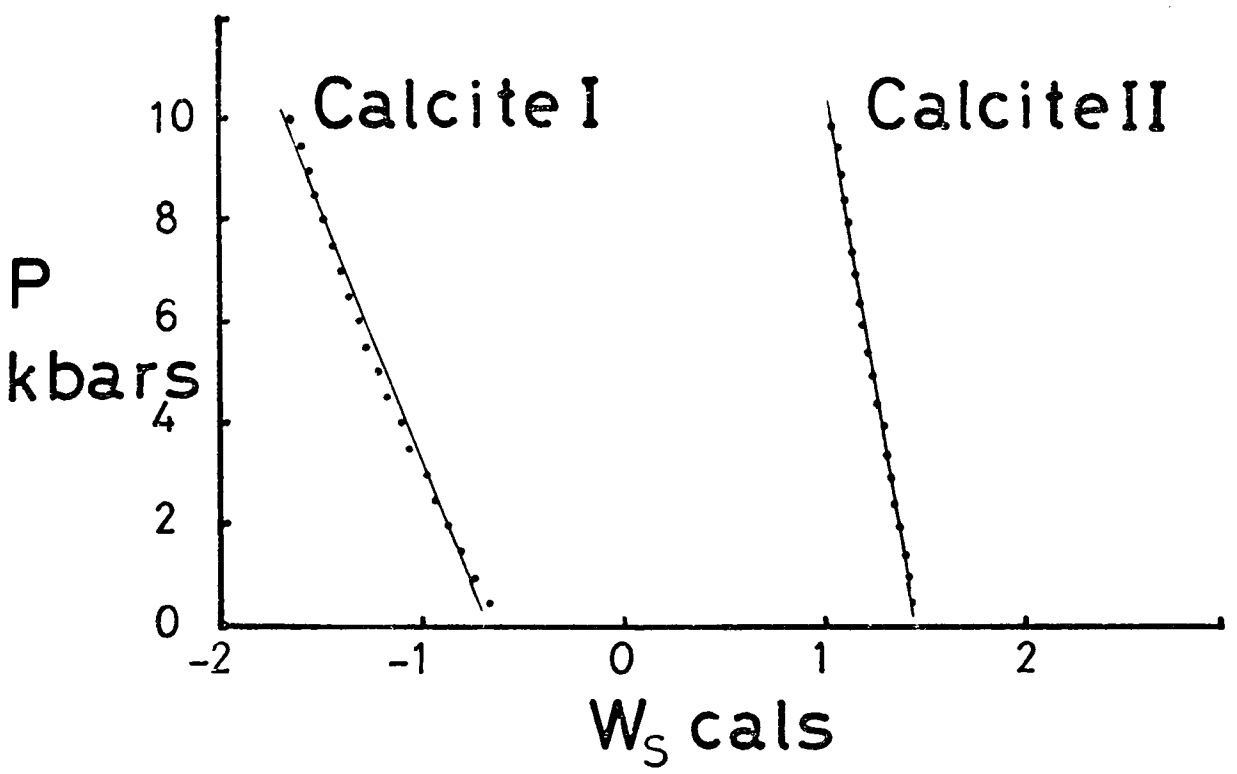


Fig 32 :- AQC model mixing parameters, W_H and W_S for calcite I and II as a function of pressure.

Gordon and Greenwood (1970) also attempted to calculate activity coefficients for coexisting calcite and dolomite using the experimental data of Graf and Goldsmith (1955) on coexisting magnesian calcites and periclase + CO_2. For the reaction

$$MgCO_3 = MgO + CO_2$$

$$-\frac{\Delta G}{RT}R = \ln f_{CO_2}$$

For the reaction

$$MgCO_3 \text{ in calcite} = MgO + CO_2$$

$$-\frac{\Delta G}{RT}R = \ln f_{CO_2}/a^{\text{calcite}}_{MgCO_3}$$

The ΔG_R in these two expressions are identical so that the activity of $MgCO_3$ in calcite can be calculated from the CO_2 fugacities for the two reactions. However many of Goldsmith and Graf's runs were shorter than the time suggested by Newton and Goldsmith for the equilibration of cold seal runs. A suggestion of some complicating factor is indicated by the lack of a discernible temperature dependence of the calculated activity coefficients, an impossible situation in a binary with a solvus. Gordon and Greenwood state that their Margules fit of the calculated activity coefficients for $MgCO_3$ in calcite are applicable only in the range $x^{\text{calcite}}_{MgCO_3}$ 0.0 to 0.18, then write an expression for the activity coefficient for $CaCO_3$ in calcite. As before, an activity coefficient equation can only be written for the second component from the equation for the first component when the mixing model applies across the complete composition range.

Enstatite - diopside

The activity coefficients for this binary are required for the retrieval of thermodynamic data for tremolite. The orthoenstatite - diopside solvus of Boyd and Schairer (1964) was used in the calculations. Equilibrium between enstatite and diopside involves cation distribution between two site phases (e.g. Blander 1972).

With (126), and a completed ordered standard state

$$\mu_{CaMgSi_2O_6} = \mu^{*}_{CaMgSi_2O_6} + RT \ln x^{M1}_{Mg}\gamma^{M1}_{Mg}x^{M2}_{Ca}\gamma^{M2}_{Ca}$$

$$\mu_{MgSiO_3} = \mu^{*}_{MgSiO_3} + RT \ln x^{M1}_{Mg}\gamma^{M1}_{Mg}x^{M2}_{Mg}\gamma^{M2}_{Mg}$$

For the approximation of complete ordering at the conditions of interest

$$x^{M1\ cpx}_{Mg} = \gamma^{M1\ cpx}_{Mg} = x^{M1\ opx}_{Mg} = \gamma^{M1\ opx}_{Mg} = 1$$

and $$x^{M2\ cpx}_{Ca} = 2x^{cpx}_{CaSiO_3}$$

$$x^{M2\ opx}_{Mg} = (x^{opx}_{MgSiO_3} - 0.5)/2$$

The activity coefficients were calculated from the solvus data with the QC program, using the assumption that the standard chemical potentials cancel in the equations

$$\mu^{M2\ cpx}_{Ca} = \mu^{M2\ opx}_{Ca}$$

$$\mu^{M2\ cpx}_{Mg} = \mu^{M2\ opx}_{Mg}$$

The mixing parameters are:-

$$w_H = 11308 \text{ cals} \qquad w_S = 2.325 \text{ cals}$$

The high pressure data of Kushiro (1969) shows that the enstatite-diopside solvus is independent of pressure so that the derived parameters should be independent of pressure.

Hercynite - magnetite

The activity coefficients for this binary are required for the retrieval of thermodynamic data for Fe-chlorite and almandine. Froese (1973) and Zen (1973) have approximated the solvus using the R model and ignoring that hercynite is a normal spinel and magnetite is a inverse spinel. The same approximation is used and the mixtures are considered in terms of the equilibrium conditions,

$$\mu^{herc}_{FeAl_2O_4} = \mu^{magt}_{FeAl_2O_4}$$

$$\mu^{herc}_{Fe_3O_4} = \mu^{mgt}_{Fe_3O_4}$$

The solvus data of Turnock and Eugster (1962) input to the QC program gave the mixing parameters:-

W_H = 2262 cals $\qquad$ W_S = -3.322 cals

These are assumed to apply over the pressure range of the experimental work in the absence of polybaric solvus data.

CHAPTER 4

THE ROCKS

The Rocks

Introduction

The aim of this chapter is to describe the assemblages in the Spean Bridge metamorphic rocks with theoretical, petrographic, textural and analytical data. The data will be used in the next chapter to calculate the conditions of metamorphism.

Lithologies

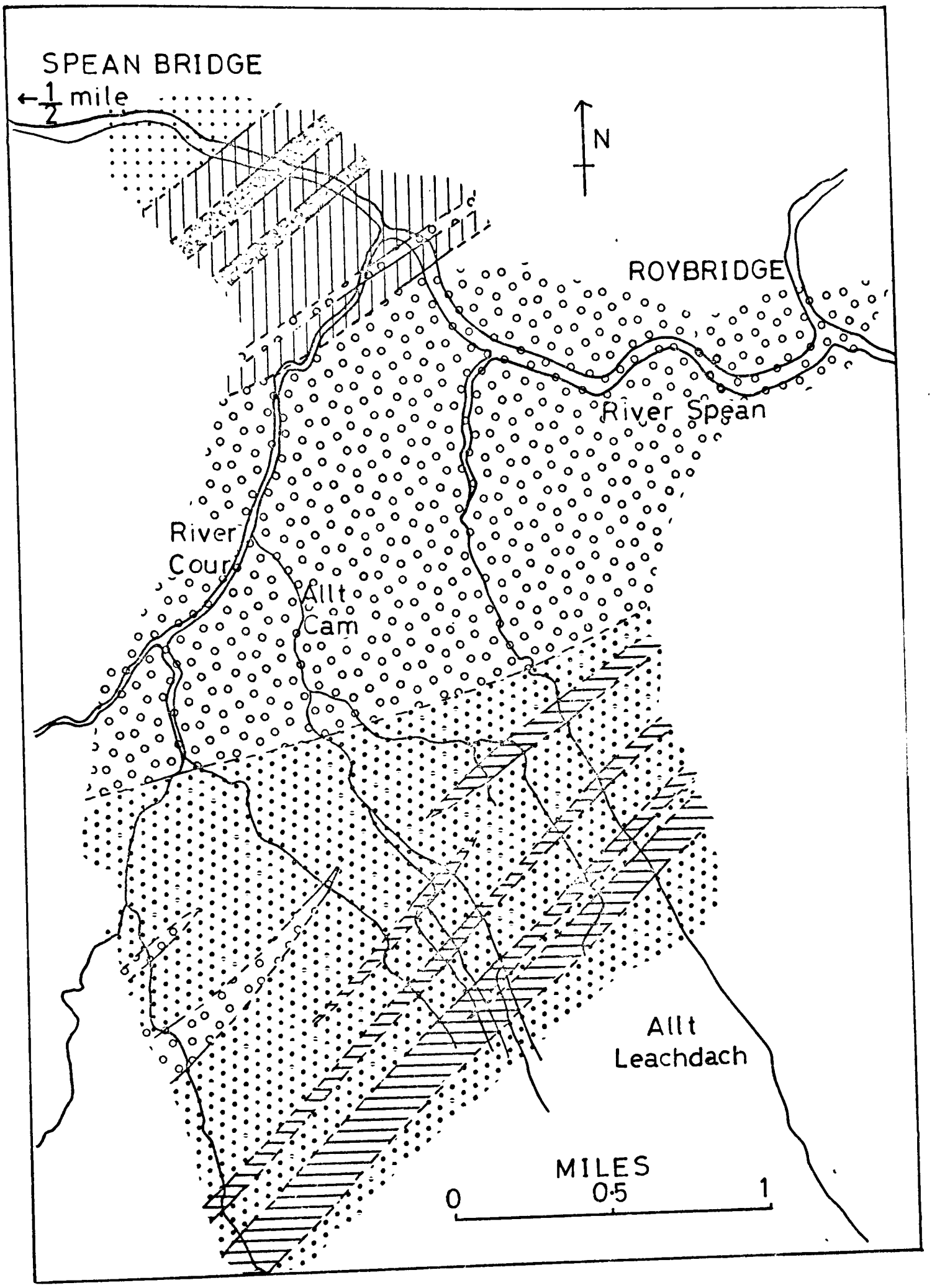
Bailey (1934) published a geological map and account of the area between Loch Leven and Glen Roy including this area. Richardson (1962, 1963) remapped the area, and, with minor corrections, this map is given in Fig. 1. Bailey's interpretation of the structure of the area is given in Fig. 2; it is based on the idea of a well-defined stratigraphy and a refolded recumbent syncline which he describes from the Ballachulish area. Discussion of this is deferred to the end of the chapter.

Four lithologies can be mapped in the field:

1. siliceous dolomite lithology: dark grey to light grey siliceous dolomites containing quartz, calcite, dolomite and talc and/or porphyroblastic tremolite (up to 4 cm. long), the latter two often in a slip strain cleavage. Some of the rocks by the mouth of the Cour contain numerous oligoclase and calcite porphyroblasts. The rocks to the west of the main graphitic lithology outcrop, contain little or no tremolite and are more cleaved than the main outcrops at the mouth of the Cour, where the quartz-calcite-dolomite-talc-tremolite assemblage is best developed.

2. graphitic lithology: black fine-grained pelitic and calc-pelitic rocks with porphyroblasts of biotite and epidote. Dark grey coarser grained rocks are interbanded with black very fine grained rocks. Some of the rocks in the main graphitic lithology outcrop

Fig. 1 :- Geological map of area studied; after Richardson (1962, 1963)



EPIDOTE PELITE LITHOLOGY with calc-pelitic bands

GARNET PELITE LITHOLOGY

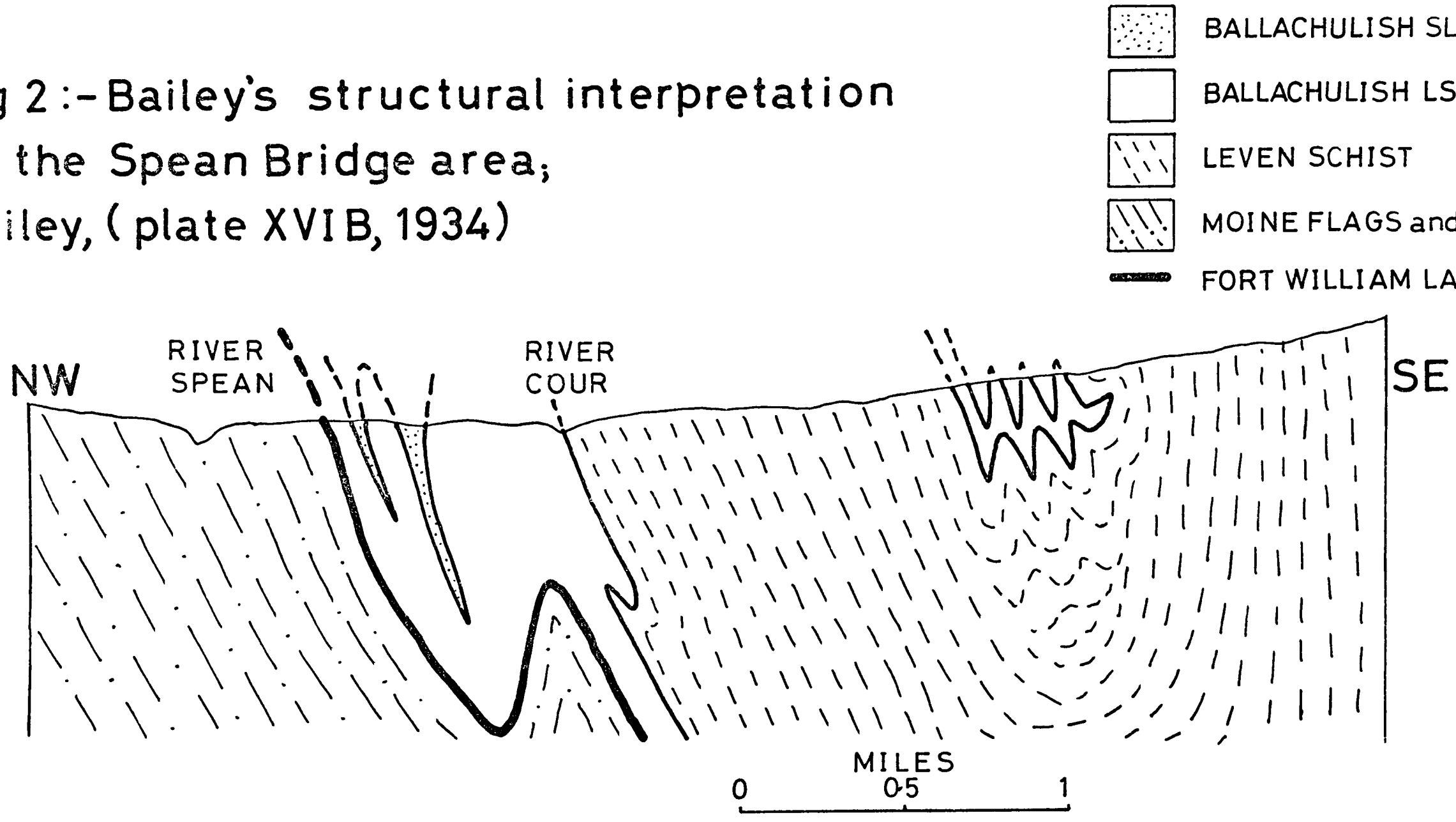
GRAPHITIC LITHOLOGY

SILICEOUS DOLOMITE LITHOLOGY

MOINE QUARTZITE

Geological boundaries:
—— observed
---- inferred

Fig 2 :- Bailey's structural interpretation of the Spean Bridge area; Bailey, (plate XVI B, 1934)



contain occasional 1.5 cm. garnet porphyroblasts. Small sulphide pods and lenses of pyrite and chalcopyrite are common. Siliceous dolomite rocks intercalate with the graphitic rocks at the margins of the graphitic lithology outcrops.

3. garnet pelite lithology: very light green to light green banded rocks with a penetrative mica cleavage, characteristically with biotite and garnet porphyroblasts up to 5 mm across. The proportion and size of porphyroblasts varies between bands. Occasional, more massive, carbonate-bearing bands occur. In the Roybridge river section hornblende joins garnet and biotite as a porphyroblast mineral. Similar rocks occur much less frequently in the Cour and Allt Leachdach sections.

The boundary with the siliceous dolomite lithology is gradational over several metres. Talc and tremolite disappear from the siliceous dolomites as the colour changes from dark grey through light grey to light green with the appearance of a penetrative mica cleavage. The transition is complete with the appearance of biotite porphyroblasts. Garnet porphyroblasts appear about 300 m. from the boundary.

4. epidote pelite lithology: white to very light green banded rocks with a penetrative mica cleavage. Biotite occurs as part of the penetrative cleavage rather than as porphyroblasts. Small pale yellow-green epidote porphyroblasts are common. Garnet porphyroblasts are less common than in the garnet pelite lithology. Abundant carbonate-bearing rocks occur and these are differentiated from the carbonate-poor and carbonate-free rocks on the map. Massive limestones, several metres thick, containing calcite-dolomite-quartz-mica occur within the calc-pelitic rocks. No talc or tremolite has been found in these rocks, whereas epidote is common.

The boundary with the garnet pelite lithology is gradational and intercalational over at least 400 m. Away from the boundary garnet

pelite lithology bands (300 m. to less than 1 m. thick) occur within the epidote pelite lithology particularly in the Cour section. The largest of these are differentiated on the map.

Table 1 is a list of the assemblages described from specimens located on Fig. 3. Most of the identification was carried out on thin sections and polished sections. X-ray diffraction was used initially to identify talc and distinguish carbonates. Secondary minerals, chlorite replacing biotite and garnet, haematite after opaques, and carbonate in veins, were omitted from the listed assemblages. Tourmaline, apatite and zircon are ubiquitous accessories and were excluded from Table 1 Table 1 also includes the abbreviation for minerals that will be used in the text and diagrams.

The most important characteristic of the assemblages is that a large proportion have many phases and therefore have a low variance. From Chapter 2, the variance of an assemblage, w, is

$$w = (C-R) + 2 - P$$

where C is the number of components

R is the number of independent reactions between the components

P is the number of phases.

In the last section of Chapter 2 it was shown that sites in a phase can be considered as virtual components and a virtual chemical potential can be written for each. In the same way oxides can be considered as virtual components of a phase and the phase rule becomes

$$w = C + 2 - P$$

where C is the number of independent virtual components (for example the number of oxides)

It is often convenient to use a mixed set of components, virtual and actual. If this is not an independent set, then a term involving

Table 1:- Assemblage lists :-
Siliceous dolomite lithology

	q	olig	phl	br.bi	gr.bi	clin	chl	mu	g	cz	ep	cc	dol	tre	hbl	ta	sph	rut	pyr	ilm	gr		
B100	O	O	O			O						O	O	O		O		O				5	A
B100a	O	O	O			O						O	O	O		O		O				5	A
B101	O	O	O			O						O	O	O		O	O					5	A
B105	O	O	O			O						O	O			O	O					4	A4
B106	O	O	O			O						O	O	O			O			O		4	A3
71·1	O	O	O			O						O	O				O	O				3	A4-3
71·4	O	O	O			O							O			O		O				3	A2-4
71·5	O	O	O			O						O	O	O		O	O	O				5	A
71·6	O	O	O			O						O	O	O		O		O				5	A
71·7	O	O	O			O						O	O			O		O	O			4	A4
71·8	O	O	O			O						O	O				O	O		O		3	A4-3
71·11	O	O	O			O						O	O				O					3	A4-3
71·12	O	O	O			O						O	O					O				3	A4-3
71·13	O	O	O			O						O	O	O			O	O				4	A3
71·14	O	O	O			O						O	O									3	A4-3
71·16	O	O	O			O						O	O				O		O	O		3	A4-3
71·19	O	O	O			O				O		O	O	O			O			O	O	5	B
71·26	O	O	O			O						O	O							O		3	A4-3
72·1	O	O	O			O						O	O			O		O				4	A4

KEY:

q — quartz
olig — oligoclase
phl — colourless biotite
br.bi — brown biotite
gr.bi — green biotite
clin — colourless chlorite
chl — green chlorite
mu — muscovite
g — garnet
cz — clinozoisite
ep — epidote
cc — calcite
dol — dolomite
tre — colourless amphibole
hbl — green amphibole
ta — talc
sph — sphene
rut — rutile
pyr — pyrite
ilm — ilmenite
gr — graphite

Table 1 (cont.):- Assemblage lists :- Garnet pelite lithology

	q	olig	phl	brbi	grbi	clin	chl	mu	g	cz	ep	cc	dol	tre	hbl	ta	sph	rut	pyr	ilm	gr		
B 86	O	O		O			O	O	O								O			O		3	D1-2
B 147	O	O		O			O	O	O		O									O		4	D13
	O	O							O				O							O		2	
B 148	O	O		O			O	O	O		O									O		4	D13
B 149	O	O		O			O	O	O		O									O		4	D13
B 150	O	O		O			O	O	O		O						O			O		4	D13
B 154	O	O		O				O	O		O									O		3	D8-9
B 234	O	O			O			O	O	O										O		3	D8-9
	O	O						O	O	O		O	O									5	D7-8-8-10
B 250	O	O						O	O				O							O		3	D 2-10
	O	O		O		O		O	O											O		3	D1-2
B 251	O	O		O		O		O	O		O									O		4	D13
	O	O						O				O					O	O		O		2	
B 252	O	O		O				O	O								O			O		2	
B 253	O	O		O			O	O	O											O		3	D1-2
B 255	O	O		O			O	O	O		O	O						O		O		5	D1-5-8-8
B 257	O	O		O				O	O				O							O		3	D 2-10
B 275	O	O		O			O	O	O				O							O		4	D 2
B 317	O	O			O		O	O	O		O									O		4	D13
B 318	O	O			O			O	O		O									O		3	D8-9
B 319	O	O		O			O	O	O		O									O		4	D13
B 320	O	O		O			O	O	O											O		3	D1-2
B 321	O	O		O				O	O		O									O		3	D8-9
	O	O	O						O				O									2	
B 322	O	O		O			O	O	O											O		3	D1-2
B 323	O	O		O				O	O		O				O					O		5	C
B 335	O	O		O			O	O	O											O		3	D1-2
B 358	O	O		O			O		O		O									O		4	D13
B 359	O	O			O		O				O	O	O							O		4	D3-5-6-7
	O	O		O			O	O	O											O		3	D1-2
70·48	O	O		O			O		O			O								O		3	D4-8
	O	O		O			O	O	O		O								O	O		4	D13
70·58	O	O			O		O	O			O									O		3	D5-6
70·64	O	O	O				O			O		O					O	O		O		3	D7-8
70·66	O	O			O			O	O		O									O		3	D8-9
70·71	O	O		O			O	O	O											O		3	D1-2
	O	O	O				O		O			O										3	D1-2
70·80	O	O		O			O	O	O		O									O		4	D13
71·53	O	O			O			O	O		O									O		3	D8-9
71·69	O	O		O					O			O								O		2	
	O	O		O				O	O											O		2	
71·72	O	O		O			O	O	O			O					O			O		4	D 2
	O	O		O				O	O											O		2	
71·79	O	O		O			O		O		O				O					O		4	

Table 1 (cont.):- Assemblage lists:-
Garnet pelite lithology (cont.)

	q	olig	phl	brbi	grbi	clin	chl	mu	g	cz	ep	cc	dol	tre	hbl	ta	sph	rut	pyr	ilm	gr		
71·81	O	O						O	O	O					O					O		4	C 3
71·84	O	O		O					O		O				O					O		3	
71·85	O	O			O			O	O		O				O					O		4	C 3
	O	O			O		O	O	O		O							O		O		4	D13
71·86	O	O		O			O	O	O											O		3	D1-2
72·3	O	O		O			O	O	O		O									O		4	D13
72·4	O	O			O		O	O	O		O									O		4	D13
72·5	O	O		O			O	O	O								O					3	D1-2
72·6	O	O		O			O	O	O		O									O		4	D13
72·7	O	O		O			O	O	O		O									O		4	D13

Graphitic lithology

	q	olig	phl	brbi	grbi	clin	chl	mu	g	cz	ep	cc	dol	tre	hbl	ta	sph	rut	pyr	ilm	gr		
B108	O	O		O			O	O		O			O					O		O	O	4	D 2
B109	O	O		O		O			O	O		O	O								O	5	D4-8-8-9
B370	O	O		O			O	O		O			O					O			O	4	D 2
B372	O	O		O				O	O											O	O	2	
B373	O	O		O		O		O											O			2	
	O	O		O				O	O									O		O	O	2	
B374	O	O		O		O		O	O										O			3	D1-2
	O	O		O				O	O									O			O	2	
B375	O	O		O			O		O	O									O		O	3	D 8-9
B376	O	O		O		O			O	O		O						O			O	4	D 8
B377	O	O		O			O	O	O	O										O	O	4	D13
70·45	O	O		O		O		O	O										O		O	3	D1-2
	O	O		O		O		O				O	O					O	O		O	4	D 3
70·47	O	O		O		O		O	O	O								O		O	O	4	D13
71·20	O	O		O		O		O		O		O	O						O		O	5	D 3-5-6-7
71·22	O	O		O			O	O	O													3	D1-2
71·25	O	O		O						O		O	O						O		O	3	D 7-8

Table 1 (cont.):- Assemblage lists:- Epidote pelite lithology

	q	olig	phl	brbi	grbi	clin	chl	mu	g	cz	ep	cc	dol	tre	hbl	ta	sph	rut	pyr	ilm	gr		
B122	O	O			O			O	O		O									O		3	D 8-9
B123	O	O			O			O	O		O									O		3	D 8-9
	O	O			O			O			O	O								O		3	D 7-8
B125	O	O		O				O			O		O							O		3	D 6-7
B126	O	O	O									O	O					O		O		2	
B127	O	O		O				O			O	O	O					O		O		4	D7
B128	O	O		O			O				O		O					O		O		3	D6-9
B129	O	O	O			O				O			O					O				3	D6-7
B134	O	O		O				O			O									O		2	
B156	O	O		O				O			O	O	O							O		4	D7
B200	O	O			O			O	O		O									O		3	D 8-9
B202	O	O			O		O	O	O									O		O		3	D1-2
B205	O	O		O			O				O		O					O		O		3	D6-9
B218	O	O			O			O			O		O					O		O		3	D6-9
B219	O	O		O			O	O												O		2	
B221	O	O		O			O	O	O		O									O		4	D13
B329	O	O			O		O	O	O		O									O		4	D13
B331	O	O			O		O	O	O		O									O		4	D13
B332	O	O	O				O			O							O	O				2	
B336	O	O			O			O	O		O									O		3	D 8-9
B338	O	O		O				O	O											O		2	
B363	O	O		O			O	O	O		O									O		4	D13
70·59	O	O		O				O			O									O		2	
70·75	O	O		O			O	O	O		O								O			4	D13
	O	O		O			O	O				O						O		O		3	D1-3
70·78	O	O			O		O	O	O		O									O		4	D13
71·41	O	O						O			O		O					O				3	D6-7
71·42	O	O																				4	D12
71·43	O	O			O		O	O			O											3	D6-7
71·44	O	O	O							O							O	O	O			3	D7-8
71·48	O	O	O		O					O		O	O				O	O				3	D12
71·54	O	O						O			O	O	O							O		4	D7
71·55	O	O	O					O			O	O	O				O			O		4	D7
71·59	O	O	O								O	O	O					O		O		4	D12
	O	O	O		O		O				O									O		3	D5-6
71·62	O	O	O					O			O	O	O				O	O				4	D7
71·63	O	O	O		O								O					O				2	
71·64	O	O																		O		4	D7
71·65	O	O	O										O							O		2	
71·67	O	O									O		O					O				3	D6-9

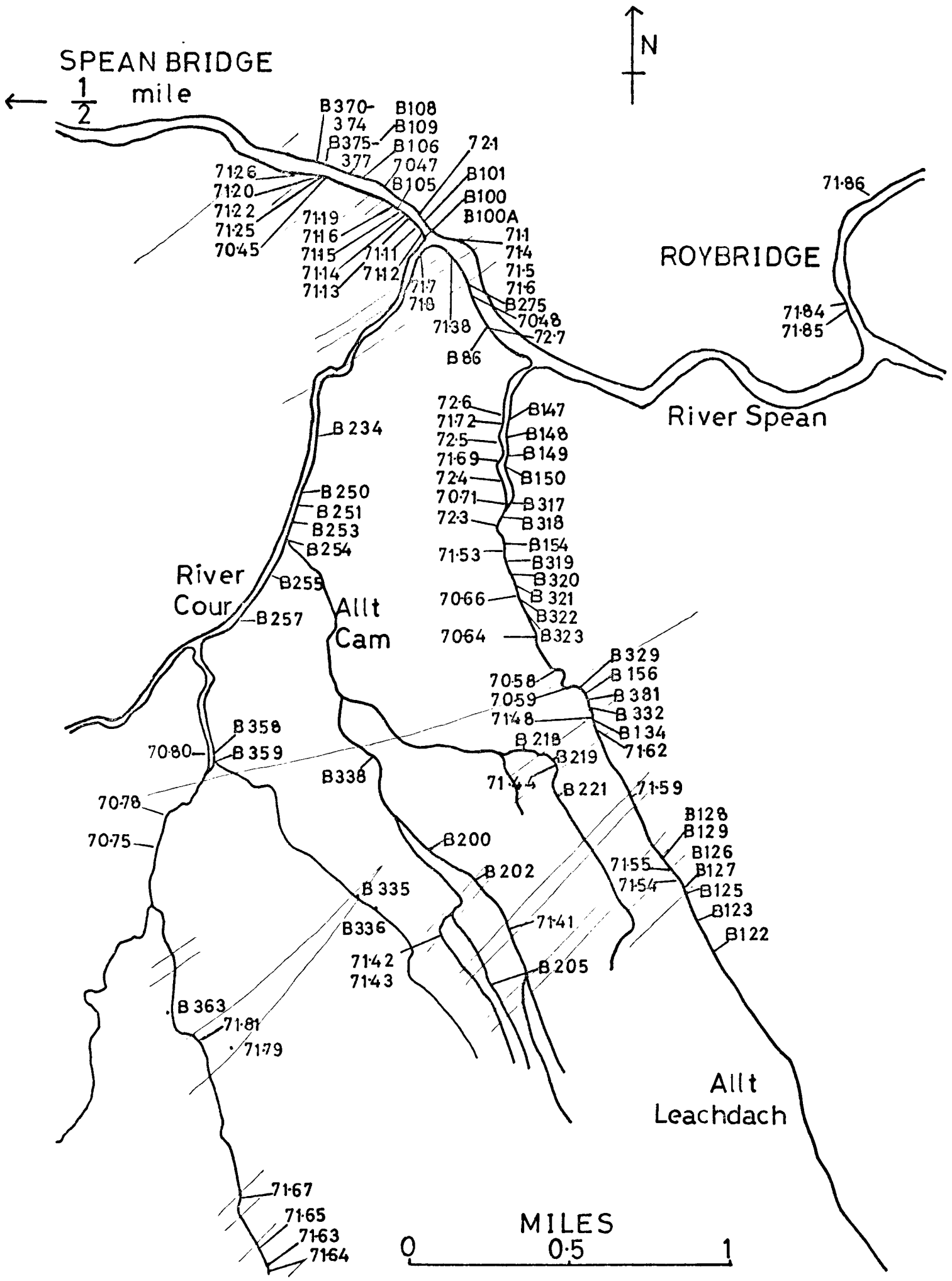


Fig. 3 :- Specimen locations of rocks in Table 1. Fine lines are geological boundaries from Fig. 1.

the number of independent reactions has to be included in the phase rule, eg. in Chapter 2. It is impossible to calculate the variance of a mineral assemblage. There is no way of telling which oxides are components in the phase rule sense. For example, in siliceous dolomites, CaO and SiO_2 are components but are MnO or SrO, There is also no way of telling if the chemical potentials of any of the components are controlled externally to the assemblage (the system). With an assemblage like B100 it is only possible to say that the variance is low, not what the variance is.

A theoretical framework is needed. The simplest approach is to choose a model system which approximately describes the assemblages. The variance of any assemblage can then be described in terms of the model, which can be called a model variance. A model provides a theoretical framework within which to calculate the conditions of metamorphism.

The model used here is the system K_2O-MgO-Al_2O_3-SiO_2-CO_2-H_2O including the following components (with their abbreviations)

calcite (cc) $CaCO_3$

dolomite (dol) $CaMg(CO_3)_2$

talc (ta) $Mg_3Si_4O_{10}(OH)_2$

clinochlore (clin) $Mg_5Al_2Si_3O_{10}(OH)_2$

tremolite (tr) $Ca_2Mg_5Si_8O_{22}(OH)_2$

phlogopite (phl) $KMg_3AlSi_3O_{10}(OH)_2$

muscovite (mn) $KAl_3Si_3O_{10}(OH)_2$

anorthite (an) $CaAl_2Si_2O_8$

grossularite (gr) $Ca_3Al_2Si_3O_{12}$

clinozoisite (cz) $Ca_2Al_3Si_3O_{12}(OH)$

quartz (q) SiO_2

One advantage of this model system is that reasonable thermodynamic data exists or has been calculated in Chapter 3 for all the above components.

The FeO analogue system suffers from the paucity of reasonable thermodynamic data. No Fe components occur which are not analogues of Mg components so that no reactions will be excluded by considering the FeO free system.

From Table 1 every assemblage contains quartz, oligoclase and biotite so that the model system can be considered in terms of excess quartz, anorthite, and phlogopite. The phase rule components can then be chosen as

$$MgO\text{-}Al_2O_3\text{-}an\text{-}phl\text{-}q\text{-}H_2O\text{-}CO_2$$

the first two of which are virtual components. H_2O and CO_2 are taken as excess components rather than mobile components (whose chemical potentials are controlled externally to the system). This is based on the predominance of very low model variance assemblages, most easily explained by the assemblage buffering the composition of the vapour phase during metamorphism. This is considered further in the next chapter.

The effect of two excess components (H_2O and CO_2) occupying one excess phase (fluid) is to make the phase rule

$$w = C + 3 - p$$

where C is the number of independent components, excluding excess components

p is the number of phases, excluding excess phases

The physical variables in this model are pressure, P, temperature T, and the mole fraction of CO_2 in the vapour phase, X_{CO_2}.

A minimum of 3 immobile components make up a non-degenerate reaction. From the above phase rule the reaction is divariant. All the possible reactions in this model system are listed in Table 2; reactions are referred to in the text and in diagrams by the number labels. These reactions were calculated by the program REACTION, listed in Appendix 3. The next to last column in Table 1 gives the number of immobile components

No.	immobile components								excess components				
	cc	dol	ta	tr	mu	cz	gr	clin	an	q	phl	H_2O	CO_2
1						-4	1		5	-1		2	
2					5		4	3	-12	3	-5	-12	
3					5	16		3	-32	7	-5	-20	
4				2			-3	-2	5	-11		6	
5				1		-6		-1	10	-7		6	
6				8	15			1	-16	-35	-15	-12	
7				-6	-10		1		9	27	10	6	
8				-3	-5	2			2	14	5	2	
9			-10				3	6	-9	31		-44	
10			-5			6		3	-12	17		-10	
11			8		3			-3		-23	-3	4	
12			2		2		1		-3	-5	-2	-2	
13			1		1	2			-4	-2	-1	-2	
14			-5	1				2	-2	10		-4	
15			-5	3			-3		3	-1		2	
16			-5	3		-12			18	-4		8	
17			1	3	6				-6	-16	-6	-4	
18		-5					3	1	-4	-4		-4	10
19		-5				12		1	-19	-1		-10	10
20		4			3			1	-4	5	-3	-4	-8
21		3			1		-1			3	-1		-6
22		3			1	-4			5	2	-1	2	-6
23		5		-2				1	-1	15		-2	-10
24		-10		2			3		-3	-19		-2	20
25		-5		1		6			-9	-8		-4	10
26		1		-2	-3				3	10	3	2	-2
27		1	-2					1	-1	7		-2	-2
28		-6	2				3		-3	-11		-2	12
29		-3	1			6			-9	-4		-4	6
30		3	2		3				-3	-2	-3	-2	-6
31		2	1	-1						4			-4
32	-2						1		-1	-1			2
33	1					-2			3			1	-1
34	8				5			3	-8	7	-5	-12	-8
35	-3			1				-1	1	-7		3	3
36	1			-3	-5				5	14	5	3	-1
37	3		-5					3	-3	17		-7	-3
38	1		1		1				-1	-2	-1	-1	-1
39	-6		-5	3						-4		2	6
40	6	-5						1	-1	-1		-4	4
41	-2	3			1				-1	2	-1		-4
42	3	-5		1						-8		-1	7
43	3	-3	1							-4		-1	3

Table 2:- All the reactions in the model system, see text.

each assemblage would have in the model system, 5 components is invariant, 4 is univariant, 3 is divariant and so on. Nearly all the assemblages in Table 1 are divariant, univariant, or invariant. The addition of FeO into the model system would increase all the variances by one. It would also increase by one the minimum number of phases in a non-degenerate reaction. Each reaction would be a combination of any 2 reactions in Table 2 with two phases in common. The reaction coefficients would depend on the Fe/Mg ratio of the minerals. In the descriptions of assemblages below, considerable importance is attached to the lowest variance assemblages because they provide potentially most information for calculating metamorphic conditions.

The assemblages are subdivided in terms of the model system and described by lithology.

Textures

The textures of low variance assemblages were examined in thin section to find evidence of the reactions which can be written between the components of the phases in the modal system. Such interpretation is usually equivocal because textures can often be interpreted in more than one way and the absence of information in the third dimension is restricting.

Cross cutting textures, particularly between poikiloblasts can be interpreted as evidence of reaction or as two minerals growing at the same time and interfering. Poikiloblast minerals have been the products of reactions, although in some cases they have become reactants at a later time.

Carmichael (1969) introduces a useful model which he uses to interpret textures at isograds involving staurolite, kyanite, and sillimanite. His initial thesis is that the diffusion range of aluminium is an order of magnitude less than elements like silicon, sodium, potassium, and

magnesium during metamorphism. This is based on his observations of the absence of Al minerals in quartz veins, the preservation of fine scale banding with different mineral assemblages, and the close associations of minerals in parts of the same band, so that, in each small volume of rock, the concentration of Al is more-or-less constant, although the concentrations of other elements are discontinuous, for example, at poikiloblast boundaries. These arguments apply equally well to my rocks. This explains why, for example, garnets growing across banding are filled with different proportions of quartz inclusions, reflecting the different concentration of Al in the different bands.

Carmichael goes on to use this model to explain textures where the products of a reaction are not growing on the reactants. Coupled reactions allow reactions to occur when the direct replacement of reactants by products has a high activation energy, for example, kyanite sillimanite. Kyanite is digested and sillimanite grows in adjacent domains of the rock, though very rarely does sillimanite replace kyanite (eg. Chinner 1961). The coupled reaction in Chinner's rocks involves muscovite and quartz as catalysts; they are produced in one domain by the digestion of kyanite, but are digested in another domain, in the production of sillimanite. Carmichael's textures show that the different parts of the coupled reaction took place at constant aluminium concentration and that many of the phases in the rock took part (as catalysts) without appearing in the net reaction. In this way Carmichael suggests that late metamorphic recrystallization, as such, might be infrequent; the common equigranular matrix textures may instead be due to coupled reactions involving the matrix minerals as catalysts.

Coupled reactions can be invoked for textures where some of the minerals involved do not appear in the net reaction which can be written for the assemblage. This applies particularly where biotite is the only potassium phase and oligoclase the only sodium phase. Coupled reactions involving most of the phases in the rock allow equilibrium to be main-

tained between the phases under pressure-temperature-fluid composition changes because the phases will be continuously digested and regrown.

The presence of reaction textures does not imply disequilibrium if the variance of the assemblage is low enough to write reactions between the phases.

The suggestion that the vapour phase composition was buffered by the assemblage, given earlier in defining a phase rule for the model system, allows an interpretation of the textures. Starting with an assemblage with a certain composition vapour phase; on increasing temperature, a divariant reaction surface will eventually be intersected. The assemblage will move up the divariant surface converting reactants to products and changing the vapour phase composition. In this way univariant lines and even invariant points can be reached. This process can explain a sequence of rocks with predominantly low variance assemblages. Textures can be interpreted in terms of reaction paths on divariant surfaces, along univariant lines and even to invariant points.

Analytical data

Minerals were analysed for two purposes:

1. calcites and dolomites were analysed to apply the calcite-dolomite geothermometer.
2. all the phases in certain low variance assemblages were analysed to find the compositional departures from the components for which thermodynamic data exists.

All the analyses given later were obtained on the University of Durham, Geology Department Geoscan Mk II electron microprobe, with the kind permission of Professor G.M. Brown. The accelerating voltage was 15 kV. A defocussed beam about 15 microns across was used for the carbonates, otherwise the beam was about 2 microns across. Nine elements were analysed Si, Ti, Al, Fe, Mg, Ca, Mn, Na, K using as standards, wollastonite, specpure TiO_2, specpure Al_2O_3, specpure Fe,

olivine, wollastonite, specpure Mn, jadeite, and potassium feldspar, respectively. The analyses of the silicates (except potassium feldspar) are given in Sweatman and Long (1969). KAP was used as an analysing crystal for Mg, Na, Si and Al, LiF for Fe, Mn, Ti and Ca, and Qtz for K. The raw probe data (counts per 10 secs) were converted to apparent weight percent by the program PROCESS, listed in Appendix 3. The procedure of Boyd et al. (1968) was used for ZAF corrections.

X-ray diffraction can give the % $MgCO_3$ in calcite using the linear change in position of the calcite peaks with % $MgCO_3$ (Goldsmith et al. 1955). The only intense peak, d_{1014}, occurs at about 29.7° 2θ, and its % $MgCO_3$ dependence is small (about 3.2% $MgCO_3$ per 0.1° 2θ) requiring precise measurements. The diffractometer is however non-linear at least between 28° and 30° 2θ, evidenced by comparative runs on well-known standards; also the non-linearity varies from day to day (pers. comm. M.J. Bickle). The method was abandoned.

The carbonates were analysed by probe for Ca, Mg, Fe and Mn. The analyses of carbonates invariably have low totals between 95.5 - 98.0%. Although polished carbonate surfaces invariably browned within 20 seconds under the electron beam, the counts per second did not change til after 2 or 3 minutes and then they decreased very slowly. A secondary standard, a clear pure calcite, was analysed and the total was 98.1%. Assuming that its total should be 100%, the 1.9% discrepancy is presumed to be due to the decomposition process under the beam. The elements of the carbonate analyses have been increased so that the totals are increased by 1.9%. Many analyses are still too low and this may be explained by the presence of fluid inclusions or that the decomposition process is composition dependent.

In assemblages where all the phases have been analysed, all 9 elements have been analysed. 'Unnecessary' elements were analysed as tracers for inclusions or adjacent grains because of the fine grain size of the rocks. Mineral separation and wet chemical analysis for Fe^{3+} was not

undertaken for the following reasons:

1. From thin sections and hand specimens, assemblages are different in adjacent bands. Moreover in homogenous assemblage rocks, compositions of coexisting minerals change over millimetre distances. At best, an analysis of a separated mineral would be an average for one assemblage; often it would be the average over several assemblages.
2. The fine grained size of the rocks and the inclusion filled nature of the poikiloblasts would provide problems for separation.
3. The minerals have been analysed so that the activities of components in the minerals can be calculated. These activities are needed in the calculation of metamorphic conditions. However, the calculation of activities from analyses is, at best, approximate (a model is adopted in the next chapter). Moreover the calculations are in the Fe free system; the amount of Mg in the recalculated analysis is not strongly dependent on the Fe^{3+}/Fe^{2+} ratio.

In the recalculation of analyses (by the program RECALC, given in Appendix 3), the amount of Fe^{3+} in epidote and garnet is calculated on a site occupancy criterion; enough Fe^{2+} is converted to Fe^{3+} to fill the 'Al' site, with Al left over from filling the 'Si' site. For the other phases, the proportion of Fe^{2+} to be converted to Fe^{3+} has been guessed; 20% for chlorite, 15% for biotite, 85% for muscovite, 5% for talc, 20% for amphibole, 50% for sphene and plagioclase.

Each mineral was usually analysed in quintuplicate; one of each set is listed (in Appendix 5) and the range of values is given in the text. Care was taken to analyse minerals within a band and, if possible, within a few millimetres of each other.

Assemblages

As stated previously all the assemblages are listed in Table 1. The basic subdivision used is

Group 1 : amphibole and/or talc bearing assemblages

Group 2 : amphibole and talc absent assemblages.

Although this subdivision is arbitrary, particularly in the garnet pelite facies, it simplifies the discussion of the assemblages. The second group includes nearly all the assemblages in the garnet pelite, epidote pelite and graphitic lithology but it is not subdivided at this stage to emphasise the coherence of the group, although the textures in each lithology are different.

The rocks in each of these groups will be divided into subgroups and described in terms of petrographical, textural, and analytical data for a few typical assemblages in each subgroup. The textures will be interpreted in terms of reactions in the model system.

Group 1

This group includes all the siliceous dolomite lithology rocks, the only rocks in the area containing talc, plus the few amphibole bearing assemblages in the garnet pelite lithology, see Fig 4.

Talc + tremolite subgroup

This subgroup includes all the normal siliceous dolomite lithology assemblages. The most important assemblage is

q + olig + phl + clin + cc + dol + ta + tre ± sph ± rut

typified by B100 and all the rocks outcropping at the mouth of the Cour and is model invariant. Closely related to B100 are the model univariant assemblages without talc (eg 71.13) or without tremolite (eg 71.7 and the model divariant assemblage without talc or tremolite (eg 71.11) (which theoretically belongs to the other main group but is texturally related to this subgroup).

Many of the Siliceous dolomite lithology rocks consist of a fine grained and a coarse grained part, eg B100, which is desribed here. see Plate 1

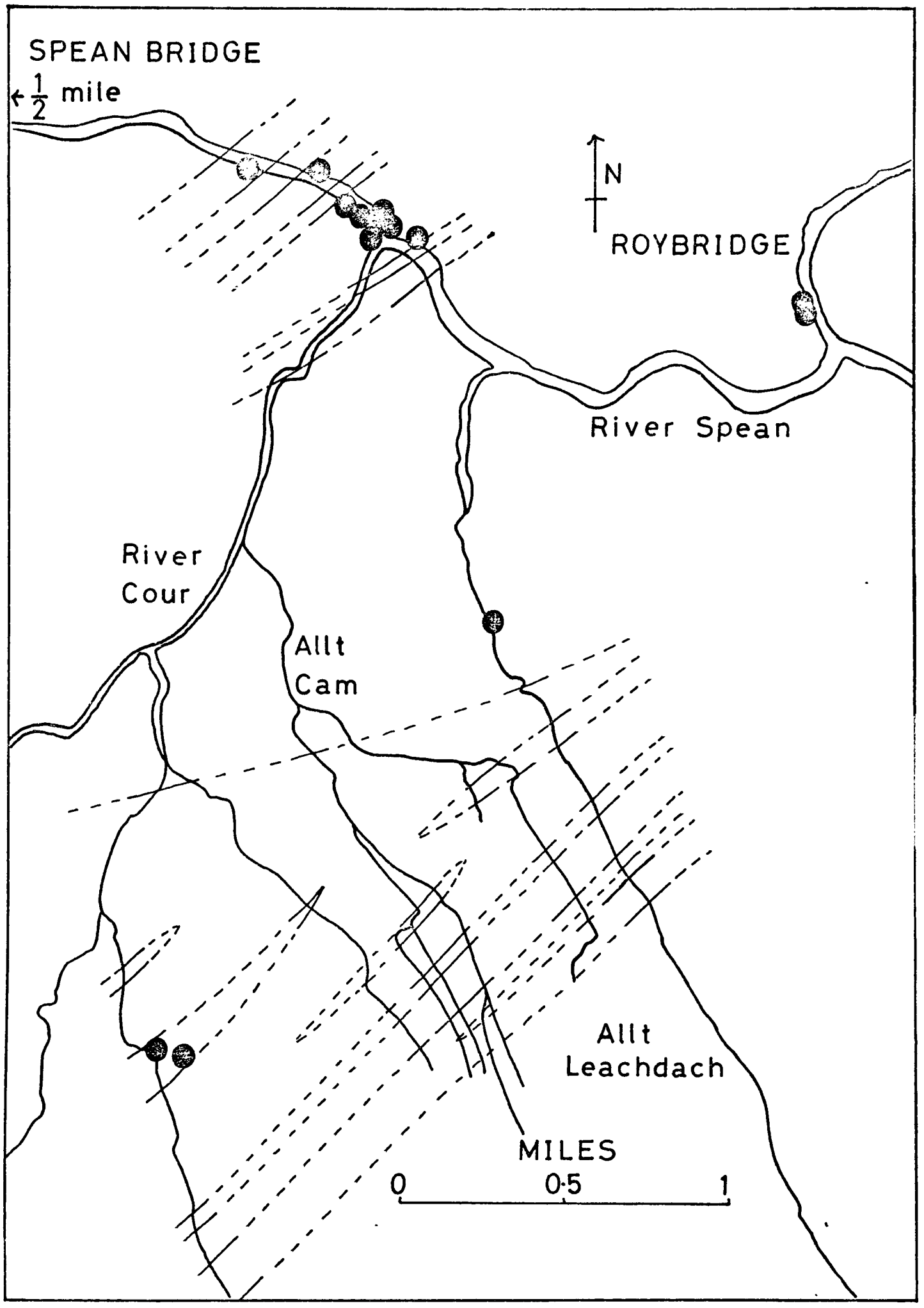


Fig. 4 :- Occurrence of amphibole bearing model univariant and divariant assemblages



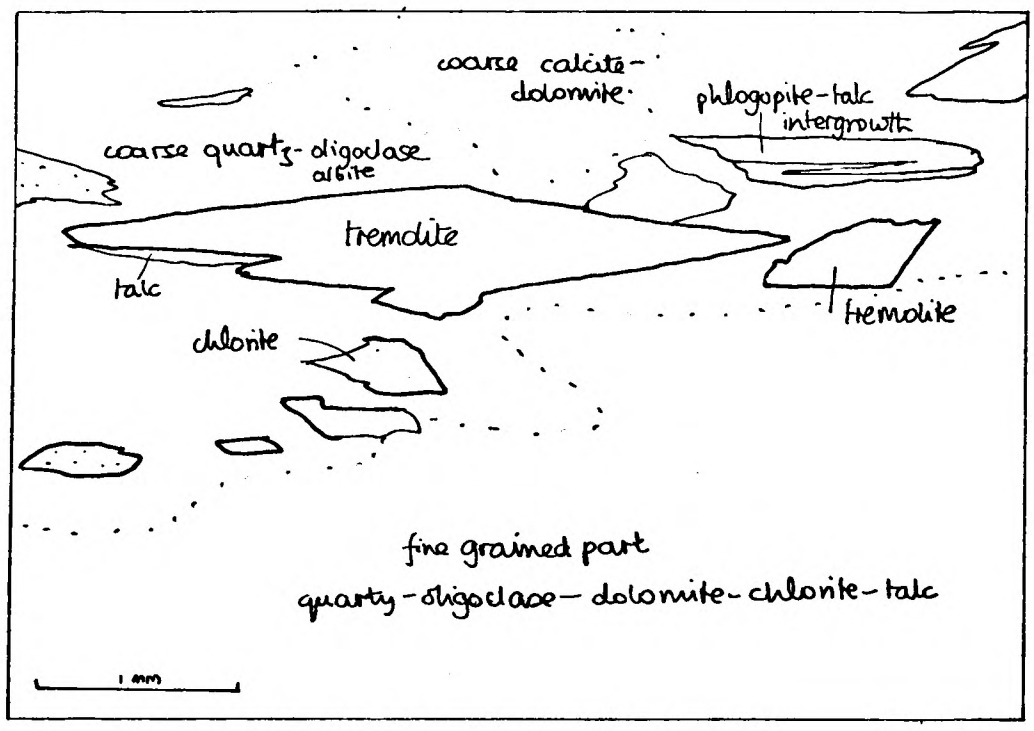


Plate 1:- B100 : an example of a siliceous dolomite.

The coarse grained part forms lenseid or elongate irregular areas within the fine grained part. It consists of coarse equigranular polygonal quartz, plagioclase, (albitic plagioclase around small oligoclase cores) calcite and dolomite (about 0.3 mm. across) with large orientated colourless laths of phlogopite, colourless chlorite, talc, phlogopite-talc intergrowths and phlogopite-chlorite intergrowths (up to 1.5 mm. long) and tremolite porphyroblasts (up to 2 cm. long).

The fine grained part consists of equigranular quartz, dolomite ± calcite (about 0.04 mm. across with small orientated colourless laiths of biotite (up to 0.06 mm. long). Calcite, oligoclase (with thin albitic rims) and tremolite poikiloblasts occur. They contain carbonate and quartz inclusions. The zoning in the plagioclase in the coarse and fine grained part is strongly discontinuous. The majority of rocks in this subgroup contain sphene and/or rutile. Sphene occurs as ragged small poikiloblasts (0.08 mm. across) with quartz inclusions. Rutile occurs as small prisms (up to 0 06 mm. long), either distributed through the rock, together in localised aggregates with quartz (after sphene?), or rarely, replacing sphene (eg. frontispiece).

The relationship between the coarse and fine grained part is not clear.

Chlorite, talc, and tremolite occur as large well-formed almost inclusion free grains in the coarse grained part and sometimes projecting from the coarse grained part into the fine grained part or within the fine grained part. These minerals also occur in domains of the fine grained part as much smaller irregular grains or as poikiloblasts. This contrast is particularly strong for tremolite, see Fig 6a.

In the fine grained part talc, chlorite, oligoclase, tremolite and calcite overgrow the matrix. They are the products of reactions involving the matrix as reactants. They do not all occur together in each domain of the fine grained part.

Oligoclase poikiloblasts, eg Fig 5a, occur when talc and/or tremolite are present and usually do not occur with calcite poikiloblasts. They contain sparse carbonate and quartz inclusions, but not phlogopite which is truncated by the poikiloblasts. Calcite poikiloblasts, eg Fig 5b, usually occur with chlorite. They contain sparse quartz and dolomite inclusions, but not phlogopite which is truncated by the poikiloblasts. Fig 6b shows a complicated texture which appears to involve the digestion of chlorite and matrix to produce talc and oligoclase.

Although cc - dol - ta - tr - clin might all occur within one domain of the fine grained part, the distribution of phases suggest that only some three or four phase combinations of these occur,

dol + ta + clin ± tr

cc + dol + clin ± tr

The above assemblages without tremolite are divariant, and a balanced reaction can be written for each,

dol + clin + q = ta + an + H_2O + CO_2 no 27

dol + an + q + H_2O = clin + cc + CO_2 no 40

Reaction 27 explains the texture in Fig 6b. Reaction 40 explains the presence of calcite poikiloblasts in different domains to oligoclase poikiloblasts.

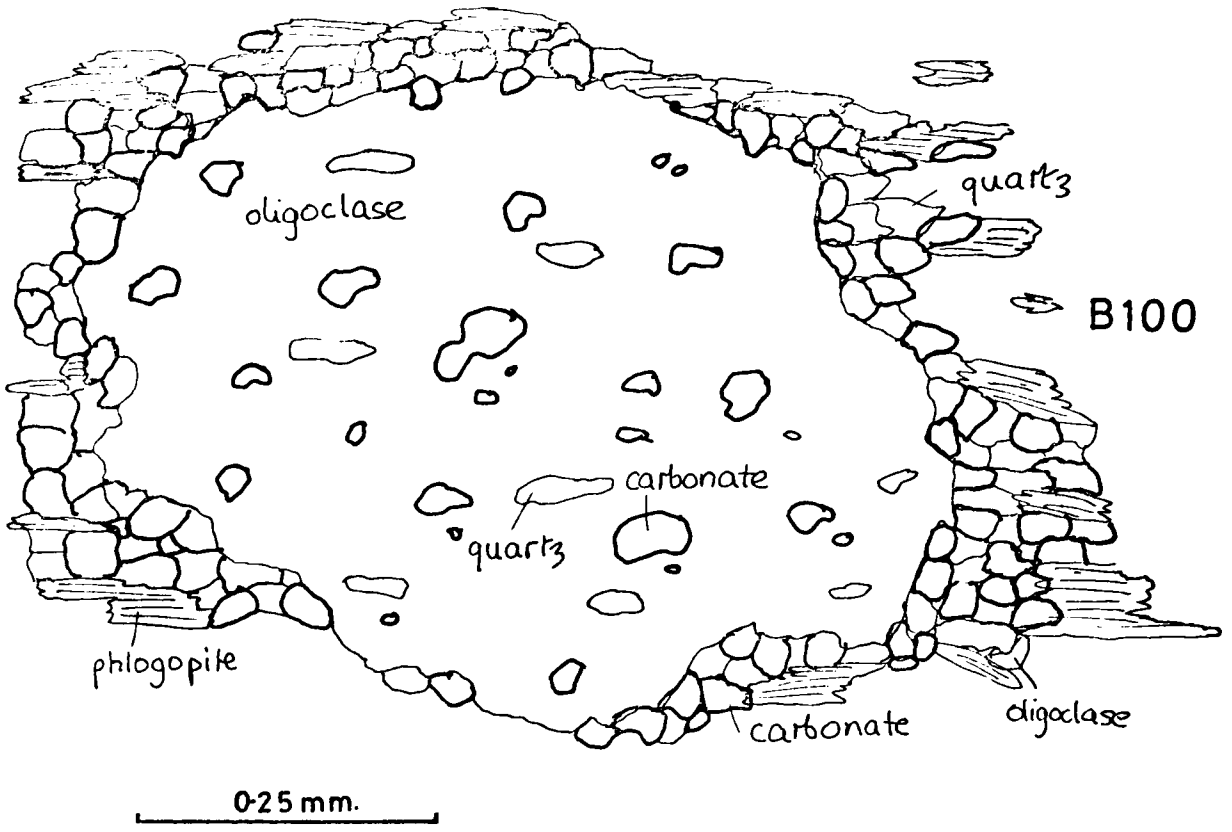
The addition of tremolite makes the assemblages model univariant. The growth of tremolite probably relates to,

dol + clin + q = tr + an + H_2O + CO_2 no 23

cc + clin + q = tr + an + H_2O + CO_2 no 35

These reactions account for the association of tremolite and oligoclase poikiloblasts. The reaction path to the model univariant assemblages probably involved reactions 27 and 40.

The coarse grained part appears to have been recrystallised in that the quartz, plagioclase, calcite and dolomite form characteristic coarse polygonal textures and the micas occur along the grain boundaries.



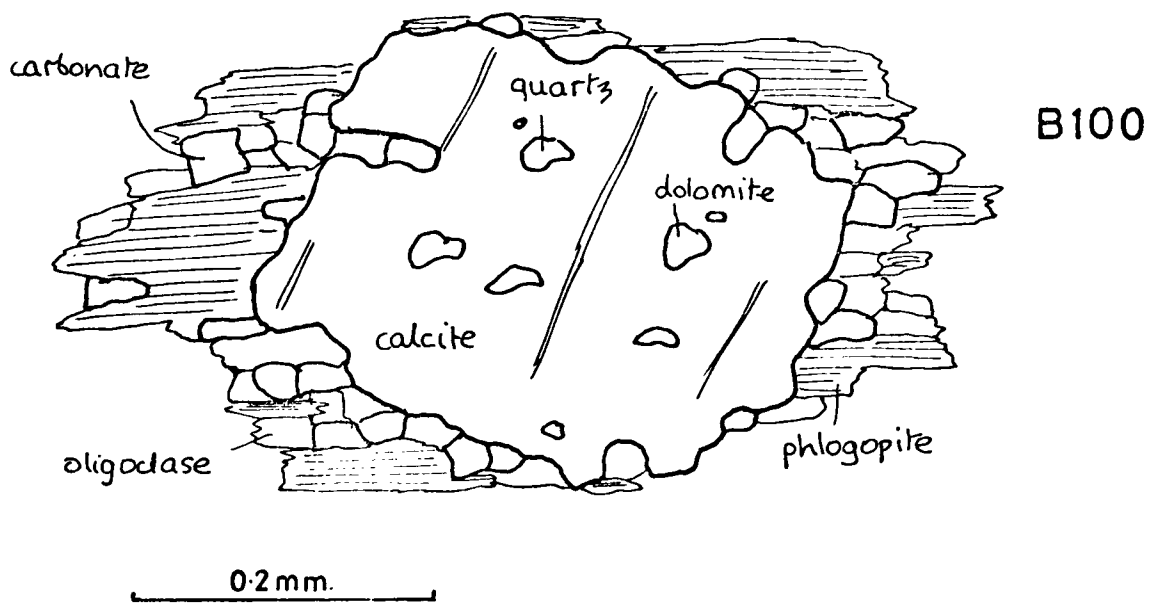
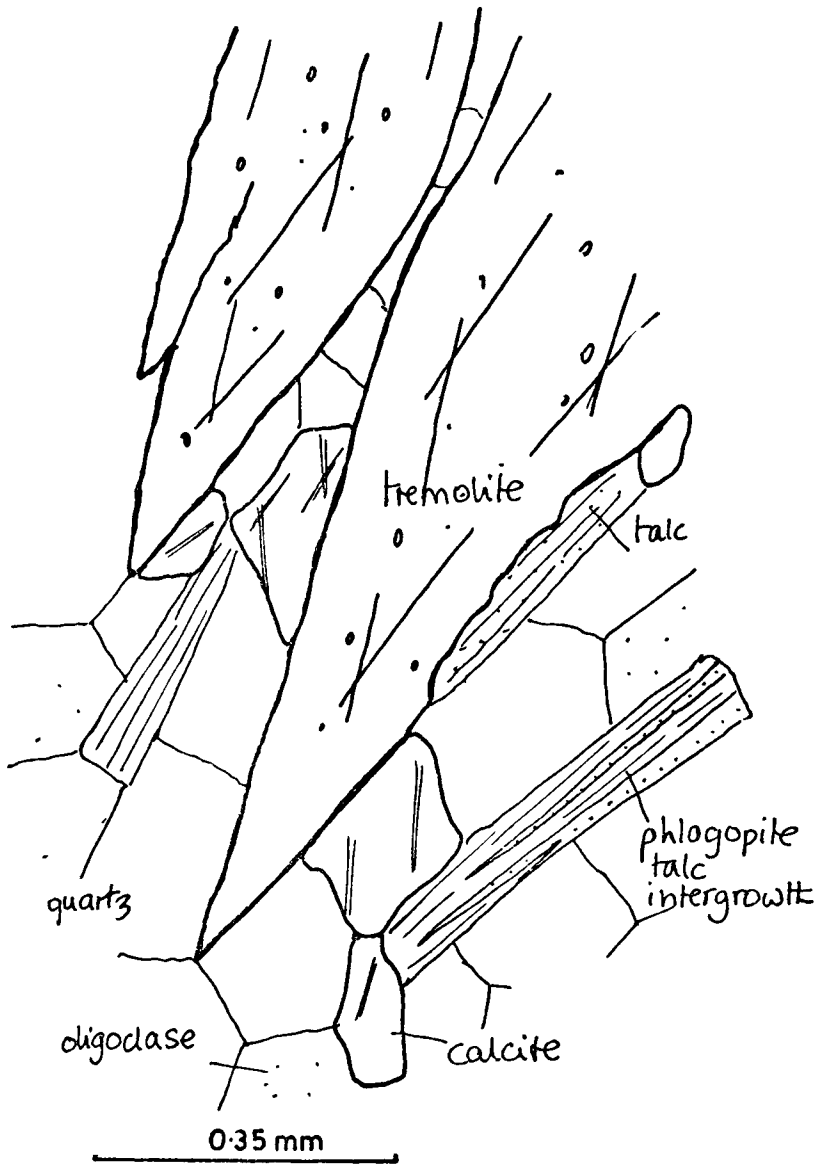
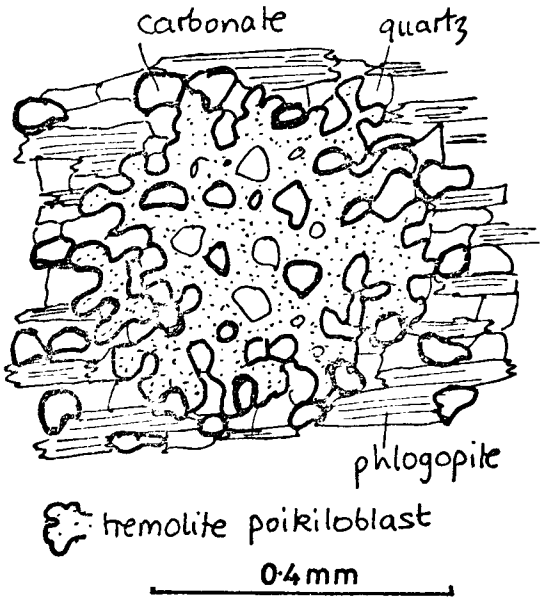


Fig. 5 :- Textures 1





B100

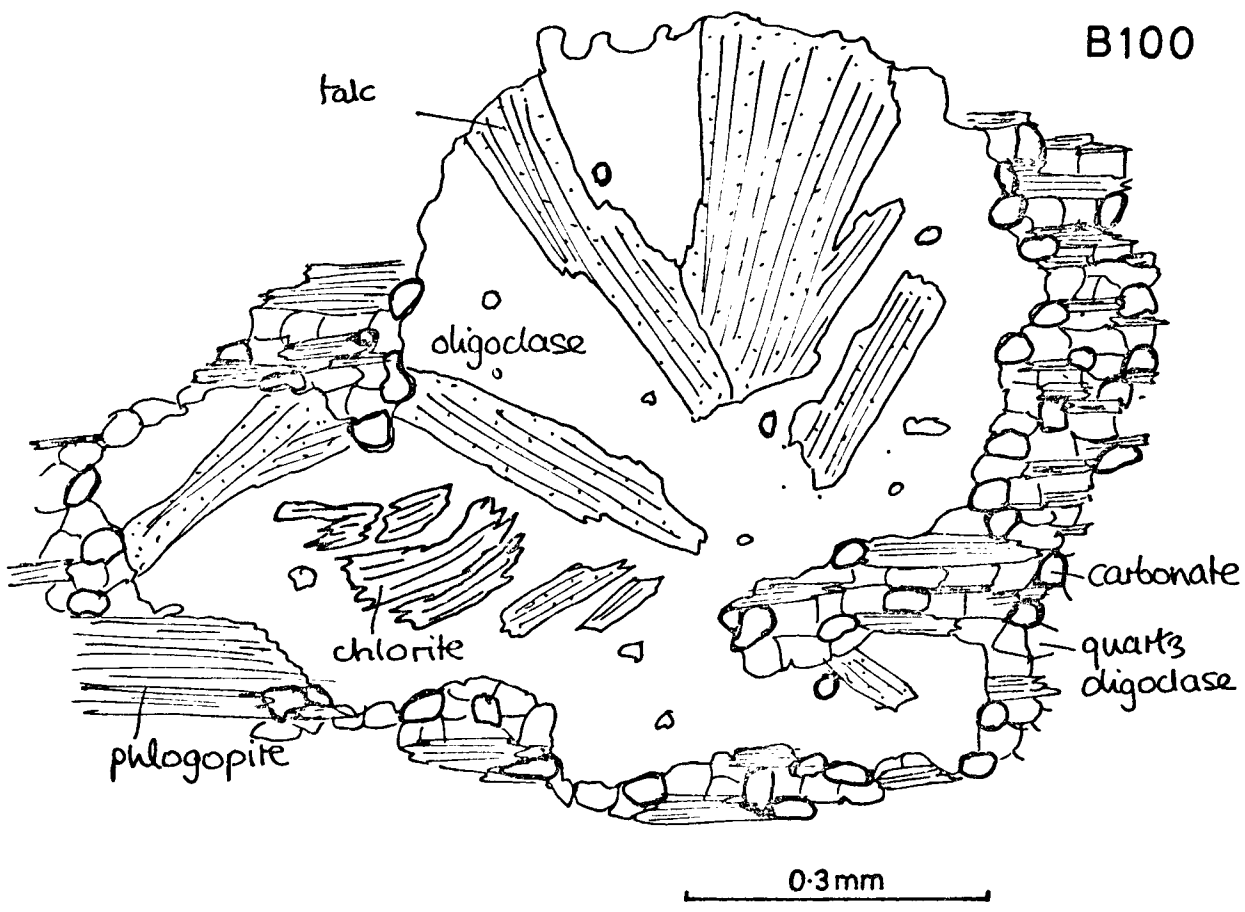


Fig. 6 :- Textures 2

As mentioned above the micas and tremolite have different forms in the coarse grained part compared with the fine grained part. There is no textural evidence for reactions. Tremolites appear to cross all minerals but this may be due to the other minerals recrystallising around them or while the tremolites were growing, rather than the late growth of tremolite. Some of the talc appears to be replacing tremolite. The calcite-dolomite geothermometer results for B100 and related rocks suggest that the recrystallisation (and reequilibration of the calcites) occurred at a lower temperature than the calcite-dolomite temperatures from unrecrystallised rocks (eg 71.19). The suggestion is made that the assemblage in the coarse grained part and the minerals with the same habit in the fine grained part formed during this lower temperature recrystallisation. This is supported in the next chapter

The analyses for the carbonates in B100, 71.16 and 71.26, are listed in Appendix 5. The compositions are discussed and used for calcite-dolomite geothermometry in the next chapter. An analysis of each of the other minerals in B100 (except quartz) are given in Appendix 5. The ranges of composition are given below in terms of the elements in the corresponding model system phases.

biotite $K_{0.87-0.90}\ Mg_{2.59-2.65}\ Al\ Si_{2.98-3.02}\ O_{10}\ (OH)_2$

chlorite $Mg_{4.50-4.58}\ Al_2\ Si_{2.80-2.85}\ O_{10}\ (OH)_8$

talc $Mg_{2.88-2.92}\ Si_{3.96-4.01}\ O_{10}\ (OH)_2$

tremolite $Ca_{1.92-1.96}\ Mg_{4.60-4.66}\ Si_{7.60-7.70}\ O_{22}\ (OH)_2$

oligoclase $Na_{0.75-0.77}\ Ca_{0.21-0.22}\ Al_{1.20-1.23}\ Si_{2.76-2.80}\ O_8$

rutile $Ti_{0.96-0.98}\ O_2$

Tremolite and clinozoisite subgroup

The assemblage in 71.19 is model invariant and contains

q - olig - brbi - clin - cz - cc - dol - tre - sph - pyr - gr.

It occurs within the siliceous dolomite lithology but is transitional to the graphitic lithology in that it contains clinozoisite and graphite but not talc.

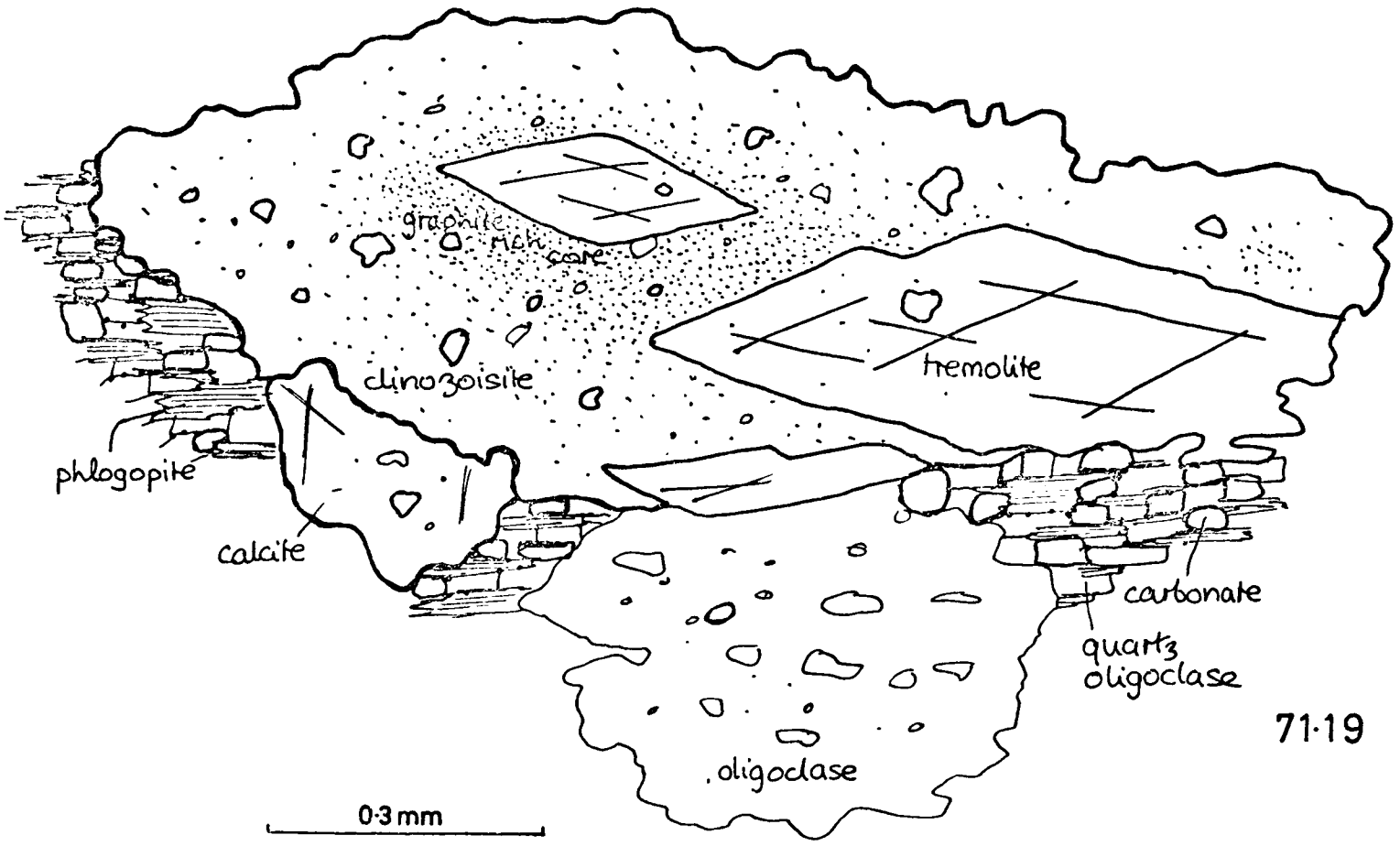
The rock is made of a coarse and a fine grained part similar to B100. The coarse grained part forms pods of graphite free equigranular polygonal texture quartz and oligoclase (0.2 mm. across) with light brown pleochroic biotite and colourless chlorite laths (up to 0.3 x 0.06 mm) alligned with the matrix micas.

The fine grained part is made of elongate quartz and oligoclase (about 0.05 x 0.01 mm) with equigranular calcite and dolomite (about 0.03 mm) with orientated light brown pleochroic biotites and colourless chlorites (0.03 x 0.3 mm) and very fine grained graphite. Oligoclase, calcite, tremolite and clinozoisite poikiloblasts overgrow the matrix. The amount of graphite in the poikiloblast cores is considerably greater than in the matrix.

The oligoclase and calcite poikiloblasts closely resemble those in B100 eg Figs 5a, b; however, calcite poikiloblasts are rarer and oligoclase poikiloblasts are more abundant. The tremolites are more prismatic and less poikiloblastic than in the fine grained part of B100.

The relations between the poikiloblast minerals indicate the reactions which took place. Figs 8a,b show two textues involving tremolite and clinozoisite. In Fig 7a, a tremolite is growing within a ragged clinozoisite poikiloblast. The core of the clinozoisite is packed with graphite yet the tremolite is graphite free. In Fig. 7b tremolite is growing around and within clinozoisite. The tremolite within the clinozoisite could be interpreted as relics of digestion but for the perfect prismatic habit. The oligoclase poikiloblast in Fig 8a may have been growing at the same time as the tremolite.

The assemblage is model invariant. The sequence of reactions producing this assemblage involved first the growth of clinozoisite



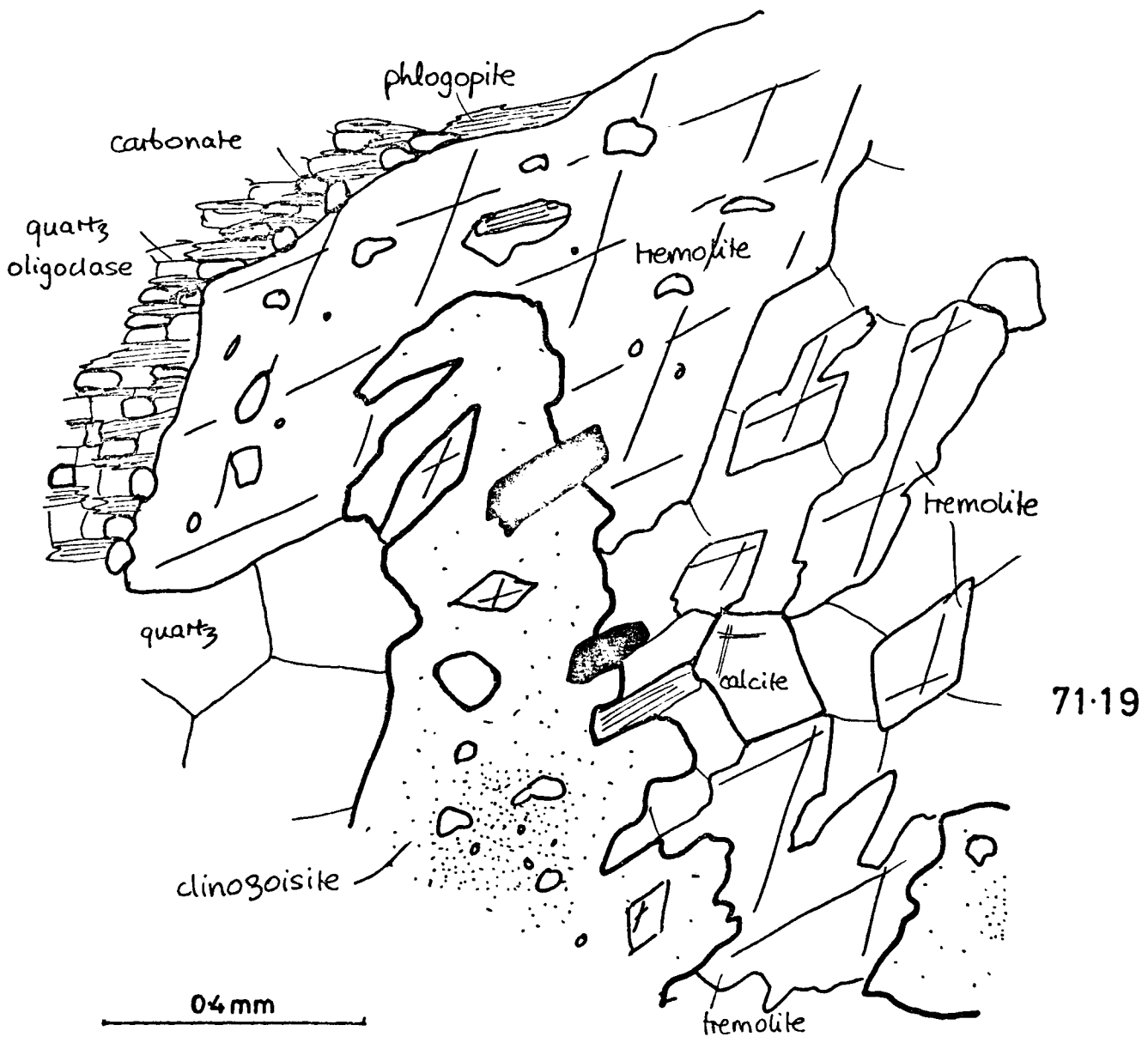


Fig. 7 :- Textures 3

from the matrix, then the growth of tremolite from the matrix and from clinozoisite and the growth of oligoclase from the matrix. The first reaction cannot be accommodated in the model system with the phases that now occur in the assemblage. If, for example, muscovite was originally present, then the clinozoisite (and phlogopite) could have grown by the reaction,

$$cz + phl + CO_2 = dol + mu + an + H_2O \qquad \text{no 22.}$$

The reaction producing tremolite from the matrix could have been

$$clin + cc + q = tr + an + CO_2 + H_2O \qquad \text{no 35}$$

$$\text{or} \quad clin + dol + q = tr + an + CO_2 + H_2O \qquad \text{no 23.}$$

The reaction represented by Fig 8a,b is probably

$$cz + clin + q = tr + an + H_2O \qquad \text{no 5}$$

These three reactions account for the tremolite and oligoclase poikiloblasts.

Another important reaction which took place is the oxidation of graphite to CO_2, evidenced by the dense graphite occuring in poikiloblast cores, and the graphite-free tremolite grown from graphite-rich clinozoisite. The presence of graphite has important consequences in the calculation of metamorphic conditions, because the vapour phase can no longer be treated as being dominantly CO_2 and H_2O in the C-H-O system. This will be considered in the next chapter.

The analysed carbonates from 71.19 are listed in Appendix 5. They are discussed and used for calcite-dolomite geothermometry in the next chapter. An analysis of each of the other minerals in 71.19 is listed in Appendix 5. The compositional ranges are given below.

biotite $K_{0.90-0.93}\ Mg_{2.24-2.27}\ Al\ Si_{2.84-2.87}\ O_{10}\ (OH)_2$

chlorite $Mg_{4.10-4.16}\ Al_2\ Si_{2.70-2.73}\ O_{10}\ (OH)_8$

tremolite $Ca_{1.80-1.83}\ Mg_{3.80-3.82}\ Si_{7.11-7.14}\ O_{22}\ (OH)_2$

clinozoisite $Ca_{1.99-2.01}\ Al_{2.87-2.90}\ Si_{2.95-2.97}\ O_{11}\ (OH)$

sphene $Ca_{0.98-1.00}\ Ti_{0\ 93-0\ 96}\ Si_{0.99-1.02}\ O_5$

oligoclase $Ca_{0.20-0.22}\ Na_{0.77-0.79}\ Al_{1.20-1.23}\ Si_{2.76-2.78}\ O_8$

Amphibole bearing garnet pelite subgroup

This subgroup contains the model invariant assemblage of B323

q - olig - brbi - mn - g - ep - cc - hbl - ilm

and the model univariant assemblage of 71.79

q - olig - gr bi - chl - g - ep - hbl - ilm

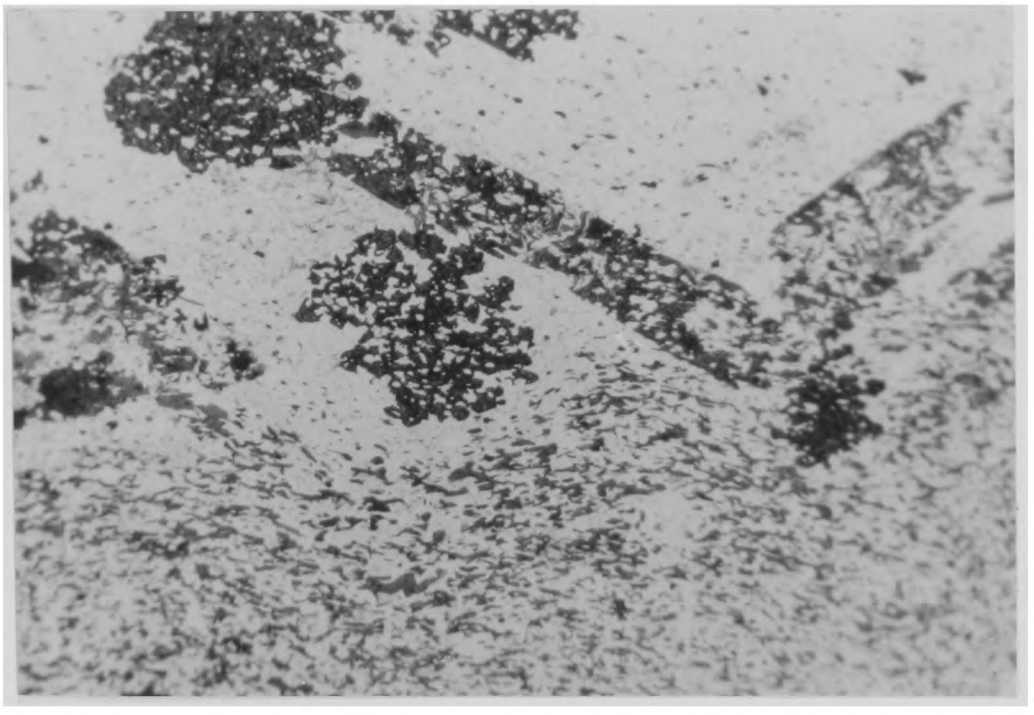
and several higher variance assemblages derived from these.

The rocks are characterised by poikiloblastic biotite, hornblende, and garnet (up to 5 mm. across) which has overgrown a matrix of fine grained equigranular polygonal oligoclase and quartz (0.1 mm. across) with orientated muscovite or chlorite laths (up to .4 x .05 mm) and small epidotes (up to .3 x 0.05 mm) usually with allanite cores, see plate 2. Matrix calcite occurs only in B323. It forms small ragged poikiloblasts often replaced by biotite. Calcite inclusions occur in the cores of garents in 71.79 and 71.85.

Because the poikiloblast biotite, hornblende and garnet overgrow the matrix and contain few inclusions; the reactions producing these phases must involve the matrix, either as reactants or as catalysts of coupled reactions. Epidote however, occurs within the hornblende and biotite poikiloblasts as well as in the matrix so may have grown later.

Where garnets would contact hornblende poikiloblasts, a coarse grained 'vein' of quartz and oligoclase occurs, see Fig. 8a. It is not clear whether this is a pressure shadow effect or evidence that garnet and hornblende are no longer stable in contact. The only textural evidence for reactions taking place is shown in Fig 8b, where biotite is replacing a calcite poikiloblast. Elsewhere, garnet poikiloblasts appear to cross-cut biotite. Although this may be two minerals that grew together, a possibility is that a coupled reaction took place. The net reaction being

$q + an + cc = gr + CO_2$ no 32.



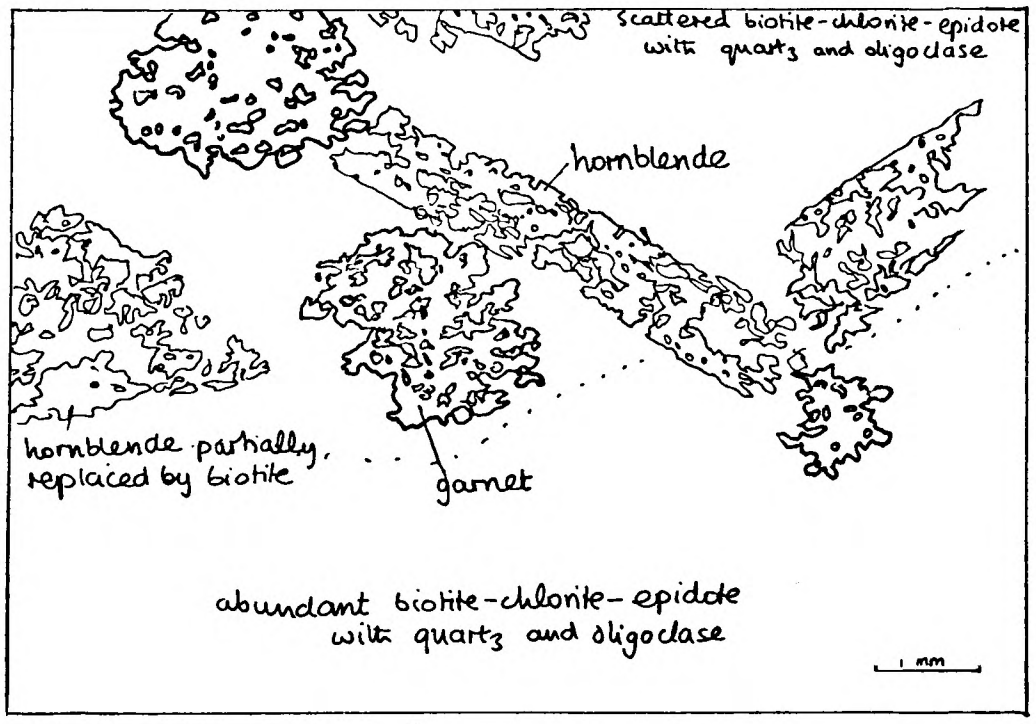
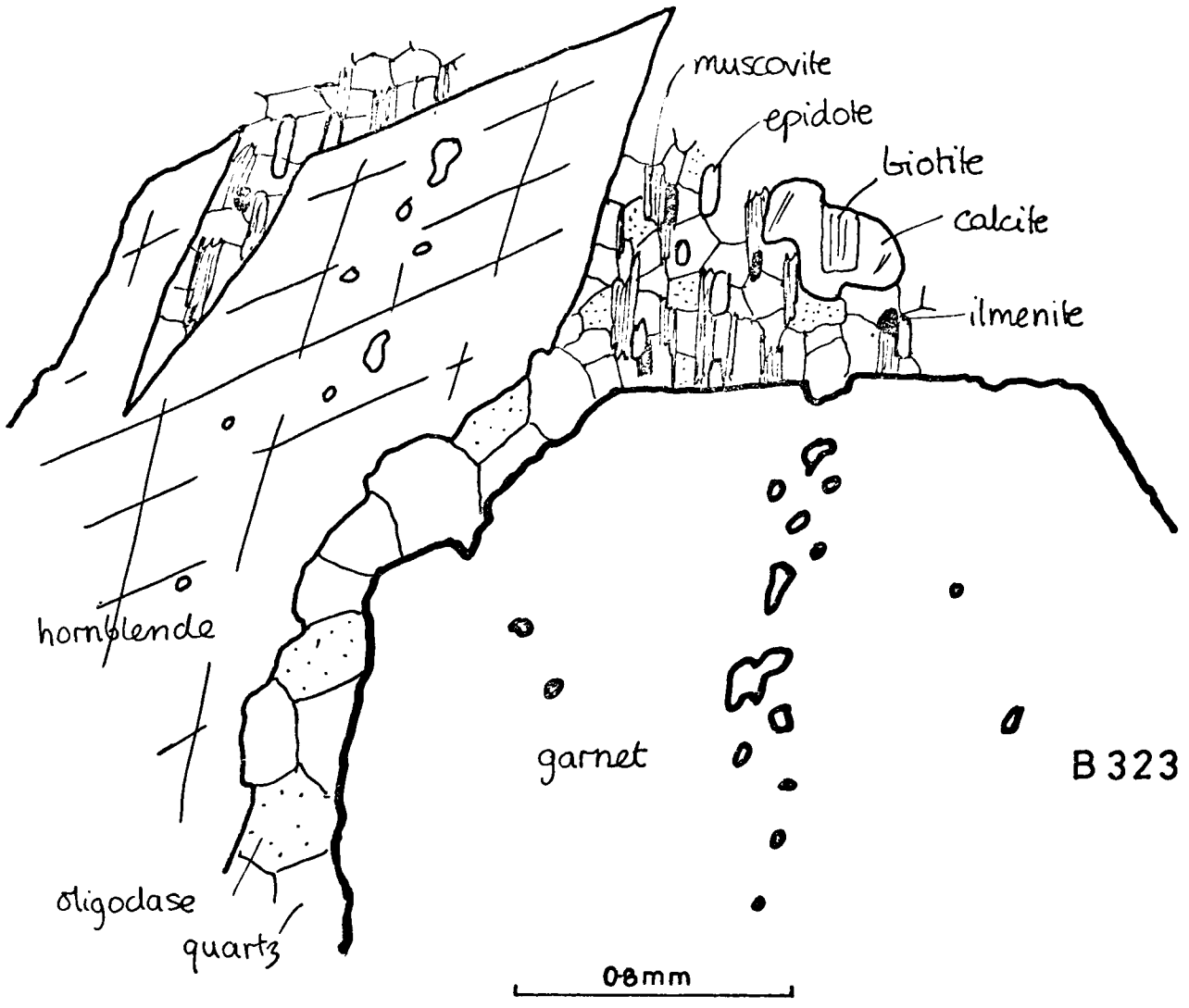


Plate 2 :- 71·79 : an example of a hornblende - bearing garnet pelite.



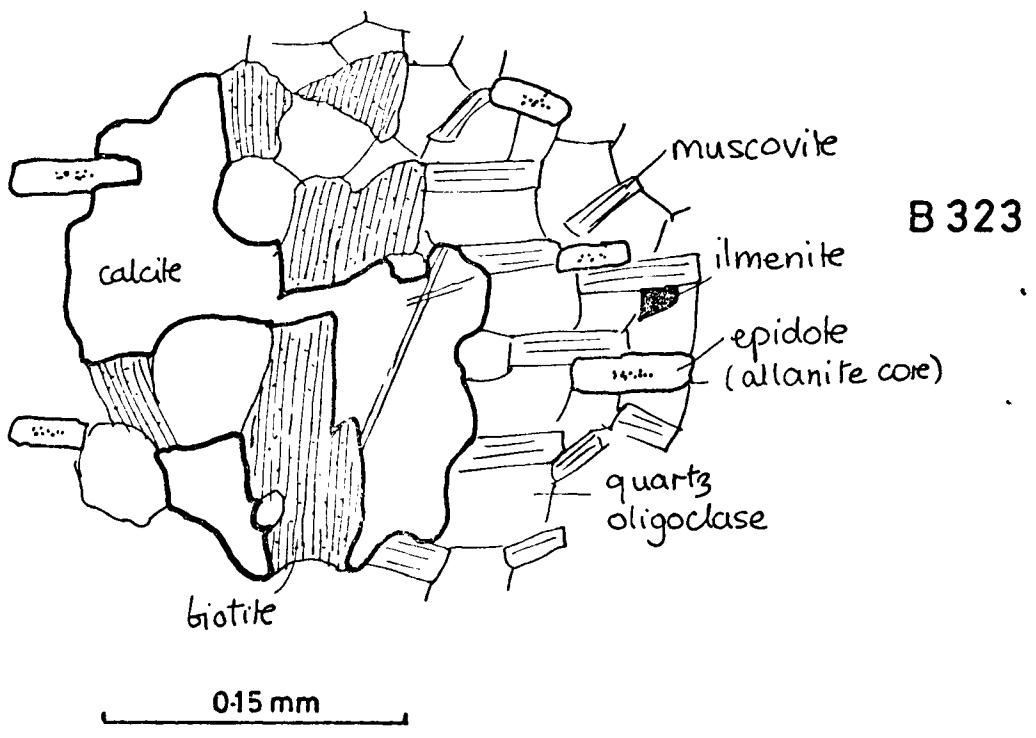


Fig. 8 :- Textures 4

The presence of carbonate in garnet cores suggests that the reaction path of the assemblage includes reactions involving carbonate which have gone to completion. Although B323 is model invariant, it shows little evidence of reactions, in contrast to B100 and 71.19. This reflects the much greater deviation of the composition of the minerals from the model system phases. The variance is therefore much higher, and, although the equilibria between the model system phases as components in the minerals still apply; there is much less evidence of reactions taking place between minerals.

An analysis of each of the minerals in 71.79 (except quartz and ilmenite) is listed in Appendix 5. The composition ranges are :

biotite	$K_{0.97\text{-}1.00}\ Mg_{1.10\text{-}1.16}\ Al\ Si_{2.50\text{-}2.54}\ O_{10}\ (OH)_2$
chlorite	$Mg_{2.37\text{-}2.40}\ Al_2\ Si_{2.36\text{-}2.40}\ O_{10}\ (OH)_8$
garnet	$Ca_{0.65\text{-}0.66}\ Al_{1.87\text{-}1.91}\ Si_{2.70\text{-}2.72}\ O_{12}$
epidote	$Ca_{1.99\text{-}2.02}\ Al_{2.58\text{-}2.60}\ Si_{2.89\text{-}2.91}\ O_{11}\ (OH)$
hornblende	$Ca_{1.60\text{-}1.66}\ Mg_{2.28\text{-}2.32}\ Si_{6.88\text{-}6.95}\ O_{22}\ (OH)_2$
oligoclase	$Na_{0.97\text{-}0.98}\ Ca_{0.24\text{-}0.21}\ Al_{1.23\text{-}1.25}\ Si_{2.69\text{-}2.72}\ O_8$

All the garnets in all the subgroups are zoned with Ca, Mn rich cores. The analyses listed are for the rims, the part of the garnet presumed to be in equilibrium with the assemblage.

Group 2

Most of the assemblages in Table 1 contain no talc or amphibole. In the model system there are 6 possible invariant assemblages, 13 possible univariant assemblages, and 13 possible divariant assemblages. Table 3 shows the variety of assemblages observed in terms of the model system.

Although the garnet pelite and epidote pelite lithologies are typically quite different in hand specimen, there is considerable overlap in the assemblages. One systematic difference is that the assemblages

		clin	mu	gr	cz	cc	ilop	GARNET PELITE	EPIDOTE PELITE	GRAPH-ITIC
invariant	D7-8-8-10		O	O	O	O	O	B234		
	D4-8-8-9	O		O	O	O	O			B109
	D3-5-6-7	O	O		O	O	O	B359		71·20
	D1-2-3-4	O	O	O		O	O			
	D2-6-9-10	O	O	O	O		O			
	D1-5-8-8	O	O	O	O	O		B255		
univariant	D7		O		O	O	O		B127 B156 71·54 71·55 71·62 71·64	
	D11		O	O		O	O			
	D10		O	O	O		O			
	D12	O			O	O	O		71·59 71·48	
	D4	O		O		O	O			
	D9	O		O	O		O			
	D8			O	O	O				B376
	D3	O	O			O	O			70·45
	D6	O	O		O		O	B359		
	D5	O	O		O	O				
	D2	O	O	O			O	B 275 71·72		B108 B370
	D1	O	O	O		O				
	D13	O	O	O	O			B147 B148 B149 B150 B251 B317	B 221 B329 B 331	B377 70·47
								B319 B356 7048 70·80 71·85 72·3	B363 70·75 70·78	
								724 72·6 72·7		
divariant	D7-8				O	O		7064	7142 7144 71·48 B123	71·25
	D3-7		O			O	O			
	D6-7		O		O		O		B125 71·41	
	D2-10		O	O			O	B250 B257		
	D8-9			O	O			B154 B234 B318 B321 7066 71·53	B122 B123 B200 B336 71·43	B375
	D3-4	O				O	O			
	D6-9	O			O		O		B128 B129 B205 B218	
	D4-9	O		O			O			
	D4-8			O		O		7048 70·71		
	D3-6	O	O				O			
	D1-3	O	O			O			70·75	
	D5-6	O	O		O			70·58	71·59	
	D1-2	O	O	O				B86 B250 B253 B320 B322 B335	B202	B374 70·45
								B359 70·71 71·86 72·5		71·22

Table 3 :- Occurrence of possible assemblages in the ta+tr free model system

with garnet and without epidote occur mainly in the garnet pelite lithology whereas the assemblages without garnet and with epidote occur mainly in the epidote pelite lithology, see Fig. 9 and 10 The assemblages with epidote and garnet are distributed between all three lithologies in Table 3. see Fig 11.

Any subdivision of this group is arbitrary. The assemblages are divided into subgroups on the basis of the presence or absence of carbonate.

Carbonate-free subgroup

This subgroup includes the important model univariant pelitic assemblage.

q - olig - bi - chl - mu - ep - g

and the model divariant assemblages without chlorite or muscovite or epidote or garnet, derived from this.

The petrographic differences between the garnet pelite and epidote pelite lithology assemblages in this subgroup involve proportions and relative grain size of the minerals.

The garnet pelite lithology assemblages have on orientated muscovite ± chlorite felt of small laths (.04 x .2 mm) with interstitial quartz, oligoclase, and ilmenite and orientated small epidote prisms (.06 x 3 mm) overgrown by biotite ± garnet poikiloblasts (up to 4 mm across) with quartz, epidote and ilmentite inclusions, see Plate 3. Varying proportions of felt to quartz- oligoclase and chlorite to muscovite give rise to fine scale banding.

The epidote pelite lithology assemblages have orientated chlorite ± muscovite scattered laths (0.05 x 0.2 mm) with equigranular polygonal quartz and oligoclase and prismatic ilmenite overgrown by epidote prisms with allanite cones (0.1 x 0.8 mm), orientated biotite laths (up to .3 x 2.0 mm) ± garnet poikiloblasts (up to 3mm across) with quartz, epidote and ilmenite inclusions.

The petrography of the graphitic lithology assemblages without

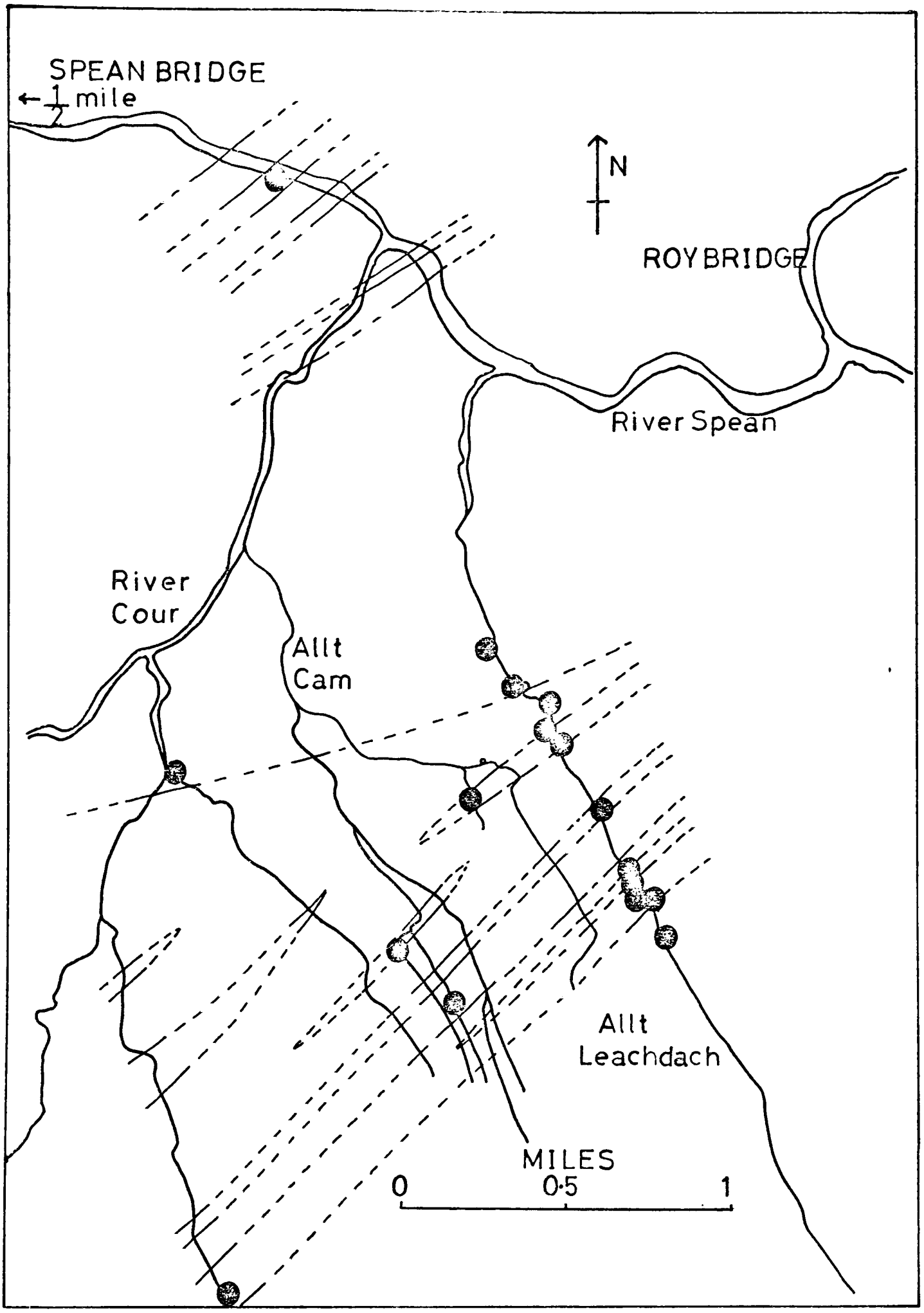


Fig 9 :- Occurrence of model univariant and divariant assemblages with epidote but without garnet.

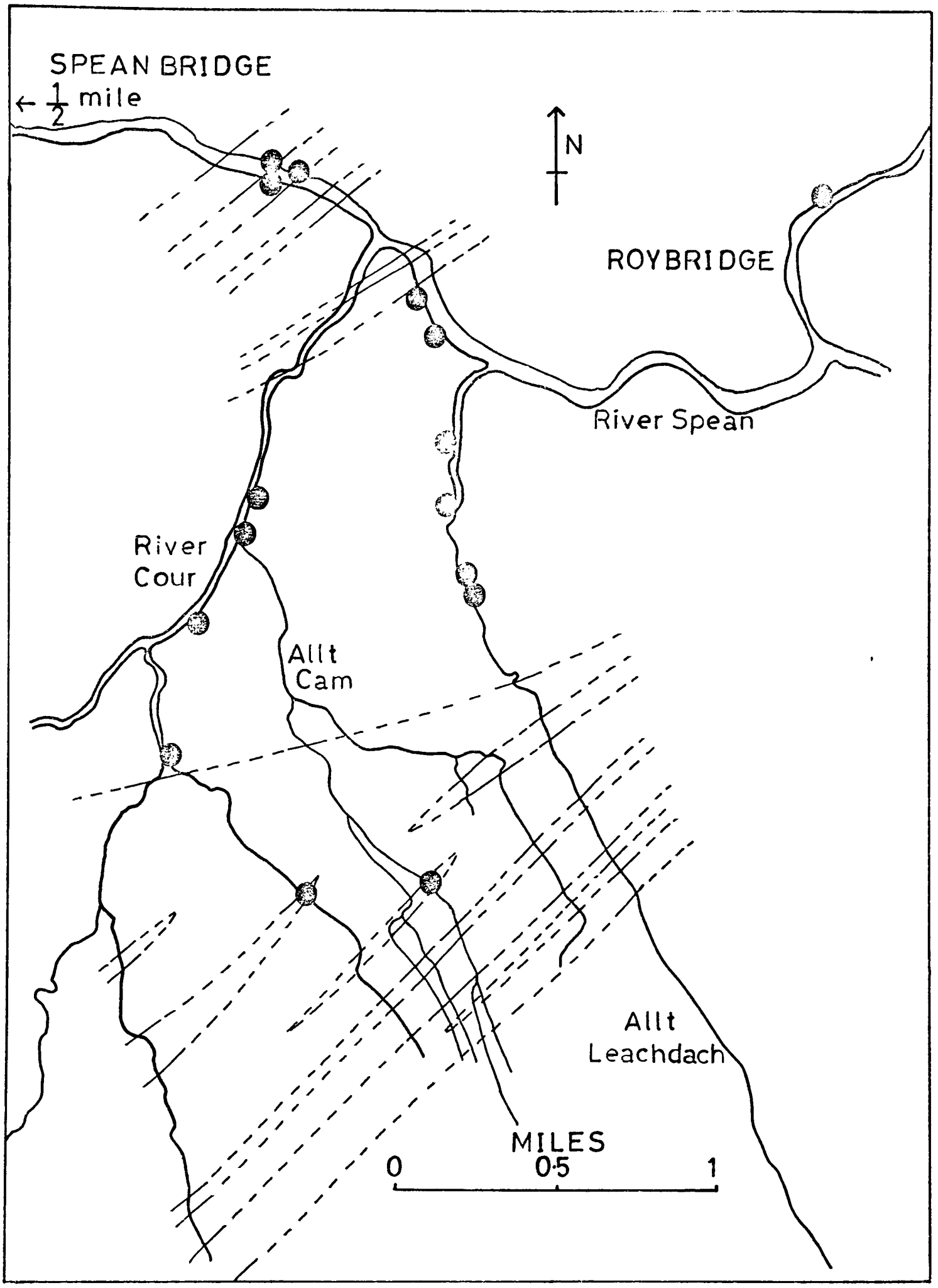


Fig. 10 :- Occurrence of model univariant and divariant assemblages with garnet but without epidote

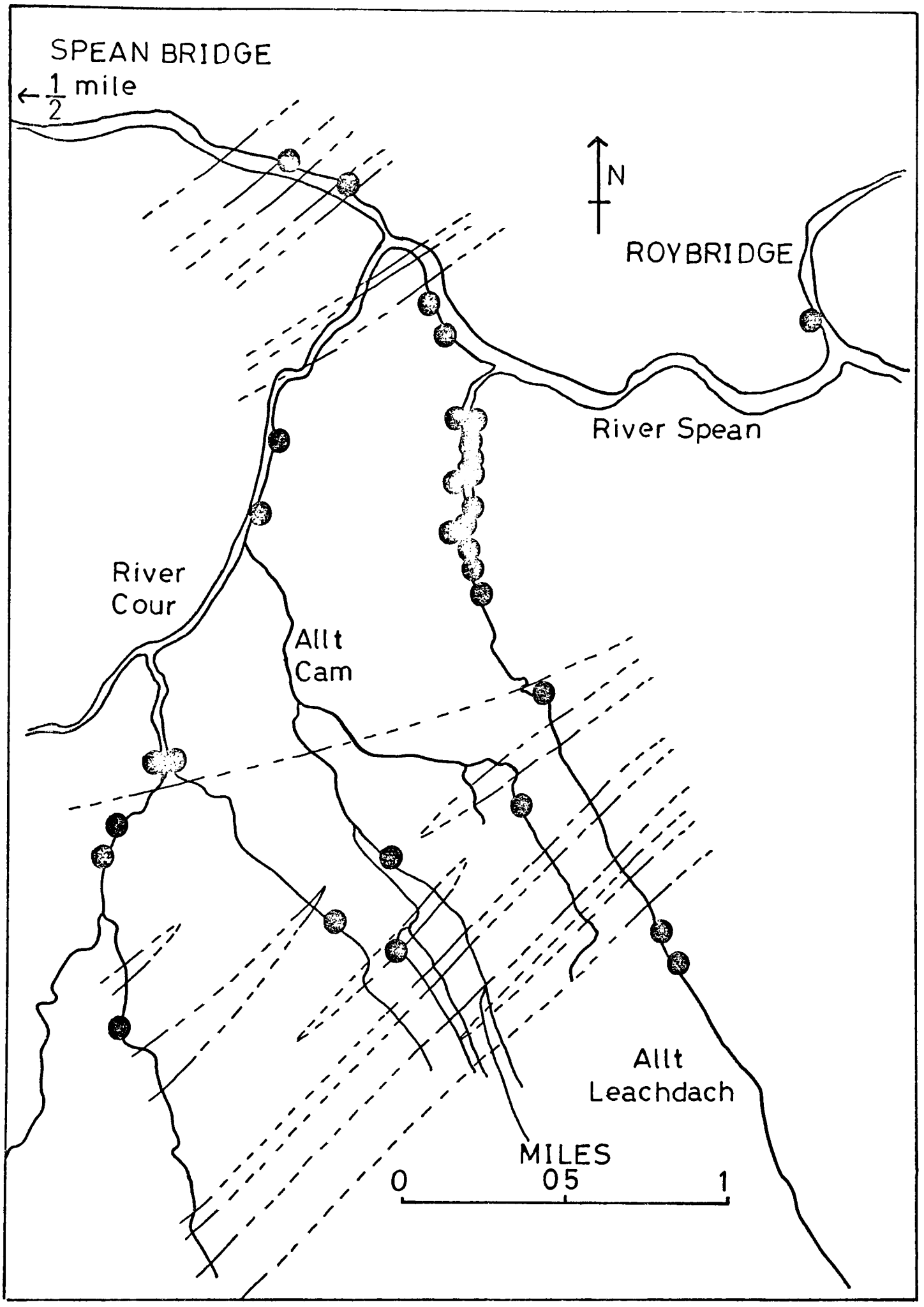
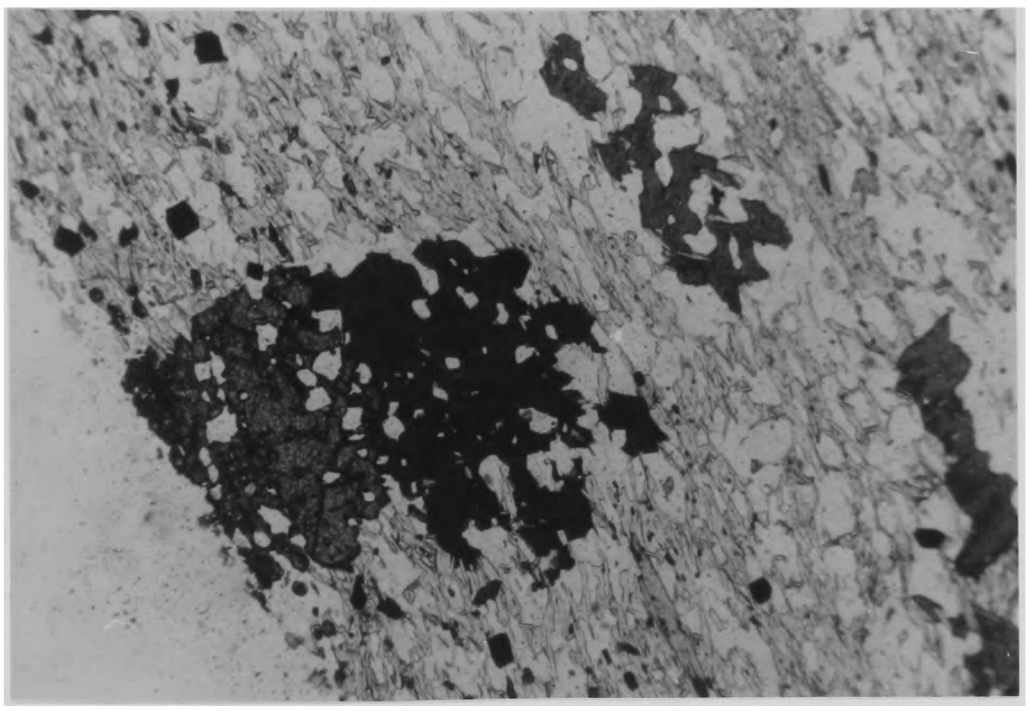


Fig 11 :- Occurrence of model univariant and divariant assemblages with garnet and epidote



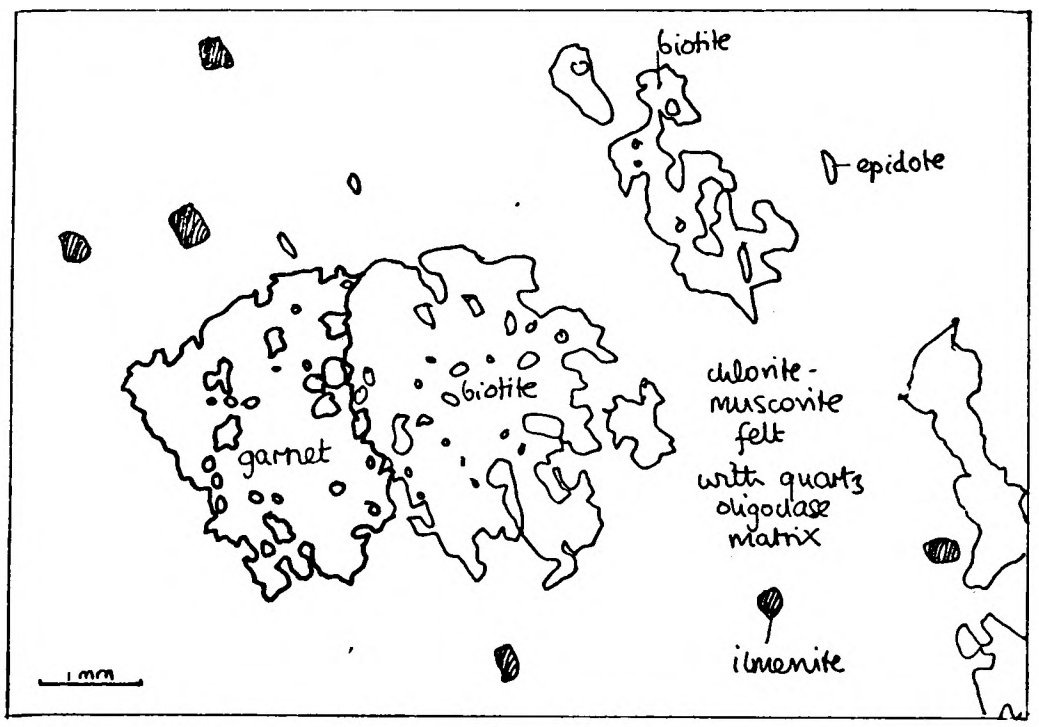


Plate 3 :- 70·80 : an example of a garnet pelite.

graphite is similar to the epidote pelite lithology, but for the characteristic reddish brown pleochroism of the biotites and the greater abundance and size of the epidotes (clinozoisite), see Plate 4. The graphitic assemblages have strongly elongate orientated quartz and feldspar (.01 x .1 mm) with minute muscovite or chlorite laths (.005 x .05 mm) overgrown with oligoclase, clinozoisite, biotite and garnet poikiloblasts. The contrast between the matrix petrography of the graphitic and non graphitic assemblages is shown in Fig 12a where the two are interbanded.

The equilibrium non-stress shape for quartz and oligoclase is polygonal, (eg. Spry 1969): it is the shape grains would take in post deformational annealing and is shown by the garnet and epidote pelite lithology rocks It is suggested that graphite inhibited annealing so that textures involving matrix minerals and oligoclase poikiloblasts are preserved in graphitic rocks. The implication that the garnet pelite and epidote pelite lithology assemblages once contained elongate quartz is supported by the presence of elongate quartz inclusions in the garnets with S-shaped inclusion trails which grew contemporaneous to deformation.

This would help to explain the absence of reaction textures in the epidote and garnet pelite lithology rocks. Part of the explanation is that the composition of the minerals is so far removed from the model system phases that the actual variance is very much higher than the model variance. However poikiloblast minerals have grown and they have replaced matrix minerals, so that the other half of coupled reactions might be expected between matrix minerals not involved in producing the poikiloblast mineral. If this is correct. the graphitic lithology graphitic assemblages should give textural evidence for reactions.

This textural evidence exists but it is difficult to interpret. The most obvious texture is shown in Fig 12b, 13a; clinozoisite cuts biotite and oligoclase appears to embay the biotite. This is a very common texture in all the graphitic rocks. If carbonate were originally



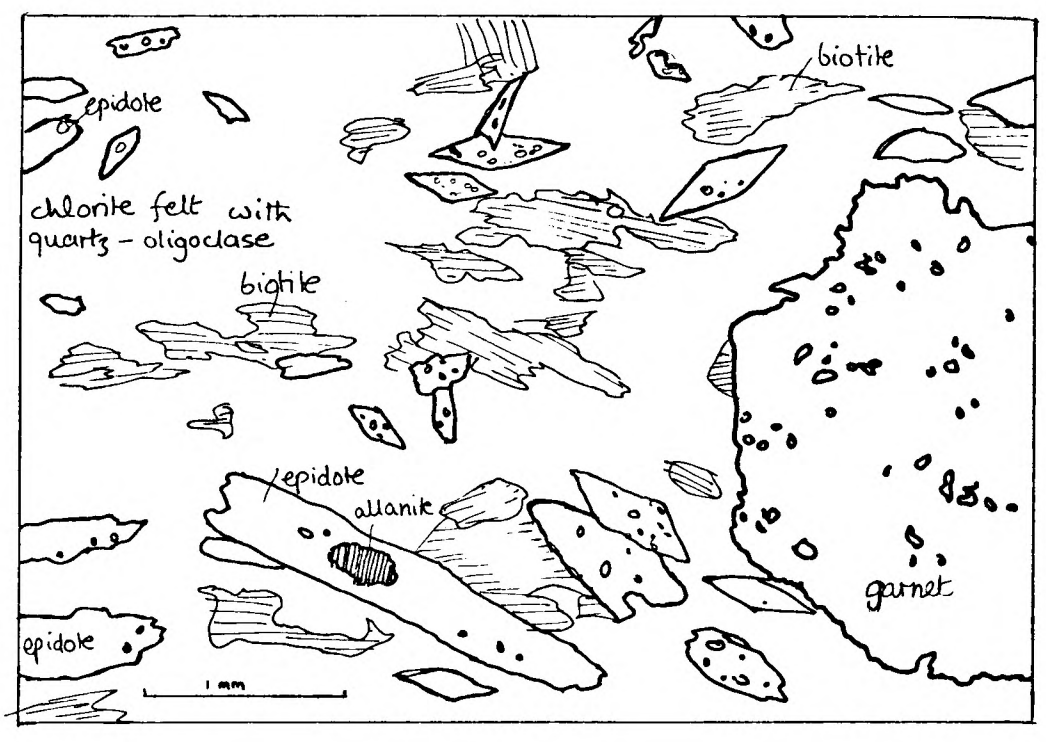
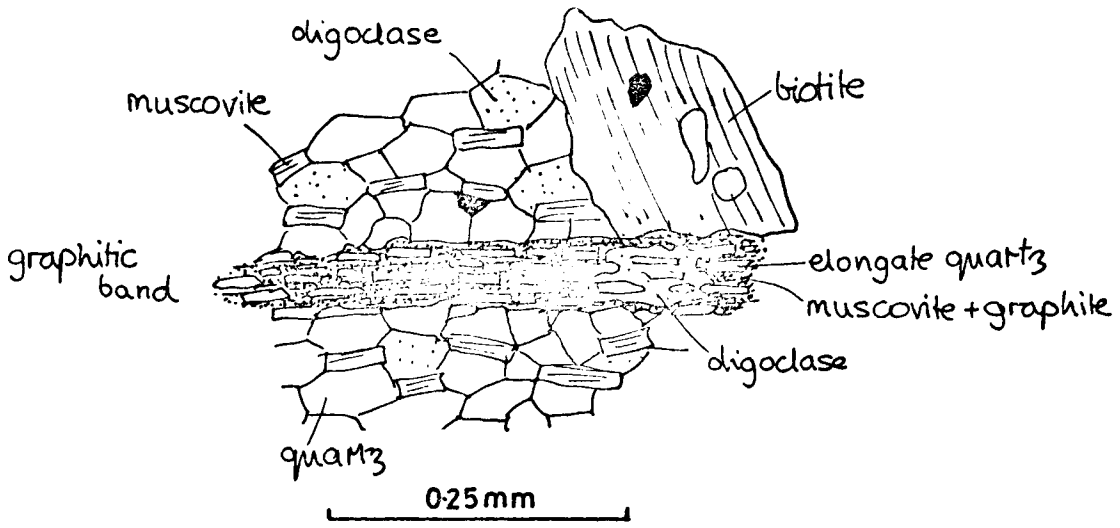
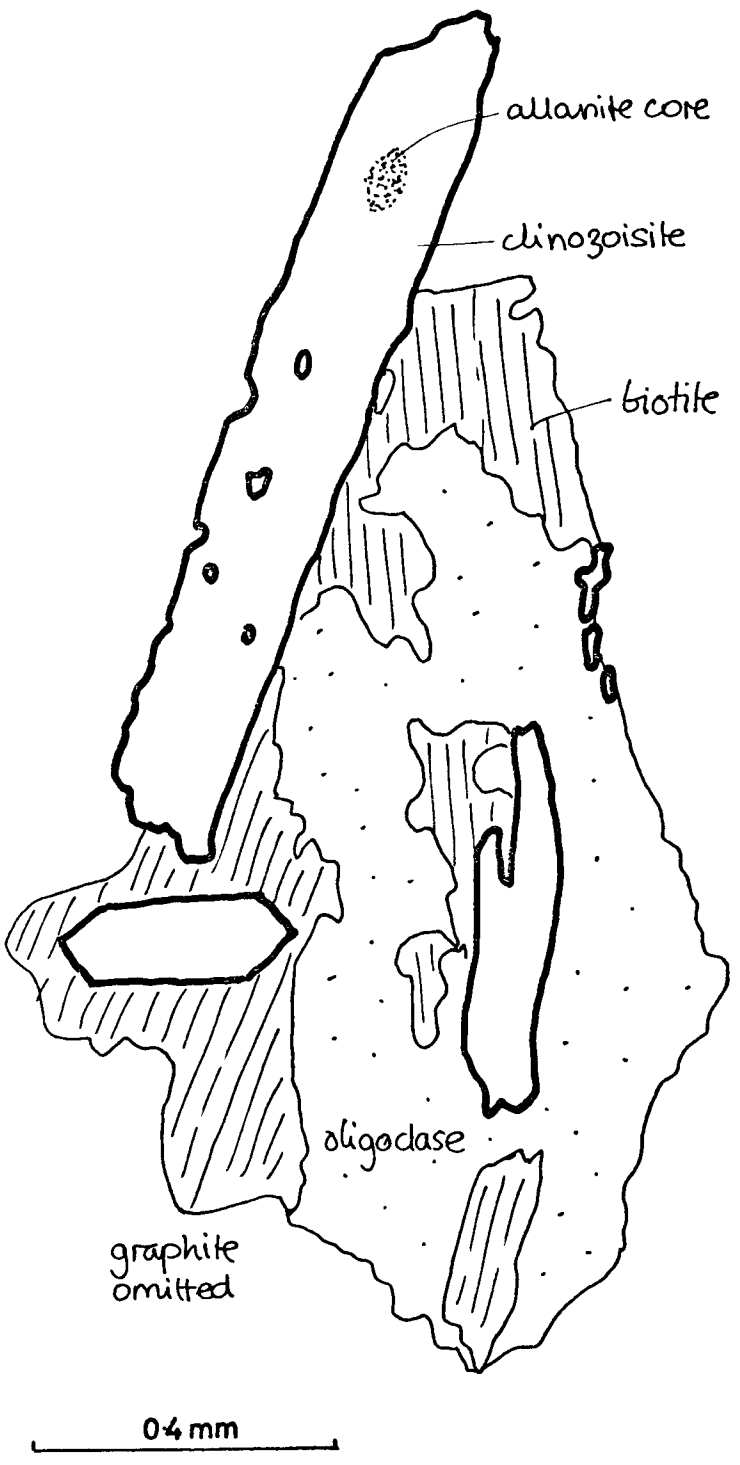


Plate 4 :- B375 : an example of a graphitic pelite.



71·22



B 376

Fig12 :- Textures 5

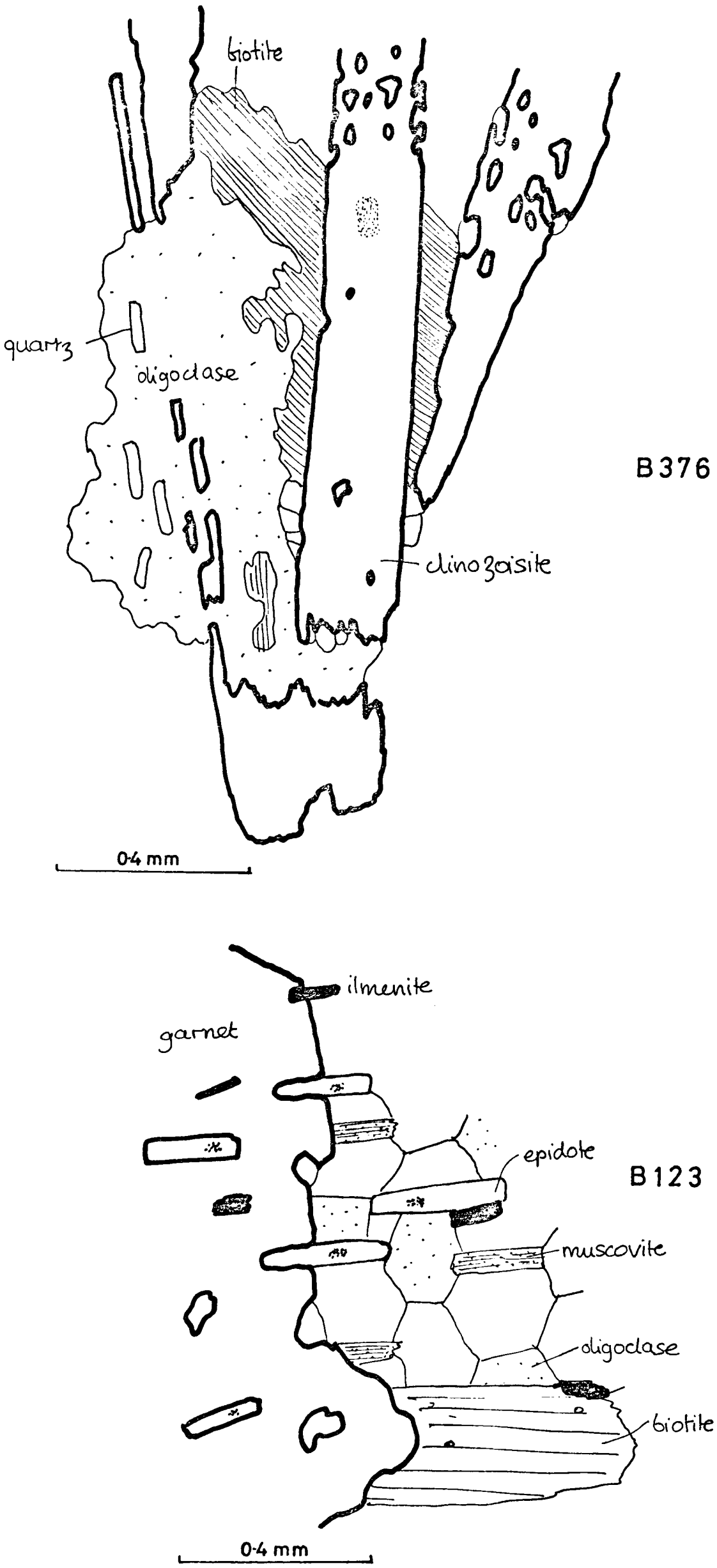


Fig.13 :- Textures 6

present, then the reaction path of the assemblage could be the same as 71.19,

$$dol + mu + an + q + H_2O = cz + phl + CO_2 \qquad \text{no 22}$$

This would explain the presence of clinozoisite and phlogopite poikiloblasts but not why clinozoisite always cross cuts biotite. The embayment of biotite by oligoclase could be related to the reaction producing garnet. If garnet grew from chlorite and quartz (in the Fe analogue of the model system), displaced oligoclase (beyond that to make the small grossularite component of the garnet) might replace biotite and the displaced biotite would grow elsewhere.

In the garnet pelite and epidote pelite lithology assemblages of this subgroup it appears that the two poikiloblast minerals grew at the same time from the matrix, as seen in Plate 3. The reaction can be found in the Fe analogue of the model system

$$chlorite + muscovite + quartz = biotite + garnet + H_2O$$

Oligoclase must provide the grossularite component of the garnet because of the absence of oligoclase inclusions and the presence of epidote inclusions, eg Fig 13b.

All the minerals (except quartz and ilmenite) were analysed in four rocks with the model univariant assemblage, 70.48, 71.85 72.3 and 72.6. The analyses are listed in Appendix 5. The ranges of composition for each rock are given below: 70.48 :

biotite	$K_{0.94-0.96}\ Mg_{1.00-1.05}\ Al\ Si_{2.62-2.64}\ O_{10}\ (OH)_2$
chlorite	$Mg_{2.00-2.04}\ Al_2\ Si_{2.44-2.48}\ O_{10}\ (OH)_8$
muscovite	$K_{0.75-0.77}\ Al_{2.75-2.78}\ Si_{2\ 99-3.03} O_{10}\ (OH)_2$
epidote	$Ca_{1.99-2.02}\ Al_{2.75-2.78}\ Si_{2.94-2.9B}\ O_{11}\ (OH)$
garnet rim	$Ca_{0.37-0.39}\ Al_{1.95-2.00}\ Si_{3.01-3.03}\ O_{12}$
oligoclase	$Na_{0.83-0.84}\ Ca_{0.15-0\ 17}\ Al_{1.16-1.19}\ Si_{2.81-2.83}\ O_8$

71.85:

biotite	$K_{0.93-0.95}\ Mg_{1.01-1.08}\ Al\ Si_{2.65-2.68}\ O_{10}\ (OH)_2$
chlorite	$Mg_{2.10-2.14}\ Al_2\ Si_{2\ 55-2.58}\ O_{10}\ (OH)_8$
muscovite	$K_{0.85-0.86}\ Al_{2.74-2.77}\ Si_{3.01-3.06}\ O_{10}\ (OH)_2$
epidote	$Ca_{1.87-1\ 92}\ Al_{2.50-2.55}\ Si_{2.98-3.05}\ O_{11}\ (OH)$
garnet rim	$Ca_{0.20-0.23}\ Al_{1.99-2.03}\ Si_{3.00-3.05}\ O_{12}$
rutile	$Ti_{0.96}\ O_2$

72.3:

biotite	$K_{0.95-0.97}\ Mg_{1.02-1.04}\ Al\ Si_{2.66-2.69}\ O_{10}\ (OH)_2$
chlorite	$Mg_{2.14-2.16}\ Al_2\ Si_{2.50-2.52}\ O_{10}\ (OH)_8$
muscovite	$K_{0.75-0.76}\ Al_{2\ 70-2.72}\ Si_{3.03-3\ 09}\ O_{10}\ (OH)_2$
epidote	$Ca_{1.93-1.96}\ Al_{2\ 35-2.38}\ Si_{2.97-3\ 04}\ O_{11}\ (OH)$
garnet rim	$Ca_{0.53-0.55}\ Al_{1.94-1.96}\ Si_{3.99-3.04}\ O_{12}$
oligoclase	$Na_{0.81-0.82}\ Ca_{0.17-0.19}\ Al_{1.18-1.20}\ Si_{2.78-2.80}\ O_8$

72.6

biotite	$K_{0.96-0.98}\ Mg_{1.00-1.05}\ Al\ Si_{2.64-2.65}\ O_{10}\ (OH)_2$
chlorite	$Mg_{1.96-1.99}\ Al_2\ Si_{2\ 49-2.53}\ O_{10}\ (OH)_8$
muscovite	$K_{0.85-0.87}\ Al_{2.70-2.75}\ Si_{2.92-2.94}\ O_{10}\ (OH)_2$
epidote	$Ca_{1.85-1.86}\ Al_{2.34-2.38}\ Si_{2.99-3.05}\ O_{11}\ (OH)$
garnet rim	$Ca_{0.33-0.35}\ Al_{1.90-1.92}\ Si_{3.00-3.03}\ O_{12}$
oligoclase	$Na_{0.81-0.83}\ Ca_{0.15-0.18}\ Al_{1.15-0.16}\ Si_{2.81-2.84}\ O_8$

Carbonate-present subgroup

Although carbonate bearing assemblages are rarer in the garnet pelite lithology than in the epidote pelite lithology, all the model invariant assemblages come from the garnet pelite (and graphitic)

lithology. However the majority of carbonate bearing model univariant and divariant assemblages come from the epidote pelite lithology. In many rocks carbonate appears to be a reactant of reactions; in other rocks, although carbonate is nolonger present in some bands, its previous presence is indicated by its preservation as inclusions in garnet cores. Textures are described that indicate the reactions that involve carbonate.

Carbonate bearing rocks in the garnet pelite lithology occur as thin bands within typical pelitic rocks of the last subgroup. They show every transition from textures like Plate 3 + carbonate (eg B255) to rocks with minor micas and dominant carbonates (eg B234). The three model invariant assemblages in this lithology are,

B255 q-olig - br bi - chl - mn - g - ep - cc - rut - ilm

B359 q - olig - br bi - chl - mn - ep - cc - dol - ilm

B234 q - olig - br bi - mn - g - ep - cc - dol - ilm

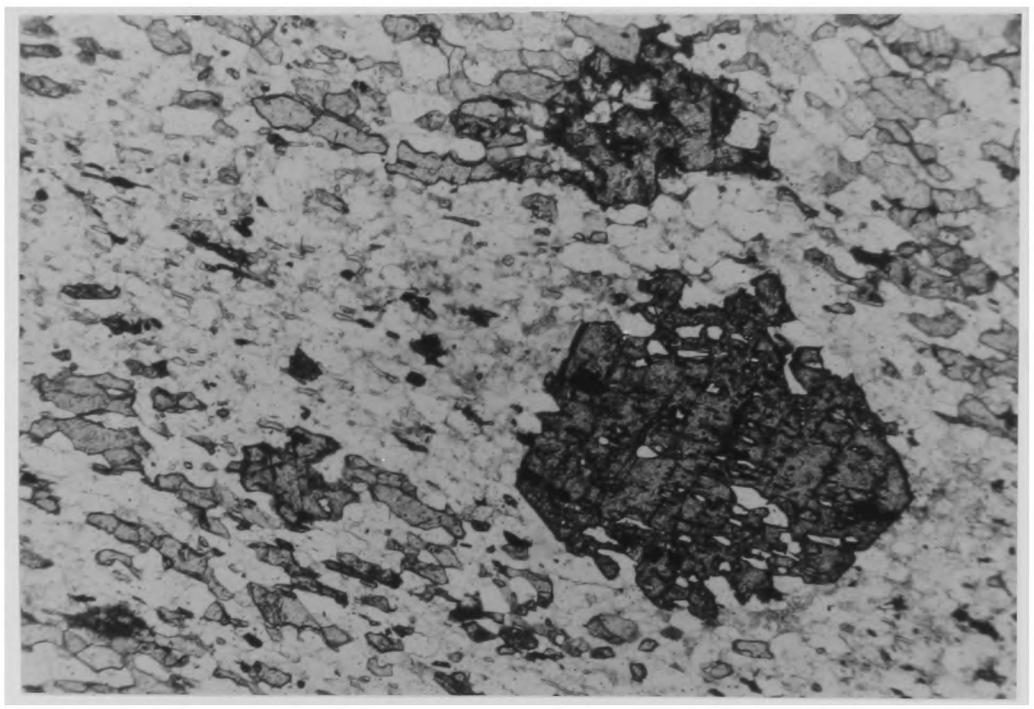
B255 is the univariant assemblage from the last subgroup plus calcite. The petrography and textures are the same with the addition of small calcite poikiloblasts (about 0.3 mm across), with no reaction relations evident.

B359 has small laths of chlorite and muscovite, small prisms of epidote and ilmenite in equigranular polygonal quartz and oligoclase with small ragged poikiloblasts of calcite and dolomite. The calcite is less ragged than dolomite which invariably has biotite replacing it.

This is the only reaction texture in the rock and is shown in Fig 14a. A possible reaction to produce both the biotite and epidote from the dolomite and matrix is

$$dol + mu + an + q + H_2O = cz + phl + CO_2 \qquad \text{no 22}$$

B234, shown in Plate 5, has very small orientated muscovite laths and epidote prisms in an equigranular polygonal quartz and oligoclase and calcite matrix (about 0.08 across) with garnet poikiloblasts and ragged dolomites being replaced by biotite. This is the only evidence



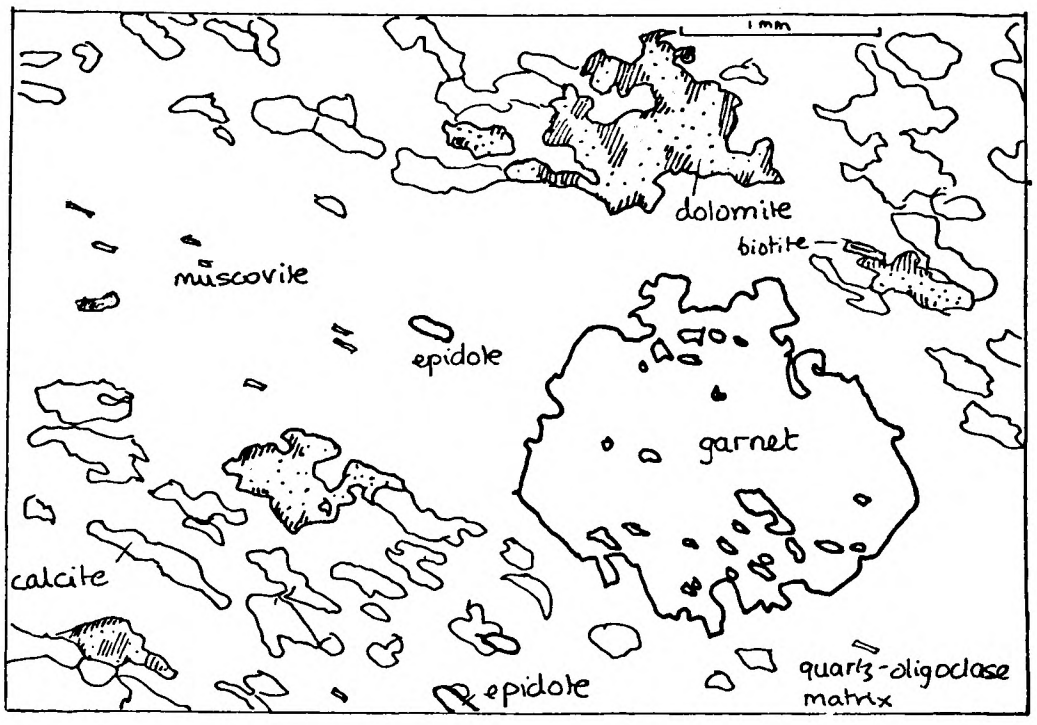
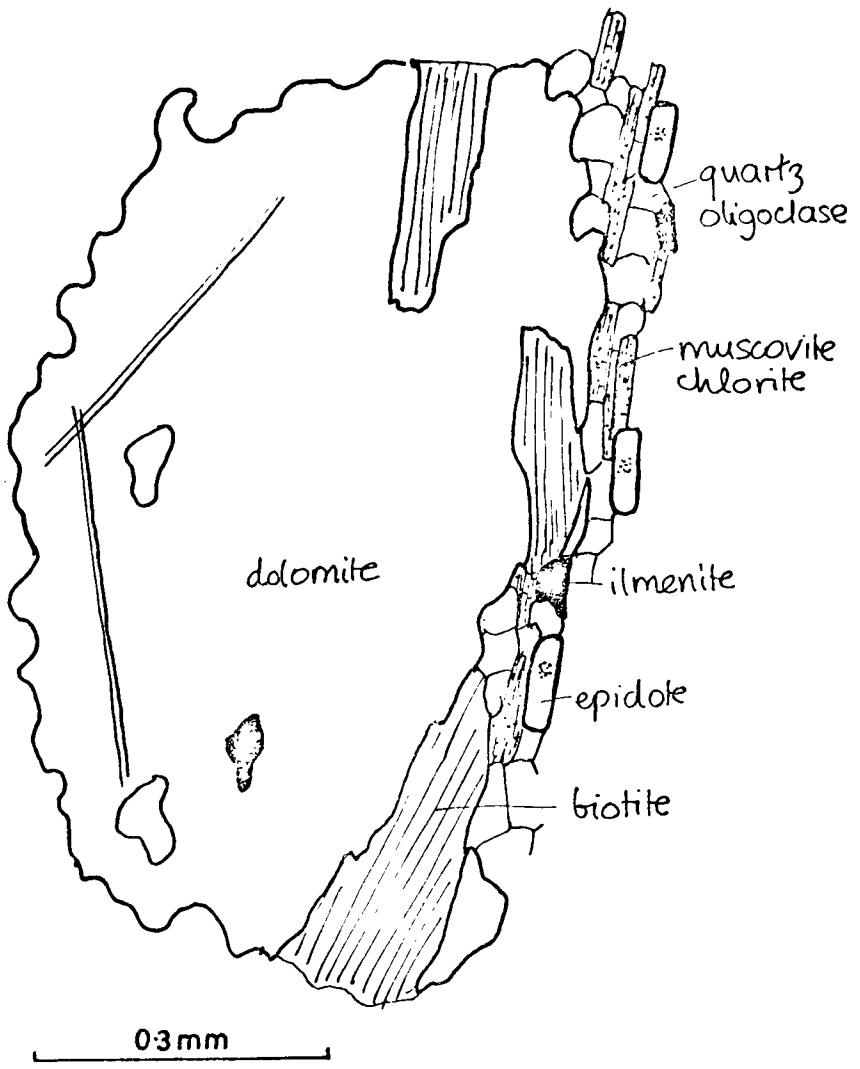
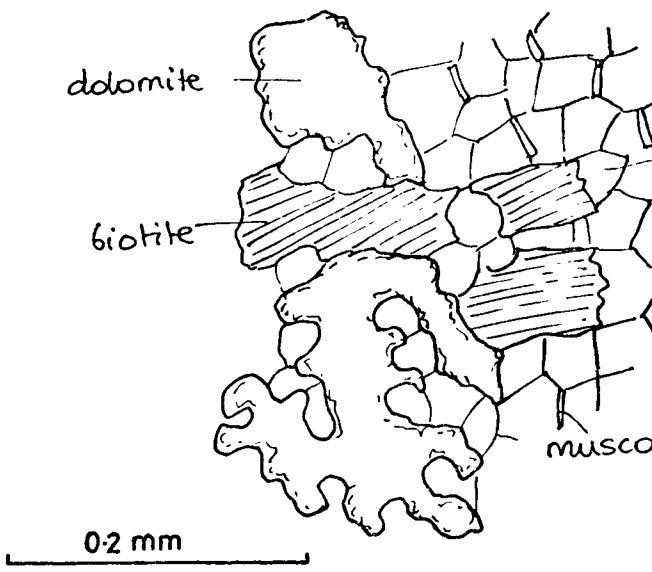


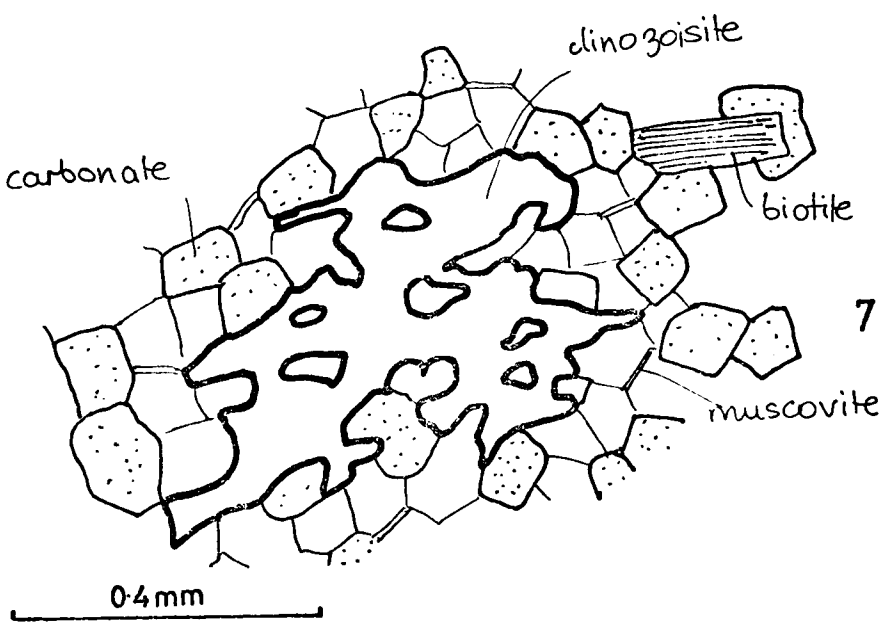
Plate 5 :- B234 : an example of a carbonate bearing garnet pelite.



B 359



B 257



71·64

Fig.14 :- Textures 7

of reactions that took place and it can be explained by reaction 22 above and

dol + mu + q = gr + phl + CO_2 no 21

A small range of higher model variance assemblages derived from these three above occur in the garnet pelite lithology. Evidence for reaction 21 comes from the presence of the dolomite → biotite texture in the model divariant assemblage corresponding to 21, see Fig 14b.

In the epidote pelite lithology the most common model univariant and derived divariant carbonate bearing assemblages are,

q - olig - br bi - chl - ep - cc - dol eg 71.42

q - olig - br bi - mu - ep - cc - dol eg 71.64

These assemblages are related to B359 above by the absence of chlorite or muscovite. They have equigranular polygonal quartz, oligoclase, calcite and dolomite (about 0.05 mm across) with orientated laths of biotite and muscovite or biotite and chlorite (0.2 x 0.03 mm) overgrown by epidote and sphene poikiloblasts (up to 0 3 mm across).

In the chlorite-bearing assemblages; calcite and dolomite do not appear in any reaction textures and the epidotes are small. In the muscovite bearing assemblages dolomite is being replaced by biotite and the epidotes are larger. The dolomite-biotite textures are less clear than in Fig 14a,b which may be due to annealing. Although epidote usually grows on allanite, in Fig 14c is an unusual texture showing a clinozoisite poikiloblast that grew from the matrix. This is excellent evidence for the reaction 22 above; clinozoisite and biotite growing from the matrix. It is possible that this reaction accounts for the epidote (and biotite) in muscovite absent assemblages; originally present muscovite has been reacted away.

The best developed reaction in these rocks took place outside the model system: it is the reaction,

sphene + CO_2 = rutile + calcite + quartz

This reaction can be seen in the frontispiece. The distribution of sphene and rutile between different assemblages appears to be random; some rocks contain sphene, sphene replaced by calcite, quartz and rutile, close groups of rutiles (after sphene), or randomly distributed rutiles. This lack of organisation is difficult to explain if the reaction was taking place at the equilibrium boundary. The implication of sphene metastability is supported in the next chapter.

The carbonate-bearing assemblages in the graphitic lithology rocks include two model invariant assemblages,

B109 q - olig - br bi - chl - ep - g - cc - dol - gr

71.20 q - olig - br bi - chl - ep - mu - cc - dol - gr

B109 is fine grained with abundant graphite; there are no graphite-free coarse grained areas. The matrix is fine grained quartz, feldspar, calcite, dolomite and graphite overgrown by calcite oligoclase, chlorite, epidote and garnet poikiloblasts. Biotite occurs as rare small reddish brown laths. Garnet forms almost inclusion free poikiloblasts up to 1.5 cm across. Epidote forms small irregular poikiloblasts growing from matrix carbonate, and is similar to Fig 14c. The calcite poikiloblasts contain dolomite and quartz inclusions.

The chlorite poikiloblasts contain graphite and a few quartz inclusions.

71.20 has a fine grained matrix of very elongate quartz, carbonate, and feldspar (about 0.04 x 0.005 mm) and graphite with small orientated muscovites and larger reddish brown biotites with chlorite, calcite, oligoclase, and epidote poikiloblasts.

The epidote cores contain more graphite than the matrix, suggesting that some of the graphite oxidised to carbon dioxide as the epidote grew. Although most epidotes grew from allanite cores, some form irregular poikiloblasts in the matrix, similar to Fig 14a. Biotite replaces dolomite as described before.

As both assemblages are model invariant it is difficult to

separate or order the reactions that took place. Reactions 21 and 22

$$dol + mu + an + q + H_2O = cz + phl + CO_2 \qquad \text{no 22}$$

$$dol + mu + q + = gr + phl + CO_2 \qquad \text{no 21}$$

account for the growth of clinozoisite and garnet from matrix. If these were preceeded with or accompanied by Reaction 40

$$dol + an + q + H_2O = clin + cc + CO_2 \qquad \text{no 40}$$

then this would account for the calcite and chlorite poikiloblasts. The oligoclase poikiloblasts may have been produced at the invariant point.

The analyses of the carbonates from 71.42, 71.44 and 71.64 from the epidote pelite lithology are listed in Appendix 5 and are discussed in the next chapter. All the minerals (except quartz and ore) were analysed in 71.42 and 71.64 and B376 from the graphitic lithology. The ranges of composition are given below.

71.42 :

biotite	$K_{0.93-0.95}\ Mg_{2.16-2.18}\ Al\ Si_{2.83-2.85}\ O_{10}\ (OH)_2$
chlorite	$Mg_{4.11-4.13}\ Al_2\ Si_{2.73-2.77}\ O_{10}\ (OH)_8$
epidote	$Ca_{1.97-1.99}\ Al_{2.70-2.72}\ Si_{2.98-3.01}\ O_{11}\ (OH)$
oligoclase	$Na_{0.76-0.77}\ Ca_{0.20-0.23}\ Al_{1.18-1.20}\ Si_{2.80-2.81}\ O_8$
sphene	$Ca_{1.00-1.01}\ Ti_{0.90-0.92}\ Si_{0.98-1.01}\ O_5$
rutile	$Ti_{0.96-0.97}\ O_2$

71.64

biotite	$K_{0.94-0.96}\ Mg_{2.01-2.04}\ Al\ Si_{2.67-2.69}\ O_{10}\ (OH)_2$
muscovite	$K_{0.90-0.91}\ Al_{2.65-2.69}\ Si_{2.97-3.01}\ O_{10}\ (OH)_2$
epidote	$Ca_{1.99-2.02}\ Al_{2.73-2.75}\ Si_{2.95-2.96}\ O_{11}\ (OH)$
oligoclase	$Na_{0.74-0.76}\ Ca_{0.21-0.24}\ Al_{1.18-1.22}\ Si_{2.79-2.83}\ O_8$

sphene	$Ca_{1.00-1.02}\ Ti_{0.90-0.93}\ Si_{0.99-1.02}\ O_5$

B376 :

biotite	$K_{0.95-0.97}\ Mg_{1.29-1.33}\ Al\ Si_{2.73-2.76}\ O_{10}\ (OH)_2$
chlorite	$Mg_{2.45-2.47}\ Al_2\ Si_{2.67-2.69}\ O_{10}\ (OH)_8$
epidote	$Ca_{1.96-1.99}\ Al_{2.57-2.60}\ Si_{3.00-3.04}\ O_{11}\ (OH)$
garnet rim	$Ca_{0.54-0.56}\ Al_{1.96-1.98}\ Si_{2.99-3.01}\ O_{12}$ see Fig 15
oligoclase	$Na_{0.74-0.76}\ Ca_{0.24-0.25}\ Al_{1.23-1.25}\ Si_{2.75-2.77}\ O_8$
calcite	$Ca_{0.96}\ CO_3$

Discussion of Bailey (1934)

Bailey (1934) interprets the area studied here with the stratigraphy and structure of the Ballachulish-Onich area. In that area Bailey recognises a well defined sequence of lithologies, including Ballachulish Slate below Ballachulish Limestone below Leven Schists. He does not conceive that lateral sedimentary facies changes are possible. In that area some of the lags and slides appear to have been created to explain departures from his expected sequence of lithologies; the missing units must have been faulted out. The large scale structure in the Ballachulish-Onich area is a refolded recumbent syncline and Bailey continues this structue into the area studied here, Fig. 2.

There is little evidence for this structure from the data presented in this chapter; in particular,

1. Bailey equates the epidote pelite lithology limestones and the siliceous dolomite lithology and calls them Ballachulish limestone. The two sets of rocks are mineralogically, texturally and compositionally quite different.
2. Bailey interprets the repeated limestone outcrops in the epidote pelite lithology are due to infolding of a separate limestone

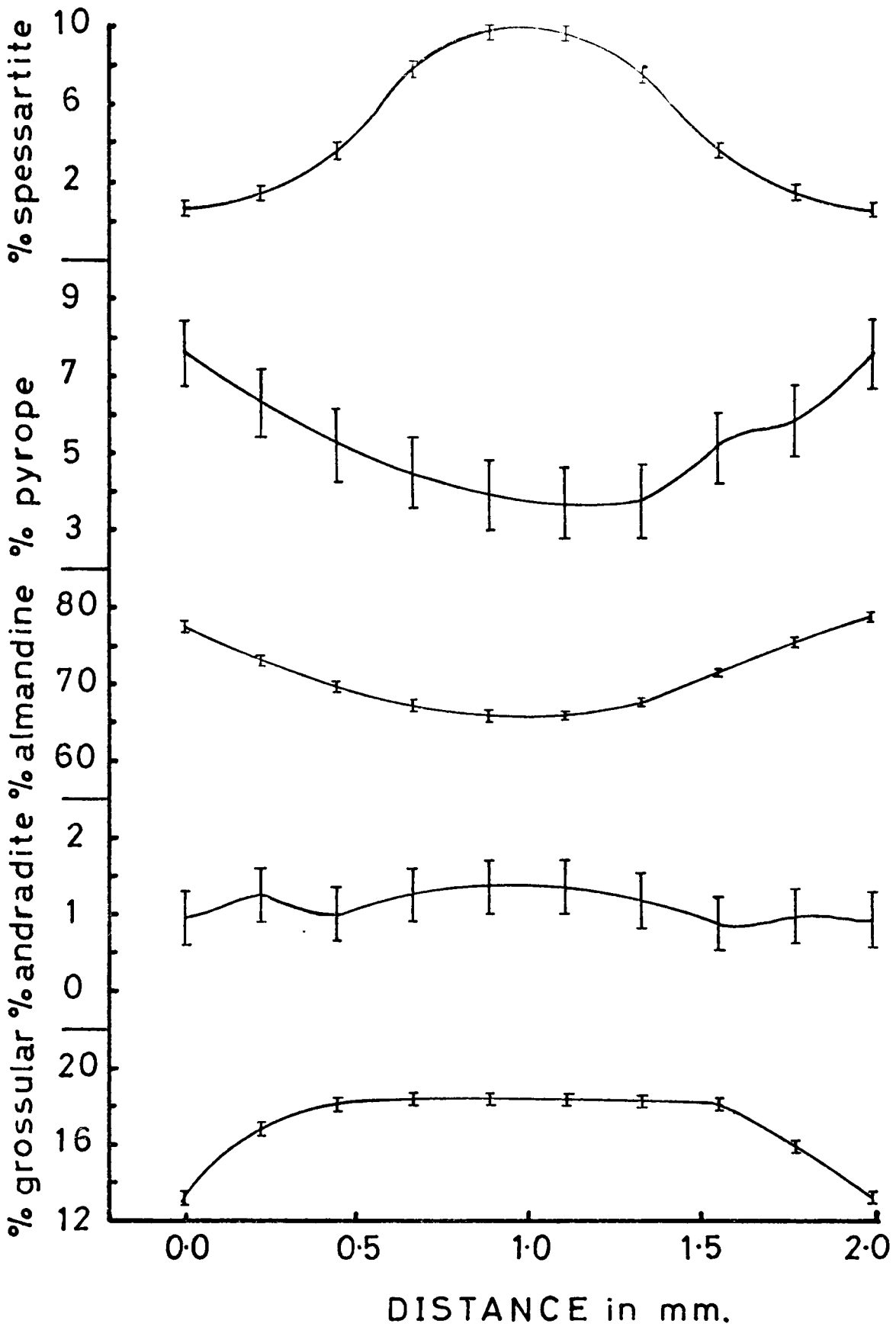


Fig.15 :- Analyses across a zoned garnet in B376.

unit. Although the limestones are similar, they grade into epidote pelite lithology pelites and there are few epidote pelite lithology rocks which lack carbonate.

3. Bailey's synclinal structure requires that the pelite lithologies be symmetrical about the limestone outcrops. This is not observed; the garnet pelite lithology rocks do not reappear immediately south of the limestones.

The stratigraphy could be a monotonic gradational and intergradational sedimentary sequence. Although large scale folds and faults may occur, there is no evidence for them in the distribution of assemblages. The sequence of rocks is referred to the Leven Schists (sensu lato).

Fluid inclusions

Mr F.W. Smith (University of Durham) kindly carried out fluid inclusion studies on a quartz sample from a semi-concordant quartz vein in the garnet pelite lithology, 400 metres east of the mouth of the Cour in the River Spean.

Homogenization temperatures of two phase primary and pseudosecondary (Yermakov (1949)) fluid inclusions were measured in doubly polished discs on a microscope heating stage. These inclusions homogenized into the liquid phase. The mean and median of 25 measurements were 350°C (std. dev. 19) and 349°C respectively. The absolute accuracy of individual measurements was not believed to be better than ± 5°C.

The concentration of dissolved salts in the inclusion liquid was established by the depression of melting point technique. During slow warming from -90°C, ice melted at approximately -22°C, very close to the eutectic temperature of -21.1°C in the NaCl-H_2O system. A high relief solid phase, believed to have been NaCl.2 H_2O, melted in the range -9°C to-5°C (16 measurements). Assuming the inclusion fluid approximates to the NaCl-H_2O system, this corresponds to a salinity of 25±2 equivalent wt.% NaCl. A shadowy low relief solid, believed to

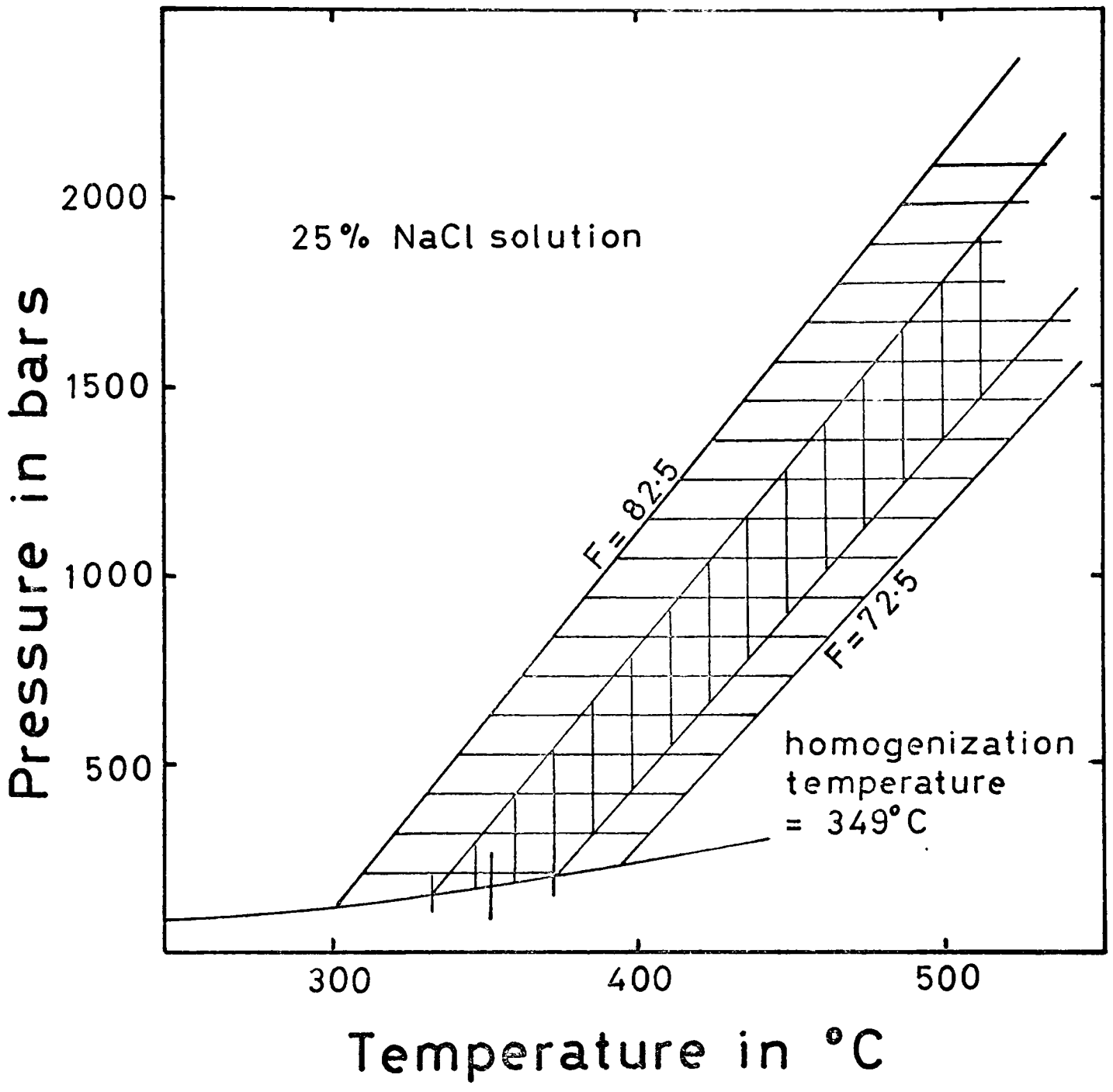


Fig.16 :- Fluid inclusion results : quartz vein probably formed within the cross-hatched area.

be CO_2 hydrate, occurred in some runs. The effect of this CO_2 on the homogenization temperatures and salinities is not known but is believed to be small.

The degree of filling (% liquid in the primary inclusions) (Sorby 1858) at room temperature was calculated (from photographs) to be 77 (std. dev. 9.0). Thus the density (Roedder (1967)) of the parent fluid was approximately 0.88 gm/cc.

The parameters, pressure of formation (P), temperature of formation (T), degree of filling (F), and salinity (X) of fluid inclusions are so interrelated that the correction of the homogenisation temperature to the actual formation temperature can only be undertaken with a knowledge of P, F and X.

Fig.16 gives the pressure effect on the measured homogenization temperatures using the data of Lemmlein and Klevtsov (1961). The fluid inclusions probably formed in the cross hatched band on this diagram.

These results will be used in the next chapter.

CHAPTER 5

METAMORPHIC CONDITIONS

Metamorphic conditions

The aim of this chapter is to calculate the conditions of metamorphism of the rocks described in the last chapter. The model system provides a framework for the calculations because thermodynamic data exists or has been calculated in chapter 3 for all the phases. The problem is how to calculate the activities of the model system phases as components in the analysed minerals. A method is presented which is based on the ionic mixing model introduced at the end of chapter 2.

A number of assumptions are required to calculate the conditions of metamorphism. These are presented as a model to be tested. Then the analytical data is ued to calculate the metamorphic conditions within this model.

Activities

There are two approximations which can be used to calculate activities of components in minerals.

1. ideal molecular mixing eg $a_{phl} = x_{phl}$

2. ideal ionic mixing, from (126)

   eg $a_{phl} = (x_K^{K \text{ site}}) (x_{Mg}^{Mg \text{ site}})^3 (x_{Al}^{Al \text{ site}}) (x_{Si}^{Si \text{ site}})^3$

   This is based on the approximation that the n atoms of a particular element in the formula unit occur randomly and ideally over n identical sites.

It will be necessary to calculate the activity of clinozoisite component in epidote, phlogopite in biotite, clinochlore in chlorite, muscovite in muscovite, tremolite in hornblende and anorthite in plagioclase.

The only data relevant to mica activities comes from the

experimental work of Wones and Eugster (1965) on biotites. They show that ideal ionic mixing is a much better approximation than ideal molecular mixing. The agreement is improved when the Fe site occupancy data of Hazen and Wones (1971) is included. Ideal ionic mixing is used to calculate the activities for all the micas.

Holdaway (1972) discusses the activity relations of epidotes and andradite-grossularite mixtures. He concludes that garnet mixtures can be approximated by ideal ionic mixing. Dollase (1971) and Burns and Strens (1971) give the distribution of Fe^{3+} and Al between the three octahedral sites in epidote. They show that about 10% of the Fe goes into M(1), 90% into M(3) and a negligible amount into M(2). The ionic mixing model then gives

$$a_{cz} = (x_{ca}^{\text{ca site}})^2 \quad (1 - 0.1 \times \frac{\text{Al site}}{\text{Fe}}) \; (1-0.9 \times \frac{\text{Al site}}{\text{Fe}})(X_{Si}^{\text{Si site}})^3$$

The ionic mixing model is used for the activity of tremolite in amphibole in the absence of any published data.

Orville (1972) experimentally determined the activity of anorthite and albite in plagioclase at 700°C and 2 kbars from cation exchange equilibria with aqueous chloride solutions. Observations on natural feldspars show that there is a solvus, the peristerite solvus, at low temperatures between albite. an_1, and oligoclase, about an_{20} (eg Brown, 1962). The presence of a solvus constrains the deviation from ideality to be positive, as found by Orville (1972). Crawford (1966) considers that the top of the solvus is at about 500°C. The positive deviation from ideality must increase with decreasing temperature below 700°C.

The composition of the analysed plagioclases falls in the region obeying Henry's law for the anorthite component. A Henry's law constant, L, must be introduced to approximate a_{an}

$$a_{an} = LX_{an}$$

L is calculated to be about 3.5 by using a very crude approximation with the temperature dependence of NaCl and KCl activities in the

NaCl-KCl binary system.

An important feature of the ionic mixing model is the rapid change of activity with composition. Using biotites again,

$K\ Mg_2Fe_1Al\ Si_3O_{10}\ (OH)_2$ $\quad a_{phl} = 0.30$

$K\ Mg_2Fe_{0.5}Al_{0.5}Al_1Si_{2.5}Al_{0.5}O_{10}\ (OH)_2$ $\quad a_{phl} = 0.17$

Decreasing an activity by an order of magnitude changes the temperature of reaction (at a particular pressure and composition of the vapour phase) by only a few tens of degrees because it is log activity rather than activity which is used in the calculation.

Model for metamorphic conditions

a. Equilibrium

Implicit in the descriptions and textural interpretations of the last chapter was that the assemblages in each small band represent a chemical system in a state of frozen equilibrium. This thesis is examined here.

The criteria available are negative, it is only possible to test for the absence of evidence of disequilibrium.

1. Textural evidence: Reaction textures, usually evidence of disequilibrium, do not demonstrate lack of equilibriaum if the variance of the assemblage is low enough for reactions to be written between the phases. The presence of recrystallised (annealed) textures in many of the rocks suggests that equilibrium may have taken place during annealing. Zoned minerals are not in chemical equilibrium with the assemblage. However it is possible that the rim of a zoned mineralwas in equilibrium with the assemblage. The core of a zoned mineral is considered to be outside the chemical system under discussion.
2. Regular distribution of cations and anions between coexisting minerals: An exchange reaction is controlled by an equilibrium

constant expression. If the compositional dependence of the activity of the components is known then it is possible to test for evidence of a lack of equilibrium from the distribution of elements between coexisting minerals for a sequence of rocks of different compositions. This compositional dependence is not well known. All that can be said is that, with the limited analytical data, the distribution of elements between the silicate minerals shows a coherent pattern. However there is a considerable spread in the compositions of calcite in equilibrium with dolomite indicating departure from equilibrium. This is interpreted in a later section.

3. Theoretical evidence: that the assemblages are consistent with experimentally determined or calculated reactions. The corollary of this approach is used here.

4. Phase rule evidence: that the assemblages do not have too many phases for the phase rule. However, as stated earlier, it is impossible to calculate the variance of an assemblage.

It is assumed that each assemblage represents frozen-in chemical equilibrium unless it can be demonstrated that this was not the case. However it is not possible to say whether this equilibrium occurred at the metamorphic maximum conditions or during annealing or later.

b. Pressure

The pressure acting on minerals during metamorphism need not have been hydrostatic or equal to the fluid pressure (eg Thompson 1955).

The rocks were acted on by non-hydrostatic pressure in that a penetrative cleavage is ubiquitous. Verhoogen (1951) has shown that there will be a negligible difference in Gibbs energy of a solid under the probable non-hydrostatic pressure than under the corresponding mean hydrostatic pressure.

It is necessary to consider the relationships of fluid pressure to solid pressure during metamorphism because nearly all the reactions considered include fluid components. There are two end member cases

(Thompson 1955),

1. $P_{fluid} = P_{total}$

2. $P_{fluid} < P_{total}$, with the fluid phase in osmotic equilibrium with a fissure system connected to the surface.

The implicit assumption in nearly all metamorphic studies outside granulites and eclogites is no.1 above. The argument for no.1 for the Spean Bridge rocks is involved with the following : that the proportions of the fluid phase components, at least H_2O and CO_2, are buffered by the assemblage (see also Greenwood 1967). The evidence for this comes from the prepondarence of low (model) variance assemblages and the association of assemblages, even on a thin section scale, which lie on opposite sides of reactions involving H_2O and CO_2 (on the assumption that the assemblages formed at the same temperature and total pressure). This means that there were chemical potential gradients for the fluid phase components between adjacent bands. This cannot occur if the fluid phase is in osmotic equilibrium with a fissure system.

An alternative explanation to No.1 above would require H_2O in osmotic equilibrium with a fissure system but CO_2 controlled by the assemblage. This would mean that rocks with associated reaction - related assemblages had P_{fluid} less than P_{total} by different amounts.

However, the simplest model, which has the minimum number of variables capable of describing the observed relations, involves $P_{fluid} = P_{total}$ and the vapour phase composition buffered by the assemblage. Fluid pressure will become equal to P_{total} with rising temperature, unless the fluid components can disappear from the system because the reactions release CO_2 and / or H_2O.

If fluid pressure is less than total pressure by as much as 50%, the actual temperature of reaction will only be a few tens of degrees lower than the calculated temperature (for fluid pressure equal to total pressure) because a log mole fraction term rather than a

mole fraction term is involved.

In graphite-free rocks the fluid phase is assumed to be H_2O and CO_2 only. There is no Fe^{3+} mineral in any of the assemblages so that there is no opportunity to calculate the fugacity of oxygen. On the other hand the assemblage had no means of changing its oxygen fugacity by oxidation reactions. The oxygen fugacity presumably changed little during metamorphism and was probably above the QFM buffer. In the C-H-O system, for these conditions, the hydrogen fugacity is very much less than the water fugacity (Wagman et al. 1945) and can be ignored.

In the graphitic rocks the fluid phase could have had methane as an important component (French 1966). Methane will act as a diluent; the reactions will take place at lower temperatures at a particular $H_2O/H_2O + CO_2$ ratio and pressure.

c. Equal distribution of conditions

The assumption is made that all the assemblages formed at the same temperature and total pressure. The longest dimension of the area, NNE - SSW, is about $2\frac{1}{2}$ miles. If the pressure gradient in this direction was horizontal, this would represent just over one Kbar. This could represent up to or over 100°C temperature difference across the area. However the calcite temperatures discussed later suggest that there is no temperature gradient in this direction. Staurolite - biotite pelites occur just east of Roybridge (R. St J. Lambert, pers. comm.) and 4 miles south of the area (S.W. Richardson, pers.comm.). The maximum temperature gradient is probably towards the south-east.

The model can now be presented :

> The assemblages in the Spean Bridge metamorphic rocks were formed under conditions of total pressure equal to fluid pressure with the fluid phase made of H_2O and CO_2 only in nongraphitic rocks. The composition of the fluid phase was buffered by the assemblage. The present compositions

of the minerals are those frozen in at or near the metamorphic maximum and can be used to calculate the conditions of metamorphism. The assemblages were formed at the same temperature and pressure over the area.

Metamorphic conditions

The above model is assumed to be correct and the metamorphic conditions are calculated from the analysed mineral assemblages using THERMOCALC. Two points must be noted:

1. the above model may be wrong,
2. the thermodynamic data and / or the calculated activities may be wrong.

Obviously both of these cannot be tested at the same time. Calculated conditions are accepted if they are geologically reasonable and if they are supported by independent calculations. When inconsistent values appear they can be interpreted in terms of 1. or 2. above.

This section is divided into parts.

Calcite-dolomite geothermometry

The analyses of coexisting calcites and dolomites from seven rocks are listed in Appendix 5. The % $MgCO_3$ in calcite in equilibrium with dolomite can be used as a geothermometer with the calibration of the calcite-dolomite solvus in the system $CaCO_3$-$MgCO_3$. (Goldsmith and Newton 1969) If they were not in equilibrium with dolomite they would contain less $MgCO_3$ so that the temperature produced would be a minimum.

The natural calcites and dolomites contain significant iron. The effect of Fe on the calcite-dolomite solvus is not clear. Rosenberg (1963) has calibrated the siderite-calcite solvus and the % siderite is about four times the % magnesite for the calcite-dolomite solvus at the same PT. There is considerable substitution of Fe for Mg in dolomite towards a theoretical $CaFe(CO_3)_2$ endmember. The boundary of the calcite only stability field in $CaCO_3$-$MgCO_3$ - $FeCO_3$ is bent at the apex of the 3

phase field, dolomite + calcite + siderite. If this bend is negligible, % magnesite + $\frac{1}{4}$% siderite should be used in the Goldsmith and Newton calibration.

The compositions of the coexisting carbonates provide evidence on the effect of Fe on the solvus, if it is assumed that the calcites were in equilibrium with dolomites in all the rocks at the same temperature and pressure. The % siderite in the carbonates have narrow ranges. Fig 1 shows this, the preference of Fe for dolomite, and the approximately linear distribution of Fe between calcite and dolomite.

Fig 2 shows the relations between % siderite and magnesite in calcite. From Figs 3 - 9, the % $MgCO_3$ in calcite shows a considerable spread. The magnesite dimension of each box in Fig 2 is four times the standard error on the microprobe counts (as calculated by PROCESS) taken from twice the standard error below the highest % $MgCO_3$ measured. This shows that % $MgCO_3$-% $FeCO_3$ should be used in the calibration. However, the rocks which control the positive slope on this graph are B100, 71.16 and 71.26.

In the last chapter is was suggested that B100 and the associated rocks (including 71.16 and 71.26) might have been involved in a late metamorphic event. The very broad calcite peaks in Figs 3, 4 and 6 suggest that the calcites partially re-equilibrated at a lower temperature. If these boxes are ignored in Fig 2 there is no significant effect of Fe on the % $MgCO_3$ in the calcite. Therefore the Fe in calcite and dolomite has no effect on the geothermometer.

The % $MgCO_3$ in calcite which was in equilibrium with dolomite is taken as 5.6% from the maximum compositions of 71.19, 71.42, 71.44 and 71.64. The temperature which this represents is pressure dependent

at 2 kbars 546°C

at 4 kbars 538°C

at 6 kbars 530°C

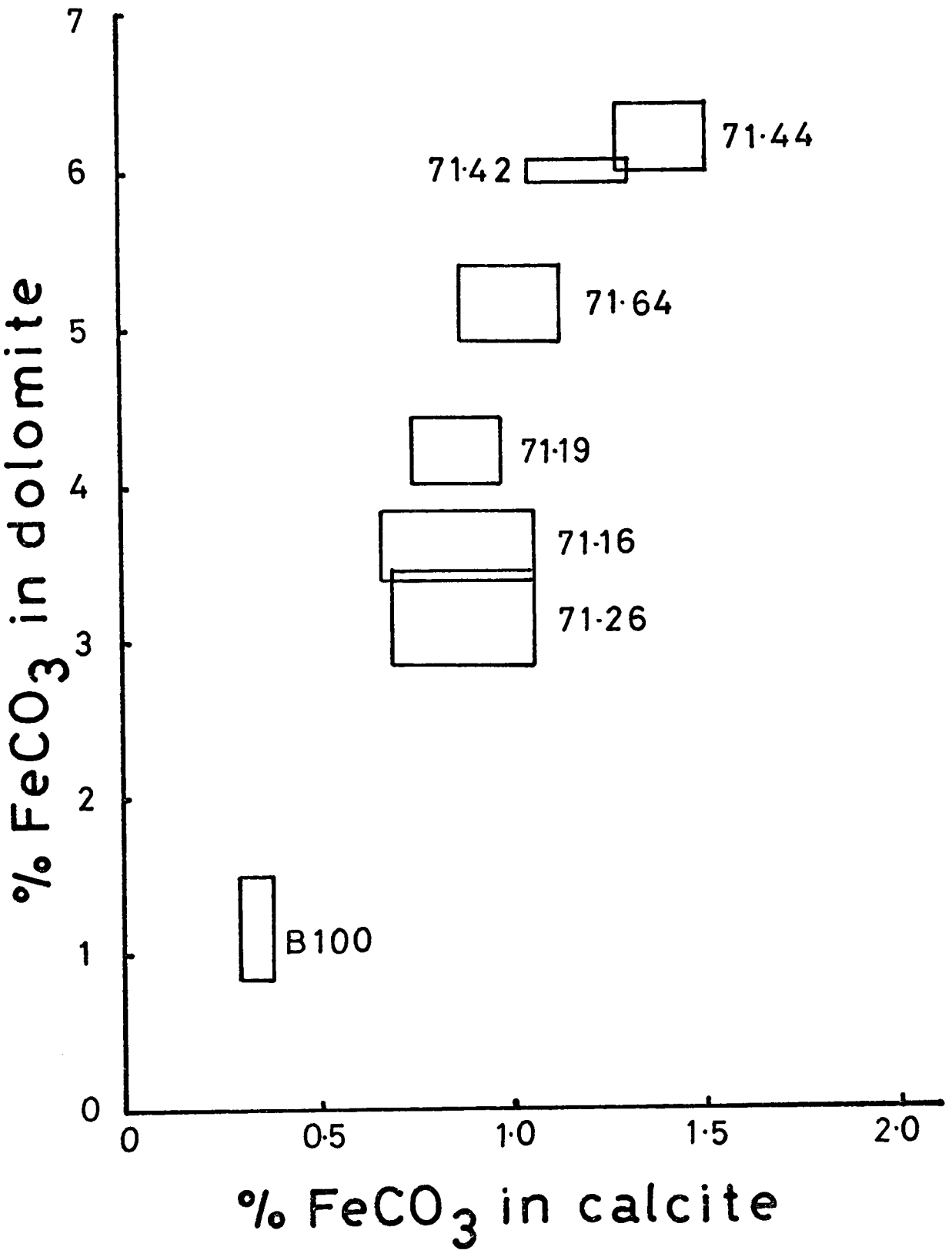


Fig 1 :- Distribution of Fe between calcite and dolomite; boxes give the range of composition for each rock.

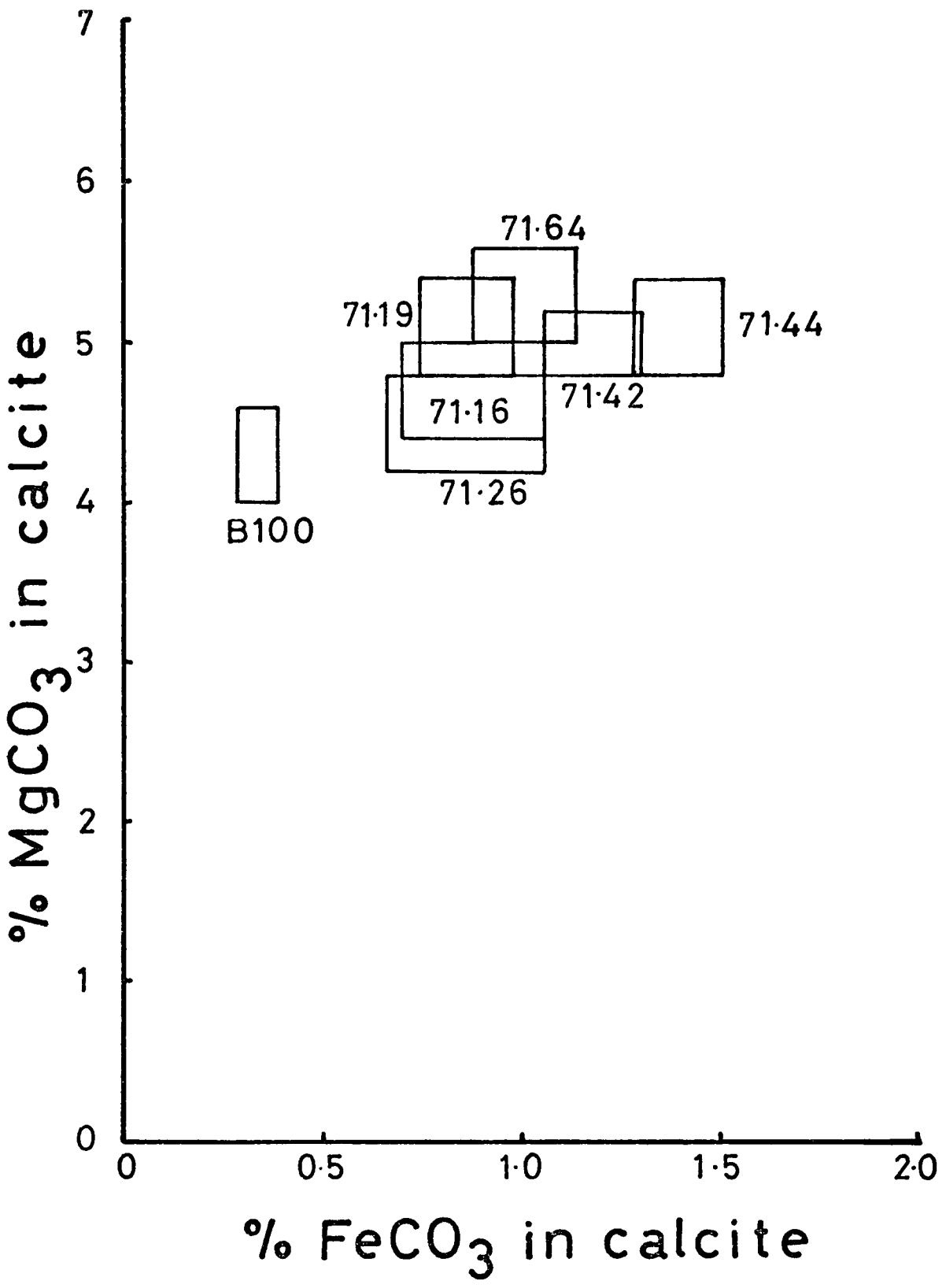


Fig 2 :- Correlation between Fe and Mg in calcite; boxes give the range of composition for each rock.

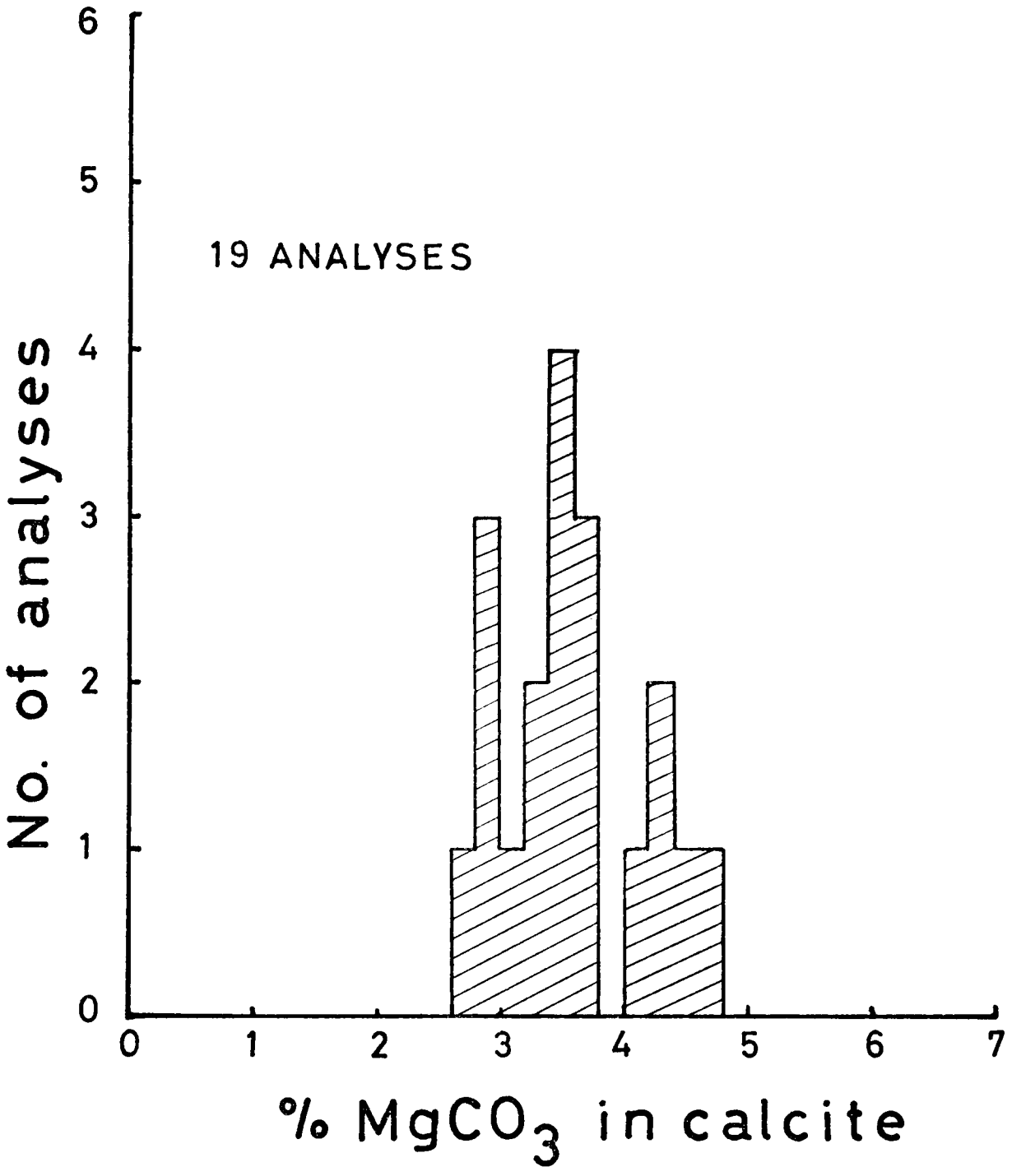


Fig 3 :- Histogram of % $MgCO_3$ in calcite : B100.

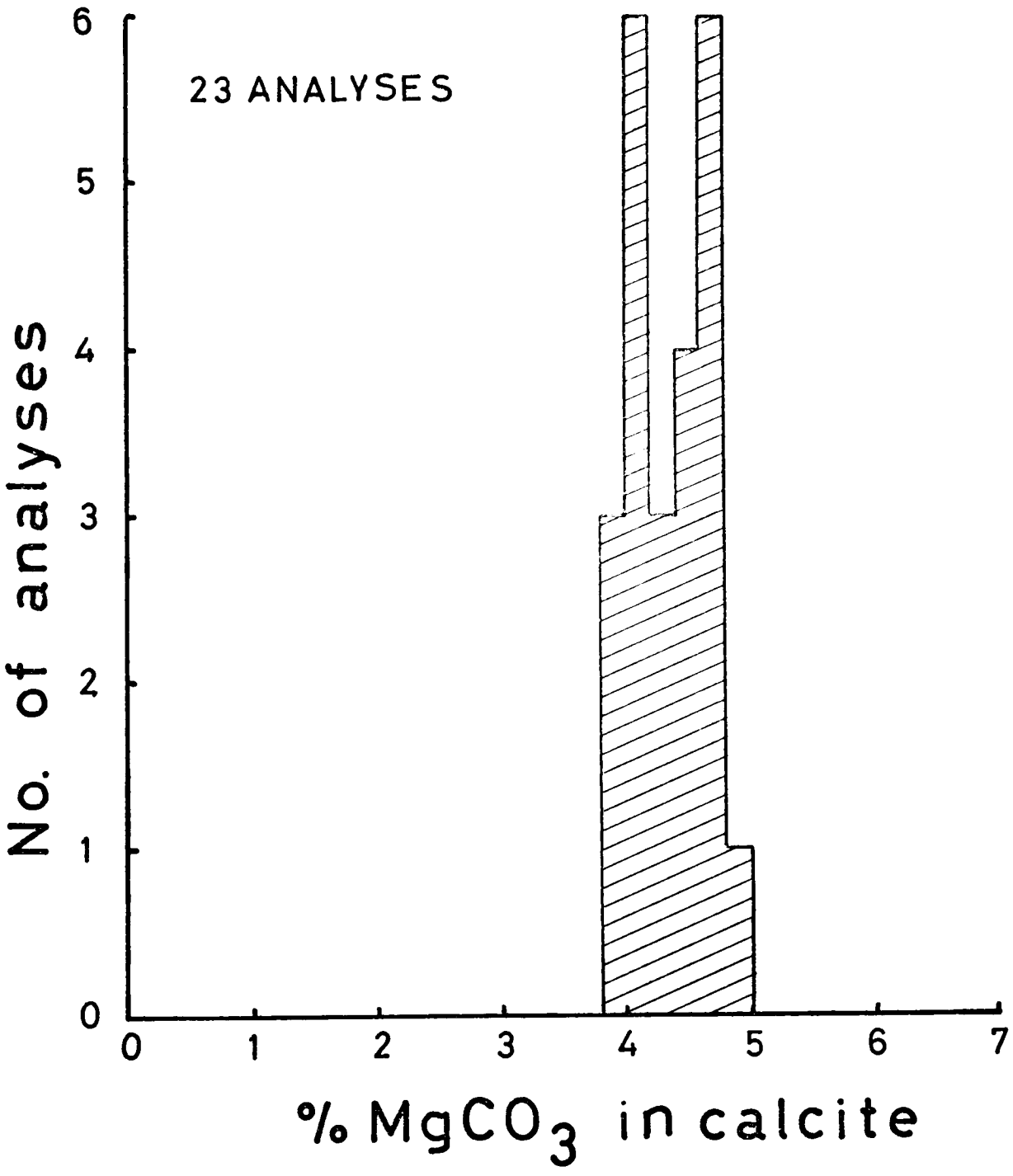


Fig 4 :- Histogram of % $MgCO_3$ in calcite :- 71·16

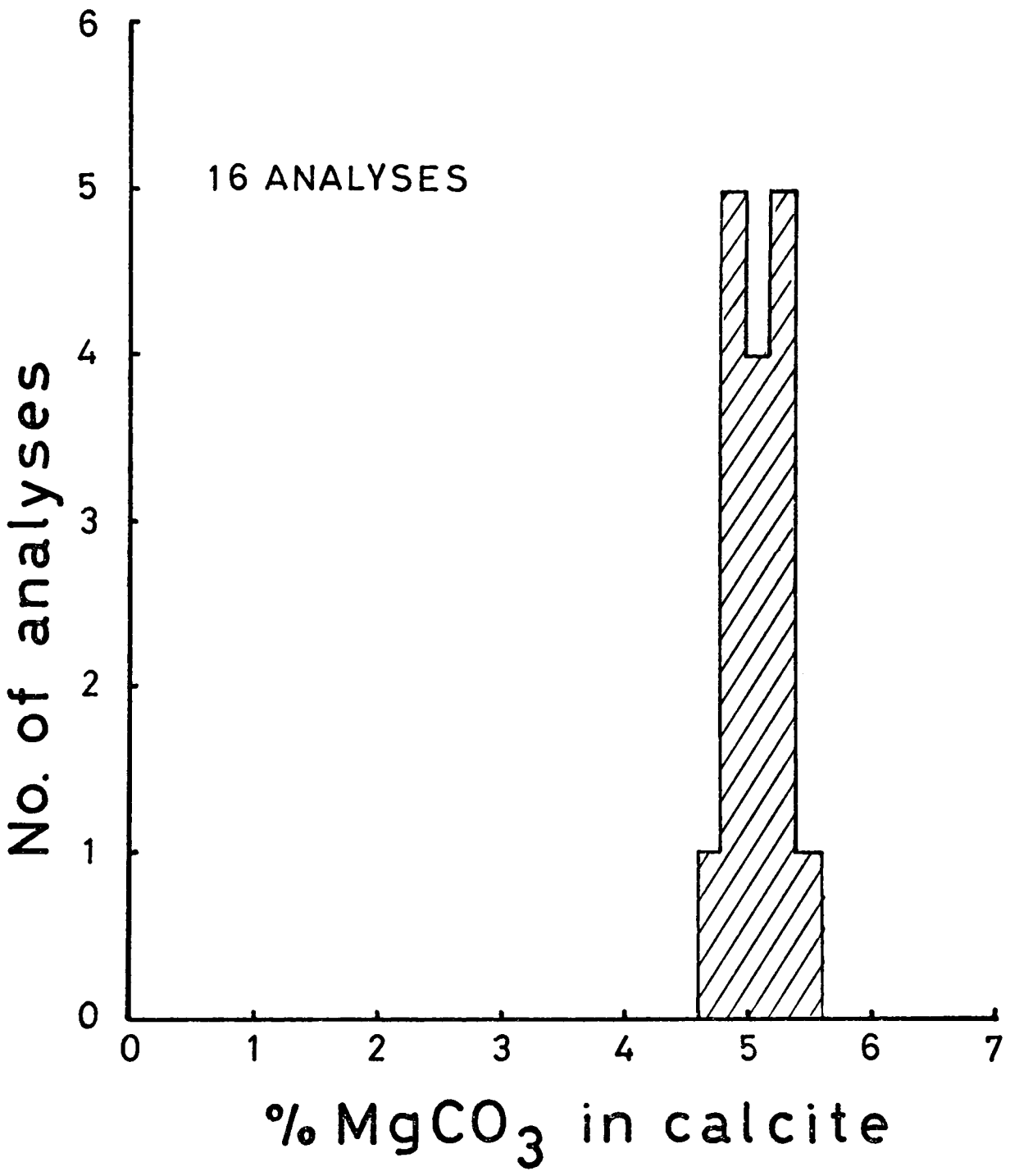


Fig 5 :- Histogram of % $MgCO_3$ in calcite : 71·19.

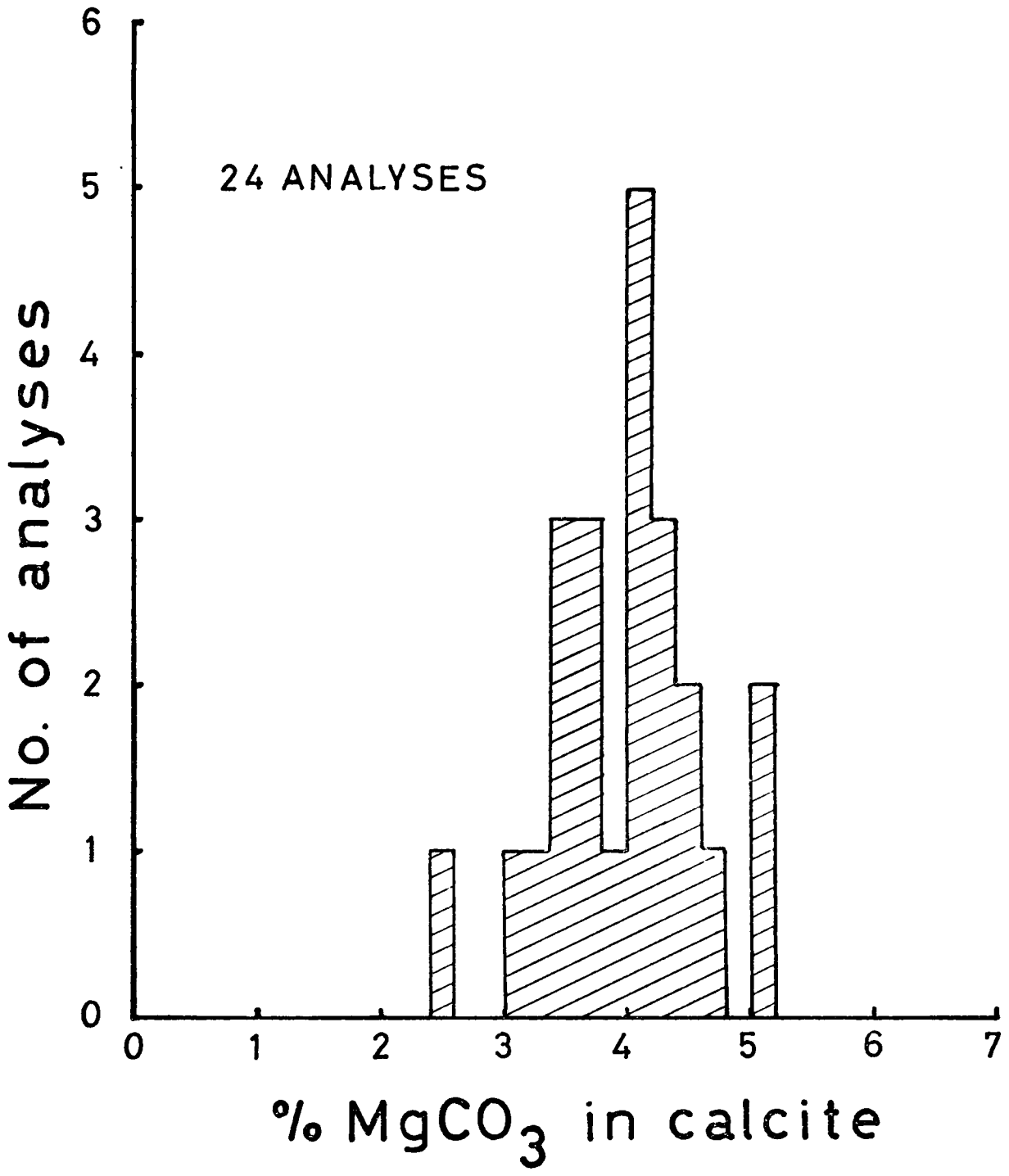


Fig 6 :- Histogram of % $MgCO_3$ in calcite : 71·26

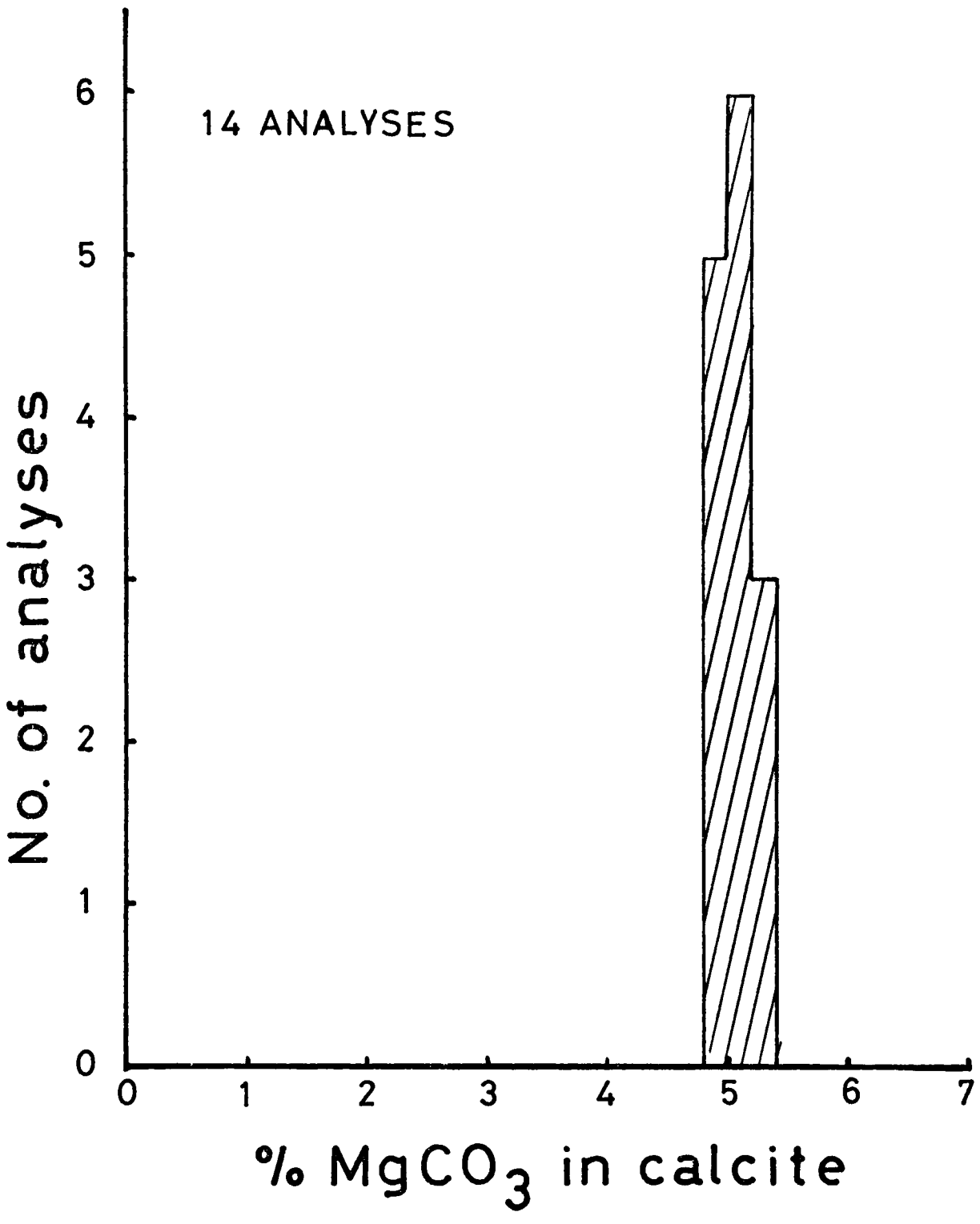


Fig 7 :- Histogram of % $MgCO_3$ in calcite : 71·42

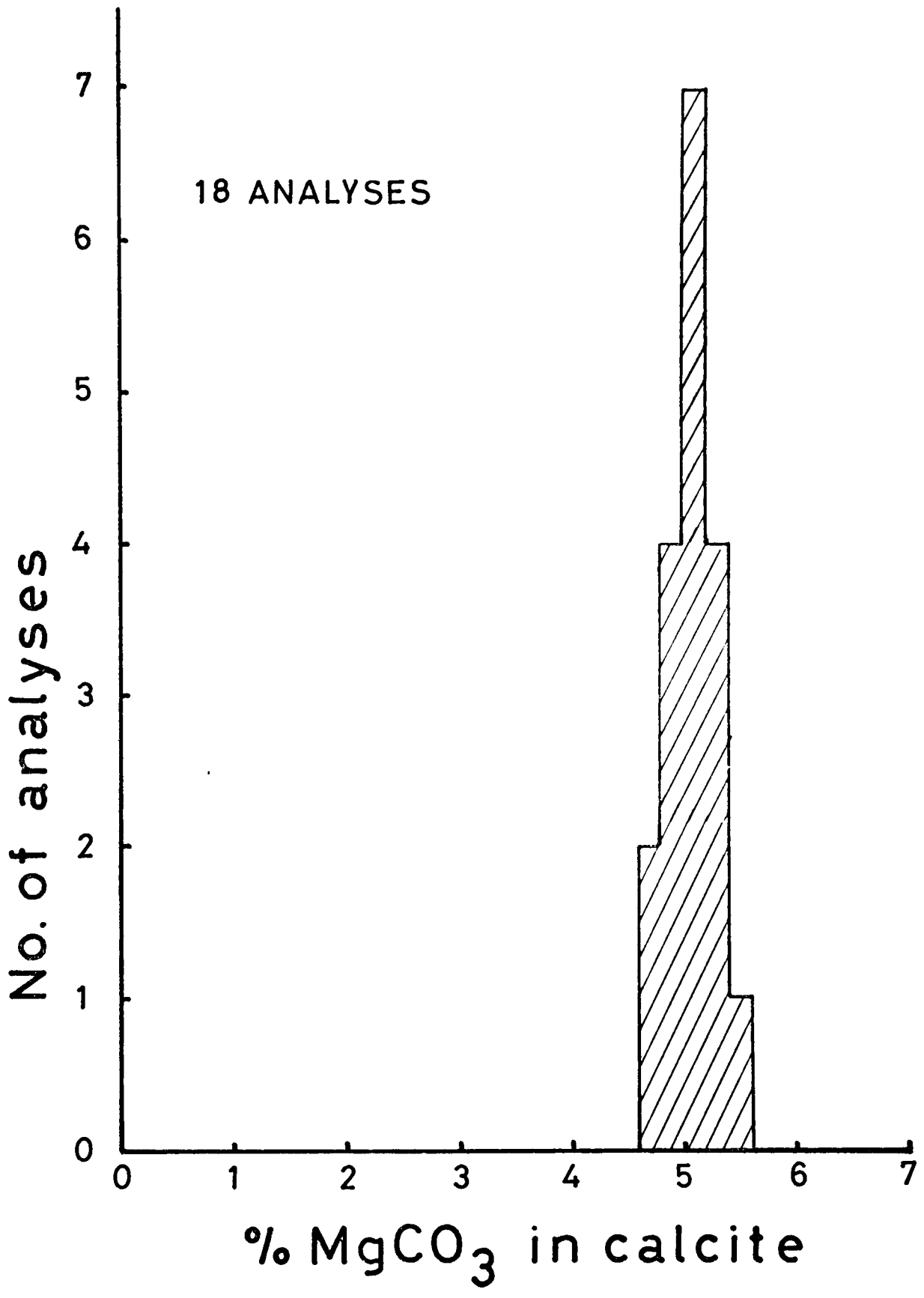


Fig 8 :- Histogram of % $MgCO_3$ in calcite : 71·44

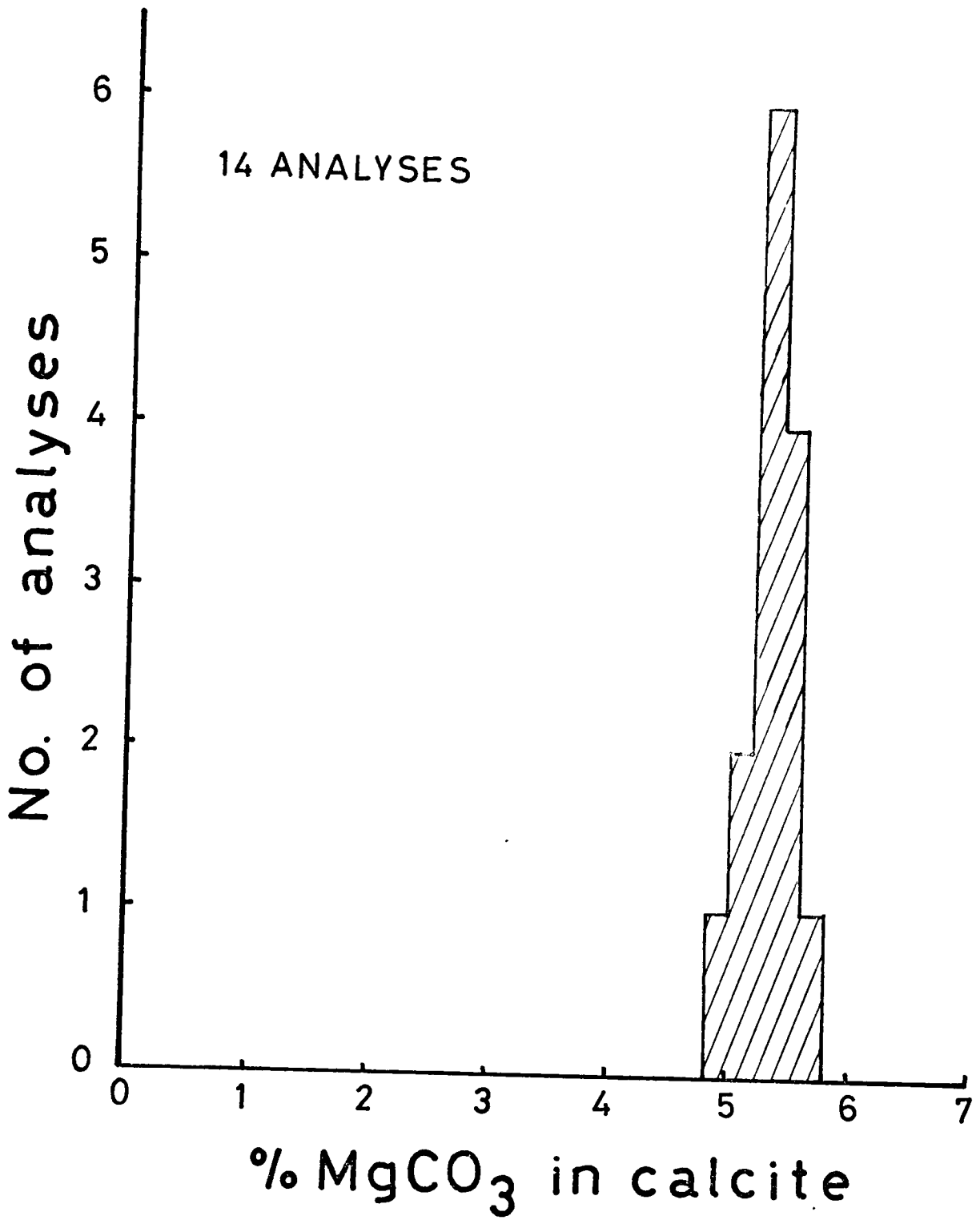


Fig 9 :- Histogram of % $MgCO_3$ in calcite : 71·64

There is no evidence for a north-south temperature gradient from the calcite temperatures because 71.19 and 71.64 are at opposite ends of the area. The temperature is a minimum for the metamorphic conditions because the calcites may have continued to equilibrate with dolomite as the temperature decreased after the metamorphic maximum.

It is difficult to give a temperature for the late metamorphic event. The range of % $MgCO_3$ compositions which probably represent the event is 2.7% to 3.5% $MgCO_3$ or between 410° and 450°C (at 2 kbars).

Model system calculations

This part is subdivided into the same groups and subgroups used in the last chapter to describe the assemblages. Each is considered in terms of chemical potential of H_2O - chemical potential of CO_2 (mu-mu) diagrams (Khorzinskii 1959) as an introduction to T - X_{CO_2} (T-X) sections (Greenwood 1967) for the model system analogue of the assemblages. T-X sections are given for the analysed mineral assemblages with activities calculated for the model system components.

Mu-mu diagrams provide a constant temperature, constant pressure representation of the relations between reactions involving H_2O and CO_2. The advantage they have over T-X sections is that the reaction lines are straight and the gradients of the lines are controlled by the reaction coefficients of H_2O and CO_2 (see (46)), thus avoiding the equivocal nature of thermodynamic data. The diagrams were constructed using Schreinemaker's rules (see Korzhinskii 1959).

The number of possible topologies is controlled by the variance of the system. For example if the variance of the system is zero, there are two topologies related by inversion. They are applicable to different regions of P-T-X space. These regions are separated by an invariant point.

On each mu-mu diagram there is a line, an arc with the origin of the diagram as its centre, on which $P_{H_2O} + P_{CO_2} = P_{total}$. Below this

line $P_{H_2O} + P_{CO_2}$ is less than P_{total}. Above the line is a physically unrealisable region with fluid pressure greater than total pressure. The line is equivalent to a constant temperature line on a T-X section. As temperature is increased the line sweeps towards the origin, relative to the reaction lines, producing the topology of a T-X section.

The last column in Table 1 of the last chapter is a code refering to model invariant, univariant and divariant assemblages on diagrams in this chapter. The letter refers to the subgroup and the numbers to the univariant points on the mu-mu and T-X sections. One number refers to the univariant point, number-number refers to a divariant line between the designated invariant points, and number-number-number-number refers to an invariant situation with the intersection of the designated univariant points.

The different subgroups are now considered in turn.

Group 1: talc-tremolite subgroup: A

The coarse grained part of the analysed assemblage B100 is model invariant. The constituent assemblages of the fine grained part are model univariant and divariant. Fig 10 and 11 are the two possible mu-mu topologies for this model invariant assemblage. The fine-grained part assemblages, A3 and A4, indicate that Topology 2 is the stable form during the main metamorphic event. The calculations, using the analyses to approximate activities, support this, Fig 12. The invariant point occurs at low pressure.

The pressure for A3 and A4 from the calcite temperature is 4.5 and 4.7 kbars respectively. These numbers could be slightly in error because the minerals analysed were in the coarse grained part. However the composition of B100 is sufficiently close to the model system that the minerals formed earlier should have similar compositions to those formed later.

Albite appears to have been the equilibrium plagioclase in the

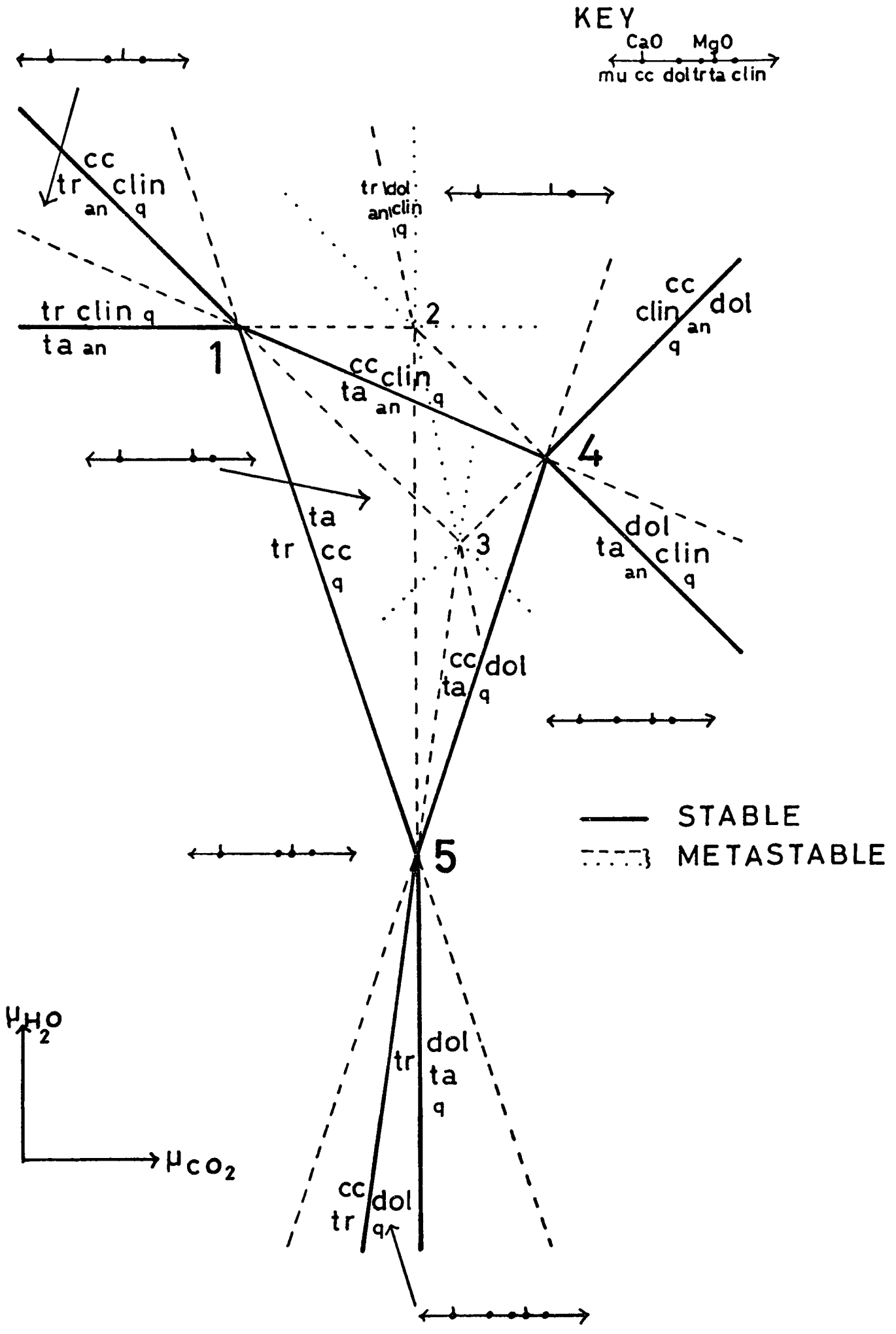


Fig 10 :- Talc + tremolite subgroup, model system, $\mu_{H_2O} - \mu_{CO_2}$, topology 1.

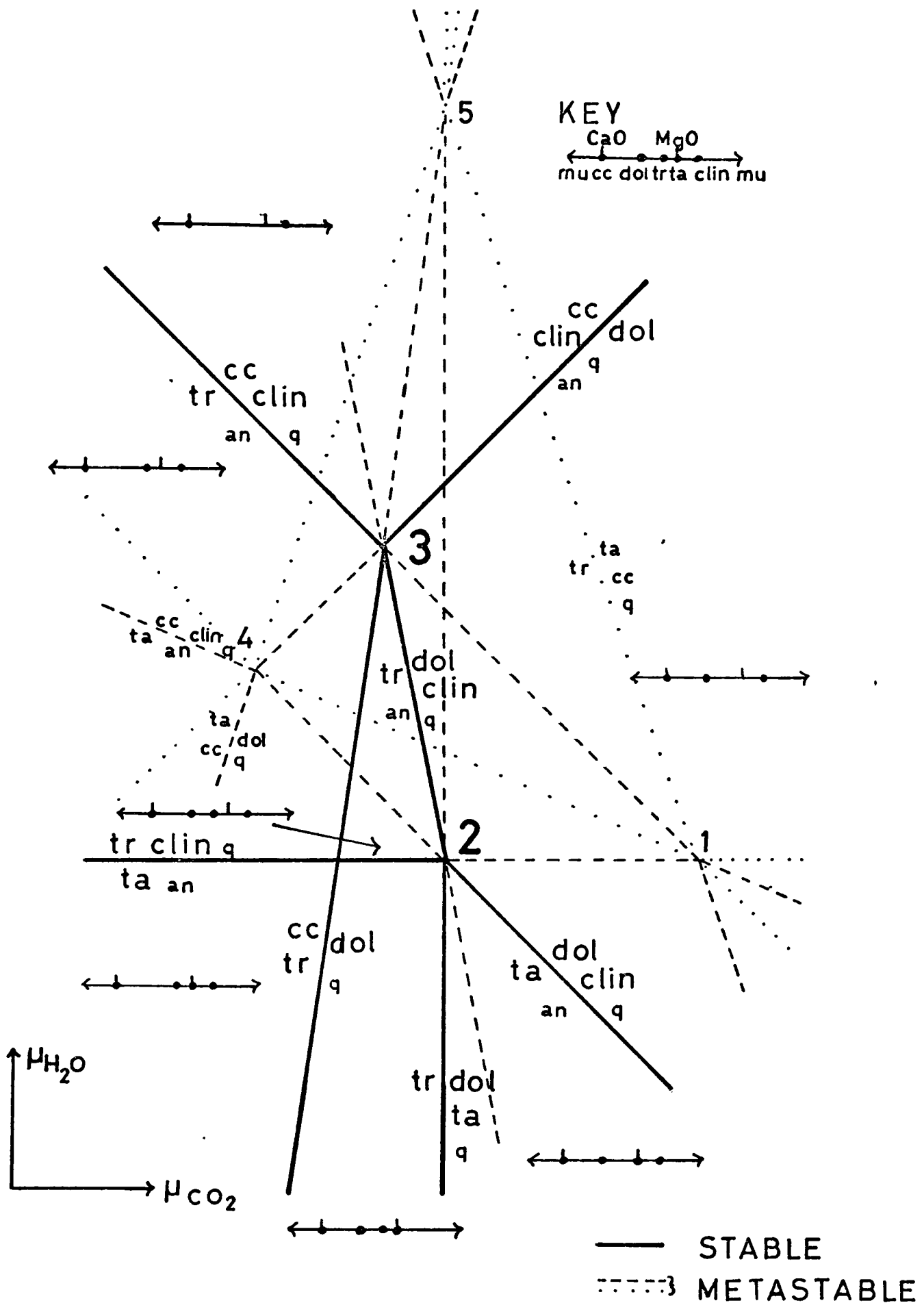


Fig 11 :- Talc + tremolite subgroup, model system, $\mu_{H_2O} - \mu_{CO_2}$, topology 2

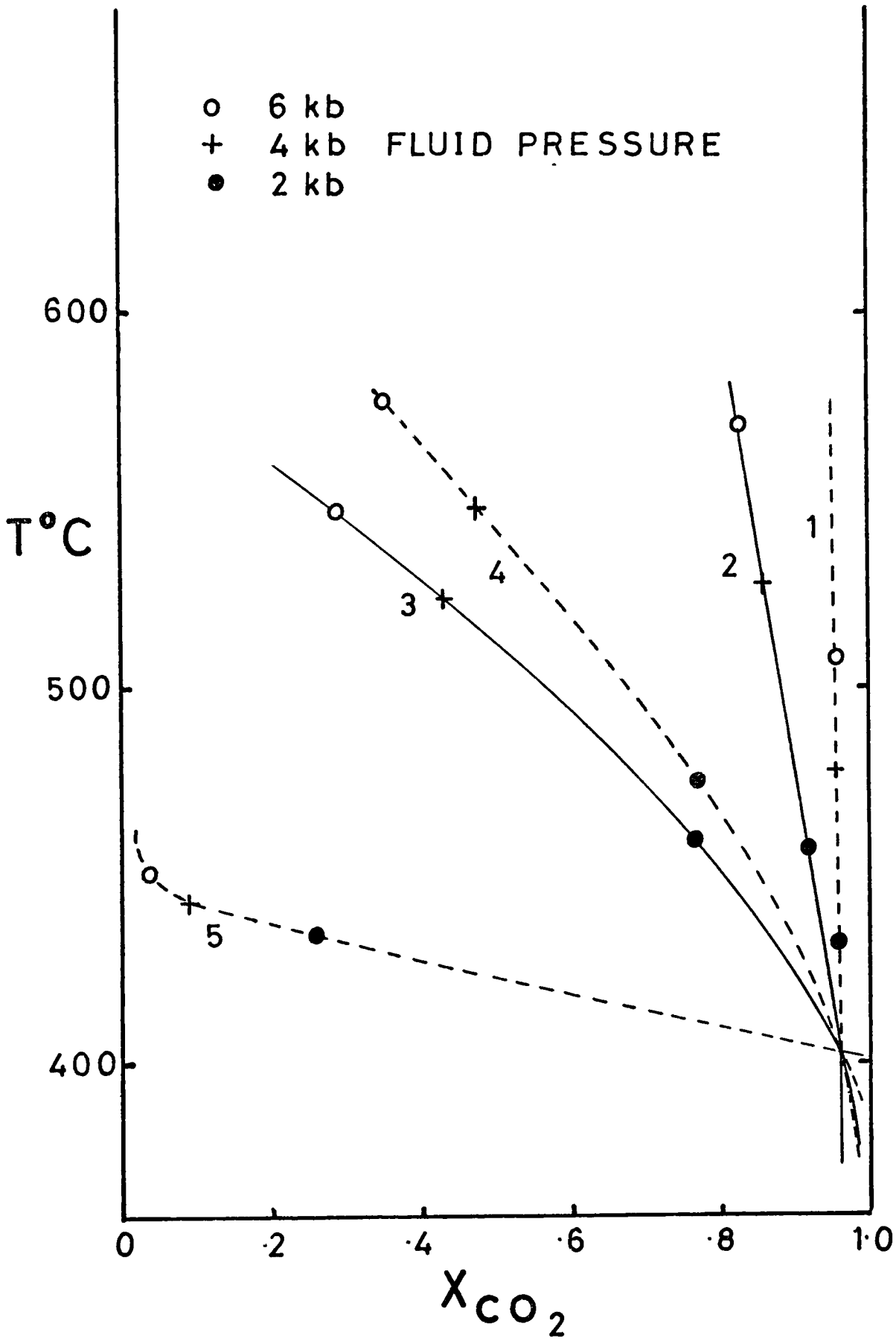


Fig 12 :- Talc + tremolite subgroup, model system, P-T-X_{CO_2}, calculated activities, plagioclase = oligoclase : B100.

late event. Although not analysed, its composition is probably close to an_1 because the peristerite solvus is effective at the temperatures indicated by the calcites. Fig 13 and 14 give the T-X sections for the late event assemblage at 1 and 1.5 kbars. Fig 13 corresponds to Topology 1 and Fig 14 to Topology 2. The invariant assemblage occurs between 1 and 1.5 kbars at about 420°C and $X_{CO_2} = 0.8$.

The evidence for the late metamorphic event is summarised in Fig 15. The calcites the fluid inclusions and the coarse grained part of the siliceous dolomites suggest a late metamorphic event at about 1 kbar and 430°C. The significance of this will be discussed later.

Group 1: tremolite + clinozoisite subgroup: B

The analysed assemblage 71.19 is model invariant. Figs 16 and 17 are the two possible topologies of the corresponding model system. Figs 18 and 19 show T-X sections for the model system at 4 kbars and 6 kbars. Topology 1 is the high pressure form. The invariant point occurs at about 5.5 kbars and 570°C. Inserting the calculated activities displaces the invariant point to about 7 kbars and 580°C, Fig 20. This tempeature is much higher than the calcite temperature.

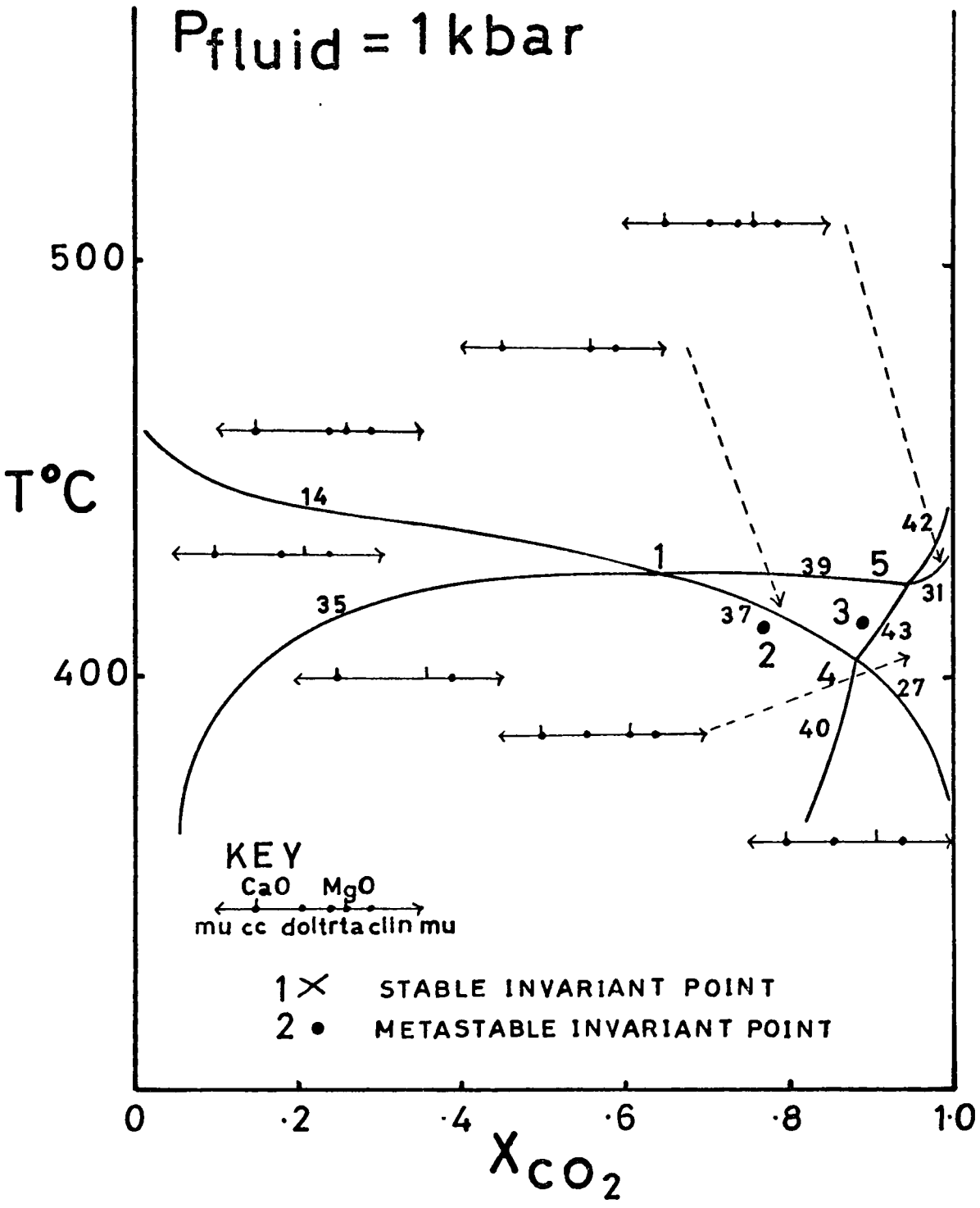
However the rock is graphitic. As suggested earlier the fluid phase of this rock could contain important methane. The calculations were repeated with 25% and 50% diluent in the fluid phase, Figs 21 and 22. This lowers the invariant point to 6 kbars and 540°C and 4.5 kbars and 490°C respectively.

This information is summarised in Fig 23. The calcite temperature gives a pressure of 5.6 kbars at $X_{CH_4} = 0.4$ and $CO_2/CO_2 + H_2O = 0.6$. This in turn means that the oxygen fugacity lies between the NNO and QFM buffer (French 1966).

Group 1 : garnet pelite amphibole subgroup : C

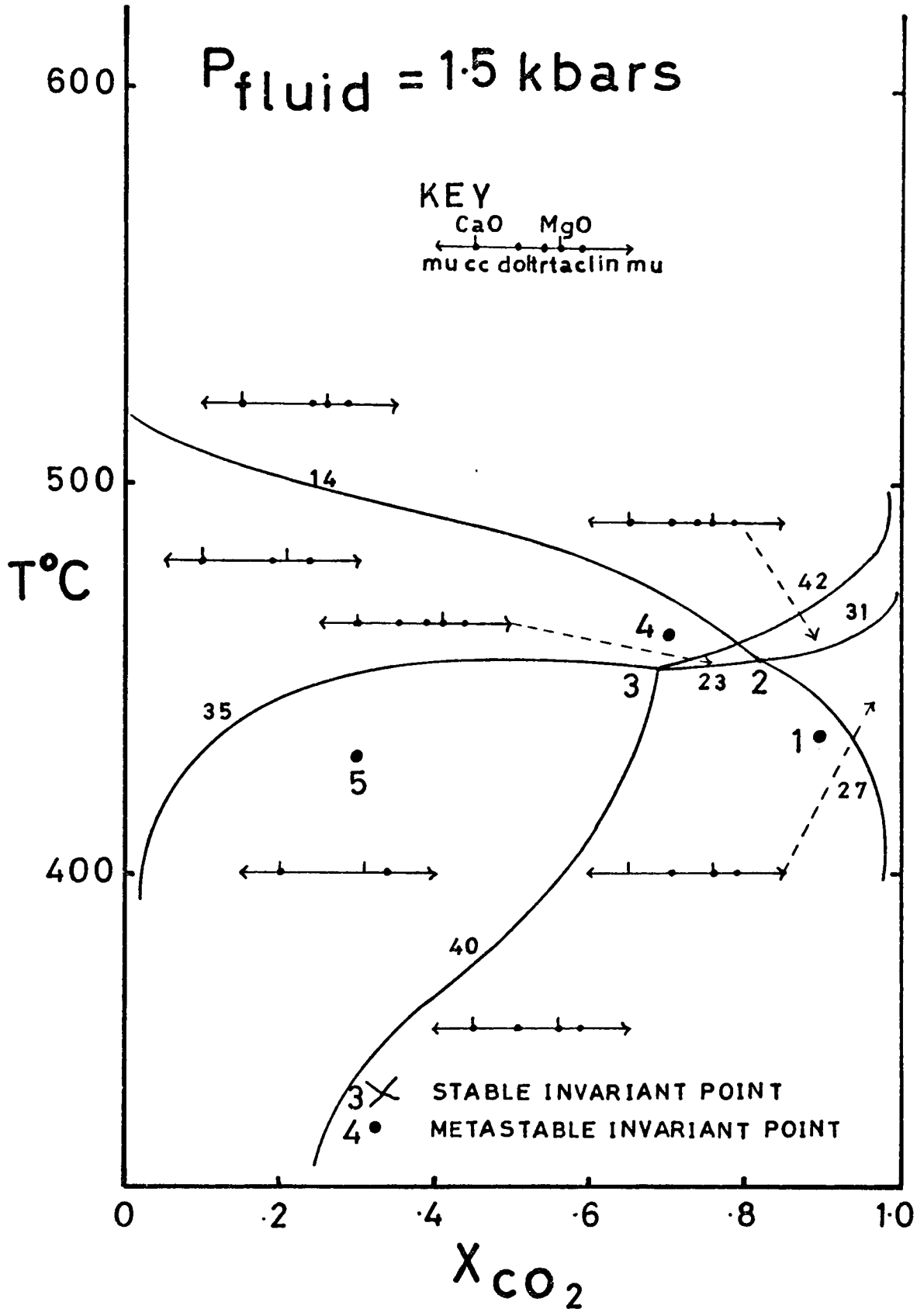
Group 2 : carbonate free subgroup : part of D

These two subgroups can be usefully considered together because



	HIGH T		LOW T
14	ta + an + H_2O	=	tr + clin + q
27	ta + an + H_2O + CO_2	=	dol + clin + q
31	tr + CO_2	=	dol + ta + q
35	tr + an + H_2O + CO_2	=	cc + clin + q
37	ta + an + H_2O + CO_2	=	cc + clin + q
39	tr + H_2O + CO_2	=	ta + cc + q
40	cc + clin + CO_2	=	dol + an + q + H_2O
42	cc + tr + CO_2	=	dol + q + H_2O
43	ta + cc + CO_2	=	dol + q + H_2O

Fig 13 :- Talc + tremolite subgroup, T-X_{CO_2} at 1 kbar, calculated activities, plagioclase = albite : B100



	HIGH T		LOW T
14	ta + an + H_2O	=	tr + clin + q
23	tr + an + H_2O + CO_2	=	dol + clin + q
27	ta + an + H_2O + CO_2	=	dol + clin + q
31	tr + CO_2	=	dol + ta + q
35	tr + an + H_2O + CO_2	=	cc + clin + q
40	clin + cc + CO_2	=	dol + an + q + H_2O
42	tr + cc + CO_2	=	dol + q + H_2O

Fig 14 :- Talc + tremolite subgroup, T-X_{CO_2} at 1·5 kbars, calculated activities, plagioclase = albite : B100

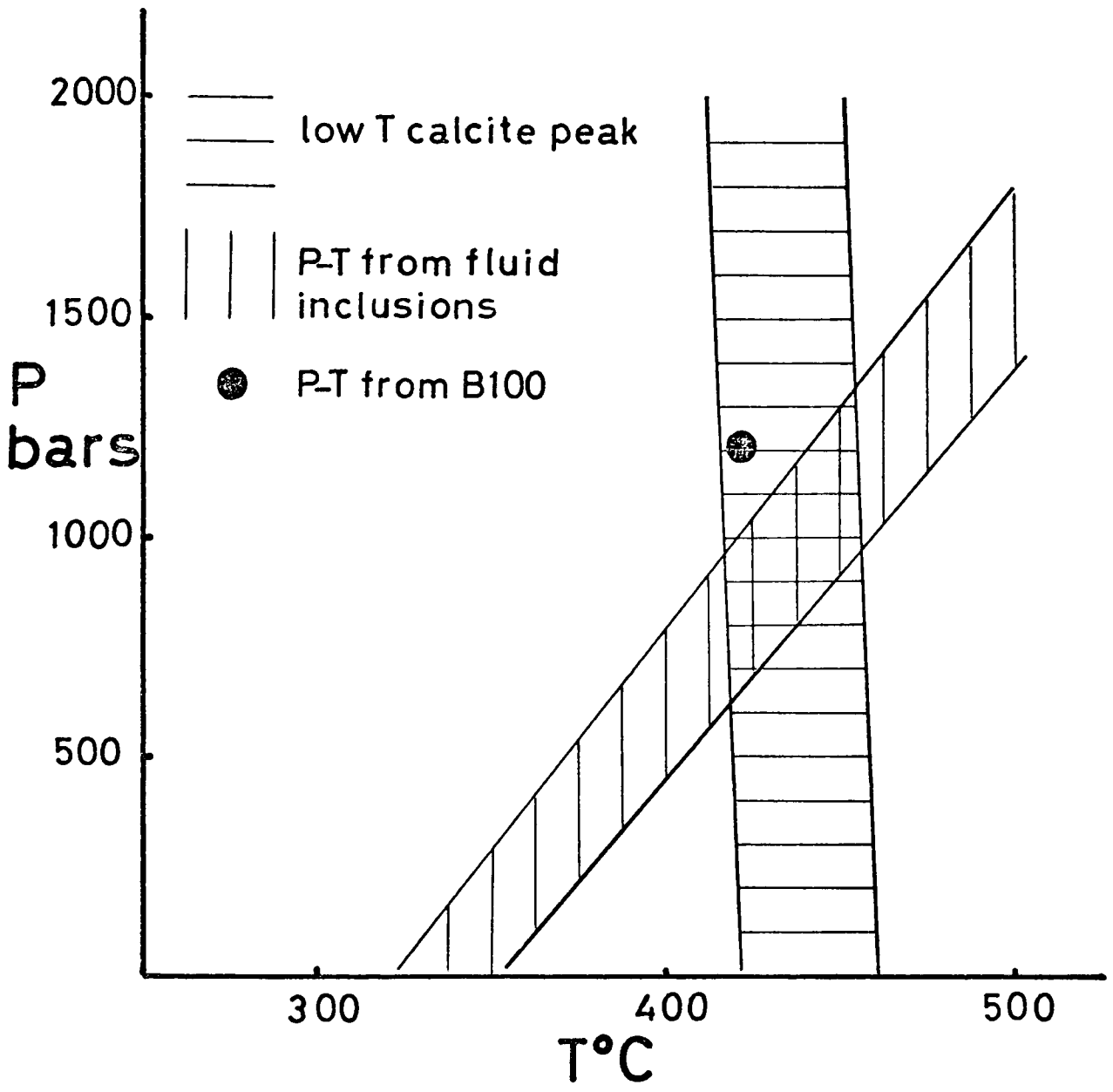


Fig15:-Summary of evidence for the late metamorphic event.

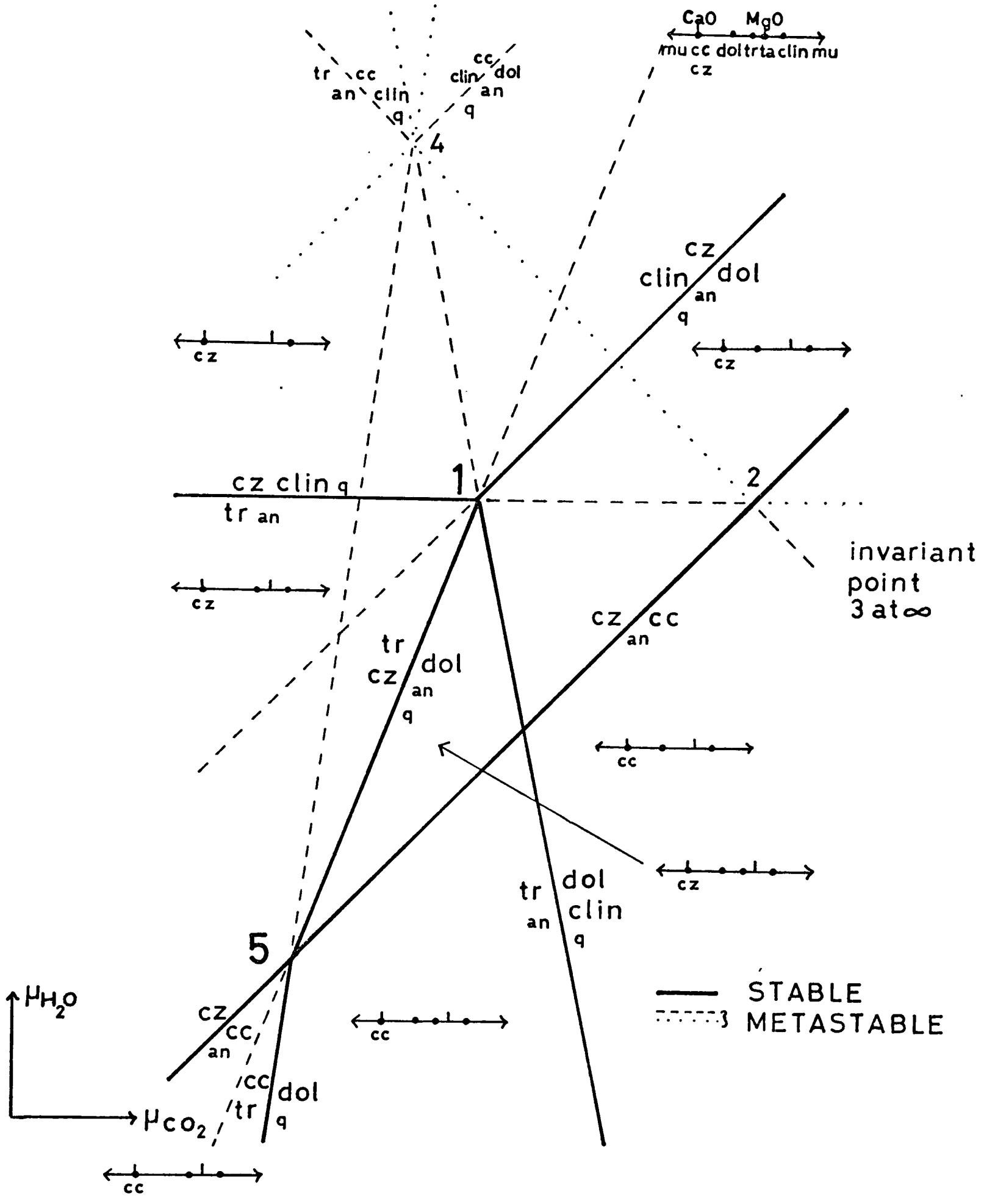


Fig 16 :- Tremolite + clinozoisite subgroup, model system, $\mu_{H_2O} - \mu_{CO_2}$, topology 1

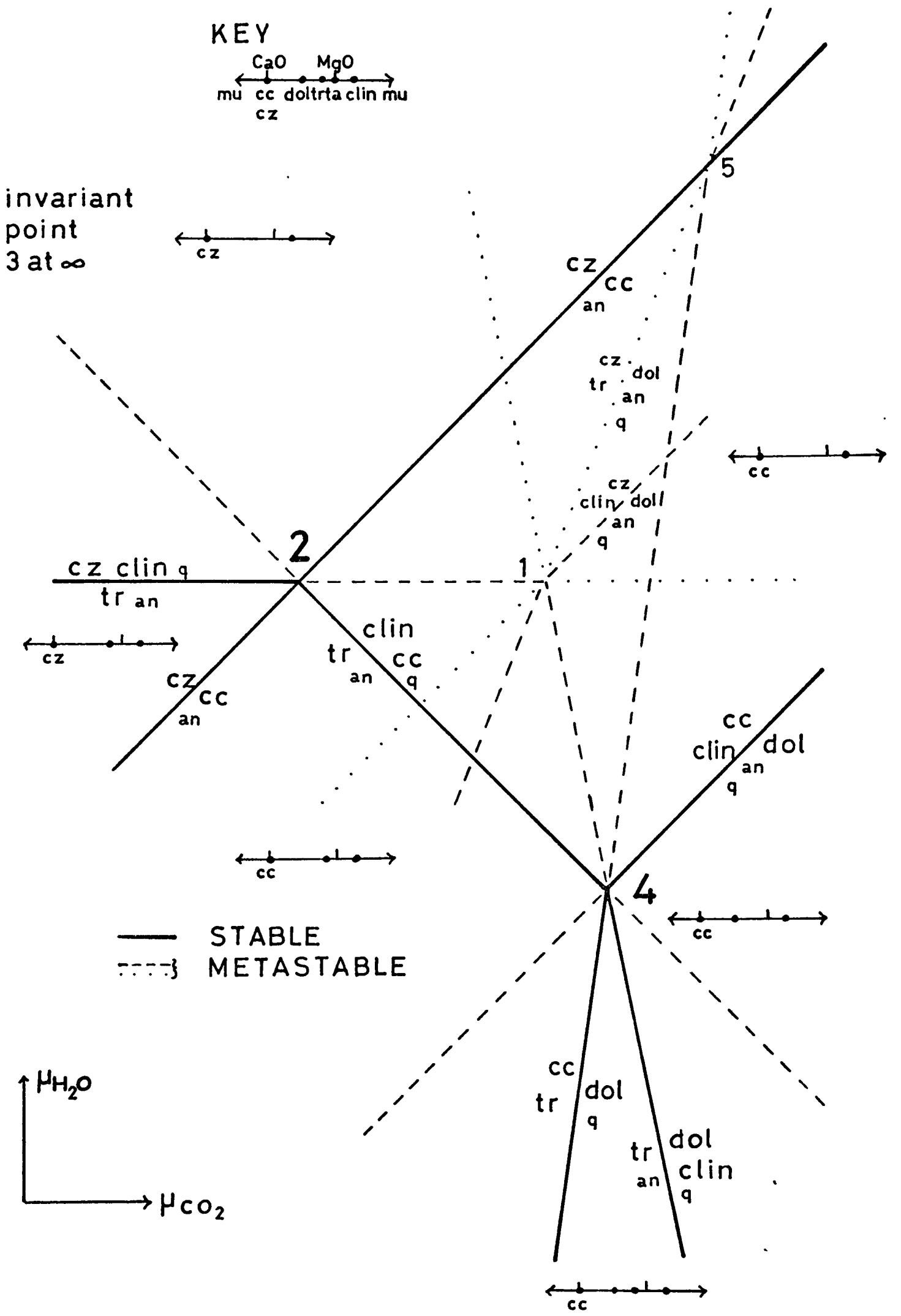
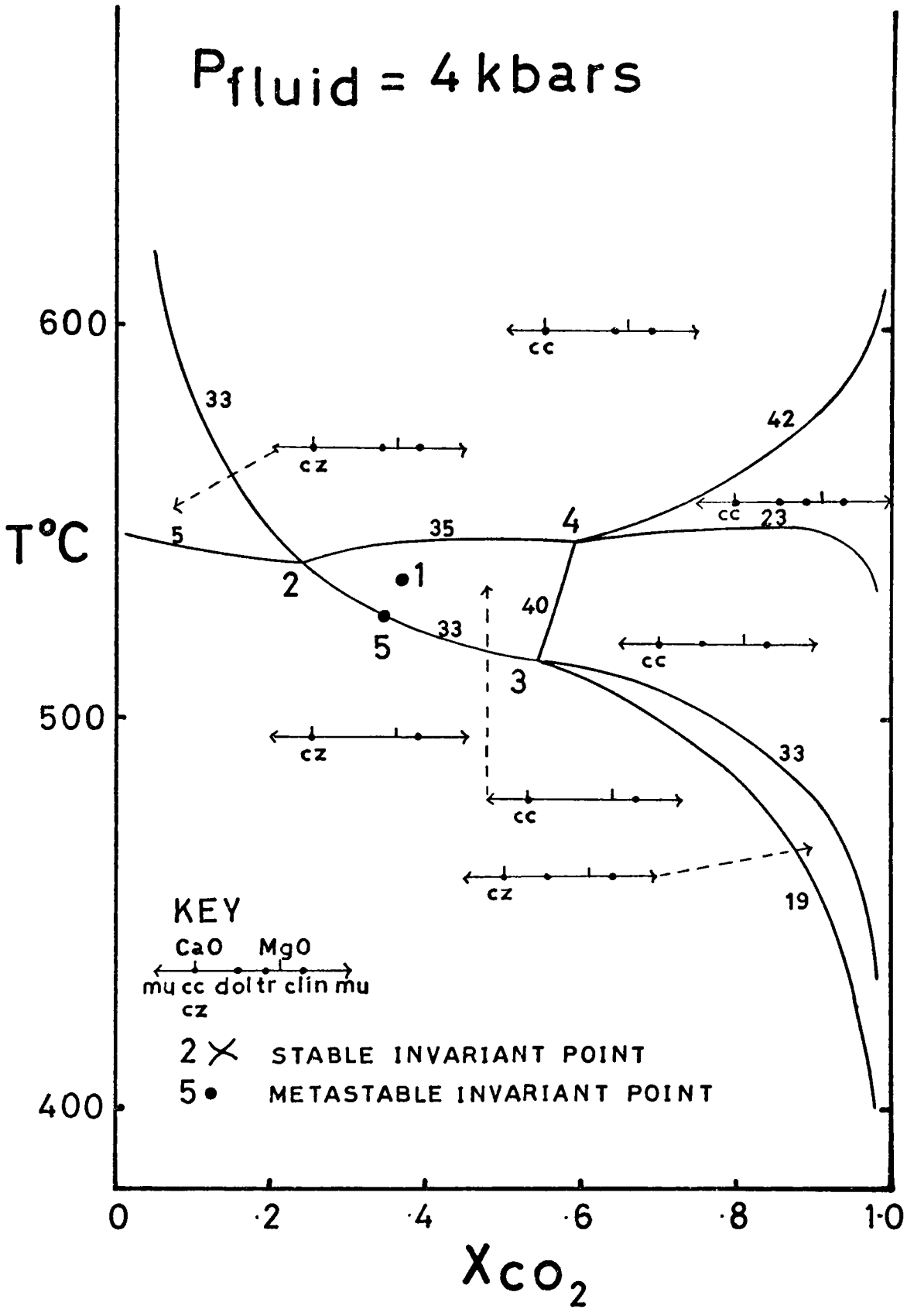
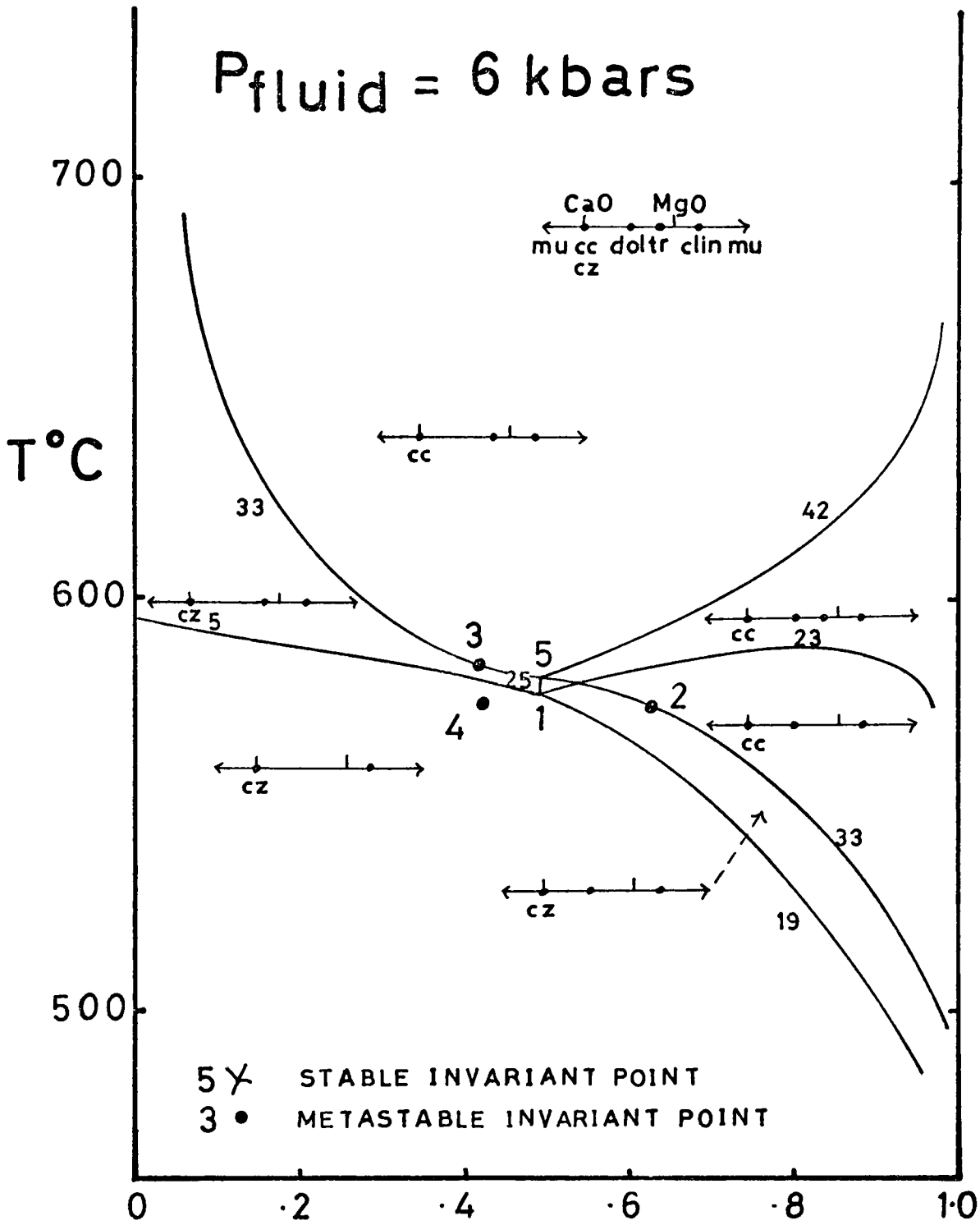


Fig 17 :- Tremolite + clinozoisite subgroup, model system, $\mu_{H_2O} - \mu_{CO_2}$, topology 2.



	HIGH T		LOW T
5	tr + an + H_2O	=	cz + clin + q
19	dol + an + q + H_2O	=	cz + clin + CO_2
23	tr + an + H_2O + CO_2	=	dol + clin + q
33	cc + an + H_2O	=	cz + CO_2
35	tr + an + H_2O + CO_2	=	cc + clin + q
40	cc + clin + CO_2	=	dol + an + q + H_2O
42	cc + tr + CO_2	=	dol + q + H_2O

Fig 18 :- Tremolite + clinozoisite subgroup, T-X_{CO_2} at 4 kbars, model system.



	HIGH T		LOW T
5	tr + an + H_2O	=	cz + clin + q
19	dol + an + q + H_2O	=	cz + clin + CO_2
23	tr + an + H_2O + CO_2	=	dol + clin + q
25	tr + cz + CO_2	=	dol + an + q + H_2O
33	cc + an + H_2O	=	cz + CO_2
42	cc + tr + CO_2	=	dol + q + H_2O

Fig 19 :- Tremolite + clinozoisite subgroup, T-X_{CO_2} at 6 kbars, model system.

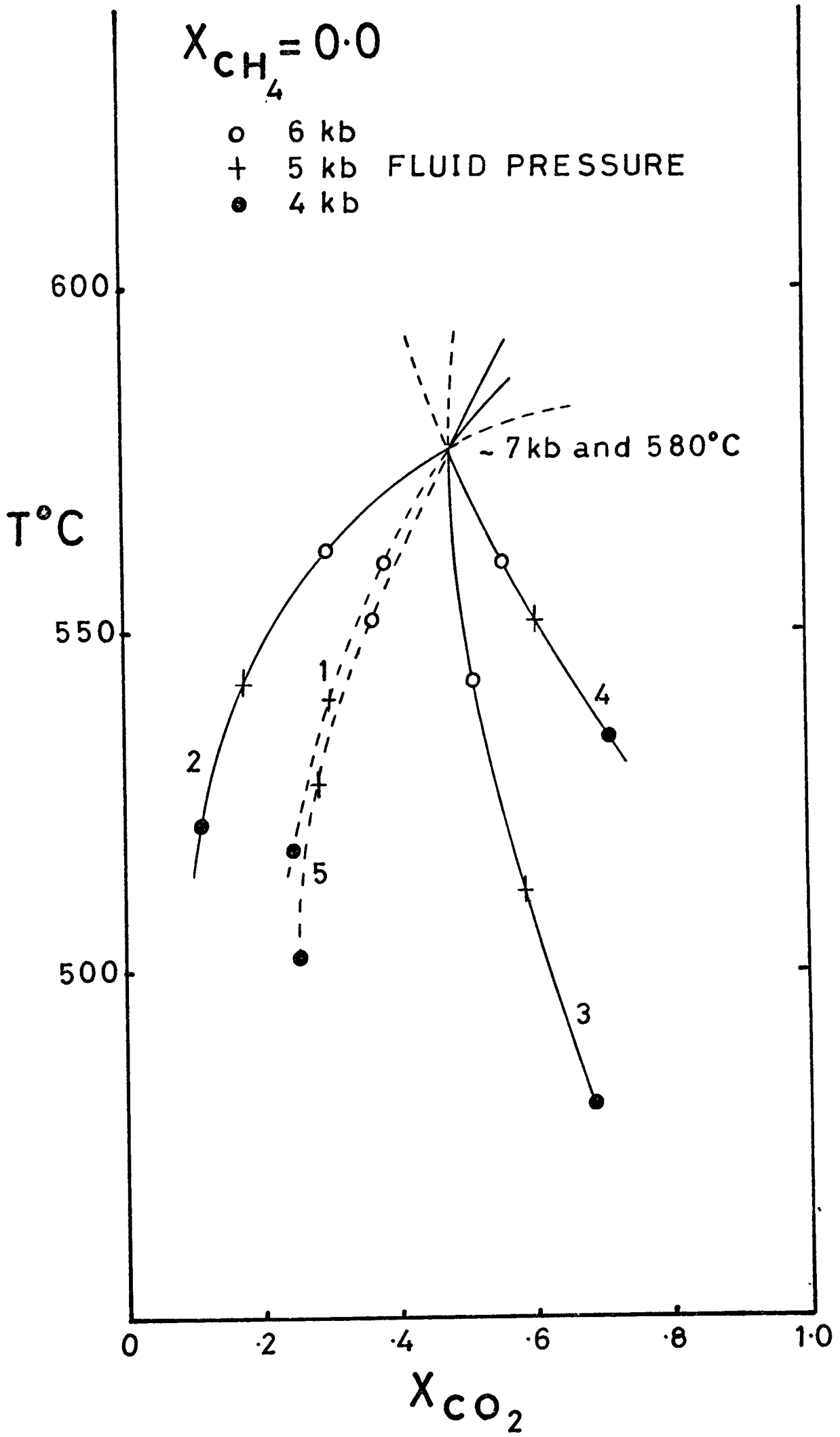


Fig 20:- Tremolite + clinozoisite subgroup, P-T-X_{CO_2}, calculated activities, 0% CH_4 diluent : 71·19.

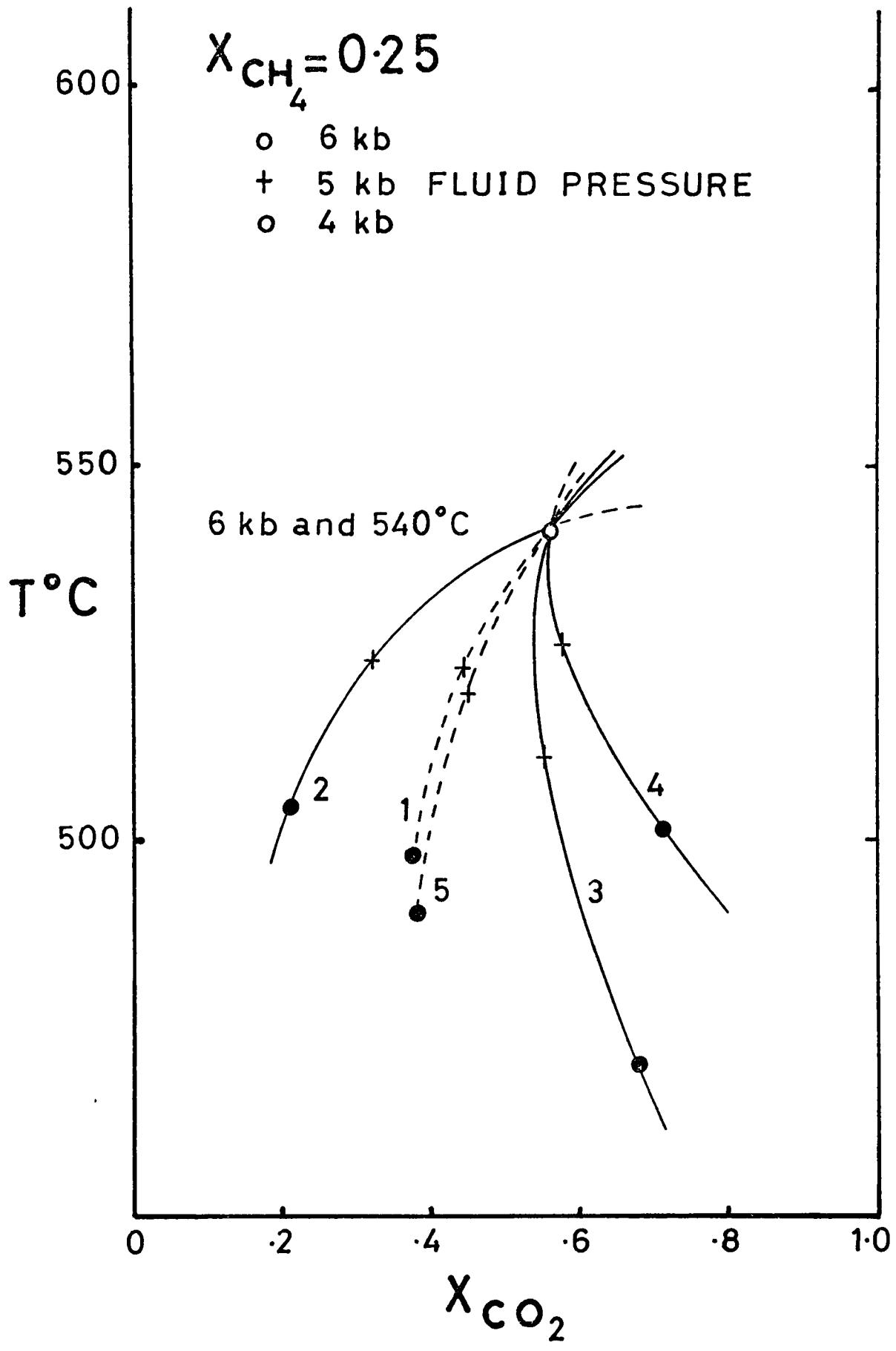


Fig 21:- Tremolite + clinozoisite subgroup, P-T-X_{CO_2}, calculated activities, 25% CH_4 diluent : 71·19.

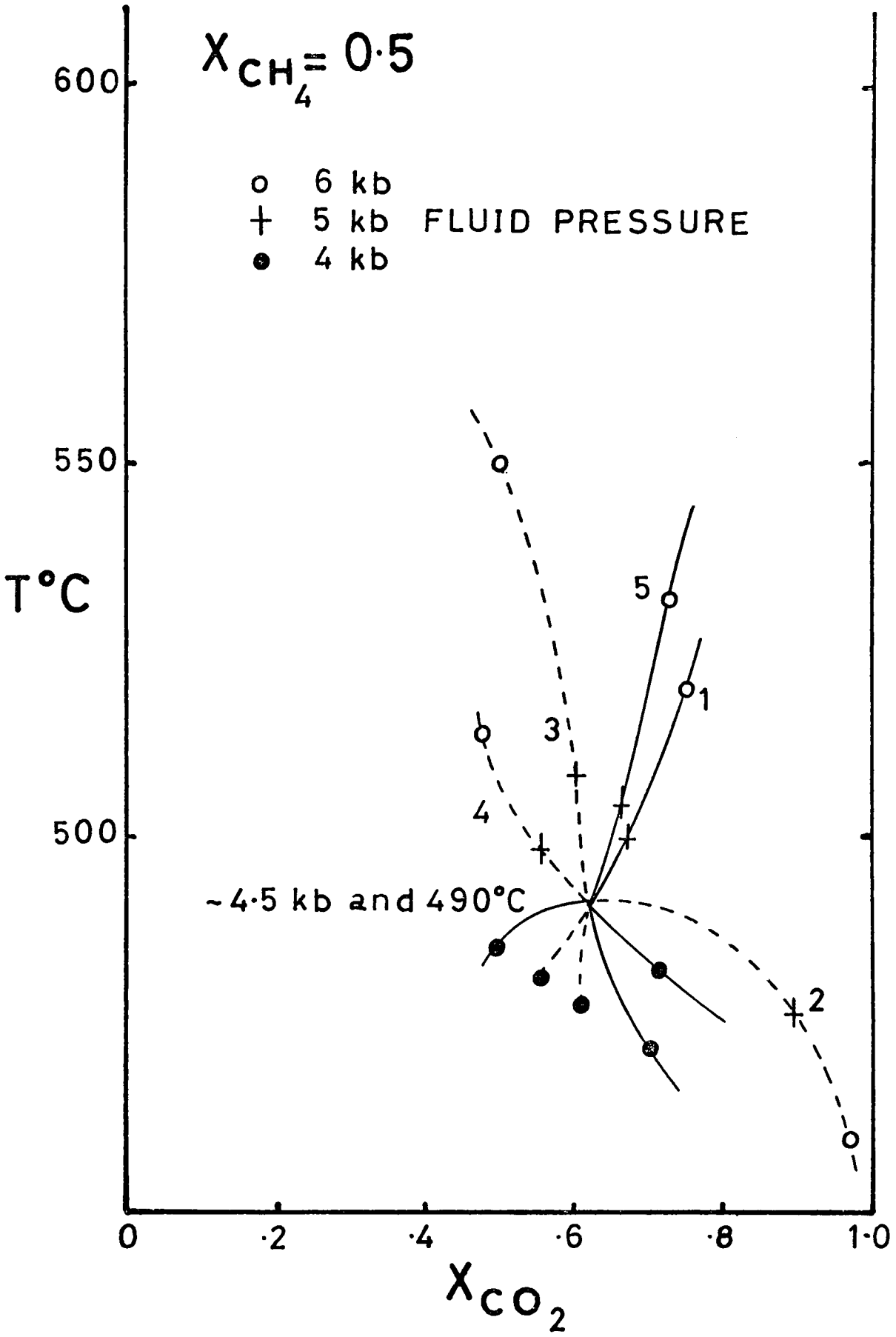


Fig.22 :- Tremolite + clinozoisite subgroup, P-T-X_{CO_2}, calculated activities, 50% CH_4 diluent : 71·19.

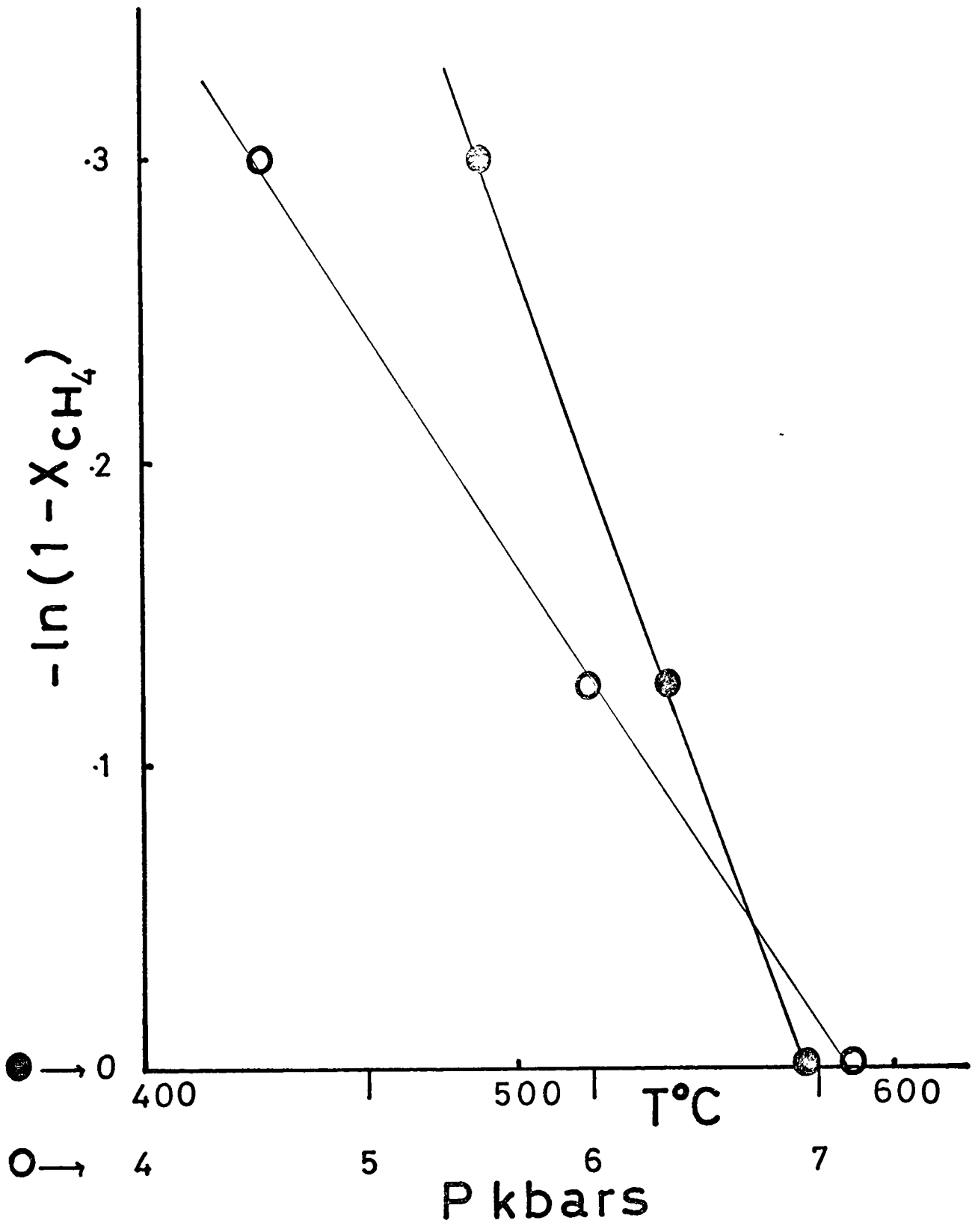


Fig. 23 :- Tremolite + clinozoisite subgroup, P and T against -ln(1-X_{CH_4}), calculated activities : 71·19.

they have several characteristics in common.

a. The assemblages are carbonate free and so all the reactions involve H_2O only. This means that mu-mu diagrams and T-X sections are not useful. Unless the assemblages once had carbonate, the coexisting fluid phase would have insignificant CO_2. 71.79 and the main pelite assemblage can be considered as P-T model invariant.

b. The minerals in these assemblages show the greatest deviation from the compositions of the model system phases. This will accentuate any error in the approximation of activities.

c. The reactions all have steep dP/dT. This means that the pressure of an invariant point is very sensitive to the temperature of the reactions.

The calculated curves for 71.79 and 70.48, 71.85, 72.3 and 72.6 are given in Figs 24 and 33. The curves for each rock should all intersect at an invariant point. The curves for 72.3 do intersect, but at about 6 kbars and 590°C. The spread of the curves and the failure to converge is interpreted as due to the failure of the activity approximations for this degree of dilution.

Group 2 : carbonate-present subgroup : D

The carbonate present subgroup, without talc and tremolite, forms a model system with a variance of -2. Figs 25-30 show the 6 possible topologies: these occur around a mu-mu-P-T invariant point involving the intersection of all univariant points on these mu-mu diagrams. By comparison with the assemblage lists, the relevant topology during the metamorphic event was either Topology 2 or 3.

Fig 31 and 32 are T-X sections at 4 kbars and 6 kbars for the model system. The invariant point involving D3, 5, 6, 7 and 12, corresponding to 71.20 and B339, occurs between 4 and 6 kbars. These T-X sections show that the model system cannot occur at low temperatures

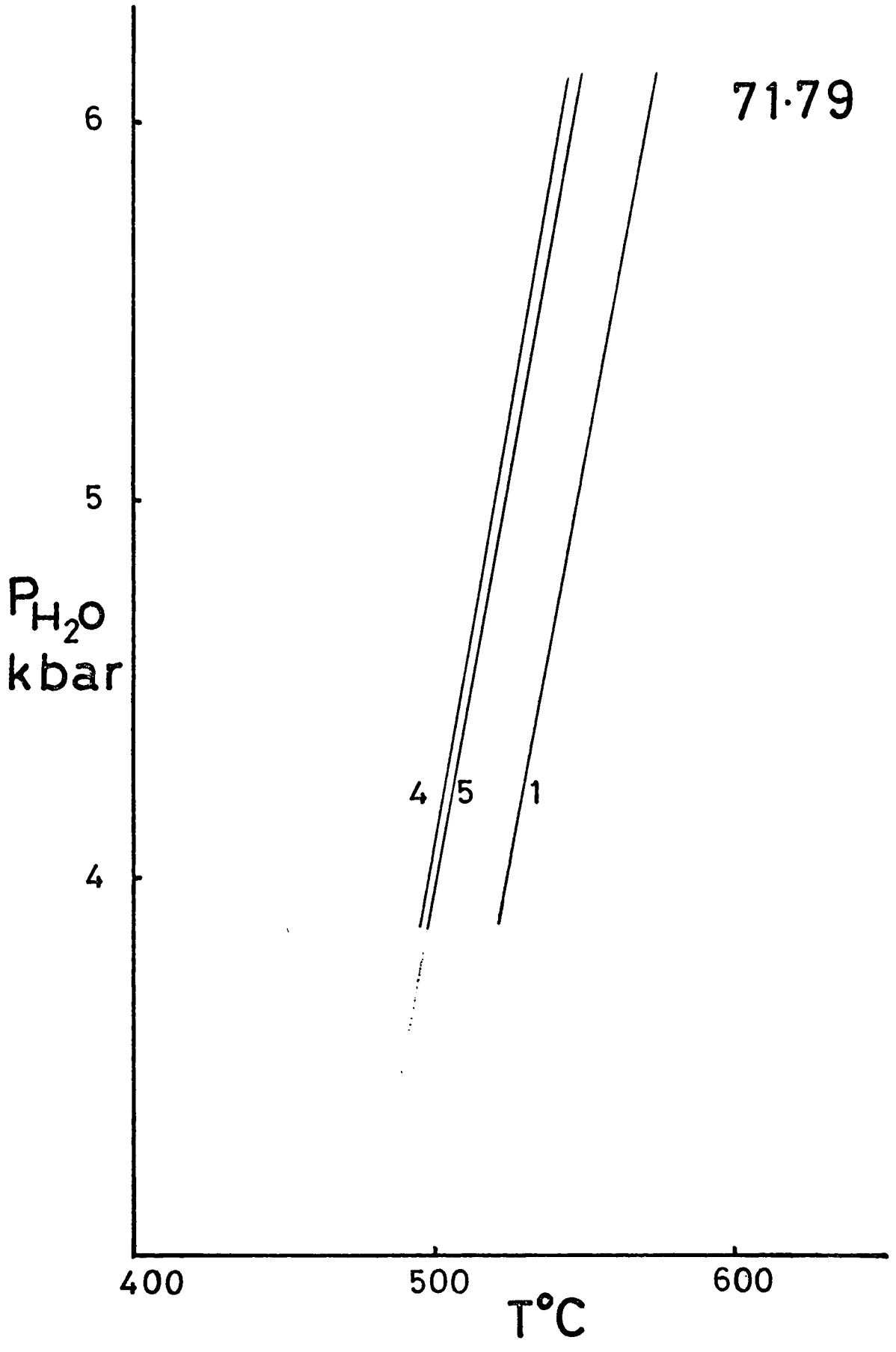


Fig. 24 :- Garnet pelite amphibole bearing subgroup, P-T at 0% CO_2, calculated activities : 71·79.

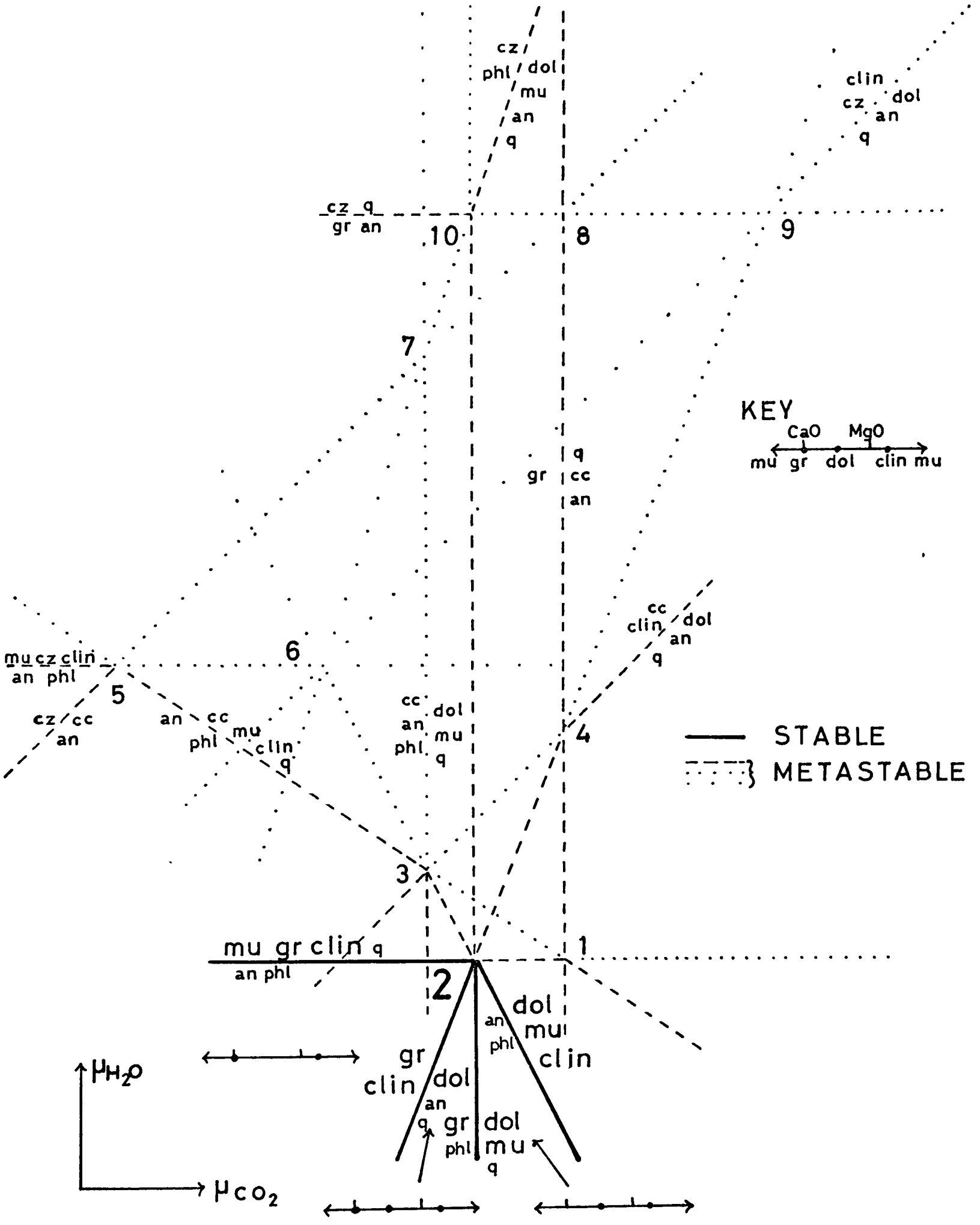


Fig 25 :- Group 2, model system, $\mu_{H_2O} - \mu_{CO_2}$, topology 1.

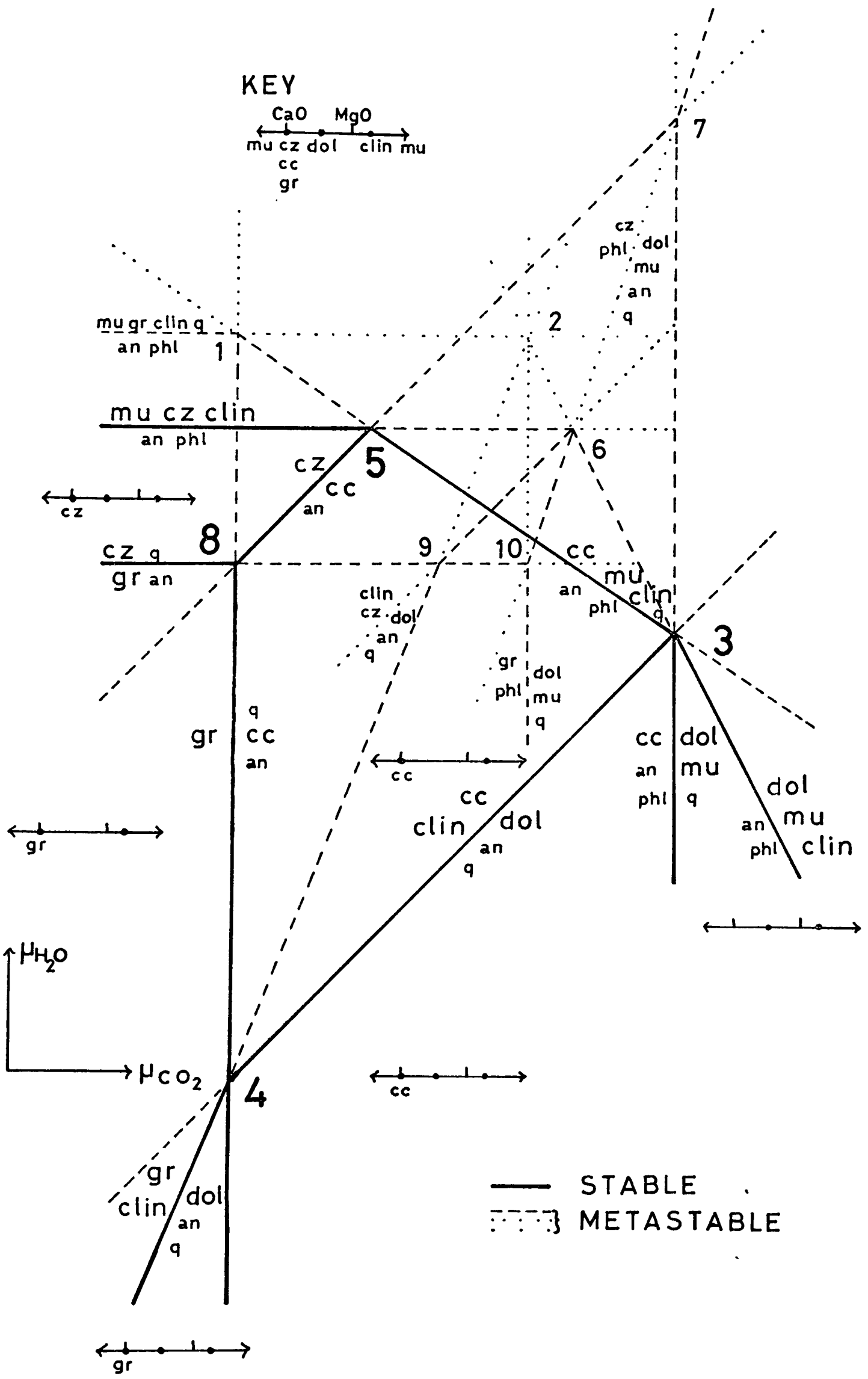


Fig. 26:- Group 2, model system, $\mu_{H_2O} - \mu_{CO_2}$, topology 2.

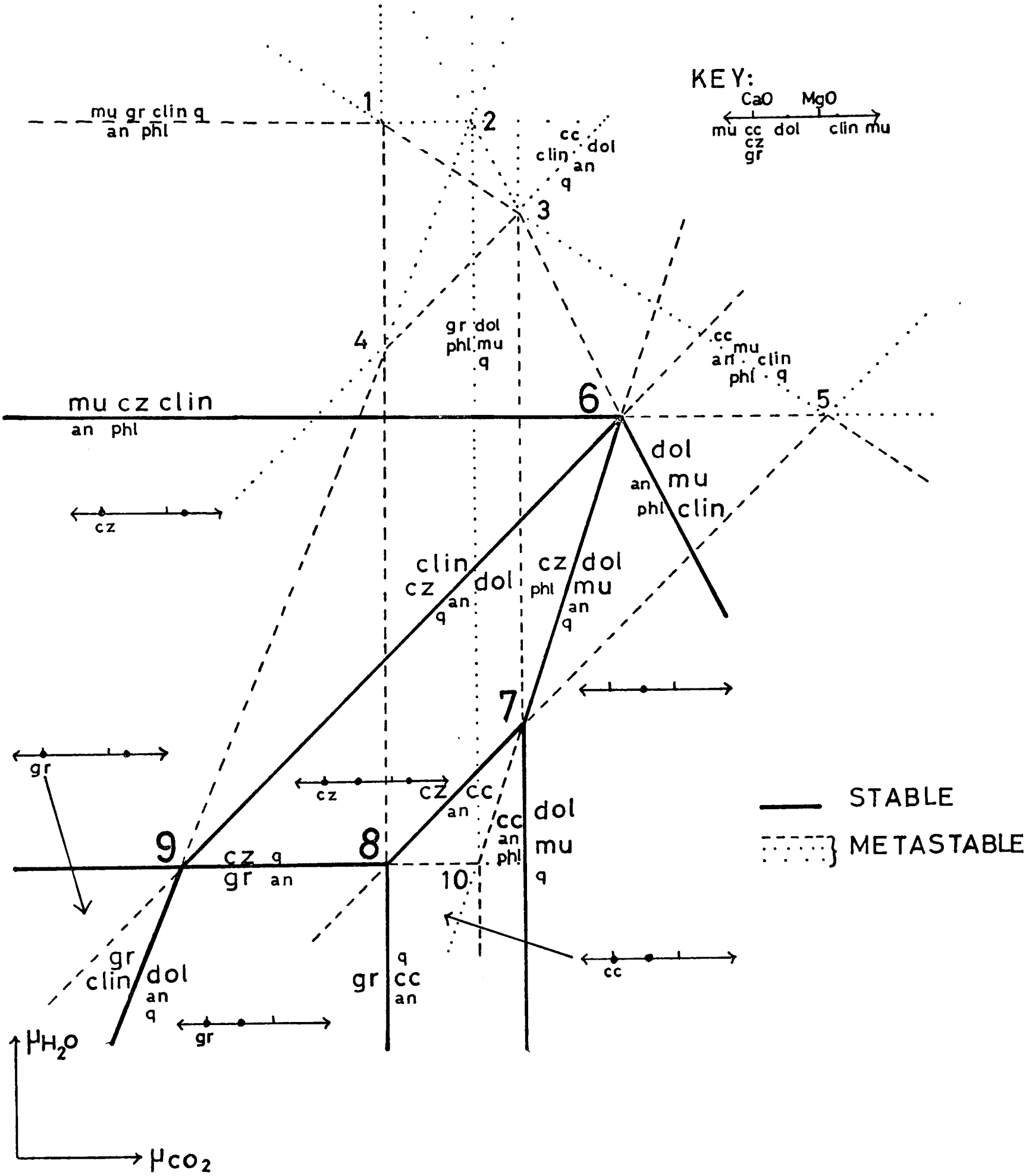


Fig. 27:- Group 2, model system, $\mu_{H_2O} - \mu_{CO_2}$, topology 3.

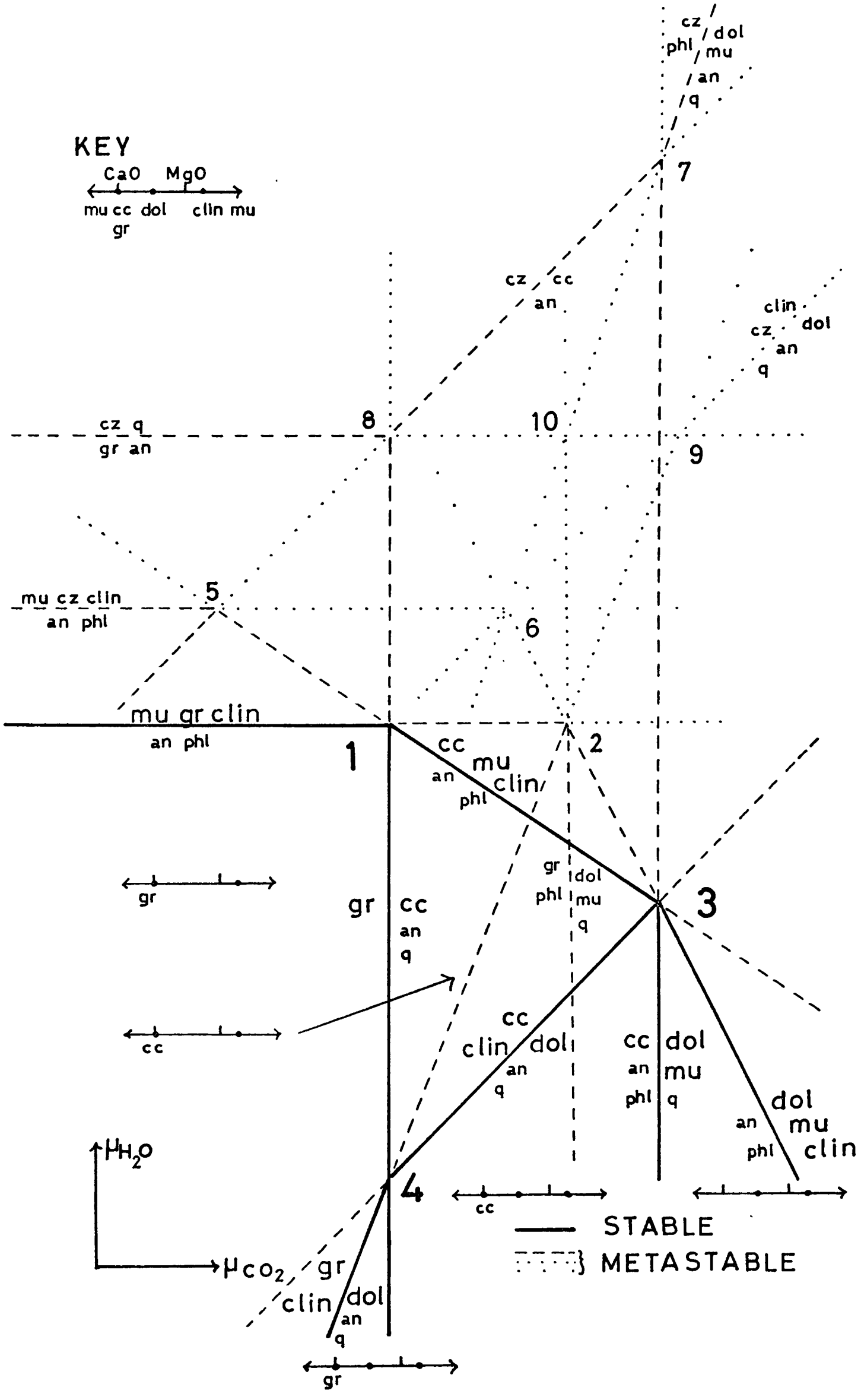


Fig.28:- Group 2, model system, $\mu_{H_2O} - \mu_{CO_2}$, topology 4.

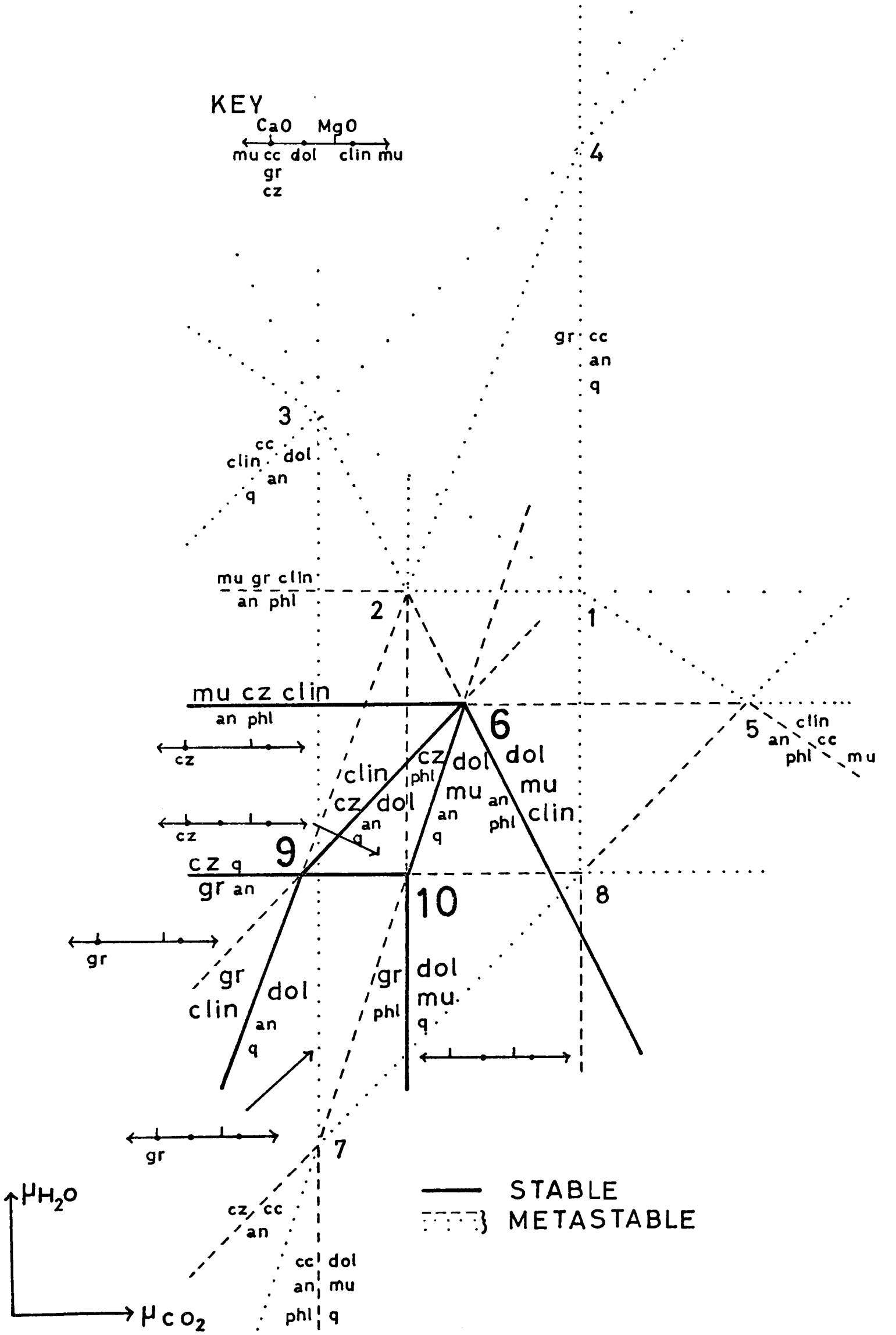


Fig.29:-Group 2, model system, $\mu_{H_2O} - \mu_{CO_2}$, topology 5.

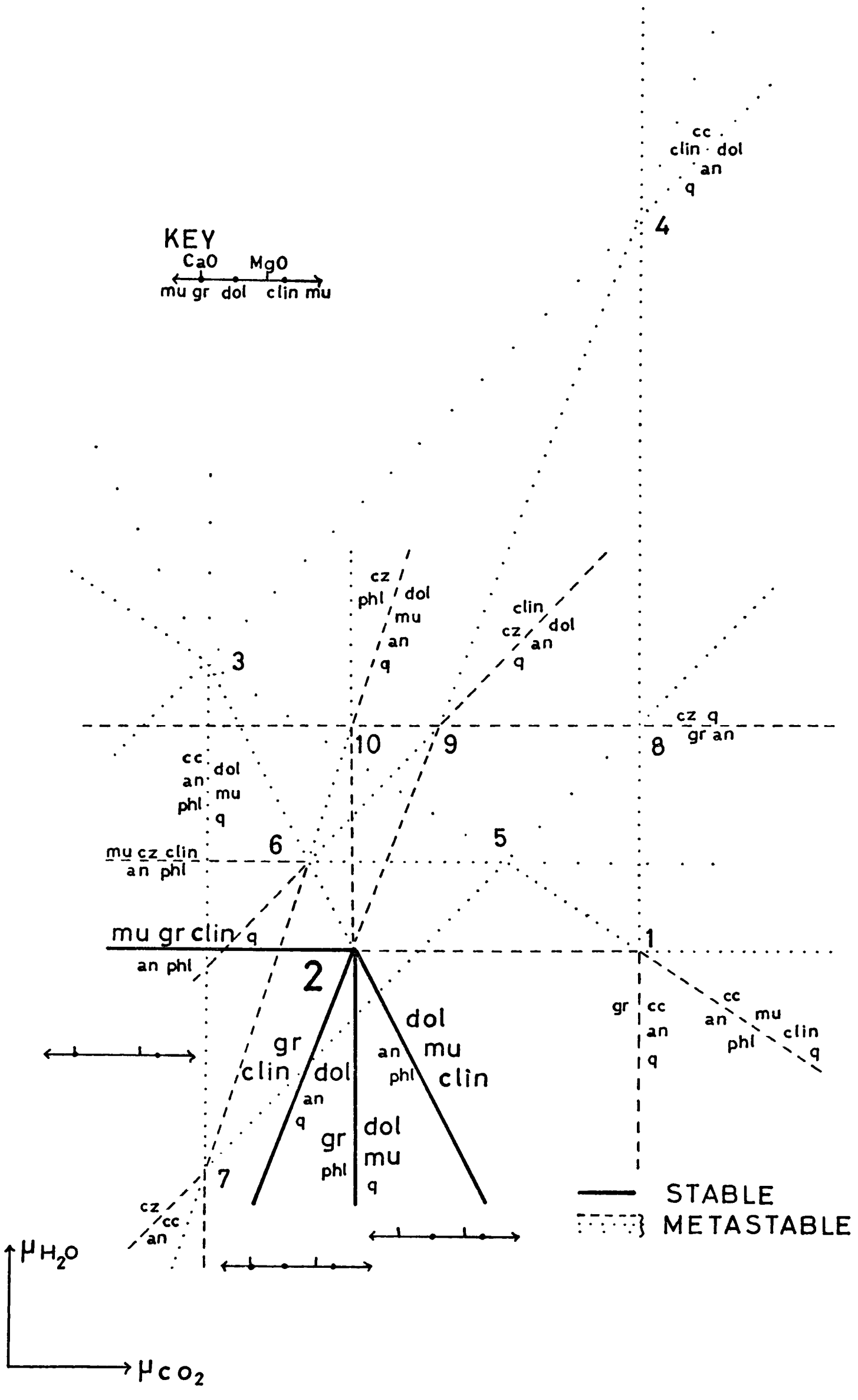
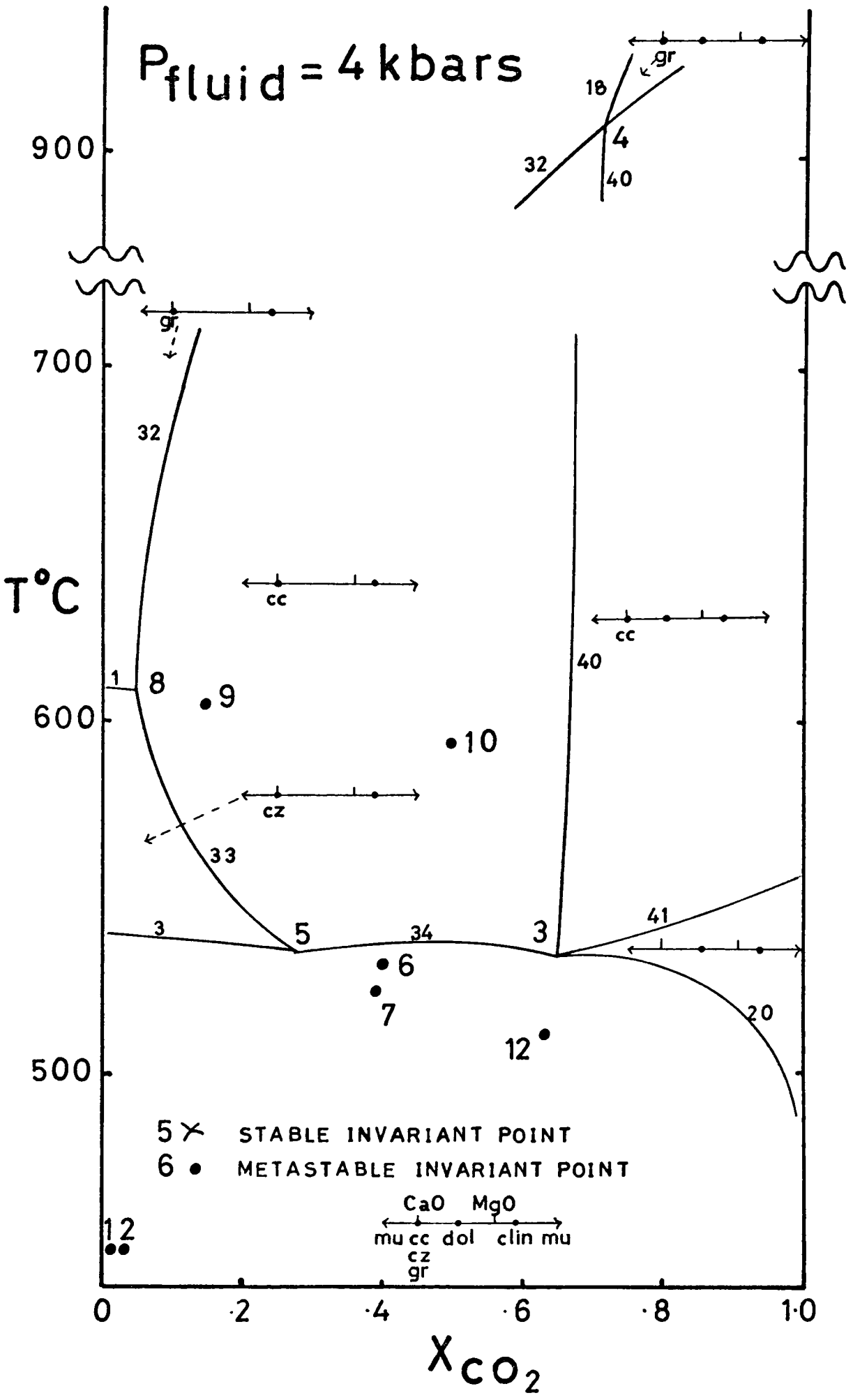
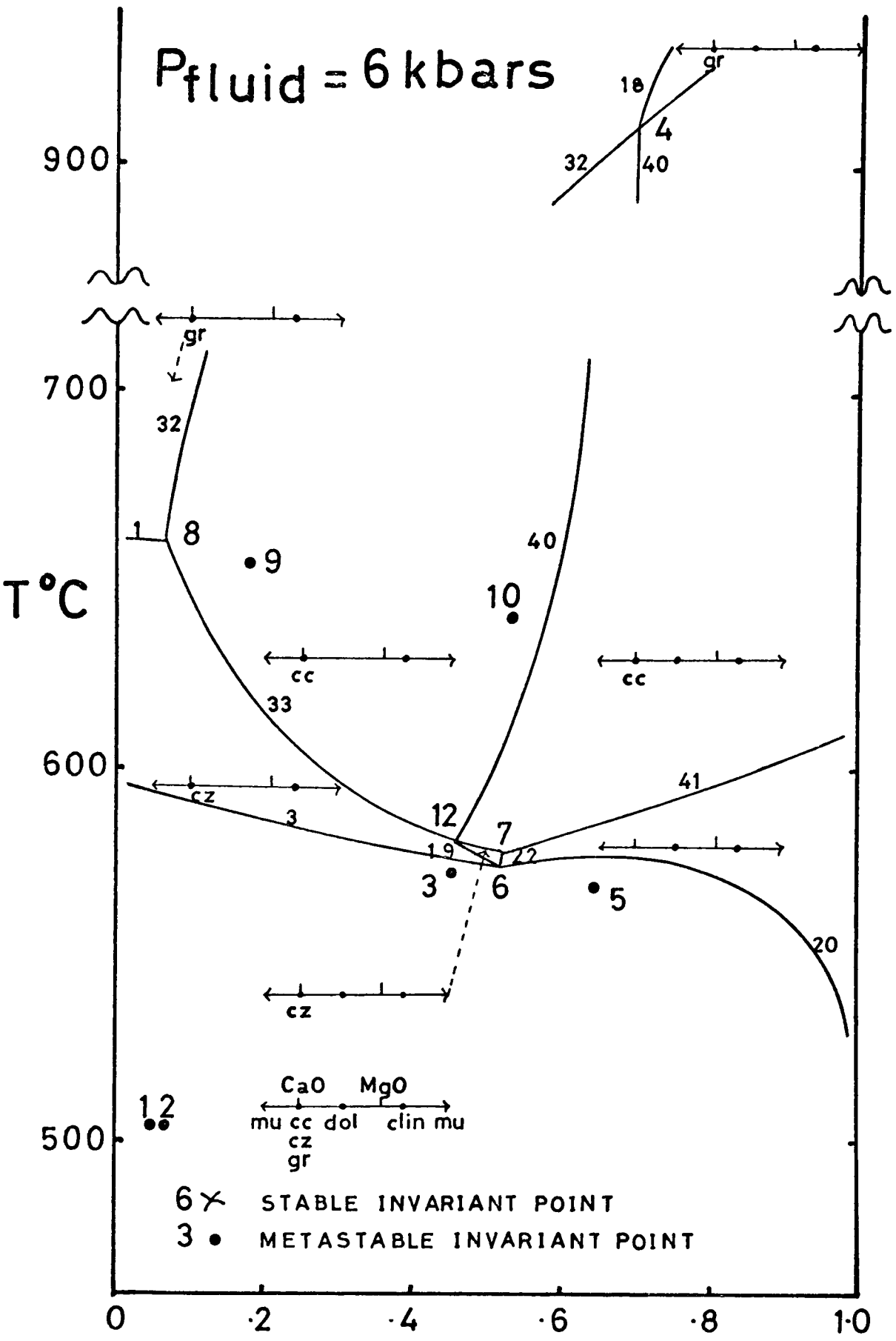


Fig.30 :- Group 2, model system, $\mu_{H_2O} - \mu_{CO_2}$, topology 6.



	HIGH T		LOW T
1	gr + an + H_2O	=	cz + q
3	an + phl + H_2O	=	mu + cz + clin + q
18	gr + clin + CO_2	=	dol + an + q + H_2O
20	an + phl + H_2O + CO_2	=	dol + mu + clin + q
32	gr + CO_2	=	cc + an + q
33	cc + an + H_2O	=	cz + CO_2
34	an + phl + H_2O + CO_2	=	cc + mu + clin + q
40	cc + clin + CO_2	=	dol + an + q + H_2O
41	cc + an + phl + CO_2	=	dol + mu + q

Fig 31:- Group 2; T-X_{CO_2} at 4 kbars, model system.



	HIGH T		LOW T
1	gr + an + H_2O	=	cz + q
3	an + phl + H_2O	=	mu + cz + clin + q
18	gr + clin + CO_2	=	dol + an + q + H_2O
19	dol + an + q + H_2O	=	cz + clin + CO_2
20	an + phl + H_2O + CO_2	=	dol + mu + clin + q
22	cz + phl + CO_2	=	dol + mu + an + q + H_2O
32	gr + CO_2	=	cc + an + q
33	cc + an + H_2O	=	cz + CO_2
40	cc + clin + CO_2	=	dol + an + q + H_2O
41	cc + an + phl + CO_2	=	dol + mu + q

Fig.32 :- Group 2, T-X_{CO_2} at 6 kbars, model system.

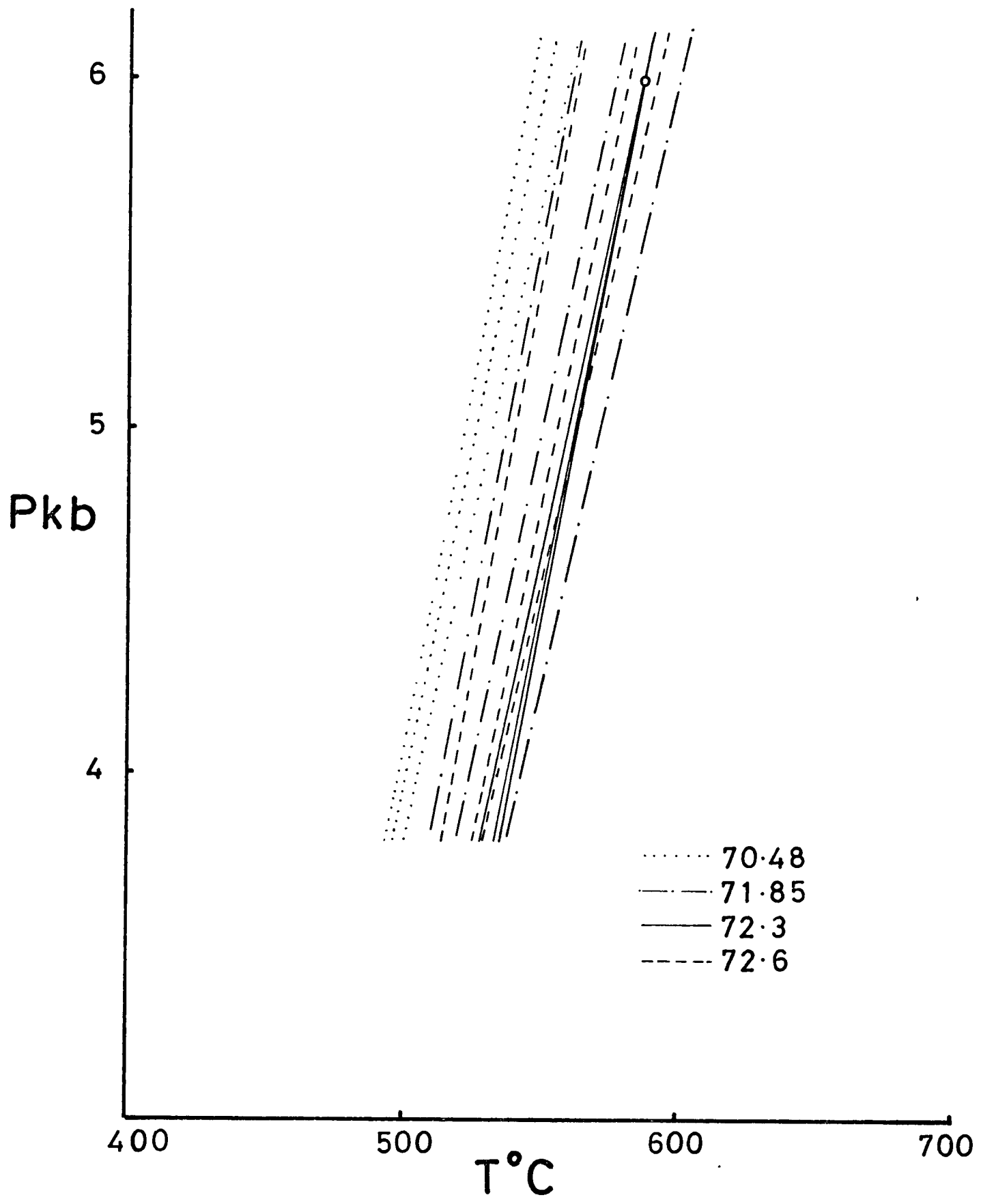


Fig 33:-Carbonate free subgroup: P-T at 0% CO_2, calculated activities: 70·48, 71·85, 72·3, 72·6.

(below 530°C at 4 kbars and 580°C at 6 Kbars, except at very high X_{CO_2}) because the stable reactions 3, 34 and 20 all have phlogopite + anorthite ± quartz and fluid on the high temperature side. To go below this reaction removes one of the characteristics of the model system, that quartz, anothite, and phlogopite are in excess. These reactions may have been very important in the development of oligoclase in these rocks.

The analysed assemblages in this subgroup, 71.42, 71.64 and B376 correspond to the univariant points D12, D7 and D8. Fig 34 shows the polybaric movement of the univariant points D12 and D7, using the activities calculated from the analyses. The calcite temperature gives a pressureof 4.8 and 5.0 kbars at an X_{CO_2} of 0.55 and 0.60 respectively for these two rocks. B376 is graphitic; Fig 35 shows the polybaric movement of this univariant point at 0%, 25%, 50% and 65% diluent in the fluid phase. Fig 36 shows that for the calcite temperature, the % diluent is 65% at 5 Kbars for $CO_2/CO_2 + H_2O = 0.30$ and is 45% at 4 kbars for $CO_2/CO_2 + H_2O = 0.70$. This corresponds to an oxygen fugacity at or just below the QFM buffer.

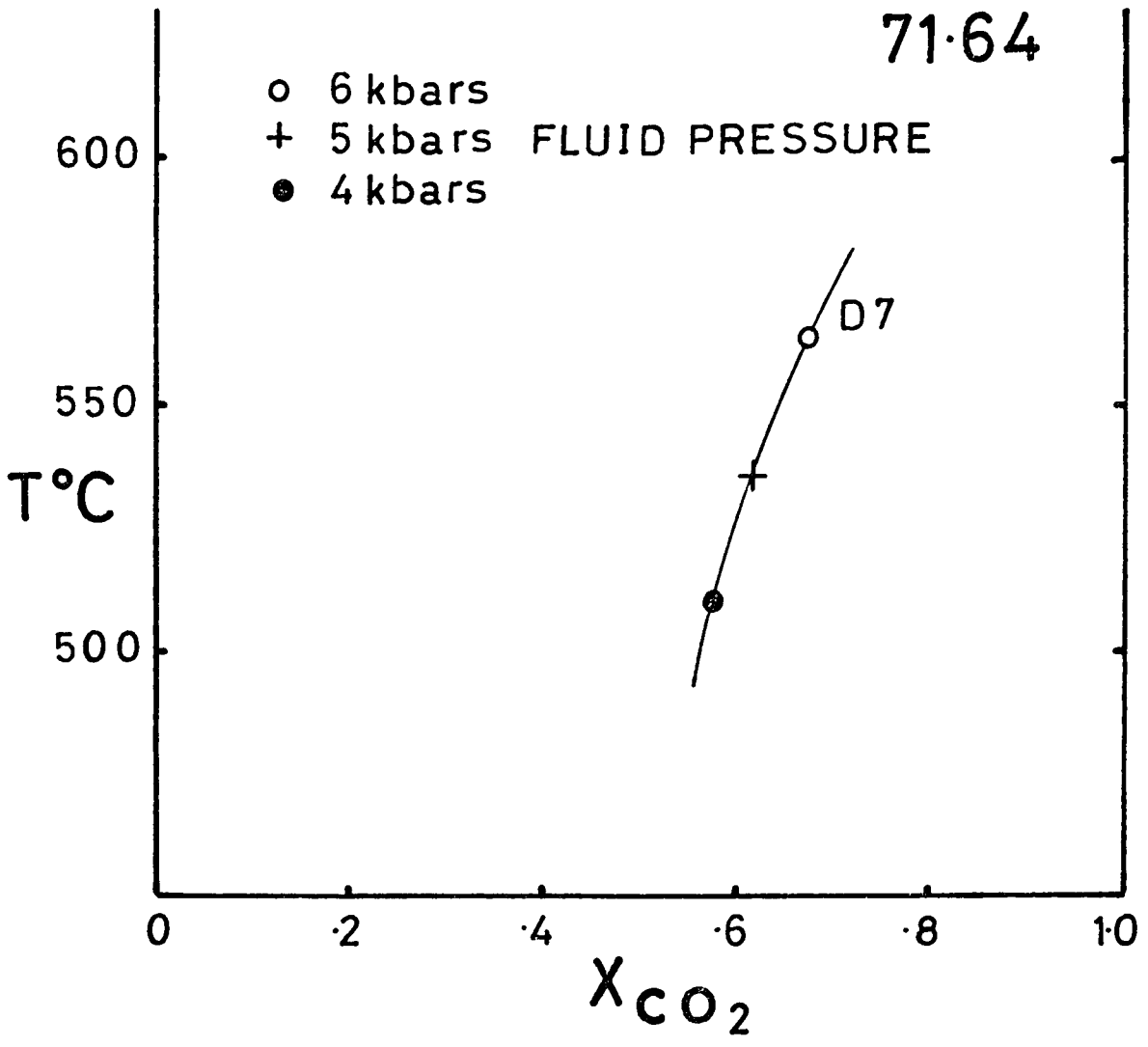
Fig 37 summarises the evidence for the pressure and temperature of the main metamorphic event from the model system calculations. The main event probably occurred at about 5 kbars and 535°C at variable X_{CO_2}.

Rutile - sphene relations

As stated in the last chapter there appears to be no pattern to the occurrence of rutile and sphene in calcite-quartz bearing assemblages. The reaction relating these phases is

rutile + calcite + quartz = sphene + CO_2

This reaction has been used by Ernst (1972) to set upper limits on the X_{CO_2} of the fluid phase during the glaucophane schist metamorphism in the Franciscan and Sanbagawa belts. Ernst used the Schuiling and Vink (1967) curve without correcting for the fact that the experimentally



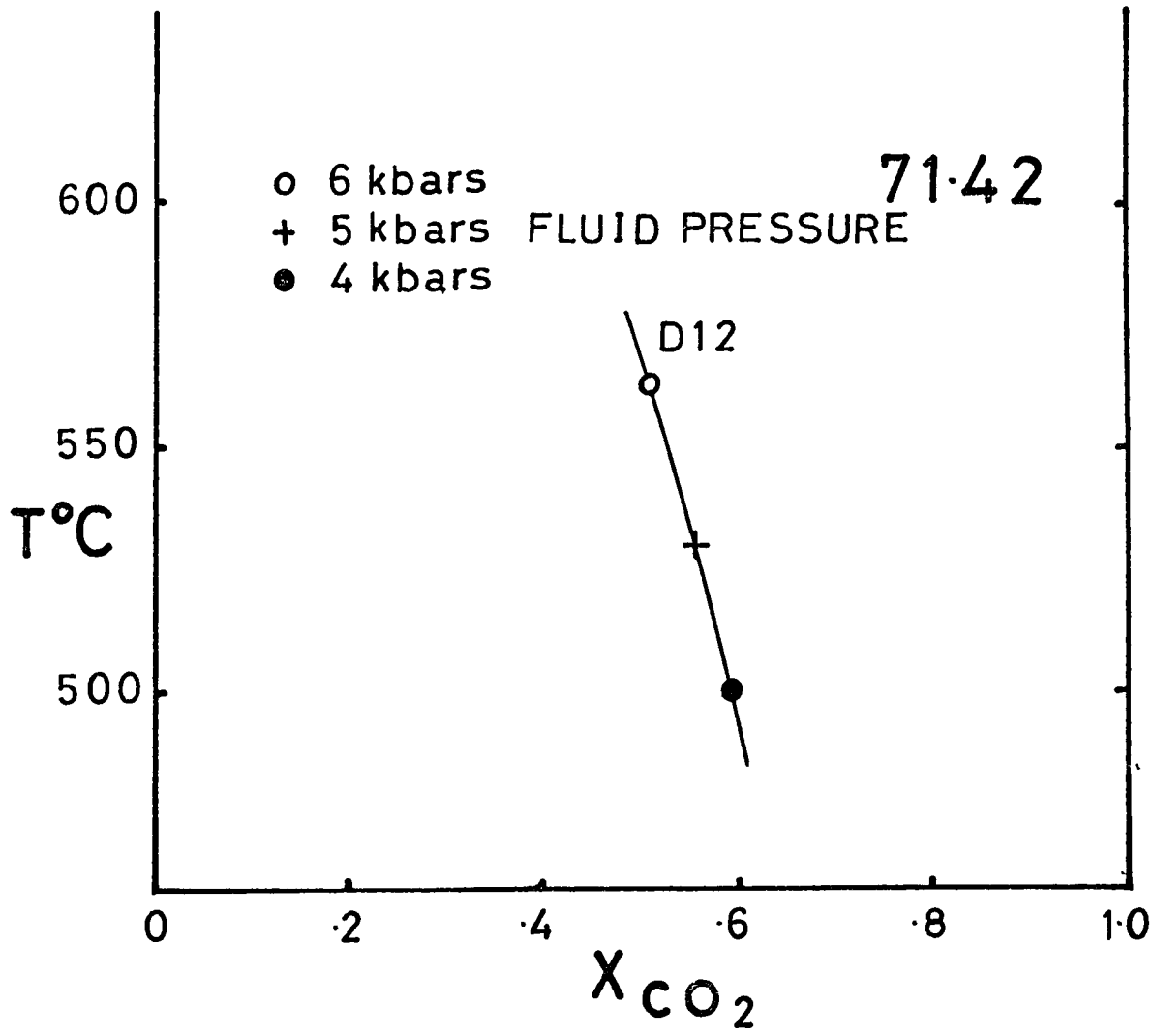


Fig 34 :- Carbonate present subgroup, P-T-X_{CO_2}, calculated activities : 71·64 and 71·42.

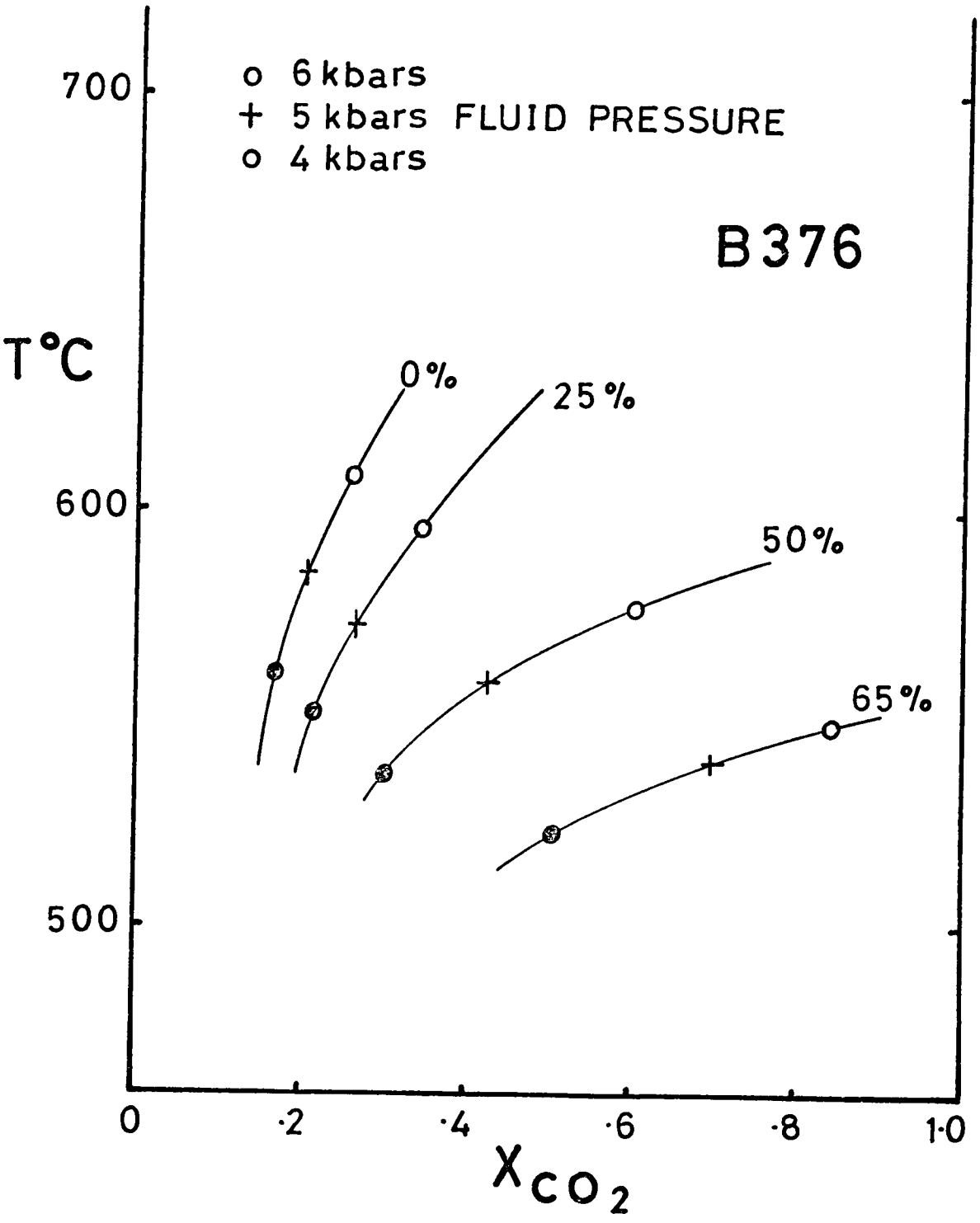


Fig.35:-Carbonate present subgroup, P-T-X_{CO_2}-X_{CH_4}, calculated activities: B376.

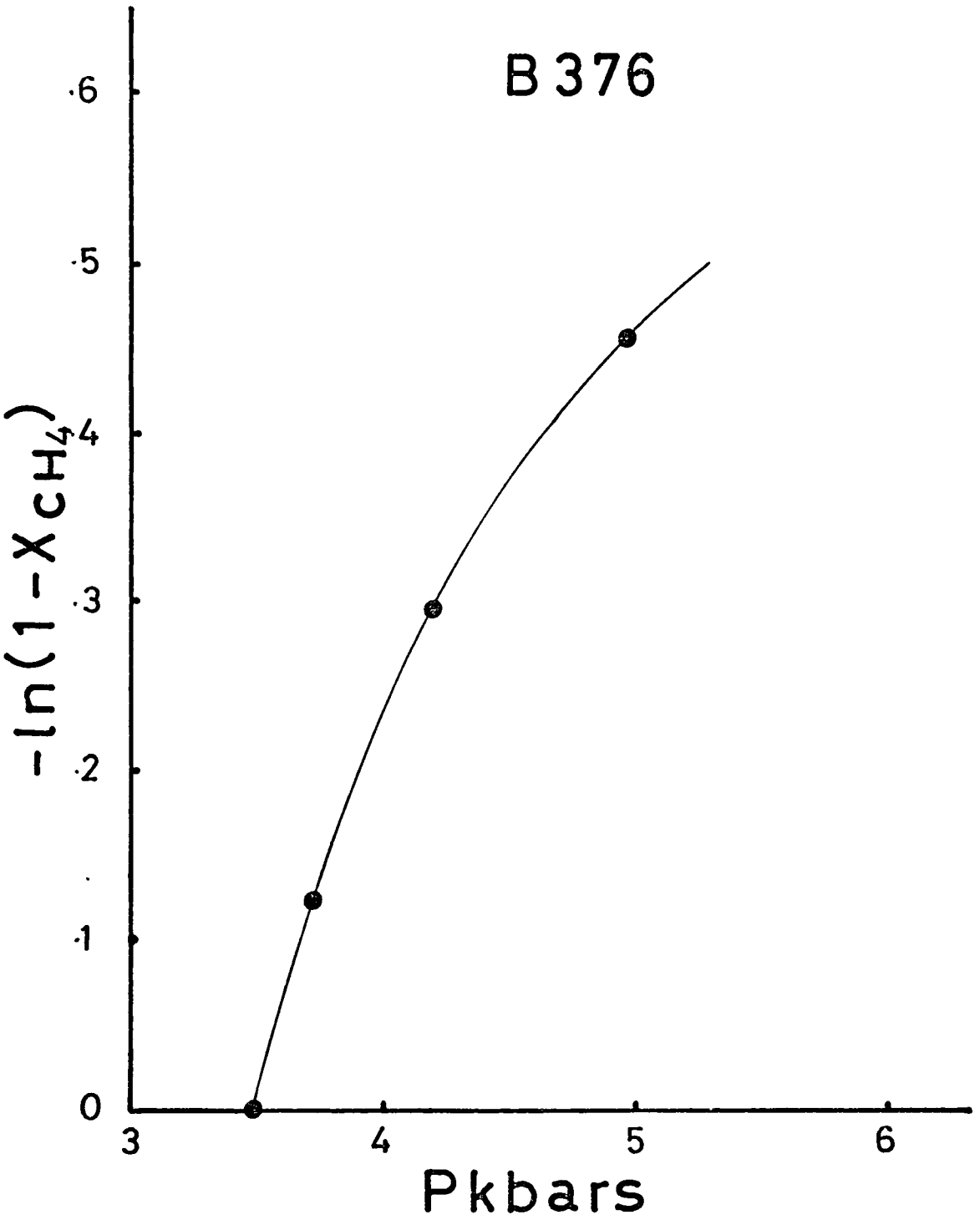


Fig.36 :- Carbonate present subgroup, $\ln(1-X_{CH_4})$ against pressure at 535°C, for B 376.

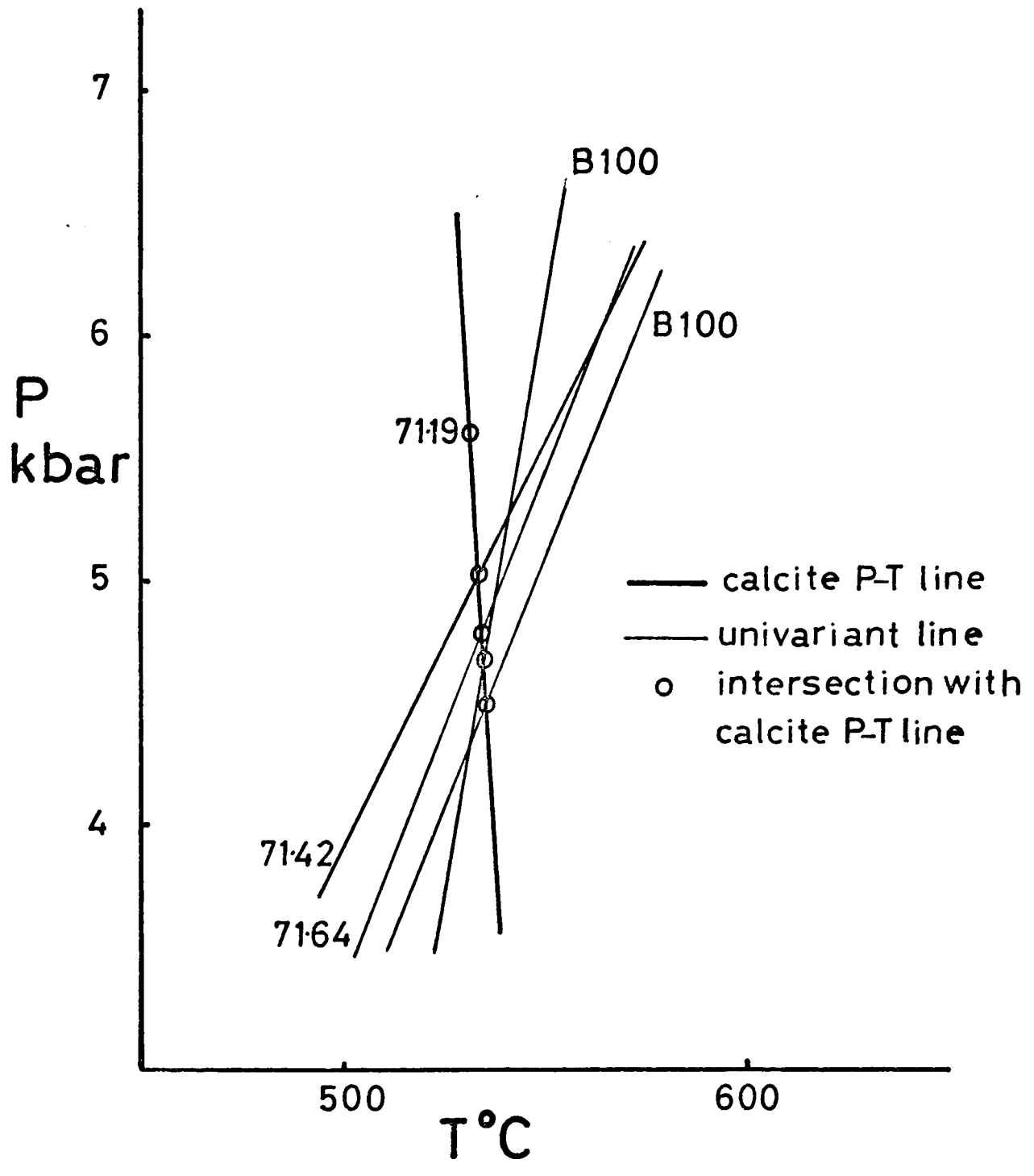


Fig.37:- Summary of evidence for the P-T conditions of the main metamorphic event.

determined reaction involved anatase rather than rutile. This increases the temperature of reaction by about 30°C.

Fig 38 shows the sphene reaction at 4,5 and 6 kbars using pure phases. The reactions are lowered by less than 10°C by using actual activities. At X_{CO_2} = 1, the dP/dT of the reaction changes from steeply positive to infinity to steeply negative between 4 and 6 kbars.

If rutile + sphene + calcite + quartz was an equilibrium assemblage, then, at the calcite temperature and 5 kbars, the X_{CO_2} was less than 0.03. But this subassemblage occurs in assemblages which correspond to the model invariant points D7 and D12. They were shown to occur at an X_{CO_2} greater than 0.50. The balance of evidence is against rutile + sphene + calcite + quartz being an equilibrium assemblage.

It is suggested that, once formed, sphene is reluctant to react to the equivalent rutile + calcite + quartz. It is not clear what controls which sphenes show the reaction taking place metastably. The conclusion here may qualify Ernst's conclusions above.

Iron analogue to the model system

The main pelitic assemblage is closer to the iron analogue to the model system than to the model system. Preliminary calculations gave temperatures of about 320°C. This can reasonably be interpreted as due to something seriously wrong with the thermodynamic data for the iron minerals, particularly Fe chlorite and almandine. This is not to suggest that the experimental work of Hsü (1968) is wrong, but more likely that the stated composition of chlorite is very incorrect. These calculations were abandoned.

Reaction paths

There is evidence from the assemblages for progressive metamorphism; that the pressure and temperature increased to the metamorphic maximum slow enough for the rocks to develop at least some of the lower pressure-temperature assemblages.

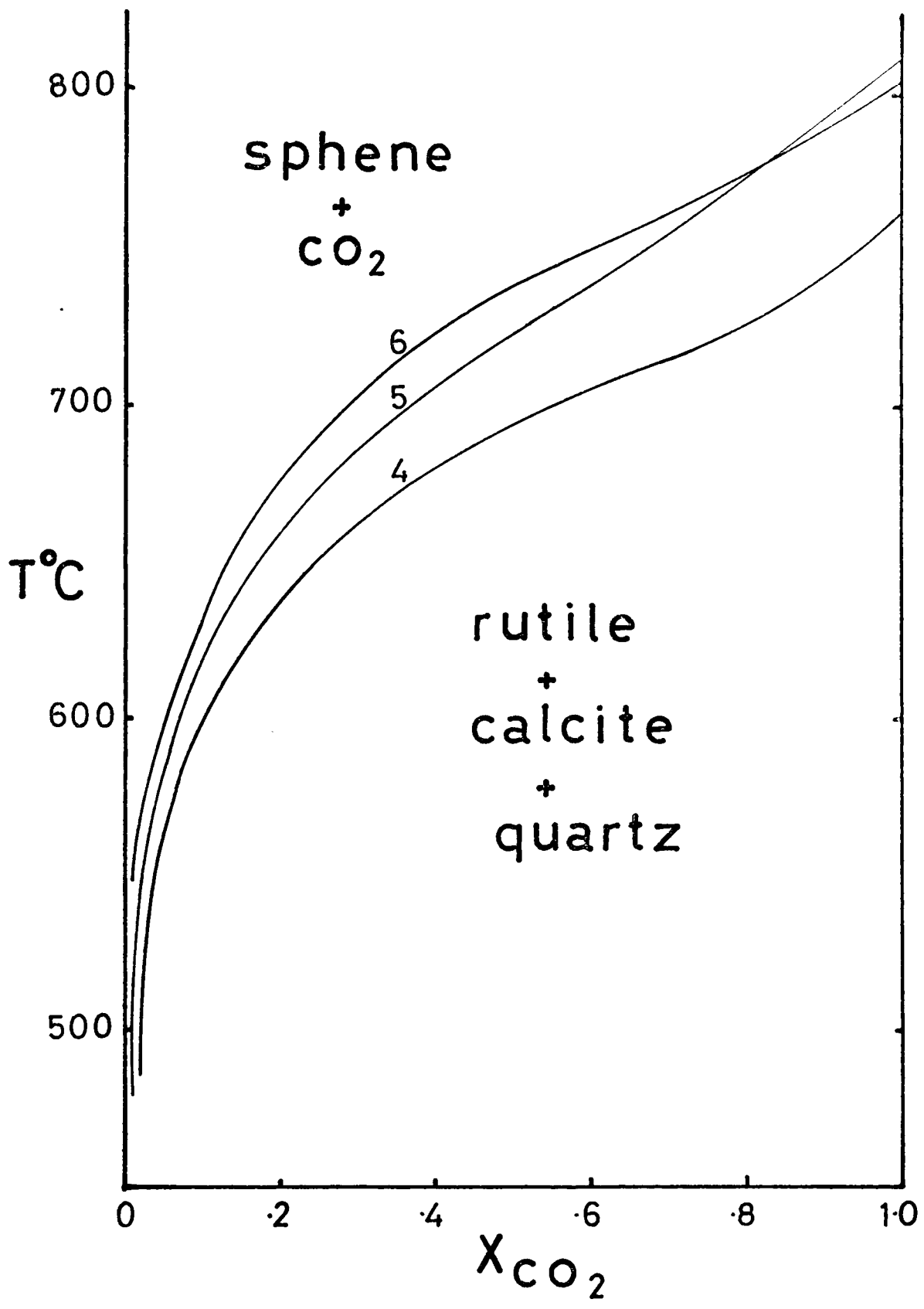


Fig. 38 :- Sphene reaction at 4, 5 and 6 kbars.

The great proportion of low variance assemblages can be explained by progressive metamorphism. As pressure and temperature is increased during metamorphism, a rock will eventually intersect a divariant reaction surface with the reactants all included in the assemblage. If the chemical potentials of H_2O and CO_2 are externally controlled (i.e. X_{CO_2} maintained constant) then the rock will pass through the divariant surface converting reactants to products at the boundary (for equilibrium). However if the chemical potentials are not externally controlled; when the rock intersects a reaction surface, it will stay on the surface converting reactants to products and changing the composition of the vapour phase. While the reactants last, the rock may follow the divariant surface to a univariant line and even to an invariant point. Reactions which release fluid components on one side of the reaction only have a maximum. If a maximum is reached, the rock has to leave the divariant surface.

The T-X sections in this chapter are approximations to the real systems, the mineral assemblages. The lines and points are smeared out as the proportions of the model system components in the minerals are decreased. As the rock moves within a smeared out surface (volume) the composition of the minerals changes as well as the composition of the fluid phase.

The original sedimentary rocks probably had an interstitial fluid with dominant H_2O. The high X_{CO_2} in the carbonate bearing assemblages can be explained by the rocks being taken rapidly, without equilibration, to the metamorphic maximum or by progressive metamorphism with reactions with positive dT/dX. However some features of the assemblages can be explained by progressive metamorphism increasing X_{CO_2}.

Sphene poikiloblasts occur in many of the epidote pelite and siliceous dolomite lithology carbonate bearing assemblages. With progressive metamorphism, sphene can grow within its stability field

before the X_{CO_2} is increased. Otherwise metastable growth of sphene must be invoked.

The different domains of the fine grained part of B100 and related siliceous dolomite lithology rocks have very different X_{CO_2} values, Fig. 12. At lower temperatures and pressures the assemblages probably were much closer to the model invariant point and so had more similar X_{CO_2} values. The different domains initially had slightly different X_{CO_2} or modal composition and progressive metamorphism has produced the big difference in X_{CO_2}.

If progressive metamorphism occurred then it should be possible to delineate reaction paths for groups of assemblages. However, without knowing the precise path of temperature and pressure to the metamorphic maximum, it is difficult to use calculated curves to suggest reaction paths. For example, on a T-X section, an assemblage may be on a divariant line above a particular univariant point; yet the univariant point will overtake the assemblage as temperature and pressure is increased, if the dP/dT of the univariant line is less than the metamorphic gradient.

In a general way the reactions 20, 22, 34 and 40 :

dol + mn + clin + q = an + phl + CO_2 + H_2O no 20

dol + mu + an + H_2O = cz + phl + CO_2 no 22

cc + mu + clin + q = an + phl + CO_2 + H_2O no 34

dol + an + q + H_2O = cc + clin + CO_2 no 40

may have been important in increasing the X_{CO_2} of the fluid phase because all the phases on the low temperature side of the reactions would be expected to occur as components of minerals in carbonate bearing rocks diagenesis and because they all have positive dT/dX at low X_{CO_2}. There is good textural evidence for reactions 22 and 40 in the pelites and siliceous dolomites respectively. Reactions 20 and 34 may have produced the orientated matrix biotites and the oligoclase

in the carbonate bearing rocks. These reactions (and others with an on the high temperature side of the reaction) occur at much lower temperature when albite is the equilibrium plagioclase. As the temperature and pressure increased X_{an} increased along with the X_{CO_2}.

Summary, implications and conclusions

The calculations and the calcite temperatures indicate that two metamorphic events affect the Spean Bridge rocks :

1. a main metamorphic event affecting the whole area at about 5 kbars (range 4.5 to 5.6 kbars from 5 independent calculations) and 535°C, at variable X_{CO_2} in the carbonate bearing pelites, variable X_{CO_2} and X_{CH_4} in the carbonate bearing graphitic rocks, and variable X_{CH_4} in the carbonate free graphitic rocks.

2. a late metamorphic event of about 1 kbar and 430°C affecting parts of the siliceous dolomite lithology rocks.

There is no evidence from the calcites or the calculation that a temperature or pressure gradient existed across the area during the main metamorphic event. It is difficult to give the size of a gradient that could definitely be detected because the calcites and dolomites in different assemblages could equilibrate to different temperatures below the metamorphic maximum. Many more analyses and calculations would be needed to look a pressure gradient across the area.

The calcite temperature of 535°C is a minimum. If the carbonates equilibrated at a lower temperature than the rest of the carbonate bearing assemblages, then the pressure of metamorphism increases. Adding 10°C to the temperature moves the pressure range up to 4.8 - 6.0kbars. If the assumption of $P_{H_2O} + P_{CO_2} = P_{total}$ is

incorrect, then the pressure from the calcite temperature increases. The suggestion that the assemblages equilibrated at or near the metamorphic maximum is supported by the order of the calcite temperature.

The main metamorphic event may have occurred contemporaneously with the metamorphism of the Dalradian to the east (eg Chinner 1966) about 530 my ago (Dewey and Pankhurst (1970)). The indicated conditions place the rocks at the bottom of the kyanite stability field (Richardson et al 1969). Rocks above the garnet-chlorite tie line should have the kyanite aluminium silicate polymorph. The pressure indicates that the rocks have been brought to the surface by the removal of about 16 km of overburden. The estimated geothermal gradient is about 35°C/km.

The evidence for the late metamorphic event comes primarily from the compositional spread of the calcites and the low calculated pressure for the siliceous dolomite model invariant assemblage. The agreement with the fluid inclusion pressure-temperature band suggests that they are the manifestation of the same process; deep metamorphic or magmatic brines flushing through the area along well defined fractures and permeating the more permeable rocks. It entered the siliceous dolomites along minor planes of weakness where it reset the calcite temperatures and created the coarse grained assemblage in B100 and related rocks. This fluid only just penetrated the siliceous dolomites because the X_{CO_2} for the coarse grained part is about 0.8, yet the fluid inclusions rarely contain liquid CO_2. The consistency of the calculated pressures for the main event suggest that this fluid did not affect the analysed assemblages from the pelite lithologies.

Of interest is the high indicated geothermal gradient of about 120°C / km for the late event. It is reasonable to suggest that the measured conditions prevailed during uplift of this part of the Caledonian belt, possibly 420 my ago (the age of Ar retention, representing uplift, from Dewey and Pankhurst (1971)).

The event may have coincided with or have been caused by the

intrusion of the Ben Nevis granite (see Haslam (1968)).

LIST OF REFERENCES

BIBLIOGRAPHY

ALTHAUS, E., KAROTKE, E., NITSCH,K.H. and WINKLER,H.G.F., 1970. An experimental re-examination of the upper stability limit of muscovite plus quartz. Neues.J.Min.Mon.7,325-336.

ANDERSON, G.M., 1970. Some thermodynamics of dehydration equilibria. Am.J.Sci.269,392-401.

ANDERSON, P.A.M., and KLEPPA, O.J., 1969. The thermochemistry of the Kyanite-sillimanite equilibrium. Am.J.Sci.267,285-290.

ATHERTON, M.P., 1968. The variation in garnet, biotite and chlorite composition in medium grade pelitic rocks from the Dalradian, Scotland, with particular reference to the zonation of garnet. Contr. Min. and Petrol. 18, 347-371.

BAIN, R.W., 1964. Steam Tables 1964. Natl.Eng.Lab, Edinb.,HMSO,147p.

BARANY, R., 1963. Heats of formation of gehlenite and talc. Rep.Invest. US Bur. Mines 6251, 9.

BARANY, R., 1964. Heat and free energy of formation of muscovite. Rep. Invest. US Bur. Mines 6356,6.

BARANY, R., and KELLEY, K.K., 1961. Heats and free energies of formation of gibbsite, kaolinite, halloysite, and dickite. Rep.Invest. US Bur. Mines 5825, 13.

BARRETT, W.T., and WALLACE, W.E., 1954. Studies of NaCl-KCl solid solutions, I. Heats of formation, lattic spacings, densities Schottky defects and mutual solubilities. J.Am.chem.Soc. 76, 366-369.

BARRET, W.T., and WALLACE, W.E., 1954. Studies of NaCl-KCl solid solutions: II Experimental entropies of formation and a comparison of certain thermodynamic properties with values calculated from Wasastjerna's theory. J.Am.chem.Soc.

BARRON, L.M., 1973. Non-ideal thermodynamic properties of H_2O-CO_2 Mixtures for 0.4 - 2 kb and 400-700°C. Contr.Min. and Petrol. 39, 184.

BARROW, G., 1893. On the intrusion of muscovite biotite gneiss in the S.E. Highlands of Scotland and its accompanying metamoprhism. Q.Jl.geol.Soc.Lond.44,330.

BARROW, G., 1912. On the geology of lower Dee-side and the southern Highland border. Proc. Geol. Ass. 23, 268-73.

BIRD, G.W., and ANDERSON, G.M., 1973. The free energy of formulation of magnesian cordierite and phlogopite. Am.J.Sci. 273, 84-91.

BIRD, G.W., and FAWCETT, J.J., 1973. Stability relations of Mg-chlorite-muscovite and quartz between 5 and 10 kb water pressure. J.Petrology in press.

BLANDER, M., 1972. Thermodynamic properties of orthopyroxenes and clinopyroxenes based on the ideal TWO-site model. Geochim. cosmochim.Acta 36, 787-799.

BOEKE, H.E., 1912. Die Schmelzerscheinungen und die umkehrbare Umwandlung des Calcium-Carbonats. Neues Jb.Miner. 1,91-212.

BOETTCHER, A.L., 1970. The system CaO-Al_2O_3-SiO_2-H_2O at high pressures and temperatures. J.Petrology. 11,337-379

BOETTCHER, A.L., and WYLLIE, P.J., 1968. The calcite-aragonite transition

measured in the system $CaO-H_2O-CO_2$. J.Geol.76,314-320.

BORN, M. 1921. Phys. Z. 22, 215-290.

BOWMAN, F. and GERARD, F.A., 1967. Higher Calculus, Camb.Univ.Press.

BOYD, F.R., 1959. Hydrothermal investigations of amphiboles in Researches in Geochemistry, vol 1 (ed. ABELSON, P.H.) N.Y.,Wiley.

BOYD, F.R. and SCHAIRER, J.F., 1964. The system $MgSio_3$ - $CaMgSi_2O_6$. J.Petrology.5, 275-309

BRADLEY, W.F., BURST, J.F., and GRAF, D.L., 1953. Crystal chemistry and differential thermal effects of dolomite. Am.Miner., 38, 207.

BRICKER, O.P., NESBITT, H.W. and GUNTER, W.D., 1973. The stability of talc. Am.Miner. 58, 64-72.

BRIDGMAN, P.W., 1935. The pressure-volume-temperature relations of the liquid, and the phase diagram of heavy water. J.chem.Phys. 3, 597-605.

BRIDGMAN, P.W., 1939. The high pressure behaviour of miscellaneous materials. Am.J.Sci.237,7-18.

BROWN, W.L. 1962. Peristerite unmixing in the plagioclases and metamorphic facies series. Norsk.geol. Tidsskr. 42,354-382.

BUNK, A.J.H. and TICHELAAR, G.W., 1953. Investigations in the systems NaCl-KCl. Kon.Ned.Akad.Wetensch.Proc.B, 56,375-384.

BURNHAM, C.W., HOLLOWAY, J.R., and DAVIS, N.F., 1969. Thermodynamic properties of water to 1,000°C and 10,000 bars. Spec.Pap. geol.Soc.Am. no 132.

BURNS, R.G., and STRENS, R.G.J., 1967. Structural interpretation of polarised absorption spectra of the Al-Fe-Mn-Cr epidotes. Min. Mag.36,204-226.

CALLEN, H.B., 1960. Thermodynamics: an introduction to the physical theories of equilibrium thermostatics and irreversible thermodynamics. N.Y., John Wiley and sons, inc.

CARATHEODORY, C., 1909. Math.Ann. 67, 355.

CARLSON, H.C., and COLBURN, A.P., 1942. Vapor-liquid equilibria of non-idealsolutions. Ind.Engng. Chem. ind. (int.) Edn 34, 581-589.

CARMICHAEL, D.M., 1969. On the mechanism of prograde metamorphic reactions in quartz bearing pelitic rocks. Contr.Mineral. and Petrol. 20, 244-267.

CHATTERJEE, N.D., 1970. Synthesis and upper stability of paragonite. Contr.Mineral.Petrol. 27, 244-257.

CHERNOVSKY, J.V., 1973. The stability of clinochlore and the free energy of Mg-cordierite. Amer. geophys.Union Trans., (abs.), 54, 479.

CHINNER, G.A., 1960. Pelitic gneisses with varying ferrous/ferric ratios from Glen Clova, Anus, Scotland. J.Petrology 1, 178-217.

CHINNER, G.A. 1961. Origin of sillimanite in Glen Clova, Angus. J. Petrology 2, 312-323.

CHINNER, G.A., 1966. The distribution of pressure and temperature during Dalradian metamorphism. Q.Jl.geol.Soc.Lond.

CHRIST, C.L., and HOSTETLER, P.B., 1970. Studies in the system MgO-SiO_2 - CO_2 - H_2O (II): The activity - product constant of magnesite. Am. J.Sci. 268, 439-453.

CLARK, S.P., Jr., 1966. Handbook of physical constants (Revised edition). Mem.geol.Soc.Am.97

CRAWFORD, M.L., 1966. Composition of plagioclase and associated minerals in some schists from Vermont, U.S.A., and South Westland, New Zealand, with inferences about the peristerite solvus. Contr. Mineral. and Petrol.13, 269-294.

DARKEN, L.S. 1967. Thermodynamics of binary metallic solutions. Trans. metall.Soc.A.I.M.E.239, 80-89.

DARKEN, L.S., and GURRY, R.W., 1945. The system iron-oxygen I. The coustite field and related equilibria. J.Am.chem.Soc.67, 1398-1412.

DAY, H.W., 1970. Redetermination of the stability of muscovite + quartz. (abstr.) Geol. Soc. Amer. Abstr. Progr., 2, 535.

DENBIGH, K. 1968. The Principles of Chemical Equilibrium. Cambridge, University Press.

DEWEY, J.F., and PANKHURST, R.J. 1970. The evolution of the Scottish Caledonides in relation to their isotopic age pattern. Trans.R. Soc.Edin. 68,361-389.

DOLLASE, W.A., 1971. Refinement of the crystal structures of epidote, allanite, and hanc ockite. Am.Miner.56, 447-464.

ELLES, G.S. and TILLEY, C.E. 1930. Metamorphism in relation to structure in the Scottish Highlands. Trans.R.Soc.Edinb.56, 621-46.

ERNST, W.G. 1972. CO_2 - poor composition of the fluid attending Franciscan and Sanbagawa low-grade metamorphism. Geochim. cosmochim.Acta 36, 497-504.

EUGSTER, H.P., 1959. Reduction and oxidation in metamorphism, in Researches

in Geochemistry, vol.1, (ed. ABELSON, P.H.) John Wiley & Sons, New York.

EUGSTER, H.P., ALBEE, A.L., BENCE, A.E., THOMPSON, J.B., and WALDBAUM, D.R., 1972. The two-phase region and excess mixing properties of paragonite-muscovite crystalline solutions. J.Petrol.13, 147-149.

EUGSTER, H.P., and SKIPPEN, G.B., 1972. Igneous and metamorphic reactions involving gas equilibria. Pp 492-520 in Researches in Geochemistry, vol 2, (ed.Abelson, P.H.) N.Y.,John Wiley & Sons Inc.

EUGSTER, H.P., and WONES, D.R., 1962. Stability relations of the ferruginous biotite, annite. J. Petrology. 3,82-125

EVANS, B.W., 1965. Application of a reaction rate method to the breakdown equilibria of muscovite and muscovity plus quartz. Am.J.Sci. 263, 647-667.

FAWCETT, J.J. and YODER, H.S., Jr., 1966. Phase relationships of chlorites in the system MgO - Al_2O_3 - SiO_2 - H_2O. Am.Miner.51, 353-380.

FISHER, J.R. and ZEN E-an., 1971. Thermochemical calculations from hydrothermal phase equilibrium data and the free energy of H_2O. Am.J.Sci.270, 297-314.

FOWLER. Sir R., and GUGGENHEIM, E.A. 1949. Statistical Thermodynamics. Cambridge Univ.Pr.

FRANK, E.U. and TOHEIDE, R. 1959. Thermische Eigenschaften über Kritischer Mischungen von Kohlendioxide und Wasser bis zu 750° und 2000 Atm. Z.phys.Chem.22.

FRENCH, B.M. 1966. Some geological implications of equilibrium between graphite and a C-H-O gas at high temperatures and pressures. Rev. geophys.4.223-253.

FROESE, E. 1973. The oxidation of almandine and iron cordierite. Can. Min. 11, 991-1002.

FYFE, W.S., TURNER, F.J. and VERHOOGEN, J. 1958. Metamorphic reactions and metamorphic facies. Mem.geol.Soc.Am 73.

GALDIN, N.Ye, 1970. Physical properties of oxides and silicates at high pressures and temperatures. Geochem.Int.7, 108-120.

GANGULY, J. 1972. Staurolite stability, and related parageneses: Theory, experiments, and applications. J. Petrology. 13,335-365

GOLDSMITH, J.R. and HEARD, H.C., 1961. Subsolidus phase relations in the system $CaCO_3$-$MgCO_3$. J.Geol.69,43-61.

GOLDSMITH, J.R. and NEWTON, R.C., 1969. P-T-X relations in the system $CaCO_3$ - $MgCO_3$ at high temperatures and pressures. Am.J.Sci. 267-A, 160-190.

GORDON, T.M., AND GREENWOOD, H.J., 1970. The reaction: Dolomite + Quartz + Water = Talc + Calcite + Carbon dioxide. Am.J.Sci.268,225-242.

GRAF, D.L. and GOLDSMITH, J.R., 1955. Dolomite-magnesian calcite relations at elevated temperatures and CO_2 pressures. Geochim.cosmochim. Acta 7, 109-128.

GREEN, E.J., 1970. Predictive thermodynamic models for mineral systems. I.Quasi-chemical analysis of the halite-sylvite subsolidus. Am. Miner.55, 1692-1713.

GREENWOOD, H.J. 1967. Mineral equilibria in the system MgO-SiO_2-H_2O-CO_2 pp 542-567 in Researches in Geochemistry, Vol 2. (ed.Abelson,P.H.) N.Y.John Wiley & Sons, Inc.

GREENWOOD, H.J., 1969. The compressibility of gaseous mixtures of carbon dioxide and water between 0 and 500 bars pressure and 450° and

800° C. Am.J.Sci.267-A, 191-208.

GROVER, J.E. and ORVILLE, P.M., 1970. Partitioning of cations between coexisiting single- and multi-site phases: A reply with incidental corrections. Geochim.cosmochim.Acta, 34, 1361-1364.

GUGGENHEIM, E.A., 1952. Mixtures. Oxford Clar.Pr.

GUGGENHEIM, E.A., 1966. Applications of statistic mechanics. Oxford: Clar.Pr.

HAAS, J.L. and ROBIE, R.A., 1973. Thermodynamic data for wustite, $Fe_{0.947}O$, magnetite, Fe_3O_4, and hematite, Fe_2O_3. Amer.geophys. Union Trans.(abs.), 54, 483.

HAASE, R. 1971. Survey of fundamental laws. pp 1-71 in Physical Chemistry; an advanced treatise, vol 1, Thermodynamics (ed.Jost, W.) N.Y., Academic Pr.

HARKER, A. 1932. Metamorphism: a study of the transormations of rock-masses. Lond.Methuen.

HAHN, W.C., Jr. and MUAN, A., 1962. Activity measurements in oxide solid solutions: The system "FeO-MgO in the temperature interval 1100° to 1300°C. Trans.metall.Soc.A.I.M.E.224, 416-420.

HARDY, H.K. 1953. A "subregular" solution model and its application to some binary alloy system. Acta metall. 1,202-209.

HARKER, R.I. and TUTTLE, O.F. 1955. Studies in the system CaO-MgO-CO_2. Part I: The thermal dissociation of calcite, dolomite and magnesite. Am.J.Sci. 253, 209-224.

HARKER, R.I. and TUTTLE, O.F. 1956. Experimental data on the P_{CO_2} - T curve for the reaction: calcite + quartz = wollastonite + CO_2. Am.J.Sci.254, 239-257.

HAYS, J.F., 1967. Lime-alumina-silica. Yb.Carnegie Instn. Wash.65, 234-9.

HAZEN, R.M. and WONES, D.R. 1972. The effect of cation substitutions on the physical properties of trioctahedral micas. Am.Miner.57, 103-129.

HEMINGWAY, B.S. and ROBIE, R.A. 1972. The heat capacties at low temperatures and entropies at 298.15°K of huntite, $CaMg_3(CO_3)_4$, and artinite, $Mg_z(OH)_2CO_3.3H_2O$. Am.Miner.57,1754-1767.

HILDEBRAND, J.H., 1927. A quantitiative treatment of deviations from Raoult's Law. Proc.Natn.Acad.Sci.U.S.A.13,267-272.

HILDEBRAND, J.H., 1929. Solubility, XII, Regular solutions. J.Am.chem. Soc.51, 66-80.

HOLDAWAY, M.J. 1966. Hydrothermal stability of clinozoisite plus quartz. Am.J.Sci. 264, 643-647.

HOLDAWAY, M.J. 1972. Thermal stability of Al-Fe Epidote as a Function of fo_2 and Fe content. Contr.Mineral. and Petrol.37, 307-340.

HOLM, J.L. and KLEPP, O.J., 1966. The thermodynamic properties of the aluminium silicates. Am.Miner.51, 1608-1522.

HOLSER, W.T. and KENNEDY, G.C., 1958. Properties of water. Part IV. Pressure-volume-temperature relations of water in the range 100-400°C and 100-1400 bars. Am.J.Sci.256, 744-753.

HOLSER, W.T. and KENNEDY, G.C. 1959. Properties of water. Part V. Pressure-volume-temperature relations of water in the range 400-1000°C and 100-1400 bars. Am.J.Sci.256, 71-77.

HOSCHEK, G. 1967. Untersuchungen zum stabilitatsbereich von chloritoid und Staurolith. Contr. Mineral. Petrol. 14, 123-62.

HOSTETLER P.B. and CHRIST, C.L., 1968. Studies in the system MgO-SiO_2-CO_2-H_2O: The activity-product constant of chrysotile. Geochim. cosmochim. Acta 32, 485-497.

HSU, L.C. 1968. Selected phase relationships in the system Al-Mn-Fe-Si-O-H: A model for garnet equilibria. J.Petrol.9,40-83.

HUANG, W.H. and KELLER, W.D. 1972. Standard free energies of formation calculated from dissolution data using specific mineral analyses. Am.Miner. 57, 1152-1162.

HUEBNER, J.S., and SATO, M., 1970. The oxygen rugacity-temperature relationships of manganese oxide and nickel oxide buffers. Am.Miner.55, 934-952.

JAMIESON, J.C., 1957. Introductory studies of high pressure polymorphism to 24,000 bars by X-ray diffraction, with some comments on calcite. J.Geol. 65, 334-344.

JOHANNES, W. 1969. An experimental investigation of the system MgO-SiO_2-H_2O-CO_2. Am.J.Sci. 267, 1083-1104.

JUZA, J., KNONICEK, V., and SIFNER, O., 1965. The specific volume of CO_2 at 700-4000 bars and 50-475°C. Physica 31.

KELLEY, K.K. 1960. Contributions to the data on theoretical metallurgy XIII. High-temperature heat-capacity, and entropy data for the elements and inorganic compounds. Bull.U.S.Bur.Mines 584,232.

KELLEY , K.K. and KING, E.G., 1961. Contributions to the data on theoretical metallurgy XIV. Entropies of the elements and inorganic compounds: Bull.U.S.Bur.Mines 592, 149.

KENNEDY, G.C. 1954. Pressure - volume - temperature relations in CO_2 at elevated temperatures and pressures. Am.J.Sci.252, 50-68.

KENNEDY, W.Q., 1948. On the significance of thermal structure in the Scottish Highlands. Geol.Mag.85, 229-34.

KERRICK, D.H. 1972. Experimental determination of muscovite + quartz + stability with $P_{H_2O} < P_{total}$. Am.J.Sci.272, 946-958.

KHORZHINSKII, D.S., 1959. Physicochemical basis of the analysis of the paragenesis of minerals N.Y., Consultants Bureau.

KING, E.G. and WELLER, W.W. 1961. Low temperature heat capacities and entropies at 298.15°K of some sodium and calcium aluminium silicates. Rept.Invest.U.S.Bur.Mines 6001,4.

KRACEK, F.C. 1953. Thermochemical properties of minerals. Yb.Carnegie Inst. Wash. 52, 69-74.

KRACEK, F.C., NEUVONEN, K.J., BURLEY, J., and GORDON, R.J., 1953. Contributions to the problem of mineral stability. Yb.Carnegie Inst. Wash.52,69.

KROGER, F.A., STIELTJES, F.H., and VINK, H.J., 1959. Thermodynamics and formulation of reactions involving imperfections in solids. Philips Res. Repts. 14, 557-601.

KRYTCHEVSKY, I.R., and MARKOV, V.P., 1940. Compressibility of gas mixtures. I. The P-V-T data for binary and ternary mixtures of hydrogen. Acta phys.-chem.URSS 12.

KUSHIRO, I., 1968. Synthesis and stability of iron-free pigeonite in the system $MgSiO_3$-$CaMgSi_2O_6$ at high pressures. Yb.Carnegie Inst, Wash. 67, 80-83.

LANGMUIR, D., 1965. Stability of carbonates in the system MgO-CO_2-H_2O. J.Geol. 73,730-754.

LEMMLEIN, G.G. and KLEVTSOV, P.V. 1961. Relations among the principal

thermodynamic parameters in a part of the system H_2O-NaCl. Geochem.2, 148-158.

LEWIS, G.N. 1901. Z.phys.Chem.38, 205.

LEWIS, G.N. and RANDALL, M. 1961. Thermodynamics. Revised by Pitzer,K.S. and Brewer, L. N.Y., McGraw-Hill Book Co.

LISTER, M.W. and MEYERS, N.F. 1958. Heats of formation of some solid solutions of alkali halides. J.phys.Chem,Wash,62,145-150.

MACKENZIE, F.T. and GARRELS, R.M., 1965. Silicates: Reactivity with sea water. Science 150, 57-58.

MAH, A.D., 1957. Heats of formation of alumina, molybdenum trioxide and molybdenum dioxide. J.phys.Chem.,Wash.61, 1572-1573.

McCORMICK, K.E. and SCHNEIDER, W.G. 1950. Carbon dioxide in the temperature range 0-600°C and pressures up to 50 atmostpheres. J.chem.Phys.18.

McNAMARA, M. 1965. The lower greenschist facies in the Scottish Highlands. Geol.För.Stockh.Förh.87,347-89.

MATHER, J.D. 1970. The biotite isograd and the lower greenschist facies in the Dalradian rocks of Scotland. J.Petrology. 11,253-275

METZ, P. and PUHAN, D. 1970. Experimentelle Untersuchung der metamorphose von Kieselig dolomitischen sedimenten I. Contr. Mineral.Petrol.26,302-314.

METZ, P. and PUHAN, D. 1970. Experimentelle Untersuchung der metamorphose von kieselig dolomitischen sedimenten I. Contr. Mineral. Petrol. 26, 302-314.

METZ, P. and PUHAN, D. 1971. Korrektur zur arbeit 'Experimentelle

Untersuchung der metamorphose von kieselig dolomitischen Sedimenten I' Contr.Mineral.Petrol.31,163-170.

METZ, P. and TROMMSDORF, V. 1968. On phase equilibria in metamorphosed siliceous dolomites. Contr.Mineral.Petrol.18,305-309.

NACKEN, R. 1918. Uber die Grenzen der Mischkristallbildung zwischen Kaliumschlorid und Natriumchlorid. Sber.Preuss.Akad.Wiss.192-200.

NAFZIGER, R.H. and MUAN, A., 1967. Equilibrium phase compositions and thermodynamic properties of olivines and pyroxenes in the system MgO-"FeO"-SiO_2. Am.Miner. 52, 1364-1385.

NAUMOV, G.B., RHZHENKO, B.N., and KHODAKOVSKIY, I.L., 1971. Spravochnik termodinamicheskikh velichin dlya geologiv. Atomizdat,Moscow.

NAVROTSKY, A. and KLEPPA, O.J. 1967. Enthalpy of the anatase-rutile transformation. J.Am.Ceram.Soc.,50, 626.

NERNST, W., 1906. Nachr. Ges.Wiss.Gottingen 1.

NEUVONEN, K.J., 1952. Thermochemical investigations of the akermanite-gehlenite series. Bull.Commn geol.Finl.158, 50.

NEWTON, R.C. 1966. Some calc-silicate equilibrium relations. Am.J.Sci. 264, 204-222.

NEWTON, R.C. 1972. An experimental determination of the high-pressure stability limits of magnesian cordierite under set and dry conditions. J.Geol., 80, 398-420.

ORVILLE, P.M., 1972. Plagioclase cation equilibria with aqueous chloride solution: results at 700°C and 2000 bars in the presence of quartz. Am.J.Sci.272, 234-272.

PANKRATZ, L.B. 1964. High temperature heat contents and entropies of

muscovite and dehydrated muscovite. Rep.Invest.U.S.Bur.Mines 6371,6.

PANKRATZ, L.B. and KELLEY, K.K., 1964. High-temperature heat contents and entropies of akermannite, cordierite, gehlenite and merwinite. Rept.Invest.U.S.Bur.Mines 6555, 7.

PARKS, G.A., 1972. Free energies of formation and aqueous solubilities of aluminium hydroxides and oxide hydroxides at 25°C. Am. Miner.57, 1163-1189.

PORTER, A.W. 1921. On the vapour-pressures of mixtures. Trans.Farady Soc. 16, 336-45.

PRESNALL, D.C. 1967. P-V-T measurements on hydrogen up to 600°C and 1800 atmospheres. Yb.Carnegie Instn Wash. 66, 539-541.

PRIGOGINE, J. and DEFAY, R. 1954. Chemical Thermodynamics. Lond., Longmans Green & Co.

READ, H.H., 1923. The geology of the country around Banff, Huntly, and Turriff (explanation of sheets 86 and 96). Mem.geol.Surv. Scotl.

READ, H.H., 1952. The Banff happe: an interpretation of the structure of the Dalradian rocks of north east Scotland. Proc.Geol.Ass. 66, 1-28.

READ, H.H., 1952. Metamorphism and migmatisation in the Ythan Valley, Aberdeenshire. Trans.Edinb.geol.Soc. 15, 265-79.

REAMER, H.H., OLD, R.H., SAGE, B.H., and LACEY, W.H., 1944. Phase equilibria in hydrocarbon systems. Ind.Engng chem.ind.(int.) Edn.36.

REESMAN, A.L. and KELLER, W.D. 1965. Calculation of apparent standard free energies of formation of six rock-forming silicate minerals from solubility data. Am.Miner.50, 1729-1739.

REESMAN, A.L. and KELLER, W.D., 1968. Aqueous solubility studies of high-alumina and clays minerals. Am.Miner.53, 929-942.

REESMAN, A.L., PICKETT, E.E. and KELLER, W.D., 1969. Aluminium ions in aqueous solutions. Am.J.Sci.267,99-113.

RICHARDSON, S.W., 1967. Composition of synthetic Fe-staurolite. Yb. Carnegie Instn.Wash., 66, 397-8.

RICHARDSON, S.W. 1968. Staurolite stability in a part of the system Fe-Al-Si-O-H. J. Petrology. 9,467-488

RICHARDSON, S.W., GILBERT, M.C. and BELL, P.M., 1969. Experimental determination of kyanite-andalusite and andalusite-sillimanite equilibria; The aluminium silicate triple point. Am.J.Sci.267,259-272.

ROBIE, R.A., BETHKE, P.M. and BEARDSLEY, K.M. 1967. Selected X-ray crystallographic data, molar volumes, and densities of minerals and related substances. Bull.U.S.geol.Surv.1248, 87.

ROBIE, R.A. and HEMINGWAY, B.S. 1972. The heat capacities at low temperatures and entropies at 298-15°K of nesquehonite, $MgCO_3$. $3H_2O$, and hydromagnesite. Am.Miner.57, 1768-1781.

ROBIE, R.A. and STOUT, J.W. 1963. Heat capacity from 12 to 305°K and entropy of talc and tremolite. J.phys.Chem.67,2252-2256.

ROBIE, R.A. and WALDBAUM, D.R. 1968. Thermodynamic properties of minerals and related substances at 298.15°K (25.0°C) and one atmosphere (1.013 bars) pressure and at higher temperatures. Bull.U.S.geol. Surv. 1259.

ROEDDER, E., 1967. Fluid inclusions of sample of ore fluid. in Geochem. of Hydrothermal ore deposits (ed.BARNES, H.L.)

RYZHENKO, B.N. and MALININ, S.D., 1971. The fugacity rule for the systems CO_2-H_2O, CO_2-CH_4, CO_2-N_2, and CO_2-H_2. Geochem.Int.8,562-574.

RYZHENKO, B.N., and VOLKOV, V.P., 1971. Fugacity coefficients of some gases in a brœad range of temperatures and pressure. Geochemistry International 8, 468-481.

SANFELD, A., 1971. Equilibrium, stability, and displacements pp 99-215. in Physical Chemistry: an advanced treatise, vol.1, (ed Jost, W.), Academic Press, London.

SAXENA, S.K., 1972. Retrieval of thermodynamic data from a study of inter-crystalline and intra-crystalline ion-exchange equilibrium. Am. Miner.57, 1782-1800.

SCHREYER, W. and YODER, H.S.Jr., 1964. The system Mg-cordierite-H_2O and related rocks. Neues Jb.Miner.Abh 101,271-342.

SCHUILING, R.D. and VINK, B.W., 1967. Stability relations of some titanium minerals (sphene, perovskite, rutile, anatase). Geochim. cosmochim.Acta 31,2399-2411.

SCHWERDTFEGER, K. and MUAN, A., 1966. Activities in olivine and pyroxenoid solid solutions of the system Fe-Mn-Si-O at 1150°C. Trans.metall. Soc.A.I.M.E. 236, 201-210.

SEIFERT, F., 1970. Low-temperature compatibility of cordierite in haplopelites of the ystem K_2O-MgO-Al_2O_3-SiO_2-H_2O. J.Petrology 11, 73-101.

SHARP, W.E., 1962. The thermodynamic functions for water in the range -10 to 1000°C and 1 to 250,000 bars. Livermore, Calif., Univ. Calif. Lacorence Radiation Lab., UCRL-7118, 51 pages.

SHAW, H.R., 1963. Hydrogen-water vapour mixtures: control of hydrothermal atmospheres by hydrogen osmosis. Science 139, 1220-1222.

SHAW, H.R., 1967. Hydrogen osmosis in hydrothermal experiments. Pp 521-541 in Researches in Geochemistry, Volume 2 (ed.Abelson, P.H.) New York: John Wiley and Sons, Inc.

SHAW, H.R. and WONES, D.R., 1964. Fugacity coefficients for hydrogen gas between 0° and 1000°C, for pressures to 3000 atm. Am.J.Sci.262, 918-929.

SKIPPEN, G.B., 1971. Experimental data for reactions in siliceous marbles. J.Geol.79,457-481.

SLAUGHTER, J., KERRICK, D.M., and WALL, V.J., 1973. Experimental and thermodynamic study of equilibria in the system CaO-MgO-SiO_2-H_2O-CO_2. Amer. geophys.Union Trans.,(abs.), 54, 479.

SORBY, H.C., 1858. On the microscopical structure of crystals, indicating the origin of minerals and rocks. Q.Jl.geol.Soc.Lond.14,453-500.

SPRY, A., 1969. Metamorphic textures. Oxford: Pergamon Press.

STOUT, J.W. and ROBIE R.A., 1963. Heat capacity from 11 to 300°K. Entropy and heat of formation of dolomite. Jour.phys.Chem. 67, 2248-2252.

STULL, D.R., and others, 1966, 1972. JANAF thermochemical tables: 1st and 2nd editions. Midland, Mich., Dow Chemical Co.

TAKENOUCHI, S., and KENNEDY, G.C., 1964. The binary system H_2O-CO_2 at high temperatures and pressures. Am.J.Sci.262, 1055-1074.

THOMPSON, J.B., 1955. The thermodynamic basis for the mineral facies concept. Am.J.Sci.253, 65-103.

THOMPSON, J.B.Jr., 1967. Thermodynamic properties of simple solutions Pp 340-361 in Researches in Geochemistry, Volume 2. C ed. Abelson, P.H.) New York: John Wiley and Sons, Inc.

THOMPSON, J.B.,Jr., and WALDBAUM, D.R., 1969. Analysis of the two-phase region halite-sylvite in the system NaCl-KCl. Geochim. cosmochim. Acta 33, 671-690.

TODD, S.S., and KELLEY, K.K., 1956. Heat and free-energy data for tricalcium dititanate, sphene, lithium metatitanate, and zinc-titanium spinel. Rep. Invest. U.S. Bur. Mines 5193, 18.

TODHEIDE, K. and FRANCK, E.U., 1963. Das Zweiphasengebiet und die Kritische Kurre im System Kohlendioxid-Wasser bis zu Drucken von 3500 bar. 37, 387-49. Z. phys.Chem.

TORGESON D.R., and SAHAMA, Th.G., 1948. A hydrofluoric acid solution calorimeter and the determination of the heats of formation of Mg_2SiO_4, $MgSiO_3$, and $CaSiO_3$. J. Am chem.Soc. 70, 2156-2160.

TSIKLIS, D.S., LINSHITS, L.R., and TSIMMERMAN, S.S., 1970. Termodinamicheskiye svoystra dvnokisi ugleroda pri vysokikh davleniyakh i temperaturakh. Zh.Fiz.Khim.44.

TUNELL, G., 1931. The definition and evaluation of the fugacity of an element or compound in the gaseous state. J.phys.Chem.35,2885.

TURNOCK, A.C., and EUGSTER, H.P., 1962. Fe-Al Oxides: Phase relationships below 1,000°C. J. Petrology 3, 533-65.

VELDE, B., 1966. Upper stability of muscovite. Am.Miner.51,924-929.

VUKALOVICH, M.P., and ALTUNIN, V.V., 1965. Thermophysical properties of carbon dioxide.Atomizdat, Moscow.

WAGMAN, D.D., EVANS, W.H., HALOW, I., PARKER, V.B., BAILEY, S.M., and SCHUMM, R.H., 1965. Selected values of chemical thermodynamic properties, Part 1 to 6. U.S. Natl.Bur.Standards Tech. Note 270-1 to 270-6.

WAGMAN, D.D., KILPATRICK, J.E., TAYLOR, W.J., PITZER, K.S. and ROSSINI, F.D., 1945. Heats, free energies, and equilibrium constants of some reactions involving O_2, H_2, H_2O, C, CO, CO_2, and CH_4. U.S. Natl. Bur. Standards J. Research 34, 143-161.

WELLER, W.W., and KELLEY, K.K., 1963. Low temperature heat capacities and entropies at 298.15°K of akermanite, cordierite, gehlenite, and merwinite. Rep. Invest. U.S. Bur.Mines 6343,7.

WELLER, W.W. and KING, E.G., 1963. Low temperature heat capacity and entropy at 298.15°K of muscovite. Rep.Invest.U.S.Bur.Mines 6281,4.

WILKS, J., 1971. The third law of thermodynamics. Pp437-486 in Physical chemistry; an advanced treatise, Vol.1, Thermodynamics. (ed.Jost, W.) New York, Academic Press.

WILLIAMS, R.J., 1971. Reaction constants in the system Fe-MgO-Sio_2-O_2 at 1 atm. between 900° and 1300°C: experimental results. Am. J.Sci 270, 334-360.

WISEMAN, J.D.H., 1934. The central and south west Highland epidiorites: a study in progressive metamorphism. Q.Jl.geol.Soc.Lond.90, 354-417.

WONES, D.R., BURNS, R.G., and CARROLL, B.M., 1971. Stability and properties of synthetic annite. Amer. geophys.Union Trans.,(abs.) 52, 369-370.

WONES, D.R., and EUGSTER, H.P., 1965. Stability of biotite: experiment,

theory and application. Am.Miner. 50, 1228-1243.

WONES, D.R., and GILBERT, M.C., 1969. The fayalite-magnetite-quartz assemblage between 600° and 800°C. Am.J.Sci. 267, 480-488.

YERMAKOV, N.P., 1949. Investigations of mineral forming solutions (in Russian). Min. sb. L'vov.geol.obshch. 3,23.

ZEN, E-an., 1969. Free energy of formation of pyrophyllite from hydrothermal data: Values, discrepancies and implications. Am. Miner. 54, 1592-1606.

ZEN, E-an., 1971. Comments on the thermodynamic constants and hydrothermal stability relations of anthophyllite. Am.J.Sci.270, 136-150.

ZEN, E-an., 1972. Gibbs free energy, enthalpy, and entropy of ten rock-forming minerals: calculations, discrepancies, implications. Am. Miner. 57, 524-553.

ZEN, E-an., 1973. Thermochemical parameters of minerals from oxygen buffered hydrothermal equilibrium data: Method, application to annite and almandine. Contr. Mineral. and Petrol. 39, 65-80.

APPENDIX 1

NOTATION

Appendix 1 : Notation

In general :

Z	a property
z	mean molar property
z_i	partial molar property of i

Applied to the following :

C_p	heat capacity at constant pressure
H	enthalpy
G	Gibbs energy
S	entry
V	volume
U	internal energy
A	Helmholz potential

Also :

q	heat
w	work
μ_i	chemical potential of i
f_i	fugacity of i
a_{ti}	activity of i for standard state t
γ_i	activity coefficient of i
n_i	mole number of i
x_i	mole fraction of i
P	pressure
p_i	partial pressure of i
T	temperature
K	equilibrium constant

In general :

Z (Pbars, $T_1 \rightarrow T_2{}^{\circ}C$) change of Z from T_1 to T_2 at P

Z ($T^{\circ}C$, $P_1 \rightarrow P_2$ bars) change of Z from P_1 to P_2 at T

Z ($T_1{}^{\circ} \rightarrow T_2{}^{\circ}C$, $P_1 \rightarrow P_2$bars) change of Z from P_1 and T_1 to P_2 and T_2

$\Delta_f Z_i$(el, $T^{\circ}C$, Pbars) change of Z at P and T for formation of i from the elements

$\Delta_f Z_i$(ox, $T^{\circ}C$, Pbars) change of Z at P and T for formation of i from the oxides

and these can be applied to H, G, S and V.

APPENDIX 2

DERIVATION OF THE FUGACITY POLYNOMIAL FOR H_2O

Appendix 2

Calculation of the polynomial for $\ln f_{H_2O}$

Burnham et al (1968) give

$$\frac{PV_{H_2O}}{M} = \sum_{j=1}^{10} \sum_{i=1}^{11-j} a_{ij} t^{i-1} P^{j-1}$$

where t is in hundreds of °C
P is in kbars
m is molecular wt of H_2O

$$\therefore \quad v_{H_2O} = \sum_{j=1}^{10} \sum_{i=1}^{11-j} 18.005 \times 1000\, a_{ij} t^{i-1} P^{j-2}$$

From (61)

$$\ln \frac{f}{f^1} = \frac{\mu - \mu^1}{RT} \quad \text{for } \frac{f}{P} \to 1 \text{ as } P \to 0$$

They consider that H_2O is nearly ideal at 0.01 bars for temperatures down to 20°C Thus

$$\ln f_{H_2O} = \Delta g_{H_2O}(T^\circ K,\ 0.01 \to P \text{ bars})$$

$$\overline{0.01} \qquad \overline{RT}$$

$$\Delta g_{H_2O}(T^\circ K,\ 0.01 \to P \text{ bars}) = \int_{0.01}^{P} v_{H_2O}\, d\,P$$

However the polynomial only applies above 1 kbar so that the integral is calculated in several parts. The origin for the integral is chosen as 2 kbars to be well within the applicable range. Thus

$$\Delta g_{H_2O}\ (T^\circ K,\ 0.01 \to P \text{ bars}) = g_{H_2O}\ (T^\circ K, 0.01 \to 2000 \text{ bars}) + \int_{2000}^{P} v_{H_2O}\, d\,P$$

The first term on the right hand side was found by least squares curve fitting, using FIT, on

$\Delta g_{H_2O}\ (T^\circ K,\ 0.0061 \to 0.01 \text{ bars})$ and

$\Delta g_{H_2O}\ (T^\circ K,\ 0\ 0061 \to 2000 \text{ bars})$

as 6th order polynomials in hundreds of °K (the fit being better than ± 0.02% over the temperature range 100 to 900°C). The coefficients are combined to form e_i, for

$$\Delta g_{H_2O}\ (T^{\circ}K,\ 0.01 \rightarrow 2000\ \text{bars}) = \sum_{i=1}^{7} e_i T^{i-1}$$

The polymonial must be expressed in hundreds of $^{\circ}K$ rather than hundreds of $^{\circ}C$, involving an awkward transformation, the resulting coefficients b_{ij} being given in Table 1

$$v_{H_2O} = \sum_{j=1}^{10} \sum_{i=1}^{11-j} 18005 a_{ij} (T-2.7315)^{i-1} P^{j-2}$$

$$= \sum_{j=1}^{10} \sum_{i=1}^{11-j} b_{ij} T^{i-1} P^{j-2}$$

Integrating this equation gives

$$\int_{2000}^{P} v_{H_2O} dP = \left| \sum_{i=1}^{10} b_{i1} T^{i-1} \ln P + \sum_{j=2}^{10} \sum_{i=1}^{11-j} \frac{b_{ij}}{j-1} T^{i-1} P^{j-1} \right|_{2000}^{P}$$

For P = 2 kbars, the coefficients and pressure term can be combined into a polynomial in T, whose coefficients C_i are given by

$$C_i = b_{i1} \ln 2 + \sum_{j=2}^{11-i} \frac{b_{ij}}{j-1} 2^{j-1} \qquad (i = 1,\ 2\ \ldots.\ 10)$$

combining the above equations

$$\frac{RT \ln f_{H_2O}}{0.01} = \sum_{i=1}^{10} b_{i1} T^{i-1} \ln P + \sum_{j=2}^{10} \sum_{i=1}^{11-j} \frac{b_{ij}}{j-1} T^{i-1} P^{j-1}$$

$$+ \sum_{i=1}^{10} C_i T^{i-1} + \sum_{i=1}^{10} e_i T^{i-1}$$

setting $m_i = b_{i1}/100\ R; i = 1,2\ \ldots.\ 10$ with R in cc bar

and $n_{ij} = b_{ij}/100\ R; j = 2,3\ \ldots.\ 10;\ i = 1,2\ \ldots.\ 11-j$

and $n_{i1} = (C_i + e_i)/100\ R;\ i = 1.2\ \ldots.\ 10$ (having set $e_i = 0,\ i = 8,10$)

also $n_{21} = n_{21} + \ln (0.01)$

$$\ln f_{H_2O} = \sum_{i=1}^{10} m_i T^{i-2} \ln P + \sum_{j=1}^{10} \sum_{i=1}^{11-j} n_{ij} T^{i-2} P^{j-1}$$

The coefficients are given in table 2. This polynomial reproduces Burnhams listed fugacities within 0.1% for the range of applicability of this equation. It gives values less than 0 5% too high in the low pressure high temperature wedge, and less than 1% too low in the 900-1000°C range.

Table 1

	b_{ij} corresponding to a_{ij}
A(1, 1) = -0.381065900E-01	-0.8543654O5E 01
A(1, 2) = 0.105646650E 01	0.143140687E 01
A(1, 3) = -0.764546830E-01	-0.167797811E 00
A(1, 4) = 0.709566000E-03	0.108409304E 00
A(1, 5) = 0.104549350E-01	-0.221942682E-01
A(1, 6) = -0.448878450E-02	0.200172157E-02
A(1, 7) = 0.905864800E-03	0.844305133E-04
A(1, 8) = -0.983132250E-04	-0.463986998E-04
A(1, 9) = 0.551474020E-05	0.427554611E-05
A(1,10) = -0.125479950E-06	-0.125479950E-06
A(2, 1) = 0.664314730E-01	0.126703509E 02
A(2, 2) = -0.426544090E-01	-0.568159487E 00
A(2, 3) = 0.821934390E-01	-0.109711294E 00
A(2, 4) = -0.460175030E-01	-0.341827016E-01
A(2, 5) = 0.154843860E-01	0.103041494E-01
A(2, 6) = -0.308094420E-02	-0.172070628E-02
A(2, 7) = 0.344626110E-03	0.255316673E-03
A(2, 8) = -0.198052880E-04	-0.182064456E-04
A(2, 9) = 0.453667980E-06	0.453667980E-06
A(3, 1) = -0.894133650E-01	-0.801586640E 01
A(3, 2) = 0.892220300E-02	0.457561816E 00
A(3, 3) = 0.197197480E-02	0.106903559E 00
A(3, 4) = -0.487960360E-02	-0.402767985E-02
A(3, 5) = 0.190171400E-02	-0.159256236E-03
A(3, 6) = -0.271553430E-03	-0.217394011E-03
A(3, 7) = 0.155187830E-04	0.171773315E-04
A(3, 8) = -0.292667470E-06	-0.292667470E-06
A(4, 1) = 0.920769930E-01	0.280391867E 01
A(4, 2) = 0.438058770E-02	-0.211469847E 00
A(4, 3) = 0.317799630E-03	-0.274251896E-01

(Table 1 continued)

A(4, 4) =	-0.141116850E-02	0.196311745E-02
A(4, 5) =	0.190879010E-03	0.303654240E-03
A(4, 6) =	-0.330168350E-05	-0.991679688E-05
A(4, 7) =	-0.202397770E-06	-0.202397770E-06
A(5, 1) =	-0.478879220E-01	-0.591871623E 00
A(5, 2) =	-0.618914870E-03	0.540221751E-01
A(5, 3) =	0.190433210E-02	0.268522565E-02
A(5, 4) =	-0.111533840E-03	-0.528818188E-03
A(5, 5) =	-0.126500680E-04	-0.799339342E-05
A(5, 6) =	0.605446950E-06	0.605446950E-06
A(6, 1) =	0.137985650E-01	0.776154942E-01
A(6, 2) =	-0.132330460E-02	-0.744626544E-02
A(6, 3) =	-0.149437770E-03	0.652950190E-04
A(6, 4) =	0.255693470E-04	0.355376416E-04
A(6, 5) =	-0.340960980E-06	-0.340960980E-06
A(7, 1) =	-0.198867890E-02	-0.630982403E-02
A(7, 2) =	0.239123440E-03	0.520267874E-03
A(7, 3) =	-0.757212920E-05	-0.186323725E-04
A(7, 4) =	-0.608230800E-06	-0.608230800E-06
A(8, 1) =	0.150644510E-03	0.310910324E-03
A(8, 2) =	-0.127915920E-04	-0.166160526E-04
A(8, 3) =	0.578449480E-06	0.578449480E-06
A(9, 1) =	-0.602113030E-05	-0.864716681E-05
A(8, 2) =	0.175016500E-06	0.175016500E-06
A(10, 1) =	0.106821100E-06	0.106871100E-06

b (1) = 0.14640217 E3

(2) = 0.30346091 E4

(3) = -0.20358190 E3

(4) = 0.38732678 E2

(Table 1 continued)

b (5) = -0.71295555 E1

(6) = 0.63823131 E0

(7) = -0.20826141 E-1

Table 2

A(1, 1) = -0.5100382393E 02

A(2, 1) = 0.5575630079E 01

A(3, 1) = 0.7681815229E 01

A(4, 1) = -0.2956561399E 01

A(5, 1) = 0.6257548091E 00

A(6, 1) = -0.83777000 43E-01

A(7, 1) = 0.7297213112E-02

A(8, 1) = -0.3975687334E-03

A(9, 1) = 0.1223219695E-04

A(10, 1) = -0.1604800416E-06

A(1, 2) = 0.3102427336E 01

A(2, 2) = -0.1231427319E 01

A(3, 2) = 0.9917182288E 00

A(4, 2) = -0.4583391675E 00

A(5, 2) = 0.1170875147E 00

A(6, 2) = -0.1613901535E-01

A(7, 2) = 0.1127627168E-02

A(8, 2) = -0.3601358689E-04

A(9, 2) = 0 3793302837E-06

A(1, 3) = -0.1818422587E 00

A(2, 3) = -0.1188939797E 00

A(3, 3) = 0.1158512411E 00

A(4, 3) = -0.2972064049E-01

A(5, 3) = 0.2909975366E-02

A(6, 3) = 0.7076012289E-04

A(7, 3) = -0.2019187659E-04

A(8, 3) = 0.6268649109E-06

A(1. 4) = 0.7832200954E-01

A(2, 4) = -0.2469583135E-01

A(3, 4) = -0.2909860764E-02

(Table 2 continued)

A(4, 4) = 0.1418285135E-02

A(5, 4) = -0.3820530319E-03

A(6, 4) = 0.2567472907E-04

A(7, 4) = -0.439425924E-06

A(1, 5) = -0.1202594904E-01

A(2. 5) = 0.5583296322E-02

A(3, 5) = -0.8629288266E-04

A(4, 5) = 0.1645348423E-03

A(5, 5) = -0.4331214760E-05

A(6, 5) = -0.1847494740E-06

A(1, 6) = -0.8677051724E-03

A(2, 6) = -0.7458908169E-03

A(3, 6) = -0.9423583716E-04

A(4, 6) = -0.4298727688E-05

A(5, 6) = 0.2624488129E-06

A(1, 7) = 0.3049907729E-04

A(2, 7) = 0.9222877659E-04

A(3, 7) = 0.6205016899E-05

A(4, 7) = -0.7311272891E-07

A(1, 8) = -0.1436634502E-04

A(2, 8) = -0.5637228636E-05

A(3, 8) = -0.9061809635E-07

A(1, 9) = 0.1158350870E-05

A(2, 9) = 0.1229098425E-06

A(1,10) = -0.3021832229E-07

E(1) = -0.185174924 3E 02

E(2) = 0.2746168381E 02

E(3) = -0.1737356692E 02

E(4) = 0.6077205652E 01

E(5) = -0.1282820938E 01

(Table 2 continued)

E(6) = 0.1682236100E 00

E(7) = -0.1367589536E-01

E(8) = 0.6738661869E-03

E(9) = -0.1874184571E-04

E(10) = 0.2315237601E-06

APPENDIX 3

COMPUTER PROGRAMS

```
      MASTER THERMOCALC
C
C
C
```

```
C
C       RL=DATA SOURCE FOR EACH PHASE
C
C       CO21=CO2 FUGACITY COEFFICIENT POLYNOMIAL COEFFICIENTS,
C            PRODUCED FROM DATA GIVEN BY RHYZENKO AND VOLKOV (1971)
C
C       O21=O2 FUGACITY COEFFICIENT POLYNOMIAL COEFFICIENTS FROM
C            RHYZENKO AND VOLKOV (1971)
C
C       H2O1=H2O FUGACITY POLYNOMIAL COEFFICIIENTS DERIVED FROM
C             EQUATION 1A OF BURNHAM ET AL (1969)
C
C       A1=NAME OF GAS PHASE
C
C       B1(1-5),(6),(7) HEAT CAPACITY POLYNOMIAL COEFFICIENTS,
C            ENTHALPY OF FORMATION, AND ENTROPY ,AS ABOVE
C
        READ(5,1003)N
        READ(5,1003)(K3(I),I=1,N)
        DO 10 I=1,N
        READ(5,1001)A(I),(B(I,J),J=1,8)
 1001   FORMAT(A4,12F0.0)
        READ(5,1008)(K1(I,J),K2(I,J),J=1,K3(I))
 1008   FORMAT(10(I0,F0.0))
   10   READ(5,1009)(RL(I,J),J=1,8)
 1009   FORMAT(10A8)
 1000   FORMAT(15F0.0)
        DO 505 I=1,3
  505   READ(5,1000)(CO21(I,J),J=1,3)
        DO 506 I=1,3
  506   READ(5,1000)(O21(I,J),J=1,3)
        DO 507 J=1,10
        DO 507 I=1,11-J
  507   READ(5,1005)H2O1(I,J)
 1005   FORMAT(E0.0)
        DO 508 I=1,10
  508   READ(5,1005)H2O1(11,I)
        DO 401 I=1,4
  401   READ(5,1001)A1(I),(B1(I,J),J=1,9)
C
C       END OF PERMANENT DATA INPUT
C
        DO 402 I=1,4
  402   C1(I)=0.0
  999   CONTINUE
C
C       FIRST PART OF VARIABLE DATA INPUT
C
C
C       VARIABLE DATA INPUT DEPENDS ON FUNCTION OF PROGRAM. FIRST
C       TIME THROUGH THE PROGRAM OR,LATER, IF CODE J6=1,NEXT 4 READ
C       STATEMENTS READ.
C
C       N1=NUMBER OF SOLID PHASES IN REACTION
C
C       N3=NUMBER OF FLUID COMPONENTS IN REACTION
```

```
C
C       J1=CODE FOR SOLID PHASES IN REACTION
C
C              DIOPSIDE=1
C              RUTILE=2
C              FORSTERITE=3
C              SPHENE=4
C              QUARTZ=5
C              WOLLASTONITE=6
C              TALC=7
C              TREMOLITE=8
C              DOLOMITE=9
C              CALCITE=10
C              ENSTATITE=11
C              MAGNESITE=12
C              ALBITE=13
C              ANORTHITE=16
C              MUSCOVITE=17
C              PHLOGOPITE=18
C              KYANITE=19
C              ANDALUSITE=20
C              SILLIMANITE=21
C              CORUNDUM=22
C              MAGNETITE=23
C              HERCYNITE=28
C              SPINEL=29
C              GROSSULARITE=30
C              CORDIERITE=32
C              SANIDINE=33
C              ZOISITE=34
C              CLINOCHLORE=35
C              ALMANDINE=38
C              FE CHLORITE=39
C              ANNITE=40
C              FE CHLORITOID=41
C              FE STAUROLITE=42
C
C       J2=CODE FOR FLUID COMPONENTS
C
C              H2O=1
C              CO2=2
C              H2=3
C              O2=4
C       C,C1=REACTION COEFFICIENTS FOR SOLID AND FLUID COMPONENTS
C            IN THE REACTION.IF THESE ARE WRONG ( IE THE REACTION
C            DOESNT BALANCE), THE PROGRAM WILL THROW THE REACTION OFF.
C
C       XM=ACTIVITIES OF SOLID COMPONENTS IN THE PHASES, OBVIOUSLY
C         EQUAL TO 1 IF THE PHASE IS PURE.
C
C
C
      READ(5,1003)N1,N3
      READ(5,1003)(J1(I),I=1,N1),(J2(I),I=1,N3)
 1003 FORMAT(50I0)
      READ(5,1000)(C(I),I=1,N1),(C1(I),I=1,N3)
      READ(5,1000)(XM(I),I=1,N1)
```

```
C
C       END OF FIRST PART OF VARIABLE DATA INPUT
C
C
C       THIS SECTION CONVERTS O2 REACTIONS TO H2,H2O REACTIONS
C       BECAUSE THE H2 AND H2O DATA IS SUPERIOR TO THE O2 DATA
C
        IKZ=0
        DO 426 I=1,N3
        IF(J2(I)-4)0,427,0
  426   CONTINUE
        GO TO 428
  427   IKZ=1
        IF(N3-1)429,0,429
        J2(1)=1
        J2(2)=3
        N3=2
        C1(1)=C1(1)*2.
        C1(2)=-C1(1)
        GO TO 428
  429   J2(2)=3
        N3=2
        C1(1)=C1(1)+2.*C1(2)
        C1(2)=-2.*C1(2)
  428   CONTINUE
C
C       END OF SECTION
C
C
C       THIS SECTION CHECKS THAT THE REACTION IS BALANCED
C
        DO 101 I=1,12
  101   XX(I)=0.0
        DO 100 I=1,N1
        DO 100 K=1,K3(J1(I))
  100   XX(K1(J1(I),K))=XX(K1(J1(I),K))+C(I)*K2(J1(I),K)
        H11=XX(5)/2.
        H22=XX(4)
        DO 104 I=1,N3
        IF(J2(I).EQ.3)XX(5)=XX(5)+C1(I)*2.
        IF(J2(I).EQ.3)XX(8)=XX(8)+2.*C1(I)
        IF(J2(I).EQ.3)XX(9)=XX(9)-C1(I)
        IF(J2(I).EQ.1)XX(5)=XX(5)+2.*C1(I)
        IF(J2(I).EQ.2)XX(4)=XX(4)-C1(I)
  104   CONTINUE
        DO 102 I=6,12
 2090   FORMAT('1      EQN DOESNT BALANCE FOR OXIDE ',I2)
  102   IF(XX(I)**2.GT.1.0E-3)WRITE(6,2090)I
C
C       END OF SECTION
C
C
C       SECOND PART OF VARIABLE DATA INPUT
C
C
C       DATA IS READ HERE FIRST TIME THROUGH THE PROGRAM OR AT A
```

```
C      LATER TIME IF J6=2; IT PROVIDES THE OPPORTUNITY TO ALTER
C      THE ENTHALPY OF FORMATION OR ENTROPY OF ANY NUMBER OF
C      THE PHASES.
C
C      N4=NUMBER OF PHASES ALTERED,MINIMUM OF 1
C
C      J5=CODE OF PHASES TO BE ALTERED
C
C      D1,T4=ENTHALPY OF FORMATION AND ENTROPY CORRECTION IN KCALS/
C              MOLE AND CALS/MOLE DEG RESPECTIVELY
C
 3001 DO 409 I=1,N
  409 D2(I),T5(I)=0.
      READ(5,1004)N4,(D1(I1),T4(I1),J5(I1),I1=1,N4)
 1004 FORMAT(I0,20(2F0.0,I0))
C
C     END OF SECOND VARIABLE DATA INPUT
C
      DO 403 I=1,N4
      DO 403 J=1,N
      IF(J5(I)-J)403,0,403
      D2(J)=D1(I)
      T5(J)=T4(I)
  403 CONTINUE
C
C      THIRD VARIABLE DATA INPUT
C
C
C      INPUT HERE WHEN J6=3 OR 4 OR 5 , DIFFERENT INPUT
C      WHEN PROGRAM USED IN DIFFERENT WAYS.
C
C      J6=3 OR 4  : WHEN PROGRAM IS BEING USED FOR CALCULATING
C             THERMODYNAMIC DATA
C
C          P=PRESSURE OF EXPERIMENTAL REVERSAL
C
C          P2=SIZE OF ENTHALPY AND ENTROPY INCREMENT (IN KCALS AND
C             CALS/MOLE DEG RESPECTIVELY) . THIS IS USED TO FIND THE
C             CORRECT ENTHALPY CORRECTION.IF ZERO INPUT THEN
C             DEFAULT 1 IS USED
C
C          XCO2=MOLE FRACTION OF DILUENT IN H2O REACTIONS
C                "        "    OF CO2 IN CO2-H2O REACTIONS
C               (1-MOLE FRACTION DILUENT) IN CO2 REACTIONS
C
C           XN5=PARTIAL PRESSURE OF H2 MEASURED IN SHAW TECHNIQUE
C             EXPERIMENTS OR CODE FOR OXYGEN BUFFER IN BUFFERED
C             EXPERIMENTS
C                        HM=1
C                        NNO=2
C                        QFM=3
C                        MW=5
C
C          TT(1),TT(2)=EXPERIMENTALLY DETERMINED BRACKETS,IF ONLY
C                      ONE TEMPERATURE KNOWN THEN SET TT(1)=TT(2)
C
```

```
C
C       J6=5 : WHEN TEMPERATURES OF REACTION ARE REQUIRED AT
C            A RANGE OF PRESSURES (500 BAR INTERVALS)
C
C            P,P2=PRESSURES BETWEEN WHICH TEMPERATURES ARE TO BE
C                 CALCULATED
C
C            XCO2,XN5=HAVE THE SAME MEANING AS ABOVE
C
 3002 IF(J6.EQ.3.OR.J6.EQ.4)READ(5,1000)P,P2,XCO2,XN5,TT(1),TT(2)
      IF(J6.EQ.5)READ(5,1000)P,P2,XCO2,XN5
C
C       END OF THIRD PART OF VARIABLE DATA INPUT
C
      IF(XN5**2.LT.1.E-4)XN5=1
      IF(IK2)0,430,0
      N5=XN5
      TTT=(TT(1)+TT(2))/2.
      TTT=TTT+273.15
      F=BUFFER(N5,P,TTT)
      XN5=WAG1(F,P,TTT)
  430 CONTINUE
      H(1)=H11
      H(3),H(4)=0
      H(2)=H22
      IF(J6-5)360,0,360
      P=P-500.
  361 P=P+500.
      IF(P2-P)230,0,0
  360 CONTINUE
C
C       THIS SECTION COMBINES THE HEAT CAPACITY EQUATIONS OF THE
C       PHASES IN THE REACTION
C
      F25,F26,Y=0.
      DO 15 J=1,N1
      F25=F25+C(J)*(B(J1(J),7)+T5(J1(J)))/1000.
      F26=F26+C(J)*(B(J1(J),8)+D2(J1(J)))
   15 Y=Y+C(J)*B(J1(J),6)*(P    -1.)/(41.92*1000.)
      IF(J6-2)712,712,0
      X(1),X(2),X(3)=0.
      F27,F28=0.
      DO 577 I=1,N3
      F27=F27+B1(J2(I),6)*C1(I)
  577 F28=F28+C1(I)*B1(J2(I),7)
      X(4)=F26+Y+F27
      X(5)=F25+F28/1000.
      DO 16 K=1,5
   17 DO 18 J=1,N3
   18 X(K)=X(K)+C1(J)*B1(J2(J),K)
      YY(K)=X(K)
      DO 576 J=1,N3
  576 YY(K)=YY(K)+H(J2(J))*B1(J2(J),K)
      DO  16 J=1,N1
   16 X(K)=X(K)+B(J1(J),K)*C(J)
C
```

```
C      END OF SECTION
C
C
C
C      FG HOLDS THE VALUE OF LOG K FOR 8 TEMPERATURES AT 100
C      DEG INTERVALS.THE NEXT SUBSECTIONS PROVIDE THE DIFFERENT
C      PARTS OF THESE VALUES
C
C      SUBSECTION 1 :EFFECT OF INPUT ACTIVITIES
C
       DO 55 J=1,10
       FG(J)=0.
       DO 53 K=1,N1
    53 FG(J)=FG(J)+C(K)*ALOG(XM(K))
C
C      SUBSECTION 2 :CALCITE DOLOMITE ACTIVITIES CALCULATED IF
C                    BOTH PHASES PRESENT. USES AQC METHOD.
C
       IYD,IYC=0
       DO 767 J=1,N1
       IF(J1(J).EQ.9)IYD=J
   767 IF(J1(J).EQ.10)IYC=J
       IF(IYC)0,768,0
        IF(IYD)0,768,0
        DO 889 I=1,10
       T1=300.+I*100.
   889 FG(I)=FG(I)+CCDOL(P,T1)
   768 CONTINUE
C
C      SUBSECTION 3 :GAS FUGACITIES
C
       IF(P-2)769,0,0
       IF(N3)0,769,0
       JK1,JK2,JK3,JK4=0
       DO 31 K=1,N3
       IF(J2(K).EQ.1)JK1=K
       IF(J2(K).EQ.2)JK2=K
       IF(J2(K).EQ.3)JK3=K
    31 CONTINUE
       DO 30 J=1,10
       T1=100.*J+300.
        XN6=XN5
C
C                              H2O=CO2
C
C
        W=0.0
        IF(XCO2.LT.0.999.AND.XCO2.GT.0.001)W=H2OCO2(P,T1)
C
C                              H2
C
C
       IF(JK3)0,35,0
       F=FH2(XN5,T1)
       IF(IK2.EQ.1)F=XN5
        FG(J)=FG(J)+C1(JK3)*ALOG(F)
    35 CONTINUE
C
C                              H2O
```

```
C
      IF(JK1)0,32,0
      F=FH2O(P,T1)
      FG(J)=FG(J)+C1(JK1)*ALOG((1.-XCO2)*F*XN6)
     1+C1(JK1)*W*XCO2**2/(0.00198726*T1)
   32 IF(JK2)0,33,0
C
C                              CO2
C
      F=FCO2(P,T1)
      FG(J)=FG(J)+C1(JK2)*ALOG(XCO2*F*XN6)
     1+C1(JK2)*W*(1.-XCO2)**2/(0.00198726*T1)
   33 CONTINUE
C
C     END OF SECTION
C
C
C     SECTION CALCULATES  TEMPERATURE OF REACTION USING THE
C     THE STORED LITERARURE AND CALCULATED DATA WITH THE
C     CORRECTIONS INPUT IN THE SECOND PART OF THE VARIABLE
C     DATA INPUT ABOVE
C
C     ZT=THE CALCULATED TEMPERATURE USING THE FULL CALCULATION
C          (IE WITH THE HEAT CAPACITY EQUATIONS)
C
C     YT=THE CALCULATED TEMPERATURE USING THE APPROXIMATION
C          OUTLINED IN THE TEXT
C
   30 CONTINUE
  769 Z=0.0
      ZT=CALC(X,FG)
      YT=CALC(YY,FG)
      IF(ZT.LT.10.0)GO TO 632
      ZT=ZT+273.15
      IF(JK3.NE.0)XN5=FH2(XN5,ZT)
      IF(JK3.NE.0)JK4=1
      IF(JK3.NE.0)XY=WAG2(XN5,P,ZT)
      ZT=ZT-273.15
C
C     SECOND PART OF OUTPUT
C
      IF(JK4.NE.0)WRITE(6,2083)XY
 2083 FORMAT(5X,'LOG 10 OXYGEN FUGACITY OF ',F7.2/)
      IF(JK3.NE.0)WRITE(6,2054)XN5
 2054 FORMAT('  F H2 = ',F11.1,' BARS'/)
      F25=F25*1000.
      IF((JK1.NE.0.OR.JK2.NE.0).AND.XCO2.LT.0.99.AND.XCO2.GT.0.01)
     1WRITE(6,2029)XCO2
  632 WRITE(6,2017)P,ZT
 2029 FORMAT(' XCO2 = ',F6.2/)
 2017 FORMAT(1X,F8.1,' BARS',F11.1,' DEGC'/)
C
C     END OF SECOND PART OF OUTPUT
C
C
C     THIS SECTION CALCULATES THE AMOUNT BY WHICH THE ENTHALPY
```

```
C       AND/OR  ENTROPY OF ONE PHASE (THE FIRST PHASE GIVEN IN THE
C       THE CODE LIST J5 ABOVE IN THE SECOND PART OF THE VARIABLE
C       DATA INPUT)HAS TO BE CORRECTED FOR THE CALCULATED
C       CURVE TO PASS THROUGH THE LIMITS
C       OF THE BRACKET
C
        IF(J6-5)0,361,0
        FA1,FA2=1.0
        IF(P2.GT.0.5)FA1,FA2=P2
        XE4=X(4)
        XE5=X(5)
        DO 65 IH=1,11
        H(IH)=(IH-6)*FA1
        X(4)=XE4
        X(4)=X(4)+(IH-6)*FA1
        DO 65 IS=1,11
        X(5)=XE5
        X(5)=X(5)+(IS-6)*FA2/1000.
   65   T6(IH,IS)=CALC(X,FG)
        DH=0.
        IJL=0
        DO 342 I=1,N1
   342  IF(J1(I).EQ.J5(1))JIK=I
        JKJ=2
        IF((TT(1)-TT(2))**2.LT.0.1)JKJ=1
        DO 666 JK=1,JKJ
        DO 344 I=2,11
        IF(T6(I,6).LT.1.0.OR.T6(I-1,6).LT.1.0)GO TO 344
        IF(TT(JK).LT.T6(I-1,6).AND.TT(JK).GE.T6(I,6))IJL=I
        IF(TT(JK).GT.T6(I-1,6).AND.TT(JK).LE.T6(I,6))IJL=I
    344 CONTINUE
        IF(IJL)343,343,0
        I=IJL
        DH=(I-7)*FA1+FA1*(TT(JK)-T6(I-1,6))/(T6(I,6)-T6(I-1,6))
        DH=DH/C(JIK)
C
C       END OF SECTION
C
C
C       THIRD PART OF OUTPUT
C
        WRITE(6,2025)A(J1(JIK)),DH,TT(JK)
    666 CONTINUE
   2025 FORMAT(' ALTER H OF ',A4,' BY ',F7.3,' KCALS FOR ',F6.0,
       1' DEGC'/)
    343 CONTINUE
        IF(J6-4)230,0,230
        WRITE(6,2019)(H(I),I=1,11)
   2019 FORMAT(/7X,11F6.1/)
        DO 66 I=1,11
        SS=(I-6)*FA2
     66 WRITE(6,2018)SS,(T6(J,I),J=1,11)
   2018 FORMAT('  S',F4.1,11F6.0)
        GO TO 230
   3459 FORMAT(//1X,72('*')//)
    712 WRITE(6,3459)
```

```
C
C       END OF THIRD PART OF OUTPUT
C
C
C       FIRST PART OF OUTPUT
C
        DO 404 I=1,N1
  404 WRITE(6,2001)A(J1(I)),C(I),A(J1(I)),XM(I),D2(J1(I)),
     1T5(J1(I))
 2001 FORMAT   (1X,A4,' = ',F5.1,' X(',A4,') = ',F5.3,5X,
     1'H = ',F6.2,' S = ',F6.2)
        DO 405 I=1,N3
  405 WRITE(6,2002)A1(J2(I)),C1(I)
 2002 FORMAT(1X,A4,' = ',F5.1)
        F25=F25*1000.
        WRITE(6,3010)F25,F26
 3010 FORMAT(/' DELTA S SOLIDS (298 K,1 BAR) = ',F9.2,' CALS'
     1//' DELTA H SOLIDS (298 K,1 BAR) = ',F9.3,' KCALS'/)
C
C       END OF FIRST PART OF OUTPUT
C
C
C       THIS SECTION READS CODE J6,THIS TELLS THE PROGRAM WHERE
C       CONTROL IS TO BE RETURNED
C
C       IF J6=0    CALCULATIONS COMPLETED,EXIT
C
C       IF J6=1    NEW REACTION TO BE CALCULATED, PROGRAM
C                  RETURNS TO FIRST PART OF VARIABLE DATA INPUT
C
C       IF J6=2    NEW ENTHALPY OF FORMATION AND/OR ENTROPY
C                  CORRECTION TO BE INPUT ; RETURNS TO SECOND PART
C                  OF VARIABLE DATA INPUT
C
C       IF J6=3    PROGRAM TO CALCULATE ENTHALPY CORRECTION WITH
C                  NO ENTROPY CORRECTION TO PASS THROUGH THE
C                  LIMITS OF AN EXPERIMENTAL BRACKET
C
C       IF J6=4    PROGRAM TO CALCULATE AS FOR J6=3,BUT ALSO TO
C                  PRINT OUT TABLE OF TEMPERATURES CALCULATED
C                  FOR ENTHALPY OF FORMATION AND ENTROPY INCREMENTS
C                  CONTROLLED BY P2 INPUT IN THIRD PART OF VARIABLE
C                  DATA INPUT
C
C       IF J6=5    PROGRAM TO CALCULATE TEMPERATORES OF REACTION
C                  FOR A RANGE OF PRESSURES CONTROLLED BY P AND P2
C                  INPUT IN THE THIRD PART OF THE VARIABLE DATA
C
  230 READ(5,1003)J6
      J8=J6+1
      GO TO(0,909,3001,3002,3002,3002),J8
C
C          END OF SECTION
C
      WRITE(6,2050)
 2050 FORMAT('1')
```

```
      STOP
      END



      FUNCTION BUFFER(N5,P,T1)
C
C     THIS FUNCTION CALCULATES THE OXYGEN FUGACITY AT ANY
C     TEMPERATURE AND PRESSURE ON 5 OXYGEN BUFFERS.
C
      IF(N5.EQ.1)F=-25680./T1+15.953+0.019*(P-1.)/T1
      IF(N5.EQ.2)F=-25680./T1+13.380+0.081*(P-1.)/T1
      IF(N5.EQ.3)F=-24930./T1+9.360+0.046*(P-1.)/T1
      IF(N5.EQ.4)F=-25738./T1+9.000+0.092*(P-1.)/T1
      IF(N5.EQ.5)F=-32730./T1+13.12+0.083*(P-1.)/T1
      BUFFER=EXP10(F)
      RETURN
      END



      FUNCTION WAG1(F,P,T)
C
C     THIS FUNCTION CALCULATES THE H2 FUGACITY FOR ANY O2
C     FUGACITY IN THE SYSTEM H-O USING WAGMAN ET AL(1945) AND
C     ZEN(1973)
C
      GK=EXP10(12447.90889/T-1.51609*ALOG10(T)+0.00016*T+2.00131)
      WAG1=FH2(P,T)*FH2O(P,T)/(FH2O(P,T)+GK*SQRT(F)*FH2(P,T))
      RETURN
      END



      FUNCTION WAG2(F,P,T)
C
C     THIS FUNCTION CALCULATES THE O2 FUGACITY FOR ANY H2
C     FUGACITY IN H-O USING WAGMAN ET AL(1945) AND ZEN(1973)
C
      GK=EXP10(12447.90889/T-1.51609*ALOG10(T)+0.00016*T+2.00131)
      A=FH2(P,T)*FH2O(P,T)-F*FH2O(P,T)
      WAG2=(A/(GK*FH2(P,T)*F))**2
      WAG2=ALOG10(WAG2)
      RETURN
      END



      FUNCTION FH2(PP,TT)
```

```
C
C       THIS FUNCTION CALCULATES THE FUGACITY OF H2 AT ANY P-T
C       USING THE DATA GIVEN BY SHAW(1963) AND PRESNALL(1968).
C       DATA PROBABLY RELIABLE TO WELL ABOVE 3KB.
C
        COMMON /GAS/CO21(3,3),H201(11,10),O21(3,3)
        P=PP
        T=TT
        A=-1.49E-5*T+0.0041
        B=EXP(-3.3699*T**0.125+0.60493)
        C=-EXP(-0.1263*T**0.5-15.9537)
        FH2=P*EXP(A+B+C)
        RETURN
        END



        FUNCTION FH2O(PP,TT)
C
C       THIS FUNCTION CALCULATES THE FUGACITY OF WATER AT ANY P-T
C       FROM AN EQUATION DERIVED FROM BURNHAM ET AL (1969, EQN 1A)
C       DATA RELIABLE 1-10 KB,50-900 DEG C.
C
        COMMON /GAS/CO21(3,3),H201(11,10),O21(3,3)
        F=0.
        P=PP/1000.
        T=TT/100.
        DO 10 I=1,10
   10   F=F+H201(11,I)*ALOG(P)*T**(I-2)
        DO 11 J=1,10
        DO 11 I=1,11-J
   11   F=F+H201(I,J)*(T**(I-2))*(P**(J-1))
        FH2O=EXP(F)
        RETURN
        END



        FUNCTION FO2(PP,TT)
C
C       THIS FUNCTION CALCULATES THE FUGACITY OF OXYGEN AT ANY P-T
C       USING THE REDUCED VARIABLE EQNS OF RHZENKO AND VOLKOV (1971)
C
        COMMON /GAS/CO21(3,3),H201(11,10),O21(3,3)
        T=TT/154.75
        P=PP/50.8
        F=0.
        DO 10 I=1,3
        DO 10 J=1,3
   10   F=F+O21(I,J)*(T**(I-1))*(P**(J-1))
        FO2=F*PP
        RETURN
        END
```

```
      FUNCTION CALC(X,FG)
C
C     THIS FUNCTION CALCULATES THE TEMPERATURE OF A REACTION
C     GIVEN  VALUES OF LOG K AT A RANGE OF TEMPERATURES AND THE
C     THE COMBINED HEAT CAPACITY EQUATION COEFFICIENTS FOR THE .
C     REACTION LINEAR INTERPOLATION GIVES THE TEMPERATURE
C     BETWEEN THE 100 DEGC VALUES.
C
      REAL X(5),TA(10),FG(10)
      XY=0.00198726
      T1=298.15
      CALC=0.
      S=X(1)*ALOG(T1)+2.0*X(2)*T1+X(3)/(2.0*T1*T1)+X(5)
      H =X(1)*T1+X(2)*T1*T1+X(3)/T1+X(4)
      DO 10 I=1,10
      T1=100.*I-300.
      S=X(1)*ALOG(T1)+2.0*X(2)*T1+X(3)/(2.0*T1*T1)+X(5)
      H =X(1)*T1+X(2)*T1*T1+X(3)/T1+X(4)
      TA(I)=H/(S-XY*FG(I))
      IF(I-1)0,10,0
      IF(TA(I)-T1)0,13,13
      IF(TA(I-1)-T1+100.)0,0,12
   13 IF(TA(I)-T1)10,10,0
      IF(TA(I-1)-T1+100.)12,0,0
   10 CONTINUE
      RETURN
   12 XT=(-T1*TA(I-1)+TA(I)*(T1-100.))/(-100.-TA(I-1)+TA(I))
      CALC=XT-273.15
   16 RETURN
      END



      FUNCTION H2OCO2(P,T)
C
C     THIS FUNCTION CALCULATES THE INTERCHANGE ENERGY W FOR
C     H2O-CO2 MIXTURES USING BARRON(1973)
C
      PP=P
      IF(P.GT.2000.)PP=2000.
      W=3116.7+0.93117*PP-3.5528*T
      H2OCO2=W/1000.
      RETURN
      END



      FUNCTION CCDOL(P,T1)
C
C     THIS FUNCTION CALCULATES THE ACTIVITY OF CALCITE DOLOMITE
C     MIXTURES USING ACTIVITY COEFFICIENTS CALCULATED BY THE AQC
```

```
C       METHOD AND GIVEN IN THE TEXT.
C
        P1=(P-1.)*(0.169E-8*T1-0.33E-6)
        IF(T1.LT.875.)W=2985.-0.1282*P-T1*(-0.664-0.000106*P)
        IF(T1.GT.874.)W=4804.-0.0725*P-T1*(1.449-0.0000429*P)
        IF(T1.LT.875.)X1=EXP(0.8469-3090.86/T1)*P1
        IF(T1.GT.874.)X1=EXP(1.9679-4020.04/T1)*P1
        FH=-300.
        W=W-0.714*FH+T1*0.614E-3*FH
        Q1=(28.018/36.934)**0.3333333
        Q2=1./Q1
        PH1=X1*Q1/(X1*Q1+(1.-X1)*Q2)
        PH2=1.-PH1
        B=SQRT(1.-4.*PH1*PH2*(EXP(2.*W/(6.*1.98717*T1))-1.))
        B=2./(B+1.)
        F=6.*Q2*ALOG((1.-B*PH1)/(1.-X1))/2.
        CCDOL=F+ALOG(1.-X1)
        RETURN
        END



        FUNCTION FCO2(PP,TT)
C
C       THIS FUNCTION CALCULATES THE FUGACITY OF CO2 USING A
C       REDUCED VARIABLE EQUATION CALCULATED FROM THE DATA GIVEN
C       IN RHZENKO AND VOLKOV(1971)
C
        COMMON /GAS/CO21(3,3),H2O1(11,10),O21(3,3)
        T=TT/304.15
        P=PP/73.8
        F=0.0
        DO 10 I=1,3
        DO 10 J=1,3
   10   F=F+CO21(I,J)*(T**(I-1))*(P**(J-1))
        FCO2=F*PP
        RETURN
        END
C
C       END OF THERMOCALC
C
        FINISH
```

EXAMPLE OF PERMANENT DATA INPUT FOR THERMOCALC

```
43
3 1 2 3 1 2 3 4 3 2 2 2 3 3 3 3 4 5 2 2 2
1 2 1 1 2 2 2 2 3 2 4 3
4 4 3 3 3 4 5 4 4 4
DI   0.05313 0.000004751 1901.5 -22.540 -0.31622
66.09 34.20 -766.59
1 1 2 1 3 2
ROBIE AND WALDBAUM  1968 BULL USGS 1259 +0.8 KCALS, SLAUGHTER 1972
RUT 0.01649 0.000000723 252.8 -5.817 -0.09581
18.820 12.04 -225.76
 10 1
ROBIE AND WALDBAUM  1968 BULL USGS 1259
FO   0.03662 0.000003078 1016.7 -14.583 -0.21620
43.79 22.75 -520.18
 2 2 3 1
ROBIE AND WALDBAUM  1968 BULL USGS 1259  ,H +0.2  JOHANNES 1970
SPH 0.04027 0.000004024 811.9 -15.056 -0.23641
55.65 30.88 -618.16
 1 1 3 1 10 1
ROBIE AND WALDBAUM  1968 BULL USGS 1259  +1.18 SCHUILING ETAL 1967
QTZ 0.01824 0.000000123 877.6 -8.348 -0.10893
22.688 9.88 -217.650
 3 1
ROBIE AND WALDBAUM  1968 BULL USGS 1259
WOLL 0.02674 0.000001776 677.9 -10.384 -0.15720
39.93 19.60 -380.740
1 1 3 1
ROBIE AND WALDBAUM  1968 BULL USGS 1259  +0.9  GREENWOOD 1967A
TALC0.08454 0.000020912 1822.0 -33.145 -0.50438
136.25 62.34 -1412.005
2 3 3 4 5 2
ROBIE AND WALDBAUM  1968 BULL USGS 1259 ,H +3.9  GORDON ET AL 1970
TREM0.18769 0.000029957 4612.8 -74.016 -1.11319
272.92 131.19 -2946.575
1 2 2 5 3 8 5 2
ROBIE AND WALDBAUM  1968 BULL USGS 1259 ,+6.36 BOYD 1959
DOL 0.04514 0.000009020 1365.4 -18.793 -0.27026
64.34 37.09 -557.063
1 1 2 1 4 2
ROBIE AND WALDBAUM  1968 BULL USGS 1259 ,H +0.55  HARKER ET AL 1955
CC   0.02421 0.000003013 558.2 -9.348 -0.14290
36.934 22.15 -238.592
1 1 4 1
ROBIE AND WALDBAUM  1968 BULL USGS 1259
EN   0.02321 0.000003221 537.4 -9.001 -0.13718
31.47 16.22 -370.03
2 1 3 1
ROBIE AND WALDBAUM  1968 BULL USGS 1259  ,H +0.1  JOHANNES 1970
MGNS0.02254 0.000004497 731.3 -9.550 -0.13524
28.018 15.70 -265.88
2 1 4 1
ROBIE AND WALDBAUM  1968 BULL USGS 1259 ,H +0.2  HARKER ET AL 1955
AB   0.06518 0.000005557 1965.2 -26.476 -0.38572
```

```
100.07 50.20 -940.396
12 1 7 1 3 3
ROBIE AND WALDBAUM  1968 BULL USGS 1259 ,H -3.25 ZEN PERS COMM
NE  0.04061 0.000001005 1425.0 -16.926 -0.24001
54.16 29.72 -500.279
12 1 7 1 3 1
ROBIE AND WALDBAUM  1968 BULL USGS 1259 ,H -3.25 ZEN PERS COMM
JD  0.05080 0.000004466 1490.1 -20.514 -0.30049
60.40 31.90 -723.121
12 1 7 1 3 2
ROBIE AND WALDBAUM  1968 BULL USGS 1259 ,H -3.25 ZEN PERS COMM
AN  0.06711 0.000005439 1972.5 -27.075 -0.39669
100.79 48.45 -1009.300
1 1 7 2 3 2
ROBIE AND WALDBAUM  1968 BULL USGS 1259
MUSC0.09936 0.000012266 2735.4 -39.855 -0.58881
140.71 69.0 -1432.73
11 1 7 3 3 3 5 2
ROBIE AND WALDBAUM  1968 BULL USGS 1259 ,H -11.55 DAY 1970
PHL 0.10533 0.000006644 2714.5 -41.052 -0.61934
149.91 76.40 -1495.65
11 1 2 3 7 1 3 3 5 2
POLY OF F-PHL, S,V OF PHL ;ROBIE ET AL 1968, H FROM BIRD ET AL 1973
KY  0.04247 0.000002957 1463.6 -17.806 -0.25199
    44.09 20.02 -619.930
7 2 3 1
ROBIE AND WALDBAUM  1968 BULL USGS 1259
AND 0.04144 0.000003184 1312.6 -17.023 -0.24542
51.53 22.28 -619.04
7 2 3 1
ROBIE AND WALDBAUM  1968 BULL USGS 1259 H +.35 HOLM AND ANDERSON 1969
SILL0.03963 0.000003827 1133.9 -15.942 -0.23444
    49.90 22.97 -618.300
7 2 3 1
ROBIE AND WALDBAUM  1968 BULL USGS 1259H +.35 HOLM AND ANDERSON
COR 0.02735 0.000001725 911.1 -11.349 -0.16200
25.575 12.18 -400.400
7 2
ROBIE AND WALDBAUM  1968 BULL USGS 1259
MAGT0.07614 -0.000009256 4250.5 -35.874 -0.45220
44.524 36.03 -267.400
8 1 9 1
ROBIE AND WALDBAUM  1968 BULL USGS 1259
HEM 0.03317 0.000003509 1149.8 -14.002 -0.19758
30.274 20.89 -197.300
9 1
ROBIE AND WALDBAUM  1968 BULL USGS 1259
PER 0.01128 0.000000621 254.2 -4.268 -0.06609
11.248 6.44 -143.800
2 1
ROBIE AND WALDBAUM  1968 BULL USGS 1259
BRUC0.02401 -0.000001919 461.0 -8.541 -0.13825
24.631 15.09 -221.200
2 1 5 2
ROBIE AND WALDBAUM  1968 BULL USGS 1259
ILM 0.02650 0.000002945 366.6 -9.389 -0.15481
```

```
31.69 25.30 -295.56
8 1 10 1
ROBIE AND WALDBAUM  1968 BULL USGS 1259
HERC0.07032 0.000007472 4011.8 -35.221 -0.41662
40.75 25.4 -475.20
8 1 7 2
ROBIE AND WALDBAUM,ZEN 1973,KUBACHEWSKI ETAL 1967
SPIN0.03678 0.000003226 986.9 -14.549 -0.21702
39.71 19.26 -552.800
2 1 7 2
ROBIE AND WALDBAUM  1968 BULL USGS 1259
GROS0.10363 0.000008789 2680. -40.591 -0.61078
125.3 57.7 -1587.193
1 3 7 2 3 3
ROBIE AND WALDBAUM  1968 BULL USGS 1259 ,H -7.5 ZEN PERS COMM
FA  0.03944 0.000003097 930.4 -15.148 -0.23182
46.39 35.45 -353.544
8 2 3 1
ROBIE AND WALDBAUM  1968 BULL USGS 1259
CORD0.21442 0.000007459 8360.22 -92.304 -1.27314
233.32 96.64 -2223.9
2 2 7 4 3 5 5 1
POLY,S,V ROBIE ET AL, ,  H FROM SIEFERT 1970
SAN 0.06215 0.000007962 1725.9 -24.975 -0.36857
109.05 56.94 -947.628
11 1 7 1 3 3
ROBIE AND WALDBAUM  1968 BULL USGS 1259 , H -3.25 ZEN PERS COMM
ZOIS0.11330 0.000003604 4047.30 -47.526 -0.67047
136.48 67.9 -1651.65
1 2 7 3 3 3 5 1
POLY FROM SUM OXIDES WITH V RATIOS, H,S ZEN 1972
CLIN0.15518 0.000010531 4392.89 -61.765 -0.91512
207.54 109.0 -2135.48
2 5 7 2 3 3 5 8
      POLY NFROM OXIDE SUM W V RATIOS,S ZEN 1972, H FAWCETT ET AL 1966
ANTH0.19939 0.000027024 5982.8 -81.734 -1.18581
264.47 133.62 -2888.0
2 7 3 8 5 2
POLY FROM SUM OXIDES WITH V RATIOS, H,S ZEN 1971
PYRP0.10458 0.000002797 3991.3 -44.666 -0.61997
113.29 50.4 -1300.
2 3 7 2 3 3
POLY FROM SUM OXIDES
ALM 0.10462 0.000005010 3307.78 -42.606 -0.61767
115.28 68.00 -1297.5
8 3 7 2 3 3
POLY FROM SUM OXIDES
FECH0.16334 0.000014795 3474.43 -61.512 -0.959
213.65 141.6 -1732.
8 5 7 2 3 3 5 8
POLY FROM SUM OXIDES
ANN 0.1207 0.000007826 3390.27 -47.911 -0.71141
154.32 97.6 -1235.
11 1 8 3 7 1 3 3 5 2
POLY FROM SUM OXIDES
FECT 0.05622 0.000004436 1562.12 -22.339 -0.29263
```

```
69.34 39.10 -748.2
8 1 7 2 3 1 5 2
POLY FROM SUM OXIDES
FEST 0.20481 0.00011196 6920.55 -85.051 -1.09414
446.760 118.4 -5717
8 4 7 18 3 7.5 5 4
POLY FROM SUM OXIDES
FECD 0.20497 0.000008227 7534.51 -86.792 -1.08920
237 125.90 -2500
8 2 7 4 3 5 5 1
POLY FROM SUM OXIDES
1.0178418 -0.14328481 0.0036866569
0.0 0.081624169 -0.001058472
0.0 -0.010527011 0.000040426609
1.0 0.0124 0.0011089
0.0 0.000254 0.0001998
0.0 -0.00005104 0.00000393
-0.5100382393E2
0.5575630079E1
0.7681815229E1
-0.2956561399E1
0.6257548091E0
-0.8377700043E-1
0.7287213112E-2
-0.3975687334E-3
0.1223219695E-4
-0.1604800416E-6
0.3102427336E1
-0.1231427319E1
0.9917182288
-0.4583391675
0.1170875147
-0.1613901535E-1
0.1127627168E-2
-0.3601358689E-4
0.3793302837E-6
-0.1818422587
-0.1188939797
0.1158512411
-0.2972064049E-1
0.2909975366E-2
0.7076012289E-4
-0.2019187659E-4
0.6268649109E-6
0.7832200954E-1
-0.2469583136E-1
-0.2909860764E-2
0.1418285135E-2
-0.3820530319E-3
0.2567472907E-4
-0.4394259244E-6
-0.1202594904E-1
0.5583296322E-2
-0.8629288266E-4
0.1645348423E-3
-0.4331214760E-5
```

```
-0.1847494740E-6
0.8677051724E-3
-0.7458908169E-3
-0.9423583716E-4
-0.4298727688E-5
0.2624488129E-6
0.3049907729E-4
0.9222877659E-4
0.6205016899E-5
-0.7311272891E-7
-0.1436634502E-4
-0.5637228636E-5
-0.9061809635E-7
0.1158350870E-5
0.1229098425E-6
-0.3021832229E-7
-0.1851749243E2
0.2746168381E2
-0.1737356692E2
0.6077205652E1
-0.1282820938E1
0.1682236100
-0.1367589536E-1
0.6738661869E-3
-0.1874184571E-4
0.2315237601E-6
H2O  0.00670 0.000001555 -37.7 -2.011 -0.03891 -57.796 45.10 221.5 374.2
CO2  0.00985 0.000001692 205.0 -3.770 -0.05831 -94.051 51.06 73.8 31.0
H2   0.00661 0.000000291 -19.3 -1.932 -0.03770 0.0 31.208 13.0 -239.9
O2   0.00685 0.000000775 39.8 -2.244 -0.03974 0.0 48.996  50.8 -118.4
```

EXAMPLE OF VARIABLE DATA INPUT FOR THERMOCALC

DATA FOR THE REACTION RUT+CC+Q=SPH+CO2
WHICH RUNS THE REACTION AT 500 BAR INTERVALS
FROM 500 TO 6000 BARS FOR 8 DIFFERENT XCO2

```
4 1
2 10 5 4 2
-1 -1 -1 1 1
1 1 1 1
1 0 0 4
5
500 6000 0.005 0
5
500 6000 0.01 0
5
500 6000 0.05 0
5
500 6000 0.1 0
5
500 6000 0.2 0
5
500 6000 0.4 0
5
500 6000 0.7 0
5
500 6000 0.95 0
0
```

```
      MASTER PROCESS
C
CCC
CCC                  **********************
CCC                  ******PROCESS*******
CCC                  **********************
CCC
CCC
CCC   THIS PROGRAM CALCULATES APPARENT WT% FROM RAW PROBE DATA
CCC   (COUNTS PER N SECS),GIVING THE STANDARD ERROR ON THE
CCC   MEAN FOR THE COUNTS. THE PROGRAM USES LINEAR INTERPOLATION
CCC   TO CALCULATE THE STANDARDS CPS FOR EACH ANALYSIS.
C
      REAL A1(8),A2(9)
      REAL D3(12,9),XX(9),X(9,25),B(9),D(9),Y1(20,9),Y2(20,9)

      DIMENSION II(15)
      REAL              D1(12,9),D2(12,9),C1(12,9),C2(12,9)
      REAL S1(12,2),S2(12,2)
C
CCC   DATA INPUT
CCC
CCC   I3=NO OF ELEMENTS
CCC
CCC   XX=WT% OF ELEMENTS IN THE STANDARDS
CCC
C     A2=NAMES OF THE ELEMENTS
C
C     CT=COUNTING TIME
C
C     DT=DEAD TIME
C
C     THEN SETS OF I3+2 CARDS ; A CODE CARD,A TITLE CARD, AND
C     I3 COUNTS CARDS, ONE CARD FOR EACH ELEMENT.SETS FOR
C     BACKGROUNDS MUST PRECEDE PEAKS.
C
C     I1,I2=CODES
C          1 1 =STANDARDS
C          2 1 =STANDARDS BACKGROUNDS
C          3 1,3 2,3 3,ETC =MINERAL BACKGROUNDS,SECOND CODE
C               FOR EACH MINERAL GROUP
C          4 1,4 2,4 3,ETC =MINERAL COUNTS,SECOND CODE SAME AS
C               FOR BACKGROUNDS
C
C     A1=TITLE CARD
C
C     N=NO OF COUNTS
C
C     X=N COUNTS FOR THE ELEMENT
C
      READ(5,1002)I3
      READ(5,1002)(XX(I),I=1,I3)
 1002 FORMAT(I0)
      READ(5,1003)(A2(I),I=1,I3)
      READ(5,1002)CT,DT
      I6=0
```

```
  102 CONTINUE
      I4=0
  105 CONTINUE
      READ(5,1000)I1,I2
 1000 FORMAT(3I0)
      IF(I1.EQ.5) GO TO 106
      READ(5,1003)(A1(I),I=1,8)
 1003 FORMAT(8A8)
      DO 10 I=1,I3
      READ(5,1001)N,(X(I,J),J=1,N)
 1001 FORMAT(I2,25F0.0)
C
C     END OF INPUT
C
      A=0.0
      DO 11 J=1,N
      X(I,J)=X(I,J)/20.0
      A=A+X(I,J)
   11 CONTINUE
      B(I)=A/N
      C=0.0
      DO 12 J=1,N
      C=C+(X(I,J)-B(I))*(X(I,J)-B(I))
   12 CONTINUE
      D(I)=SQRT(C/(N*(N-1)))
      B(I)=B(I)/(1.0-B(I)*0.000002)
   10 CONTINUE
      IF(I1.EQ.2.OR.I1.EQ.3) GO TO 100
      GO TO 101
  100 CONTINUE
      DO 13 I=1,I3
      Y1(I2,I)=B(I)
      Y2(I2,I)=D(I)
   13 CONTINUE
      GO TO 102
  101 CONTINUE
      IF(I1.EQ.1) GO TO 103
      GO TO 104
  103 CONTINUE
      I6=I6+1
      I7=0
      IF(I6.EQ.3)I7=1
      IF(I6.EQ.3)I6=2
      DO 14 I=1,I3
      IF(I6.EQ.1) GO TO 107
      IF(I7.EQ.1)S2(I,1)=S2(I,2)
      IF(I7.EQ.1)S1(I,1)=S1(I,2)
  107 CONTINUE
      S2(I,I6)=SQRT(D(I)*D(I)+Y2(1,I)*Y2(1,I))
      S1(I,I6)=B(I)-Y1(1,I)
      IF(I4.EQ.0)GO TO 14
      IF(I6.EQ.1.AND.I.EQ.I3)GO TO 105
      IF(I6.EQ.1)GO TO 14
      X2C=S2(I,1)
      X2M=SQRT(S2(I,1)*S2(I,1)+S2(I,2)*S2(I,2))/(I6+1)
      X1C=S1(I,1)
```

```
      X1M=(S1(I,2)-S1(I,1))/(I4+1)
      DO 15 J=1,I4
      Z1=X1M*J+X1C
      Z2=SQRT(J*J*X2M*X2M+X2C*X2C)
      D1(J,I)=C1(J,I)*XX(I)/Z1
      D2(J,I)=(SQRT(C2(J,I)*C2(J,I)+((C1(J,I)*C1(J,I)*Z2*Z2)/(Z1*Z1)))*
     1XX(I))/Z1
      D3(J,I)=C2(J,I)*XX(I)/Z1
      D3(J,I)=D3(J,I)*2.0
      D2(J,I)=D2(J,I)*2.0
   15 CONTINUE
   14 CONTINUE
      IF(I4.EQ.0) GO TO 102
      IF(I6.EQ.1)GO TO 14
      DO 16 J=1,I4
      WRITE(6,2000)J,(A2(I),I=1,I3)
 2000 FORMAT(3X,'NO',I4,11X,10A8)
C
C     OUTPUT
C
C     1ST STANDARD ERROR INCLUDES LINEAR INTERPOLATION,
C     2ND OMITS IT
C
C     WT X OUTPUT IS THE APPARENT WTX OF THE ELEMENT
C
403   CONTINUE
      WRITE(6,2001)(D1(J,I),I=1,I3)
      WRITE(6,2002)(D2(J,I),I=1,I3)
      WRITE(6,2002)(D3(J,I),I=1,I3)
2002  FORMAT(1X,'TWICE STD ERR,MEAN',1X,10F8.3)
2001  FORMAT(15X,'WTX',1X,10F8.3)
   16 CONTINUE
      WRITE(6,2008)
 2008 FORMAT(1X,'**********************************************************
     1**************************************')
      GO TO 102
  104 CONTINUE
      I4=I4+1
      DO 17 I=1,I3
      F1=B(I)
      F2=D(I)
      C1(I4,I)=F1-Y1(I2,I)
      C2(I4,I)=SQRT(D(I)*D(I)+Y2(I2,I)*Y2(I2,I))
   17 CONTINUE
      WRITE(6,2004)I4,(A1(I),I=1,8)
 2004 FORMAT(1X,'NO ',I2,5X,8A8)
      GO TO 105
  106 CONTINUE
      WRITE(6,2003)
 2003 FORMAT('1',10X,'END OF OUTPUT')
      STOP
      END
C
C     END OF PROCESS
C
      FINISH
```

```
      MASTER ACTIVITY
C
CCC
CCC                  **************************
CCC                  ******ACTIVITY*********
CCC                  **************************
CCC
CCC
CCC     THIS PROGRAM COMPARES THE VARIOUS MIXING MODELS, R,QC,
CCC     AQC AND SR FOR BINARY SYSTEMS FOR WHICH ACTIVITIES HAVE
CCC     BEEN EXPERIMENTALLY DETERMINED, BY PLOTTING THE MIXING
CCC     PARAMETERS CALCULATED FOR EACH PAIR OF ACTIVITIES AND
CCC     CONCENTRATIONS AGAINST CONCENTRATION. THE MIXING
CCC     PARAMETER MUST BE INDEPENDENT OF COMPOSITION.
C
      REAL X1(50),Y(50),M,X2(50),AA(50),X11(50),W11(50),W21(50),
     1W31(50)
      R=1.98726
      IA=0
C
CCC   INPUT DATA
CCC
CCC   T=TEMPERATURE OF EXPERIMENTS IN DEGK
CCC
CCC   V1,V2=MOLAR VOLUME OF THE TWO COMPONENTS OF THE BINARY.
CCC
CCC   Z=COORDINATION NUMBER OF THE MIXED CATIONS IN THE PHASES.
C
CCC   X,A=CONCENTRATION AND ACTIVITY AT TEMPERATURE T
C
      READ(5,1000)Z,T,V1,V2
   10 READ(5,1000,END=11)X,A
 1000 FORMAT(10F0.0)
C
CCC   END OF INPUT
C
      IA=IA+1
      FC=A/X
C
CCC   W11=R MODEL MIXING PARAMETER
C
      W11(IA)=R*T*ALOG(FC)/((1.-X)**2.)
      X11(IA)=X
C
CCC   W21=QC MODEL MIXING PARAMETER
C
      B=X*(FC**(2./Z)-1.)/(1.-X)
      C=(1.+B)/(1.-B)
      D=(C**2-1.)/(4.*X*(1.-X))+1.
      W21(IA)=Z*R*T*ALOG(D)/2.
C
CCC   W31=AQC MODEL MIXING PARAMETER
C
      Q1=V1**0.33333/V2**0.33333
      Q2=V2**0.33333/V1**0.33333
      PH1=Q1*X/(Q1*X+Q2*(1.-X))
```

```
      B1=-(X*FC**(2./(Z*Q1))-1.)/(1.-PH1)
      C1=(((2.-B1)/B1)**2-1.)/(4.*PH1*(1.-PH1))+1.
      X2(IA)=X
      W31(IA)=Z-R*T*ALOG(C1)/2.
C
C     SR MODEL : X1 AGAINST Y SHOULD BE LINEAR IF MODEL IS
C     CORRECT
C
      Y(IA)=ALOG(FC)/((1.-X)**2)
      X1(IA)=2.-X
      WRITE(6,2000)X,A,W11(IA),W21(IA),W31(IA),X1(IA),Y(IA)
 2000 FORMAT(1X,'X=',F6.3,'    A=',F6.3,'    R W=',F11.3,
     1'    QC W=',F11.3,'    AQC W=',F11.3,'S    SR X=',F11.3,
     2'    SR Y=',F11.3)
      GO TO 10
   11 CONTINUE
C
C     GRAPHICAL OUTPUT
C
      CALL GRAPH(X11,W11,IA,0,'  X    ',' W R  ',1)
      CALL GRAPH(X11,W21,IA,0,'  X    ','W QC  ',1)
      CALL GRAPH(X11,W31,IA,0,'  X    ','W AQC ',1)
      CALL GRAPH(X1,Y,IA,0,'FC/X↑2',' 2X  ',1)
      A=Y(1)
      M=Y(2)+A
      WRITE(6,2001)A,M
 2001 FORMAT(///10X,'SR MODEL :-    W G1=',F11.3,'    W G2=',
     1F11.3/'1')
      STOP
      END
C
C     END OF ACT
C
      FINISH
```

```
      MASTER QC
C
CCC
C                  ********************
C                  ********QC********
C                  ********************
C
C
C     THIS PROGRAM CALCULATES THE AQC MIXING PARAMETER W FROM
C     EXPERIMENTALLY DETERMINED SOLVUS DATA, USING THE EQUATIONS
C     DERIVED IN GUGGENHEIM(1953), WHEN R1=R2
C
C
      REAL T(50),AB(8),AA1(50),BB1(50),
     1A(4,50)
C
CCC   INPUT DATA
C
C
C     AB=NAME OF BINARY SYSTEM AND SOURCE OF SOLVUS DATA
C
C     T=TEMPERATURE IN DEGC
C
C     V1,V2=MOLAR VOLUME OF COMPONENT 1 AND 2
C
C     A1,B1=MOLE FRACTION OF COMPONENT 2 IN PHASES A AND B,IN
C              THE SAME ORDER AS IN AB
C
      READ(5,1001)(AB(I),I=1,8)
 1001 FORMAT(8A8)
      READ(5,1000)V1,V2
      IK=0
   21 CONTINUE
      IK=IK+1
      READ(5,1000,END=22)T(IK),A1,B1
 1000 FORMAT(10F0.0)
      T(IK)=1./(T(IK)+273.15)
C
CC    END OF INPUT DATA
C
C
C     PROGRAM WORKS ON TWO SEPARATE ITERATIVE CYCLES, EACH ONE
C     CALCULATING A VALUE FOR W,THE MIXING PARAMETER, FROM THE
C     TWO EQUILIBRIUM EQUATIONS FOR COEXISTING PHASES ACROSS A
C     BINARY SOLVUS
C
      A(4,IK)=1.-B1
      A(3,IK)=B1
      A(2,IK)=1.-A1
      A(1,IK)=A1
      Z=6
      Q1=(V1/V2)**0.333333
      Q2=1./Q1
      PH1A=1./(1.+A2*Q2/(A1*Q1))
      PH2A=1./(1.+A1*Q1/(A2*Q2))
      PH1B=1./(1.+B2*Q2/(B1*Q1))
```

```
      PH2B=1./(1.+B1*Q1/(B2*Q2))
      IA=0
      Y1,Y2=0.
      WG=0.
      X=0.2
C
C     BEGINNING OF FIRST CYCLE
C
   10 WG=WG+X
      IA=IA+1
      IF(IA-1000)0,0,24
      BB=SQRT(1.-4.*PH1B*PH2B*(1.-EXP(WG*2./Z)))
      BA=SQRT(1.-4.*PH1A*PH2A*(1.-EXP(WG*2./Z)))
      T1=ALOG(A1)+Z*Q1*ALOG((PH1A/A1)*(1.+PH2A*(BA-1.)/(PH1A*(BA
     1+1.))))/2.
      T2=ALOG(B1)+Z*Q1*ALOG((PH1B/B1)*(1.+PH2B*(BB-1.)/(PH1B*(BB
     1+1.))))/2.
      Y=T1-T2
      IF(IA-1)0,12,0
      IF(Y1.GE.0..AND.Y.LE.0..OR.Y1.LE.0..AND.Y.GE.0.)GO TO 11
      GO TO 12
   11 CONTINUE
      WG=WG-1.5*X
      X=X/2.
      IF(X.LT.0.0000001)STOP
   12 CONTINUE
      Y1=Y
      IF(ABS(T1-T2).LT.0.00001)GO TO 13
      GO TO 10
C
C     CONVERGED AND DROPPED OUT OF THE FIRST CYCLE
C
C
C
C     ENTER SECOND CYCLE
C
   13 AA1(IK)=WG
      WG=0.
      X=0.2
      IA=0
   14 WG=WG+X
      IA=IA+1
      IF(IA-1000)0,0,24
      BA=SQRT(1.-4.*PH1A*PH2A*(1.-EXP(WG*2./Z)))
      BB=SQRT(1.-4.*PH1B*PH2B*(1.-EXP(WG*2./Z)))
      T4=ALOG(B2)+Z*Q2*ALOG((PH2B/B2)*(1.+PH1B*(BB-1.)/(PH2B*(BB
     1+1.))))/2.
      T3=ALOG(A2)+Z*Q2*ALOG((PH2A/A2)*(1.+PH1A*(BA-1.)/(PH2A*(BA
     1+1.))))/2.
      Y=T3-T4
      IF(IA-1)0,15,0
      IF(Y2.GE.0..AND.Y.LE.0..OR.Y2.LE.0..AND.Y.GE.0.)GO TO 16
      GO TO 15
   16 CONTINUE
      WG=WG-1.5*X
      X=X/2.
   15 CONTINUE
```

```
      Y2=Y
      IF(ABS(T3-T4).LT.0.00001)GO TO 20
      GO TO 14
C
C     CONVERGED AND DROPPED OUT OF THE SECOND CYCLE
C
   20 CONTINUE
      AA1(IK)=(AA1(IK)+WG)/2.
      GO TO 21
C
C     RETURNS FOR MORE DATA
C
   22 CONTINUE
      IK1=IK-1
      G2=AA1(2)
      G1=AA1(1)
      CALL GRAPH(T,AA1,IK1,0,'WG/RT ','1/T    ',1)
      WS=AA1(1)*1.98726
      WH=AA1(2)*1.98726
C
C      OUTPUT
C
      WRITE(6,2010)(AB(I),I=1,8)
 2010 FORMAT('1',1X///' QC APPROXIMATION FOR  ',8A8)
      DO 62 I=1,IK1
   62 T(I)=1./T(I)-273.15
      WRITE(6,2011)
 2011 FORMAT(//10X,'T',5X,'A1',5X,'A2',5X,'B1',5X,'B2',5X,
     1'WG/RT')

      AA1(2)=G2
      AA1(1)=G1
      DO 23 I=1,IK-1
   23 WRITE(6,2012)T(I),(A(J,I),J=1,4),AA1(I)
 2012 FORMAT(4X,F8.1,5(F6.3,1X))
      WS=-WS
      WRITE(6,2020)WH,WS
 2020 FORMAT(//'  WH = ',F8.3,'     WS = ',F7.3///)
   24 CONTINUE
   25 WRITE(6,3333)
 3333 FORMAT('1')
      STOP
      END
C
C     END OF QC
C
      FINISH
```

```
      MASTER SR
C
C
C                ******************
C                *******SR********
C                ******************
C
C
C     THIS PROGRAM CALCULATES THE SR MODEL MIXING PARAMETERS
C     WS1,WS2,WH AND WH2 FROM EXPERIMENTAL SOLVUS DATA
C
      DATA A1,A2,A3/' BG    ',' 1/T  ',' CG    '/
C
C     DATA INPUT
C
C     BB=NAME OF BINARY SYSTEM
C
C     T=TEMPERATURE IN DEGC
C
C     XA,XB=MOLE FRACTION OF COMPONENT 2 IN THE COEXISTING
C           PHASES. COMPONENT 1 IS RICHEST IN PHASE GIVEN
C           FIRST IN BB
C
      READ(5,1001)(BB(I),I=1,8)
 1001 FORMAT(8A8)
      WRITE(6,2002)(BB(I),I=1,8)
 2002 FORMAT('1'///10X,8A8///)
      J=0
   10 CONTINUE
      J=J+1
      READ(5,1000,END=11)T,XA,XB
 1000 FORMAT(3F0.0)
C
C     END OF DATA INPUT
C
C
C     CALCULATION METHOD  FOLLOWS THOMPSON AND WALDBAUM
C     S,R,BG,CG HAVE THE SAME MEANING AS IN THEIR PAPERS.
C
      T=T+273.15
      S=XB-XA
      R=XB+XA-1
      P1=ATANH(2.0*S/(1.0+S*S-R*R))
      P2=-ATANH(2.0*S*R/(1.0-S*S-R*R))
      CG=(R*P1+P2)/S**3
      BG=3.0*R*CG+P1/S
      TT=1000.0/T
      WRITE(6,2000)BG,CG,T,TT,XA,XB
 2000 FORMAT(' BG = ',F6.2,'  CG = ',F6.2,'  T = ',F6.1,
     1'  INV T = ',F6.4,'   X OF 2 IN A=',F6.3,'   X OF 2 IN B=',
     2F6.3)
      XBG(J)=BG
      XCG(J)=CG
      T1(J)=T
      T2(J)=TT
      GO TO 10
```

```
   11 J=J-1
C
C      GRAPHICAL OUTPUT TO SEE LINEARITY OF BG AND CG. IF THEY
C      ARE LINEAR THEN WH1,WH2,WS1 AND WS2 ARE INDEPENDENT OF
C      TEMPERATURE
C
       CALL GRAPH(T2,XCG,J,' CG    ','1/T    ')
       CALL GRAPH(T2,XBG,J,' BG    ','1/T    ')
       R=1.98726
       WS2=-R*(XBG(1)+XCG(1))
       WS1=-R*(XBG(1)-XCG(1))
       WH2=R*(XBG(2)+XCG(2))*1000.
       WH1=R*(XBG(2)-XCG(2))*1000.
       A=WH1/R
       B=-WS1/R
       C=2*(WH2-WH1)/R
       D=-2.*(WS2-WS1)/R
C
C      OUTPUT OF WS1,WS2,WH1 AND WH2 AND THE EQUATIONS FOR
C      THE FUGACITY COEFFICIENTS OF THE 2 COMPONENTS
C
       WRITE(6,2002)(BB(I),I=1,8)
       WRITE(6,2001)WS1,WS2,WH1,WH2
 2001  FORMAT(//1X,'WS1',F10.4,' CAL/S2',F10.4,
     1' CAL/DEG',5X,'WH1',F10.1,' CAL',5X,'WH2',F10.1,' CAL')
       WRITE(6,2004)A,B,C,D
       D=-D
       C=-C
       B=-WS2/R
       A=WH2/R
       WRITE(6,2005)A,B,C,D
 2005  FORMAT(//' LN(FC)2 = (1-X2)**2(',F8.2,' /T + ',F8.4,
     1' + X2(',F8.2,'/T + ',F8.4,' ))')
 2004  FORMAT(//' LN(FC)1 = (1-X1)**2(',F8.2,' /T + ',F8.4,
     1' + X1(',F8.2,'/T + ',F8.4,' ))')
       WRITE(6,2003)
 2003  FORMAT('1')
       STOP
       END
C
C      END OF SR
C
       FINISH
```

```
      MASTER REACTION
C
C
C                  **********************
C                  ******REACTION*******
C                  **********************
C
C
C     THIS PROGRAM CALCULATES ALL THE POSSIBLE BALANCED REACTIONS
C     BETWEEN A SET OF PHASES FOR SYSTEMS WITH VARIANCE BETWEEN
C     1 AND -5.  THE PROGRAM COPES WITH DEGENERATE REACTIONS,
C     PRINTING THEM OUT ONCE ONLY WITH AN IDENTIFYING *.
C
      COMMON/FGH2/A(15,15),IX(15),D(5,15)
      COMMON/FGH12/IRL,F(15),V(5),PX(15),IGG,NX3,IJK(20,10)
      INTEGER MI5(10),MI6(10,20)
      DIMENSION C(20,20),JJ(6)
C
C     DATA INPUT AND OUTPUT
C
C     N=NO OF PHASES EXCLUDING EXCESS PHASES.THESE ARE
C       THE PHASES WHICH ARE OMITTED IN TURN TO MAKE EACH
C       BALANCED REACTION (FOR SYSTEMS WITH VARIANCE LESS THAN 1)
C
C     NO=NO OF IMMOBILE COMPONENTS. THESE ARE THE COMPONENTS
C        WHICH CONTROL THE REACTION COEFFICIENTS OF THE ABOVE
C        PHASES.
C
C     L=NO OF EXCESS COMPONENTS. THESE ARE THE COMPONENTS WHICH
C        ARE BALANCED FOR THE REACTION AFTER THE CALCULATION
C        OF THE REACTION COEFFICIENTS FOR THE ABOVE PHASES
C
C     F=NAMES OF THE IMMOBILE COMPONENTS
C
C     V=NAMES OF THE EXCESS COMPONENTS
C
C     PX=NAME OF EACH PHASE
C
C     C=COMPOSITION OF EACH PHASE
C
      READ(5,4003)N,NO,L
 4003 FORMAT(6I0)
      READ(5,1002)(F(I),I=1,NO),(V(I),I=1,L)
 1002 FORMAT(15A4)
      IGG,IRL=0
      NX3=N
      WRITE(6,7777)
 7777 FORMAT(' ~~~~~~~~~~~~~~~~~~~~')
      WRITE(6,2000)NO,L,(F(I),I=1,NO),(V(I),I=1,L)
 2000 FORMAT('1    '//,2X,'  NO OF IMMOBILE COMPONENTS = ',I2,
     110X,'NO OF MOBILE COMPONENTS = ',I2////5X,20(3X,A4))
      DO 1 I=1,J
      READ(5,4001)PX(I),(C(J,I),J=1,NO+L)
 4001 FORMAT(A4,15F0.0)
      DO 8052 J=1,NO+L
      X1=C(J,I)
```

```
      CALL SUBS(X1,7,3,MI5)
      DO 8052 K=1,7
 8052 MI6(K,J)=MI5(K)
      WRITE(6,2001)PX(I),((MI6(K,J),K=1,7),J=1,NO+L)
 2001 FORMAT(/1X,A4,114A1)
 4001 FORMAT(A4,15F0.0)
    1 IX(I)=I
      DO 2 I=1,NO
      DO 2 J=1,N
    2 A(I,J)=C(I,J)
      DO 3 I=1,L
      DO 3 J=1,N
    3 D(I,J)=C(NO+I,J)
C
C     THIS SECTION CALCULATES THE VARIANCE OF THE SYSTEM (IVAR)
C     AND DECIDES ON A DO LOOP WITHIN WHICH TO LEAVE OUT THE
C     NECESSARY NO OF PHASES TO MAKE A BALANCED REACTION
C
      NN=NO
      IVAR=NO+2-N
      IF(IVAR.EQ.1)GO TO 510
      DO 500 J1=1,N+IVAR
      JJ(1)=J1
      IF(IVAR.EQ.0) GO TO 511
      DO 501 J2=J1+1,N+IVAR+1
      JJ(2)=J2
      IF(IVAR.EQ.-1) GO TO 512
      DO 502 J3=J2+1,N+IVAR+2
      JJ(3)=J3
      IF(IVAR.EQ.-2)GO TO 513
      DO 503 J4=J3+1,N+IVAR+3
      JJ(4)=J4
      IF(IVAR.EQ.-3)GO TO 514
      DO 504 J5=J4+1,N+IVAR+4
      JJ(5)=J5
      IF(IVAR.EQ.-4)GO TO 515
      DO 505 J6=J5+1,N+IVAR+5
      JJ(6)=J6
      CALL FORM(N,NO,L,JJ)
  505 CONTINUE
      GO TO 504
  515 CALL FORM(N,NO,L,JJ)
  504 CONTINUE
      GO TO 503
  514 CALL FORM(N,NO,L,JJ)
  503 CONTINUE
      GO TO 502
  513 CALL FORM(N,NO,L,JJ)
  502 CONTINUE
      GO TO 501
  512 CALL FORM(N,NO,L,JJ)
  501 CONTINUE
      GO TO 500
  511 CALL FORM(N,NO,L,JJ)
  500 CONTINUE
      GO TO 7000
```

```
  510 CALL FORM(N,NO,L,JJ)
C
C       END OF SECTION
C
 7000 CONTINUE
      WRITE(6,8059)
 8059 FORMAT('1')
      STOP
      END



      SUBROUTINE FORM(N,NO,L,JJ)
C
C       THIS SUBROUTINE ASSEMBLES THE SET OF SIMULTANEOUS
C       EQUATIONS FOR SUBROUTINE EQN TO SOLVE
C
      COMMON/FGH12/IRL,F(15),V(5),PX(15),IGG,NX3,IJK(20,10)
      COMMON/FGH2/A(15,15),IX(15),D(5,15)
      REAL T(5),A1(15,15),D1(5,15)
      INTEGER P(15),JJ(6)
      IA=-NO-1+N
      ID,IC=0
      IB=1
      DO 100 I=1,N
      IF(IB-IA-1)0,101,101
      IF(I-JJ(IB))0,102,0
      GO TO 101
  102 IB=IB+1
      GO TO 105
  101 IC=IC+1
      P(IC)=IX(I)
      DO 103 J=1,NO
  103 A1(J,IC)=A(J,I)
      DO 104 J=1,L
  104 D1(J,IC)=D(J,I)
      GO TO 100
  105 ID=ID+1
      T(ID)=P(I)
  100 CONTINUE
      IF(IRL)0,10,0
      DO 11 I=1,IRL
      IXY=0
      DO 12 J=1,IJK(I,10)
      DO 12 K=1,IC
   12 IF(P(K).EQ.IJK(I,J))IXY=IXY+1
      IF(IXY-IJK(I,10))0,15,0
   11 CONTINUE
   10 CONTINUE
      CALL EQN(NO,L,A1,D1,P,T,IA)
   15 RETURN
      END
```

```
      SUBROUTINE EQN(NO,L,A,D,P,T,IA)
C
C     THIS SUBROUTINE SOLVES THE SET OF SIMULTANEOUS EQUATIONS
C     TO CALCULATE THE REACTION COEFFICIENTS BY
C     GAUSSIAN ELIMINATION. MOST OF THE SUBROUTINE IS INVOLVED
C     WITH THE DEGENERATE CASE
C
      COMMON/FGH12/IRL,F(15),V(5),PX(15),IGG,NX3,IJK(20,10)
      REAL A(15,15),T(5),D(5,15),R(12),X(12),XYY(20),GRAD(8)
      INTEGER MI5(10),MI6(10,15),II(6),JJ(6),P(15)
      NN=NO
      NB=NO+1
      IF(NO-1)601,601,0
      DO 16 N=1,NO-1
      Z=0.0
      KT=0
      DO 17 K=N,NO
      IF((A(K,N)*A(K,N)).LE.(Z*Z)) GO TO 17
      KT=K
      Z=A(K,N)
   17 CONTINUE
      NC=N+1
      IA=0
      IF(KT)0,60,0
      DO 18 M=N,NB
      TEMP=A(N,M)
      A(N,M)=A(KT,M)
   18 A(KT,M)=TEMP
      DO 100 M=N,NB
  100 A(N,M)=A(N,M)/Z
      DO 96 J=NC,NB
      DO 96 I=NC,NO
   96 A(I,J)=A(I,J)-A(I,N)*A(N,J)
      IF(N-NO+1)16,0,16
      IF(A(NO,NB)**2-1.E-8)121,121,0
      IF(A(NO,NO)**2-1.E-8)97,97,0
   16 CONTINUE
      GO TO 400
   60 IA=0
      DO 50 I=N+1,NB
      IA=IA+1
   50 JJ(IA)=I
      IA=0
      DO 160 I=N,NO
      IA=IA+1
  160 II(IA)=I
      IXX=2
      GO TO 98
   97 CONTINUE
      IXX=2
      N=NO
      IA,IE=0
      IA=1
```

```
      II(1)=NO
      JJ(1)=NB
      DO 125 I=1,NO-1
      IU=0
        DO 126 J=I+1,NO
      IF((A(I,J)*A(I,J)).GT.1.0E-8)IU=IU+1
      IF(J.EQ.NO.AND.IU.EQ.0) GO TO 127
      GO TO 126
  127 IA=IA+1
      JJ(IA),II(IA)=I
      IF(IA-1)0,126,0
      IF(JJ(IA-1)-JJ(IA))0,0,141
      GO TO 126
  141 TEMP=JJ(IA-1)
      SEMP=II(IA-1)
      JJ(IA-1)=JJ(IA)
      II(IA-1)=II(IA)
      JJ(IA)=TEMP
      II(IA)=SEMP
  126 CONTINUE
  125 CONTINUE
      GO TO 98
  121 IA=IA+1
      IXX=2
      N,JJ(1),II(1)=NO
      DO 122 I=1,NO-1
      IR=0
      DO 123 J=I+1,NB
      IF(J-NO)0,123,0
      IF((A(I,J)*A(I,J)).GT.1.0E-8)IR=IR+1
      IF(J.EQ.NB.AND.IR.EQ.0) GO TO 124
      GO TO 123
  124 IA=IA+1
      JJ(IA),II(IA)=I
      IF(IA-1)0,123,0
      IF(JJ(IA-1)-JJ(IA))0,0,130
      GO TO 123
  130 TEMP=JJ(IA-1)
      SEMP=II(IA-1)
      JJ(IA-1)=JJ(IA)
      II(IA-1)=II(IA)
      JJ(IA)=TEMP
      II(IA)=SEMP
  123 CONTINUE
  122 CONTINUE
   98 ND=N-1
      IC=0
      IB=1
      DO 51 I=1,NO
      IF(IB-IA-1)0,52,52
      IF(I-II(IB))0,102,0
      GO TO 52
  102 IB=IB+1
      GO TO 51
   52 IC=IC+1
      DO 53 J=1,NB
```

```
 53 A(IC,J)=A(I,J)
 51 CONTINUE
    ID,IC=0
    IB=1
    DO 54 I=1,NB
    IF(IB-IA-1)0,55,55
    IF(I-JJ(IB))0,103,0
    GO TO 55
103 IB=IB+1
    GO TO 600
 55 IC=IC+1
    P(IC)=P(I)
    DO 56 J=1,NO
 56 A(J,IC)=A(J,I)
    DO 113 J=1,L
113 D(J,IC)=D(J,I)
    GO TO 54
600 ID=ID+1
    T(ID)=P(I)
 54 CONTINUE
    NO =NO-IA
    NB=NB-IA
400 DO 19 N=1,NO
    X(NB-N)=A(NB-N,NB)/A(NB-N,NB-N)
    IF(N-NO)0,36,0
    DO 19 M=1,NO-N
    IF((A(M,NB-N)*A(M,NB-N)).LT.1.0E-8.AND.(X(NB-N)*X(NB-N)).LT.
   11.0E-8) GO TO 19
    A(M,NB)=A(M,NB)-A(M,NB-N)*X(NB-N)
 19 CONTINUE
 36 IV=IA
    IX=ID
    IA,IC,ID=0
    DO 163 I=1,NB
    X(NB)=1.0
    IF(X(I)**2-1.E-8)165,165,0
    IC=IC+1
    X(IC)=X(I)
    P(IC)=P(I)
    DO 168 J=1,L
168 D(J,IC)=D(J,I)
    GO TO 163
165 ID=ID+1
    T(ID)=P(I)
163 CONTINUE
    IA=NO-IC+1
    NO=NO-IA
    NB=NB-IA
    X(NB)=-1.000
 94 GO TO 602
601 X(NB)=-1.0
    IF(A(1,1)**2.LT.1E-4)GO TO 765
    GO TO 766
765 X(1)=0
    GO TO 602
766 CONTINUE
```

```
      X(1)=A(1,2)/A(1,1)
  602 U=2.0
      DO 43 I=1,NB
      IF(X(I)**2-1.E-8)43,43,0
      IF((X(I)*X(I)).LT.(U*U))U=X(I)
   43 CONTINUE
      UU=1.0
      IF(U.LT.1.)UU=1./U
      DO 44 I=1,NB
   44 X(I)=X(I)*UU
      DO 40 J=1,L
      R(J)=0.0
      DO 40 I=1,NB
   40 R(J)=R(J)-D(J,I)*X(I)
      IGG=IGG+1
      I5=4260880
      IF(NN-NO)8060,8060,0
      IRL=IRL+1
      DO 8061 I=1,NO+1
 8061 IJK(IRL,I)=P(I)
      IJK(IRL,10)=NO+1
      I5=6882320
 8060 NX=NX3
      DO 8070 I=1,5
      IF(IGG-I*28+27)0,8071,0
 8070 CONTINUE
      GO TO 8053
C
C     OUTPUT OF REACTIONS
C
 8071 WRITE(6,5012)(PX(I),I=1,NX),(V(I),I=1,L)
 5012 FORMAT('1'//6X,20(4X,A4))
 8053 DO 5006 J=1,NX
      XYY(J)=0.0
      DO 5006 I=1,NO+1
 5006 IF(P(I).EQ.J)XYY(J)=X(I)
      DO 5008 I=1,L
 5008 XYY(I+NX)=R(I)
      DO 8051 I=1,NX+L
      X1=XYY(I)
      CALL SUBS(X1,8,2,MI5)
      DO 8051 J=1,8
 8051 MI6(J,I)=MI5(J)
      WRITE(6,5011)I5,((MI6(J,I),J=1,8),I=1,NX+L)
 5011 FORMAT(/1X,A1,4X,114A1)
C
C     END OF OUTPUT
C
 7062 CONTINUE
  461 NO=NN
      RETURN
      END
C
C     END OF REACTION
C
      FINISH
```

EXAMPLE OF DATA INPUT FOR REACTION

DATA TO FIND ALL THE BALANCED REACTIONS BETWEEN
CALCITE DOLOMITE QUARTZ TALC TREMOLITE

```
5 3 2
CAO MGO SIO2H2O CO2
CC     1 0 0 0 1
DOL    1 1 0 0 2
TA     0 3 4 1 0
TR     2 5 8 1 0
Q      0 0 1 0 0
```

```
      MASTER RECALC
C
C
C                  **********
C                  ******RECALC********
C                  **********
C
C
C     THIS PROGRAM RECALCULATES ANALYSES FROM WT % TO CATIONS
C     PER N OXYGENS. THE PROGRAM CAN  BE RUN ON A VOLATILE FREE
C     BASIS (WHEN H2O AND CO2 HAVE NOT BEEN ANALYSED) OR WITH
C     VOLATILES INCLUDED. THE PROGRAM CAN ALSO BE RUN WITH
C     A % OF THE INPUT WT % FEO CONVERTED TO FE2O3,OR WITH
C     ANALYSED WT %FE2O3. THERE ARE 16 MINERAL SUBROUTINES;
C     EACH CALCULATING  % ENDMEMBERS FOR THE PARTICULAR
C     MINERAL GROUP; MORE SUBROUTINES CAN BE ADDED IF NECESSARY.
C
      INTEGER M5(6),M6(3,6)
      INTEGER J3(25),ZY(25,8,2),ZZ(4,8,2),DES(4,7)
      REAL XO22(25),XO21(25),TXWT(15),TT(25),WT(4,15),RC(4,15),
     1TOT(4),ZV(4,25),XJ(25)
      COMMON /A/AM(15),TEXT(15),XME(15),XOX(15),OXWT(15),T
      COMMON /B/II,ANS(25),R,S,ZX(8),J,JT(25),IK,TOTAL,X5,X6,XO2
      II=1
      J=12
C
C     DATA INPUT
C
C     TEXT=NAME OF OXIDE
C
C     AM=MOLECULAR WT
C
C     XME=NO OF CATIONS IN FORMULA
C
C     XOX=NO OF OXYGENS IN FORMULA
C
C     TT=NAMES OF CATIONS
C
C     N1=NO OF MINERAL GROUPS FOR WHICH SUBROUTINES ARE INCLUDED
C
C     ZY=NAMES OF ENDMEMBERS FOR EACH MINERAL GROUP,MAXIMUM OF
C        8, IN A8 FORMAT
C
C     JT=NO OF CATIONS IN TETRAHEDRAL POSITION FOR EACH MINERAL
C        GROUP
C
C     XO22=NO OF OXYGENS TO RECALCULATE EACH MINERAL GROUP
C
C     XJ=FRACTION OF FEO WT% TO BE CONVERTED TO FE2O3, IF NO
C        CONVERSION REQUIRED SET ALL XJ=0
C
C     MM=1   NO VOLATILES ANALYSED
C       =0   VOLATILES ANALYSED
C
C     M=NO OF ELEMENTS ANALYSED
C
```

```
C       J3=CODE GIVING THE ORDER OF THE ELEMENTS ANALYSED.
C              SIO2=1
C              AL2O3=2
C              TIO2=3
C              FE2O3=4
C              FEO=5
C              MGO=6
C              MNO=7
C              CAO=8
C              NA2O=9
C              K2O=10
C              H2O=11
C              CO2=12
C
C       THEN PAIRS OF CARDS GIVING THE TITLE OF THE ANALYSIS AND
C       M WT% OXIDES IN THE ORDER GIVEN BY J3
C
C       IK=CODE FOR EACH MINERAL GROUP, IT DIRECTS THE
C          PROGRAM TO THE CORRECT SUBROUTINE
C              CARBONATE=1
C              CHLORITE=2
C              GARNET=3
C              BIOTITE=4
C              EPIDOTE=5
C              MUSCOVITE=6
C              TALC=7
C              AMPHIBOLE=8
C              RUTILE=9
C              FELDSPAR=10
C              SPHENE=11
C
C       DES=TITLE, PREFERABLY LESS THAN 16 CHARACTERS LONG,
C          THOUGH IT CAN BE UP TO 28 CHARACTERS LONG
C
C       TXWT=WT% OXIDES
C
        DO 60 I=1,J
   60   READ(5,1001)TEXT(I),AM(I),XME(I),XOX(I)
 1001   FORMAT(A6,15F0.0)
        READ(5,1031)(TT(I),I=1,12)
 1031   FORMAT(12A6)
        READ(5,1020)N1
        DO 24 I=1,N1
   24   READ(5,1030)((ZY(I,K,K1),K1=1,2),K=1,8)
 1030   FORMAT(20A4)
        READ(5,1020)(JT(I),I=1,N1)
 1020   FORMAT(5010)
        READ(5,1032)(XO22(I),I=1,N1)
 1032   FORMAT(50F0.0)
        READ(5,1032)(XJ(I),I=1,N1)
        READ(5,1020)MM,M,(J3(I),I=1,M)
        IF(MM.EQ.1)J=10
 5676   CONTINUE
        I4=0
 5677   CONTINUE
        I4=I4+1
```

```
      DO 63 I=1,15
      IF(I.LE.8)ZX(I)=-0.000001
   63 ANS(I),OXWT(I)=-0.000001
      READ(5,1022,END=5678)IK,(DES(I4,I),I=1,7)
 1022 FORMAT(I0,8A4)
      READ(5,1021)(TXWT(I),I=1,M)
 1021 FORMAT(50F0.0)
C
C     END OF INPUT
C
      XO2=XO22(IK)
      IF(MM.EQ.1)J=10
      DO 61 I=1,M
      DO 61 K=1,J
   61 IF(J3(I).EQ.K)OXWT(K)=TXWT(I)
      WTSUM,SUMO,T=0.0
      XX=OXWT(5)
      OXWT(5)=XX*(1.-XJ(IK))
      OXWT(4)=OXWT(4)+XX*XJ(IK)*1.1113
      DO 11 I=1,J
      WTSUM=WTSUM+OXWT(I)
   11 CONTINUE
      TOTAL =WTSUM
      T=0.0
      DO 13 I=1,J
      XX=XOX(I)*OXWT(I)/AM(I)
      SUMO=SUMO+XX
      IF(I.EQ.4.OR.I.EQ.5)GO TO 13
      T=T+XX
   13 CONTINUE
      FACTOR=XO2/SUMO
      DO 14 I=1,J
      AT=XME(I)*OXWT(I)/AM(I)
   14 ANS(I)=AT*FACTOR
      R=0.0
      IF(ANS(1).LT.JT(IK))R=JT(IK)-ANS(1)
      S=ANS(2)-R
      IF(S.LT.0.0)R=JT(IK)-ANS(1)+S
      IF(S.LT.0.0)S=0.0
      IF(IK.EQ.1)CALL CARBONATE
      IF(IK.EQ.2)CALL CHLORITE
      IF(IK.EQ.3)CALL GARNET
      IF(IK.EQ.4)CALL BIOTITE
      IF(IK.EQ.5)CALL EPIDOTE
      IF(IK.EQ.6)CALL MUSCOVITE
      IF(IK.EQ.7)CALL TALC
      IF(IK.EQ.8)CALL AMPHIBOLE
      IF(IK.EQ.9)CALL RUTILE
      IF(IK.EQ.10)CALL PLAG
      IF(IK.EQ.11)CALL SPHENE
      DO 82 I=1,8
      ZV(I4,I)=ZX(I)
      XO21(I4)=XO2
      DO 82 K=1,2
   82 ZZ(I4,I,K)=ZY(IK,I,K)
      DO 83 I=1,J
```

```
   83 WT(I4,I)=OXWT(I)
      DO 84 I=1,12
      II=I
      IF(I.EQ.2)RC(I4,I)=R
      IF(I.EQ.4)RC(I4,I)=S
      IF(I.EQ.2.OR.I.EQ.3.OR.I.EQ.4)GO TO 84
      IF(I.GT.4)II=I-2
      RC(I4,I)=ANS(II)
   84 CONTINUE
      TOT(I4)=TOTAL
      IF(I4.LT.3)GO TO 5677
C
C     OUTPUT
C
      WRITE(6,2000)((DES(K,I),I=1,7),K=1,I4)
 2000 FORMAT('1'/////////20X,3(7A4,2X))
      WRITE(6,2001)
 2001 FORMAT(/20X,3('OXIDE',8X,'WT %',13X)/)
      I5=1
      DO 40 I=1,10
      IJK=1
      IF(I.EQ.4)IJK=0
       DO 42 J=1,3
       X=WT(J,I)
       CALL SUBS(X,6,2,M5,IJK)
       DO 42 K=1,6
   42 M6(J,K)=M5(K)
   40 WRITE(6,3000)(TEXT(I),(M6(J,K),K=1,6),J=1,3)
 3000 FORMAT(21X,3(A6,4X,6A1,14X))
      WRITE(6,2004)(TOT(I),I=1,I4)
 2004 FORMAT(/20X,3('TOTAL',5X,F7.2,13X)/)
      WRITE(6,2002)(XO21(I),I=1,I4)
 2002 FORMAT(/20X,3('RECALCULATED ON',15X)/20X,3('BASIS OF ',F4.1,' (O)
     1',13X)/)
      I5=2
       DO 41 I=1,12
      IKJ=1
      IF(I.EQ.2 .OR.I.EQ.6)IJK=0
      IF(I.EQ.3)WRITE(6,3001)
 3001 FORMAT(1X)
      IF (I.EQ.3)GO TO 41
      DO 44 J=1,3
      X=RC(J,I)
      CALL SUBS(X,6,3,M5,IJK)
      DO 44 K=1,6
   44 M6(J,K)=M5(K)
      WRITE(6,3000)(TT(I),(M6(J,K),K=1,6),J=1,3)
   41 CONTINUE
      WRITE(6,2003)
 2003 FORMAT(/20X,3('ENDMEMBERS',20X)/)
      DO 45 I=1,8
       DO 46 J=1,3
      X=ZV(J,I)
      CALL SUBS(X,6,2,M5,0)
      DO 46 K=1,6
   46 M6(J,K)=M5(K)
```

```
   45 WRITE(6,3002)((ZZ(J,I,K),K=1,2),(M6(J,K),K=1,6),J=1,3)
 3002 FORMAT(20X,3(2A4,3X,6A1,13X))
      GO TO 5676
 4000 FORMAT('1')
 5678 WRITE(6,4000)
      STOP
      END
      SUBROUTINE FIDDLE
C
C     THIS SUBROUTINE CALCULATES THE AMOUNT OF FEO NEEDED TO BE
C     CONVERTED TO FE2O3 SO THAT A PARTICULAR SITE IS FULL
C     VARIABLE PASSED FROM MINERAL SUBROUTINE (IN COMMON)
C     IS THE SIZE OF THE SITE TO BE FILLED .
C     THE ASSUMPTION IS MADE THAT SIO2 AND ENOUGH AL2O3 FILLS THE
C     TETRAHEDRAL SITE,THEN THE REST OF THE AL2O3 + TIO2 AND
C     THE CALCULATED FE2O3 FILL XS.  SUBROUTINES GARNET AND EPIDOTE
C     USE THIS SUBROUTINE.
C
      COMMON /A/AM(15),TEXT(15),XME(15),XOX(15),OXWT(15),T
      COMMON /B/II,ANS(25),R,S,ZX(8),J,JT(25),IK,TOTAL,X5,X6,XO2
      X1=XO2*(2.2226*OXWT(5)/159.7+2.*OXWT(2)/101.94+
     1OXWT(3)/79.9+OXWT(1)/60.09)
      X2=(X5+JT(IK))*(T+3.3339*OXWT(5)/159.70)
      X3=OXWT(5)*(-XO2*2.2226/159.7+(X5+JT(IK))*3.3339/159.70-
     1(X5+JT(IK))/71.85)
      X=(X2-X1)/X3
      XX=OXWT(5)
       OXWT(5)=XX*X
      OXWT(4)=XX*(1.-X)
      SUMO,T,TOTAL,TOTAL1=0.0
      DO 85 I=1,J
      XX=XOX(I)*OXWT(I)/AM(I)
      SUMO=SUMO+XX
      IF(I.EQ.4.OR.I.EQ.5)GO TO 85
      T=T+XX
   85 CONTINUE
      FACTOR=XO2/SUMO
      DO 86 I=1,J
      AT=XME(I)*OXWT(I)/AM(I)
      ANS(I)=AT*FACTOR
   86 TOTAL =TOTAL+OXWT(I)
      R=0.0
      IF(ANS(1).LT.JT(IK))R=JT(IK)-ANS(1)
      S=ANS(2)-R
      IF(S.LT.0.0)R=JT(IK)-ANS(1)+S
      IF(S.LT.0.0)S=0.0
      RETURN
      END



      SUBROUTINE EPIDOTE
C
C     THIS SUBROUTINE CALCULATES  EPIDOTE AND CLINOZOISITE
C     ENDMEMBERS.
```

```
C
      COMMON /A/AM(15),TEXT(15),XME(15),XOX(15),OXWT(15),T
      COMMON /B/II,ANS(25),R,S,ZX(8),J,JT(25),IK,TOTAL,X5,X6,XO2
       X6=3.-S-ANS(3)
       X5=3.
       IF(X6.LT.0.)GO TO 10
       CALL FIDDLE
   10 CONTINUE
   12 C1=ANS(1)/3.
      C2=ANS(8)/2.
      C3=(S*ANS(4))/3.
      X=AMIN1(C1,C2,C3)
      ZX(1)=ANS(4)*X*100./(C3*3.)
      ZX(2)=S*X*100./(C3*3.)
      RETURN
      END
      SUBROUTINE GARNET
C
C     THIS SUBROUTINE CALCULATES GROSSULAR,ANDRADITE,PYROPE,
C     ALMANDINE AND SPESSARTITE ENDMEMBERS
C
      COMMON /A/AM(15),TEXT(15),XME(15),XOX(15),OXWT(15),T
      COMMON /B/II,ANS(25),R,S,ZX(8),J,JT(25),IK,TOTAL,X5,X6,XO2
       X6=2.-S-ANS(3)
         X5=2.
       IF(X6.LT.0.0)GO TO 10
       CALL FIDDLE
   10 CONTINUE
      CC=ANS(8)-2.*ANS(3)-1.5*ANS(4)
      CD=ANS(8)-CC
      C1=(ANS(8)+ANS(5)+ANS(6)+ANS(7))/3.
      C2=(S*ANS(3)+ANS(4))/2.
      C3=ANS(1)/3.0
      X=AMIN1(C1,C2,C3)
      F=X*100./(C1*3.)
      ZX(1)=ANS(6)*F
      ZX(2)=ANS(5)*F
      ZX(3)=ANS(7)*F
      ZX(5)=CC*F
      ZX(4)=CD*F
      RETURN
      END



       SUBROUTINE CHLORITE
C
C     THIS SUBROUTINE CALCULATES MG AND FE CLINOCHLORE
C     ENDMEMBERS
C
      COMMON /A/AM(15),TEXT(15),XME(15),XOX(15),OXWT(15),T
      COMMON /B/II,ANS(25),R,S,ZX(8),J,JT(25),IK,TOTAL,X5,X6,XO2
      C1=(ANS(6)+ANS(5))/5.
      C2=ANS(1)/3.0
```

```
      X=AMIN1(C1,C2)
      ZX(1)=ANS(6)*X*100./(5.*C1)
      ZX(2)=ANS(5)*X*100./(5.*C1)
      RETURN
      END



      SUBROUTINE TALC
C
CC    THIS SUBROUTINE CALCULATES MG AND FE TALC ENDMEMBERS
C
      COMMON /A/AM(15),TEXT(15),XME(15),XOX(15),OXWT(15),T
      COMMON /B/II,ANS(25),R,S,ZX(8),J,JT(25),IK,TOTAL,X5,X6,XO2
      X1=ANS(1)/4.
      X2=(ANS(6)+ANS(5))/3.0
      X=AMIN1(X1,X2)
      IF(X.GT.1.)X=1.
      ZX(1)=ANS(6)*X*100./(ANS(6)+ANS(5))
      ZX(2)=ANS(5)*X*100./(ANS(6)+ANS(5))
      RETURN
      END
```

```
      SUBROUTINE BIOTITE
C
CC    THIS SUBROUTINE CALCULATES ANNITE AND PHLOGOPITE
C      ENDMEMBERS
C
      COMMON /A/AM(15),TEXT(15),XME(15),XOX(15),OXWT(15),T
      COMMON /B/II,ANS(25),R,S,ZX(8),J,JT(25),IK,TOTAL,X5,X6,XO2
      C1=ANS(10)
      C2=(ANS(5)+ANS(6))/3.
      C3=ANS(1)/3.0
      C4=S
      X=AMIN1(C1,C2,C3,C4)
      IF(X.GT.1.)X=1.
      ZX(1)=ANS(6)*X*100./(3.*C2)
      ZX(2)=ANS(5)*X*100./(3.*C2)
      RETURN
      END



      SUBROUTINE MUSCOVITE
C
CC    THIS SUBROUTINE CALCULATES MUSCOVITE AND PARAGONITE
C     ENDMEMBERS
C
```

```
      COMMON /A/AM(15),TEXT(15),XME(15),XOX(15),OXWT(15),T
      COMMON /B/II,ANS(25),R,S,ZX(8),J,JT(25),IK,TOTAL,X5,X6,X02
      C1=ANS(10)*ANS(9)
      C2=ANS(1)/3.0
      C3=S/3.0
      X=AMIN1(C1,C2,C3)
      ZX(1)=ANS(10)*X*100./C1
      ZX(2)=ANS(9)*X*100./C1
      RETURN
      END
C
C
C
      SUBROUTINE SPHENE
C
C     THIS SUBROUTINE CALCULATES SPHENE ENDMEMBER
C
      COMMON /A/AM(15),TEXT(15),XME(15),XOX(15),OXWT(15),T
      COMMON /B/II,ANS(25),R,S,ZX(8),J,JT(25),IK,TOTAL,X5,X6,X02
      C1=ANS(1)
      C2=ANS(8)
      C3=ANS(3)
      X=AMIN1(C1,C2,C3)
      ZX(1)=X*100.
      RETURN
      END
C
C
C     THIS SUBROUTINE CALCULATES RUTILE ENDMEMBER
C
      SUBROUTINE RUTILE
      COMMON /A/AM(15),TEXT(15),XME(15),XOX(15),OXWT(15),T
      COMMON /B/II,ANS(25),R,S,ZX(8),J,JT(25),IK,TOTAL,X5,X6,X02
      ZX(1)=ANS(3)*100./3.
      RETURN
      END
C
C
C
      SUBROUTINE PLAG
C
C     THIS SUBROUTINE CALCULATES THE ANORTHITE,ALBITE AND
C     ORTHOCLASE ENDMEMBERS
C
      COMMON /A/AM(15),TEXT(15),XME(15),XOX(15),OXWT(15),T
      COMMON /B/II,ANS(25),R,S,ZX(8),J,JT(25),IK,TOTAL,X5,X6,X02
      C1=ANS(8)+ANS(9)+ANS(10)
      X2=ANS(8)/C1
      C2=ANS(2)/(1.+X2)
      C3=ANS(1)/(3.-X2)
      X=AMIN1(C1,C2,C3)
      DO 10 I=8,10
   10 ZX(I-7)=ANS(I)*X*100./C1
```

```
      RETURN
      END



      SUBROUTINE AMPHIBOLE
C
CC    THIS SUBROUTINE CALCULATES THE TREMOLITE ENDMEMBER
C
      COMMON /A/AM(15),TEXT(15),XME(15),XOX(15),OXWT(15),T
      COMMON /B/II,ANS(25),R,S,ZX(8),J,JT(25),IK,TOTAL,X5,X6,X02
      Y1=ANS(6)
      Y=S+Y1
      IF(Y.GT.5.)Y1=ANS(6)-(Y-5.0)
      X1=ANS(8)/2.
      X2=Y1/5.0
      X3=ANS(1)/8.0
      X4=AMIN1(X1,X2,X3)
      ZX(1)=X4*100.
      RETURN
      END
      SUBROUTINE CARBONATE
C
CC    THIS SUBROUTINE CALCULATES THE CALCITE,MAGNESITE,
C     SIDERITE AND RHODOCHROSITE ENDMEMBER
C
      COMMON /A/AM(15),TEXT(15),XME(15),XOX(15),OXWT(15),T
      COMMON /B/II,ANS(25),R,S,ZX(8),J,JT(25),IK,TOTAL,X5,X6,X02
      OXWT(10)=OXWT(5)*0.6126+OXWT(7)*0.6204+OXWT(6)*1.0918+OXWT(8)*
     10.7853
      TOTAL=TOTAL+OXWT(10)
      DO 64 I=1,4
   64 ZX(I)=ANS(I+4)*100./(ANS(5)+ANS(6)+ANS(7)+ANS(8))
      RETURN
      END



      FINISH
```

EXAMPLE OF INPUT FOR RECALC

PERMANENT DATA FOLLOWED BY VARIABLE DATA

```
SIO2      60.09   1. 2.
AL2O3    101.94 2. 3.
TIO2      79.90 1. 2.
FE2O3    159.70 2. 3.
FEO       71.85 1. 1.
MGO       40.32 1. 1.
MNO       70.94   1. 1.
CAO      56.08   1. 1.
NA2O      61.982   2. 1.
K2O       94.20    2. 1.
H2O       18.016   2. 1.
CO2      44.010 1. 2.
SI     AL            AL     TI     FE3+   FE2+   MG     MN     CA     NA     K
11
% SID    % MAGN  % RHOD  % CALC
% MGCLIN% FECLIN
% PYROPE% ALM    % SPESS % ANDR  % GROSS
% PHLOG % ANNITE
% EP     % CZ
% MUSC   % PARAG
% MGTALC% FETALC
% TREM
% RUT
% AN     % AB     % OR
% SPHENE
0 4 3 3 3 3 4 8 0 8 5
4. 14. 12. 11. 12.5 11. 11. 23. 6.  8. 5.
0. 0.2 0. 0.15 0. 0.85 0.05 0.2 0. 0.5 0.5
1 9  1 2 3 5 6 7 8 9 10
4 B100 2 BIOTITE
44.25 13.55 0.46 2.27 25.88 0.02 0.04 0.15 10.35
2 B100 7 CHLORITE
30.05 20.68 0.04 3.07 32.49 0.01 0.05 0.02 0.03
7 B100 11 TALC
62.85 0.42 0.01 1.10 30.59 0.01 0.05 0.01 0.02
```

```
      MASTER
C
C
C                  **********
C                  *******FIT*********
C                  **********
C
C     GENERAL BUILD-IT-YOURSELF PROGRAM FOR LEAST SQUARES CURVE
C     FITTING. IT CAN CALCULATE UP TO 8 POLYNOMIAL
C     COEFFICIENTS IN ANY NO OF DIMENSIONS (THE RESTRICTION IS
C     A MATHEMATICAL ONE. THE MATRIX THAT IS INVERTED IN THE
C     CALCULATION IS ILL-CONDITIONED).
C
      REAL A(50,10),B(10,10),D(10),C(50),X(50),Y(50)
C
C     DATA INPUT
C
C     N=NO OF DATA POINTS
C
C     II=NO OF POLYNOMIAL COEFFICIENTS
C
C     X,Y,ETC=COORDINATES OF THE POINTS TO BE FITTED
C
      READ(5,1000)(X(I),I=1,N)
      READ(5,1000)(Y(I),I=1,N)
 1000 FORMAT(50F0.0)
C
C     AN EXAMPLE IS SET UP IN THE PROGRAM. THE INTENTION IS TO
C     FIT Y=F(X) AS  Y=A+BE↑X+CSQRT(X) ,WHERE A,B,C ARE
C     THE POLYNOMIAL COEFFICIENTS.
C
      IA=0
      DO 14 I=1,N
      IA=IA+1
      A(IA,1)=1.
      A(IA,2)=EXP(X(I))
      A(IA,3)=SQRT(X(I))
      C(IA)=Y(IA)
   14 CONTINUE
      DO 16 J=1,II
      DO 16 I=1,II
      B(I,J)=0.
      DO 16 K=1,IA
   16 B(I,J)=B(I,J)+A(K,J)*A(K,I)
      DO 17 I=1,II
      D(I)=0.
      DO 17 K=1,IA
   17 D(I)=D(I)+C(K)*A(K,I)
C
C     A SUBROUTINE IS REQUIRED HERE TO SOLVE THE SET OF NORMAL
C     EQUATIONS.(THE ROUTINE USED WAS COPYRIGHT).ANY ROUTINE
C     WILL SURFICE. THE PROGRAM IS SET UP WITH THE COEFF-
C     ICIENTS TO BE RETURNED IN THE RHS.  INPUT TO THE
C     ROUTINE IS B AND D ; THE LHS AND RHS OF THE NORMAL
C     EQUATIONS
C
```

```
      CALL SOLVES
      DO 18 I=1,IA
      X1=0.
      DO 19 J=1,II
   19 X1=X1+D(J)*A(I,J)
      FF=(X1-C(I))*100./C(I)
C
C     OUTPUT GIVES INPUT Y,CALCULATED Y AND % DIFFERENCE
C     AND THE POLYNOMIAL COEFFICIENTS
C
   18 WRITE(6,2000)C(I),X1,FF
 2000 FORMAT(1X,4F12.5)
      WRITE(6,2001)(D(I),I=1,II)
 2001 FORMAT(//1X,10E19.12)
      STOP
      END
C
C     END OF FIT
C
      FINISH
```

```
      SUBROUTINE SUBS(X1,J3,J1,M1,IY)
C
CC
CC                  **********
CC                  *******SUBS********
CC                  **********
CC
CC    THIS GENERAL SUBROUTINE PROVIDES THE MEANS OF CLARIFYING
CC    OUTPUT.THE MAIN USE IS TO REPLACE ZEROS BY BLANKS.
CC    THERE ARE OTHER POSSIBILITIES WHICH CAN BE IMPLEMENTED
CC    AT THE WHIMS OF THE USER
CC
CC    THE METHOD OF THE SUBROUTINE IS TO REPLACE THE
CC    INPUT NUMBER BY A CHARACTER STRING CONTAINING THE DIGITS
CC    OF THE NUMBER
CC
CC
CC    X1=THE NUMBER TO BE PROCESSED
CC
CC    J3,J1=THE FORMAT WHICH THE NUMBER WILL BE OUTPUT IN THE
CC          CALLING SEGMENT , EG FJ3.J1. IF THE NUMBER IS AN
CC          INTEGER THEN SET J1=0. IF THE INPUT NUMBER IS TOO
CC          TOO BIG FOR THE FORMAT, THE SUBROUTINE RETURNS M1
CC          FULL OF *
CC
CC    M1=INTEGER ARRAY OF LENGTH J3 HOLDING X1 AS A CHARACTER
C           STRING
C
C     IY=1 SECTION WITH OPORTUNITY FOR SUBSTITUTING
C          ALPHANUMERICS FOR NUMBERS.
C       =0 ZEROS ALWAYS REPLACED BY BLANKS
C
      INTEGER M3(20),M1(J3)
           BB=0.5
      X=ABS(X1)
      J2=J3-J1-1
      DO 33 I=1,J3
   33 M1(I)=4260880
      J4=J2
      IF(X1)0,32,32
      J4=J2-1
   32 IF(IFIX(X)-10.**J4)30,0,0
      DO 31 I=1,J3
   31 M1(I)=6882320
      RETURN
   30 M3(J3),M3(J3+1)=0
      DO 10 I=1,J2+J1
      II=J2+J1+1-I
      M3(II)=IFIX(X*10.**(J1-I+1)+BB)-IFIX(X*10.**(J1-I)+BB)*10
      IF(M3(II+1).GE.5)M3(II)=M3(II)-1
   10 IF(M3(II).LT.0)M3(II)=10+M3(II)
      IX=0
      DO 20 I=1,J2+J1
      IF(M3(I))0,20,0
      IX=1
```

```
      GO TO 24
   20 CONTINUE
C
C        SECTION TO SUBSTITUTE ALPHANUMERICS FOR NUMBERS.
C        ZEROS NOT RETURNED AS BLANKS
C
   24 IF(IY-1)50,0,50
C
C        EG. NO  INPUT WITH J3-1 IS 8'S;RETURNS BLANKS
C
         DO 18 I=1,J2+J1
         IF(M3(I)-8)16,0,16
   18 CONTINUE
         RETURN
C
C        EG. NO IS INPUT WITH J3=1 9'S;RETURNS INF(INFINITY)
C
   16 DO 13 I=1,J2+J1
         IF(M3(I)-9)14,0,14
   13 CONTINUE
         M1(4)=-5962736
         M1(5)=-4652016
         M1(6)=-6749168
         RETURN
C
C        END OF SECTION
C
   50 IF(IX)0,0,22
         DO 21 II=1,J3
   21 M1(II)=4260880
         RETURN
   22 IX=0
   14 DO 11 II=1,J2+J1
         I=II
         IF(I.EQ.J2+1.AND.J1.NE.0)M1(I)=7930896
         IF(I.GE.J2+1)I=II+1
         IF(I.EQ.J2.OR.I.GT.J2+1)M1(I)=66576
         IF(M3(II))11,11,0
         IX=IX+1
         IF(X1)0,0,15
         IF(IX-1)15,0,15
         IF(I-J2)0,17,17
         M1(I-1)=7668752
         GO TO 15
   17 M1(J2-1)=7668752
   15 DO 12 J=1,10
         IF(M3(II)-J+1)12,0,12
         M1(I)=66576+(J-1)*262144
   12 CONTINUE
   11 CONTINUE
         RETURN
C
C        END OF SUBS
C
         END
```

```
      SUBROUTINE GRAPH(X,Y,NXY,NXY1,AA,BA,IM)
C
C                  **********
C                  ******GRAPH*******
C                  **********
C
C
C     GENERAL PURPOSE GRAPHICAL SUBROUTINE WHICH PLOTS Y AGAINST
C     X AND CALCULATES THE STRAIGHT LINE REGRESSION OF Y ON X
C     AS AN OPTION. THE PROGRAM WORKS OUT ITS OWN AXES. THERE IS
C     AN OPTION FOR TWO DIFFERENT SYMBOLS.
C
C
C     INPUT PARAMETERS :-
C
C     X,Y=ARRAYS HOLDING X AND Y VALUES TO BE PLOTTED
C
C     NXY=NUMBER OF POINTS TO BE PLOTTED
C
C     NXY1=NUMBER OF POINTS TO BE PLOTTED WITH SYMBOL X,
C          THE REST ARE PLOTTED WITH *; IF ALL POINTS TO BE
C          PLOTTED WITH THE SAME SYMBOL, THEN SET NXY=NXY1
C
C     AA=LABEL FOR X AXIS
C
C     BA=LABEL FOR Y AXIS
C
C     IM=0  IF NO REGRESSION REQUIRED
C       =1  IF REGRESSION REQUIRED
C
      DIMENSION NX(200),NY(200),FG(11),M(101),X(NXY),Y(NXY)
      DATA I1,I2,I3,I4/'X',' ','O','*'/
      WRITE(6,4000)
 4000 FORMAT('1')
 2003 FORMAT(//12X,A6/)
      XMAX,YMAX=-1.E10
      XMIN,YMIN=1.E10
C
C     CHOOSES AXES
C
      DO 100 I=1,NXY
      IF(X(I).GT.XMAX)XMAX=X(I)
      IF(X(I).LT.XMIN)XMIN=X(I)
      IF(Y(I).GT.YMAX)YMAX=Y(I)
  100 IF(Y(I).LT.YMIN)YMIN=Y(I)
      XX=(XMAX-XMIN)/90.
      YY=(YMAX-YMIN)/40.
      STX=XMIN-(XMAX-XMIN)/150.
      STY=YMIN-(YMAX-YMIN)/150.
      A1,B1=0.
C
C     REGRESSION SECTION
C
      IF(IM.EQ.0)GO TO 98
      A,B,C,D,E=0.0
      DO 10 I=1,NXY
```

```
      A=A+X(I)
      B=B+Y(I)
      C=C+X(I)*Y(I)
      D=D+X(I)*X(I)
   10 E=E+Y(I)*Y(I)
      XD=NXY*D-A*A
      A1=(B*D-A*C)/XD
      B1=(NXY*C-B*A)/XD
      R=(NXY*C-A*B)/SQRT(XD*(NXY*E-B*B))
      Y3=0.0
      DO 70 I=1,NXY
      Y2=A1+B1*X(I)
   70 Y3=Y3+(Y(I)-Y2)**2
      SY=SQRT(Y3/(NXY-2))
      SY=SY*2.
      WRITE(6,2013)BA,A1,B1,AA,R,SY
 2013 FORMAT(/' LINE    ',A6,' = ',F12.4,' + ',F12.4,1X,A6,
     1'    WITH R = ',F8.4,'    WITH TWOSIGMA = ',F8.4/)
C
C     END OF REGRESSION SECTION
C
C
C     PLOTTING SECTION
C
   98 CONTINUE
      WRITE(6,2003)BA
      DO 30 I=1,NXY
      NX(I)=(X(I)-STX)/XX
      NY(I)=(Y(I)-STY)/YY
      NX(I)=NX(I)+5
   30 NY(I)=NY(I)+5
      DO 40 IJK=1,51
      I=52-IJK
      DO 41 J=1,101
   41 M(J)=I2
      DO 44 JJ=1,11
      M(1+(JJ-1)*10)=I3
      IF(I.EQ.1+(JJ-1)*5)GO TO45
   44 CONTINUE
      GO TO 99
   45 DO 46 IJ=1,51
   46 M(1+(IJ-1)*2)=I3
   99 CONTINUE
      DO 43 II=1,NXY
      IF((NX(II)+1).LT.1.OR.(NX(II)+1).GT.101)GO TO 43
      IF((NY(II)+1).LT.1.OR.(NY(II)+1).GT.51)GO TO 43
      IJ=I1
      IF(II.GE.NXY+1-NXV1)IJ=I4
      IF(NY(II)+1.EQ.I)M(NX(II)+1)=IJ
   43 CONTINUE
      DO 50 JJ=1,11
      F=STY+(5*JJ-5)*YY
      IF(I.EQ.1+(JJ-1)*5)WRITE(6,2011)F,(M(KK),KK=1,101)
 2011 FORMAT(1X,F9.3,101A1)
      IF(I.EQ.1+(JJ-1)*5)GO TO 40
   50 CONTINUE
```

```
      WRITE(6,2010)(M(KK),KK=1,101)
 2010 FORMAT(10X,101A1)
   40 CONTINUE
      DO 51 K=1,11
   51 FG(K)=STX-(10*K-10)*XX
      WRITE(6,2012)(FG(K),K=1,11)
 2012 FORMAT(5X,11(F8.3,2X))
      WRITE(6,2000)AA
 2000 FORMAT(/35X,A6)
C
C     END OF PLOTTING SECTION
C
C
C     REGRESSION COEFFICIENTS RETURNED IN Y(1),Y(2)
C
      IF(IM.EQ.0)RETURN
      Y(1)=A1
      Y(2)=B1
      RETURN
C
C     END OF GRAPH
C
      END
```

APPENDIX 4

THERMODYNAMIC DATA

KEY FOR THERMODATA IN FOLLOWING PAGES

A, B, C, D, E are heat capacity polynomial coefficients giving entropy and heat contents in Kcals / mole :—

s (1bar, 298.15 → T°K) = A ln T + 2 B T + C / 2 T^2 + E

h (1bar, 298.15 → T°K) = A T + B T^2 + C / T + D

H is $\Delta_f h$ (el, 298.15°K, 1bar) in kcals / mole

S is s (298.15°K, 1bar) in cals / mole °C

V is molar volume in cc.

columns labelled S, HC, HFN are :

S is s (1bar, 298.15 → T°K)

HC is h (1bar, 298.15 → T°K)

HFN is $\Delta_f h$ (el, 298.15°K, 1bar) + h(1bar, 298.15 → T°K)

Appendix 4 : Thermodynamic data

Correction scheme for mineral enthalpies of formation

The following scheme allows the correction of enthalpies in the light of improved determinations of reactions relevant to dependent enthalpies. The mineral name is used to represent the enthalpy correction for that mineral,

eg., talc = 3 dolomite

or; the talc enthalpy is to be corrected by an amount equal to three times the difference between the enthalpy of dolomite listed here and that calculated for a redetermination of the dolomite reaction.

talc = 3 dolomite

diopside = dolomite

forsterite = $\frac{1}{4}$ talc + magnesite

enstatite = forsterite

tremolite = 2 diopside + 3 enstatite

clinochlore = forsterite + enstatite

phlogopite = 0.6 clinochlore + muscovite

cordiente = 0.4 clinochlore

grossularite = 2 wollastonite

zoisite = $\frac{1}{4}$ grossularite

iron chlorite = hercynite

almandine = iron chlorite

iron staurolite = 1.333 almandine

iron chloritoid = $\frac{1}{4}$ iron staurolite

If, for example, the enthalpy of dolomite is to be corrected, then this will necessitate correcting the enthalpies of talc, diopside, forterite, enstatite, tremolite, clinochlore, phlogopite and cordierite.

DIOPSIDE DATA

A =	0.05313	H =	-766.590
B =	0.000004751	S =	34.200
C =	1901.50	V =	66.09000
D =	-22.540		
E =	-0.31622		

DEGK	S	HC	HFN
298.1	0.00	0.000	766.590
350.0	8.95	2.070	768.660
400.0	14.71	4.226	770.816
450.0	20.19	6.356	773.146
500.0	25.37	9.016	775.606
550.0	30.25	11.576	778.166
600.0	34.85	14.218	780.808
650.0	39.18	16.927	783.517
700.0	43.29	19.695	786.285
750.0	47.18	22.515	789.105
800.0	50.88	25.382	791.972
850.0	54.40	28.290	794.880
900.0	57.77	31.238	797.828
950.0	61.00	34.223	800.813
1000.0	64.10	37.243	803.833
1050.0	67.08	40.295	806.885
1100.0	69.95	43.380	809.970
1150.0	72.72	46.496	813.086
1200.0	75.39	49.642	816.232

RUTILE DATA

A =	0.01649	H =	-225.760
B =	0.000000723	S =	12.040
C =	252.80	V =	18.82000
D =	-5.817		
E =	-0.09581		

DEGK	S	HC	HFN
298.1	0.00	0.000	225.760
350.0	3.55	0.765	226.525
400.0	5.58	1.527	227.287
450.0	7.43	2.312	228.072
500.0	9.12	3.114	228.874
550.0	10.68	3.931	229.691
600.0	12.12	4.759	230.519
650.0	13.46	5.596	231.356
700.0	14.71	6.441	232.201
750.0	15.89	7.294	233.054
800.0	17.00	8.154	233.914
850.0	18.05	9.019	234.779
900.0	19.04	9.891	235.651
950.0	19.99	10.767	236.527
1000.0	20.89	11.649	237.409
1050.0	21.76	12.535	238.295
1100.0	22.59	13.427	239.187
1150.0	23.39	14.322	240.082
1200.0	24.15	15.223	240.983

FORSTERITE DATA

A =	0.03662	H =	-520.180
B =	0.000003078	S =	22.750
C =	1016.70	V =	43.79000
D =	-14.583		
E =	-0.21620		

DEGK	S	HC	HFN
298.1	0.00	0.000	520.180
350.0	6.91	1.516	521.696
400.0	11.14	3.099	523.279
450.0	15.09	4.779	524.959
500.0	18.78	6.530	526.710
550.0	22.22	8.338	528.518
600.0	25.45	10.192	530.372
650.0	28.48	12.085	532.265
700.0	31.34	14.012	534.192
750.0	34.04	15.969	536.149
800.0	36.60	17.954	538.134
850.0	39.04	19.964	540.144
900.0	41.36	21.998	542.178
950.0	43.58	24.054	544.234
1000.0	45.72	26.132	546.312
1050.0	47.76	28.230	548.410
1100.0	49.73	30.348	550.528
1150.0	51.63	32.485	552.665
1200.0	53.47	34.641	554.821

SPHENE DATA

A =	0.04027	H =	-618.160
B =	0.000004024	S =	30.880
C =	811.90	V =	55.65000
D =	-15.056		
E =	-0.23641		

DEGK	S	HC	HFN
298.1	0.00	0.000	618.160
350.0	8.51	1.851	620.011
400.0	13.51	3.726	621.886
450.0	18.12	5.685	623.845
500.0	22.39	7.709	625.869
550.0	26.34	9.786	627.946
600.0	30.04	11.908	630.068
650.0	33.50	14.069	632.229
700.0	36.75	16.265	634.425
750.0	39.82	18.493	636.653
800.0	42.74	20.750	638.910
850.0	45.51	23.036	641.196
900.0	48.15	25.349	643.509
950.0	50.68	27.687	645.847
1000.0	53.11	30.050	648.210
1050.0	55.43	32.437	650.597
1100.0	57.68	34.848	653.008
1150.0	59.84	37.282	655.442
1200.0	61.93	39.739	657.899

QUARTZ DATA

A =	0.01824	H =	-217.650
B =	0.000000123	S =	9.880
C =	877.60	V =	22.68800
D =	-8.348		
E =	-0.10893		

DEGK	S	HC	HFN
298.1	0.00	0.000	217.650
350.0	2.25	0.558	218.208
400.0	3.86	1.162	218.812
450.0	5.45	1.835	219.485
500.0	6.97	2.558	220.208
550.0	8.41	3.317	220.967
600.0	9.78	4.103	221.753
650.0	11.07	4.910	222.560
700.0	12.29	5.734	223.384
750.0	13.45	6.571	224.221
800.0	14.54	7.420	225.070
850.0	15.58	8.277	225.927
900.0	16.57	9.143	226.793
950.0	17.52	10.015	227.665
1000.0	18.42	10.893	228.543
1050.0	19.28	11.775	229.425
1100.0	20.10	12.663	230.313
1150.0	20.90	13.554	231.204
1200.0	21.66	14.448	232.098

WOLLASTONITE DATA

A =	0.02674	H =	-389.740
B =	0.000001776	S =	19.600
C =	677.90	V =	39.93000
D =	-10.384		
E =	-0.15720		

DEGK	S	HC	HFN
298.1	0.00	0.000	389.740
350.0	5.15	1.129	390.869
400.0	8.25	2.291	392.031
450.0	11.13	3.515	393.255
500.0	13.80	4.786	394.526
550.0	16.30	6.093	395.833
600.0	18.62	7.429	397.169
650.0	20.80	8.790	398.530
700.0	22.85	10.173	399.913
750.0	24.78	11.574	401.314
800.0	26.61	12.992	402.732
850.0	28.35	14.426	404.166
900.0	30.01	15.874	405.614
950.0	31.59	17.335	407.075
1000.0	33.10	18.810	408.550
1050.0	34.55	20.297	410.037
1100.0	35.94	21.795	411.535
1150.0	37.29	23.305	413.045
1200.0	38.58	24.826	414.566

TALC DATA

A =	0.08454	H =	-1412.005
B =	0.000020912	S =	62.340
C =	1822.00	V =	136.25000
D =	-33.145		
E =	-0.50438		

DEGK	S	HC	HFN
298.1	0.00	0.000	1412.005
350.0	19.46	4.211	1416.216
400.0	31.10	8.572	1420.577
450.0	41.95	13.182	1425.187
500.0	52.10	17.997	1430.002
550.0	61.61	22.991	1434.996
600.0	70.58	28.144	1440.149
650.0	79.06	33.444	1445.449
700.0	87.12	38.883	1450.888
750.0	94.81	44.452	1456.457
800.0	102.16	50.148	1462.153
850.0	109.21	55.966	1467.971
900.0	116.00	61.904	1473.909
950.0	122.54	67.959	1479.964
1000.0	128.87	74.129	1486.134
1050.0	135.00	80.413	1492.418
1100.0	140.96	86.809	1498.814
1150.0	146.74	93.316	1505.321
1200.0	152.37	99.935	1511.940

TREMOLITE DATA

A =	0.18769	H =	-2946.575
B =	0.00002995	S =	131.190
C =	4612.80	V =	272.92000
D =	-74.016		
E =	-1.11319		

DEGK	S	HC	HFN
298.1	0.00	0.000	2946.575
350.0	39.18	8.525	2955.100
400.0	62.83	17.385	2963.960
450.0	84.90	26.761	2973.336
500.0	105.51	36.544	2983.119
550.0	124.79	46.662	2993.237
600.0	142.90	57.071	3003.646
650.0	159.97	67.736	3014.311
700.0	176.13	78.636	3025.211
750.0	191.47	89.753	3036.328
800.0	206.08	101.074	3047.649
850.0	220.04	112.591	3059.166
900.0	233.42	124.296	3070.871
950.0	246.27	136.181	3082.756
1000.0	258.65	148.244	3094.819
1050.0	270.58	160.479	3107.054
1100.0	282.13	172.884	3119.459
1150.0	293.30	185.457	3132.032
1200.0	304.14	198.194	3144.769

DOLOMITE DATA

A =	0.04514	H =	-557.063
B =	0.000009020	S =	37.090
C =	1365.40	V =	64.34000
D =	-18.793		
E =	-0.27026		

DEGK	S	HC	HFN
298.1	0.00	0.000	557.063
350.0	9.04	2.012	559.075
400.0	14.66	4.120	561.183
450.0	19.98	6.381	563.444
500.0	25.00	8.763	565.826
550.0	29.73	11.245	568.308
600.0	34.20	13.814	570.877
650.0	38.44	16.460	573.523
700.0	42.46	19.175	576.238
750.0	46.30	21.956	579.019
800.0	49.97	24.799	581.862
850.0	53.48	27.699	584.762
900.0	56.86	30.656	587.719
950.0	60.12	33.668	590.731
1000.0	63.26	36.732	593.795
1050.0	66.30	39.849	596.912
1100.0	69.25	43.016	600.079
1150.0	72.11	46.234	603.297
1200.0	74.89	49.502	606.565

CALCITE DATA

A =	0.02421	H =	-288.592
B =	0.000003013	S =	22.150
C =	558.20	V =	36.93400
D =	-9.348		
E =	-0.14290		

DEGK	S	HC	HFN
298.1	0.00	0.000	288.592
350.0	5.02	1.089	289.681
400.0	8.02	2.214	290.806
450.0	10.81	3.397	291.989
500.0	13.40	4.627	293.219
550.0	15.82	5.894	294.486
600.0	18.08	7.193	295.785
650.0	20.20	8.520	297.112
700.0	22.21	9.873	298.465
750.0	24.10	11.249	299.841
800.0	25.91	12.646	301.238
850.0	27.63	14.064	302.656
900.0	29.27	15.502	304.094
950.0	30.85	16.958	305.550
1000.0	32.36	18.433	307.025
1050.0	33.82	19.926	308.518
1100.0	35.22	21.436	310.028
1150.0	36.58	22.964	311.556
1200.0	37.89	24.508	313.100

ORTHOENSTATITE DATA

A =	0.02321	H =	-370.030
B =	0.000003221	S =	16.220
C =	537.40	V =	31.47000
D =	-9.001		
E =	-0.13718		

DEGK	S	HC	HFN
298.1	0.00	0.000	370.030
350.0	4.86	1.053	371.083
400.0	7.76	2.142	372.172
450.0	10.47	3.290	373.320
500.0	12.98	4.484	374.514
550.0	15.33	5.716	375.746
600.0	17.53	6.980	377.010
650.0	19.60	8.273	378.303
700.0	21.55	9.592	379.622
750.0	23.41	10.935	380.965
800.0	25.17	12.300	382.330
850.0	26.85	13.687	383.717
900.0	28.46	15.094	385.124
950.0	30.00	16.521	386.551
1000.0	31.49	17.967	387.997
1050.0	32.92	19.432	389.462
1100.0	34.30	20.916	390.946
1150.0	35.63	22.418	392.448
1200.0	36.92	23.937	393.967

MAGNESITE DATA

A =	0.02254	H =	-265.880
B =	0.000004497	S =	15.700
C =	731.30	V =	28.01800
D =	-9.550		
E =	-0.13524		

DEGK	S	HC	HFN
298.1	0.00	0.000	265.880
350.0	4.38	0.979	266.859
400.0	7.14	2.014	267.894
450.0	9.76	3.129	269.009
500.0	12.25	4.307	270.187
550.0	14.59	5.537	271.417
600.0	16.81	6.812	272.692
650.0	18.91	8.126	274.006
700.0	20.91	9.476	275.356
750.0	22.82	10.860	276.740
800.0	24.65	12.274	278.154
850.0	26.40	13.718	279.598
900.0	28.08	15.191	281.071
950.0	29.70	16.691	282.571
1000.0	31.27	18.218	284.098
1050.0	32.78	19.771	285.651
1100.0	34.25	21.350	287.230
1150.0	35.68	22.954	288.834
1200.0	37.07	24.583	290.463

L-ALBITE DATA

A =	0.06518	H =	-940.396
B =	0.000005557	S =	50.200
C =	1965.20	V =	100.07000
D =	-26.476		
E =	-0.38572		

DEGK	S	HC	HFN
298.1	0.00	0.000	940.396
350.0	11.91	2.633	943.029
400.0	19.29	5.398	945.794
450.0	26.24	8.347	948.743
500.0	32.74	11.434	951.830
550.0	38.83	14.627	955.023
600.0	44.53	17.908	958.304
650.0	49.90	21.262	961.658
700.0	54.97	24.680	965.076
750.0	59.76	28.155	968.551
800.0	64.31	31.681	972.077
850.0	68.64	35.254	975.650
900.0	72.78	38.871	979.267
950.0	76.73	42.529	982.925
1000.0	80.53	46.226	986.622
1050.0	84.17	49.961	990.357
1100.0	87.68	53.733	994.129
1150.0	91.06	57.539	997.935
1200.0	94.33	61.380	1001.776

ANORTHITE DATA

A =	0.06711	H =	-1009.300
B =	0.000005439	S =	48.450
C =	1972.50	V =	100.79000
D =	-27.075		
E =	-0.39669		

DEGK	S	HC	HFN
298.1	0.00	0.000	1009.300
350.0	12.35	2.715	1012.015
400.0	19.97	5.570	1014.870
450.0	27.13	8.609	1017.909
500.0	33.82	11.785	1021.085
550.0	40.07	15.067	1024.367
600.0	45.93	18.437	1027.737
650.0	51.44	21.879	1031.179
700.0	56.64	25.385	1034.685
750.0	61.55	28.947	1038.247
800.0	66.22	32.560	1041.860
850.0	70.65	36.219	1045.519
900.0	74.89	39.921	1049.221
950.0	78.93	43.665	1052.965
1000.0	82.81	47.447	1056.747
1050.0	86.54	51.266	1060.566
1100.0	90.13	55.120	1064.420
1150.0	93.58	59.010	1068.310
1200.0	96.92	62.933	1072.233

MUSCOVITE DATA

A =	0.09936	H =	-1432.730
B =	0.000012266	S =	69.000
C =	2735.40	V =	140.71000
D =	-39.855		
E =	-0.58881		

DEGK	S	HC	HFN
298.1	0.00	0.000	1432.730
350.0	19.42	4.239	1436.969
400.0	31.30	8.690	1441.420
450.0	42.43	13.420	1446.150
500.0	52.85	18.362	1451.092
550.0	62.59	23.477	1456.207
600.0	71.74	28.736	1461.466
650.0	80.36	34.120	1466.850
700.0	88.50	39.615	1472.345
750.0	96.23	45.212	1477.942
800.0	103.57	50.902	1483.632
850.0	110.58	56.681	1489.411
900.0	117.28	62.544	1495.274
950.0	123.70	68.486	1501.216
1000.0	129.88	74.506	1507.236
1050.0	135.83	80.601	1513.331
1100.0	141.57	86.770	1519.500
1150.0	147.11	93.009	1525.739
1200.0	152.48	99.320	1532.050

PHLOGOPITE DATA

A =	0.10533	H =	-1495.650
B =	0.000006644	S =	76.400
C =	2714.50	V =	149.91000
D =	-41.052		
E =	-0.61934		

DEGK	S	HC	HFN
298.1	0.00	0.000	1495.650
350.0	20.10	4.383	1500.033
400.0	32.23	8.929	1504.579
450.0	43.52	13.724	1509.374
500.0	54.01	18.703	1514.353
550.0	63.77	23.825	1519.475
600.0	72.88	29.062	1524.712
650.0	81.42	34.396	1530.046
700.0	89.45	39.812	1535.462
750.0	97.02	45.302	1540.952
800.0	104.19	50.857	1546.507
850.0	111.00	56.472	1552.122
900.0	117.48	62.143	1557.793
950.0	123.67	67.865	1563.515
1000.0	129.59	73.637	1569.287
1050.0	135.27	79.455	1575.105
1100.0	140.72	85.318	1580.968
1150.0	145.97	91.225	1586.875
1200.0	151.04	97.173	1592.823

KYANITE DATA

A =	0.04247	H =	-619.930
B =	0.000002957	S =	20.020
C =	1463.60	V =	44.09000
D =	-17.806		
E =	-0.25199		

DEGK	S	HC	HFN
298.1	0.00	0.000	619.930
350.0	7.17	1.602	621.532
400.0	11.74	3.314	623.244
450.0	16.07	5.157	625.087
500.0	20.16	7.095	627.025
550.0	23.99	9.108	629.038
600.0	27.60	11.180	631.110
650.0	30.99	13.301	633.231
700.0	34.20	15.465	635.393
750.0	37.23	17.661	637.591
800.0	40.11	19.892	639.822
850.0	42.85	22.152	642.082
900.0	45.46	24.438	644.368
950.0	47.96	26.750	646.680
1000.0	50.36	29.085	649.015
1050.0	52.66	31.441	651.371
1100.0	54.87	33.820	653.750
1150.0	57.00	36.218	656.148
1200.0	59.06	38.636	658.566

ANDALUSITE DATA

A =	0.04144	H =	-619.060
B =	0.00000318d	S =	22.280
C =	1312.60	V =	51.53000
D =	-17.023		
E =	-0.24542		

DEGK	S	HC	HFN
298.1	0.00	0.000	619.040
350.0	7.35	1.621	620.661
400.0	11.94	3.344	622.384
450.0	16.28	5.187	624.227
500.0	20.35	7.118	626.158
550.0	24.16	9.119	628.159
600.0	27.74	11.175	630.215
650.0	31.11	13.278	632.318
700.0	34.28	15.420	634.460
750.0	37.29	17.598	636.638
800.0	40.14	19.808	638.848
850.0	42.85	22.046	641.086
900.0	45.44	24.310	643.350
950.0	47.92	26.600	645.640
1000.0	50.29	28.914	647.956
1050.0	52.57	31.249	650.289
1100.0	54.76	33.607	652.647
1150.0	56.88	35.985	655.025
1200.0	58.92	38.384	657.424

SILLIMANITE DATA

A =	0.03963	H =	-618.300
B =	0.00000382	S =	22.970
C =	1133.90	V =	49.90000
D =	-15.942		
E =	-0.23444		

DEGK	S	HC	HFN
298.1	0.00	0.000	618.300
350.0	7.47	1.637	619.937
400.0	12.06	3.357	621.657
450.0	16.36	5.186	623.486
500.0	20.39	7.098	625.398
550.0	24.15	9.074	627.374
600.0	27.69	11.104	629.406
650.0	31.01	13.179	631.479
700.0	34.14	15.294	633.594
750.0	37.11	17.445	635.745
800.0	39.93	19.629	637.929
850.0	42.61	21.843	640.143
900.0	45.18	24.085	642.385
950.0	47.63	26.354	644.654
1000.0	49.98	28.649	646.949
1050.0	52.25	30.969	649.269
1100.0	54.43	33.312	651.612
1150.0	56.53	35.680	653.980
1200.0	58.57	38.070	656.370

CORUNDUM DATA

A =	0.02735	H =	-400.400
B =	0.000001725	S =	12.180
C =	911.10	V =	25.57500
D =	-11.349		
E =	-0.16200		

DEGK	S	Hc	HFN
298.1	0.00	0.000	400.400
350.0	4.67	1.038	401.438
400.0	7.62	2.145	402.545
450.0	10.42	3.332	403.732
500.0	13.05	4.579	404.979
550.0	15.51	5.872	406.272
600.0	17.82	7.201	407.600
650.0	20.00	8.559	408.959
700.0	22.05	9.943	410.343
750.0	23.99	11.349	411.749
800.0	25.83	12.774	413.174
850.0	27.58	14.217	414.617
900.0	29.24	15.676	416.076
950.0	30.84	17.149	417.549
1000.0	32.36	18.637	419.037
1050.0	33.83	20.138	420.538
1100.0	35.24	21.652	422.052
1150.0	36.59	23.177	423.577
1200.0	37.90	24.714	425.114

MAGNETITE DATA

A =	0.07614	H =	-267.400
B =	-0.000009256	S =	36.030
C =	4250.50	V =	44.52400
D =	-35.874		
E =	-0.45220		

DEGK	S	HC	HFN
298.1	0.00	0.000	267.400
350.0	6.35	1.785	269.185
400.0	11.53	3.727	271.127
450.0	16.78	5.960	273.360
500.0	21.89	8.383	275.783
550.0	26.74	10.931	278.331
600.0	31.32	13.562	280.962
650.0	35.62	16.246	283.646
700.0	39.64	18.961	286.361
750.0	43.41	21.692	289.092
800.0	46.94	24.427	291.827
850.0	50.25	27.158	294.558
900.0	53.36	29.877	297.277
950.0	56.28	32.580	299.980
1000.0	59.03	35.260	302.660
1050.0	61.62	37.916	305.316
1100.0	64.07	40.544	307.944
1150.0	66.38	43.142	310.542
1200.0	68.56	45.707	313.107

HERCYNITE DATA

A =	0.07032	H =	-475.200
B =	0.000007472	S =	25.400
C =	4011.80	V =	40.75000
D =	-35.221		
E =	-0.41662		

DEGK	S	HC	HFN
298.1	0.00	0.000	475.200
350.0	8.10	1.769	476.969
400.0	14.40	4.132	479.332
450.0	20.79	6.851	482.051
500.0	27.07	9.831	485.031
550.0	33.13	13.009	488.209
600.0	38.93	16.347	491.547
650.0	44.48	19.816	495.016
700.0	49.79	23.395	498.595
750.0	54.86	27.071	502.271
800.0	59.71	30.832	506.032
850.0	64.37	34.669	509.869
900.0	68.83	38.577	513.777
950.0	73.13	42.549	517.749
1000.0	77.27	46.583	521.783
1050.0	81.26	50.674	525.874
1100.0	85.11	54.819	530.019
1150.0	88.85	59.017	534.217
1200.0	92.46	63.266	538.466

SPINEL DATA

A =	0.03678	H =	-552.800
B =	0.000003226	S =	19.260
C =	986.90	V =	39.71000
D =	-14.549		
E =	-0.21702		

DEGK	S	HC	HFN
298.1	0.00	0.000	552.800
350.0	7.05	1.539	554.339
400.0	11.34	3.146	555.946
450.0	15.34	4.848	557.648
500.0	19.08	6.621	559.421
550.0	22.57	8.450	561.250
600.0	25.83	10.325	563.125
650.0	28.89	12.239	565.039
700.0	31.78	14.188	566.988
750.0	34.51	16.166	568.966
800.0	37.10	18.173	570.973
850.0	39.56	20.206	573.006
900.0	41.91	22.263	575.063
950.0	44.16	24.342	577.142
1000.0	46.32	26.444	579.244
1050.0	48.39	28.567	581.367
1100.0	50.38	30.710	583.510
1150.0	52.31	32.873	585.673
1200.0	54.16	35.055	587.855

GROSSULARITE DATA

A =	0.10363	H =	-1587.193
B =	0.000008789	S =	57.700
C =	2680.00	V =	125.30000
D =	-40.591		
E =	-0.61078		

DEGK	S	HC	HFN
298.1	0.00	0.000	1587.193
350.0	20.08	4.413	1591.606
400.0	32.23	8.967	1596.160
450.0	43.56	13.778	1600.971
500.0	54.10	18.781	1605.974
550.0	63.92	23.937	1611.130
600.0	73.11	29.218	1616.411
650.0	81.74	34.605	1621.798
700.0	89.86	40.085	1627.278
750.0	97.53	45.649	1632.842
800.0	104.81	51.288	1638.481
850.0	111.73	56.997	1644.190
900.0	118.34	62.773	1649.966
950.0	124.65	68.611	1655.804
1000.0	130.70	74.508	1661.701
1050.0	136.51	80.463	1667.656
1100.0	142.10	86.473	1673.666
1150.0	147.49	92.537	1679.730
1200.0	152.70	98.654	1685.847

MG-CORDIERITE DATA

A =	0.21442	H =	-2223.900
B =	0.000007459	S =	96.640
C =	8360.22	V =	233.32000
D =	-92.304		
E =	-1.27314		

DEGK	S	HC	HFN
298.1	0.00	0.000	2223.900
350.0	32.50	7.543	2231.443
400.0	53.88	15.558	2239.458
450.0	74.40	24.274	2248.174
500.0	93.81	33.491	2257.391
550.0	112.09	43.084	2266.984
600.0	129.29	52.967	2276.867
650.0	145.48	63.082	2286.982
700.0	160.75	73.388	2297.288
750.0	175.19	83.854	2307.754
800.0	188.88	94.456	2318.356
850.0	201.88	105.178	2329.078
900.0	214.25	116.005	2339.905
950.0	226.06	126.927	2350.827
1000.0	237.35	137.935	2361.835
1050.0	248.17	149.023	2372.923
1100.0	258.56	160.184	2384.084
1150.0	268.54	171.413	2395.313
1200.0	278.15	182.708	2406.608

SANIDINE DATA

A =	0.06215	H =	-947.628
B =	0.000007962	S =	56.940
C =	1725.90	V =	109.05000
D =	-24.975		
E =	-0.36857		

DEGK	S	HC	HFN
298.1	0.00	0.000	947.628
350.0	12.17	2.684	950.312
400.0	19.61	5.474	953.102
450.0	26.60	8.440	956.068
500.0	33.13	11.542	959.170
550.0	39.25	14.754	962.382
600.0	45.00	18.058	965.686
650.0	50.42	21.442	969.070
700.0	55.54	24.897	972.525
750.0	60.39	28.417	976.045
800.0	65.01	31.998	979.626
850.0	69.42	35.636	983.264
900.0	73.64	39.327	986.955
950.0	77.69	43.070	990.698
1000.0	81.58	46.863	994.491
1050.0	85.33	50.704	998.332
1100.0	88.95	54.593	1002.221
1150.0	92.45	58.528	1006.156
1200.0	95.83	62.509	1010.137

CLINOZOISITE DATA

A =	0.11330	H =	-1651.650
B =	0.000003604	S =	67.900
C =	4047.30	V =	136.48000
D =	-67.526		
E =	-0.67047		

DEGK	S	HC	HFN
298.1	0.00	0.000	1651.650
350.0	18.11	4.134	1655.784
400.0	29.72	8.489	1660.139
450.0	40.78	13.183	1664.833
500.0	51.17	18.120	1669.770
550.0	60.93	23.238	1674.888
600.0	70.08	28.497	1680.147
650.0	78.68	33.868	1685.518
700.0	86.77	39.332	1690.982
750.0	94.42	44.873	1696.523
800.0	101.66	50.480	1702.130
850.0	108.52	56.144	1707.794
900.0	115.06	61.860	1713.510
950.0	121.29	67.622	1719.272
1000.0	127.24	73.425	1725.075
1050.0	132.94	79.267	1730.917
1100.0	138.41	85.144	1736.794
1150.0	143.66	91.055	1742.705
1200.0	148.72	96.997	1748.647

CLINOCHLORE DATA

A =	0.15518	H =	-2135.480
B =	0.000010531	S =	109.000
C =	4392.89	V =	207.54000
D =	-61.765		
E =	-0.91512		

DEGK	S	HC	HFN
298.1	0.00	0.000	2135.480
350.0	28.69	6.389	2141.869
400.0	46.26	12.974	2148.454
450.0	62.71	19.961	2155.441
500.0	78.05	27.244	2162.724
550.0	92.37	34.757	2170.237
600.0	105.77	42.456	2177.936
650.0	118.34	50.310	2185.790
700.0	130.18	58.297	2193.777
750.0	141.36	66.401	2201.881
800.0	151.95	74.610	2210.090
850.0	162.02	82.915	2218.395
900.0	171.62	91.308	2226.788
950.0	180.78	99.784	2235.264
1000.0	189.56	108.339	2243.819
1050.0	197.98	116.968	2252.448
1100.0	206.07	125.669	2261.149
1150.0	213.87	134.439	2269.919
1200.0	221.39	143.276	2278.756

ALMANDINE DATA

A =	0.10462	H =	-1297.500
B =	0.000005010	S =	68.000
C =	3307.78	V =	115.28000
D =	-42.606		
E =	-0.61767		

DEGK	S	HC	HFN
298.1	0.00	0.000	1297.500
350.0	18.11	4.076	1301.576
400.0	29.42	8.313	1305.813
450.0	40.07	12.838	1310.338
500.0	50.04	17.572	1315.072
550.0	59.37	22.465	1319.965
600.0	68.10	27.483	1324.983
650.0	76.29	32.603	1330.103
700.0	84.01	37.808	1335.308
750.0	91.29	43.087	1340.587
800.0	98.19	48.431	1345.931
850.0	104.74	53.832	1351.332
900.0	110.97	59.285	1356.785
950.0	116.92	64.786	1362.286
1000.0	122.61	70.332	1367.832
1050.0	128.06	75.919	1373.419
1100.0	133.29	81.545	1379.045
1150.0	138.33	87.209	1384.709
1200.0	143.18	92.909	1390.409

FE-CHLORITE DATA

A =	0.16334	H =	-1732.000
B =	0.000014795	S =	141.600
C =	3474.43	V =	213.65000
D =	-61.512		
E =	-0.95900		

DEGK	S	HC	HFN
298.1	0.00	0.000	1732.000
350.0	33.81	7.396	1739.396
400.0	53.77	14.877	1746.877
450.0	72.21	22.708	1754.708
500.0	89.27	30.806	1762.806
550.0	105.11	39.118	1771.118
600.0	119.89	47.609	1779.609
650.0	133.73	56.255	1788.255
700.0	146.75	65.039	1797.039
750.0	159.04	73.948	1805.948
800.0	170.69	82.972	1814.972
850.0	181.76	92.104	1824.104
900.0	192.31	101.338	1833.338
950.0	202.40	110.671	1842.671
1000.0	212.07	120.097	1852.097
1050.0	221.36	129.615	1861.615
1100.0	230.30	139.223	1871.223
1150.0	238.92	148.917	1880.917
1200.0	247.24	158.696	1890.696

ANNITE DATA

A =	0.12070	H =	-1235.000
B =	0.000007826	S =	97.600
C =	3390.27	V =	154.32000
D =	-47.911		
E =	-0.71141		

DEGK	S	HC	HFN
298.1	0.00	0.000	1235.000
350.0	22.34	4.979	1239.979
400.0	36.00	10.097	1245.097
450.0	48.77	15.523	1250.523
500.0	60.68	21.176	1256.176
550.0	71.79	27.005	1262.005
600.0	82.18	32.977	1267.977
650.0	91.93	39.066	1274.066
700.0	101.10	45.257	1280.257
750.0	109.77	51.536	1286.536
800.0	117.98	57.895	1292.895
850.0	125.77	64.327	1299.327
900.0	133.20	70.825	1305.825
950.0	140.30	77.386	1312.386
1000.0	147.09	84.005	1319.005
1050.0	153.60	90.681	1325.681
1100.0	159.86	97.411	1332.411
1150.0	165.89	104.192	1339.192
1200.0	171.70	111.024	1346.024

FE-CHLORITOID DATA

A =	0.05622	H =	-748.200
B =	0.000004436	S =	39.100
C =	1562.12	V =	69.34000
D =	-22.339		
E =	-0.29263		

DEGK	S	HC	HFN
298.1	0.00	0.000	748.200
350.0	10.57	2.345	750.545
400.0	17.02	4.764	752.964
450.0	23.06	7.330	755.530
500.0	28.70	10.004	758.204
550.0	33.96	12.764	760.964
600.0	38.88	15.593	763.793
650.0	43.50	18.481	766.681
700.0	47.86	21.420	769.620
750.0	51.97	24.404	772.604
800.0	55.88	27.429	775.629
850.0	59.59	30.491	778.691
900.0	63.13	33.588	781.788
950.0	66.52	36.718	784.918
1000.0	69.76	39.879	788.079
1050.0	72.87	43.070	791.270
1100.0	75.87	46.291	794.491
1150.0	78.76	49.539	797.739
1200.0	81.54	52.815	801.015

FE-STAUROLITE DATA

A =	0.20481	H =	-5717.000
B =	0.000111960	S =	118.400
C =	6920.55	V =	446.76000
D =	-35.051		
E =	-1.09414		

DEGK	S	HC	HFN
298.1	0.00	0.000	5717.000
350.0	49.97	20.121	5737.121
400.0	81.90	32.088	5749.088
450.0	112.68	45.164	5762.164
500.0	142.20	59.185	5776.185
550.0	170.52	74.045	5791.045
600.0	197.71	89.675	5806.675
650.0	223.88	106.026	5823.026
700.0	249.12	123.063	5840.063
750.0	273.54	140.761	5857.761
800.0	297.21	159.102	5876.102
850.0	320.20	178.070	5895.070
900.0	342.59	197.655	5914.655
950.0	364.42	217.847	5934.847
1000.0	385.75	238.640	5955.640
1050.0	406.61	260.026	5977.026
1100.0	427.06	282.003	5999.003
1150.0	447.12	304.565	6021.565
1200.0	466.81	327.711	6044.711

APPENDIX 5

ANALYSES

CARBONATE ANALYSES

NAME		FEO	MGO	MNO	CAO	CO2	TOTAL	XSID	XMAGN	XRHOD	XCALC
B100 1	DOL	1.10	20.81	0.05	29.95	46.95	98.86	1.436	48.412	0.069	50.083
B100 2	CC	0.24	1.90	0.25	52.85	43.87	99.10	0.333	4.718	0.352	94.597
B100 3	DOL	0.74	21.01	0.05	29.09	46.27	97.15	0.977	49.601	0.063	49.359
B100 4	DOL	0.96	19.72	0.09	30.67	46.26	97.70	1.266	46.549	0.125	52.060
B100 5	CC	0.24	1.71	0.03	53.15	43.77	98.90	0.334	4.264	0.044	95.358
B100 6	CC	0.25	1.49	0.16	53.84	44.15	99.88	0.345	3.688	0.218	95.749
B100 7	CC	0.28	1.21	0.03	53.66	43.65	98.82	0.393	3.032	0.037	96.538
B100 8	CC	0.23	1.51	0.02	53.98	44.19	99.93	0.316	3.736	0.029	95.919
B100 9	CC	0.22	1.26	0.02	54.19	44.08	99.77	0.302	3.130	0.032	96.536
B100 10	CC	0.25	1.37	0.02	54.15	44.18	99.97	0.345	3.378	0.029	96.248
B100 11	CC	0.21	1.14	0.02	54.31	44.04	99.72	0.288	2.835	0.026	96.851
B100 12	CC	0.28	1.41	0.03	54.11	44.22	100.05	0.387	3.477	0.044	96.092
B100 13	CC	0.24	1.78	0.02	53.72	44.29	100.05	0.330	4.391	0.029	95.250
B100 14	CC	0.27	1.23	0.01	54.30	44.16	99.97	0.374	3.047	0.015	96.565
B100 15	CC	0.23	1.45	0.02	54.12	44.24	100.06	0.316	3.579	0.028	96.078
B100 16	CC	0.26	1.50	0.03	53.91	44.15	99.85	0.359	3.714	0.044	95.883
B100 17	CC	0.28	1.46	0.02	54.08	44.24	100.08	0.387	3.603	0.022	95.988
B100 18	CC	0.23	1.41	0.02	54.04	44.13	99.83	0.316	3.485	0.029	96.170
B100 19	CC	0.27	1.33	0.02	54.13	44.14	99.89	0.374	3.279	0.032	96.315
B100 20	CC	0.92	20.41	0.06	30.31	46.69	98.40	1.213	47.733	0.083	50.972
B100 21	DOL	0.86	19.79	0.05	30.25	45.92	96.87	1.151	47.059	0.070	51.720
B100 22	DOL	0.81	20.87	0.07	30.46	47.25	99.46	1.050	48.238	0.095	50.617
B100 23	DOL	0.72	20.63	0.06	29.77	46.37	97.54	0.947	48.573	0.083	50.397
B100 24	CC	0.26	1.67	0.02	53.85	44.28	100.08	0.358	4.111	0.029	95.502
B100 25	CC	0.27	1.84	0.02	53.52	44.22	99.87	0.373	4.552	0.029	95.045
B100 26	CC	0.27	1.13	0.03	54.36	44.11	99.90	0.374	2.794	0.044	96.788

CARBONATE ANALYSES

NAME		FEO	MGO	MNO	CAO	CO2	TOTAL	%SID	%MAGN	%RHOD	%CALC
71.16 1	CC	0.69	1.81	0.01	53.02	44.05	99.58	0.965	4.493	0.007	94.534
71.16 2	CC	0.66	1.81	0.01	52.32	43.47	98.26	0.933	4.540	0.015	94.512
71.16 3	DOL	2.59	19.31	0.05	29.98	46.24	98.17	3.439	45.594	0.070	50.898
71.16 4	CC	0.69	1.88	0.01	52.47	43.69	98.73	0.966	4.700	0.015	94.319
71.16 5	DOL	2.50	18.92	0.05	30.03	45.80	97.29	3.348	45.109	0.063	51.479
71.16 6	DOL	2.70	19.12	0.06	29.53	45.75	97.16	3.616	45.625	0.085	50.675
71.16 7	CC	0.61	1.91	0.01	53.07	44.14	99.73	0.848	4.714	0.010	94.427
71.16 8	CC	2.62	18.73	0.02	30.01	45.63	97.01	3.514	44.830	0.021	51.635
71.16 9	CC	0.75	1.79	0.00	51.82	43.11	97.47	1.061	4.542	0.000	94.397
71.16 10	CC	0.66	1.72	0.01	52.05	43.16	97.60	0.942	4.353	0.015	94.691
71.16 11	CC	0.62	1.78	0.01	52.80	43.79	99.00	0.870	4.443	0.010	94.677
71.16 12	CC	0.71	1.82	0.01	51.90	43.19	97.64	1.015	4.611	0.015	94.359
71.16 13	CC	0.51	1.93	0.01	52.57	43.71	98.72	0.712	4.833	0.010	94.445
71.16 14	CC	0.48	1.91	0.01	52.28	43.43	98.10	0.673	4.791	0.015	94.521
71.16 15	CC	0.54	1.66	0.01	52.49	43.37	98.08	0.767	4.179	0.012	95.042
71.16 16	CC	0.70	1.72	0.01	52.87	43.83	99.13	0.985	4.284	0.012	94.720
71.16 17	CC	0.69	1.66	0.01	52.87	43.76	98.99	0.972	4.144	0.009	94.876
71.16 18	CC	0.69	1.55	0.01	52.52	43.37	98.15	0.981	3.913	0.007	95.098
71.16 19	CC	0.85	1.91	0.01	52.40	43.77	98.94	1.189	4.779	0.009	94.023
71.16 20	CC	0.67	1.63	0.01	53.21	43.98	99.50	0.938	4.037	0.013	95.012
71.16 21	DOL	2.87	18.86	0.05	31.25	46.92	99.95	3.752	43.886	0.069	52.293
71.16 22	CC	0.66	1.55	0.01	53.11	43.81	99.14	0.927	3.862	0.009	95.202
71.16 23	CC	0.71	1.86	0.02	52.90	44.03	99.52	0.995	4.624	0.022	94.360
71.16 24	CC	0.72	1.66	0.01	53.07	43.93	99.39	1.011	4.126	0.009	94.854
71.16 25	CC	0.72	1.68	0.01	52.88	43.81	99.09	1.014	4.183	0.012	94.791
71.16 26	CC	0.66	1.56	0.01	52.74	43.54	98.52	0.933	3.924	0.013	95.130
71.16 27	CC	0.71	1.61	0.01	52.60	43.50	98.43	1.007	4.031	0.012	94.950
71.16 28	CC	0.73	1.68	0.01	52.68	43.65	98.74	1.018	4.199	0.013	94.770

CARBONATE ANALYSES

NAME	FEO	MGO	MNO	CAO	CO2	TOTAL	%SID	%MAGN	%RHOD	%CALC
71.19 27 CC	0.62	1.89	0.04	52.08	43.36	97.99	0.879	4.749	0.059	94.313
71.19 28 CC	0.58	1.95	0.04	51.66	43.07	97.30	0.826	4.940	0.052	94.182
71.19 29 CC	0.60	1.98	0.04	52.26	43.59	98.47	0.845	4.957	0.059	94.139
71.19 30 CC	0.64	2.18	0.05	51.80	43.48	98.14	0.906	5.466	0.067	93.562
71.19 31 CC	0.66	1.98	0.04	51.83	43.29	97.80	0.939	4.993	0.059	94.009
71.19 32 CC	0.67	2.06	0.05	51.67	43.27	97.73	0.954	5.204	0.074	93.768
71.19 33 CC	0.60	2.06	0.04	51.57	43.14	97.41	0.854	5.221	0.060	93.865
71.19 34 DOL	3.20	18.99	0.09	29.83	46.18	98.29	4.242	44.916	0.126	50.716
71.19 35 DOL	2.99	18.73	0.11	29.63	45.63	97.10	4.017	44.833	0.155	50.995
71.19 36 DOL	3.23	19.15	0.08	29.76	46.31	98.53	4.271	45.153	0.111	50.464
71.19 37 DOL	3.13	18.70	0.10	29.91	45.88	97.72	4.187	44.496	0.140	51.176
71.19 38 CC	0.66	2.00	0.03	51.92	43.38	97.99	0.937	5.035	0.044	93.984
71.19 39 CC	0.68	2.08	0.05	51.88	43.47	98.17	0.964	5.232	0.074	93.730
71.19 40 DOL	3.33	18.78	0.12	29.80	46.02	98.05	4.437	44.555	0.168	50.860
71.19 41 CC	0.65	1.96	0.03	51.92	43.33	97.89	0.923	4.936	0.045	94.096
71.19 42 CC	0.66	2.13	0.04	52.00	43.60	98.43	0.932	5.366	0.052	93.670
71.19 43 CC	0.62	1.99	0.05	51.81	43.27	97.74	0.881	5.022	0.074	94.023
71.19 44 CC	0.64	2.02	0.04	51.73	43.25	97.68	0.911	5.103	0.059	93.927
71.19 45 CC	0.69	2.06	0.05	51.69	43.30	97.79	0.983	5.201	0.067	93.749
71.19 46 CC	0.60	2.03	0.04	51.92	43.38	97.97	0.849	5.113	0.059	93.979
71.19 47 CC	0.62	1.96	0.05	51.87	43.28	97.78	0.880	4.942	0.074	94.104

CARBONATE ANALYSES

NAME		FEO	MGO	MNO	CAO	CO2	TOTAL	XBID	XMAGN	XRHOD	XCALC
71.26 1	CC	0.48	1.60	0.05	52.82	43.54	98.48	0.671	4.001	0.071	95.257
71.26 2	CC	0.57	1.49	0.08	52.71	43.42	98.27	0.804	3.752	0.117	95.326
71.26 3	CC	0.58	1.73	0.06	52.25	43.32	97.94	0.821	4.363	0.089	94.727
71.26 4	DOL	2.20	19.71	0.06	30.24	46.65	98.86	2.890	46.132	0.083	50.895
71.26 5	CC	0.66	1.99	0.11	51.95	43.45	98.17	0.935	5.000	0.163	93.902
71.26 6	CC	0.57	1.86	0.07	52.12	43.36	97.98	0.806	4.698	0.095	94.402
71.26 7	CC	0.62	1.77	0.11	52.33	43.48	98.32	0.876	4.449	0.163	94.512
71.26 8	CC	0.61	1.64	0.09	52.86	43.73	98.94	0.856	4.100	0.132	94.912
71.26 9	CC	0.56	1.46	0.11	53.20	43.78	99.11	0.783	3.645	0.162	95.411
71.26 10	DOL	2.63	19.95	0.13	30.01	47.05	99.78	3.432	46.305	0.178	50.085
71.26 11	DOL	2.60	19.95	0.09	30.09	47.07	99.81	3.390	46.285	0.123	50.202
71.26 12	CC	0.75	2.03	0.06	52.28	43.77	98.89	1.044	5.066	0.088	93.802
71.26 13	CC	0.60	1.42	0.07	52.49	43.18	97.76	0.853	3.590	0.104	95.452
71.26 14	CC	0.66	1.81	0.08	53.25	44.25	100.06	0.918	4.471	0.115	94.496
71.26 15	CC	0.70	1.79	0.12	53.05	44.12	99.79	0.978	4.434	0.175	94.414
71.26 16	CC	0.60	1.72	0.09	53.25	44.12	99.78	0.834	4.255	0.131	94.780
71.26 17	DOL	2.72	20.14	0.10	29.68	47.02	99.66	3.542	46.763	0.137	49.558
71.26 18	DOL	2.47	20.28	0.08	29.89	47.18	99.90	3.207	46.945	0.109	49.739
71.26 19	CC	0.61	1.63	0.07	53.52	44.22	100.05	0.847	4.014	0.096	95.043
71.26 20	CC	0.62	1.53	0.01	53.42	44.01	99.59	0.865	3.803	0.013	95.318
71.26 21	CC	0.68	1.72	0.11	53.20	44.15	99.87	0.949	4.252	0.160	94.639
71.26 22	CC	0.60	1.51	0.07	52.97	43.66	98.82	0.843	3.783	0.103	95.271
71.26 23	CC	0.61	1.29	0.06	53.22	43.62	98.81	0.859	3.241	0.088	95.812
71.26 24	CC	0.52	0.96	0.06	53.71	43.58	98.83	0.728	2.414	0.089	96.770
71.26 25	CC	0.57	1.68	0.04	53.04	43.86	99.19	0.796	4.178	0.059	94.968
71.26 26	CC	0.57	1.51	0.07	52.87	43.56	98.58	0.802	3.792	0.103	95.303
71.26 27	CC	0.76	1.27	0.09	53.28	43.75	99.15	1.059	3.180	0.132	95.629
71.26 28	CC	0.51	1.38	0.06	53.82	44.12	99.88	0.705	3.409	0.080	95.806
71.26 29	CC	0.57	1.63	0.12	52.97	43.80	99.09	0.797	4.055	0.176	94.972

CARBONATE ANALYSES

NAME		FEO	MGO	MNO	CAO	CO2	TOTAL	XSID	XMAGN	XRHOD	XCALC
71.42 1	DOL	4.50	17.39	0.09	30.34	45.63	97.96	6.048	41.620	0.127	52.205
71.42 2	DOL	4.60	17.40	0.16	30.15	45.59	97.89	6.180	41.688	0.212	51.920
71.42 3	CC	0.88	1.95	0.06	51.88	43.45	98.22	1.242	4.896	0.089	93.773
71.42 4	CC	0.85	1.96	0.07	51.91	43.46	98.25	1.198	4.920	0.096	93.786
71.42 5	CC	0.96	2.02	0.07	52.00	43.68	98.74	1.352	5.050	0.103	93.495
71.42 6	CC	0.84	2.10	0.07	51.89	43.60	98.50	1.179	5.268	0.103	93.450
71.42 7	CC	0.88	2.05	0.07	52.10	43.73	98.83	1.234	5.122	0.096	93.549
71.42 8	CC	0.93	2.07	0.07	51.94	43.67	98.69	1.308	5.181	0.103	93.407
71.42 9	CC	4.45	17.45	0.13	30.20	45.58	97.82	5.985	41.816	0.184	52.015
71.42 10	CC	0.84	2.15	0.07	51.79	43.59	98.45	1.180	5.399	0.103	93.317
71.42 11	CC	0.82	1.91	0.06	51.79	43.29	97.87	1.159	4.809	0.089	93.943
71.42 12	DOL	4.57	17.53	0.12	30.32	45.82	98.36	6.105	41.784	0.169	51.942
71.42 13	CC	0.83	1.99	0.07	51.90	43.48	98.27	1.168	4.996	0.104	93.732
71.42 14	CC	0.81	1.95	0.07	51.89	43.41	98.13	1.141	4.900	0.096	93.863
71.42 15	CC	0.85	2.10	0.07	51.92	43.63	98.57	1.193	5.264	0.103	93.440
71.42 16	DOL	4.48	17.65	0.17	30.40	45.98	98.67	5.972	41.906	0.224	51.898
71.42 17	CC	0.83	2.07	0.07	52.03	43.67	98.66	1.163	5.181	0.096	93.560
71.42 18	CC	0.76	1.93	0.07	52.15	43.57	98.48	1.064	4.830	0.103	94.003
71.42 19	CC	0.84	2.01	0.06	51.81	43.43	98.15	1.184	5.054	0.089	93.673

CARBONATE ANALYSES

NAME	FEO	MGO	MNO	CAO	CO2	TOTAL	XSID	XMAGN	XRHOD	XCALC
71.44 22 CC	1.06	2.08	0.05	51.01	43.01	97.21	1.506	5.290	0.075	93.129
71.44 23 CC	0.97	1.84	0.04	51.28	42.91	97.05	1.392	4.696	0.060	93.852
71.44 24 CC	1.02	2.04	0.06	51.65	43.45	98.22	1.432	5.130	0.089	93.349
71.44 25 CC	0.96	1.94	0.05	51.91	43.50	98.35	1.357	4.864	0.067	93.712
71.44 26 CC	0.97	2.02	0.06	51.88	43.58	98.52	1.369	5.062	0.081	93.487
71.44 27 DOL	4.53	16.74	0.12	30.48	45.06	96.93	6.155	40.375	0.172	53.099
71.44 28 CC	0.92	1.84	0.05	52.34	43.71	98.87	1.292	4.606	0.074	94.028
71.44 29 CC	0.92	2.09	0.04	51.87	43.61	98.54	1.296	5.240	0.059	93.405
71.44 30 CC	1.01	2.13	0.05	51.24	43.22	97.65	1.425	5.395	0.074	93.105
71.44 31 CC	0.93	1.93	0.05	52.15	43.66	98.71	1.309	4.820	0.066	93.805
71.44 32 CC	0.94	1.96	0.05	52.11	43.67	98.73	1.323	4.896	0.074	93.707
71.44 33 CC	0.99	2.11	0.04	51.53	43.41	98.09	1.404	5.318	0.059	93.219
71.44 34 CC	1.05	2.06	0.05	51.06	43.02	97.24	1.491	5.236	0.075	93.198
71.44 35 CC	0.96	2.02	0.05	51.58	43.33	97.95	1.363	5.092	0.067	93.478
71.44 36 CC	0.99	2.13	0.04	51.01	43.02	97.20	1.417	5.420	0.060	93.103
71.44 37 CC	0.99	2.00	0.05	51.71	43.44	98.20	1.403	5.028	0.074	93.495
71.44 38 CC	0.97	2.02	0.05	51.68	43.42	98.14	1.375	5.082	0.067	93.477
71.44 39 DOL	4.44	17.04	0.10	30.77	45.55	97.90	5.975	40.850	0.141	53.034
71.44 40 DOL	4.52	16.71	0.09	30.56	45.07	96.95	6.140	40.494	0.129	53.237
71.44 41 CC	0.95	2.07	0.04	51.88	43.62	98.57	1.339	5.188	0.059	93.414
71.44 42 CC	0.98	2.00	0.05	51.80	43.50	98.34	1.387	5.020	0.074	93.520
71.44 43 DOL	4.57	17.00	0.12	30.30	45.23	97.22	6.188	41.048	0.171	52.593
71.44 44 DOL	4.45	16.79	0.10	31.01	45.47	97.82	5.999	40.322	0.142	53.537
71.44 45 CC	1.05	1.95	0.04	51.68	43.38	98.10	1.478	4.904	0.059	93.559
71.44 46 DOL	4.34	17.43	0.11	30.66	45.83	98.37	5.798	41.529	0.155	52.518
71.44 47 CC	1.02	2.07	0.04	51.80	43.59	98.52	1.427	5.191	0.059	93.323
71.44 48 CC	1.00	2.03	0.06	51.68	43.46	98.24	1.417	5.103	0.089	93.391

CARBONATE ANALYSES

NAME		FEO	MGO	MNO	CAO	CO2	TOTAL	XSID	XMAGN	XRHOD	XCALC
71.64 1	DOL	3.97	18.24	0.09	30.72	46.53	99.56	5.231	42.812	0.125	51.832
71.64 2	DOL	3.81	18.15	0.10	30.85	46.44	99.35	5.023	42.684	0.139	52.154
71.64 3	CC	0.67	2.28	0.07	52.23	43.96	99.21	0.939	5.661	0.102	93.298
71.64 4	CC	0.76	1.96	0.06	52.21	43.64	98.63	1.062	4.899	0.088	93.950
71.64 5	CC	0.70	2.08	0.06	51.89	43.49	98.23	0.993	5.229	0.081	93.696
71.64 6	CC	0.73	2.19	0.06	51.91	43.63	98.51	1.019	5.471	0.088	93.422
71.64 7	CC	0.75	2.06	0.05	52.10	43.65	98.61	1.047	5.158	0.066	93.729
71.64 8	CC	0.70	2.12	0.05	51.88	43.52	98.28	0.992	5.329	0.074	93.605
71.64 9	CC	0.78	2.22	0.06	52.11	43.86	99.03	1.085	5.519	0.088	93.307
71.64 10	DOL	3.86	18.31	0.10	30.55	46.41	99.23	5.096	43.082	0.139	51.683
71.64 11	DOL	4.10	17.97	0.09	30.70	46.29	99.15	5.424	42.379	0.125	52.072
71.64 12	CC	0.74	2.16	0.05	52.02	43.70	98.67	1.032	5.411	0.074	93.484
71.64 13	CC	0.65	2.23	0.05	52.12	43.79	98.83	0.913	5.554	0.066	93.466
71.64 14	CC	0.81	2.06	0.06	52.00	43.62	98.54	1.135	5.162	0.081	93.622
71.64 15	CC	0.63	2.11	0.05	51.93	43.51	98.24	0.890	5.305	0.074	93.731
71.64 16	CC	0.68	2.26	0.05	52.19	43.90	99.08	0.954	5.617	0.073	93.355
71.64 17	CC	0.73	2.10	0.06	52.11	43.70	98.70	1.017	5.255	0.088	93.640
71.64 18	CC	0.63	2.19	0.05	52.22	43.81	98.90	0.884	5.448	0.073	93.595
71.64 19	DOL	3.75	18.25	0.10	30.91	46.57	99.59	4.941	42.808	0.138	52.113
71.64 20	CC	0.68	2.07	0.05	51.89	43.46	98.16	0.964	5.207	0.074	93.755

B100 2 BIOTITE

OXIDE	WT %
SIO2	44.25
AL2O3	13.55
TIO2	0.46
FE2O3	0.38
FEO	1.93
MGO	25.88
MNO	0.02
CAO	0.04
NA2O	0.15
K2O	10.35
TOTAL	97.01

RECALCULATED ON BASIS OF 11.0 (O)

SI	3.031
AL	
AL	1.094
TI	0.024
FE3+	0.020
FE2+	0.111
MG	2.642
MN	0.001
CA	0.003
NA	0.020
K	0.895

ENDMEMBERS

% PHLOG	86.83
% ANNITE	3.63

B100 7 CHLORITE

OXIDE	WT %
SIO2	30.05
AL2O3	20.68
TIO2	0.04
FE2O3	0.68
FEO	2.46
MGO	32.40
MNO	0.01
CAO	0.15
NA2O	0.02
K2O	0.03
TOTAL	86.51

RECALCULATED ON BASIS OF 14.0 (O)

SI	2.841
AL	1.159
AL	1.146
TI	0.003
FE3+	0.049
FE2+	0.194
MG	4.573
MN	0.001
CA	0.005
NA	0.004
K	0.004

ENDMEMBERS

% MGCLIN	90.75
% FECLIN	3.85

B100 11 TALC

OXIDE	WT %
SIO2	62.85
AL2O3	0.42
TIO2	0.01
FE2O3	0.06
FEO	0.95
MGO	30.59
MNO	0.01
CAO	0.05
NA2O	0.01
K2O	0.02
TOTAL	95.07

RECALCULATED ON BASIS OF 11.0 (O)

SI	3.985
AL	0.005
AL	0.020
TI	
FE3+	0.003
FE2+	0.056
MG	2.897
MN	0.001
CA	0.003
NA	0.001
K	0.002

ENDMEMBERS

% MGTALC	96.58
% FETALC	1.85

B100 17 TREMOLITE

OXIDE	WT %
SIO2	56.40
AL2O3	3.10
TIO2	0.08
FE2O3	0.39
FEO	1.42
MGO	22.78
MNO	0.03
CAO	13.27
NA2O	0.32
K2O	0.11
TOTAL	97.90

RECALCULATED ON BASIS OF 23.0 (O)

SI	7.694
AL	0.306
AL	0.192
TI	0.008
FE3+	0.040
FE2+	0.162
MG	4.631
MN	0.003
CA	1.940
NA	0.075
K	0.019

ENDMEMBERS

% TREM	92.62

B100 20 OLIGOCLASE

OXIDE	WT %
SIO2	63.25
AL2O3	23.19
TIO2	0.00
FE2O3	0.01
FEO	0.01
MGO	0.06
MNO	0.00
CAO	4.52
NA2O	9.05
K2O	0.10
TOTAL	100.18

RECALCULATED ON BASIS OF 8.0 (O)

SI	2.791
AL	1.206
AL	
TI	
FE3+	
FE2+	
MG	0.004
MN	
CA	0.214
NA	0.774
K	0.006

ENDMEMBERS

% A_N	21.35
% AB	77.37
% O_R	0.56

B100 24 RUTILE

OXIDE	WT %
SIO2	1.28
AL2O3	0.53
TIO2	97.59
FE2O3	
FEO	0.10
MGO	0.15
MNO	0.01
CAO	0.15
NA2O	0.15
K2O	0.06
TOTAL	100.02

RECALCULATED ON BASIS OF 6.0 (O)

SI	0.051
AL	
AL	0.015
TI	2.917
FE3+	
FE2+	0.003
MG	0.009
MN	
CA	0.006
NA	0.012
K	0.003

ENDMEMBERS

% RUT	97.15

71.19 1 BIOTITE

OXIDE	WT %
SIO2	40.81
AL203	17.34
TIO2	0.74
FE203	0.86
FEO	4.39
MGO	21.57
MNO	0.03
CAO	0.04
NA2O	0.15
K2O	10.10
TOTAL	96.04

RECALCULATED ON BASIS OF 11.0 (O)

SI	2.862
AL	0.138
AL	1.296
TI	0.039
FE3+	0.045
FE2+	0.258
MG	2.254
MN	0.002
CA	0.003
NA	0.020
K	0.904

ENDMEMBERS

% PHLOG	75.05
% ANNITE	8.59

71.19 7 CHLORITE

OXIDE	WT %
SIO2	28.09
AL203	22.03
TIO2	0.04
FE203	1.74
FEO	6.28
MGO	28.64
MNO	0.02
CAO	0.06
NA2O	0.01
K2O	0.00
TOTAL	86.91

RECALCULATED ON BASIS OF 14.0 (O)

SI	2.709
AL	1.291
AL	1.213
TI	0.003
FE3+	0.127
FE2+	0.506
MG	4.116
MN	0.002
CA	0.006
NA	0.002
K	

ENDMEMBERS

% MGCLIN	80.39
% FECLIN	9.89

71.19 15 TREMOLITE

OXIDE	WT %
SIO2	51.37
AL203	9.20
TIO2	0.15
FE203	1.10
FEO	3.95
MGO	18.39
MNO	0.05
CAO	12.21
NA2O	1.28
K2O	0.07
TOTAL	97.77

RECALCULATED ON BASIS OF 23.0 (O)

SI	7.125
AL	0.865
AL	0.641
TI	0.016
FE3+	0.105
FE2+	0.459
MG	3.807
MN	0.006
CA	1.817
NA	0.335
K	0.012

ENDMEMBERS

% TREM	76.13

71.19 16 CLINOZOISITE

OXIDE	WT %
SIO2	39.07
AL203	32.99
TIO2	0.09
FE203	1.78
FEO	0.00
MGO	0.23
MNO	0.06
CAO	24.56
NA20	0.10
K20	0.01
TOTAL	98.89

RECALCULATED ON BASIS OF 12.5 (O)

SI	2.952
AL	0.048
AL	2.891
TI	0.005
FE3+	0.101
FE2+	
MG	0.026
MN	0.004
CA	1.988
NA	0.005
K	0.001

ENDMEMBERS

% EP	3.32
% CZ	95.08

71.19 19 OLIGOCLASE

OXIDE	WT %
SIO2	63.30
AL203	23.45
TIO2	0.00
FE203	0.01
FEO	0.01
MGO	0.05
MNO	0.00
CAO	4.53
NA20	9.06
K20	0.10
TOTAL	100.50

RECALCULATED ON BASIS OF 8.0 (O)

SI	2.775
AL	1.216
AL	
TI	
FE3+	
FE2+	
MG	0.003
MN	
CA	0.214
NA	0.773
K	0.006

ENDMEMBERS

% AN	21.35
% AB	77.28
% OR	0.56

71.19 24 SPHENE

OXIDE	WT %
SIO2	30.59
AL203	2.07
TIO2	38.51
FE203	0.01
FEO	0.01
MGO	0.14
MNO	0.01
CAO	28.49
NA20	0.01
K20	0.00
TOTAL	99.83

RECALCULATED ON BASIS OF 5.0 (O)

SI	0.996
AL	0.079
AL	
TI	0.943
FE3+	
FE2+	
MG	0.007
MN	
CA	0.994
NA	0.001
K	

ENDMEMBERS

% SPHENE	94.32

71.64 2 BIOTITE

OXIDE	WT %
SIO2	37.36
AL2O3	18.29
TIO2	1.18
FE2O3	1.66
FEO	8.46
MGO	18.96
MNO	0.06
CAO	0.05
NA2O	0.12
K2O	10.34
TOTAL	96.48

RECALCULATED ON BASIS OF 11.0 (O)

SI	2.689
AL	0.311
AL	1.240
TI	0.064
FE3+	0.090
FE2+	0.509
MG	2.033
MN	0.004
CA	0.004
NA	0.017
K	0.949

ENDMEMBERS

% PHLOG	67.78
% ANNITE	16.97

71.64 6 MUSCOVITE

OXIDE	WT %
SIO2	45.01
AL2O3	33.96
TIO2	0.55
FE2O3	3.36
FEO	0.53
MGO	1.53
MNO	0.02
CAO	0.09
NA2O	0.74
K2O	10.61
TOTAL	96.41

RECALCULATED ON BASIS OF 11.0 (O)

SI	3.000
AL	
AL	2.669
TI	0.028
FE3+	0.169
FE2+	0.030
MG	0.152
MN	0.001
CA	0.006
NA	0.096
K	0.902

ENDMEMBERS

% MUSC	80.43
% PARAG	8.53

71.64 10 EPIDOTE

OXIDE	WT %
SIO2	38.74
AL2O3	30.94
TIO2	0.17
FE2O3	4.29
FEO	0.07
MGO	0.17
MNO	0.05
CAO	24.49
NA2O	0.00
K2O	0.03
TOTAL	98.95

RECALCULATED ON BASIS OF 12.5 (O)

SI	2.954
AL	0.046
AL	2.736
TI	0.010
FE3+	0.246
FE2+	0.004
MG	0.019
MN	0.003
CA	2.001
NA	
K	0.003

ENDMEMBERS

% EP	8.14
% CZ	90.34

71.64 16 OLIGOCLASE

OXIDE	WT %
SIO2	63.26
AL2O3	22.89
TIO2	0.01
FE2O3	
FEO	0.00
MGO	0.03
MNO	0.00
CAO	4.60
NA2O	8.83
K2O	0.30
TOTAL	99.92

RECALCULATED ON BASIS OF 8.0 (O)

SI	2.800
AL	1.194
AL	
TI	
FE3+	
FE2+	
MG	0.002
MN	
CA	0.218
NA	0.758
K	0.017

ENDMEMBERS

% AN	21.52
% AB	74.74
% OR	1.67

71.64 20 SPHENE

OXIDE	WT %
SIO2	30.45
AL2O3	2.80
TIO2	36.65
FE2O3	0.01
FEO	0.01
MGO	0.00
MNO	0.00
CAO	28.69
NA2O	0.02
K2O	0.00
TOTAL	98.62

RECALCULATED ON BASIS OF 5.0 (O)

SI	1.003
AL	0.109
AL	
TI	0.908
FE3+	
FE2+	
MG	
MN	
CA	1.013
NA	0.001
K	

ENDMEMBERS

% SPHENE	90.82

71.42 3 BIOTITE

OXIDE	WT %
SIO2	40.57
AL2O3	16.95
TIO2	0.88
FE2O3	1.23
FEO	6.27
MGO	20.66
MNO	0.03
CAO	0.04
NA2O	0.06
K2O	10.53
TOTAL	97.22

RECALCULATED ON BASIS OF 11.0 (O)

SI	2.848
AL	0.152
AL	1.251
TI	0.046
FE3+	0.055
FE2+	0.368
MG	2.161
MN	0.002
CA	0.003
NA	0.008
K	0.943

ENDMEMBERS

% PHLOG	72.04
% ANNITE	12.28

71.42 7 CHLORITE

OXIDE	WT %
SIO2	28.59
AL2O3	21.73
TIO2	0.04
FE2O3	1.74
FEO	6.28
MGO	28.74
MNO	0.02
CAO	0.06
NA2O	0.00
K2O	0.01
TOTAL	87.21

RECALCULATED ON BASIS OF 14.0 (O)

SI	2.745
AL	1.345
AL	1.195
TI	0.003
FE3+	0.126
FE2+	0.504
MG	4.113
MN	0.002
CA	0.006
NA	
K	0.001

ENDMEMBERS

% MGCLIN	81.51
% FECLIN	9.99

71.42 14 EPIDOTE

OXIDE	WT %
SIO2	39.33
AL2O3	30.35
TIO2	0.13
FE2O3	4.80
FEO	0.06
MGO	0.15
MNO	0.01
CAO	24.39
NA2O	0.06
K2O	0.03
TOTAL	99.31

RECALCULATED ON BASIS OF 12.5 (O)

SI	2.990
AL	0.010
AL	2.710
TI	0.007
FE3+	0.274
FE2+	0.004
MG	0.017
MN	0.001
CA	1.987
NA	0.009
K	0.003

ENDMEMBERS

% EP	9.13
% CZ	90.20

71,42 16 OLIGOCLASE

OXIDE	WT %
SIO2	63.56
AL2O3	22.59
TIO2	0.00
FE2O3	0.01
FEO	0.01
MGO	0.04
MNO	0.00
CAO	4.52
NA2O	8.86
K2O	0.26
TOTAL	99.84

RECALCULATED ON BASIS OF 8.0 (O)

SI	2.813
AL	1.179
AL	
TI	
FE3+	
FE2+	
MG	0.003
MN	
CA	0.214
NA	0.760
K	0.005

ENDMEMBERS

% AN	20.99
% AB	74.46
% OR	1.44

71,42 18 SPHENE

OXIDE	WT %
SIO2	30.57
AL2O3	3.01
TIO2	36.75
FE2O3	0.01
FEO	0.01
MGO	0.00
MNO	0.00
CAO	28.67
NA2O	0.58
K2O	0.01
TOTAL	99.60

RECALCULATED ON BASIS OF 5.0 (O)

SI	0.999
AL	0.116
AL	
TI	0.903
FE3+	
FE2+	
MG	
MN	
CA	1.004
NA	0.037
K	

ENDMEMBERS

% SPHENE	90.30

71,42 20 RUTILE

OXIDE	WT %
SIO2	1.58
AL2O3	0.46
TIO2	97.83
FE2O3	
FEO	0.05
MGO	0.10
MNO	0.01
CAO	0.12
NA2O	0.16
K2O	0.04
TOTAL	100.35

RECALCULATED ON BASIS OF 6.0 (O)

SI	0.063
AL	
AL	0.021
TI	2.911
FE3+	
FE2+	0.002
MG	0.006
MN	
CA	0.005
NA	0.012
K	0.002

ENDMEMBERS

% RUT	97.04

71.79 1 BIOTITE

OXIDE	WT %
SIO2	32.52
AL2O3	19.06
TIO2	1.65
FE2O3	3.57
FEO	18.18
MGO	10.01
MNO	0.05
CAO	0.04
NA2O	0.07
K2O	10.11
TOTAL	95.26

RECALCULATED ON BASIS OF 11.0 (O)

SI	2.520
AL	0.480
AL	1.260
TI	0.096
FE3+	0.208
FE2+	1.178
MG	1.156
MN	0.003
CA	0.003
NA	0.011
K	0.999

ENDMEMBERS

% PHLOG	38.53
% ANNITE	39.27

71.79 7 CHLORITE

OXIDE	WT %
SIO2	21.96
AL2O3	21.82
TIO2	0.09
FE2O3	5.97
FEO	21.50
MGO	14.79
MNO	0.06
CAO	0.07
NA2O	0.00
K2O	0.01
TOTAL	86.28

RECALCULATED ON BASIS OF 14.0 (O)

SI	2.373
AL	1.627
AL	1.153
TI	0.007
FE3+	0.486
FE2+	1.944
MG	2.382
MN	0.005
CA	0.008
NA	
K	0.001

ENDMEMBERS

% MGCLIN	43.56
% FECLIN	35.54

71.79 14 HORNBLENDE

OXIDE	WT %
SIO2	41.77
AL2O3	17.72
TIO2	0.30
FE2O3	4.22
FEO	15.18
MGO	6.09
MNO	0.06
CAO	10.55
NA2O	1.92
K2O	0.20
TOTAL	98.01

RECALCULATED ON BASIS OF 23.0 (O)

SI	6.190
AL	1.810
AL	1.286
TI	0.033
FE3+	0.470
FE2+	1.882
MG	1.335
MN	0.008
CA	1.675
NA	0.552
K	0.038

ENDMEMBERS

% TREM	26.90

71.79 16 GARNET RIM

OXIDE	WT %
SIO2	33.05
AL203	22.71
TIO2	0.09
FE203	1.66
FEO	31.40
MGO	1.78
MNO	1.82
CAO	7.53
NA2O	0.07
K2O	0.01
TOTAL	100.12

RECALCULATED ON BASIS OF 12.0 (O)

SI	2.700
AL	0.300
AL	1.888
TI	0.006
FE3+	0.102
FE2+	2.145
MG	0.217
MN	0.126
CA	0.659
NA	0.011
K	0.001

ENDMEMBERS

% PYROPE	6.20
% ALM	61.36
% SPESS	3.60
% ANDR	4.70
% GROSS	14.15

71.79 19 EPIDOTE

OXIDE	WT %
SIO2	36.75
AL203	28.69
TIO2	0.29
FE203	6.55
FEO	0.47
MGO	0.14
MNO	0.09
CAO	23.56
NA2O	0.06
K2O	0.05
TOTAL	96.65

RECALCULATED ON BASIS OF 12.5 (O)

SI	2.906
AL	0.094
AL	2.581
TI	0.017
FE3+	0.390
FE2+	0.031
MG	0.016
MN	0.006
CA	1.996
NA	0.009
K	0.005

ENDMEMBERS

% EP	12.72
% CZ	84.05

71.79 22 OLIGOCLASE

OXIDE	WT %
SIO2	60.16
AL203	23.44
TIO2	0.08
FE203	0.03
FEO	0.03
MGO	0.01
MNO	0.00
CAO	4.53
NA2O	11.16
K2O	0.33
TOTAL	99.76

RECALCULATED ON BASIS OF 8.0 (O)

SI	2.706
AL	1.243
AL	
TI	0.003
FE3+	0.001
FE2+	0.001
MG	0.001
MN	
CA	0.218
NA	0.973
K	0.019

ENDMEMBERS

% AN	17.31
% AB	77.17
% OR	1.50

71,85 5 BIOTITE

OXIDE	WT %
SIO2	35.45
AL2O3	18.46
TIO2	1.62
FE2O3	2.50
FEO	17.83
MGO	9.66
MNO	0.05
CAO	0.03
NA2O	0.25
K2O	9.75
TOTAL	96.60

RECALCULATED ON BASIS OF 11.0 (O)

SI	2.665
AL	0.325
AL	1.317
TI	0.092
FE3+	0.199
FE2+	1.125
MG	1.086
MN	0.003
CA	0.002
NA	0.037
K	0.939

ENDMEMBERS

% PHLOG	36.21
% ANNITE	37.51

71,85 6 CHLORITE

OXIDE	WT %
SIO2	24.12
AL2O3	22.30
TIO2	0.09
FE2O3	5.86
FEO	21.08
MGO	13.35
MNO	0.08
CAO	0.05
NA2O	0.00
K2O	0.02
TOTAL	86.95

RECALCULATED ON BASIS OF 14.0 (O)

SI	2.557
AL	1.443
AL	1.343
TI	0.007
FE3+	0.467
FE2+	1.869
MG	2.109
MN	0.007
CA	0.006
NA	
K	0.003

ENDMEMBERS

% MGCLIN	42.18
% FECLIN	37.37

71,85 14 MUSCOVITE

OXIDE	WT %
SIO2	46.35
AL2O3	35.30
TIO2	0.24
FE2O3	1.72
FEO	0.27
MGO	0.72
MNO	0.00
CAO	0.01
NA2O	1.32
K2O	10.23
TOTAL	96.16

RECALCULATED ON BASIS OF 11.0 (O)

SI	3.061
AL	
AL	2.749
TI	0.012
FE3+	0.085
FE2+	0.015
MG	0.071
MN	
CA	0.001
NA	0.169
K	0.862

ENDMEMBERS

% MUSC	76.60
% PARAG	15.02

71,85 16 EPIDOTE

OXIDE	WT %
SIO2	39.69
AL2O3	27.44
TIO2	0.13
FE2O3	6.49
FEO	1.53
MGO	0.01
MNO	2.10
CAO	22.92
NA2O	0.27
K2O	0.02
TOTAL	97.54

RECALCULATED ON BASIS OF 12.5 (O)

SI	3.086
AL	
AL	2.515
TI	0.008
FE3+	0.380
FE2+	0.010
MG	0.001
MN	0.138
CA	1.909
NA	0.041
K	0.002

ENDMEMBERS

% EP	12.52
% CZ	82.96

71,85 20 GARNET RIM

OXIDE	WT %
SIO2	38.07
AL2O3	21.53
TIO2	0.05
FE2O3	
FEO	36.01
MGO	1.78
MNO	0.23
CAO	2.60
NA2O	0.15
K2O	0.01
TOTAL	100.43

RECALCULATED ON BASIS OF 12.0 (O)

SI	3.042
AL	
AL	2.028
TI	0.003
FE3+	
FE2+	2.406
MG	0.212
MN	0.016
CA	0.223
NA	0.023
K	0.001

ENDMEMBERS

% PYROPE	7.07
% ALM	80.21
% SPESS	0.52
% ANDR	0.20
% GROSS	7.22

71.85 26 RUTILE

OXIDE	WT %
SIO2	1.55
AL2O3	0.64
TIO2	96.14
FE2O3	
FEO	0.84
MGO	0.15
MNO	0.00
CAO	0.09
NA2O	0.17
K2O	0.08
TOTAL	99.66

RECALCULATED ON BASIS OF 6.0 (O)

SI	0.062
AL	
AL	0.030
TI	2.891
FE3+	
FE2+	0.028
MG	0.009
MN	
CA	0.004
NA	0.013
K	0.004

ENDMEMBERS

% RUT	96.36

72.3 3 BIOTITE

OXIDE	WT %
SIO2	35.17
AL2O3	18.03
TIO2	1.54
FE2O3	3.68
FEO	18.74
MGO	9.38
MNO	0.08
CAO	0.03
NA2O	0.24
K2O	10.08
TOTAL	96.97

RECALCULATED ON BASIS OF 11.0 (O)

SI	2.666
AL	0.334
AL	1.277
TI	0.088
FE3*	0.210
FE2*	1.188
MG	1.060
MN	0.005
CA	0.002
NA	0.035
K	0.965

ENDMEMBERS

% PHLOG	35.32
% ANNITE	39.61

72.3 6 MUSCOVITE

OXIDE	WT %
SIO2	46.83
AL2O3	34.80
TIO2	0.20
FE2O3	2.06
FEO	0.33
MGO	0.47
MNO	0.02
CAO	0.04
NA2O	2.06
K2O	9.02
TOTAL	95.83

RECALCULATED ON BASIS OF 11.0 (O)

SI	3.092
AL	
AL	2.709
TI	0.010
FE3*	0.102
FE2*	0.018
MG	0.046
MN	0.001
CA	0.003
NA	0.264
K	0.760

ENDMEMBERS

% MUSC	67.03
% PARAG	23.26

72.3 9 CHLORITE

OXIDE	WT %
SIO2	25.90
AL2O3	22.03
TIO2	0.10
FE2O3	6.17
FEO	22.21
MGO	13.77
MNO	0.11
CAO	0.05
NA2O	0.01
K2O	0.02
TOTAL	88.37

RECALCULATED ON BASIS OF 14.0 (O)

SI	2.513
AL	1.487
AL	1.244
TI	0.008
FE3*	0.488
FE2*	1.953
MG	2.158
MN	0.010
CA	0.006
NA	0.002
K	0.003

ENDMEMBERS

% MGCLIN	43.16
% FECLIN	39.06

72.3 14 EPIDOTE

OXIDE	WT %
SIO2	38.25
AL2O3	25.98
TIO2	0.13
FE2O3	9.92
FEO	0.13
MGO	0.37
MNO	0.14
CAO	23.30
NA2O	0.16
K2O	0.01
TOTAL	98.39

RECALCULATED ON BASIS OF 12.5 (O)

SI	2.993
AL	0.007
AL	2.390
TI	0.008
FE3+	0.584
FE2+	0.008
MG	0.043
MN	0.009
CA	1.954
NA	0.024
K	0.001

ENDMEMBERS

% EP	19.19
% CZ	78.49

72.3 20 GARNET RIM

OXIDE	WT %
SIO2	38.65
AL2O3	19.75
TIO2	0.07
FE2O3	0.59
FEO	33.37
MGO	1.76
MNO	0.62
CAO	5.33
NA2O	0.11
K2O	0.01
TOTAL	100.26

RECALCULATED ON BASIS OF 12.0 (O)

SI	3.085
AL	
AL	1.864
TI	0.004
FE3+	0.036
FE2+	2.234
MG	0.210
MN	0.042
CA	0.457
NA	0.017
K	0.001

ENDMEMBERS

% PYROPE	6.79
% ALM	72.26
% SPESS	1.36
% ANDR	2.00
% GROSS	12.79

72.3 26 OLIGOCLASE

OXIDE	WT %
SIO2	63.24
AL2O3	22.93
TIO2	0.00
FE2O3	0.07
FEO	0.06
MGO	0.27
MNO	0.00
CAO	3.73
NA2O	9.47
K2O	0.23
TOTAL	100.00

RECALCULATED ON BASIS OF 8.0 (O)

SI	2.797
AL	1.196
AL	
TI	
FE3+	0.002
FE2+	0.002
MG	0.018
MN	
CA	0.177
NA	0.812
K	0.013

ENDMEMBERS

% AN	17.48
% AB	80.30
% OR	1.28

72,6 2 BIOTITE

OXIDE	WT %
SIO2	34.61
AL2O3	18.19
TIO2	1.80
FE2O3	3.78
FEO	19.27
MGO	8.84
MNO	0.06
CAO	0.01
NA2O	0.12
K2O	9.98
TOTAL	96.66

RECALCULATED ON BASIS OF 11.0 (O)

SI	2.640
AL	0.360
AL	1.276
TI	0.103
FE3+	0.217
FE2+	1.229
MG	1.005
MN	0.004
CA	0.001
NA	0.018
K	0.971

ENDMEMBERS

% PHLOG	33.50
% ANNITE	40.98

72,6 7 MUSCOVITE

OXIDE	WT %
SIO2	44.47
AL2O3	35.88
TIO2	0.24
FE2O3	3.47
FEO	0.55
MGO	1.38
MNO	0.01
CAO	0.00
NA2O	1.13
K2O	10.13
TOTAL	97.26

RECALCULATED ON BASIS OF 11.0 (O)

SI	2.934
AL	0.066
AL	2.724
TI	0.012
FE3+	0.172
FE2+	0.030
MG	0.136
MN	0.001
CA	
NA	0.135
K	0.853

ENDMEMBERS

% MUSC	77.64
% PARAG	13.16

72,6 11 CHLORITE

OXIDE	WT %
SIO2	23.55
AL2O3	21.95
TIO2	0.09
FE2O3	6.42
FEO	23.11
MGO	12.43
MNO	0.07
CAO	0.03
NA2O	0.32
K2O	0.00
TOTAL	87.97

RECALCULATED ON BASIS OF 14.0 (O)

SI	2.506
AL	1.494
AL	1.260
TI	0.007
FE3+	0.514
FE2+	2.057
MG	1.971
MN	0.006
CA	0.003
NA	0.066
K	

ENDMEMBERS

% MGCLIN	39.43
% FECLIN	41.14

72,6 16 EPIDOTE

OXIDE	WT %
SIO2	38.05
AL2O3	24.48
TIO2	0.11
FE2O3	11.22
FEO	0.03
MGO	0.37
MNO	0.14
CAO	23.01
NA2O	0.13
K2O	0.01
TOTAL	97.55

RECALCULATED ON BASIS OF 12.5 (O)

SI	3.016
AL	
AL	2.288
TI	0.007
FE3+	0.669
FE2+	0.002
MG	0.044
MN	0.009
CA	1.954
NA	0.020
K	0.001

ENDMEMBERS

% EP	22.11
% CZ	75.60

72.6 21 GARNET RIM

OXIDE	WT %
SIO2	37.46
AL2O3	20.17
TIO2	0.07
FE2O3	1.16
FEO	35.70
MGO	1.86
MNO	0.29
CAO	3.96
NA2O	0.15
K2O	0.02
TOTAL	100.84

RECALCULATED ON BASIS OF 12.0 (O)

SI	3.011
AL	
AL	1.912
TI	0.004
FE3+	0.070
FE2+	2.400
MG	0.223
MN	0.020
CA	0.341
NA	0.023
K	0.002

ENDMEMBERS

% PYROPE	7.41
% ALM	79.87
% SPESS	0.66
% ANDR	3.78
% GROSS	7.57

72.6 24 OLIGOCLASE

OXIDE	WT %
SIO2	64.75
AL2O3	22.59
TIO2	0.05
FE2O3	0.04
FEO	0.04
MGO	0.30
MNO	0.00
CAO	3.34
NA2O	9.68
K2O	0.01
TOTAL	100.79

RECALCULATED ON BASIS OF 8.0 (O)

SI	2.830
AL	1.164
AL	
TI	0.002
FE3+	0.001
FE2+	0.001
MG	0.020
MN	
CA	0.156
NA	0.820
K	0.001

ENDMEMBERS

% AN	15.64
% AB	82.04
% OR	0.06

70.48 5 BIOTITE

OXIDE	WT %
SIO2	34.87
AL203	18.38
TIO2	1.54
FE203	3.78
FEO	19.25
MGO	9.12
MNO	0.06
CAO	0.08
NA20	0.22
K20	9.88
TOTAL	97.18

RECALCULATED ON BASIS OF 11.0 (O)

SI	2.642
AL	0.358
AL	1.284
TI	0.088
FE3+	0.215
FE2+	1.220
MG	1.030
MN	0.004
CA	0.006
NA	0.032
K	0.955

ENDMEMBERS

% PHLOG	34.33
% ANNITE	40.67

70.48 9 CHLORITE

OXIDE	WT %
SIO2	24.17
AL203	24.24
TIO2	0.05
FE203	6.37
FEO	22.94
MGO	13.28
MNO	0.03
CAO	0.07
NA20	0.09
K20	0.10
TOTAL	91.35

RECALCULATED ON BASIS OF 14.0 (O)

SI	2.457
AL	1.543
AL	1.363
TI	0.004
FE3+	0.488
FE2+	1.951
MG	2.012
MN	0.003
CA	0.008
NA	0.018
K	0.013

ENDMEMBERS

% MGCLIN	40.24
% FECLIN	39.02

70.48 6 MUSCOVITE

OXIDE	WT %
SIO2	46.03
AL203	35.60
TIO2	0.23
FE203	2.56
FEO	0.41
MGO	0.90
MNO	0.00
CAO	0.01
NA20	0.92
K20	10.13
TOTAL	96.79

RECALCULATED ON BASIS OF 11.0 (O)

SI	3.027
AL	
AL	2.760
TI	0.011
FE3+	0.127
FE2+	0.022
MG	0.088
MN	
CA	0.001
NA	0.117
K	0.750

ENDMEMBERS

% MUSC	80.83
% PARAG	11.16

70.48 11 EPIDOTE

OXIDE	WT %
SIO2	38.56
AL203	31.49
TIO2	0.15
FE203	3.78
FEO	0.20
MGO	0.16
MNO	0.05
CAO	24.49
NA20	0.01
K20	0.03
TOTAL	98.92

RECALCULATED ON BASIS OF 12.5 (O)

SI	2.939
AL	0.061
AL	2.768
TI	0.009
FE3+	0.217
FE2+	0.013
MG	0.018
MN	0.003
CA	2.000
NA	0.001
K	0.003

ENDMEMBERS

% EP	7.11
% CZ	90.75

70.48 19 GARNET RIM

OXIDE	WT %
SIO2	37.86
AL203	20.99
TIO2	0.09
FE203	0.20
FEO	35.04
MGO	2.02
MNO	0.29
CAO	4.51
NA20	0.20
K20	0.01
TOTAL	101.21

RECALCULATED ON BASIS OF 12.0 (O)

SI	3.013
AL	
AL	1.969
TI	0.005
FE3+	0.012
FE2+	2.332
MG	0.240
MN	0.020
CA	0.375
NA	0.031
K	0.001

ENDMEMBERS

% PYROPE	7.99
% ALM	77.73
% SPESS	0.65
% ANDR	0.96
% GROSS	11.86

70.48 20 OLIGOCLASE

OXIDE	WT %
SIO2	64.55
AL203	22.69
TIO2	0.00
FE203	0.03
FEO	0.03
MGO	0.31
MNO	0.00
CAO	3.26
NA20	9.88
K20	0.01
TOTAL	100.76

RECALCULATED ON BASIS OF 8.0 (O)

SI	2.815
AL	1.170
AL	
TI	
FE3+	0.001
FE2+	0.001
MG	0.020
MN	
CA	0.153
NA	0.838
K	0.001

ENDMEMBERS

% AN	15.28
% AB	83.82
% OR	0.06

B376 2 BIOTITE

OXIDE	WT %
SIO2	37.05
AL2O3	17.79
TIO2	1.55
FE2O3	3.00
FEO	15.28
MGO	11.81
MNO	0.05
CAO	0.03
NA2O	0.13
K2O	10.35
TOTAL	97.04

RECALCULATED ON BASIS OF 11.0 (O)

SI	2.745
AL	0.345
AL	1.299
TI	0.086
FE3+	0.167
FE2+	0.947
MG	1.304
MN	0.003
CA	0.002
NA	0.019
K	0.978

ENDMEMBERS

% PHLOG	43.47
% ANNITE	31.57

B376 5 CHLORITE

OXIDE	WT %
SIO2	26.31
AL2O3	21.77
TIO2	0.07
FE2O3	5.29
FEO	19.06
MGO	16.23
MNO	0.08
CAO	0.00
NA2O	0.01
K2O	0.06
TOTAL	88.88

RECALCULATED ON BASIS OF 14.0 (O)

SI	2.680
AL	1.320
AL	1.294
TI	0.005
FE3+	0.406
FE2+	1.623
MG	2.464
MN	0.007
CA	
NA	0.002
K	0.008

ENDMEMBERS

% MGCLIN	49.28
% FECLIN	32.47

B376 8 EPIDOTE

OXIDE	WT %
SIO2	38.41
AL2O3	28.06
TIO2	0.19
FE2O3	5.94
FEO	0.18
MGO	0.10
MNO	0.11
CAO	23.49
NA2O	0.05
K2O	0.16
TOTAL	96.33

RECALCULATED ON BASIS OF 12.5 (O)

SI	3.023
AL	
AL	2.603
TI	0.011
FE3+	0.352
FE2+	0.008
MG	0.012
MN	0.007
CA	1.981
NA	0.008
K	0.016

ENDMEMBERS

% EP	11.73
% CZ	86.77

B376 13 GARNET RIM

OXIDE	WT %
SIO2	37.76
AL203	20.99
TIO2	0.12
FE203	0.21
FEO	32.17
MGO	1.37
MNO	1.73
CAO	6.52
NA2O	0.16
K2O	0.02
TOTAL	101.05

RECALCULATED ON BASIS OF 12.0 (O)

SI	3.008
AL	
AL	1.971
TI	0.007
FE3+	0.012
FE2+	2.144
MG	0.163
MN	0.117
CA	0.557
NA	0.015
K	0.002

ENDMEMBERS

% PYROPE	5.42
% ALM	71.45
% SPESS	3.89
% ANDR	1.10
% GROSS	17.45

B376 16 OLIGOCLASE

OXIDE	WT %
SIO2	61.89
AL203	23.51
TIO2	0.00
FE203	0.02
FEO	0.02
MGO	0.25
MNO	0.00
CAO	5.22
NA2O	8.78
K2O	0.11
TOTAL	99.80

RECALCULATED ON BASIS OF 8.0 (O)

SI	2.752
AL	1.232
AL	
TI	
FE3+	0.001
FE2+	0.001
MG	0.017
MN	
CA	0.249
NA	0.757
K	0.006

ENDMEMBERS

% AN	24.31
% AB	73.99
% OR	0.61

B376 20 CALCITE

OXIDE	WT %
SIO2	0.03
AL203	0.05
TIO2	0.01
FE203	
FEO	0.79
MGO	1.07
MNO	0.02
CAO	53.84
NA2O	0.00
K2O	43.94
TOTAL	99.76

RECALCULATED ON BASIS OF 4.0 (O)

SI	0.002
AL	
AL	0.004
TI	0.001
FE3+	
FE2+	0.044
MG	0.106
MN	0.001
CA	3.838
NA	
K	0.001

ENDMEMBERS

% SID	1.10
% MAGN	2.65
% RHOD	0.03
% CALC	96.22